

# SAFIR2018 – The Finnish Research Programme on Nuclear Power Plant Safety 2015–2018

Interim Report



# **SAFIR2018 – The Finnish Research Programme on Nuclear Power Plant Safety 2015–2018**

Interim Report

---

Jari Hämäläinen & Vesa Suolanen (eds.)



ISBN 978-951-38-8524-3 (URL: <http://www.vttresearch.com/impact/publications>)

VTT Technology 294

ISSN-L 2242-1211

ISSN 2242-122X (Online)

<http://urn.fi/URN:ISBN:978-951-38-8524-3>

Copyright © VTT 2017

JULKAISIJA – UTGIVARE – PUBLISHER

Teknologian tutkimuskeskus VTT Oy

PL 1000 (Tekniikantie 4 A, Espoo)

02044 VTT

Puh. 020 722 111, faksi 020 722 7001

Teknologiska forskningscentralen VTT Ab

PB 1000 (Teknikvägen 4 A, Esbo)

FI-02044 VTT

Tfn +358 20 722 111, telefax +358 20 722 7001

VTT Technical Research Centre of Finland Ltd

P.O. Box 1000 (Tekniikantie 4 A, Espoo)

FI-02044 VTT, Finland

Tel. +358 20 722 111, fax +358 20 722 7001

## Preface

The Finnish Research Programme on Nuclear Power Plant Safety 2015–2018, SAFIR2018, continues a series of Finnish national research programmes in nuclear energy that started in 1989. The programmes were initially carried out separately in the fields of operational aspects of safety (YKÄ 1990–1994, RETU 1995–1998) and structural safety (RATU 1990–1994, RATU2 1995–1998, OHA 1995–1998), and then in combined programmes (FINNUS 1999–2002, SAFIR2003–2006, SAFIR2010 2007-2010, SAFIR2014 2011-2014). Simultaneously research has been carried out in the national nuclear waste management programmes (KYT2018 runs in parallel with SAFIR2018).

SAFIR2018 consist of four main research areas: (1) Plant safety and systems engineering; (2) Reactor safety; (3) Structural safety and materials; and (4) Research infrastructure. Research has been carried out annually in 28 projects that are guided by six reference groups. The research results of the projects are published in scientific journals, conference papers and research reports.

The programme management structure consists of the Management Board, three Steering Groups managing the research areas, six Reference Groups, and programme administration. SAFIR2018 Management Board consists of representatives of the Radiation and Nuclear Safety Authority (STUK), Ministry of Economic Affairs and Employment (MEAE), Fennovoima Oy, Fortum, Teollisuuden Voima Oyj (TVO), Technical Research Centre of Finland Ltd (VTT), Aalto University (Aalto), Lappeenranta University of Technology (LUT), the Finnish Funding Agency for Innovation (Tekes), and the Swedish Radiation Safety Authority (SSM).

The research in the programme has been carried out by VTT, LUT, Aalto, University of Oulu, Finnish Meteorological Institute, Finnish Institute of Occupational Health, SP Technical Research Institute of Sweden, Risk Pilot AB, Finnish Software Measurement Association FISMA, and IntoWorks. A few subcontractors have also contributed to the work in the projects.

This report has been prepared by the programme management in cooperation with the project leaders and project staff.

More information on SAFIR2018 can be found on the programme website <http://safir2018.vtt.fi/>.

# Contents

<b>Preface</b> .....	<b>3</b>
<b>1. Introduction</b> .....	<b>6</b>
<b>2. Automation, organisation and human factors</b> .....	<b>16</b>
2.1 Crafting operational resilience in nuclear domain (CORE) .....	16
2.2 Management principles and safety culture in complex projects (MAPS) ...	29
2.3 Integrated safety assessment and justification of nuclear power plant automation (SAUNA).....	40
<b>3. Severe accidents and risk analysis</b> .....	<b>66</b>
3.1 Comprehensive analysis of severe accidents (CASA).....	66
3.2 Chemistry and transport of fission products (CATFIS) .....	78
3.3 Experimental and numerical methods for external event assessment improving safety (ERNEST).....	89
3.4 Extreme weather and nuclear power plants (EXWE) .....	104
3.5 Fire risk evaluation and Defence-in-Depth (FIRED) .....	124
3.6 Safety of new reactor technologies (GENXFIN).....	135
3.7 Probabilistic risk assessment method development and applications (PRAMEA).....	143
<b>4. Reactor and fuel</b> .....	<b>162</b>
4.1 Nuclear criticality and safety analyses preparedness at VTT (KATVE) ....	162
4.2 Development of a Monte Carlo based calculation sequence for reactor core safety analyses (MONSOON).....	175
4.3 Neutronics, burnup and nuclear fuel (NEPAL15) .....	186
4.4 Physics and chemistry of nuclear fuel (PANCHO) .....	192
4.5 Safety analyses for dynamical events (SADE).....	203
<b>5. Thermal hydraulics</b> .....	<b>215</b>
5.1 Comprehensive and systematic validation of independent safety analysis tools (COVA) .....	215
5.2 Couplings and instabilities in reactor systems (INSTAB).....	223
5.3 Integral and separate effects tests on thermal-hydraulic problems in reactors (INTEGRA).....	236
5.4 Development and validation of CFD methods for nuclear reactor safety assessment (NURESA).....	253
5.5 Uncertainty and sensitivity analyses for reactor safety (USVA) .....	266

<b>6. Structural integrity</b> .....	<b>274</b>
6.1 Condition monitoring, thermal and radiation degradation of polymers inside NPP containments (COMRADE).....	274
6.2 Analysis of fatigue and other cumulative ageing to extend lifetime (FOUND) .....	286
6.3 Long term operation aspects of structural integrity (LOST) .....	307
6.4 Mitigation of cracking through advanced water chemistry (MOCCA) .....	313
6.5 Thermal ageing and EAC research for plant life management (THELMA) .....	319
6.6 Non-destructive examination of NPP primary circuit components and concrete infrastructure (WANDA).....	331
<b>7. Research infrastructure</b> .....	<b>343</b>
7.1 Development of thermal-hydraulic infrastructure at LUT (INFRAL) .....	343
7.2 JHR collaboration & Melodie follow-up (JHR).....	354
7.3 Radiological laboratory commissioning (RADLAB) .....	362

**Abstract**

## 1. Introduction

In accordance with Chapter 7a of the Finnish Nuclear Energy Act enacted in 2004, the objective of SAFIR2018 National Nuclear Power Plant Safety Research programme 2015-2018 is to ensure that should new matters related to the safe use of nuclear power plants arise, the authorities possess sufficient technical expertise and other competence required for rapidly determining the significance of the matters.

National research programmes on nuclear safety have had a significant role in the maintenance of expertise and the training of new experts. Since 1990 the programmes (YKÄ & RATU 1990–1994, RETU&RATU2 1995–1998, OHA 1995-1998, FINNUS 1999–2002, SAFIR 2003–2006, SAFIR2010 2007–2010 and SAFIR2014 2011-2014) have had a total volume of 144 M€ and 1 170 person years.

The total volume of the SAFIR2018 programme has been 8,5 M€ (63 person years) and 7,0 M€ (50 person years) in 2015 and 2016, respectively. The main funding organisations were the Finnish State Waste Management Fund (VYR) and Technical Research Centre of Finland Ltd (VTT). Research has been carried out annually in 28 projects. The results are utilised by the Radiation and Nuclear Safety Authority (STUK), Teollisuuden Voima Oyj (TVO), Fortum and Fennovoima Oy, in addition to the research organisations carrying out the projects. However, international co-operation is involved in most of the projects and thus the results are also more widely utilised.

VYR funding is collected from the Finnish utilities Fennovoima, Fortum and TVO based on their MWth shares in Finnish nuclear power plants (units in operation, under construction, and in planning phase according to the decisions-in-principle). VYR funding was smaller in 2016 as compared with 2015 due to the stopping of Olkiluoto 4 (OL4) project in 2015 before entering the construction license phase, which made its funding proportion not to be available since 1.1.2016. In addition to VYR and VTT, other key organisations operating in the area of nuclear safety also fund the programme.

SAFIR2018 Management Board was nominated in September 2014. It consists of representatives of STUK, Ministry of Economic Affairs and Employment (MEAE), Fennovoima, Fortum, TVO, VTT, Aalto University (Aalto), Lappeenranta University of Technology (LUT), and the Finnish Funding Agency for Innovation (Tekes). In 2015 the management board was completed with a representative of Swedish Radiation Safety Authority (SSM).

SAFIR2018 has four main research areas that are managed by *the steering groups* (SG1-SG3 and RG6): plant safety and systems engineering, reactor safety, structural safety and materials, and research infrastructure (see <http://safir2018.vtt.fi/> and [3]).

*The plant safety and systems engineering* research area considers topics of operational resilience in nuclear domain, management principles and safety culture, PRA methods including Defence-in-Depth (DiD), integrated safety assessment of nuclear power automation (I&C), and electrical systems. The goal of the work is to increase the understanding and management of issues significant to overall safety throughout the life cycle of nuclear power plants.

In *the reactor safety research area*, experimental and computational methods are developed for ensuring that the plant and its systems satisfy the safety requirements. The research focuses on thermal-hydraulic problems, development and validation of computational fluid dynamics (CFD) methods, development of Monte Carlo based methods for reactor core safety analyses, fuel behaviour studies, reactor dynamics, severe accidents and fission product transport, and uncertainty and sensitivity analyses for reactor safety.

The aim of the research in *the structural safety and materials area* is to increase knowledge supporting the long-term and reliable use of nuclear power plants, particularly with respect to the integrity of barriers and material issues that affect safety. The aging phenomena of structures and equipment, experimental and numerical methods for external event assessment, and fire risk evaluation are important research topics.

In addition, *infrastructure related research* is funded in SAFIR2018 in order to ensure modern research facilities and equipment. Funding is allocated to the Centre for Nuclear Safety at VTT, to national thermal-hydraulic experimental facilities at LUT, and to the participation in the Jules Horowitz Reactor (JHR) development.

Recently a Memorandum of Understanding (MoU) on scientific and technical co-operation in the area of nuclear safety research was signed between NUGENIA and SAFIR2018 programmes. Co-operation and research results exchange has already started particularly in the material research area.

The SAFIR2018 programme's planning group, nominated by the MEAE in March 2014, defined the following mission for national nuclear safety programmes:

*National nuclear safety research develops and creates expertise, experimental facilities as well as computational and assessment methods for solving future safety issues.*

The vision of SAFIR2018 was defined as follows:

*The SAFIR2018 research community is a vigilant, internationally recognised and strongly networked competence pool that carries out research on topics relevant to the safety of Finnish nuclear power plants on a high scientific level and with modern methods and experimental facilities.*

The Framework Plan [1] describes the research to be carried out in SAFIR2018 that essentially also covers the themes of the preceding SAFIR2014 programme [2].

During the first half 2015–2016 of the SAFIR2018 programme period, research was carried out under the guidance of six *reference groups*:

1. Automation, organisation and human factors
2. Severe accidents and risk analysis
3. Reactor and fuel
4. Thermal hydraulics
5. Structural integrity
6. Research infrastructure.

The results achieved by all SAFIR2018 projects in each year and their full research plans for the next year are reported in the annual reports and plans (see, e.g., [4] and [5]).

Table 1 shows the actualised costs and volumes of SAFIR2018 projects in 2015–2016.

**Table 1.** SAFIR2018 projects 2015–2016.

Project	Acronym	Participating organisations	Total funding (k€)		Volume in person years 2015-2016
			2015	2016	
<b>1. Plant safety and systems engineering</b>					
Crafting operational resilience in nuclear domain	CORE	VTT, FIOH	414	243	5,6
Extreme weather and nuclear power plants	EXWE	FMI	323	327	7,3
Management principles and safety culture in complex projects	MAPS	VTT, Aalto, University of Oulu, University of Jyväskylä	285	203	3,8
Probabilistic risk assessment method development and applications	PRAMEA	VTT, Aalto, Risk Pilot	403	342	5,8
Integrated safety assessment and justification of nuclear power plant automation	SAUNA	VTT, Aalto, FISMA, Risk Pilot, IntoWorks	560	473	8,2
Safety of new reactor technologies	GENXFİN**	VTT		112	0,6
<b>2. Reactor safety</b>					
Comprehensive analysis of severe accidents	CASA	VTT	280	228	3,8
Chemistry and transport of fission products	CATFIS	VTT	262	158	2,9
Comprehensive and systematic validation of independent safety analysis tools	COVA	VTT	305	278	4,3
Couplings and instabilities in reactor systems	INSTAB	LUT	213	167	3,3
Integral and separate effects tests on thermal-hydraulic problems in reactors	INTEGRA	LUT	322	360	5,5
Nuclear criticality and safety analyses preparedness at VTT	KATVE	VTT	231	178	3,4
Development of a Monte Carlo based calculation sequence for reactor core safety analyses	MONSOON	VTT	149	126	2,2
Neutronics, burnup and nuclear fuel	NEPAL15*	Aalto	96		1,0
Development and validation of CFD methods for nuclear reactor safety assessment	NURESA	VTT, Aalto, LUT	257	236	3,4
Physics and chemistry of nuclear fuel	PANCHO	VTT	340	277	5,0
Safety analyses for dynamical events	SADE	VTT	156	100	2,2
Uncertainty and sensitivity analyses for reactor safety	USVA	VTT, Aalto	215	140	3,5

3. Structural safety and materials					
Experimental studies on projectile impacts against concrete structures	ESPIACS*	VTT	44		0,3
Experimental and numerical methods for external event assessment improving safety	ERNEST**	VTT		90	0,5
Fire risk evaluation and Defence-in-Depth	FIRED	VTT, Aalto	220	195	3,4
Analysis of fatigue and other cumulative ageing to extend lifetime	FOUND	VTT, Aalto	542	409	6,4
Long term operation aspects of structural integrity	LOST	VTT	77	245	2,0
Mitigation of cracking through advanced water chemistry	MOCCA	VTT	96	148	1,4
Numerical methods for external event assessment improving safety	NEST*	VTT	334		2,0
Thermal ageing and EAC research for plant life management	THELMA	VTT, Aalto	359	277	4,3
Non-destructive examination of NPP primary circuit components and concrete infrastructure	WANDA	VTT, Aalto	347	91	2,7
Condition monitoring, thermal and radiation degradation of polymers inside NPP containments	COMRADE**	VTT, SP		194	0,8
4. Research infrastructure					
Development of thermal-hydraulic infrastructure at LUT	INFRAL	LUT	313	314	4,2
JHR collaboration & Melodie follow-up	JHR	VTT	40	30	0,4
Renewal of Hot Cell infrastructure	REHOT*	VTT	1008		5,8
Radiological laboratory commissioning 2016	RADLAB**	VTT		751	4,5
0. Programme administration					
SAFIR2018 administration and information	ADMIRE	VTT	324	330	2,1
Total:			8517	7022	112,4

*The costs of ADMIRE are for periods 1.1.15–31.3.16 and 1.1.16–31.3.17. The costs include subcontracted small study projects (50 k€ per year) and value-added tax 24%.*

\*) Project carried out only during the year 2015.

\*\*) Project started from the year 2016 (ESPIACS and NEST were continued as ERNEST and REHOT as RADLAB).

## Financial and statistical information

The total volume of the SAFIR2018 programme in 2015–2016 was 15,5 M€ and 112 person years. The funding partners were VYR with 9,340 M€, VTT with 3,474 M€, Lappeenranta University of Technology with 0,430 M€, Aalto University with 0,412 M€, NKS with 0,327 M€, SSM with 0,277 M€, Halden Reactor Project in-kind with 0,196 M€, TVO with 0,130 M€, Fennovoima with 0,119 M€, Fortum with 0,053 M€, and several other partners with 0,781 M€. The funding proportions of the major funding partners are illustrated in Figure 1.

The costs structure of the projects is shown in Figure 2. The personnel costs make up the major share.

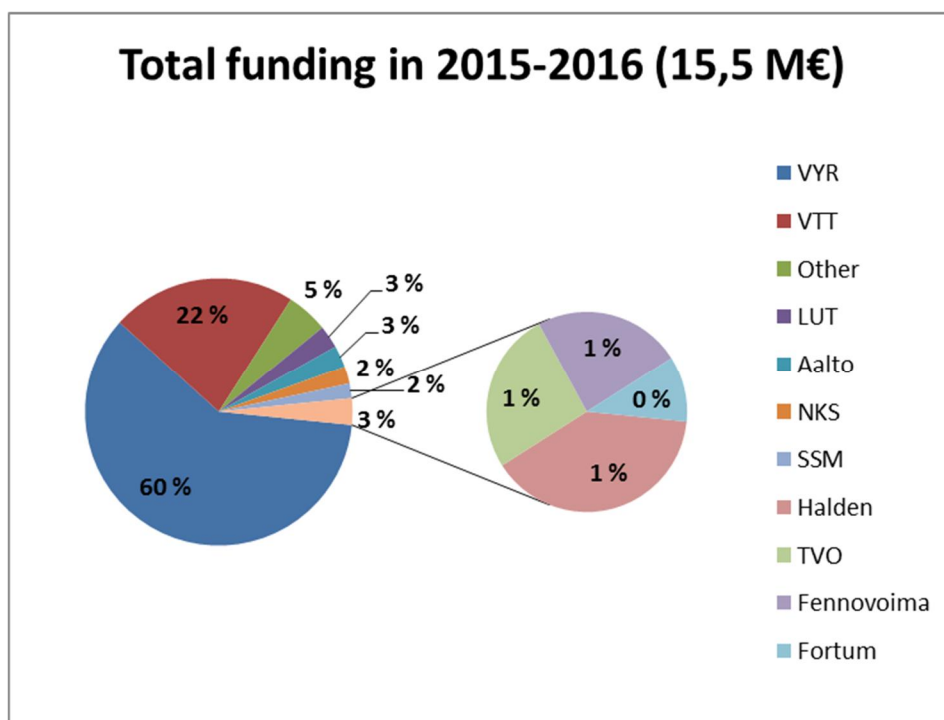


**Figure 1.** Funding of the SAFIR2018 programme in 2015–2016.

Figures 3–5 show the funding and volumes of SAFIR2018 research areas in 2015–2016. In the area Research infrastructure (RG6) the share of person-years was lower than the share of total funding because of infrastructure investments (Figures 3–4). In SG1 and SG2 the shares of the person-years were bigger and in SG3 slightly smaller than the shares of the total funding, respectively.

The effect of the decrease in VYR funding in the beginning of 2016 can clearly be seen in Figure 5. The total funding of SG1, SG2, SG3, and RG6 areas decreased 285 k€, 578 k€, 371 k€, and 267 k€, respectively. In 2017 there was no substantial change in the available VYR funding.

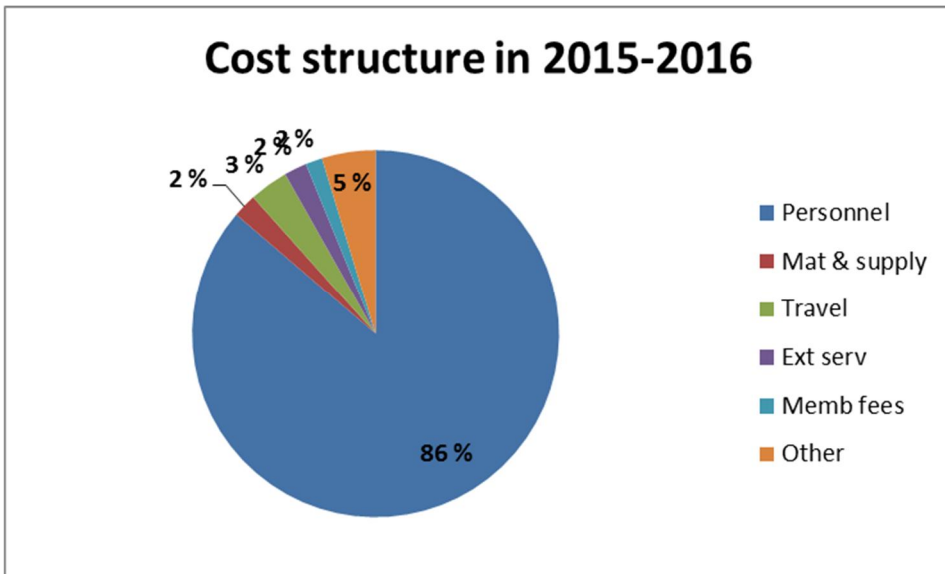


**Figure 2.** Cost structure of SAFIR2018 in 2015–2016.

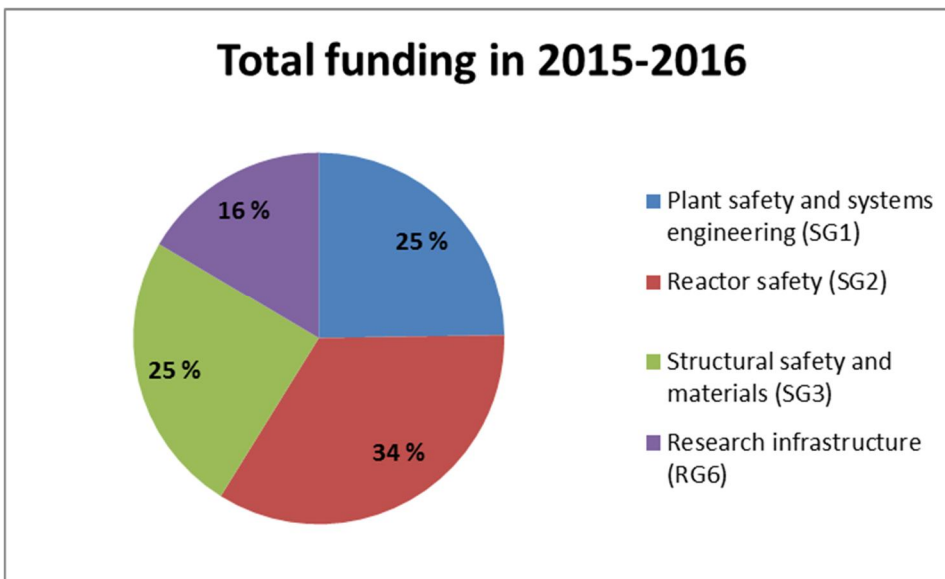


**Figure 3.** Division of funding to the research areas in 2015–2016.

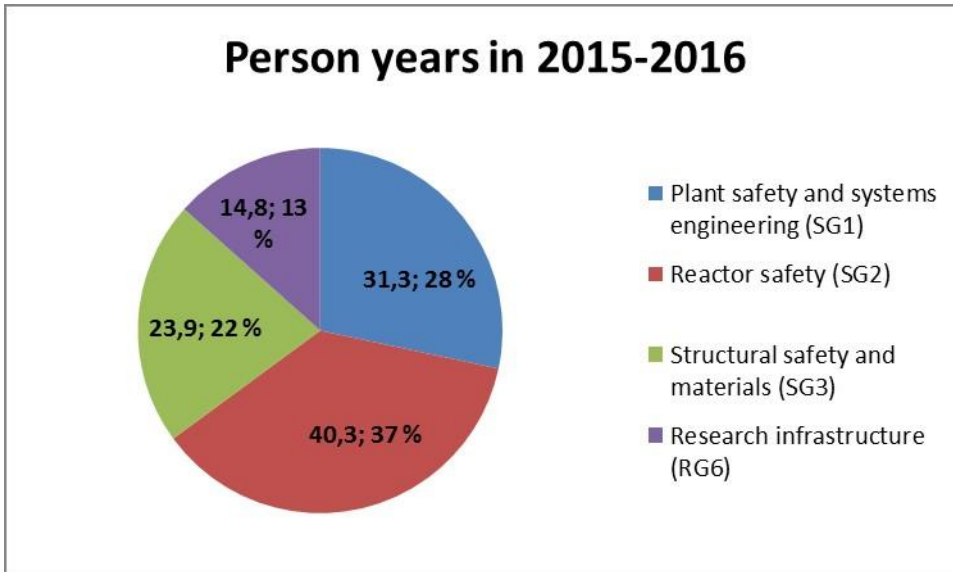


**Figure 4.** Volumes of the research areas in 2015–2016.

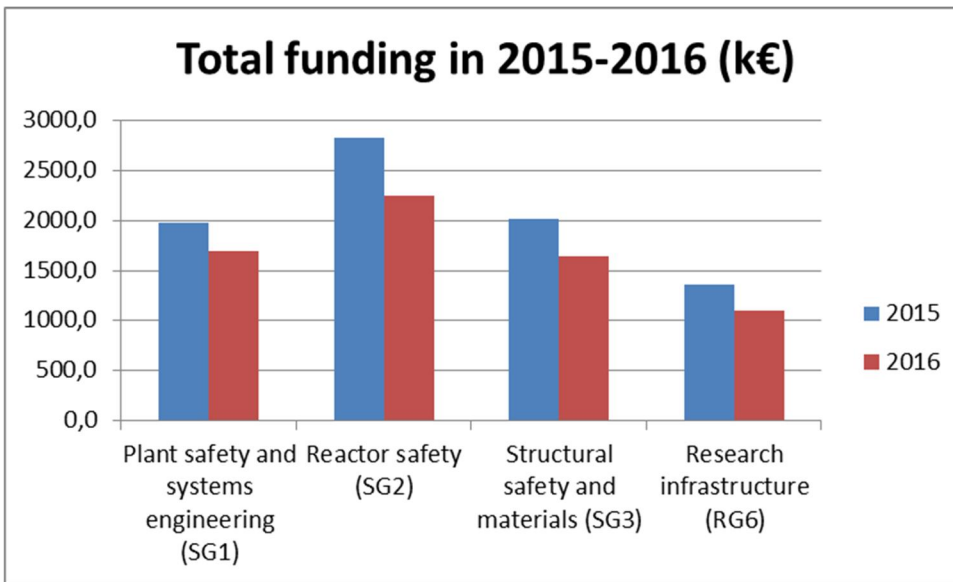


**Figure 5.** Total funding of the research areas in 2015–2016.

The projects of the programme have produced 552 publications in 2015–2016 (Table 2). Major part of the publications consisted of public research reports and conference articles. A total of 89 scientific journal articles were made. The average number of publications was 5,0 per person year, and the average number of scientific journal articles was 0,8 per person year (administration project excluded). The projects had different scopes and there were also clear differences in the number of publications between the projects even when the project volumes are taken into account. Some projects also mainly published the results as research reports that allow more extensive reporting and are useful for the end-users of the results of certain research areas.

**Table 2.** Publications in the SAFIR2018 projects in 2015–2016.

Project acronym	Volume in person years	Research reports	Scientific journal articles	Conference articles	Others	Total
CORE	5,6	5	2	21	4	32
EXWE	7,3	15	14	10	11	50
MAPS	3,8	2	7	8	9	26
PRAMEA	5,8	17	5	7	6	35
SAUNA	8,2	12	3	17	18	50
GENXFIN	0,6	2	1	0	4	7
CASA	3,8	10	3	1	8	22
CATFIS	2,9	6	8	9	4	27
COVA	4,3	14	0	0	0	14
INSTAB	3,3	8	2	1	1	12
INTEGRA	5,5	5	1	1	1	8
KATVE	3,4	9	2	4	5	20
MONSOON	2,2	1	7	0	4	12
NEPAL15	1,0	0	6	0	2	8
NURESA	3,4	15	1	2	1	19
PANCHO	5,0	11	5	5	7	28
SADE	2,2	2	4	4	6	16
USVA	3,5	3	4	3	3	13
ESPIACS	0,3	1	1	1	0	3
ERNEST	0,5	2	0	2	0	4
FIRED	3,4	5	2	1	2	10
FOUND	6,4	22	0	3	5	30
LOST	2,0	8	3	1	1	13
MOCCA	1,4	6	3	1	0	10
NEST	2,0	2	1	4	2	9
THELMA	4,3	5	3	4	10	22
WANDA	2,7	7	1	8	1	17
COMRADE	0,8	6	0	0	0	6
INFRAL	4,2	2	0	2	2	6
JHR	0,4	2	0	0	1	3
REHOT	5,8	8	0	1	1	10
RADLAB	4,5	0	0	0	5	5
ADMIRE	2,1	3	0	0	2	5
<b>TOTAL</b>	<b>112,4</b>	<b>216</b>	<b>89</b>	<b>121</b>	<b>126</b>	<b>552</b>

Altogether 17 higher academic degrees were obtained in the research projects in 2015-2016: 6 Doctoral degrees and 11 Master's degrees (Table 2).

**Table 3.** Academic degrees obtained in the projects in 2015–2016.

Project acronym	Doctor	Master
MAPS	0	1
SAUNA	1	2
CASA	1	1
MONSOON	1	0
NURESA	0	1
PANCHO	1	0
SADE	0	1
USVA	0	1
FOUND	1	3
THELMA	1	0
WANDA	0	1
<b>Total</b>	<b>6</b>	<b>11</b>

## Structure of the report

This report describes on the main scientific achievements of the projects during 2015–2016. Chapters 2–7 include summaries of the projects in the six reference groups of SAFIR2018. More detailed statistical information of the programme and lists of project publications as well as the members of the Management Group, Steering Groups, and Reference Groups can be found in annual plans and reports on SAFIR2018 website.

## Acknowledgements

The results of the SAFIR2018 programme during the first half 2015–2016 period have been produced by all who have been involved in the research projects. Their work is highly esteemed.

The contributions of project managers and researchers that form the essential contents of this report are acknowledged with gratitude.

The work of the persons in the Management Group, Steering Groups, and Reference Groups that has been carried out with the expense of their own organisations is highly appreciated.

*Jari Hämäläinen and Vesa Suolanen*

## References

- [1] National Nuclear Power Plant Safety Research 2015-2018. SAFIR2018 Framework Plan. Publications of the Ministry of Employment and the Economy, Energy and the climate 34/2014. (in Finnish, an English version available on <http://safir2018.vtt.fi/>).
- [2] Hämäläinen J. & Suolanen, V. (eds) SAFIR2014 - The Finnish Research Programme on Nuclear Power Plant Safety 2010-2014. Final Report. VTT Technology 213. Espoo 2015. 722 p. (available on <http://safir2018.vtt.fi/> and <http://safir2014.vtt.fi/>).
- [3] SAFIR2018 – The Finnish Research Programme for Nuclear Power Plant safety 2015-2018. Operational Management Handbook. 2015. 19 p + 26 app (available on <http://safir2018.vtt.fi/> ).
- [4] Hämäläinen, J. & Suolanen, V. (eds) SAFIR2018 Annual Report 2015. Research Report VTT-R-01745-16. 106 p + 76 app (available on <http://safir2018.vtt.fi/> ).
- [5] Hämäläinen, J. & Suolanen, V. (eds) SAFIR2018 Annual Plan 2016. Research Report VTT-R-02463-16. 46 p + 637 app (available on <http://safir2018.vtt.fi/> ).

## 2. Automation, organisation and human factors

### 2.1 Crafting operational resilience in nuclear domain (CORE)

Jari Laarni<sup>1</sup>, Hannu Karvonen<sup>1</sup>, Jussi Korpela<sup>2</sup>, Hanna Koskinen<sup>1</sup>, Timo Kuula<sup>1</sup>, Marja Liinasuo<sup>1</sup>, Kristian Lukander<sup>2</sup>, Satu Pakarinen<sup>2</sup>, Markus Porthin<sup>1</sup>, Vuokko Puro<sup>2</sup>, Henriikka Ratilainen<sup>2</sup>, Marika Schaupp<sup>2</sup>, Laura Seppänen<sup>2</sup>, Anna-Mari Teperi<sup>2</sup>, Maria Tiikkaja<sup>2</sup>, Jari Tornainen<sup>2</sup>, Kaupo Viitanen<sup>1</sup>, Mikael Wahlström<sup>1</sup>

<sup>1</sup>VTT Technical Research Centre of Finland Ltd  
P.O. Box 1000, FI-02044 Espoo

<sup>2</sup>Finnish Institute of Occupational Health (FIOH)  
P.O. Box 40, FI-00251 Helsinki

#### Abstract

The CORE project aims to identify the key characteristics of operational resilience at three defence levels of prevention, preparation, and consequence management and to study how these characteristics are manifested in operator behaviour and how they can be operationalized and measured. The project is divided into six work packages with the aim to consider resilience from various perspectives. We have developed 1) tools and practices for gathering positive operating experiences from challenging operational situations; 2) training interventions and guidance to promote reflective thinking and learning and effective interruption management and troubleshooting among operators; 3) interventions and guidance for the management of acute stress and fatigue; and 4) guidance for the promotion of communication and coordination of activities in emergency exercises. In addition, a safety management procedure, Human Factors tool, has been developed to analyse human contribution to nuclear safety.

#### Introduction

The aim of the CORE project is to improve safe operation of nuclear power plants (NPPs) by developing guidance, training interventions, and other practical solutions that promote resilience for the three general defence levels of prevention, preparation, and consequence management. Regarding *prevention*, the aim is to support operating personnel to succeed better in challenging work tasks by being more reflexive, engaged, and self-conscious and aware of high-level operational goals, instead of being solely guided by fixed and predetermined procedures. To that aim, we have developed new Human Factors (HF) guidelines, models and tools and interventions that are tested and examined in simulated test environments and in workshops. Regarding *preparation*, operating personnel needs generic skills and abilities to master difficult, unfamiliar, and knowledge-intensive operational situations. Therefore, we have investigated the

effects of acute stress on operator performance in simulated accident situations and collected operating experiences from successful actions and decisions and analysed the lessons learned from these experiences. Regarding *consequence management and recovery*, it is required that risk is efficiently detected, recognized, interpreted, and communicated so that a collective response is mobilized promptly. Therefore, we have also developed methods and tools for crisis management that help stakeholders with different responsibilities to coordinate their actions to achieve a common operational picture. The chapter presents the findings of the research conducted in each work package of the project.

## **Learning from successes in nuclear power plant operation to enhance organizational resilience**

Efficient organisational learning is an important constituent for ensuring and sustaining the competence, performance and success of organisations (e.g., Argote, 2013; Senge, 1990). The ability of the organization to learn is especially important in safety-critical organizations in order to achieve and maintain an acceptable level of safety and reliability of operations. In safety-critical domains there has thus been great interest in facilitating learning within and between organisations. One of the essential means to ensure organizational learning – and ultimately avoiding the recurrence of adverse events – is to utilize operating experience. Operating experience activities at nuclear power plants primarily consist of analysing events and providing corrective action plans and lessons learned to own organisation and peer organisations. Modern developments in safety science, such as Resilience Engineering, have questioned the efficiency of failure-oriented approaches to learning and safety management and have presented alternatives. Complementary to the traditional approaches to safety management that emphasize avoiding things that “go wrong”, it is proposed that in order to sustain safety effectively, the organisation also needs to ensure that things “go right”, i.e. an organisation should focus on understanding the reasons behind successful activities (Hollnagel, 2014). Due to the likely void of such approaches in the nuclear industry (cf. Pietikäinen et al., 2010) and the general lack of practical guidelines, tools or other means for learning from successful experiences, the overall objective has been to improve nuclear safety through organizational learning from successful actions and decisions. We have focused on supporting operating experience activities, including developing principles and tools to help detect and analyse successes in NPP operations, and to generalize and share the lessons learned from successes.

We carried out a literature review in the fields of leadership, project management literature, and safety science to identify theories that define success and provide insight into learning from successful experiences. In addition, two case studies were carried out at two Nordic NPPs. Two approaches were utilized in the empirical data collection: one that was based on document analysis of incident reports and another based on field observations. Both of them involved interviewing relevant personnel to gain more insight. These findings are reported in more detail in a research report (Viitanen et al., 2016) and a conference paper (Viitanen et al., 2016).

We found that success is a complex and multidimensional concept that can take many forms. This means, for example, that viewing success as just a “non-failure” may mean that many important and potentially informative aspects to success would be overlooked. Within the context of this project, we defined success as matching, exceeding or returning to an expected performance level. In order to capture successes, a range of metrics was also identified. These were associated with processes, project management (i.e., cost, budget, and scope), product acceptance, organization (e.g., creating financial, technological, social or structural benefit for the organization), preparation for future scenarios, socio-affective impact, as well as lagging and leading safety metrics. Success can also have properties such as time and situation-dependence, and it relates to the objective or subjective expectations of multiple stakeholders. We also found that successes are often less salient and less likely to trigger intentional learning processes than failures. For example, we noticed that in contexts where a failure had taken place (i.e., when discussing event reports), it is often somewhat difficult to find the successes (e.g., recoveries), because the interviewees tended to focus on the failures instead. Striving towards understanding the failures can be seen as a desirable trait in safety-critical organisations; however, if the successes achieved in adverse situa-

tions are ignored, it may also mean that some useful learning opportunities may be missed. We observed similar tendencies in normal situations where a task had been executed as expected: in such cases further investigation into how exactly the success was achieved (to create lessons) was often not found motivating – the successes were “business as usual”. Figure 1 illustrates these situations.

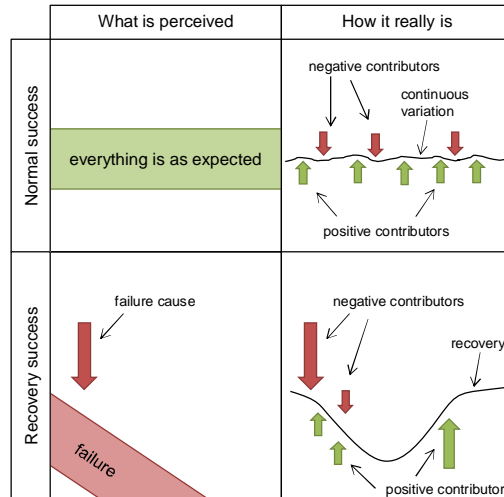


**Figure 1.** Illustration of how positive contributors are often neglected in normal or recovery situations.

In our empirical studies we observed that there was clear interest in successes at the power plants: existing methods, albeit not very refined, were already in place that could be utilized to learn from successes in a more systematic way. Various promising forums existed for sharing experiences that could be harnessed for discussing successes, and to some extent the case organisations have even initiated their own projects that intend to promote or facilitate learning from successes. Altogether, this suggests that there is a need to create means for organized and systematic learning from successes. This may include, for example, improving or creating investigation methods that acknowledge or explicitly analyse successes, or creating awareness of and sensitizing to successes. In practice, implementing tools that facilitate learning from success requires deliberate effort and organizational commitment, and it needs to be carefully carried out in order to ensure efficiency and to avoid negative side effects and to overcome implementation challenges (e.g., socio-cultural acceptability).

In addition, a guideline has been produced that proposes eight basic principles on how to learn from successes and describes a generic process for performing an analysis of successes. The guideline was reported as a conference paper for academic audience (Skjerve et al., 2017) and as a set of PowerPoint slides for practitioner audience. This guideline was based on the insights from the theoretical and empirical work conducted within this project, and the feedback received from the case study organizations. The purpose of this guideline is to provide insights to practitioners working at safety-critical organizations on how to promote learning from successes and to help develop practical tools to achieve this goal. In the upcoming years, we plan to develop pilotable tools to aid learning from successes based on the principles and process description of this guideline. These tools can include, for example, augmented event investigation methods with a success analysis to identify recovery successes, observation techniques to identify successes in daily work, and improving the practices for sharing of lessons learned from successes.

## Developing work-based learning in the NPP domain

### Shortcomings in operator performance and training

We assume that an important aspect in system resilience is the quality of operators' work practices. More specifically, as suggested by Savioja et al. (2014), being able to consider situations *interpretatively* in NPP operations provides a good basis for handling various kinds of challenges. Being interpretative entails, for instance, a profound understanding of the plant dynamics as well as consideration of various information sources and dialogue within the operator crews prior executing operating procedures. According to Savioja et al. (2014), there are differences between operator crews in the interpretativeness of their work practices. In order to reduce these differences and to refine operators' work practices, operator training has to be improved.

However, we have identified challenges in the existing training practices, which can be seen as being at odds with generating interpretive workers (Wahlström & Kuula, 2016). For example, at one specific NPP, training is performed tightly in accordance of the official training curriculum, while more time would be needed for freely "playing" with the simulator; allowing understanding of plant dynamics holistically as considered necessary by the operators themselves. To allow the proliferation of good practices between the work shifts, the crews would also need opportunities to witness and exchange the practices with other crews. Furthermore, in terms of learning, it is problematic that the current safety procedures determine operator activity in detail – capability to handle new kinds of situations is not, thus, efficiently developed in the emergency training where these procedures are applied. Overall, training is a top-down guided process, while exchange and creation of good work practices should be emphasized. Transition from the kind of training where learners are more or less "passive objects" to active and critical subjects is necessary. It is possible that some of these challenges are typical to the nuclear power plant work, because of safety critical and hierarchical nature of the domain (Wahlström & Kuula, 2016).

### Developing simulator training through a novel self-evaluation method

We assume that new training methods for the NPP domain could be developed by drawing from the Finnish Change Laboratory tradition (Engeström et al., 2014) and from the French Activity Clinic approach (Clot, 2009). To simplify, some of the main ideas of these approaches can be summarized as follows:

1. Double-stimulation: in dialogical workshops with workers, certain problem area or question can be considered with a new kind of presentation (or "stimulus"), such as, map or model; this technique enhances problem solving, concept formation and worker agency (Engeström et al., 2014)
2. Simple self-confrontation: the worker reviews sequences of his/her work activity together with the researcher, by using video material or other means of representation (Clot, 2009).
3. Crossed self-confrontation: a group or duo of workers review sequences of their work activity and discuss this together, with the guidance of a researcher (Clot, 2009; Seppänen et al., 2016).

More specifically, for enhancing simulator training, we have generated a self-evaluation method that aims to disseminate good practices by the means of guided dialogue among the operators. It consists of 1) personal evaluation, 2) group evaluation and 3) inter-group learning. Two questionnaires were constructed for self-evaluation in first two phases, including simulator task performance related open-ended questions and statements with rating scales. The group discussions were recorded for later analysis.

The operator crews' reflections on the simulator tasks have been preliminarily analysed. In short, reflection here indicates an activity in which the operators are analysing or commenting on themes prompted by their simulation experience or by the self-evaluation guideline. Reflection is expressed as uncertainty or doubt, dilemmatic speech, expressions of challenges, evaluation or questioning, and expressions of feelings (Heikkilä & Seppänen, 2014). As a preliminary result on the method introduced, we have found that reflection was quite abundant, consisting of more than a half of all discussions. In this sense, self-evaluations were efficient in enhancing operators' reflection: they involved dialogue and reflection among

operator crews about their own work practices and capability in emergency situations. Overall, findings portray a vivid discussion among the operator shifts encompassing the following themes: work practices, collaboration, plant dynamics and stress at emergency situations.

In future, new digital technologies could also be used in a post-simulator self-study: automatically created video representation of the performance can be imagined, including video clips synchronized with time-line of simulator events. This would require a synchronization of a video-observation system with the simulator system. With the various current software applications, audio could be represented visually for indicating collaboration. With this kind of media representation of the simulator performance, the operators could be able to better reflect and compare activity in discussion after simulator sessions.

## **Supporting operational resilience in complex and dynamic environments**

### **Multitasking in operator work**

The rate of interruptions has increased during the last decades in many work domains. Multitasking, interruptions and distractions are also a natural part of operator and maintenance personnel work in NPPs. Multitasking in operator and maintenance personnel work is a direct consequence of goal conflicts that are characteristic to the work in industrial organizations. We have studied the impact of multitasking and interruptions/distractions on work performance in safety-critical domains by preparing a literature review, and a method has been developed for the identification and classification of distractions in operator work, and it has been tested in the analysis of simulated accidents. According to the literature review, interruptions and distractions that divert attention away from the task at hand to another task have typically a detrimental effect on performance (Laarni et al., 2016). However, if the distraction is related to the primary task and add new information that is helpful in task execution, its effect can be positive. Even in the latter case the effect may be negative, if the information is not directly associated with the task the worker is just performing.

In nuclear domain, multitasking and task interruptions are quite common in 'normal' operational conditions, and operators have also told that the amount of multitasking has increased during recent years (Laarni et al., 2016). In (simulated) accident situations operators focus on accident management, and therefore interruptions that hinder the execution of the primary task are especially harmful. We have observed main control room (CR) operators' work in order to investigate the effects of interruptions and task switching in simulated accident management situations and the management of multiple parallel tasks (Laarni et al., 2016). In the analysis, we have utilized video data from head-mounted cameras. It was found that the shift supervisors were interrupted somewhat more often than the other operators in loss-of-coolant accident (LOCA) simulation runs (Laarni et al., 2016). For the shift supervisors, there also seemed to be somewhat more interruptions in the first part of the scenario than in the latter part. On the other hand, the interruptions were longer for reactor operators than for the other operators. Tasks that were most often interrupted were screen monitoring and procedure handling activities and panel operations (Laarni et al., 2016). A response to an interruption was typically immediate, indicating that the operators considered it necessary to respond immediately to the interrupter so that the latter does not need to wait for a long time. In general, external interruptions were caused by alarms, phone calls and other operators' comments. The shift supervisors interrupted reactor and turbine operators by asking questions or providing updates about important issues more frequently than the other way around (Laarni et al., 2016). This finding can be understood in that the shift supervisor is responsible for making the final operational decisions, and he/she also has the main responsibility of co-ordinating the operators' work and communicating with personnel outside the CR. We also studied the operators' procedure usage from the perspective of multitasking, and we found that self-initiated interruptions were a characteristic feature of operators' multitasking behaviour (Laarni et al., 2016). However, the operators wanted to minimize the time they spend on multitasking, and they tried to execute each procedure path from the beginning to the end before they moved to another path (Laarni et al., 2016).

## Troubleshooting in operator work

There is evidence that control room operators have problems in diagnosing complicated events and multiple simultaneous events in process industry (e.g., Kim et al., 1999). Even though there is a lot of research on finding faults in complex incident situations, there is quite little knowledge of the problem solver's cognitive strategies, states and activities in troubleshooting situations (see, however, e.g., Patrick, 1999). We have conducted a literature review on diagnostic reasoning and troubleshooting in process industry. With regard to nuclear domain, better methods have to be developed to study diagnostic reasoning and troubleshooting in simulator or plant environments. For example, the process tracing approach based on Newell and Simon's (1972) work has to be tailored to suit better the analysis of team collaboration and co-operation in incident and accident situations.

One of our main aims in the CORE project has been to develop new modelling tools for the analysis of distributed cognition in general and collaborative troubleshooting in particular. To that aim, we have proposed a modelling approach suitable for analyzing collaborative diagnostic reasoning and troubleshooting of a NPP control room crew which is based on existing methods and tools. The approach describes the progress and evolution of a CR operator crew's knowledge states and communication throughout the critical sections of a simulator run. The model would be useful, for example, in the analysis of operator collaborative fault-finding behaviour in the Human Factors validation of CR systems.

## Supporting operator performance in extreme stress

### Effects of acute stress on operator work

Acute stress affects cognition and performance roughly according to an inverted U-shaped function (Lupien et al., 2007). Whereas low-to-moderate amounts of stress may improve cognitive performance, high stress typically has an impairing effect: attention is more focused but narrower (e.g., Skosnik et al, 2000), working memory capacity decreases (Hsu et al., 2003) and encoding to and retrieval from long-term memory becomes impaired (de Quervain et al., 2000). Encoding of emotionally arousing information, in turn, may be amplified sometimes producing the so called "flashbulb memories" (Diamond et al., 2007). Effects of acute stress are also seen at the team-level: in attention, communication, and decision-making. Crew members typically shift their focus from the team to themselves and decrease communication (Gladstein & Reilly, 1985) reducing the situational awareness of the team. Stressed team members also focus on information they consider important or that is the most salient, and tend to ignore secondary or peripheral tasks (Gladstein & Reilly, 1985). This can lead to a possible loss of relevant information or neglecting important tasks. Decision-making may become delayed (Kerstholt, 1996) and a tendency to pass the responsibility upwards in a chain of commands increases (LeBlac, 2009). The optimal level of stress is inversely related to the complexity of the task, i.e., higher levels of arousal are optimal for simple tasks whereas lower levels of arousal are optimal with complex tasks (Diamond et al., 2007). Hence, performance impairments tend to increase with increasing task complexity. In NPP operator work, the stress-induced impairments of problem solving and executive functions are most evident and detrimental in the most critical, highest-risk situations where maintaining the best possible level of performance is of highest importance.

We conducted a literature review on the effects of stress on cognition and performance, with the applied focus on NPP operator work and some examples from other safety critical domains such as mining and aviation. We have disseminated the findings to the NPP personnel in the form of a research report and several lectures at both TVO Olkiluoto and Fortum Loviisa facilities.

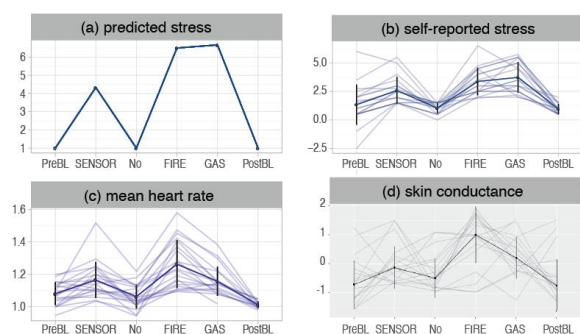
## Quantifying acute stress on operator work

Typically, stress is evaluated by collecting self-reports of experienced stress. While these subjective reports have been found indicative, there is a substantial risk that the subjective perception is biased. Another major limitation of subjective measures is that the operator can often only assess the overall experience of their workload post-hoc, but cannot reflect changes in workload during the execution of specific activities. Moreover, collecting self-reports during a task can disrupt task performance. Continuous, non-invasive physiological recordings, instead, can provide temporal information on the build-up and recovery from stress at different time points, and are not dependent on stress awareness and memory of the individual. Thus, objective and unobtrusive measurements of workload and stress levels are needed to provide more accurate information on the state of the individual within the desired time frame, without disturbing the primary task. Once this is achieved, the evaluation of the effects of stress on operator performance becomes more reliable.

One of the main goals of our study has been to quantify the stress of NPP operators during simulated incident and accident scenarios. With the lead of the operator instructors of the power plant, we first identified different types of incident and accident situations varying in their expected cognitive demands, and their perceived level of threat/health outcome. The scenarios selected for the simulations were 1) malfunction of an oil pressure sensor, 2) fire and 3) radioactive steam leakage. We quantified the level of stress of 22 NPP operators during these simulated scenarios by questionnaires and ambulatory measurements of electrocardiography (ECG) and electrodermal activity (EDA). We also used accelerometers to separate the effects of stress on physiology from the effects of physical activity, i.e., operators moving in the simulator. All the measures, namely self-reports and the physiological recordings of mean heart rate (HR), heart rate variability (HRV), and skin conductance response (SCR) indicated that the operators' stress was mild to moderate during the malfunctioning oil pressure sensor incident, and moderate to high during the accident scenarios of fire and radioactive gas leakage. The perceived and physiologically measured stress were low after the scenarios and during normal operation. We also detected signs of pretest excitement in the cardiac signal during the baseline period preceding the simulations.

Before the simulations were carried out, we also built a model of the predicted stress from the operator instructor's rating on the stressfulness of the task and our assumption that the baseline periods and normal run would not be stressful. Further, we examined the relationship between predicted stress, and the physiological stress response of operators during the simulated scenarios. Interestingly, the predicted stress better matched the physiological responses of the operators, than did the operators' self-evaluated stress, apparently because of some operators' self-reports were in conflict with their physiological results (Figure 2).

**Figure 2.** (a) Predicted stress (b) self-reported stress (c) mean heart rate and (d) skin conductance during different parts of the simulator training: pre and post baselines (PreBL, PostBL), normal operation (No), malfunction of the oil pressure sensor (SENSOR), fire and radioactive steam leakage (FIRE, GAS).



We have presented the results at the Enlarged Halden Research Project Meeting (EHPG2016) and published in the Proceedings of the 39<sup>th</sup> EHPG meeting (Pakarinen et al., 2016; Torniainen et al., 2016).

## Benefits of stress management for operator work outside extreme situations

Besides extreme stress during severe accidents, and preparing for them by simulator training, NPP operators face challenging, stress inducing situations repeatedly in their everyday work activities, such as when managing deviations in normal operation and outages, and at their periodical license examination, critical for practising their profession as an NPP operator. Also, with increasing use of renewable energy, prone to large supply fluctuations, the pressure to move from base-load mode towards the load-following mode of operation is increasing. The load-following mode is expected to increase the workload and regulative activities of the operators, and the amount of deviations in the production process, placing further demand on effective stress management and mitigation of stress-related performance decline in the future.

## Supporting resilience in emergency management

Vital functionalities of the society need to be secured in case of emergency. Emergency preparedness means readiness to act in case of emergency, supported by precautionary measures. Emergency exercises are an important part of such measures, maintaining and developing preparedness for emergencies which could have devastating consequences. We studied emergency exercises by interviewing members of NPPs' emergency organisations, to clarify the practises related to exercises and to identify development needs.

Emergency exercises, in accordance with all activities in the nuclear domain, are to be conducted according to regulation. In Finland, emergency exercise activity is described in YVL C.5 4.3. We found out that these requirements are well fulfilled; the emergency organisations are established, the exercises conducted and evaluated as required by regulation in the both operating NPPs in Finland. NPPs organise also training to support effective emergency management. Emergency exercises are organised in three-year periods so that a regular exercise takes place once a year in minimum, whereas a large emergency exercise with several participating organisations takes place every third year.

We identified several development needs (Figure 3). The main developmental need identified was the lack of clearly defined objectives for the exercises. With such objectives, exercises could be planned and evaluated in a systematic way. In this way, the participating personnel would know what they are expected to do and eventually, the performance in exercises and consequently in a potential emergency situation as well would improve. Another, almost equally important issue is that the proceeding of emergency exercises is predefined. The question of correctness of actions can therefore be raised.

The criticality of evaluation is also reflected in the concept of resilience (Hollnagel, 2006). When evaluation is guided to focus on critical matters, it is possible to learn the important lessons of what is beneficial, inefficient or harmful in some specific situation, depending on the performance and hence, lessons in the respective situations (exercises). This learning, in turn, supports resilient performance which in this case means successful management of an emergency situation. Thus, the lack of clear objectives probably leaves the basis for emergency exercises too vague – a matter which should be concentrated on to improve the effectiveness of emergency exercises in the future.

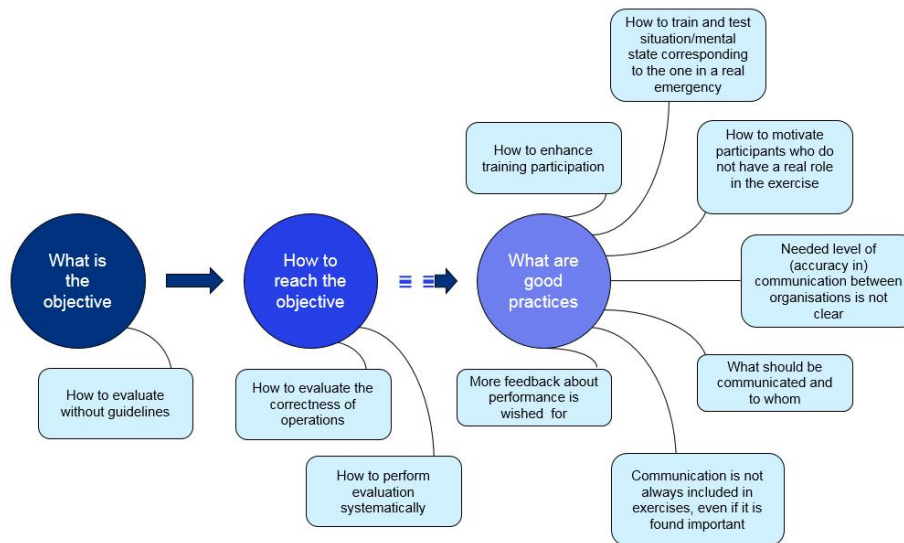


Figure 3. Developmental needs related to emergency exercises.

## Applying a HF tool to learn to analyse human contribution to nuclear safety

### Human factors in the nuclear industry

The mastery of Human Factors (HF) is known to be a necessary area of expertise, while human contribution to the safety incidents and accidents has been recognized already for a long time (Dekker, 2002; Reason, 2008). Still, technological and procedural contribution to safety have been dominated, and the human has not been in focus (Teperi, 2012). The system safety models and frameworks have been changing during the decades, from technical analysis to human factors, safety culture and system analysis (Hollnagel, 2006; Reiman & Oedewald, 2009), i.e., self-reflection by learning to analyse variability of human action during operational experiences.

Nuclear safety guidelines recommend incorporating systematic methods in the management system in order to identify and manage human and organisational factors affecting safety. According to the guidelines, personnel's individual competence should be developed in the identification and management of human factors and potential errors. The strengths, weaknesses, and areas for improvement of the safety culture could be best identified in connection with operational events (OEs). (YVL A3, 303, 311, 319-320, 315).

In the nuclear industry, the lessons learnt from OEs are critical in HF thinking for future prevention of accidents and other events. In addition, national nuclear guidelines highlight identifying and analysing HF more correctly (YVL A10, 2013; YVL A3, 2014). Especially in safety critical domains, like the nuclear industry, it is known that the management of HF is a necessary area of expertise and the human contribution to safety incidents and accidents has to be taken account (Dekker, 2002; Reason, 2008). At the same time, several HF tools have been used to improve operative performance at nuclear power plants (NPPs). Most of the currently known HF investigation techniques are, however, designed for larger accident or case investigations, and to be used by investigation professionals and thus need a strong training input and can be time consuming. It was not clear for us, which HF procedures are currently in active use in NPPs and by authority, and if the currently used HF models and tools support the mastery of HF in a sufficiently concrete way.

In our study, we have identified the current HF conceptions, practices and tools used by the nuclear safety organisations in the two NCPs and by Radiation and Nuclear Safety Authority (STUK), as well as

tested a new HF tool for OE analyses. The data have been collected with document analyses (e.g. YVL guide, guidelines at each NPP), interviews at NPP and STUK (overall 22 interviewees), as well as three workshops with safety experts of two NPPs

## New HF tool for nuclear industry

We found that there was no systematic OE analysis method in use, and that there is a need for positive safety thinking and more concrete and holistic (system view) HF tools and models. In this study, we modified the HF tool for nuclear industry based on the experiences of NPC safety experts. The HF tool was originally developed in Finnish Air Navigation Services to examine the human contribution to work and safety, and aims to improve users' understanding and identification of the HF contributing to their work and OEs (Teperi, 2012).

The HF tool consists of several items at four levels (individual-, work-, group- and organizational factors), which all have been stated relevant as background factors of mishaps in safety critical work (Figure 4). In our study, the HF tool was used by safety experts of two NPPs, to recognize and analyse both positive (successes) and negative (risks, errors) contributing factors to OEs.

We then wanted to evaluate appropriateness and use of the HF tool as an investigation method in OE analysis of nuclear industry. We also studied how safety experts and supervisors define HF and if they would benefit from the usage of a new HF tool as a part of its safety management.

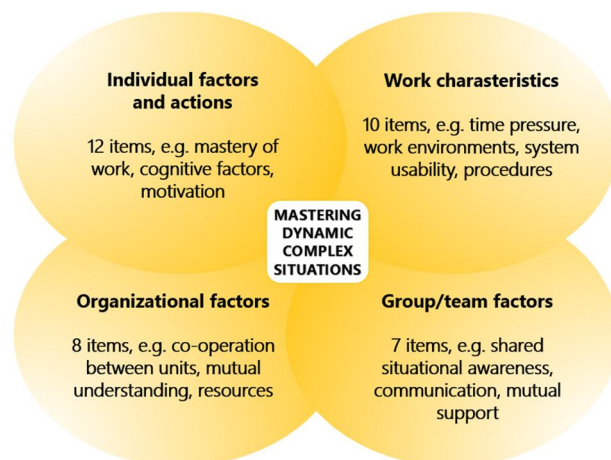


Figure 4. HF tool basic idea and contents.

Furthermore, we are evaluating the implementation process of the HF tool - its effects on safety thinking and practices, as well as supporting and hindering factors of the implementation process. We also have started to validate and test HF tool, and recognized HF needs at NPPs.

## Broader conception of HF and system thinking are needed

In our study, we have found that in the nuclear industry, the field of HF is viewed as an abstract issue. The conceptions regarding HF are individual and error based which may hinder the awareness and improvements at the organizational and system level of nuclear industry. The safety procedures, reporting and analysis of OEs mainly focuses on technical and risk aspects and HF is not very concrete. The HF procedures are seen as a way to inhibit individual errors. There is a clear need to concretize the conception of HF, as well as to improve the knowledge of HF, i.e., what does it mean in everyday life of the organization in individual-, work-, group- and at the organisational level. For example, research participants (both at the regulator and NPP side) recognized the need to improve the capability of summarizing the most evident findings revealed via SMS practices, as well as the activities in decision making, implementation and putting actions in practice, which should emerge as an agile process after identifying the development needs and recommendations in reporting and event analysis.

In NPPs, several human performance tools have been implemented, but none of them highlight human success factors. The current HF tools are not actively used to analyse OEs and no tools are used to summarise information from reports and their analysis for higher management purposes. No model is used to normalise personnel's capacity after unwanted events at work and consequence management was seen more as correcting operative items. Finally, we found that the newly offered HF tool was regarded as clear

and easy-to-use, and it was considered a useful tool especially at OE analysis, reporting and training as well as to self-evaluation and for monitoring safety trends. It was found to offer a more accurate picture of the analysed OEs and HFs affecting OEs including the success factors, than current OE analysis methods.

## Conclusion

The CORE project has developed operational practices that promote resilience in different levels of defence and that can be utilized by design organizations, NPPs and regulatory bodies. We have developed guidelines for prevention, preparation and consequence management at the operational level and training interventions and tools that complement the existing guidance and training procedures. The project provides solutions and practices for better management of severe unanticipated accidents and challenging incident situations. These results will further improve nuclear safety at the national level by improving ability to respond, monitor and anticipate to potentially disruptive situations at the operational level. The aim is that the research will produce new tools and practices that are immediately exploitable by NPPs and the Finnish regulator. Our aim is also to develop new work practices to promote collaboration and communication between researchers and different stakeholders. We will continue this path also in the following two project years.

## References

- Argote, L. 2013. *Organizational Learning*. Boston, MA: Springer US.
- Clot, Y. 2009. Clinic of activity: the dialogue as an instrument. In A. Sannino, H. Daniels, & K. Gutiérrez (Eds.), *Learning and expanding with activity theory* (pp. 286–302). Cambridge: Cambridge University Press.
- de Quervain D.J., Dominique, J. F., Roozendaal, B., Nitsch, R. M., McGaugh, J. L., & Hock, C. 2000. Acute cortisone administration impairs retrieval of long-term declarative memory in humans. *Nature neuroscience*, 3(4), 313-314.
- Dekker, S. 2002. Reconstructing the human contribution to accidents: The new view of human error and performance. *Journal of Safety Research*, 33, 371-385.
- Dekker, S. 2007. *Just culture. Balancing safety and accountability*. Cornwall, UK: Ashgate.
- Diamond, D. M., Campbell, A. M., Park, C. R., Halonen, J., & Zoladz, P. R. 2007. The temporal dynamics model of emotional memory processing: a synthesis on the neurobiological basis of stress-induced amnesia, flashbulb and traumatic memories, and the Yerkes-Dodson law. *Neural plasticity*, 2007.
- Engeström, Y., Sannino, A., & Virkkunen, J. 2014. On the methodological demands of formative interventions. *Mind, Culture, and Activity*, 21(2), 118–128.
- Gladstein, D. L., & Reilly, N. P. 1985. Group decision making under threat: The tycoon game. *Academy of Management Journal*, 613-627.
- Heikkilä, H., & Seppänen, L. 2014. Examining Developmental Dialogue: the Emergence of Transformative Agency. *Outlines: Critical Practice Studies*, 15(2), 5–30.
- Hollnagel, E., 2006. Resilience: The challenge for the unstable. In E. Hollnagel et al. (eds.) *Resilience Engineering. Concepts and Precepts*. Aldershot: Ashgate.

- Hollnagel, E. 2014. *Safety-I and Safety-II: The Past and Future of Safety Management*. Farnham, Surrey: Ashgate.
- Hsu, F. C., Garside, M. J., Massey, A. E., & McAllister-Williams, R. H. 2003. Effects of a single dose of cortisol on the neural correlates of episodic memory and error processing in healthy volunteers. *Psychopharmacology*, 167(4), 431-442.
- Kerstholt, J. 1996. The effect of information costs on strategy selection in dynamic tasks. *Acta Psychologica*, 94(3), 273-290.
- Kim, H., Yoon, W. C., & Choi, S. (1999). Aiding fault diagnosis under symptom masking in dynamic systems. *Ergonomics*, 42, 1472-1481.
- Laarni, J., Karvonen, H., Pakarinen, S., & Torniainen, J. 2016. Multitasking and interruption management in control room operator work during simulated accidents. In: *Proceedings of HCI International 2016*, Toronto, Canada, July 17 - 22, 2016.
- LeBlanc, V. R. 2009. The effects of acute stress on performance: implications for health professions education. *Academic Medicine*, 84(10), S25-S33.
- Lupien, S. J., Maheu, F., Tu, M., Fiocco, A., & Schramek, T. E. 2007. The effects of stress and stress hormones on human cognition: Implications for the field of brain and cognition. *Brain and cognition*, 65(3), 209-237.
- Newell, A., & Simon, H. A. (1972). *Human Problem Solving*. Englewood Cliffs, NJ: Prentice-Hall.
- Pakarinen S, Korpela J, Torniainen J, Laarni J, Karvonen H. 2016. Control room operator stress and cardiac activity in simulated incident and accident situations. In: *Proceedings of the 39th Enlarged Halden Research Project Meeting*, Fornebu, Norway, May 9th – 12th, 2016.
- Patrick, J. (1999). Analysing operators' diagnostic reasoning during multiple events. *Ergonomics* 42, 493-515.
- Pietikäinen, E., Oedewald, P., Haavisto, M.-L., Reiman, T., Ruuhilehto, K., & Heikkilä, J. 2010. Pyrkivätkö turvallisuuskriittiset organisaatiot oppimaan kokemuksistaan? Kokemustiedon käsittelyä ohjaavat oletukset ydinvoimateollisuudessa ja terveydenhuollossa. In: *Työelämän tutkimus - Arbetslivsforskning* (Vol. 8, pp. 279–290).
- Reason, J., 2008. *The human contribution: unsafe acts, accidents and heroic recoveries*. Cornwall, UK: Ashgate.
- Reiman, T., & Oedewald, P., 2009. Evaluating safety critical organizations. Focus on the nuclear industry. Swedish Radiation Safety Authority. Research Report, 2009:12. <http://www.stralsakerhetsmyndigheten.se/Publikationer/Rapport/Sakerhat-vid-karnkraftverken/2009/200912/>
- Savioja, P., Norros, L., Salo, L., & Aaltonen, I. 2014. Identifying resilience in proceduralised accident management activity of NPP operating crews. *Safety Science*, 68, 258–274. <http://doi.org/10.1016/j.ssci.2014.04.008>.
- Senge, P. M. 1990. *The Fifth Discipline: The Art and Practice of the Learning Organization*. New York: Doubleday/Currency.

- Seppänen, L., Kloetzer, L., Riikonen, J., & Wahlström, M. (2016). A developmental perspective to studying objects in robotic surgery (pp. 229–245). [http://doi.org/10.1007/978-3-319-49733-4\\_14](http://doi.org/10.1007/978-3-319-49733-4_14).
- Skjerve, A. B., Viitanen, K., Axelsson, C., Bisio, R., Koskinen, H., & Liinasuo, M. 2017. Learning from successes in nuclear operations – A Guideline. Presented at the ESREL2017, Portorož, Slovenia.
- Skosnik, P. D., Chatterton, R. T., Swisher, T., & Park, S. 2000. Modulation of attentional inhibition by norepinephrine and cortisol after psychological stress. *International Journal of Psychophysiology*, 36(1), 59-68.
- Teperi, A.-M., 2012. Improving the mastery of human factors in a safety critical ATM organization. *Cognitive Science*, Institute of Behavioural Sciences, Faculty of Behavioural Sciences, University of Helsinki, Finland. Doctoral dissertation.
- Teperi, A.-M., Leppänen, A., Norros, L., 2015. Application of the HF tool in the air traffic management organization. *Safety Science*, 73, 23-33.
- Torniainen J, Korpela J, & Pakarinen S. 2016. Control room operator stress and electrodermal activity in simulated incident and accident situations. In: Proceedings of the 39th Enlarged Halden Research Project Meeting, Fornebu, Norway, May 9th – 12th, 2016.
- Viitanen, K., Bisio, R., Axelsson, C., Koskinen, H., Liinasuo, M., & Skjerve, A. B. 2016. Learning from Successes in Nuclear Power Plant Operation - Intermediate Report from the NKS-R LESUN (No. NKS-354). NKS. Retrieved from [http://www.nks.org/en/nks\\_reports/view\\_document.htm?id=111010213330253](http://www.nks.org/en/nks_reports/view_document.htm?id=111010213330253)
- Viitanen, K., Koskinen, H., Axelsson, C., Bisio, R., Liinasuo, M., & Skjerve, A. B. 2016. Learning from successful experiences: An undeveloped potential in the nuclear industry? Presented at the Enlarged Halden Programme Group Meeting, Fornebu, Norway.
- Wahlström, M., & Kuula, T. (2016). Organizational self-determination and new digital self-study applications as means for developing nuclear power plant operation training. *International Conference on Learning and Collaboration Technologies*. Retrieved from [http://link.springer.com/chapter/10.1007/978-3-319-39483-1\\_59](http://link.springer.com/chapter/10.1007/978-3-319-39483-1_59).
- YVL A.10. Guide, 2013. Operating experience feedback of a nuclear facility. 15 November 2013. Helsinki, STUK.
- YVL A.3. Guide, 2014. Management system for a nuclear facility. 2 June 2014. Helsinki, STUK.

## 2.2 Management principles and safety culture in complex projects (MAPS)

Nadezhda Gotcheva<sup>1</sup>, Kaupo Viitanen<sup>1</sup>, Marja Ylönen<sup>1</sup>, Pertti Lahdenperä<sup>1</sup>, Joonas Tuovinen<sup>1</sup>, Sampsa Ruutu<sup>1</sup>, Jaakko Kujala<sup>2</sup>, Kirsi Aaltonen<sup>2</sup>, Karlos Arto<sup>3</sup>

<sup>1</sup>VTT Technical Research Centre of Finland Ltd  
P.O. Box 1000, FI-02044 Espoo

<sup>2</sup>University of Oulu  
P.O. Box 4610, FI-90014 Oulu

<sup>3</sup>Aalto University  
P.O. Box 15500, FI-00076 Espoo

### Abstract

MAPS aims at enhancing nuclear safety by supporting high quality execution of complex nuclear industry projects. The conceptual governance model for inter-organizational networks we developed provides insight in practical relevance of project governance approaches for enhancing safety. The ongoing case studies identify the need to pay more attention to non-technical aspects of complexity and understand the implications from unexpected events and changes in projects. Benchmarking the Norwegian oil & gas industry proved useful for sharing best practices and challenges on management of complex projects. The co-existence of different subcultures in projects calls for recognizing and aligning emerging tensions to manage cultural complexity. Identifying practical methods to assure and improve safety culture culminated in a preliminary framework for evaluating their applicability in temporary environment. System dynamics modelling represented reinforcing loops that can explain issues, such as delays, in complex nuclear industry projects.

### Introduction

Complex projects are large-scale temporal undertakings, subject to high levels of uncertainty with major financial, environmental and social implications for project stakeholders and society. *Project governance* aims at aligning multiple diverse project stakeholders' interests to work together towards shared goals (Turner & Sinister, 2001). Existing evidence suggests that inability to manage the increasing complexity in projects may be a significant factor in deficient project performance (Flyvbjerg et al., 2003).

Safety-critical projects are increasingly carried out by a multinational network of companies. In Finland, various nuclear industry projects are currently executed, including new builds and modernization projects in the operating plants. Some of the project parties might have little experience with the Finnish nuclear regulatory requirements or nuclear industry practices in general. In this context, it is challenging to ensure that the safety and quality requirements are adequately understood and fulfilled by every organization involved in the project network throughout the project lifecycle. Safety research has so far paid insufficient attention to *project management* because delays have usually been perceived mainly as economic problems and not safety concerns as such. However, safety cannot be separated from other performance issues when a *systemic approach* is applied, that is, when human, technological, organizational and cultural factors are seen as interrelated elements (Reiman & Rollenhagen, 2014).

*Safety* is an emerging property of the sociotechnical system, continuously created in daily activities (Hollnagel 2009; Reiman & Oedewald, 2009; Oedewald et al., 2011). Current safety culture and safety management models are largely focused on a single organisation and it is far from clear how to apply them in dynamic temporary project networks. Some characteristics of complex project networks challenge the very usability of the safety culture concept: cultural approaches emphasize that it takes time and certain

amount of continuity to create a culture, both of which may be in short supply in projects. In essence, *safety culture* is an organization's potential for safety, or the ability and willingness of organizations to *understand* safety, hazards and means of preventing them, and the ability and willingness to *act* on safety in practice by actively preventing hazards from actualizing and promoting safety, both in routine daily activities and unexpected situations (Reiman & Oedewald 2009, Oedewald et al. 2011). Recently, the need to connect safety culture research to project governance has been identified, recognizing the potential for a novel perspective towards the way culture is developing, and nuclear project activities are coordinated (Oedewald & Gotcheva, 2015).

## Objectives of the MAPS project

The overall *research question* of the MAPS project is: what are the safety management principles that should be applied in managing complex projects in the nuclear industry, and how these principles can be implemented in practice? The ultimate *goal of the MAPS project* (2015–2018) is to enhance nuclear safety by supporting high quality execution of complex nuclear industry projects, including modernisations and new builds. Three objectives are formulated according to this goal, as presented at Figure 1:

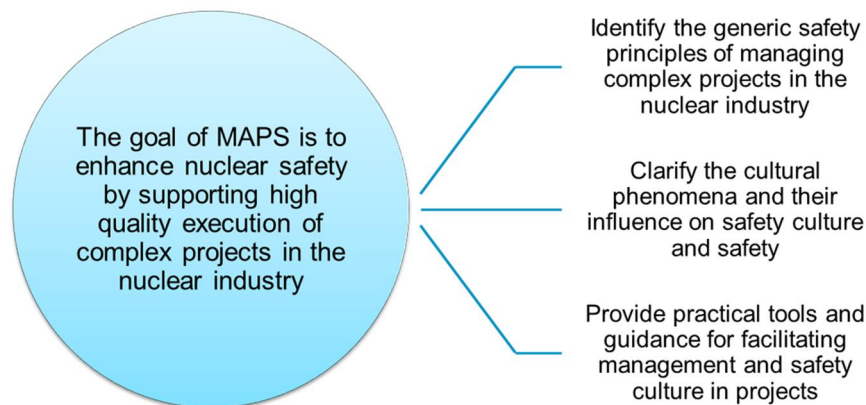


**Figure 1.** The ultimate goal and objectives of the MAPS project (2015–2018).

The project brings together expertise in safety culture, complexity, project governance and network management, societal research on safety regimes and system dynamics modelling, and integrates in a novel way theories and concepts from these different disciplines to advance theoretical understanding and provide practical guidance for the nuclear industry and potentially other safety-critical industries as well.

The overall research structure follows the logics that conceptual and empirical works interact in a meaningful way. MAPS project consists of five work packages (WPs), each consisting of work tasks, which have been identified as scientifically understudied and practically challenging topics:

WP1: Characteristics of complex projects from nuclear safety point of view/Project governance

WP2: Nuclear specific requirements for complex projects/Benchmarking the Norwegian oil & gas industry

WP3: Safety culture in complex networked organizations

WP4: Applying system dynamics modelling in complex projects

WP5: Integration and dissemination of results

The first (WP1) and the last (WP5) work packages are integrative and thus crucial for creating a shared view on management and safety culture principles of complex projects among the researchers. The other work packages complement the integrative approach by paying attention to the regulator's role and benchmarking the Norwegian oil & gas industry (WP2), and the role of cultural complexity and safety culture development and assurance in project networks (WP3). WP4 focuses on system dynamics modelling,

which is a practical approach to test and visualise the dynamics in a complex project. Since WP5 focuses on internal cooperation, integration and dissemination of results, the following chapters provide a cohesive picture of the main research results as summarized for work packages WP1-WP4.

## Understanding typical project governance models and their effects on safety

During the first two years of the project we developed a conceptual governance model for inter-organizational project networks and focused on validating and refining the model to take into account the characteristics of different types of projects and governance approaches. The research work was conducted through theoretical development, literature reviews, case studies and workshops. We analysed practical empirical examples in which decision-making and activities of the project actors have a significant influence on safety, and how the underlying set of governance approaches applied in a project influence the actors' behaviour. This builds understanding of the practical relevance of project governance approaches with regard to enhancing safety.

Based on a systematic literature review on project governance literature, we developed a conceptual framework to identify the key dimensions and mechanisms of project governance. Three leading journals were selected for the purpose of capturing relevant research: the *International Journal of Project Management*, the *Project Management Journal* and *International Journal of Managing Projects in Business* (Kujala, Aaltonen, Gotcheva & Pekuri, 2016). The framework categorizes *governance in project networks* under six key dimensions: goal setting, rewarding, monitoring, coordination, roles and decision-making power, and capability building (Fig. 2).

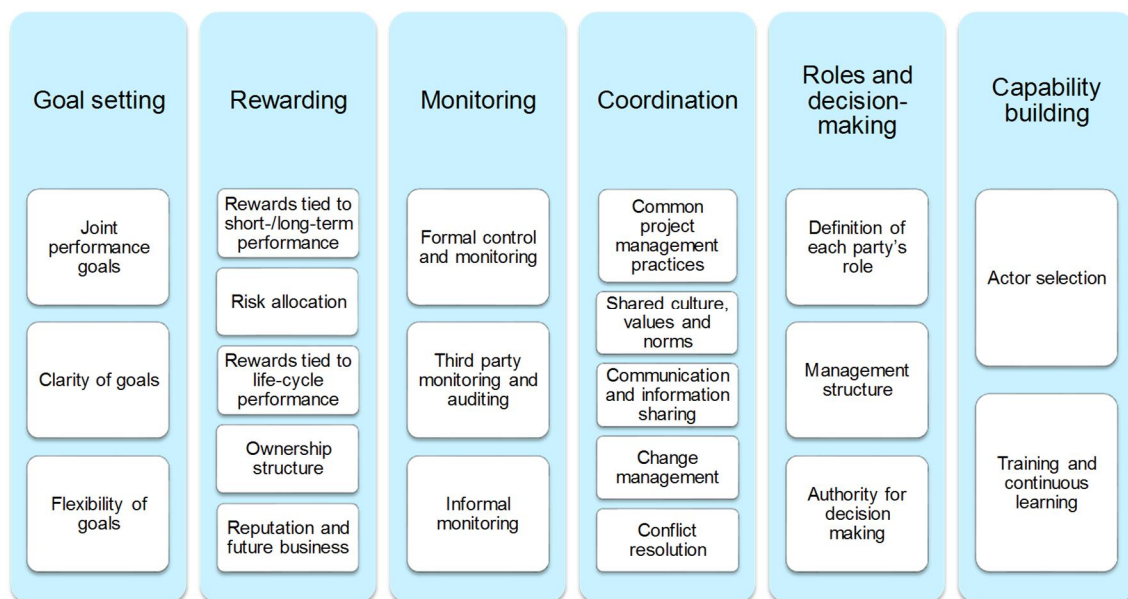


**Figure 2.** Dimensions and mechanisms of governance in inter-organizational project networks (adapted from Kujala et al., 2016).

*Goal setting* focuses on creating shared performance goals for the project that will be understood by all project actors in the network. *Rewarding* refers to aligning actors' goals with the project goals by means of incentives: provided that contracts cannot identify every potential contingency, relational governance approach is useful to adjust actors' behavior (Lu et al., 2015), and creating a sense of ownership among participating organizations (Guo et al., 2014). *Monitoring* seeks to ensure that all project actors act as expected in terms of achieving project milestones and performance targets (Nisar, 2013). *Coordination* is

required to align the activities of the project actors for example by adapting tools and work processes and making them compatible across different organizations. *Roles and decision making* refers to providing actors with the necessary information to enable them to make appropriate decisions and to understand the effect of decisions on overall performance. Although the formal roles and responsibilities of each party are defined contractually, effective governance also requires suitable project management structures and decentralized decision-making principles (Pitsis et al., 2014). *Capability building* ensures that project actors have adequate capabilities and resources to meet performance expectations.

Governance of safety critical projects was explored theoretically and empirically in a Master's thesis, focusing on key elements in project governance and how they affect nuclear safety (Starck, 2016). The objective of the thesis was to evaluate how different project governance mechanisms are related to safety in the context of nuclear industry projects. The study was based on a systematic literature review of two leading safety scientific journals, *Safety Science* and *Reliability Engineering and System Safety*, and analysis of interviews and observations of a focus group. The results indicated that an overarching goal for all actors involved in the studied nuclear industry projects was to complete the project in budget and on schedule and get the end-product (a nuclear power plant) working safely and efficiently. According to Arto et al. (2011), when discussing governance in a complex project, the project network can be seen as an organization of its own. The empirical findings indicated that the project was rather seen as carried out by each of the project actors, and not as a shared entity consisting of multiple actors. However, a shared project culture was seen as something to strive for. The findings also indicated that the key dimensions of project governance (Kujala et al., 2016) exist also in the safety literature, and two additional sub-dimensions were found: coordination tools and informal roles. The findings highlighted the importance of a project organization, leaders' participation in safety related issues, and sharing a common view of safety in the project network (Starck, *ibid*).

The applicability of governance approaches related to project alliancing and its influence on safety in nuclear industry projects was discussed during an international cross-industry MAPS project seminar. Project alliancing is a particular type of project delivery method based on strong inter-organizational integration (Lahdenperä, 2012). We explored the challenges and opportunities associated with different contractual arrangements and the applicability of project alliancing or collaborative contract arrangements in the nuclear industry context, based on experiences from Finland (Lahdenperä, 2016) and Australia (Walker, 2016).

A contract, which effect is based upon a relationship of trust between the parties, and in which responsibilities and benefits are apportioned fairly and transparently, is called *relational* as opposed to *transactional* (Lahdenperä, 2012). In practice, relational and contractual mechanisms are complementary parts of the governance continuum of a project. While explicit contracts are needed to reduce uncertainty and minimize opportunism, they can only cover foreseeable contingencies – specifying everything for the contract would increase transaction costs and prevent a flexible and quick response to unforeseen events.

A key feature of project alliancing is *effective collaboration* and creating and developing a common best-for-project mindset and culture (Walker, 2016). It is a "painshare/gainshare" type of incentive with added focus on committed relationships and early contractor involvement. From that perspective, it was suggested that possibilities to apply alliancing in subsections of a nuclear industry project could be explored. Moreover, lessons learned from managing complex megaprojects was another topic for discussion during the seminar, focusing on comparative analysis between Heathrow Terminal 5 and the 2012 London Olympics projects. These two megaprojects had to deal with three types of complexity: structural, socio-political and emergent (Brady, 2016; Brady & Davies, 2014).

The main empirical data collection is focused in this work package: first, we carried out and analysed nine baseline interviews, and the results provided basic theoretical background of project complexity and brief descriptions of selected complex projects in the Finnish nuclear industry. The results identified the need to pay more attention to non-technical aspects of complexity (e.g. organizational, emergent, institutional) and their implications for safety (Gotcheva et al., 2015). Furthermore, in-depth case studies in two Finnish nuclear power companies have been proceeding. We carried out a total of 15 interviews to study events or "critical incidents" in different projects from project governance and safety culture perspective,

i.e., disruptive events that involve different project actors, and make a significant contribution, either positively or negatively, to the general aim of the project or activity. Based on the data analysis, we investigated drivers of complexity in inter-organizational nuclear industry project networks, focusing on the implications for safety. A preliminary integrated framework for governance in complex nuclear power industry project networks is proposed, which presents key factors that influence the complexity of such project networks. The conceptual framework builds upon and extends the IAEA's integrated framework for management systems in a nuclear power environment (IAEA, 2012) to reflect governance in complex project networks (Gotcheva et al., to be submitted).

## **Benchmarking the Norwegian oil & gas industry**

Benchmarking between the nuclear industry and the Norwegian oil & gas industry in terms of governance of safety and management of complex projects was in the focus in the beginning of the project: first we studied the regulatory perspective concerned governance practices of Norwegian Petroleum Safety Authority and Finnish Radiation and Nuclear Safety Authority, then the industry perspective, e.g. oil & gas and the nuclear industry experiences and management of complex projects and related innovations. Both the regulatory and industry perspectives are required to get better insights into the complexity and the recent developments in handling complex projects and safety.

Criteria for comparison between Finnish and Norwegian regulatory regimes were the following: safety philosophy, stakeholder involvement, regulatory practices, and the role of inspectors. Findings indicate that Norwegians have adopted safety philosophy that includes also economic aspects. Broad definition of safety indicates strong national interest in oil revenues, and a willingness to safeguard profit. Safety and the creation of economic value for society are regarded as a win-win situation. Instead, in Finland the economic aspects are excluded from the safety regulation (Ylönen & Engen, to be submitted).

The Norwegian Petroleum Safety Authority (PSA) has adopted a tripartite system, in which different stakeholders, including trade unions and the industry, participate in the improvement of safety. For instance, 'working together for safety' is one of the most extensive collaboration projects and forums for improving safety. Participants are oil companies and supplier companies represented by the Oil Industry Association, the Norwegian Confederation of Trade Unions, the energy industry, the PSA, etc. The Norwegian regulatory regime is risk-informed, function-based, trust and dialogue-based and where regulation and inspection practises is mainly characterised by authority enforced self-regulation of the industry. Enforced self-regulation means that authorities set upper level requirements and the licensees are free to show how they meet the requirements. Self-regulation is considered very demanding and it requires much competence, knowledge and skills, from both the inspectors and the industry. Therefore, capability building among the regulators and industry is emphasized (Ylönen & Engen 2016).

The Finnish regulatory regime can be characterized as a command and control type of regulation. Finnish regime includes risk-informed, trust and dialogue-based regulation, like the Norwegian regime. What is typical of Finnish inspectors' regulatory practices is the grass-roots level interaction. It seems that within the nuclear industry, the paramount importance of safety is well emphasised, whilst in the oil and gas industry, the win-win situation between safety and profit making is underlined. In economic hard times, the win-win thinking creates vulnerabilities in Norwegian regime. In addition, tripartite system is also vulnerable in the sense that political and economic issues can easily undermine the existing trust between the parties and ruin the climate of cooperation. In such contexts, it is a demanding role for the regulatory body to act as a navigator and as mediator.

The Finnish nuclear and Norwegian petroleum industries are very different branches, yet they share similar goals, such as continuous improvement of safety. In addition, both industries have faced similar challenges, such as dealing with economically hard times, ageing of personnel and infrastructure, decommissioning, managing complex projects with long supply chains as well as increasing automation and related safety and security concerns. We identified the challenges that the oil & gas industry in Norway has faced in managing complex chains of multiple stakeholders, as well as solutions that the oil & gas industry and the regulatory body (Petroleum Safety Authority) have created to tackle these issues. In addition,

recent developments in the oil & gas industry in terms of handling of risk and safety are analysed, and comparisons were made with the nuclear industry in Finland.

The case studies on complex projects in Norwegian oil & gas industry were based on documentary analysis and interviews with representatives of the oil & gas industry. The results of this work indicated that Norwegian oil companies have mostly adopted hands-on strategy in managing their relationship with the contractors and sub-suppliers, due to failed projects based on the hands-off strategy (i.e. giving freedom to contractor to realize the project) (Ylönen, 2017). The lessons learned from the failed projects can be crystallised as a citation of a project manager “never trust fully the contractor” (Ylönen, to be submitted). Since the industry has taken responsibility and active role in managing its relationship with the contractors, the regulatory body in Norway plays a minor role in that respect.

A joint cross-industry video-seminar, organized by MAPS project, attracted representatives of the Norwegian oil & gas industry, the Finnish nuclear industry and the regulator. The discussions highlighted the importance of listening to those people in a project who have concerns, and the challenge to capture the dynamic interfaces between different project actors and their effects on safety. The oil & gas companies have adopted mainly hands-on strategy, i.e. taking control over the project and the contractors. Managing increasing documentation was another topic for discussion, emphasizing the need for grading approach in documentation - what to be documented and how thoroughly - and the importance of ensuring availability of high-level competence to understand what is the purpose of each document and how it relates to other design documents. In terms of communication, it was reminded that questioning our own understanding is especially important in complex safety-critical project environments.

## **Understanding safety culture in complex networked organisations**

The research in this work package focused on modelling the cultural complexity and safety culture challenges in projects, as well as on identifying and specifying methods to improve and facilitate safety culture in complex projects. We carried out a literature review on the concept of cultural complexity and provided an overview of incidents in high-risk industries, related to cultural complexity. Subcultures could be classified in three categories: 1) enhancing, with more intense adherence to the beliefs and values of the dominant culture; 2) orthogonal (independent), adherence both to the dominant culture and to other set of beliefs, and 3) counterculture, which is challenging the dominant values and beliefs (Martin & Siehl, 1983). Cultural complexity contributes to asymmetries in power and social distribution of meaning and knowledge. On the one hand, fragmentation that stems from differences in roles, responsibilities, perceptions of time or areas of expertise may trigger tensions, decision-making issues and thus increased risk (Hannerz, 1992). On the other hand, subcultural dynamics provide potential advantages for enhancing safety through variety and richness of perspectives, flexibility, responsiveness or identification of emergent risks and coping with uncertainties (Boisnier & Chatman, 2003).

In the safety literature, there has been many studies on identifying the features of a good safety culture and evaluating it, yet empirical studies on culture improvement in high-risk industries are scarce (Hale et al., 2010). Thus, our research work on safety culture assurance and improvement methods in complex nuclear industry projects in the SC AIM subproject is producing new and relevant knowledge (see Viitanen, Gotcheva & Rollenhagen, 2017). The study provided an overview of the characteristics of temporary project organizations from the perspective of safety culture improvement, which were related to time, team, task, and context (Bakker, 2010). A literature review was conducted to identify the practical methods to assure and improve safety culture. The predominant approaches for safety culture development are based on the assumption that the context is stable and relatively homogeneous, which often does not apply to dynamic project networks. Although a variety of approaches was identified in the literature, practical methods intended specifically for project environments were scarce. The safety culture improvement and assurance methods were classified into seven categories, based on their objectives (see Fig. 3).

Three empirical case studies in Nordic nuclear industry organizations were conducted as a part of this study. The first case study focused on Safety Culture Ambassadors group as a method. It was found that this method could influence safety culture through multiple mechanisms. Furthermore, the flexibility of this

method can potentially balance some of the challenges posed by the project environment, and even benefit from them. The findings indicated that the Safety Culture Ambassadors group could facilitate the development and assurance of safety culture by improving the information flow, enabling bidirectional communication, encouraging and facilitating participation of personnel and ensuring that safety is taken into consideration in various activities in the project.



**Figure 3.** Examples of safety culture improvement methods categorized by objective (figure adapted from Viitanen et al., 2017).

The second case study focused on a safety-oriented project management seminar as a method, which indicated the potential of this method for influencing safety culture through providing a shared forum for dialogue between different stakeholders.

The third case study consisted of information exchange sessions with human and organizational factors experts, which provided additional insights into the current challenges and opportunities of safety culture improvement in projects. A variety of methods were applied rather implicitly in projects, including development of working processes, organizing training sessions, seminars and workshops, also with top man-

agement, and encouraging people to speak openly if they have safety concerns. As a result of the theoretical and empirical work, a preliminary framework for evaluating the applicability of safety culture assurance and improvement methods in projects was developed (Viitanen et al., 2017).

## **Applying system dynamic modelling in complex projects**

System dynamics modelling is a methodology for modelling complex systems: the focus is on dynamic behaviour over time of the system, not on individual events. To understand the dynamic behaviour over time, one must understand the structure of the system, that is, aspects such as feedback mechanisms, time delays, and accumulations. Using diagramming tools such as causal loop and stock/flow diagrams can help in improving the holistic understanding of a system. In non-linear systems, simulations can reveal e.g. tipping points in which the behaviour of a system changes qualitatively after a certain threshold.

We conducted a literature review of the use of system dynamics modelling of complex safety critical projects (Ruutu, 2015). The literature review provided an understanding of the existing uses of system dynamics to project management issues in general, as well as the applications of system dynamics for analysing and improving safety culture in order to focus the work for the system dynamics modelling. The review indicated that although there are many existing studies of applying system dynamics to project management, and the key feedback mechanisms have been discovered (Lyneis & Ford 2007), governance of multiple stakeholders is not typically primary focus in these studies. Furthermore, safety issues in existing models are typically not taken into account explicitly. The existing models often include key variables, such as the number of undiscovered errors in a project that affect safety issues, and these models could be used as a basis for more detailed examinations of safety-related phenomena.

The study identified two ways, in which the simulation modelling can be of practical relevance. First, the modelling can be done interactively within a workshop setting, which means that the models can be used as boundary objects to get people to form a common understanding of a complex issue. Second, the models can be used for theory building and generation of insights based on which practical policy recommendations for companies can be drawn.

An interactive workshop was held with experts in a complex nuclear industry project in Finland to support the simulation modelling. The focus was on delays in creating and handling design documents: this is a topical issue since small delays and disruptions in document handling processes can cause complex projects to suffer massive cost and time overruns. The causal loop diagram of how governance and safety aspects related in a nuclear industry project has been prepared. In nuclear industry projects efficient document management system and processes are both crucial and challenging due to the huge amount of documents. They can also have potential safety implications if design-related information is lost, unclear or incomplete, e.g. during consequent maintenance in the plant. The study highlighted that in order to evaluate and mitigate the cumulative impact of a number of delays in complex projects, a system dynamics perspective is beneficial for proactively understanding how in a complex project delays and disruptions may reinforce themselves over time (Tuovinen & Gotcheva, 2017).

## **Conclusion**

MAPS project contributes to an improved understanding and applicability of the concept of safety culture in temporary and dynamic inter-organizational project networks. During the first two years of the project we have developed a set of theoretical frameworks and collected and analysed empirical data, which resulted in a richer understanding of the phenomena under study and links between them. In the next phase of the project, we continue the cooperation with nuclear industry practitioners to further refine and validate these preliminary insights and to integrate them into practical guidance for facilitating governance and safety culture in complex projects. Ultimately, the results presented in this report provide a foundation to identify and describe the safety management principles and their associated attributes, that should be adopted and implemented in complex projects in the nuclear industry to support the development of a healthy safety culture.

## Acknowledgements

MAPS project is funded by the Finnish Nuclear Waste Management Fund (VYR) and other organisations operating in the field of nuclear energy via SAFIR2018, the Finnish Research Programme on Nuclear Power Plant Safety (2015-2018), the Nordic Nuclear Safety Research (NKS) and VTT. The authors are grateful to the nuclear power companies for their cooperation.

## References

- Artto, K., Martinsuo, M. & Kujala, J., 2011. *Project Business*. 1st ed. Helsinki: WSOY.
- Bakker, R. M. 2010. Taking stock of temporary organizational forms: a systematic review and research agenda: temporary organizational forms. *International Journal of Management Reviews* 12: 466-486.
- Boisnier, A. & Chatman, J. 2003. The role of subcultures in agile organizations. In R. Peterson & E. Mannix (Eds.), *Leading and managing people in the dynamic organization* (pp. 87-112). Mahwah, NJ.
- Brady, T. & Davies, A. 2014. Managing structural and dynamic complexity: A tale of two projects. *Project Management Journal* 45: 21-38.
- Brady, T. 2016. Lessons learned in managing complex projects, presented at the International MAPS seminar "Relational contracting for improved network performance in complex projects", May 24, 2016, Aalto University, Espoo.
- Flyvbjerg, B., Bruzelius, N. & Rothengatter, W. 2003. *Megaprojects and risk: An anatomy of ambition*. Cambridge University Press.
- Gotcheva, N., Aaltonen, K. & Kujala, J. Project complexity and implications for management of safety: nuclear industry practitioners' perspective, Manuscript to be submitted to *Safety Science*.
- Gotcheva, N., Ylönen, M., Kujala, J. & Aaltonen, K. 2015. Characteristics of complex projects in the Finnish nuclear industry: Interview study of three cases. Unpublished research report.
- Guo, F., Chang-Richards, Y., Wilkinson, S. & Li, T.C. 2014. Effects of project governance structures on the management of risks in major infrastructure projects: A comparative analysis. *International Journal of Project Management* 32: 815-826.
- Hale, A. R., Guldenmund, F. W., van Loenhout, P. L., & Oh, J. I. 2010. Evaluating safety management and culture interventions to improve safety: Effective intervention strategies. *Safety Science* 48: 1026–1035.
- Hannerz, U., 1992. *Cultural complexity: Studies in the social organization of meaning*, New York: Columbia University Press.
- Hollnagel, E. 2009. The four cornerstones of resilience engineering. In Nemeth, C., Hollnagel, E., Dekker, S. (Eds.) *Resilience Engineering Perspectives, Volume 2. Preparation and Restoration*. Ashgate.
- IAEA, 2012. *Safety culture in pre-operational phases of nuclear power plant projects*. Vienna: International Atomic Energy Agency.

- Kujala, J., Aaltonen, K., Gotcheva, N. & Pekuri, A. 2016. Key dimensions of project network governance and implications for safety in nuclear industry projects, European Academy of Management (EURAM), 1-4 June 2016, Paris, France.
- Kujala, J., Aaltonen, K., Gotcheva, N. & Pekuri, A. 2016. Key dimensions of project network governance and implications for safety in nuclear industry projects, presented at the European Academy of Management (EURAM), 1-4 June 2016, Paris, France.
- Lahdenperä, P. 2012. Making sense of the multi-party contractual arrangements of project partnering, project alliancing and integrated project delivery, *Construction Management and Economics*, 30:1, 57-79.
- Lahdenperä, P. 2016. Project Alliancing Experiences in Finland, presented at the International MAPS seminar "Relational contracting for improved network performance in complex projects", May 24, 2016, Aalto University, Espoo.
- Lu, P., Guo, S., Qian, L., He, P. & Xu, X. 2015. The effectiveness of contractual and relational governances in construction projects in China. *International Journal of Project Management* 33: 212-222.
- Lyneis, J. & Ford, D. 2007. System dynamics applied to project management: a survey, assessment, and directions for future research, *System Dynamics Review*, 23 (2-3),157-189.
- Nisar, T.M. 2013. Implementation constraints in social enterprise and community Public Private Partnerships. *International Journal of Project Management* 31: 638-651.
- Oedewald, P. & Gotcheva, N. 2015. Safety culture and subcontractor network governance in a complex safety critical project, *Reliability Engineering and System Safety*, Special Issue "Resilience Engineering",141, 106-114. <http://www.sciencedirect.com/science/article/pii/S0951832015000824>
- Oedewald, P., Pietikäinen, E. & Reiman, T. 2011. A Guidebook for Evaluating Organizations in the Nuclear Industry – an example of safety culture evaluation, *SSM: The Swedish Radiation Safety Authority*, 2011: 20.
- Pitsis, T.S., Sankaran, S., Gudergan, S. & Clegg, S. 2014. Governing projects under complexity: theory and practice in project management. *International Journal of Project Management* 32: 1285-1290.
- Reiman, T. & Rollenhagen, C. 2014. Does the concept of safety culture help or hinder systems thinking in safety? *Accident Analysis and Prevention*, 68, 5-15.
- Reiman, T., & Oedewald, P. 2009. Evaluating safety critical organizations: focus on the nuclear industry. Swedish Radiation Safety Authority, Research Report 2009:12.
- Ruutu, S. 2015. System dynamics modelling of complex safety critical projects. VTT Research Report, VTT-R-05827-15, Espoo, 2015.
- Starck, M. 2016. Key dimensions of project governance and their relation to nuclear safety-An explorative study of nuclear industry projects, Master's thesis, Department of Management and Organization, Hanken School of Economics, Helsinki.
- Tuovinen, J. & Gotcheva, N. 2017. Delays in creating and handling design documents: A case study of a complex nuclear industry project. VTT Research Report, VTT-R-00892-17, Espoo.

- Turner J.R. & Simister S. 2001. Project contract management and a theory of organization. *International Journal of project management* 19(8): 457-464.
- Viitanen, K., Gotcheva, N. & Rollenhagen, C. 2017. Safety Culture Assurance and Improvement Methods in Complex Projects – Intermediate Report from the NKS-R SC\_AIM, NKS-381, [http://www.nks.org/en/nks\\_reports/view\\_document.htm?id=111010214063661](http://www.nks.org/en/nks_reports/view_document.htm?id=111010214063661)
- Walker, D. 2016. Project alliancing practices and experiences in Australia, presented at the International MAPS seminar “Relational contracting for improved network performance in complex projects”, May 24, 2016, Aalto University, Espoo.
- Woods, D.D. 2006. Essential characteristics of resilience. In Hollnagel, Woods and Leveson (Ed.), *Resilience Engineering: Concepts and Precepts* (pp.21-33). Aldershot. UK: Ashgate Publishing.
- Ylönen, M & Engen O. A. Regulation of sociotechnical systems: Characteristics of safety regulation: Comparison between Finnish nuclear industry and Norwegian petroleum industry, Manuscript to be submitted.
- Ylönen, M. & Engen, O. A. 2016. Sociotechnical aspects in safety regulation in the high-risk industries. In Walls, Lesley, Mathew Revie, Tim Bedford (Eds). *Risk, Reliability and Safety. Innovating theory and practice: Proceedings of ESREL 2016, Glasgow, Scotland, 25-29 September*.
- Ylönen, M. 2017. Licensee’s relationship with the suppliers – Simple rules, lessons learned. Paper accepted to ESREL 2017 conference.
- Ylönen, M. Simple rules and lessons learned in the complex project management in the nordic oil and gas and nuclear industries, Manuscript to be submitted.

## 2.3 Integrated safety assessment and justification of nuclear power plant automation (SAUNA)

Antti Pakonen<sup>1</sup>, Jarmo Alanen<sup>1</sup>, Kim Björkman<sup>1</sup>, Igor Buzhinsky<sup>2</sup>, Atte Helminen<sup>1</sup>, Arttu Hirvonen<sup>5</sup>, Jan-Erik Holmberg<sup>4</sup>, Hanna Koskinen<sup>1</sup>, Jari Laarni<sup>1</sup>, Joonas Linnosmaa<sup>1</sup>, Risto Nevalainen<sup>3</sup>, Nikolaos Papakonstantinou<sup>1</sup>, Markus Porthin<sup>1</sup>, Teemu Tommila<sup>1</sup>, Tero Tyrväinen<sup>1</sup>, Eero Uusitalo<sup>5</sup>, Janne Valkonen<sup>1</sup>, Timo Varkoi<sup>3</sup>, Valeriy Vyatkin<sup>2</sup>

<sup>1</sup>VTT Technical Research Centre of Finland Ltd  
P.O. Box 1000, FI-02044 Espoo

<sup>2</sup>Aalto University, Department of Electrical Engineering and Automation  
P.O. Box 15500, FI-00076 Aalto

<sup>3</sup>Finnish Software Measurement Association FiSMA ry  
Tekniikantie 14, FI-02150 Espoo

<sup>4</sup>Risk Pilot AB Suomen sivuliike  
P.O.Box 72, FI-02101 Espoo

<sup>5</sup>IntoWorks Oy  
Huvilatie 40, FI-90940 Jääli

### Abstract

The general objective of SAUNA (2015-2018) is to develop an integrated framework for safety assessment and transparent safety demonstration of nuclear power plant instrumentation and control (I&C) systems. In the first two project years, SAUNA has specified reference models for Systems Engineering life-cycle processes, with focus on I&C qualification. We have also developed concepts and models for analysing I&C architectures and Defence-in-Depth. In terms of analysis methods and tools, SAUNA has created ways of integrating a formal verification method called model checking with requirement engineering, plant simulation, testing, and probabilistic assessment. We have also developed methods for assessing engineering processes, and studied an interdisciplinary hazard analysis method called STPA. On the topic of structured safety demonstration, a Nordic expert network has been established for collecting and reporting licensing practices, and developing methods for justifying overall safety of nuclear I&C in a transparent way.

### Introduction

Overall plant safety of nuclear power plant instrumentation and control systems (I&C) cannot be addressed by focusing only on technical solutions, deterministic or probabilistic analysis, or single faults. The key challenge is to account for 1) all types of hazards, including rare and extreme conditions, 2) all disciplines and types of system elements (technical, human, environmental...), and 3) all life-cycle phases and activities. While the scope of SAUNA is plant operations (I&C systems and their human users), we consider the power plant and the people involved in its development, licensing and maintenance as a sociotechnical system.

Accordingly, the overall objective of SAUNA (2015-2018) is to create an integrated framework for safety assessment and transparent safety demonstration of nuclear I&C systems. We aim to develop multidisciplinary

plinary ways to build confidence in system safety. In addition to contributing to nuclear safety, we expect the utilities, the systems suppliers, as well as the regulator to benefit from cost-effective and timely licensing processes, built upon integrated analysis methods and tools, and structured ways of justifying safety.

As the basis for integrating different aspects and disciplines of safety into a consistent framework, we look to adapt good Systems Engineering practices to the needs of the nuclear domain. To facilitate collaboration, SAUNA develops common terminologies, documentation practices, and information models. Specific effort is placed on safety-related topics such as Defence-in-Depth (DiD) architectures. A key example of a shared model is the virtual plant originally used in the DIGREL project (2010-2014), and further developed in the MODIG (Modellind of DIGital I&C) project, a subtask of SAUNA.

When looking into assessment methods and tools, SAUNA emphasises that the methods should apply structured argumentation, and produce results that can be used as evidence in safety demonstration. To meet these demands, we will extend existing methods with other suitable methods and documentation practices. As an example, a formal verification method called model checking has been one of the success stories of the previous SAFIR programmes, as evidenced by its practical application in the Finnish nuclear industry. In SAUNA, the focus is not on developing the actual model checking algorithms and tools, but on an integrated approach — co-use with probabilistic assessment methods, integration into I&C requirement specification processes, and the use of simulators to validate the results. SAUNA will also develop other novel methods and tools, supporting a more multidisciplinary approach. Examples of topics include System-Theoretic Process Analysis (STPA), systems and safety engineering process assessment, Human Factors evaluation of control room systems, and DiD assessment.

On the research theme of safety justification, SAUNA aims at providing recommendations and new viewpoints for planning, documenting, and communicating the safety demonstration. Instead of a traditional, document-based approach, we hope to promote model-based, structured ways of arguing safety, and capturing the traceability links to requirements, design artefacts and analysis results in a transparent manner. We aim to showcase these concepts using case studies from real ongoing or past projects.

Below, we report the results of the first two project years. First, we review the work done on the conceptual basis of research on NPP I&C system safety. SAUNA has developed reference models for Systems Engineering processes, multidisciplinary models for DiD architecture assessment, and shared example models for working on I&C risk assessment. Next, we look at research activities on analysis methods and tools. On one hand, SAUNA has focused on integrating formal analysis methods (model checking) with related methods like simulation, testing and PRA. On the other hand — in addition to analysing the technical solutions — SAUNA has also looked at methods and tools related to engineering process assessment, human factors, and societal issues. Finally, we review the research activities on safety demonstration practices. Together with Nordic partners, SAUNA has collected and defined guidelines for arguing the safety of I&C systems in a structured, model-based way.

## **Safety systems engineering**

### **Towards model-based I&C safety engineering processes and data**

The governance of complex projects, such as nuclear power plant (NPP) investments, requires that engineering activities are well planned and their outcomes are well managed. The main motivation for this comes from the stringent safety requirements and the long lifetime of nuclear power plants. Accordingly, we have applied the Systems Engineering methodology to provide a life cycle management framework that supports overall safety in I&C systems, which involve multi-disciplinary teams.

Systems Engineering can be thought of as systematic engineering of a system through its whole life cycle. To achieve a demonstrably safe design, the NPP organisations should possess the following: a) a systematic model of the engineering processes and system's life cycle (obtained e.g. from ISO/IEC/IEEE 15288 and its daughter standards), b) a systematic model for the information items (such as safety requirements and the corresponding verification and validation results), c) an effective project organisation

model and d) well-planned use of project management and systems engineering tools. In the SAUNA project, we have addressed especially the first two success factors with the intention to improve safety engineering practices and to provide a basis for tool development.

To define engineering processes in a systematic and model-based way, we have created an enhanced process constructs model. This model relates the processes, their activities and tasks to process inputs, outcomes, enablers and controls in a traceable way. For example, the qualification process is traced to the corresponding process requirements stated by the regulators; the qualification engineers that apply and customise the process can easily see the original rationale for the process description. Furthermore, an impact analysis can be carried out to indicate the processes, activities and tasks that are affected by changes in the process requirements. Or, vice versa, if a process description is modified, the corresponding process requirements can be flagged to indicate that it shall be checked that the updated process satisfies the relevant requirements. The enhanced process constructs model is presented in (Alanen & Salminen 2016), and its updated version in (Alanen & Tommila 2016). Using the enhanced process constructs model, we created an example implementation of a Systems Engineering Management Plan template (Alanen & Salminen 2016). We also created two example processes, Stakeholder Requirements Definition process (Alanen & Salminen 2016) and Qualification process (Alanen & Tommila 2016).

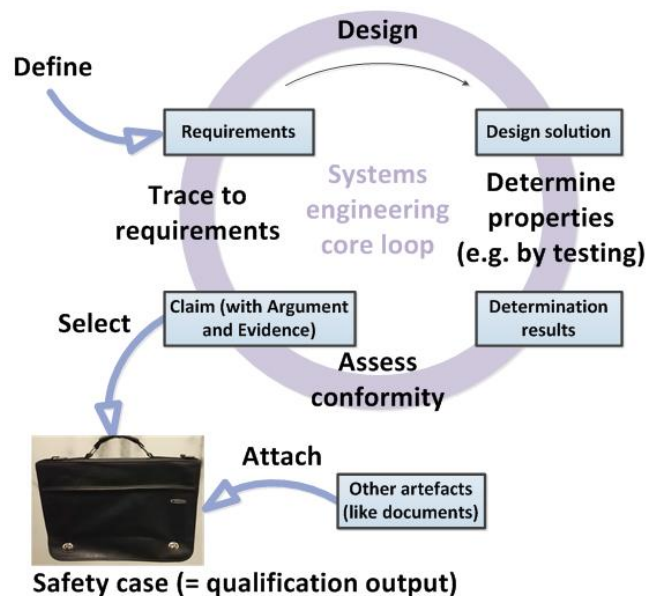


**Figure 1.** Systems engineering core loop.

To provide a systematic information model of engineering artefacts, we elicited the systems engineering core loop (see Figure 1) that is carried out by engineers, either consciously or unconsciously, systematically or in an ad-hoc manner. The loop starts with the definition of requirements; then a design solution is created to satisfy the requirements; thereafter the actual properties of the design solution are determined e.g. by testing or analysis; and finally the conformity assessor claims that the particular design solution satisfies (or does not satisfy) the relevant requirements based on the determination results. The claims needed for qualification are then collected into a safety case to demonstrate safe design solution (see also Chapter Safety demonstration methods and practices).

Using the idea of SE core loop, we created a data model to support model-based safety demonstration with traces to requirements, design artefacts and to the determination results that are used as evidence for the assurance claims. The data model depicted in Figure 2 can be implemented using a structured data repository such as a relational database or XML files to facilitate traceability of artefacts and impact analysis. See (Alanen & Tommila 2016) for a detailed description of the model.

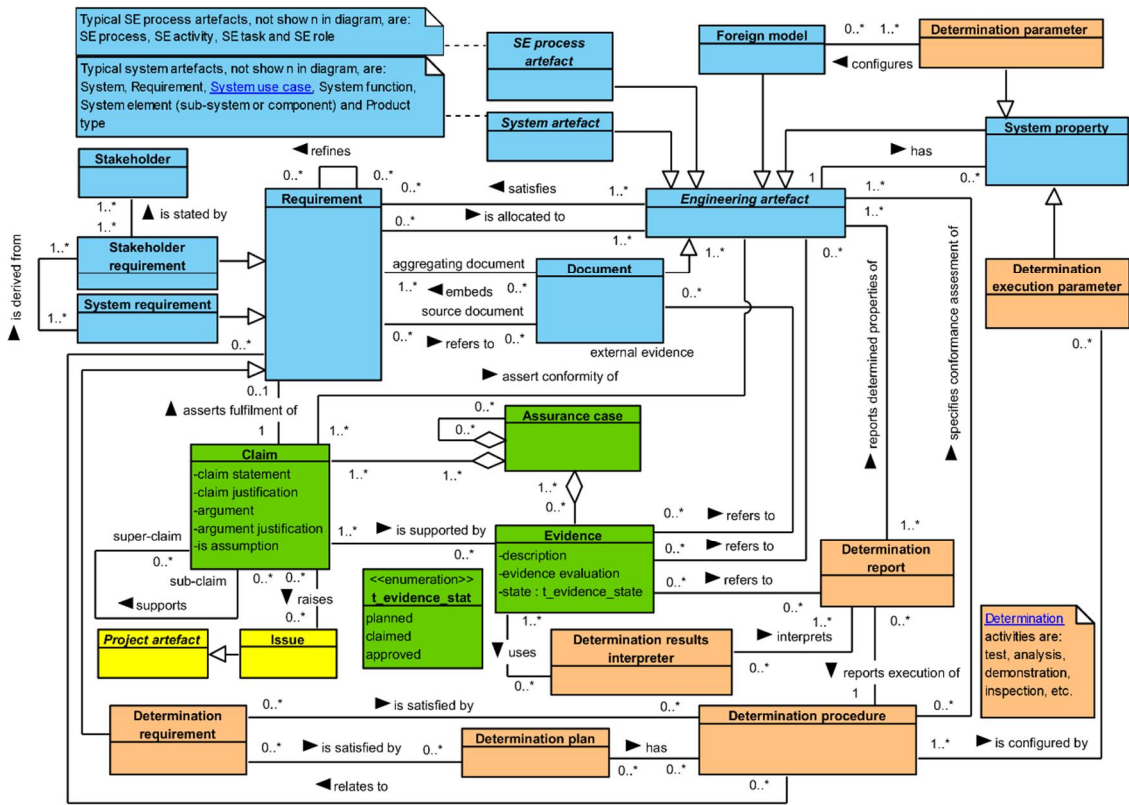


**Figure 2.** Our suggested data model for the main development artefacts, determination artefacts and conformity artefacts.

Our experiences so far indicate that applying model-based engineering as presented here helps assuring the safety of complex systems, such as the I&C systems of nuclear power plants. This is because the engineering and conformity assessment effort can be managed more systematically. The systematic process and data models help identify gaps in fulfilling the process and product safety requirements. To do this in practice, tool support is however needed. As a next step, our plan is to verify the feasibility of the approach by applying it for the I&C architecture definition process with an (preferably real) industrial example.

## Modelling and analysing defence-in-depth

Defence in depth (DiD) is a key design principle of complex systems for enabling overall safety. This task's first focus was to establish the state of the art in DiD, based on literature and on interviews with power utilities and STUK. Our effort then focused on developing methods to support the early assessment of DiD attributes (such as redundancy, isolation, diversity, etc.) in complex systems.

One of the crosscutting topics in the SAUNA project is overall safety which, when looked from the safety engineering perspective, is concretized in the plant-level DiD architecture. A second main topic in SAUNA, instrumentation and control (I&C), has a major role in the DiD implementation. Therefore, the design decisions concerning DiD and I&C architecture, for example independence of DiD levels and redundancies, are critical and should be verified as early as possible.

In order to provide a basis for modelling and model-based safety assessment, we started by reviewing the principles, challenges, terminology and assessment methods related to DiD (Tommila & Papa-

konstantinou 2016). We learned that DiD continues to be a major design principle for nuclear power plants. Partly due to the Fukushima disaster, there is a debate going on its scope and interpretations concerning, for example, human and organisational factors and extreme conditions. The concrete challenge is to find good technical solutions and practices for development and assessment. Moreover, many terms related to DiD (e.g. physical separation and functional isolation) and failure behaviour (active failure, failure mode, etc.) would still need clarification to provide a good basis for computer tools. As a complement to Probabilistic Risk Analysis (PRA) of digital automation (see below), also other kinds of models and simulation and reasoning algorithms would be needed for analysing the DiD solutions at early stages of development. With this in mind, as described in the sections below, we have explored various approaches and proposed methodologies for the analysis of hidden dependencies and failure propagation paths.

### **Failure propagation between redundant systems**

We developed a method for estimating the failure propagation risk between uncoupled systems in constructed environments (O'Halloran et al. 2015). The system components are given 3D coordinates (placed in the environment) and a list of potential failure modes and related probabilities is generated. We developed a software tool called Uncoupled Failure Flow State Reasoner (UFFSR) which traverses through all the components and based on the nature of the failure mode (e.g. water leak, steam leak, explosion) and the location it calculates the propagation probability of that fault through the environment to a component belonging to a redundant subsystem. The UFFSR tool provides a report of the failure propagation paths and a total risk estimation for the design.

### **Cable routing when redundant systems are present**

In complex systems with multiple redundancy (e.g., 4 redundant systems), it may not be possible to completely isolate the cabling required for the redundant systems. This introduces a risk of failure propagation. We proposed the Cable Routing Function Failure Analysis (CRFFA) functional model based method for cable routing aiming to minimize this risk of failure propagation between redundant systems (O'Halloran et al. 2016). This method calculates all the possible arrangements of cable bundles, rejects the ones that lead to risk higher than a set threshold and ranks the acceptable routing solutions.

### **Model driven approach for early assessment the reliability of Emergency Operating Procedures**

Human factors are an important aspect when considering complex system safety. We proposed the early Model-based HRA (eMHRA), an early safety assessment method for Emergency Operating Procedures (EOPs) (Papakonstantinou et al., 2016). We developed a metamodel (Figure 3) that can be used to model EOPs with the addition of SPAR-H Human reliability attributes. These EOPs can be automatically assessed and the total Human Error Probability can be calculated using a software tool.

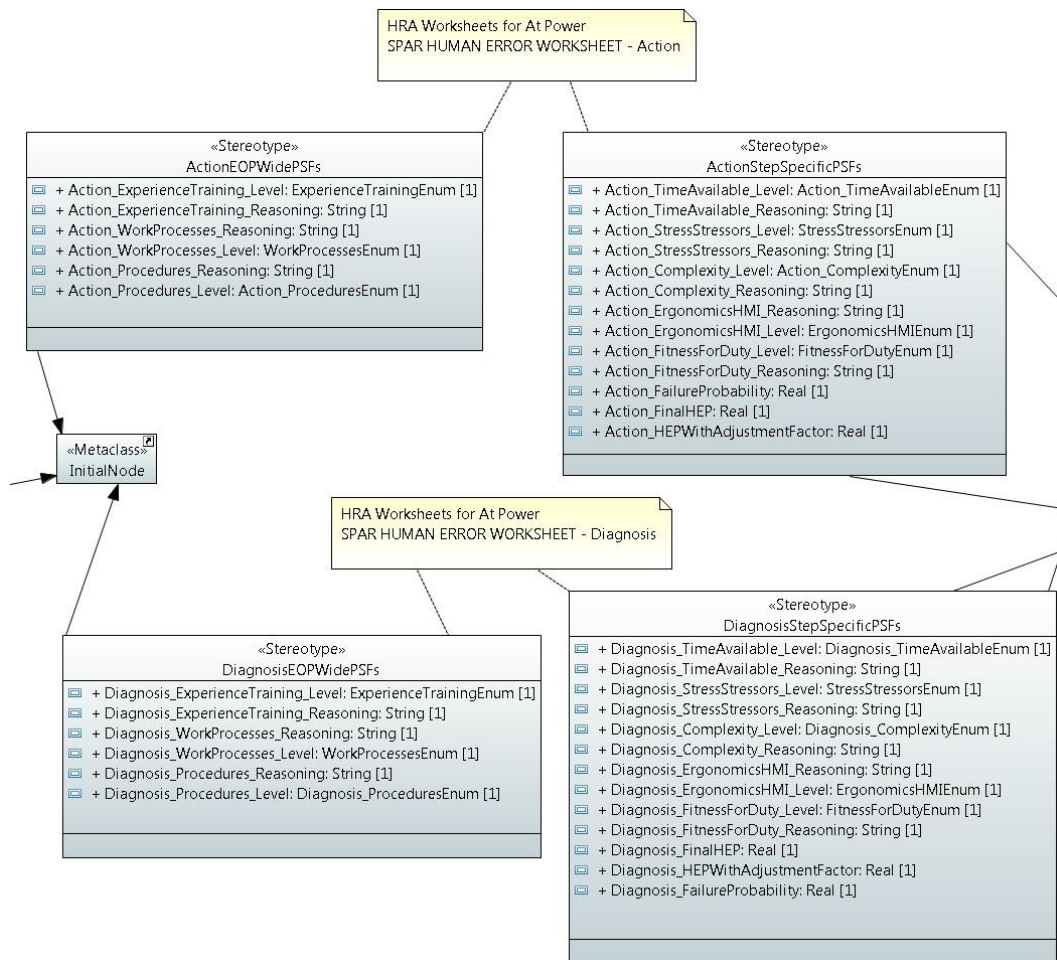


**Figure 3.** The partial UML profile with the stereotypes that include as UML attributes the SPAR-H Performance Shaping Factors (PSFs) used to calculate the overall Human Error Probability (HEP) of an Emergency Operating Procedure (EOP). The EOP models created following this profile can include partial Human Reliability Analysis (HRA) information early on in order to provide feedback to the EOP designer using a prototype software tool we developed.

### Model driven early assessment of Defence in depth

The practical early application and assessment of DiD is a challenging task. Based on the state of the art report on DiD we proposed a metamodel for creating High Level Interdisciplinary Models (HLIMs) which also include DiD attributes which help the assessment of the design (Papakonstantinou et al. 2017). A HLIM is a dependency model that captures the human factors, electrical, automation, process and environment aspects of a complex system. We developed a set of DiD guidelines which should be followed early on in the design process. A software tool can parse the HLIM and assess these rules. The results can be used to improve the design until it is acceptable.

### Future research directions

We are planning to extend the metamodel for the HLIMs introduced in our work for early DiD assessment with additional information related to the I&C aspect of the system. In collaboration with other SAUNA tasks, we are aiming to be able to use the enriched case study for producing reports that can be utilized in

task T3.1 as safety demonstration artefacts. Extensions to the case study will also provide connections to early HRA (using the eMHRA method) and potentially to PRA in collaboration with task T1.3.

### Modelling of digital automation systems

The objective with the MODIG (Modelling of DIGital I&C) subproject is to get a consensus approach for a reliability analysis of a plant design with digital I&C, improved integration of probabilistic and deterministic approaches in licensing of digital I&C, improved failure data collection including software failure probability quantification, and a practical application of PRA to compare design alternatives.

### Assessment of defence-in-depth

Defence-in-depth (DiD) can be seen as a deterministic design principle with multiple barriers associated with accident prevention and mitigation. Ideally, barriers should be independent of each other to ensure that single failures or common cause failures (CCF) do not cause a failure of multiple barriers. In practice, it is not possible to achieve such a design. PRA can be used to show that the risk is acceptable despite of dependences, as indicated in Figure 4. PRA can also indicate risk important dependences. PRA is as such capable of assessing risk of core damage and radioactive release, as well as the effectiveness of an individual DiD level. PRA can also be used in a “deterministic” manner, by utilizing the logic model to analyse the failure criteria defined in the deterministic safety requirements (Holmberg et al. 2017).

Initiating event Level 1 PRA		Safety functions Level 1 PRA	Safety functions Level 2 PRA	Consequence Level 3 PRA	
DID level 1 Prevention of abnormal operation and failures	DID level 2 Control of abnormal operation and detection of failures	DID level 3 Control of accidents within the design basis	DID level 4 Severe accident management	DID level 5 Mitigation of the radiological consequences	Consequence

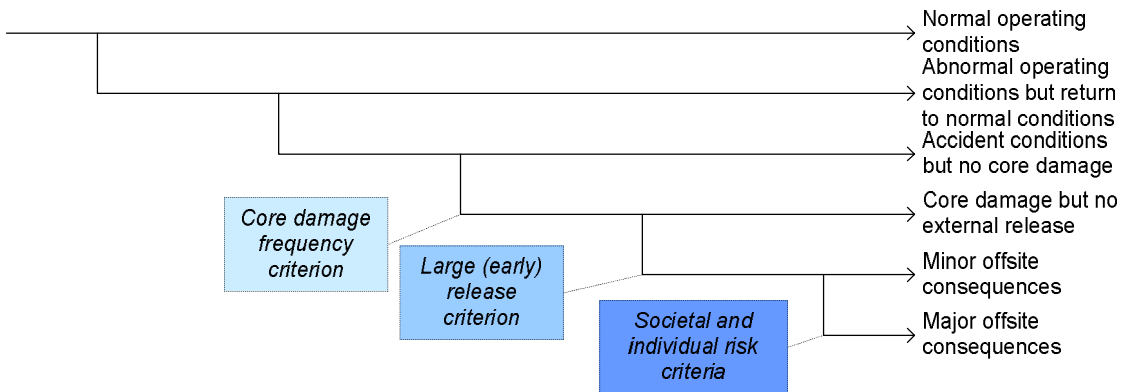


**Figure 4.** Levels of defence-in-depth, PRA and risk criteria.

DiD requirements can be grouped into the following categories:

- deterministic plant condition category related requirements (deterministic safety analyses, DSA)
- probabilistic plant condition category related requirements (probabilistic risk analysis, PRA)
- independence requirements between DiD levels
- individual DiD level strength requirements.

The first two categories rely on identification and assessment of a number of scenarios that form the so called design basis of the plant. DiD level independence assessments form a heterogeneous group of various assessments. Independence is a desired property of DiD concept but cannot be fully achieved. Individual DiD level strength requirements consists of a set of specific requirements which vary between levels of DiD and types of systems (e.g. rules for electric power supply and I&C in various safety classes).

The overall DiD assessment approach can be defined in five major steps, see Figure 5. DSA and PRA should be carried in an integrated manner to save analysis resources as well as to reach a common and broad understanding on issues important to safety. Due to different acceptance criteria, there are some differences in the set of analysed scenarios and also in the way the thermo-hydraulic analyses are carried out. The logic model of PRA provides a powerful tool to complement the deterministic assessments.

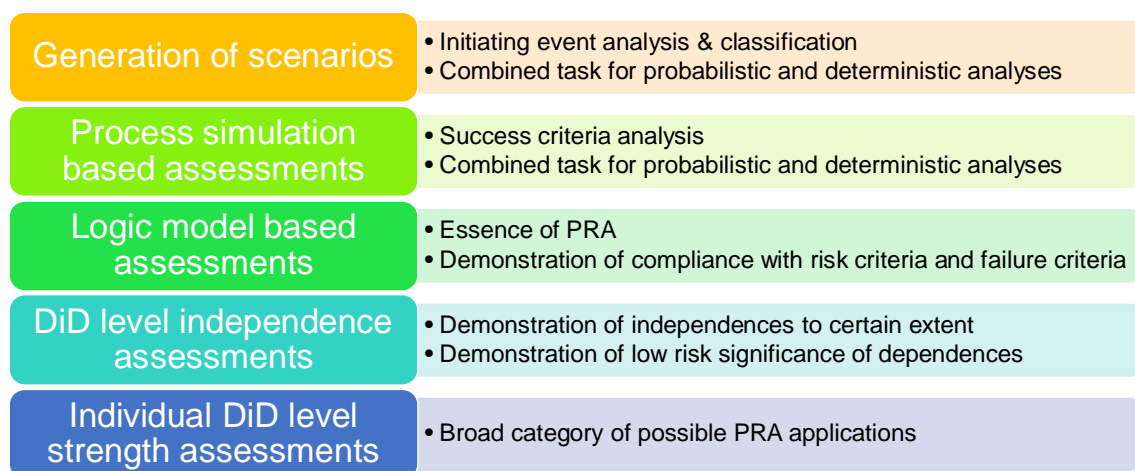


**Figure 5.** Role of PRA in DiD assessment steps.

We have discussed the assessment of preventive safety functions, which belong to the DiD level 2 responsible for the preventive safety functions (Holmberg et al. 2017). DiD level 2 overlaps with DiD level 1 and 3 both functionally and system arrangements. The role of DiD level 2 has been somewhat diffuse both in the context of DSA and PRA, and there are, e.g., differences in the design requirements for DiD level 2 functions and systems, e.g., redundancy requirements and safety classification. In current PRA models, only a fraction of DiD level 2 functions and associated systems are included in the model. Some functions are explicitly modelled, some can be implicitly included in the initiating event frequencies, and there can also be DiD level 2 functions which are not credited or are not typically analysed in PRA.

There is clearly an opportunity to refine PRA models by explicitly analysing and modelling DiD level 2 functions, which would make the PRA model more realistic and would provide insights concerning the importance of preventive safety functions. We have made an example on the implementation of DiD level 2 to the DIGREL PRA model. Based on the example, it is evident that the preventive safety function of DiD level 2 can be implemented to PRA models. For PRA event trees, the implementation is quite straightforward procedure. The main challenges are expected in the initiating event analysis and system analysis parts of PRA modelling.

Generally, failure analysis of I&C is a demanding task. Previous Nordic and international research work has given guidance for the definition of failure modes but there are still open issues in this task (Authén et al 2015, OECD 2015). Failure propagation can be analysed only in a limited manner following on some analysis assumptions. A crucial issue is which CCF should be postulated and how CCF should be defined. This is a difficult question for, e.g., software reliability analysis as discussed below.

The assessment of spurious actuations is another challenging topic. Spurious actuation is a functional failure mode where a component performs a function without a real demand. The topic is of special interest for I&C due to complex effects via system dependences and due to a huge number of possible failure locations. We have compiled analysis requirements for DSA and PRA, and defined a generic failure modes taxonomy based on von Wright's theory on concept of action (Authén et al. 2016).

### **Software reliability**

Assessment of software reliability is a controversial issue. It is mostly agreed that software could and should be treated probabilistically but the question is to agree on a feasible approach. Software reliability estimation methods described in academic literature are not applied in real industrial PRAs for NPPs. Software failures are either omitted in PRA or modelled in a very simple way as common cause failures related to the application software of operating system (platform). It is difficult to find any basis for the numbers used except the reference to a standard statement that  $1E-4$  per demand is a lower limit to reliability claims, which limit is often suggested as a screening value for software CCF (IEC 2005, Common Position 2014).

As a solution to software reliability analysis, we propose an approach based on categorisation of software into modules, as can be found in digital reactor protection systems (Authén et al. 2016): System software, data communication software, data link configuration, application software modules, elementary functions in application software modules, and proprietary software in I&C in various hardware components.

Depending on the type of software, we suggest different assessment approaches. For system software and related generic (not plant-specific modules) operating experience could be used (three first cases above). For application software modules, expert judgements and operating experience could be used together in a Bayesian manner. Faults in elementary functions can be assumed to be covered by application software failures. Proprietary software faults are included in the hardware modules failures.

In the failure modes and effects analysis, we distinguish between fatal and non-fatal failures. A fatal failure causes the I&C unit or hardware module to stall. The functional impact of fatal failure depends on the fail-safe design of the concerned I&C system. In a non-fatal failure, the unit or module continues functioning but produces a wrong output. Functionally, the wrong output can lead to a failure to actuate a safety function or a spurious actuation. This categorisation of software failure modes and association of them with software modules provides us a manageable way to handle software failures in the context of PRA.

### **Extending the DIGREL plant example with functional architecture**

Assessing I&C architectures presents two challenges. Firstly, it is difficult to demonstrate I&C architecture safety because of lack of acknowledged methodologies. Secondly, there is no acknowledged methodology to measure the "goodness" of I&C architecture, or even to make a comparison between two architectural solutions. However, at the root of the problem is the issue that in order to develop and test such methodologies, a functional reference architecture is required.

In 2015, we started the task of designing such a functional reference I&C architecture based on the DIGREL model. The DIGREL nuclear power plant model currently models the protection system of a fictional boiling water reactor. However, we soon found out that extending the model was severely hindered by lack of input on plant process system design. Rescoping the task to suit the allocated resources, we adapted tasks of I&C architecture design based on (EPRI 2014) in order to create a roadmap on how to produce such a reference architecture for a non-existing plant given the limitations of the context. Based on this roadmap, we performed initial design tasks in sequence.

Besides the roadmap, contribution of this work was forming a requirements base for building the reference I&C architecture, forming architectural rules, and performing initial design work based on the established rules. As one of the initial steps, we presented a prioritization concept for I&C architecture that is compliant with YVL B.1 (Uusitalo & Koskela 2015).

## Formal verification methods

### Closed-loop model checking

Formal verification is an alternative to simulation-aided testing and other conventional verification and validation (V&V) approaches. It is capable of proving the correctness of the model of the system. The corresponding V&V procedures are commonly automated, but their user is responsible to provide the formal model of the system and the formal representation of requirements to be checked. We have studied the ways to develop new V&V approaches related to a particular kind of formal verification – model checking (Clarke et al. 1999), which explores the state space of the formal model to verify a requirement. In the previous SAFIR programmes — as well as VTT’s practical customer work (Pakonen et al. 2013) — model checking has been proven a highly useful method (Lahtinen et al. 2012). Notably, in previous SAFIR research, as well as other relevant studies (Yoo et al. 2008) this technique has been applied to nuclear I&C systems in open loop – that is, the automation logic is provided with free, unconstrained inputs, and certain requirements (for example, of the response-request or the invariant types) are checked. However, in this case the plant, or the environment where the controller operates, is disregarded. This leads to the following consequences:

- The controller is checked for correctness under the presence of plant behaviours (represented as input sequences) which are not possible for real life. This can result into irrelevant counterexamples generated by the employed model checker.
- Certain requirements cannot be checked without the plant models, including requirements involving internal plant parameters and the ones constraining output plant parameters. For example, instead of actually verifying that the value of some NPP parameter is within certain interval, in the open-loop scenario we would check that the controller attempts to return this parameter to normal values when dangerous values are reached.
- For explicit-state model checkers, arbitrary input values to the controller quickly lead to the “state explosion” problem if the size of the checked system grows.

In contrary, in closed-loop model checking, the plant and the controller models are composed into a closed-loop system, which eliminates the aforementioned problems. Thus, we decided to investigate the application of this technique in the nuclear automation industry.

In the beginning of the project work, due to the lack of a proper case study for closed-loop model checking, we worked on closed-loop model checking approaches using a model of a laboratory-scale heat production plant. Then, we migrated to the generic pressurised water reactor (PWR) model provided by Fortum Power and Heat Oy, which is implemented in the Apros continuous process simulator, and contains basic components of an NPP. To obtain the formal model of the controller, we used the MODCHK tool (Pakonen et al. 2013) developed in VTT. After preparing a library of basic function blocks, we modelled several Apros automation networks in this tool. Corresponding formal models were automatically generated by MODCHK in the format of the NuSMV symbolic model checker. This approach follows the methodology outlined in (Pakonen et al. 2013).

We could have applied the same approach to the plant model, but due to the reasons explained below, we chose another path. Since the computational complexity of verification depends on the complexity of the verified system and, for explicit-state model checkers, on the number of states in it, for complex plants closed-loop model checking may become computationally infeasible. Moreover, manual modelling of complex plants requires much effort and is an error-prone task. Thus, to achieve reasonable model complexity and to reduce manual effort, we investigated ways to obtain the plant model using heuristic and/or artificial intelligence approaches. The input data for such methods is often a set of behaviour examples, or traces, of the system that shall be identified. In our case, we were able to use the traces generated by simulating the generic PWR model. As a result, we developed three formal plant model construction methods and a methodology (Buzhinsky et al. 2017) of closed-loop model checking involving the generated plant models.

The first plant model generation method (the explicit-state method) generates the plant model in the form of a nondeterministic Moore machine and is thus most suitable for explicit-state model checking. The second method (the symbolic method) generates the plant model in the form of constraints over its input and output parameters, which makes it more suitable for symbolic model checking. Since the employed model checker (NuSMV) was symbolic, we found that model checking with models generated by the second method runs significantly faster. The third plant model generation method (the SAT-based method) (Buzhinsky & Vyatkin 2016) generates plant models in the form similar to the one of the explicit-state method, but supports additional requirements for the plant model to be constructed in the form of linear temporal logic (LTL) properties, which may facilitate the exclusion of irrelevant behaviours from the plant model. On the other hand, the SAT-based method is based on Boolean satisfiability (SAT) solvers, which limits the size of plant models it can generate and the length of traces it supports.

The developed methodology of closed-loop model checking (Figure 6) is built around the application of the developed plant model generation methods. In addition, it considers the issues of trace acquisition, measuring the sufficiency of the recorded traces, and adjusting the level of detail of the formal model to make model checking computationally feasible. Using the developed methodology, we verified eight sub-systems of the generic PWR model. It is especially important that among the verified temporal properties the ones which cannot be meaningfully verified in the open-loop case were present. However, we found that the anticipated model checking complexity reduction was not achieved, but instead closed-loop model checking required more CPU time than open-loop one. This result can be explained by using a symbolic model checker (NuSMV), which cannot benefit from state space reduction. Then, the developed plant model generation methods were not suitable for verification of timing requirements, but other, more elaborate methods can be potentially developed and integrated into the methodology.

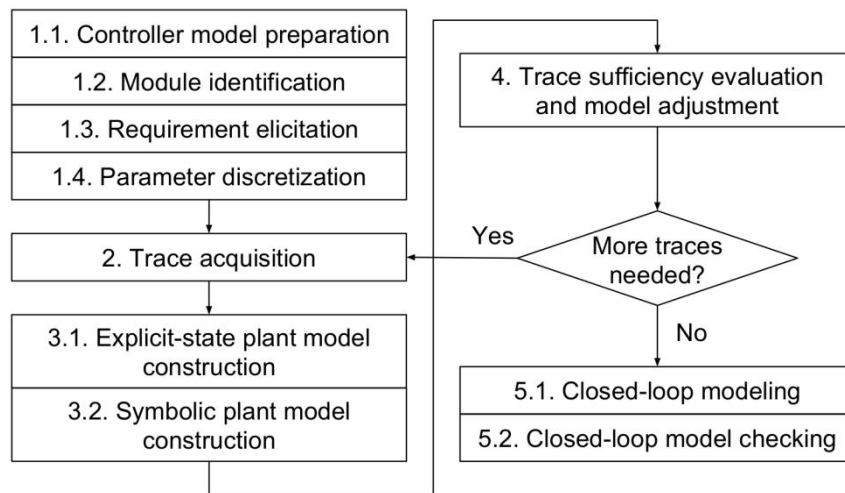


**Figure 6.** Overview of the closed-loop model checking methodology.

In future work, we plan to explore the possibility of extending the existing verification framework to make it support explicit-state verification. We will consider the possibility of translating controller block diagrams to the format of the SPIN verifier, and generating formal plant models in the same format. This will allow to gain the benefit achieved by the small state space of explicit-state plant models, and thus, potentially, speed up the verification process. Explicit-state open-loop model checking will be also considered. Moreover, we plan to improve the reliability of the library of basic function block formal models. For this purpose, we will formally synthesize these models from behaviour examples and temporal properties using existing techniques, and compare the synthesized models with manually created ones by means of model checking.

## User-friendly requirement representation and editing for formal verification

To apply formal verification methods, such as model checking, in industrial practice, experts need profound knowledge and experience, and the lack of such them may be dangerous (Holzmann 2002) since the experts may miss certain software faults by writing erroneous formal specifications. These requirements hinder the adoption of formal methods in industry (Dwyer et al. 1999), and in particular in the I&C systems industry. Meanwhile, in different domains different requirement types, or patterns, may prevail. Understanding the cost common requirement patterns in the I&C systems industry may suggest ideas for user-friendly and/or visual requirement representation and editing.

We started with the examination of existing approaches of user-friendly requirement representations (Pang et al. 2016). We identified two groups of approaches: (1) approaches for textual representation of requirements according to predefined rules and templates; (2) visual formal specification languages. We also explored works on achieving and measuring the usability of user-friendly specification languages. Based on the performed examination, we found that tool support and visual representation are crucial in reducing the gap between existing specification practices in the nuclear I&C industry and existing formal languages and methods.

As the next step, we examined which temporal property patterns are the most common in the nuclear I&C industry by collecting formal properties from VTT's practical customer projects (Pakonen et al. 2016). Our study showed that a relative small set of Linear Temporal Logic (LTL) and Property Specification Language (PSL) patterns could be used to capture about 93% of the 1079 collected properties. PSL, in particular, offered many advantages in capturing properties that deal with timing and sequencing issues, common in functional I&C requirements.

Bringing together the results of our studies, we applied visual specification languages for temporal requirements to represent the patterns common in the I&C systems industry (Buzhinsky 2016). We also we used the generic pressurised water reactor (PWR) model provided by Fortum Power and Heat Oy to provide examples of requirements which can be represented by previously identified temporal specification patterns, and as a source of new patterns. As a result, we found that five languages are potentially applicable in thus field, but may require some modification prior to that.

In the future work, we intend to focus on requirements that cannot be expressed compactly using a small set of templates and which deal with timing and sequencing issues (according to our findings, about 24% can be attributed to this class). PSL is a possible solution to represent such temporal properties. Thus, we intend to develop a concept of a tool to visually express PSL requirements. Next, we aim to improve visualisation of counterexamples, which would facilitate understanding the results of verification. This can be done by showing whether and how each of the subformulas of the temporal requirement is satisfied or violated.

Ultimately, we would wish to combine the results on user-friendly requirement representation and editing with the results on closed-loop model checking, uniting them into a comprehensive, tool-supported framework which would allow formulating requirements, generating formal models, performing model checking, and understanding its results for persons without or with limited expertise in formal methods.

## Model checking in structure-based test design

System testing often focuses on verifying the design against system specification. To improve coverage, test cases can also be based on the structure of the software code. In white-box testing (where the software implementation is known), structure-based techniques can be used to either assess the test coverage (by keeping track of how many software components or lines of code have been executed in the tests), or increase test coverage by generating additional test cases. In many safety-critical applications and standards, structure-based testing is required.

In the CORSICA project of the previous SAFIR programme, a concept technique was developed, where model checking was used to generate structure-based test cases and efficient test suites. For making the

technique feasible, it was still necessary to develop the methodology and tools, and overall reduce the manual work that was required. In SAUNA, the objective was to extend the test coverage methodology to allow for a wider range of function block diagram based systems. In particular, the goal was to better take into account the time-dependent behaviour of function blocks.

We defined three test coverage metrics for function block diagrams, by using the metrics introduced in (Jee et al. 2014), and modifying them to include delayed input-output dependencies for elements such as delay blocks. We then used model checking to generate the test cases (Lahtinen 2015). Our approach is based on adding Boolean monitor variables in the system model that indicate if a certain test requirement is true. A model checker can then be used to generate a test case for that requirement, as a property stating that the test requirement shall not be true will result in a counterexample that represents a suitable test case.

We tested our approach on fictitious function block diagrams, as well as a set of vendor-specific, real-world industrial examples. The tests indicated that while the developed technique is scalable to most nuclear safety systems, the time required for generating the tests becomes excessive (Lahtinen 2015). Partition of the tested logic into smaller subsystems might alleviate the computational cost. The results also showed that vast majority test requirements became infeasible in the context of the industrial examples, as vendor-specific features such as signal validity processing lead to a large number of different input-output dependencies. As in model checking, mathematically complex functions are also difficult to analyse.

We also compared the three coverage metrics by using variations of the target systems, altered to contain errors. Two of the three metrics proved as capable in detecting the faults, with one of those metrics (MICC, or modified input condition coverage) being more lightweight computationally.

In the overall methodology, the test generation process should be coupled with an automated test oracle — a system that is capable of distinguishing whether the outcome of a test is correct or not. Creating a test oracle for an arbitrary system is unfortunately very difficult.

## Integration of model checking and probabilistic risk assessment

Due to many unique features of digital systems, the safety and reliability analysis of such systems can be challenging, and a range of techniques is used for analysing the systems. We have primarily focused on model checking and fault tree analysis (FTA) in the context of probabilistic risk assessment (PRA).

PRA is an efficient method for handling both hardware failures and software failures. However, there are challenges on how to handle complex failure modes. It can be challenging to capture with static fault trees all the relevant issues of a software logic design. In PRA, it might not be relevant or practical to model the software logic designs at the function block level of detail. An issue is to define functional impacts of possible software errors from the safety function's point of view.

In the model-checking approach developed for modelling hardware failures (see e.g. Lahtinen 2014), the situation is different to PRA. Software errors, especially errors in the logic design, can be analysed in fairly large models, but the method does not scale well to large systems when hardware failures are assumed as well. Currently, both approaches contain limitations in analysis of situations in the middle ground that involve both software design errors and hardware failures.

We have studied different ways to handle this middle ground, and to integrate PRA and model checking to enable more extensive or practical safety analysis of digital systems. An ultimate goal of this work is to develop an integration approach that utilizes both of the methods and provides results that cannot be computed with either of the methods alone.

We identified 12 different approaches to couple model checking and PRA, and discussed their feasibility (Lahtinen & Björkman 2016a). Many of the coupling approaches relate somehow to fault tolerance analysis. The ways to couple model checking and PRA can roughly be divided into three groups; 1) the two tools are used together for a more extensive safety analysis, 2) model checking is used to support PRA analysis, or 3) PRA is used to support model checking.

We developed a concrete concept-level coupling approach for the coupling of model checking and PRA (Lahtinen & Björkman 2016b). The general approach is illustrated in Figure 7. The main idea of the ap-

proach is that the model checking analysis is restricted to a smaller set of postulated component failures based on PRA results. Model checking is used to thoroughly analyse the System behaviour under the failures and then the results are again compared against the PRA model. The results of the model checking can facilitate the definition of functional impacts of possible errors in the logic design for PRA purposes. We performed a simple case study in order to demonstrate the usability of the developed approach.

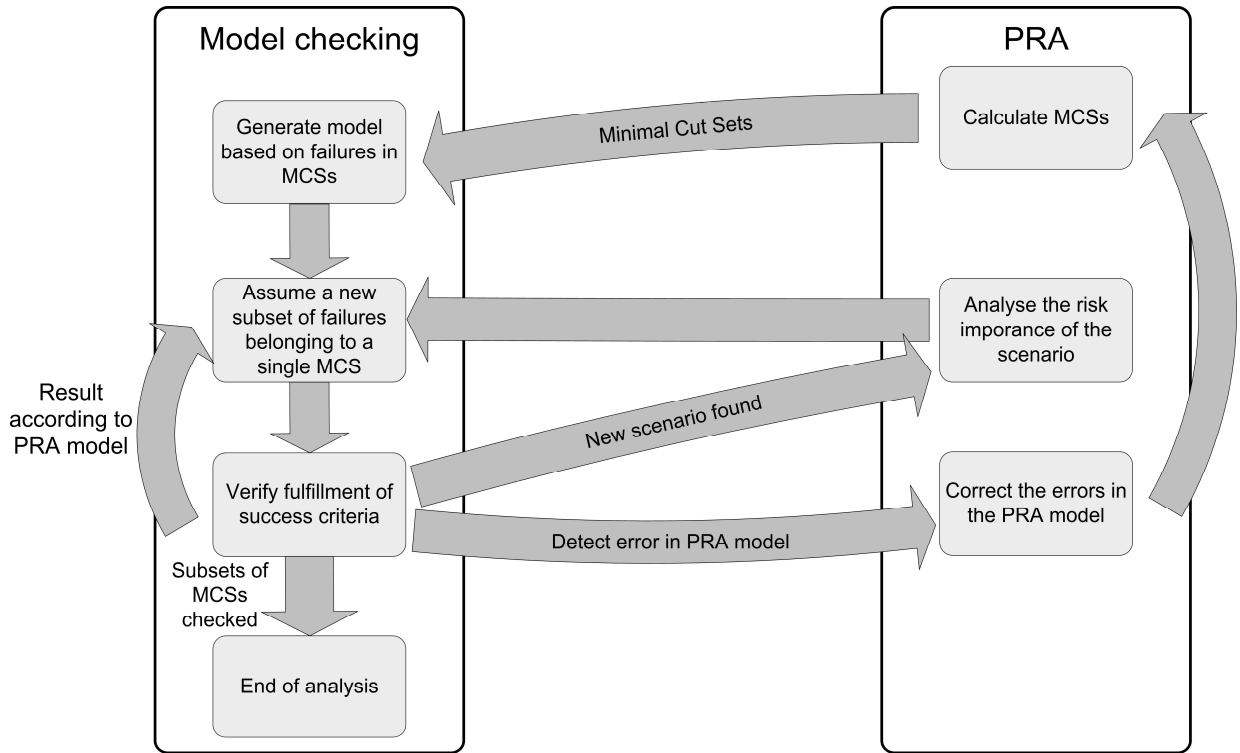


**Figure 7.** An approach for integration of model checking and PRA (Lahtinen & Björkman 2016b).

During the upcoming project years, the plan is to develop and perform a more complex case study to test the applicability of the approach on a larger scale model. The development of the case study can also benefit the development PRA level 1 method development in the PRAMEA SAFIR2018 project in the future, which can benefit both PRA I&C model construction and verification. In addition, the following issues can be addressed from the integrated approach point of view; deterministic analysis of failure criteria and failure mode definitions.

The integration of model checking and probabilistic risk assessment is closely related to the modelling of digital automation systems research done in the SAUNA project. Therefore, the integration of model checking and PRA has been included as part of the MODIG work for the rest of the project to further facilitate the cooperation between the tasks.

## Multidisciplinary assessment of automation

### Process assessment

The first statement in SAFIR2018 Framework Plan for Plant safety and systems engineering research area reads: “Plant overall safety is analysed from the perspectives of the system (ISO 15288) and its operating environment and with respect to the system of systems, also known as the system architecture.” This in

mind, we planned a task to develop a process assessment model (PAM) for performing ISO/IEC 15288 based systems engineering process assessments.

The foundation for this work is the Nuclear SPICE process assessment method that was already developed in SAFIR2014. However, as ISO/IEC 15288 was largely renewed in 2015, the existing software engineering oriented (ISO/IEC 12207 based) PAM could not sufficiently address the systems engineering approach. Our aim was that the Nuclear SPICE method would be based on the newest international standards and represent the strictest approach in process assessment. The method aims to ensure trustworthy systems development by identifying the risks related to the development processes, and to increase confidence and trust between acquirers, suppliers and regulators. The overall goal of this task is to establish a domain specific interpretation of process quality that sustains achievement of safety goals in systems engineering. A key benefit is cost-effectiveness when using process assessments in qualification.

We started the task by defining the requirements for a new systems engineering PAM (Nevalainen & Varkoi 2015). We described a prototype process assessment model (PAM) for performing systems engineering process assessment in safety-critical environments. We used as an example one fully defined process, Architecture definition. We identified four use cases for the Nuclear SPICE assessment method: process improvement; process capability determination; safety demonstration; and conformity with requirements (Figure 8). Evidence types for these use cases were defined using Architecture definition process as an example.

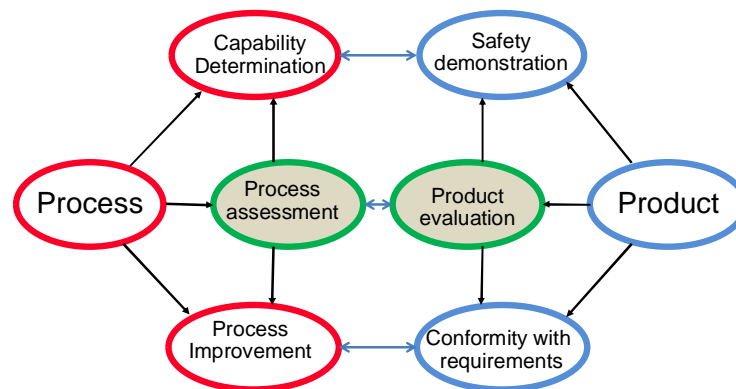


**Figure 8.** Nuclear SPICE use cases.

Next we continued by developing a new PAM based on the ISO/IEC 15288:2015 standard (Nevalainen & Varkoi 2016). The revised ISO/IEC 15288 standard provides the process reference model (Figure 9) including activities, tasks and information products as assessment indicators. In addition, we supplemented the process assessment process with a new activity for conformity evaluation. Based on our assessment experiences, we defined example process sets for two typical applications: supplier selection and project evaluation. These applications improve the usability of the Nuclear SPICE method. We used the IAEA Management Guide and ISO/IEC Assurance standards as input to consider emerging topics that may link up with future Nuclear SPICE development. Topics include safety culture, leadership, quality and safety management, cybersecurity, and quality and safety assurance.

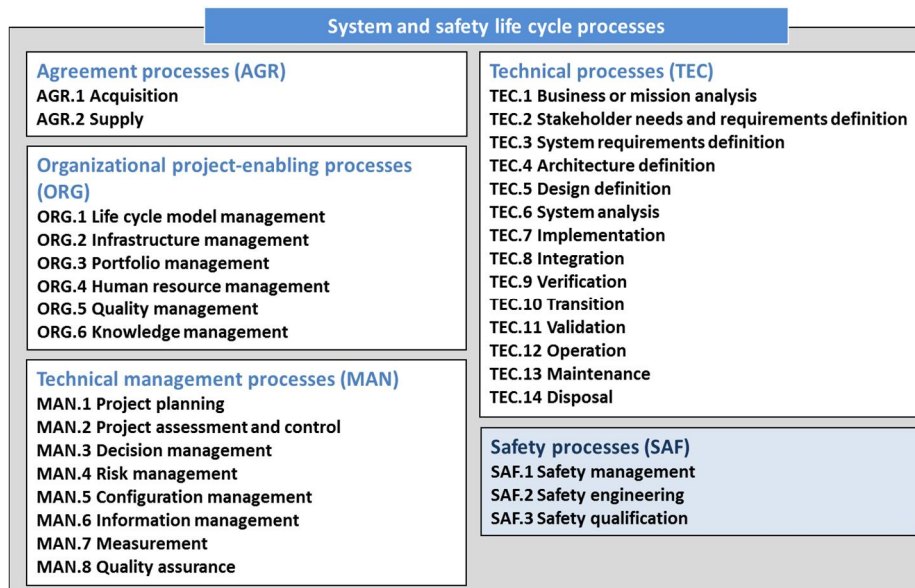


**Figure 9.** Nuclear SPICE Systems and Safety Engineering Process Reference Model.

To collect feedback from stakeholders, we organized two workshops. The first one, on Nov 25<sup>th</sup> 2015, focused on relevant process assessment needs. This workshop had extensive participation from all major stakeholders: STUK, TVO, Fortum, Fennovoima, VTT and FiSMA. The second, on Nov 23<sup>rd</sup> 2016, was named FiSMA Safety Panel and had close to 20 participants. We presented the updated Nuclear SPICE method and other safety assurance topics to promote co-operation and information exchange for researchers and industry.

We described the Nuclear SPICE development work in (Nevalainen & Varkoi 2015) and (Nevalainen & Varkoi 2016). In addition, we discussed systems and software engineering related process assessments in safety-critical domains, including nuclear, automotive and medical devices (Varkoi & Nevalainen 2015). Based on the key stakeholder requirements, we should extend the SPICE framework to take into account also safety demonstration and conformity with requirements use cases. To achieve this, product evaluation should be considered in conjunction with process assessment. Another issue is how process assessment method and results can be used as evidence in safety assurance. We presented a detailed mapping of assurance case elements to process assessment in (Varkoi et al. 2016). A conclusion is that process assessment output can also serve assurance needs, but requires tool support to be efficient. Finally, we proposed situational factors (Nevalainen et al. 2016) that can be used as a high level profile and starting point for more detailed process and safety assessment. The proposed safety situational factors contribute mainly to quality. The selected factors are applied to the medical device and nuclear power domains.

International collaboration had high priority in the task. As a result of the successful presentation in the QUATIC conference (Varkoi et al. 2016), we were able to invite a safety case expert to give a presentation in our FiSMA Safety Panel workshop. In addition, we received an invitation to participate the AMASS External Advisory Board. AMASS (Architecture-driven, Multi-concern and Seamless Assurance and Certification of Cyber-Physical Systems) is an ECSEL Joint Undertaking (<http://www.amass-ecsel.eu/>).

The systems engineering assessment model describes now the generic ISO/IEC 15288 based assessment indicators, but does not yet contain the domain specific, IEC 60880/61513 based assessment indicators. Next year, we will focus on extending the use of the Nuclear SPICE method, and to studying novel solutions for collection, management and reuse of the evidence data.

## System-Theoretic Process Analysis (STPA)

Safety of a NPP and its safety systems shall be assessed analytically and experimentally. Analytical methods include for example transient and accident analyses, analysis of internal and external hazards, strength analyses, failure tolerance analyses, failure mode and effects analyses (FMEA) and probabilistic risk assessment (PRA). These analyses must be maintained and revised throughout the plant's life cycle. The methods to demonstrate compliance with safety requirements shall be reliable and well qualified for the purpose (STUK Y/1/2016, 3§).

The fast pace of technological change, changing nature of accidents, and increasing complexity and coupling of systems have been stretching the limits of traditional safety engineering. Hazard analysis methods such as FMEA or Fault Tree Analysis (FTA) are mainly based on reliability theory, which evaluates systems and their components by failure rate. According to reliability theory, accidents are seen as a chain of component failures, an approach that is not relevant with complex designs anymore. Accidents could also be caused by component interactions where no components have failed but the system design has (Leveson 2011).

Instead of breaking systems into components, in systems theory, they are examined as a hierarchy of organizational levels, which are described by emergent properties. A new causality model, Systems-Theoretic Accident Model and Processes (STAMP), has been developed to take into account also cyber and physical interactions between several controllers in the system, in addition to component failures and unreliability. STAMP also accounts human as a component of the system (Leveson 2011). Based on the STAMP framework, a new hazard assessment technique based on called Systems-Theoretic Process Analysis (STPA) has been created (Leveson 2011). We evaluated the use of STPA in a safety-critical design process of a reactor service bridge (RSB), also known as refuelling machine. We wanted to find out whether using STPA in a safety-critical design process contributes to creating justifiable design solutions that can be traced to relevant artefacts in upper levels. Another research question was whether the functionality of the system can be analysed even at the early stages of design.

In the course of the work, we initially defined the system context, process model and operating conditions for RSB, including fixed structures, overall system requirements and operations performed. Then, we were able to define the STAMP Systems Engineering Foundation, consisting of accidents, system level hazards, system level safety constraints and the overall safety control structure of the RSB. This was followed by analysis of possible elimination or mitigation of system level hazards.

With this basis, we were able to start the two steps of STPA safety-critical design process: Identifying unsafe control actions and mitigating them as part of the design, and then identifying causal factors leading to those unsafe control actions.

Our findings from the use of STPA as part of safety-critical design process were as follows. Top-down reasoning together with systemic approach provides an effective background for the design process. The design path proceeds from the accidents and hazards and continues step by step into the final architecture. Every decision in every stage of the design has a clear trace upward back to related hazards and accidents. The required safety functions are constructed according to unsafe control actions, which can also be traced back to hazards. Then design decisions can be made in such a way that they fulfil the requirements to properly implement the safety functions. Safety classification can be made and justified according to these aspects. Therefore STPA based safety guided design provides traceable justifications for the design decisions of safety-related components and functions. This traceable design material can be used also to justify safety classification. The traceability also promotes the verification of the materials by external parties, including regulatory verification.

The application of STPA needs only the systems engineering foundation and a concept of the system. The systems engineering foundation includes accidents, hazards and control structure of the system. STPA as a systemic top-down technique supports early analysis of functionality by nature. In addition, the strength of the method is that the results can easily be refined when more details are added to the system or system modifications are made during operations (Hirvonen 2016).

In 2017, we aim to disseminate the lessons learned from applying STPA as part of a safety-critical design process in order to provide easily approachable guides for the practitioners. In 2016, we found that there seems to exist little guidance on how to apply STPA as part of a design process. Additionally, we aim to provide guidance also from the points of view peculiar to the nuclear industry in Finland, namely regarding the specific life cycles and licensing model. In 2018, we aim to find a more complex case in order to perform assessment on the effectiveness of STPA in a broader scope.

## Safety demonstration of control room systems

Human factors evaluation is a critical activity in ensuring the proper functioning of the control room (CR) systems and human-system interfaces. We have developed a Systems Usability Case (SUC) approach to support continuous, early-stage evaluation of CR systems. An early version of the SUC approach has been applied in the analysis of the results of individual validation tests at the Fortum Loviisa NPP.

The SUC is based on the Safety Case approach and on the Systems Usability (SU) construct. It provides a requirements-based approach to CR system verification and validation (V&V), in which general human-factors and plant-specific requirements are systematically used as a reference in the assessment of acceptability of the CR system solutions.

One of the main aim of establishing a SUC is to bring to the front the arguments and evidence for safety in such a way that the reasoning may support the work of both a regulator and licensing organization. Another aim of the SUC is to better manage and organize the validation evidence and make decisions about safety traceable throughout the lifecycle of a CR system product.

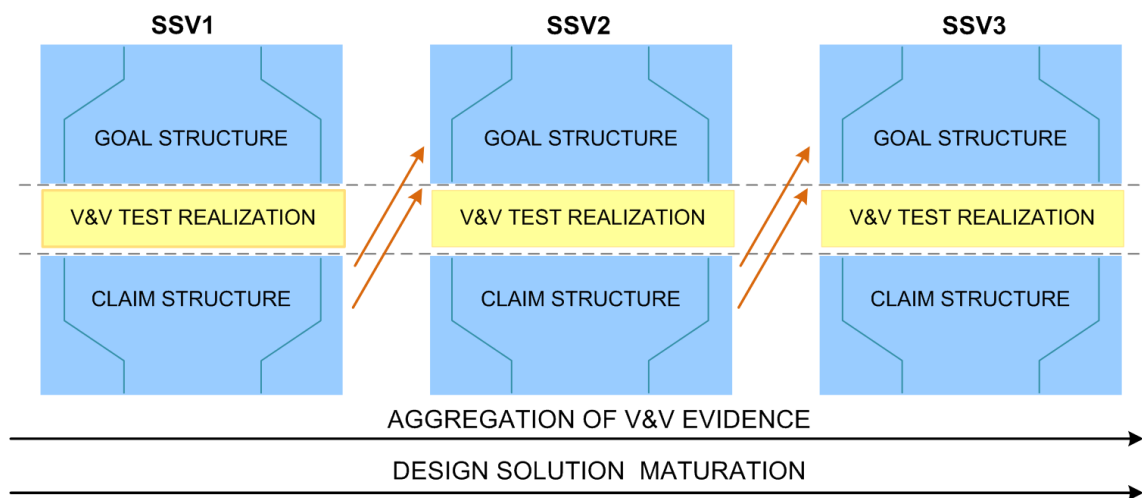


**Figure 10.** SUC development process illustrating the aggregation of V&V evidence and maturation of the design solution over sub-system validation (SSV) tests.

Figure 10 demonstrates how the validation evidence is aggregated and design solutions are matured over V&V test activities and how the individual SSV activities are interrelated. There is a progression of fulfilment of human factors requirements through the time of validation. Some of the design flaws are resolved in one stage or the revised design solutions has to be retested in the next stage. Also requirements may change: new requirements may be identified during the validation process. But the idea is that at the end of the process all the design flaws are resolved, and new requirements do not emerge any more. Figure also indicates that SUC provides support both for the continuous evaluation of the design solutions and for the independent validation of the CR systems. As can be seen, SUC development is divided into two main efforts: the first part of the SUC (i.e., goal structure) is established before the accomplishment of

V&V test activities, the latter part (i.e., claim structure) is established after the implementation of the validation tests.

We have applied the SUC method to real data from a stepwise CR system validation. The results suggest that the SUC has some clear advantages: it helps us to conduct the evaluation activities in a more systematic fashion, and it makes the reasoning process more explicit and transparent. In addition, we are able to build a longitudinal view of the progress of the design process, and constructing the SUC enables monitoring of the fulfilment of the requirements from the human factors that is SU perspective.

We plan to further develop the SUC approach, and especially concerning the goal structure part of the SUC there is a need to develop/improve the processing and handling of requirements. Regarding the claim structure part we plan to pilot/demonstrate the accumulation of evidence over SSVs and further over the different stages if the modernization is realized in stage-wise manner. We also aim to study the application of case-based approach to form a human factors case (HFC) that would cover also other human factors topics such as Human Reliability Analysis, training and procedure design.

## **Safety demonstration methods and practices**

One of the goals of the SAUNA project has been to identify development needs and possible solutions in the design and safety assessment of nuclear I&C systems. The aim has been to integrate various engineering disciplines under the concept of overall safety and to develop a good basis for model-based, computer-assisted tools. As one part of the project, we have evaluated feasibility of the structured safety demonstration approach in the Finnish engineering practice. Within the framework of the Nordic Nuclear Safety Research (NKS) we have collaborated with the Halden Reactor Project (HPR). The work has been mostly based on interviews of industrial experts, review of literature and available qualification documentation. Moreover, the SAUNA project has organised two workshops on safety demonstration and qualification of I&C systems. We have published the collected insights in (Valkonen et al. 2016a), (Valkonen et al. 2016b) and (Valkonen et al. 2017).

### **The need for better justification of I&C safety**

Nuclear power plants are large-scale and long-term investments with specific risk potential. Therefore, their reliability and safety are important for both the industry and the society. Use of nuclear power is controlled by national regulations and international standards. Responsible utilities are required to submit a justification of the safety of the plant and its systems – a “safety demonstration” – to the local regulatory body. The fundamental questions are, is the plant sufficiently safe and is it reasonable to rely on its safety demonstration. Because of the complexity of nuclear power plants and the emergent nature of safety, these questions are hard to answer. In particular, digital instrumentation and control (I&C) systems have turned out to be a challenge. Firstly, it is due to their interdisciplinary role as a link between several plant systems, human operators and engineering disciplines. Secondly, the complexity and failure mechanisms of software have introduced additional difficulties in safety analysis and demonstration.

When looking, for example, at the Finnish YVL guides, it becomes clear that some sort of justification is required for decisions having potential safety impacts. As an example, YVL guides require that the licensee prepare a Preliminary Safety Analysis Report (PSAR) in the construction license application phase of a newbuild project and a Final Safety Analysis Report (FSAR) in the operation license phase. Our experience is that SARs typically contain a limited amount of explicit safety justification. No detailed requirements are given in the YVL guides on how argumentation should be made (Tommila et al. 2014).

One starting point of the SAUNA project has been that the safety justification must be understandable, transparent and logically sound. Therefore, we adopt the term safety demonstration defined by the safety critical task force in (Common position 2014): “*The set of arguments and evidence elements which support a selected set of claims on the safety of the operation of a system important to safety used in a given plant environment.*” While this looks rather formal (Figure 11), Common position (2014) states that a safety

demonstration may or may not use a structured formalism. However, the reasoning should be clearly visible.

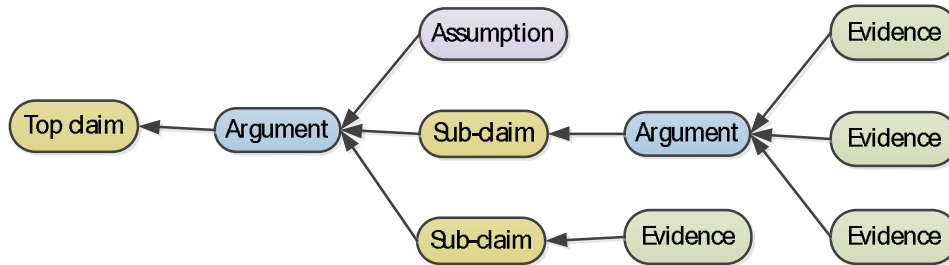


**Figure 11.** Claim, arguments and evidence structure [adapted from Common position 2014 and ISO/IEC 15026-2: 2015]. Claims are statements about a system’s safety properties. Arguments express why the claims are true (or false) based on the sub-claims, evidence items and explicit assumptions.

Developing an understandable, transparent, convincing and complete safety demonstration in a cost-effective way is a difficult task, especially in the context of complex systems and varying regulatory environment. From the viewpoint of safety authorities, submittals of licensing documentation for regulatory review and approval could have more explicit argumentation, better traceability and clearer structure. From the licensee viewpoint, it has been a problem to collect and understand a complete set of requirements and to demonstrate compliance to them.

Therefore, we come to the conclusion that the nuclear power industry would benefit from more structured, systematic and harmonised practices in engineering I&C systems and justifying their safety. Possible solutions can be found, e.g., from other safety-critical domains, Systems Engineering (SE) principles and standards.

### Challenges in the current practice

Some of the challenges in safety justification that we have identified in our interviews and literature review are caused by the inevitable difficulty of assuring safety of complex systems. Some others are related to practical issues, such as working practices and training. The challenges can be summarised as follows:

- Assuring safety of complex system in difficult in principle
  - Systems have dependencies and may behave in unexpected ways that are hard to analyse (I&C architecture & Defence in Depth (DiD))
  - Safety is emergent, many disciplines and aspects (e.g. product + process) must be integrated and many disciplines and organisations need to collaborate and coordinate their work
  - There are uncertainties, e.g. with completeness and relevance of the evidence
  - Good arguments are difficult to write, e.g. logical flaws and natural language limitations
- The amount of information is large
  - The cost of reviewing the material, e.g. by the regulator or a third party
  - Many participants in the supply chain, allocation of responsibilities
  - Changes and configuration management
  - Preservation of the accumulated safety knowledge over the whole system life
- Variations in standardization and regulatory practices.
  - Different requirements and expectations, regulatory uncertainty
  - Different licensing processes

- Need for interpretations in terminology and requirements
- Number and overlaps in possibly relevant standards

### Role of structured safety demonstration

Even if the idea of structured safety demonstration is rather old, there is some confusion concerning the terminology. Safety demonstration is easily mixed with terms like “safety case”, “assurance case” and “safety assessment”. We advocate here the relatively formal definition of safety demonstration in (Common position 2014) above. Its main purpose is to present a transparent argumentation for the claimed compliance to regulatory requirements. Consequently, safety demonstration is an artefact, e.g. set of documents, not an engineering process. Figure 12 illustrates the role of safety demonstration in the overall documentation. Herein the term safety case is an overall term referring to totality of the safety justification and all the supporting material. In addition to safety demonstration, it includes, for example, system descriptions, testing reports, hazard analysis and PRA results etc. (see ONR 2013). Safety Analysis Reports (SAR) can be written as summaries of the whole safety case. We use the word justification as a general term for any kind of safety argumentation.

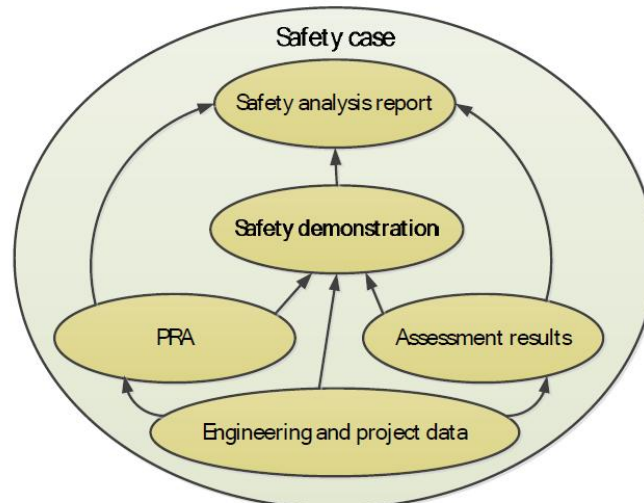


**Figure 12.** Position of safety demonstration in the overall safety justification material.

Safety demonstrations and complete safety cases are results of various engineering and licensing processes. In YVL terminology, licensing applies to the whole plant only. In the case of I&C, the term qualification (of systems and components) refers to a “process to demonstrate the ability to fulfil specified requirements”. As it is defined, qualification is about “demonstrating safety” and therefore (primarily) carried out by the license applicant and its contractors. Therefore, the process of developing a safety demonstration can be called qualification with its broadest meaning (Alanen & Tommila 2016). Safety demonstration planning (resulting in a safety demonstration plan or a qualification plan) is part of licensing planning or qualification planning.

Our findings so far support the initial assumption that systematic engineering and safety justification methods are increasingly important. Changing established practices is, however, not straightforward and may lead to increased costs and delays. Fortunately, many other safety-critical domains face similar challenges and there are existing solutions that might be applicable also in the nuclear industry. The simplest solutions are improvements in documentation practices and “everyday” working methods. On the other hand, the implementation of conceptual, organisation wide changes, e.g. in the design or documentation

philosophy, will require remarkable efforts and pilot projects to allow a smooth transition. It is evident that this would also require extensive utilization of computerised tools to support the new working processes. Some of the solutions are discussed below.

### **Possible solutions**

Systems Engineering principles: Safety is an emergent property that requires seamless and resilient co-operation of all system elements. Therefore, a systematic and multi-disciplinary approach is needed. By definition of International Council on Systems Engineering, (INCOSE), Systems Engineering (SE) is one answer to that need. SE principles and related standards and guidelines can provide an overall framework also for the design of nuclear I&C. Of course, they need to be adapted to the specific requirements of nuclear power, for example in the form of reference models for design (e.g. (EPRI 2014)), safety management and licensing (Alanen & Tommila 2016). While SE is mostly concerned with the principles, artefacts and activities of engineering design, it should be seen in the wider context of the life cycle processes as defined, e.g., in ISO/IEC 15288 (2015). Therefore, SE is closely related to and partly overlapping with project management. For comprehensive safety demonstration, both systems and components and their development processes and organisations need to be assessed (see above). So, we should have a consistent set of concepts, documents and models that link together technical I&C and safety engineering, project management and operation and maintenance processes.

Document and information management: Design documentation, safety analysis and V&V results, safety demonstrations, as well as the underlying regulations and standards, are a knowledge asset that must be communicated and maintained throughout the system life cycle. The solutions available today include, for example, good practices of technical writing and drawing, document and configuration management systems and design and plant databases. Irrespective of any formal structure for safety argumentation, these methods can be applied for preparing better safety demonstrations.

Harmonization and standardization: As stated in the NUGENIA roadmap, there is a need for further harmonisation and standardisation. Already now, there are many international and national groups sharing information and exploring opportunities for convergence of requirements and practices. For example, Common position (2014) gives guidance that licensees can follow in preparing a safety demonstration and Elforsk has provided a report on safety demonstration planning (Elforsk 2013). Due to different traditions and complexity of the issues, harmonisation takes time and effort. However, harmonization is necessary and must be continued, also concerning safety demonstration, by sharing best practices in the nuclear domain and in other critical areas. Besides harmonisation, standardisation bodies are moving towards electronic publication, online databases, modularisation and formalisation. With distributed intelligence, internet and semantic technologies, “smart” standards and regulations can lead to a new way of engineering safety-critical products and applications. For example, relevant requirements can be found and fetched easily and used for defining system requirements, assessment criteria and claims in a safety demonstration.

Assurance case approach: A safety justification should be easily understandable, transparent, traceable, complete and logically flawless. It should also have a clear, modular structure that enables its efficient maintenance and allocation of responsibilities in the project organisation and supply chain. Traditional documentation practices do not support these goals very well. More structure is needed to do that. Similar to a safety demonstration, an assurance case (ISO/IEC 15026-2: 2015) includes one or more top-level claims for properties of a system, argumentation regarding truth of the claims, and evidence and assumptions used as the basis of the argumentation. Multiple levels of sub-claims and argumentation connect the top-level claims to the evidence. Assurance cases usually concern properties such as safety, human factors, and security. They would be useful in nuclear power, for example in the assessment of engineering artefacts, organisations and working processes, suitability analysis of equipment and components, system and plant level safety assessments, and in assessment of safety demonstrations themselves. While being internally traceable, an assurance case/safety demonstration should be also linked to all relevant engineering artefacts used, for example, as evidence. This includes system specifications, project and V&V

plans, V&V results, etc. In other words, an assurance case can't be planned and implemented afterwards or separately from the normal engineering work. In computer-assisted engineering, this means that the model-based assurance case is integrated with system models and project models. Such a solution would provide several opportunities, for example related to application-specific terms, change management and design automation.

Model-based approaches: One attractive solution is to move from documents based design and safety justification towards Model-Based Systems Engineering (MBSE) which can be defined as the formalised application of modelling to support system requirements, design, analysis, verification and validation activities beginning in the conceptual design phase and continuing throughout development and later life cycle phases (Friedental et al. 2007). Models can be used to guide designers in their work, and to enable design automation and computer-assisted system analysis, such as formal verification (e.g. model checking, see above) and simulation-assisted I&C testing. Moreover, structured models help to link I&C specifications and PRA models.

### Conclusions and next steps

Especially in preparing a safety demonstration, model-based analysis tools provide means to generate high-quality evidence. In particular, the structured assurance case described above is also a “model”, which creates the opportunity to integrate the safety demonstration and models of I&C systems and their design processes. Automatic generation of assurance cases based on a formal Architecture Description Language (ADL) has been reported in (Hawkings et al. 2015). Despite being of limited size and outside nuclear (security of safety-critical software-based system), this example is an indication that similar approaches could be investigated also within nuclear industry.

### References

- Alanen, J. & Salminen K. 2016. Systems Engineering Management Plan template - V1. Espoo: VTT. VTT Research Report: VTT-R-00153-16. 78 p. + app. 12 p.
- Alanen, J. & Tommila, T. 2016. A reference model for the NPP I&C qualification process and safety demonstration data, VTT. VTT Research Report; VTT-R-00478-16. 43 p. + app. 21 p.
- Authén, S., Holmberg, J.-E., Tyrväinen, T., Zamani, L. 2015. Guidelines for reliability analysis of digital systems in PSA context – Final Report, NKS-330, Nordic nuclear safety research (NKS), Roskilde. 101 p.
- Authén, S., Bäckström, O., Holmberg, J.-E., Porthin, M., Tyrväinen, T. 2016. Modelling of Digital I&C, MODIG — Interim report 2015, NKS-361, Nordic nuclear safety research (NKS), Roskilde. 83 p.
- Buzhinsky, I. & Vyatkin, V. 2016. Plant model inference for closed-loop verification of control systems: Initial explorations. IEEE International Conference on Industrial Informatics (INDIN 2016). IEEE, pp. 736–739.
- Buzhinsky, I. 2016. Visual formalisms applied to temporal logic property patterns in the nuclear automation domain. Research report, Aalto University. 40 p.
- Buzhinsky, I., Pakonen, A. & Vyatkin, V. 2017. Methodology for building discrete plant models for closed-loop model checking: nuclear plant case. Submitted to IEEE Transactions on Industrial Informatics.

- Common position 2014. Licensing of safety critical software for nuclear reactors - Common position of seven European nuclear regulators and authorised technical support organisations.
- Clarke, E. M., Grumberg, O. & Peled, D. 1999. Model checking. MIT press.
- Dwyer, M. B., Avrunin, G. S. & Corbett, J. C. 1999. Patterns in property specifications for finite-state verification. In International Conference on Software Engineering (ICSE 1999), IEEE, pp. 411–420.
- Elforsk 2013. Safety Demonstration Plan Guide A general guide to Safety Demonstration with focus on digital I&C in Nuclear Power Plant modernization and newbuild projects. Elforsk rapport 13:86, 63 p.
- EPRI 2014. Principles and Approaches for Developing Overall Instrumentation and Control Architectures that Support Acceptance in Multiple International Regulatory Environments. Electric Power Research Institute, Inc. (EPRI), technical report 3002002953, 366 p.
- Friedental, S., Griego, R. & Simpson, M. 2007. INCOSE Model Based Systems Engineering (MBSE) Initiative. INCOSE2007, San Diego, June 24-29 2007. A presentation. 29 p.
- Hawkins, R., Habli, I., Kolovos, D., Paige, R. & Kelly, T. 2015. Weaving an Assurance Case from Design: A Model-Based Approach. IEEE 16th International Symposium on High Assurance Systems Engineering (HASE), pp. 110-117. DOI: 10.1109/HASE.2015.25
- Hirvonen, A. 2016. Implementing systems-theoretic process analysis (STPA) in safety-critical system design. Master's Thesis, University of Oulu / IntoWorks. 112 p.
- Holmberg, J.-E., Helminen, A. & Porthin, M. 2017. Using PSA to assess defence-in-depth — case study on level 2 of defence-in-depth, Report 14127\_R002, Risk Pilot Ab, Espoo. 33 p.
- Holzmann, G. J. 2002. The logic of bugs. 10th ACM SIGSOFT Symposium on Foundations of Software Engineering, ACM, pp. 81–87.
- IEC 2005. Nuclear power plants – Instrumentation and control systems important to safety – Classification of instrumentation and control functions, IEC 61226. Second edition, Geneva: International Electrotechnical Commission.
- ISO/IEC 15026-2:2015, Systems and software engineering – Systems and software assurance – Part 2: Assurance case.
- Jee, E., Shin, D., Cha, S., Lee, J.-S., & Bae, D.H. 2014. Automated test case generation for FBD programs implementing reactor protection system software. Software Testing, Verification and Reliability, 24(8), pp. 608–628.
- Lahtinen, J., Valkonen, J., Björkman, K., Frits, J., Niemelä, I. & Heljanko, K. 2012. Model checking of safety-critical software in the nuclear engineering domain. Reliability Engineering & System Safety, 105, pp. 104–113.
- Lahtinen, J. 2014. Hardware failure modelling methodology for model checking. Technical report, VTT Technical Research Centre of Finland. Research report: VTT-R-00213-14. 36p.
- Lahtinen, J. 2015. Supporting structure-based test design using model checking, VTT. VTT Research Report; VTT-R-04004-15, 19 p.

- Lahtinen, J. & Björkman, K. 2016a. Feasibility study on the integration of PRA methods and model checking. Technical report, VTT Technical Research Centre of Finland Ltd. Research report: VTT-R-04924-15, 26 p.
- Lahtinen, J. & Björkman, K. 2016b. Integrating model checking and PRA: a novel safety assessment approach for digital I&C systems, 26th European Safety and Reliability, ESREL 2016, 25 - 29 September 2016, Glasgow, UK Risk, Reliability and Safety: Innovating Theory and Practice, Walls, Lesley etc. eds.. CRC Press (2016), 486.
- Leveson, N., 2011. Engineering A Safer World. MIT Press. ISBN:9780262016629
- Nevalainen, R., Clarke, P., McGaffery, F., O'Connor, R. V. & Varkoi, T. 2016. Situational Factors in Safety Critical Software Development. Kreiner, C. et al. (Eds.): EuroSPI 2016, Graz, Austria, September 14–16, 2016, CCIS 633, Springer 2016, pp.132-147.
- Nevalainen, R. & Varkoi, T. 2015. FiSMA report 2015-1: Requirements for an extended process assessment model in systems and safety engineering. Research report, 48 p.
- Nevalainen, R. & Varkoi, T. 2016. FiSMA report 2016-1: Systems and safety engineering process assessment. Research report, 80 p.
- O'Halloran, B., Papakonstantinou, N. & L. Van Bossuyt, D. 2015. Modeling of Function Failure Propagation Across Uncoupled Systems, Reliability and Maintainability Symposium (RAMS) 2015, Palm Harbor, FL, January 26–29, 2015.
- O'Halloran, B., Papakonstantinou, N. & L. Van Bossuyt, D. 2016. Cable Routing Modeling in Early System Design to Prevent Cable Failure Propagation Events, Reliability and Maintainability Symposium (RAMS) 2016, Tucson, AZ, USA, January 25–28, 2016.
- OECD 2015. Failure modes taxonomy for reliability assessment of digital I&C systems for PRA, NEA/CSNI/R(2014)16, OECD Nuclear Energy Agency, Paris.
- ONR 2013. The purpose, scope, and content of safety cases. Office for Nuclear Regulation (ONR, an agency of HSE), guide NS-TAST-GD-051 rev. 3, 26 p. Available at: [http://www.onr.org.uk/operational/tech\\_asst\\_guides/ns-tast-gd-051.pdf](http://www.onr.org.uk/operational/tech_asst_guides/ns-tast-gd-051.pdf)
- Pakonen, A., Mätäsniemi, T., Lahtinen, J. & Karhela, T. 2013. A toolset for model checking of PLC software. 18th IEEE Conference on Emerging Technologies & Factory Automation (ETFA). IEEE, pp. 1–6.
- Pakonen, A., Pang, C., Buzhinsky, I. & Vyatkin, V. 2016. User-friendly formal specification languages — conclusions drawn from industrial experience on model checking. 21st IEEE Conference on Emerging Technologies & Factory Automation (ETFA). IEEE, pp. 1–8.
- Pang, C., Pakonen, A., Buzhinsky, I. & Vyatkin, V. 2016. A Study on User-Friendly Formal Specification Languages for Requirements Formalization. IEEE International Conference on Industrial Informatics (INDIN 2016), IEEE, pp. 676–68.
- Papakonstantinou, N., Porthin, M., O'Halloran, B. & L. Van Bossuyt, D. 2016. A model-driven approach for incorporating human reliability analysis in early emergency operating procedure development, Reliability and Maintainability Symposium (RAMS) 2016, Tucson, AZ, USA, January 25–28 2016.
- Papakonstantinou, N., Tommila, T., O'Halloran, B., Alanen, J. & L. Van Bossuyt, D. 2017. A Model Driven Approach For Early Assessment Of Defence in Depth Capabilities Of Complex Sociotechnical

- Systems, ASME 2017 International Design Engineering Technical Conferences & Computers and Information in Engineering Conference (IDETC/CIE 2017), Cleveland, Ohio, USA, August 6-9 2017. (Submitted, under review)
- Tommila, T., Savioja, P. & Valkonen, J. 2014. Role of requirements in safety demonstrations Version 2, 31.1.2014. SAFIR 2014 programme, Working report of the SAREMAN project, 49 p.
- Tommila, T. & Papakonstantinou, N. 2016. Challenges in defence in depth and I&C architectures, Research Report, VTT-R-00090-16, VTT 2016, 54 p. + app. 5 p.
- Uusitalo, E. & Koskela, M. 2015. Towards a functional nuclear I&C reference architecture based on the DIGREL plant model, IntoWorks research report, IW2015-001. 25 p.
- Valkonen, J., Tommila, T., Linnosmaa, J. & Varkoi, T. 2016a. Safety demonstration of nuclear I&C - an introduction. VTT Research Report: VTT-R-00167-16. 38 p.
- Valkonen, J., Tommila, T., Alanen, J., Linnosmaa, J. & Varkoi, T. 2016b. Views on safety demonstration and systems engineering for digital I&C. 39th Enlarged Halden Programme Group Meeting, EHPG 2016, 8 - 13 May 2016, Fornebu, Norway, 13 p.
- Valkonen, J., Tommila, T., Linnosmaa, J., Karpati, P. & Katta, V. 2017. Demonstrating and arguing safety of I&C systems — challenges and recent experiences. Submitted to the 10th International Topical Meeting on Nuclear Plant Instrumentation, Control, and Human-Machine Interface Technologies (NPIC & HMIT), June 11-15, 2017.
- Varkoi, T. & Nevalainen, R. 2015. Extending SPICE for Safety Focused Systems Engineering Process Assessment. R.V. O'Connor et al. (Eds.): EuroSPI 2015, Ankara, Turkey, September 30 – October 2, 2015, CCIS 543, Springer 2015, pp. 1–13.
- Varkoi, T., Nevalainen, R. & Mäkinen, T. 2016. Process Assessment in A Safety Domain - Assessment Method and Results as Evidence in An Assurance Case. In Proceedings of the 10th International Conference on the Quality of Information and Communications Technology - QUATIC 2016, Lisbon, Portugal, September 6-9, 2016, pp. 52-58.
- Yoo, J., Cha, S. & Jee, E. 2008. A verification framework for FBD based software in nuclear power plants. 15th Asia-Pacific Software Engineering Conference (APSEC). IEEE, pp. 385–392.

## **3. Severe accidents and risk analysis**

### **3.1 Comprehensive analysis of severe accidents (CASA)**

Anna Nieminen, Tuomo Sevón, Magnus Strandberg, Eveliina Takasuo, Veikko Taivassalo, Mikko Ilvonen,  
Jukka Rossi

VTT Technical Research Centre of Finland Ltd  
P.O. Box 1000, FI-02044 Espoo

#### **Abstract**

Overall understanding of the progress and mitigation of severe accidents was strengthened by simulating the Fukushima accidents for all three units with the integral code MELCOR. A good correspondence was achieved to the available measurement data. Cooling the core melt is the primary objective in all of its locations. Multi-dimensional flooding increases the dryout heat flux of a debris bed but the benefit is lost if the conical bed is more than 1.5 times higher than the cylindrical bed. However, the coolability of a conical bed could be estimated less conservatively by establishing a temperature-based coolability criterion. In the case of an ex-vessel melt pool, the correlations were found to overestimate heat transfer coefficients and that heat flux was proven to be more biased upwards than expected. The new water ingress model in MELCOR produced good results when gas is bubbling through the melt pool. All these findings increase the understanding of core melt management. The biggest threats for the containment integrity in addition to core melt are highly energetic events of steam and hydrogen explosions. The melt drop size, that depends on physical properties of the melt, was found to have the strongest effect on the steam explosion strength. Hydrogen explosions in the Nordic BWR containments were proven to be very unlikely. Well-founded dose estimates are needed for example when licensing the operation of instrumentation and automation systems. Dose rates calculated with the ASTEC and NRC methods were compared. In all cases the total dose rate estimates are within a factor of two that can be considered rather acceptable. If the containment integrity is lost, it is necessary to assess the transport of radioactive release to evaluate environmental consequences. It is important to include ingestion dose to offsite dose assessment because its contribution dominates the total dose. Calculations indicate that if the release magnitude corresponds to the national severe accident release limit (100 TBq of Cs-137), countermeasures are improbable beyond the distance of 20 km.

#### **Analysing Fukushima accidents**

The Fukushima accident provides a unique opportunity for gaining more information on the progress of severe accidents and their prevention and mitigation. Finland was accepted to participate phase 2 of the OECD NEA BSAF (Benchmark Study of the Accident at Fukushima) project. The objective in analysing the accidents are 1) improving expertise in severe accident modelling, using data from a real full-scale reactor

accident; 2) gaining a better understanding of the events in the Fukushima reactors; 3) getting insights into the capabilities and weaknesses of the integral codes in simulating severe accidents.

VTT has MELCOR models for all three units that have been updated when new plant data has been published (Sevón 2015a; Sevón 2016; Sevón, 2017b). Some additional plant data was obtained from the OECD BSAF project. New MELCOR best practice guidelines have been also taken into use.

The unit 2 model reproduces the measured pressures in the reactor and in the containment well during the first 81 h. This required manual adjustment of the RCIC system flow rates and flooding rate of the torus room, so that a good match to the measurements is obtained. MELCOR result for the reactor pressure from 75 to 83 h is compared to available measurement data in Figure 1. According to this calculation, the core was uncovered for 14 h. The actual time may have been longer because the calculation underestimates the reactor pressure between 83 and 89 h and therefore the water injection rate with the fire engine may be overestimated.

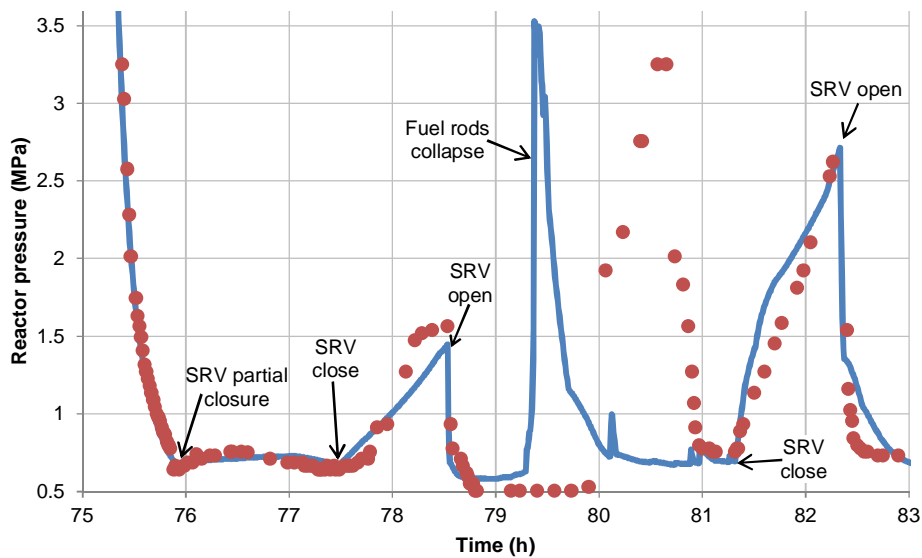


**Figure 1.** Fukushima unit 2 Reactor pressure from 75 to 83 h. Red dots indicate the measured values. Operation of SRV (Safety Relief Valve) was adjusted based on measurement data.

24% of the fuel mass was relocated to the bottom of the reactor at unit 2, but the RPV did not fail in this calculation. 547 kg of hydrogen was generated during the accident, and 29% of zirconium was oxidized. The maximum calculated hydrogen concentration in the reactor building is 5%, and hydrogen explosion did not take place at unit 2. The major radioactive release to the environment started at 89 h when the containment pressure started decreasing and a large leak from the drywell was assumed. Almost all radioactive noble gases were released to the environment during the accident. The calculated cesium release was 0.1% of the core inventory.

In Unit 3 the reactor was cooled by the RCIC and HPCI systems for the first 36 hours. In the model the RCIC and HPCI flow rates were manually adjusted so that the measured water level and pressure in the reactor are reproduced. The rise of the containment pressure accelerated after 6 h. This might be caused by stratification of the wetwell water, but it could not be reproduced by a simple stratification model. A small leak from the recirculation pump seal to the drywell was assumed, starting at 6 h 20 min, in order to reproduce the measured pressure increase.

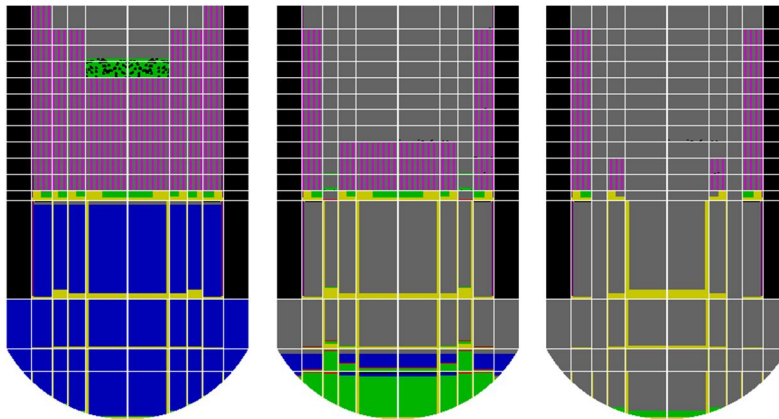


**Figure 2.** State of the reactor in Unit 3 at three instants of time: 41 h 52 min, 43 h 44 min, and 72 h. The pink color shows fuel rods, yellow is steel structures, green particulate debris, and blue is water.

RPV lower head penetration failure was calculated to occur at 43 h 44 min at unit 3. It is uncertain whether a failure of an instrument penetration is sufficiently large to cause a discharge of debris out of the reactor, but that is what happened in this calculation. The lower head was cool at this time, and removing the penetrations from the model would delay the RPV failure to a much later time. At the end of the calculation, 31% of the fuel was still in the reactor, while 69% of the fuel had been discharged to the containment. The state of Unit 3 reactor at three instants is illustrated in Figure 2.

The calculated hydrogen concentration in the unit 3 reactor building at the time of the explosion was 9.4%. Almost all of the radioactive noble gases and 3.2% of the caesium inventory were released to the environment during the accident. Almost all of the radioactive release was caused by the containment venting because the venting system was not equipped with filters.

Many of the uncertainties in the Fukushima analyses are still caused by the lack of plant data. Some uncertainties are caused by uncertain boundary conditions. For example the rate of water injection with fire engine was not accurately measured. Other uncertainties are inherent in any severe accident calculation because Fukushima was the first severe accident in a BWR and the physical models are based on small-scale experiments. Therefore it is necessary to continue updating the models.

### Debris bed coolability

The coolability of ex-vessel core debris has been studied at VTT with the COOLOCE test facility which is the only existing test facility in which the debris bed shape and its variations are taken into account. The final synthesis of the results of the experiments was made (Takasuo, 2015; Takasuo, 2016a). The dryout heat fluxes for the six geometry variations are collected in Figure 3. The experiments show that multi-dimensional flooding increases the dryout heat flux compared to top flooding by 47–73%. For heap-like geometries, which include a conical bed and a conical bed with a flattened top, the increase is 47–58%.

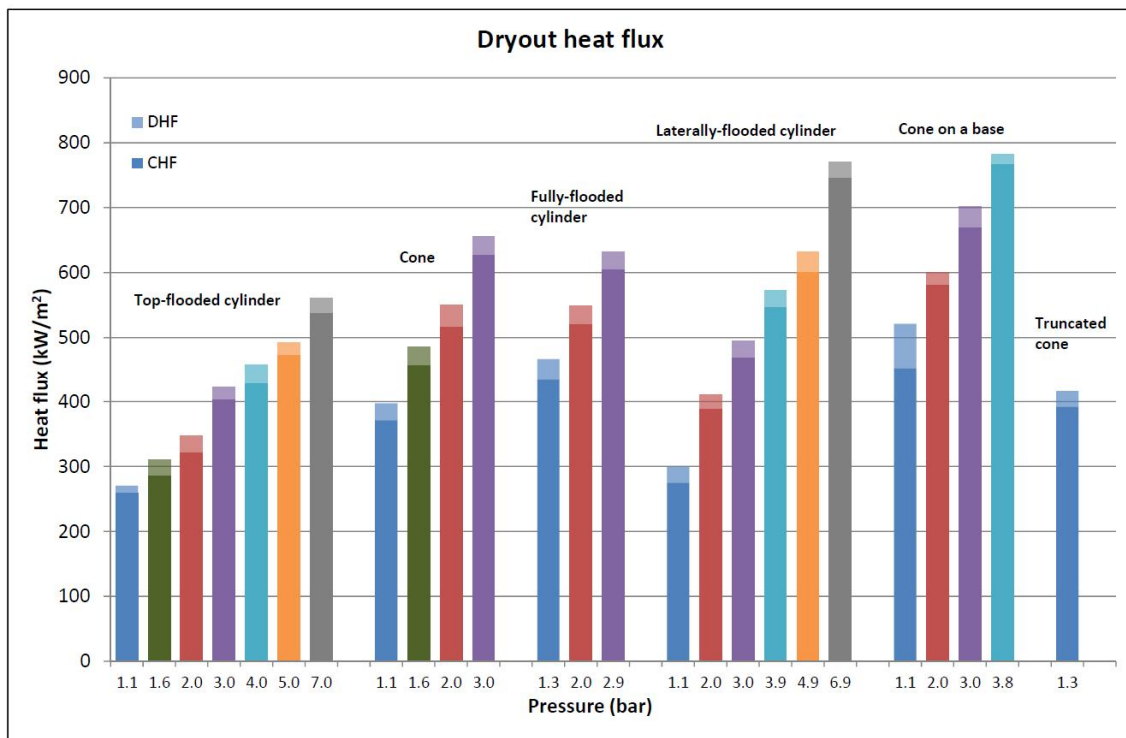


**Figure 3.** The dryout heat flux (DHF) in the COOLOCE experiments for the different geometries and pressures. The critical heat flux (CHF) is the maximum coolable power and the zone with a lighter colour at the bar top end is the error margin DHF-CHF.

The results also suggest that the benefit from the multi-dimensional flooding is lost if a heap-shaped bed is more than about 1.5-1.6 times higher than the top-flooded bed. This is because the heat flux in the bed increases linearly as a function of height, making dryout possible at the top of a heap-shaped bed. Thus, the heap-like geometry has a twofold effect on coolability: it increases the dryout heat flux by facilitating multi-dimensional infiltration of water into the bed, but it also decreases the dryout power by having a greater height.

In addition to synthesising the experimental results, a simulation case of a conical bed for a reference BWR reactor was presented (Takasuo, 2016b). It was found that, in general, the large-scale bed behaves similarly to the small-scale bed of the geometry variation experiments. With the simulation case, the post-dryout behaviour of the multi-dimensionally flooded bed was demonstrated. Even though dryout has been reached, the solid temperature in the dryout zone is clearly stabilized if the excess power is small.

The coolability limit based on the minimum dryout heat flux might be overly conservative, since the temperature may remain on an acceptable level even in the dry zone. Instead of the dryout heat flux, it has been proposed that the coolability limit should be based on the increase of the particle temperature. To analyse this, the behaviour of conical debris beds was studied by performing MEWA simulations (Tavassalo & Takasuo, 2017). Influences of the bed particle size, heating power and porosity were examined. Different heat transfer models available in MEWA and important in predicting the post-dryout temperature field were tested.

Due to the lack of experimental data that could be directly used for code validation, the MEWA results were compared to the DECOSIM results by Yakush & Kudinov (2014) in Figure 4. The simulation results of the MEWA code are not in fully agreement with the DECOSIM results. For small particle cases without temperature stabilization, the codes agree satisfactorily. On the other hand, these cases are not interesting

because the maximum particle temperature eventually exceeds the temperatures where zirconium oxidation or even corium remelting begins.

In the other conical bed cases the beds are coolable but MEWA and DECOSIM predict different transient behaviours and final steady-state conditions. Therefore, before trying to quantify the temperature-based dryout criterion, the origin of the significant differences between the MEWA and DECOSIM results needs to be identified. Some differences in the simulation setups and models are known or probable but most likely they do not cause those large differences in simulation results for post-dryout conditions.

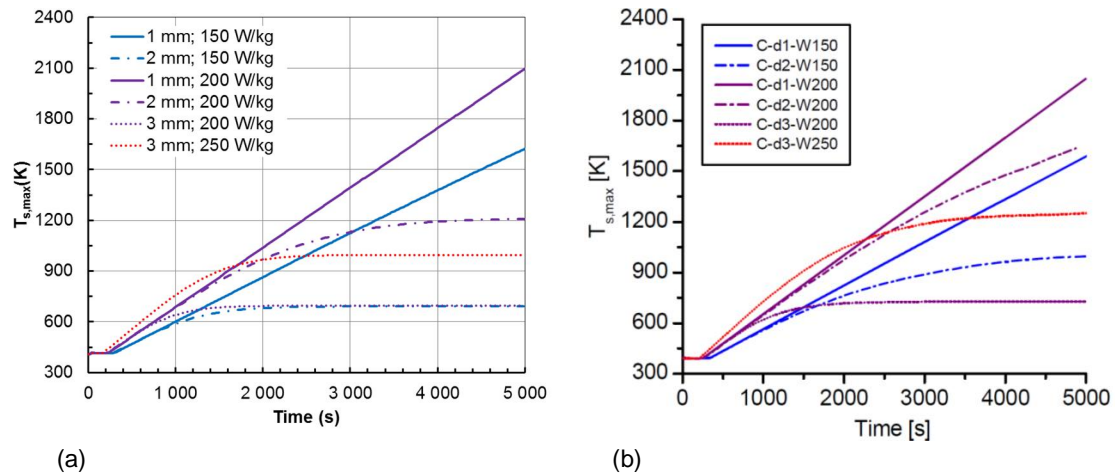


**Figure 4.** Maximum solid particle temperature as a function of time in the MEWA simulations (a) and in the DECOSIM simulations according to Yakush & Kudinov (2014) (b) for the same conical bed.

## Predicting heat transfer in ex-vessel melt pools

Methods for analysing operation of core catchers should be readily available. Distribution of heat between the different surfaces is an important factor in evaluating the core catcher performance. The melt stabilization phase of the Water-Cooled Basemat (WCB-1) experiment, which is the only public experiment of water-cooled basemat with real reactor materials, was analysed to improve expertise in assessing performance of various core catcher designs (Sevón, 2015b).

Heat transfer coefficients upwards and downwards from the melt to crusts were calculated from the measured heat fluxes. It was assumed that the melt–crust interface is at the solidus temperature. After transient effects had ceased, the heat transfer coefficient upwards stabilized to around 220 W/m<sup>2</sup>K, and the heat transfer coefficient downwards reached 40 W/m<sup>2</sup>K. Thus, the heat flux was heavily biased upwards.

Heat transfer coefficients in the experiment were compared with free convection correlations. At the period when conditions were relatively stable, Steinberner & Reineke correlations overestimate the average heat transfer coefficient upwards by a factor of 2 and downwards by a factor of 3. Consequently, the correlations underestimate the up/down power split by a factor of 1.5. Accident analyses based on these correlations would be conservative with respect to containment pressure and heat flux to cooling channels, but non-conservative with respect to melt temperature and solidification.

Mechanisms that also affect melt ex-vessel heat transfer are water ingress, i.e. penetration of water to cracks in the crust, and melt eruptions caused by gases released from hot concrete. These phenomena may enhance the coolability of the melt, and on the other hand increase the containment pressure. Water ingress and melt eruption models became recently available in MELCOR and they were tested and validated (Sevón, 2017a).

Seven SSWICS (Small-Scale Water Ingression and Crust Strength) experiments and two CCI (Core-Concrete Interaction) experiments were analysed with three variants of the MELCOR model: (1) old code version 1.8.6 default model that does not take water ingression into account; (2) new code version 2.1 default model that attempts to model water ingression by heat transfer multipliers for the boiling heat transfer coefficient and thermal conductivity and (3) with the new water ingression model.

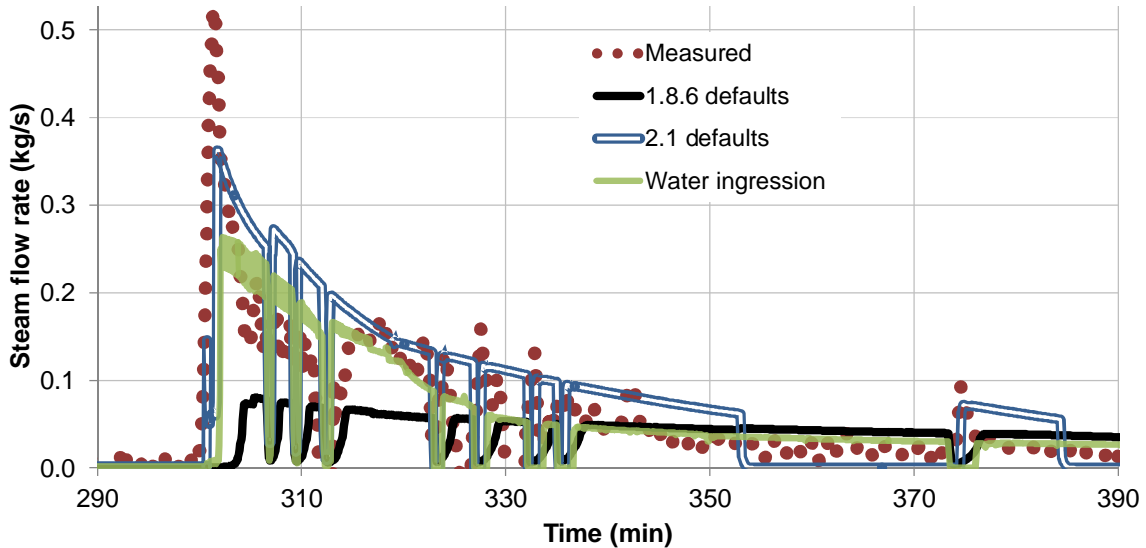


**Figure 5.** Steam flow rate in the CCI-2 test, measurement compared with three variants of the MELCOR model.

1.8.6 defaults underestimated melt pool coolability in seven of the calculated cases as expected. 2.1 defaults significantly overestimated the melt pool coolability in all analysed cases. The new water ingression model performed satisfactorily in CCI experiments in which gas bubbles were released to the melt from decomposing concrete as illustrated in Figure 5. The new model had little effect in the SSWICS experiments that were done without gas bubbling through the melt. When applied to the Fukushima Daiichi Unit 1 accident, the water ingression model slowed down concrete ablation by 19% but did not quench the melt.

## Ex-vessel steam explosion analyses with MC3D

Preserving of knowledge of steam explosions is important still today, since the risk of steam explosions during a severe nuclear accident cannot be excluded in our current nuclear power plants. The steam explosion loads in a Nordic BWR containment were assessed with the MC3D code studying the sensitivity of the results for some key input parameters (Strandberg, 2016). The effect of some key input parameters on the steam explosion loads was examined. The main focus of the analysis was on the dynamic loads on the cavity wall imposed by the explosion.

Simulations were firstly made to analyse the effect of different triggering times on a standard case with central break location. In Figure 6 is illustrated the premixing conditions at a time just before the triggering at the time of the highest explosivity. The results showed that as long as the mixture is triggerable, the resulting explosions are fairly similar. Different side breaks scenarios were also tested but here the mixture did not trigger. This result, which is considered unphysical, still gives indication on how complex problem steam explosions are and how large role the mesh geometry has in the simulations.

The sensitivity analysis was done for melt temperature, coolant subcooling, cavity water level and melt drop size. Simple MELCOR calculations were made to find realistic boundary condition limits for the parameters. Based on the sensitivity analysis, the drop size has the largest and most predictable impact on both explosion strength and probability. When assuming larger drops, explosion becomes more probable and also stronger.

Another interesting result was that when analysing the melt temperature sensitivity, there was no clear correlation between higher melt temperatures and stronger explosions. This was explained by the fact that the melt in all cases was overheated and that the time span is so short that no solidification takes place. However, it should be noted that the melt temperature does still have a significant impact on the outcome as melt temperatures below the liquidus temperature did not result in steam explosions.

Based on the water level analysis it seems clear that a larger water volume is able to generate a stronger explosion, as there is a larger region with drops in coolant compared to the lower water level cases. The coolant temperature analysis did not offer clear results but it seems likely that a higher subcooling level could cause stronger explosions.

A case that is likely to cause the most triggerable premixture which at the same time yields the strongest explosion would include: (1) a melt temperature well above the melt liquidus temperature, (2) a well filled cavity (12 or more meters of water), (3) a subcooling of the coolant to at least 50K, (4) melt fragmentation into large drops. Drop size is dependent on melt physical properties. Basically melt having lower density produces larger drops, which would mean metallic melt that has lower liquidus temperature than oxidic melt. Therefore a combination of melt producing large drops and having high temperature is unlikely, since overheating of the melt is limited. As a result, cases threatening the containment integrity the most are unlikely.

## Hydrogen fire risk in the containment

Accidents that may lead to bypassing the filtered containment venting should be practically eliminated in Nordic BWRs that are inerted with nitrogen to avoid hydrogen explosions. However, if the inertion is lost, hydrogen explosions may be possible in the containment. This is most probable during the shutdown or start-up. In the reactor hall hydrogen explosion could occur after the loss of containment integrity. This still has an effect on the timing of the radioactive release and on the quantity also by resuspension of deposited fission products. Hydrogen explosions may also occur in the reactor hall even if the containment is intact if containment pressure evolves to a high level increasing the leak.

The risk of a flammable mixture of hydrogen and air to be formed in the reactor building was studied analysing a SBO scenario for the Nordic BWR plant with MELCOR (Strandberg, 2017). Without assuming an increase in the containment design leak, the results showed such low concentrations that a hydrogen fire is considered very unlikely. The total mass of hydrogen also remained low, so that if the local

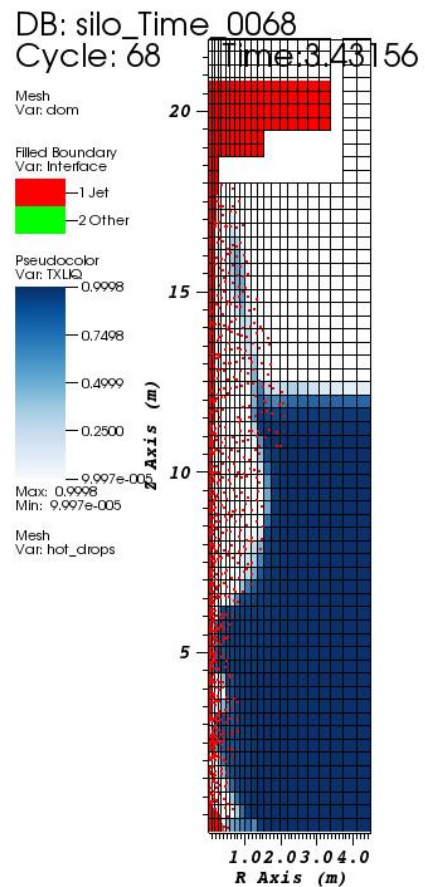


Figure 6. Premixing conditions at a time just before the triggering.

concentrations could be high enough to be theoretically able to cause a hydrogen fire, the assorted energy release would not be very high and this event could not be considered as an explosion.

Also a SBO accident with a non-inerted containment was analysed and this resulted in hydrogen deflagrations in the containment. However, this did not proceed into detonation i.e. into an explosion. Despite the hydrogen deflagrations caused an increase in the temperature, the pressure remained even on a lower level than in the previous accident analysis, where there was no hydrogen deflagration in the containment. This could be because the burning of hydrogen consumes gas which decreases the pressure.

## Defining in-containment dose rates

Estimating the dose rates inside the containment during a hypothetical severe accident is important since the radiation dose might affect the operation of instrumentation and automation systems and leak-tightness of containment penetration seal materials. To be able to assess the operation of these systems and structures in all circumstances, reliable evaluations on fission product behaviour in the containment are needed. Dose rate affects also the formation of nitric acid ( $\text{HNO}_3$ ) in the containment that reduces the pool pH decreasing iodine retention in pools.

Previously the capability of the integral code ASTEC to produce the dose rates in the containment was tested (Nieminen, 2016) and then the ASTEC dose rates were compared to the dose rates produced by NRC method (Nieminen & Rossi, 2017). The selected test case was a large LOCA in a Nordic BWR. The source term to the containment was defined based on NUREG-1465 report. Fission product distribution for NRC method dose calculations was obtained from ASTEC.

The basic assumption was that the dose rates produced by NRC method are higher than the ASTEC dose rates because the deposited fission products were included in the gas phase inventory and because ASTEC assumes that 50% of the radiation from the deposited fission products is absorbed by the wall. The difference was higher than expected for all but drywell beta dose rate.

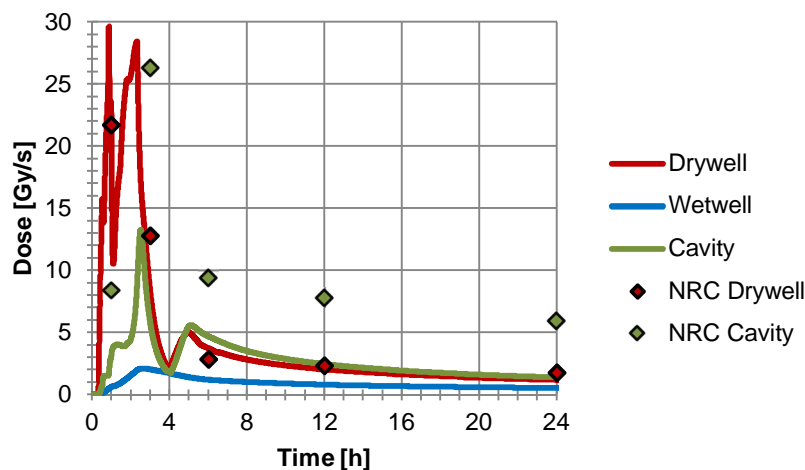


**Figure 7.** Comparison of dose rates in the gas phase calculated with ASTEC and NRC method.

As seen from Figure 7, NRC beta dose rate in the cavity is nearly approximately twice the ASTEC dose rate in cavity atmosphere but in drywell they are more or less equal. In ASTEC the beta dose rate is inversely proportional to the volume of the zone. It is assumed that ASTEC does not take into account the decreasing gas phase volume due to cavity flooding when defining the dose rate. With NRC method the dose peaks are difficult to observe, due to few datapoints. However, in all cases the total dose rate esti-

mates were within a factor of two that can be considered rather acceptable difference taking into account different approach in the methods.

ASTEC input was also changed by increasing the wet painted wall area in the containment. It was expected that this would increase the mass of organic iodide, but it increased more notably the mass of gaseous iodine and iodine oxides. This is assumed to result from organic iodides radiolytically destructing into gaseous iodine that then reacts with air radiolysis products to form iodine oxides. The effect of increased wet painted wall area on iodine behaviour is illustrated in Figure 8.

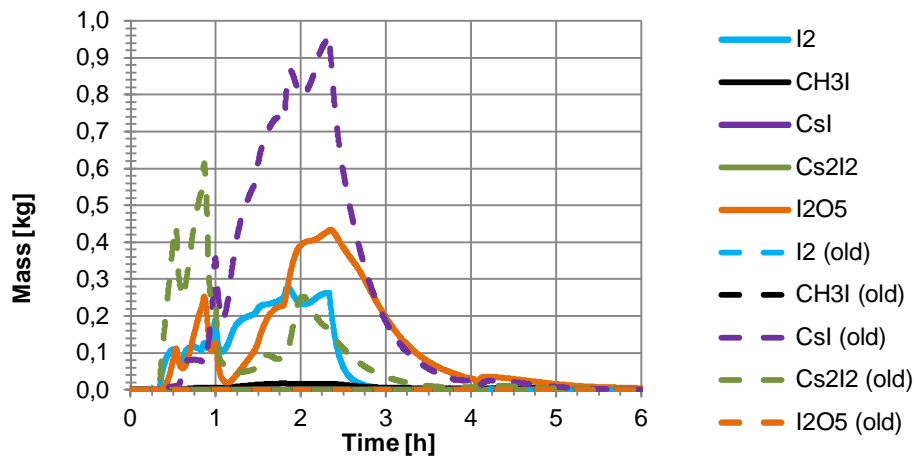


**Figure 8.** Iodine compounds in the drywell. Dashed lines indicate previous analysis results, where the area of wet painted wall was defined notably smaller.

The change in iodine behaviour resulted slightly higher dose peaks in the containment gas phase but notably smaller dose rates on walls. In total 98.71% of fission products were retained in the containment, which is 1.5% more than in previous analysis. This is mostly because the amount of dissolved fission products is higher.

## Environmental consequences

The Fukushima Daiichi accident caused remarkable radiation dose levels in the environment of the power plant, even at longer distances. As a consequence of this event IAEA started to develop recommendations which consider emergency planning outside the protection and emergency planning zones. Therefore studies of the expected doses beyond 20 km are needed. The proposed two new zones are planned to be extended to the distances from 20 km up to 100 km and from 100 km up to 300 km from a power plant.

Probability distributions of radiation doses from different exposure pathways at distances up to 300 km from the power plant were determined (Rossi & Ilvonen, 2016) using three different release magnitudes: (1) 1% of noble gas inventory, 1000 TBq for  $I^{131}$  and 100 TBq for  $Cs^{137}$ ; (2) 20% of noble gas inventory and 2% of iodine and caesium inventory and (3) 100% of noble gas inventory and 20% of iodine and caesium inventory. The first source term corresponds to the maximum release of activity in the case of a severe accident according to the YVL-guide.

The weather data used in the calculations consists of FMI's winding trajectory data of Oulkuoto for one year. Figure 9 illustrates the areas affected by the plume on the map indicating how the prevailing wind fields affect the plume dispersion. The calculated dose estimates were compared with the threshold values for countermeasure actions given in the recommendations of IAEA. In short, countermeasures are needed when the dose level exceeds 100 mSv in a week or in a year (exposure duration) at the distances of 20 to 100 km or if it exceeds 10 mSv in a year (consumption duration) from ingestion at the distances of 100 to 300 km.

In the case of the smallest source term the dose levels at the distance of 20 km remain clearly below the limit value of 100 mSv. In the second release case the expected distance for exceeding the dose criterion for countermeasures is less than 50 km but if the maximum doses (plume centerline) are considered, the distance might be nearly 100 km. In the third release case the expected distance for exceeding the dose criterion for countermeasures is about 200 km but if the maximum doses are considered, the distance might be even beyond 300 km. Early health effects are not expected so the aim of the countermeasures is to reduce the risk of statistical health effects.

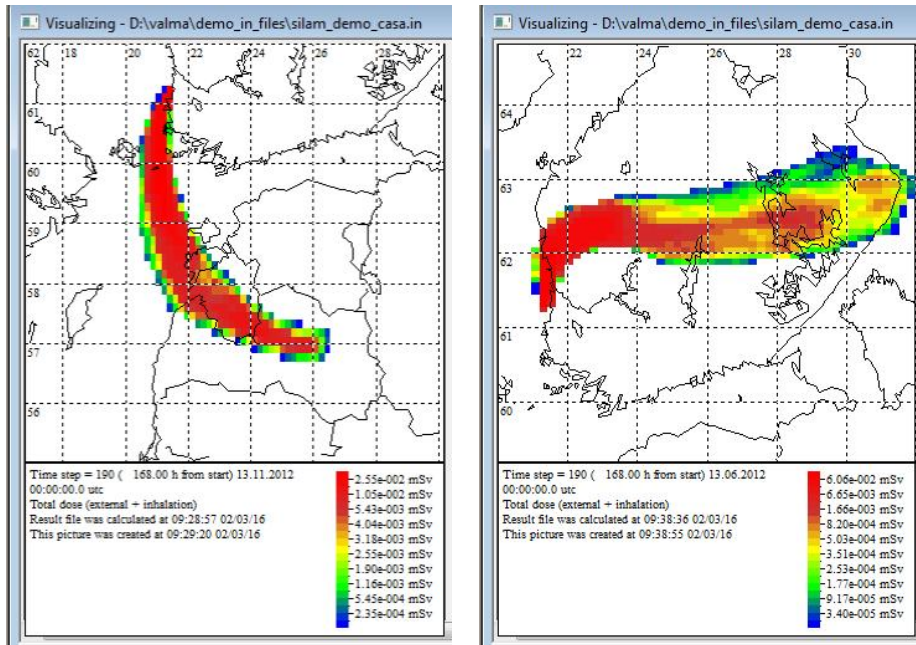


**Figure 9.** Examples of the VALMA GUI outputs. Total dose in one week is presented with two different release starting times.

VALMA was also further developed (Ilvonen & Rossi, 2017) by implementing there the ingestion dose pathways (green vegetables, grain, root vegetables, cow milk and cow meat) based on coefficients acquired from the AGRID nutrition dose model. Ingestion dose is important when the release includes notably iodine and caesium. If deposition occurs during a growing season, potential doses from contaminated foodstuffs may be significant. The difference between summertime and wintertime doses can be orders of magnitude, as in the summer the deposition may arrive directly on the edible plant parts, used for humans or cattle. In Figure 10 is compared the mean non-zero values of the total non-ingestion dose and the ingestion dose at the distance of 100 km.

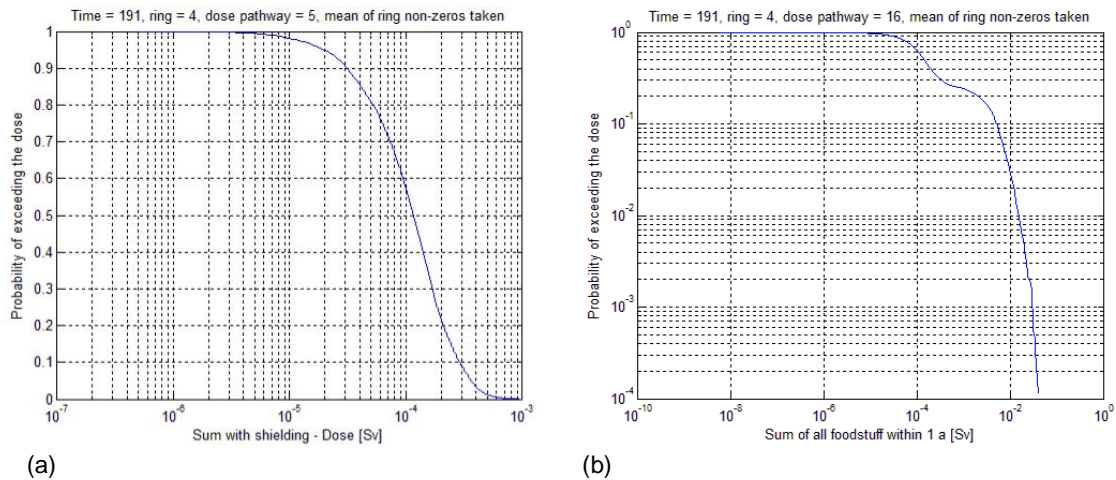


**Figure 10.** Mean non-zero value of the total dose at distance of 100 km from the severe accident release limit (a) non-ingestion and (b) ingestion. Exposure / ingestion of one year.

The total ingestion dose is approximately 20 times higher than the dose from non-ingestion pathways, when the integration / consumption time period is one year for both. Ingestion dose remains under 10 mSv with the probability level of 95% which indicates that countermeasures on food consumption would not be necessary at the distance of 100 km in the case of the release magnitude corresponding to the severe accident limit value. Also it was found that the total dose is little below 100 mSv at the distance of 20 km which results in the similar conclusion that the prevailing release limit is reasonable.

If the release magnitude exceeds significantly the criterion of the severe accident, ingestion dose may increase over the level of 10 mSv at 100 km. Besides the dose level of 100 mSv from non-ingestion pathways might be exceeded beyond 20 km and countermeasures should be recommended in both cases.

## References

- Ilvonen, M. & Rossi, J. 2017. VALMA extension with ingestion doses assessment. Espoo: VTT. VTT Research Report VTT-R-00695-17. 42 p. + app. 42 p.
- Nieminen, A. 2016. Defining dose rates in Nordic BWR containment with ASTEC. Espoo: VTT. VTT Research Report VTT-R-00673-16. 25 p.
- Nieminen, A. & Rossi, J. 2017. Comparing in-containment dose rates calculated with ASTEC and NRC method. Espoo: VTT. VTT Research Report VTT-R-00760-17. 31 p. + app. 8 p.
- Rossi, J. & Ilvonen, M. 2016. Dose estimates at long distances from severe accidents. Espoo: VTT. VTT Research Report VTT-R-00589-16. 41 p.
- Sevón, T. 2015a. A MELCOR model of Fukushima Daiichi Unit 1 accident. *Annals of Nuclear Energy*, Volume. 85, p. 1–11.
- Sevón, T. 2015b. An Analysis of Core Catcher Experiment WCB-1. Espoo: VTT. VTT Research Report VTT-R-02476-15. 24 p.

- Sevón, T. 2016. Fukushima Unit 2 Accident Modeling with MELCOR, Version 2. Espoo: VTT. VTT Research Report VTT-R-00829-16. 49 p.
- Sevon, T. 2017a. Modeling of Water Ingression Mechanism for Corium Cooling with MELCOR. Nuclear Technology. Volume 197, Number 2. 9 p.
- Sevón, T. 2017b. Fukushima Unit 3 Accident Modeling with MELCOR, Version 2. Espoo: VTT. VTT Research Report VTT-R-00461-17. 50 p.
- Strandberg, M. 2016. Ex-Vessel Steam Explosion Analysis with MC3D. Master's Thesis. 68 p. + app. 15 p.
- Strandberg, M. 2017. Hydrogen fire risk in BWR simulations with MELCOR. Espoo: VTT. VTT Research Report VTT-R-00669-17. 21 p.
- Taivassalo, V. & Takasuo, E. 2017. Predicting debris bed behaviour in post-dryout conditions. Espoo: VTT. VTT Research Report VTT-R-00762-17. 28 p.
- Takasuo, E. 2015. Coolability of porous core debris beds: Effects of bed geometry and multi-dimensional flooding. VTT Science 108. Teknologian tutkimuskeskus VTT Oy. Juvenes Print, Tampere 2015. ISBN 978-951-38-8344-7. 112 p. + app. 72 p.
- Takasuo, E. 2016a. An experimental study of the coolability of debris beds with geometry variations, Annals of Nuclear Energy, Volume 92, p. 251-261.
- Takasuo, E. 2016b. A summary of studies on debris bed coolability and multidimensional flooding. . Espoo: VTT. VTT Research Report VTT-R-00432-16. 27 p.
- Yakush, S. & Kudinov, P., 2014. A model for prediction of maximum post-dryout temperature in decay-heated debris bed. In 22nd International Conference on Nuclear Engineering. July 7-11, 2014, Prague, Czech Republic.

## 3.2 Chemistry and transport of fission products (CATFIS)

Teemu Kärkelä, Mélyany Gouëlle, Jouni Hokkinen, Karri Penttilä, Tommi Kekki, Petri Kotiluoto

VTT Technical Research Centre of Finland Ltd  
P.O. Box 1000, FI-02044 Espoo

### Abstract

The aim in the CATFIS project during 2015-2016 was to investigate the transport and chemistry of gaseous and particulate fission products in severe accident conditions. The main focus was on the behaviour of iodine and ruthenium which are highly radiotoxic and the mitigation of their possible source term is of utmost importance. It was observed that the fission product deposits on the reactor coolant system surfaces act as an important source of gaseous iodine, which can enhance the iodine source term. In air ingress conditions, the oxidizing air radiolysis products had a significant impact on the formation of gaseous ruthenium, which was observed to exist even at the low temperatures of containment building. Similarly, airborne CsI reacted with ruthenium oxides and increased the gaseous ruthenium fraction. The follow-up of OECD/NEA STEM-2 and BIP-3 projects was carried out.

### Introduction

In Fukushima Daiichi nuclear plant cooling of the reactor cores at units 1, 2 and 3 was lost due station black out. Since the cooling could not be restored in time, fuel damage took place in all three reactors and fission products were partly released from the core. As expected in a such severe accident, the highest contribution to the source term to the environment was from iodine isotopes. In case of the Chernobyl accident, a high release of fission products to the environment took place and fission products (FPs) were spread e.g. across the continent of Europe. In this accident, a fall-out of radioactive FPs containing also ruthenium was detected as far away as in Finland [Pöllänen, 1997].

Traditionally, it has been assumed that in a severe accident most iodine would be released from the fuel. Release to the containment would take place mostly as aerosol particles with gaseous fraction of about 5%. Concerning studies on iodine chemistry in the primary circuit, it is typically assumed that caesium iodide is the main iodine compound formed in the reactor coolant system. This assumption leads to a low release of gaseous iodine into the containment, because the current severe accident (SA) integral codes do not take into consideration the effect of FP deposits chemical reactions on the primary circuit surfaces. Also, the previous studies have mainly focused on the reactions taking place in the gas phase [Gouëlle, 2013; Grégoire, 2012]. However, the importance of surface reactions as a source of volatile iodine is even increased at the late phase of accident when the thermalhydraulic conditions of the circuit are changing.

Along with iodine, low-volatile ruthenium is released from the fuel in oxidizing conditions. The most important volatile forms of ruthenium are  $\text{RuO}_3$  and  $\text{RuO}_4$ . Currently, the fraction of ruthenium which can be transported to the containment atmosphere in gaseous form is not well-known. VTT's previous studies [Kärkelä, 2014] indicated that the gaseous fraction can be significantly higher than what is expected based on thermodynamic equilibrium calculations. In general, the experimental work on international level has focused on pure air or air-steam atmospheres. The effect of oxidizing air radiolysis products and airborne aerosols on the chemistry of ruthenium and on the formation of gaseous Ru compounds has not been studied in detail. Nevertheless, most ruthenium in a severe accident would be expected to transport mainly as  $\text{RuO}_2$  aerosol e.g. as a consequence of a reactive condensation of  $\text{RuO}_3$  at ca. 1000 K.

The follow-up of OECD/NEA STEM-2 (Source Term Evaluation and Mitigation Issues) and OECD/NEA BIP-3 (Behaviour of Iodine) projects, which both began in January 2016, is being conducted. The four-year

STEM-2 project is focused on the transport of ruthenium in the primary circuit conditions and on the reactions of particulate iodine on the painted and metal containment surfaces. The three-year BIP-3 project is focused on the behaviour of gaseous inorganic and organic iodine on the painted containment surfaces, especially the adsorption and desorption phenomena.

### Primary circuit chemistry of iodine

After fission products have been released from the overheated and molten fuel, they are transported through the reactor coolant system and FPs will reach areas at lower temperature. As a consequence, vapour condensation and particle nucleation processes takes place in the gas flow. If vapour condensation takes place close to the surfaces of primary circuit, a layer of condensate can be formed on it. Particles in the gas flow may also deposit on the circuit surfaces together with control rod and structural materials. The study on the release of gaseous iodine from precursor mixtures simulating deposits in primary circuit conditions have been performed with EXSI-PC facility [Kärkelä, 2009; Kalilainen, 2011] and the results of years 2015-2016 have been summarized in [Gouëlle, 2016a; Gouëlle, 2016b]. The set-up of the experimental EXSI-PC facility used for experiments is presented in Figure 1. Inactive materials have been used to simulate fission products. The precursor materials were CsI, B<sub>2</sub>O<sub>3</sub> and CsOH and they were placed into an alumina crucible. The choice of the crucible material, non-representative of primary circuit surface, was selected because the purpose of the following experiments is to study reaction between the precursor materials at the surface of the crucible and not with the surfaces of the crucible. Since it was previously shown that the CsI precursor reacts with iron oxide layer on the stainless steel crucible surface [Kalilainen, 2011], it was preferred to work with an alumina crucible.

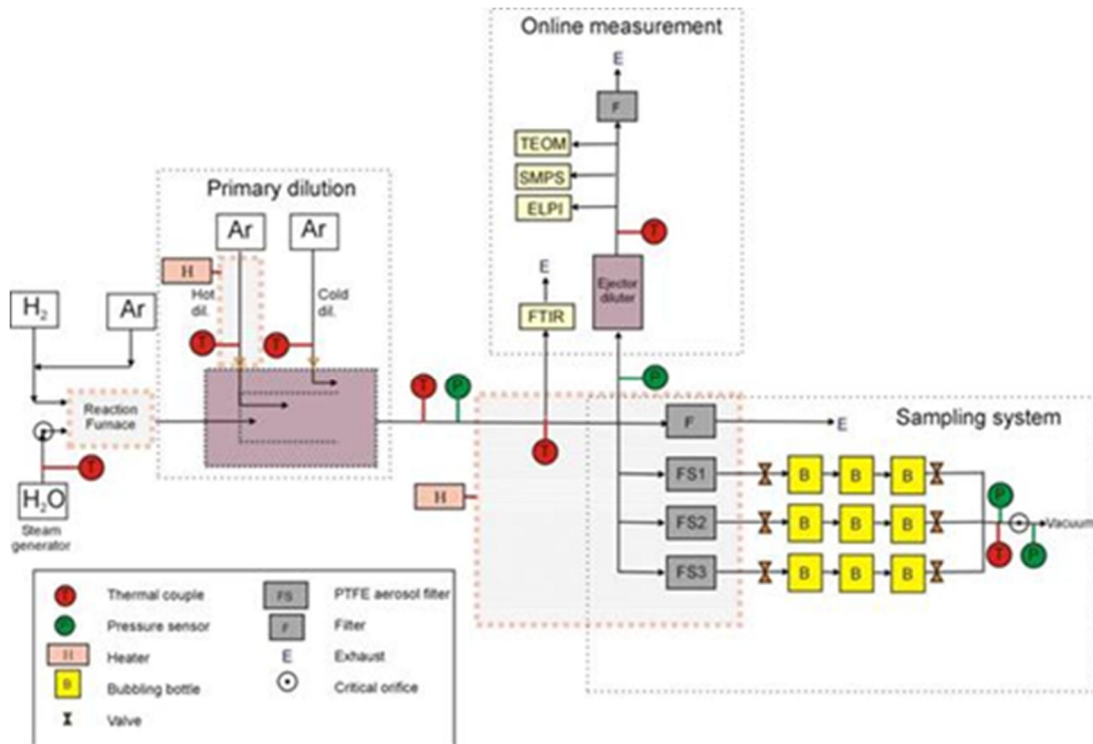


**Figure 1.** Schematics of the experimental EXSI-PC facility.

The evaporation crucible containing the precursor material(s) is placed in a tube inside the reaction furnace. The furnace tube used in the experiments was made of stainless steel (AISI 304), which was pre-

oxidized before the experiment. The furnace is heated to 400 °C or 650 °C. The carrier gas is then fed into the heated furnace, where the source materials react with each other, with gas and with the surface of the crucible. Reaction products are then transported with the gas flow into the primary diluter where the sample mixture is diluted and cooled down to 120 °C. The sampling furnace contains three sampling lines, each is equipped with a polytetrafluoroethylene (PTFE) membrane filter (hydrophobic, poral grade 5.0 µm, 47 mm, Mitex®) and two glass scrubbers assembled in series (0.1 M NaOH and 0.02 M Na<sub>2</sub>S<sub>2</sub>O<sub>3</sub> water solution). Additional toluene trap was used in some experiments. The elemental composition of both samples was analysed with Inductively Coupled Plasma Mass Spectrometer (ICP-MS). A list of the recently conducted experiments is presented in Table 1. Experiments included three or four different gaseous atmosphere conditions, with different fractions of steam, argon, hydrogen and air, shown in Table 2.

**Table 1.** Experiments conducted on primary circuit chemistry of iodine during the past 2 years.

Precursors	Temperature [°C]	Crucible material	Atmosphere*
CsI	650	Al <sub>2</sub> O <sub>3</sub>	A, B, C and D
CsI	400	Al <sub>2</sub> O <sub>3</sub>	A, B, C and D
CsI + B <sub>2</sub> O <sub>3</sub>	650	Al <sub>2</sub> O <sub>3</sub>	A, B, C and D
CsI + B <sub>2</sub> O <sub>3</sub>	400	Al <sub>2</sub> O <sub>3</sub>	A, B, C and D
CsI + CsOH	650	Al <sub>2</sub> O <sub>3</sub>	A and C
CsI + CsOH + B <sub>2</sub> O <sub>3</sub>	650	Al <sub>2</sub> O <sub>3</sub>	A, B and D
CsI + CsOH + B <sub>2</sub> O <sub>3</sub>	400	Al <sub>2</sub> O <sub>3</sub>	A, C and D

\* The composition of atmosphere is explained in Table 2.

**Table 2.** Volume percentage of gases fed to the reaction furnace.

		Atmosphere composition			
		A	B	C	D
Gas vol-%	Argon	86.7	83.9	76.1	86.7
	Steam	13.3	13.5	13.4	0
	Hydrogen	0	2.6	10.5	0
	Air	0	0	0	13.3

The work performed during the past years has been particularly focused on determining how significant effect the presence of boron at the primary circuit surfaces can have on the physical and chemical form and on the transport of iodine and caesium, under different gas composition.

The addition of boron to caesium iodide resulted in lower caesium and iodine release fractions and a higher gaseous iodine fraction. The devices used in the EXSI-PC facility and the choice of analytical techniques allowed to quantify the amount and proportion of gas/aerosols formed. Furthermore, it was observed that the higher the steam concentration in the carrier gas, the higher was the gaseous iodine release. As a consequence of the caesium borate glass formation, the transport of caesium from the crucible through the facility was drastically decreased (Figure 2).

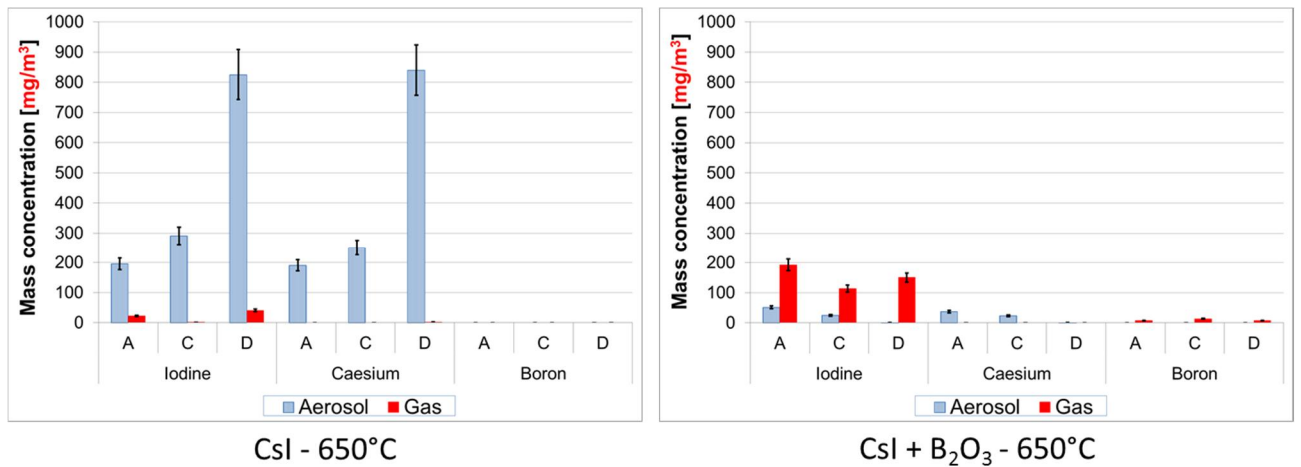


**Figure 2.** Iodine, caesium and boron mass concentrations, transported in gaseous and particulate forms, in the experiments at 650 °C [Gouëlle 2016c]

The results of the Csl/B<sub>2</sub>O<sub>3</sub>/CsOH experiments at 650 °C revealed that the composition of the carrier gas had no influence on the formation of boron and caesium compounds. Different caesium borate glasses were formed from Csl/B<sub>2</sub>O<sub>3</sub>/CsOH mixture and Csl/B<sub>2</sub>O<sub>3</sub> mixture. In addition, the mass of released iodine was lower than for the Csl/B<sub>2</sub>O<sub>3</sub> experiments (Figure 3).

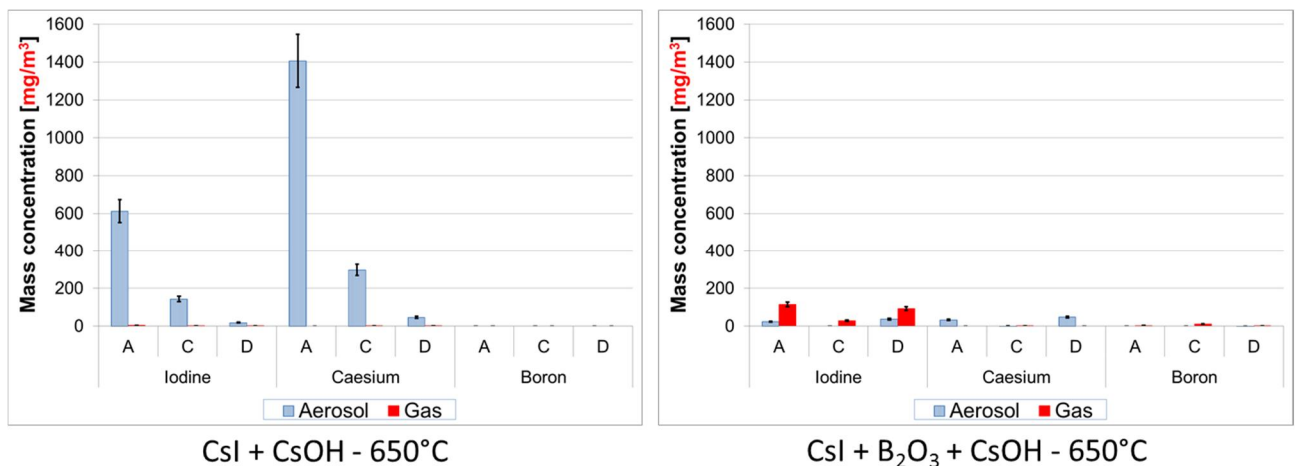


**Figure 3.** Iodine, caesium and boron mass concentrations, transported in gaseous and particulate forms, in the experiments at 650 °C [Gouëlle 2016c]

### Primary circuit chemistry of ruthenium

Most of the international experiments on the transport of ruthenium through a reactor coolant system have been conducted in a flow of pure air and/or steam with Ru oxides [Kärkelä, 2014]. The focus in the CAT-FIS project was to find out the effect of other components, such as aerosols and air radiolysis products, on the transport of gaseous and particulate ruthenium species through a model RCS in air ingress conditions. Thus this study gave a possibility to study the speciation of ruthenium in more realistic conditions. The study was performed in collaboration with Chalmers University of Technology (Sweden) within SAFIR2014/SAFIR2018 and Nordic Research on Nuclear Safety NKS-R (ATR activity) programs. This collaboration received also travel assistance from NUGENIA for researcher mobility between the organisa-

tions. The results of this collaboration are summarized in scientific publications [Kajan, 2017] and [Kärkelä, 2017].

The work was conducted with “VTT’s Ru transport facility” simulating a primary circuit, see Figure 4. The configuration of the facility for the experiments can be seen in Figure 1. The main component of the facility was the horizontal, tubular flow furnace (Entech, ETF20/18-II-L), which was used to heat the anhydrous RuO<sub>2</sub> powder (99.95%, Alfa Aesar). The furnace was 110 cm long and it had two heating sections, each 40 cm long. These zones were separated by a 38 mm layer of insulation. At both ends of the furnace, there was 131 mm of thermal insulation. The furnace tube was made of high purity alumina (Al<sub>2</sub>O<sub>3</sub>, 99.7%) and its inner diameter was 22 mm. The alumina crucible (length 20 cm) with the RuO<sub>2</sub> powder (mass. 1 or 2 g depending on the temperature used in the experiment) was placed in the beginning of the second heated zone of the furnace. As a new feature in these experiments, inside the furnace tube was inserted a second alumina tube (Al<sub>2</sub>O<sub>3</sub>, 99.7%, outer diameter 6 mm with a wall thickness of 1 mm), which outlet was located directly after the crucible. The RuO<sub>2</sub> powder was heated to 1300 K, 1500 K or 1700 K in an oxidizing flow in order to produce gaseous ruthenium oxides.

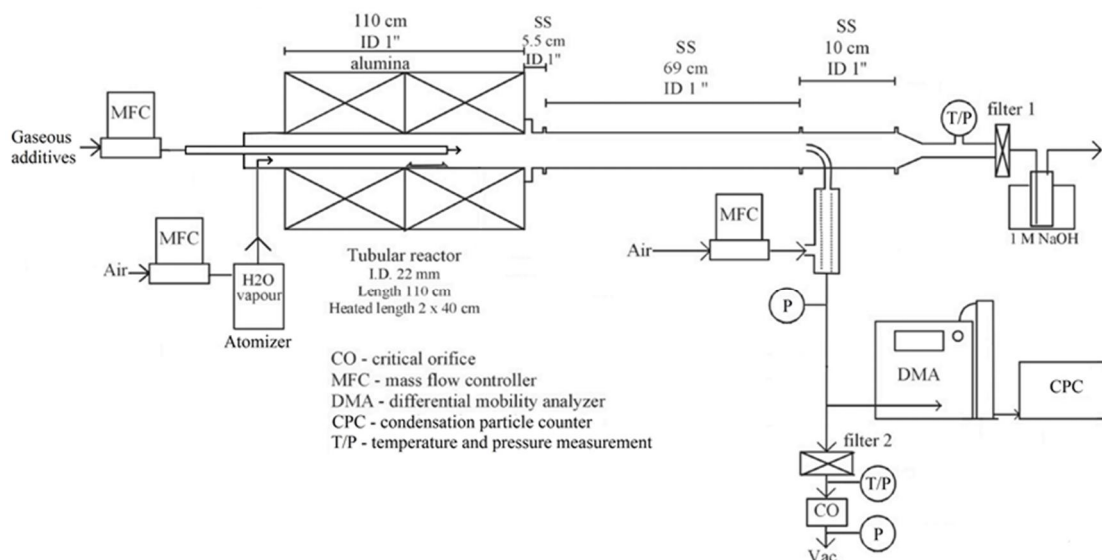


**Figure 4.** Schematics of the experimental facility for ruthenium transport studies.

The total flow rate through the facility was 5.0 l/min (NTP; NTP conditions 0 °C, 101325 Pa, measured with Thermal Mass Flowmeter TSI 3063, TSI Incorp.). Half of the total flow was directed through the inner furnace tube and the rest of the flow was passing through the furnace tube. The pressure inside the facility ranged from 102 to 104 kPa. The air flow (2.5 l/min, NTP) directed to the furnace tube was fed through an atomizer (TSI 3076). The air flow transported the water droplets (Milli-Q, ultrapure water, resistivity of 18.2 MΩ·cm at 25 °C) produced by atomizer via the heated line (120 °C) into the inlet of the furnace. Water evaporated when the droplets were heated and thus it led to an increase in the steam concentration within the furnace. A flow of N<sub>2</sub>O, NO<sub>2</sub> or HNO<sub>3</sub> gases (2.5 l/min, NTP) was fed through the inner furnace tube. NO<sub>2</sub> was diluted with N<sub>2</sub> to obtain a similar concentration of precursor as in case of N<sub>2</sub>O. As HNO<sub>3</sub> was fed with an additional atomizer (located then before the inlet of inner furnace tube, not presented in Figure 4), a carrier gas of nitrogen was used to transport HNO<sub>3</sub> droplets (solution of HNO<sub>3</sub> and Milli-Q water) via the heated line (120 °C) into the inlet of the inner furnace tube. CsI additive was also fed with an atomizer, but the inner furnace tube was removed in those experiments.

After the vaporization of Ru and the following reactions within the gaseous atmosphere, the gaseous and particulate reaction products were trapped in a NaOH solution and collected on planer filters, respectively (see Figure 5). The diameter, number concentration and the number size distribution of particles was analysed online with a combination of DMA and CPC. The experimental matrix is presented in Table 3.

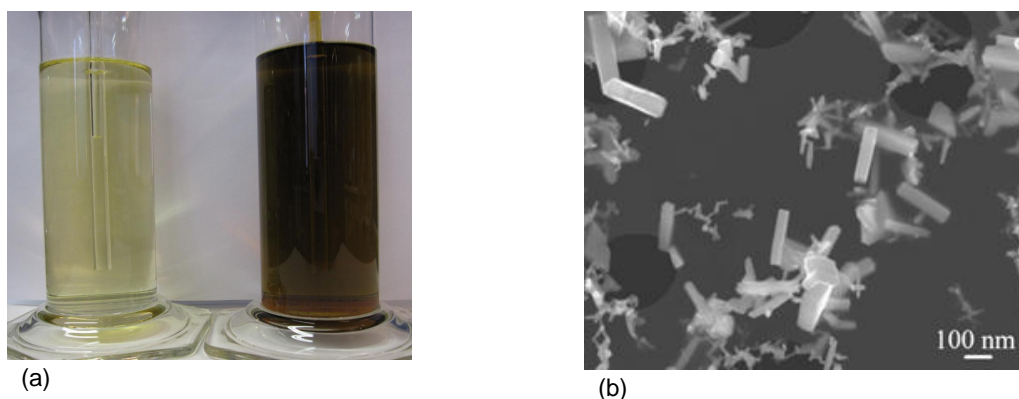


**Figure 5.** (a) Gaseous ruthenium trapped in two sequential bubblers with NaOH solution. (b) A SEM micrograph of the typical, crystalline, needle-shaped form of RuO<sub>2</sub> particles.

**Table 3.** Matrix of Ru transport experiments (air atmosphere; 1300 to 1700 K).

Exp	T [K]	Precursor	Gas phase	Additive precursor conc.	Humidity
1	1300	RuO <sub>2</sub>	Air	-	dry
2	1500	RuO <sub>2</sub>	Air	-	dry
3	1700	RuO <sub>2</sub>	Air	-	dry
4	1300	RuO <sub>2</sub>	Air	-	humid
5	1500	RuO <sub>2</sub>	Air	-	humid
6	1700	RuO <sub>2</sub>	Air	-	humid
7	1300	RuO <sub>2</sub>	Air+NO <sub>2</sub>	50 ppmV NO <sub>2</sub>	humid
8	1500	RuO <sub>2</sub>	Air+NO <sub>2</sub>	50 ppmV NO <sub>2</sub>	humid
9	1700	RuO <sub>2</sub>	Air+NO <sub>2</sub>	50 ppmV NO <sub>2</sub>	humid
10	1300	RuO <sub>2</sub>	Air+N <sub>2</sub> O	50 ppmV N <sub>2</sub> O	humid
11	1500	RuO <sub>2</sub>	Air+N <sub>2</sub> O	50 ppmV N <sub>2</sub> O	humid
12	1700	RuO <sub>2</sub>	Air+N <sub>2</sub> O	50 ppmV N <sub>2</sub> O	humid
13	1300	RuO <sub>2</sub>	Air+HNO <sub>3</sub>	5 ppmV HNO <sub>3</sub>	humid
14	1500	RuO <sub>2</sub>	Air+HNO <sub>3</sub>	5 ppmV HNO <sub>3</sub>	humid
15	1700	RuO <sub>2</sub>	Air+HNO <sub>3</sub>	5 ppmV HNO <sub>3</sub>	humid
16	1300	RuO <sub>2</sub>	Air+Csl	4 wt.% of Csl solution	humid
17	1500	RuO <sub>2</sub>	Air+Csl	4 wt.% of Csl solution	humid
18	1700	RuO <sub>2</sub>	Air+Csl	4 wt.% of Csl solution	humid

Experiments were conducted at 1300 to 1700 K with air as the carrier gas which was mixed with steam, air radiolysis products ( $\text{NO}_2$ ,  $\text{N}_2\text{O}$ ,  $\text{HNO}_3$ ) or CsI particles. The quantification of ruthenium transport showed significant impact of the experimental conditions on both the absolute amount as well as on the partitioning of the transported ruthenium between gaseous and aerosol compounds (see Figure 6). In general, the increase in temperature resulted in higher release of ruthenium from the precursor and also to higher transport of ruthenium downstream the furnace. The gaseous fraction of transported ruthenium was significantly increased under all temperatures due to  $\text{NO}_2$ . At temperatures of 1300 and 1700 K the overall transport of ruthenium was significantly increased when compared to the humid air atmosphere. The diameter of particles seemed to increase in the course of experiments, whereas the particle number concentration was low. It is suggested, that part of the formed gaseous Ru compounds was condensing on the surface of the existing particles and thus increased the particle diameter. Introduction of  $\text{N}_2\text{O}$  into the gas phase led to a decrease of gaseous ruthenium transport through the facility as well as to an increased fraction of ruthenium transported in form of aerosols. Nearly 100% increase in the total amount of transported ruthenium was detected at temperature of 1500 K when compared to the humid air atmosphere. An interesting observation was also done in the experiments with  $\text{HNO}_3$  in the humid air flow. The transport of gaseous ruthenium increased at all studied temperatures. However, the overall transport of ruthenium was fairly similar than in humid air atmosphere. Thus, the partitioning of ruthenium to gaseous and aerosol compounds was influenced by the fed  $\text{HNO}_3$ . Likely, the concentration of  $\text{HNO}_3$  was too low in order to observe a higher increase in ruthenium transport. The feed of CsI into the flow of ruthenium oxides had a significant effect on the thermodynamic equilibrium of Ru species. The transport of gaseous ruthenium increased from 0.2% up to 16% and 6% at 1500 K and 1700 K, respectively, whereas the aerosol transport of ruthenium decreased significantly. This is the highest amount of Ru ever observed in gaseous form in the experiments with this facility. At 1300 K the transport of ruthenium was rather similar to that in an air atmosphere, as it has been reported previously. At all studied conditions (Table 3), most of the released ruthenium was deposited inside the facility.

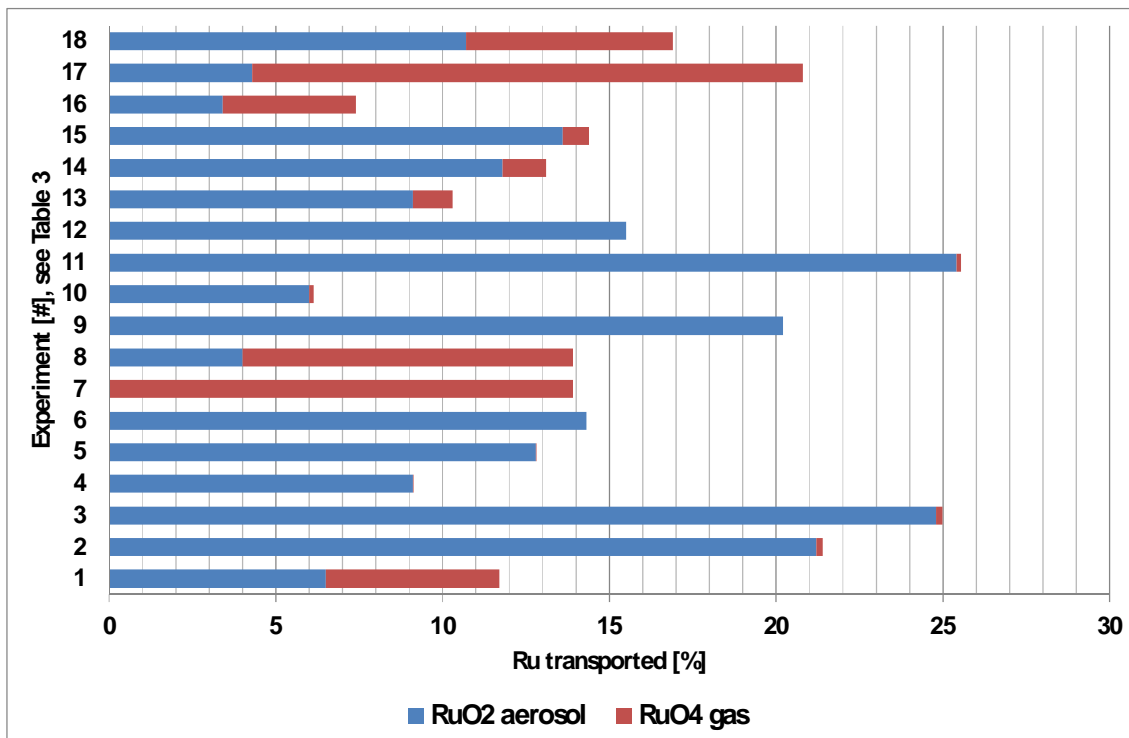


**Figure 6.** Ruthenium transport as aerosol and gaseous compounds through the experimental facility. Note the numbering of experiments on y-axis (see Table 3).

## The follow-up of OECD/NEA STEM-2 and BIP-3 projects

The follow-up of both OECD/NEA STEM-2 and BIP-3 projects [OECD, 2017] is performed as part of CAT-FIS. Both projects started in 2016 and the duration of STEM-2 is four years and BIP-3 three years. The experimental work is ongoing currently. The OECD/NEA STEM-2 project composes of two experimental main topics (iodine and ruthenium chemistry) and an analytical working group:

- 1) Iodine topics
  - a. **Paint ageing by irradiation:** For paints, natural ageing in normal operating conditions as well as their change during a nuclear accident (under irradiation, high temperature and humidity) might modify the paint capacity to trap iodine. There are some experimental evidences on this phenomenon. In STEM-2 project the aim is to experimentally verify if high doses ( $> 100 - 1000$  kGy) lead to significant chemical modifications in the paint, and to assess to what extent the iodine release kinetics ( $I_2$  and  $CH_3I$ ) can be modified by the dose received by the paint before and all along the accident.
  - b. **Iodine oxides radiolytic decomposition:** It has been shown that iodine oxides particles ( $IO_x$  of  $I_xO_y$ ) partly decompose under irradiation. Due to the lack of knowledge on the precise composition of  $I_xO_y$  species, a more analytical study, based on surface characterizations analysis, is also needed in order to better estimate the size and composition of such aerosols under different conditions and above all their potential chemical evolution as a function of time. Thus a set of irradiation tests will be performed by measuring on-line the release kinetics of gaseous  $I_2$  and  $CH_3I$  from the particles with the objective to study the influence of the dose, temperature and specifically higher humidity rates in order to reach and/or exceed the deliquescence point.
  - c. **Radiolytic oxidation of multi-component iodine aerosols:** According to PHEBUS-FP tests, multi-component iodine aerosols are formed and/or transported in the Reactor Coolant System (RCS) to the containment building during the accident. Their radiolytic stability has never been checked and they might contribute to iodine volatility before settling or once deposited onto surfaces, thus leading in this case to a potential direct impact on ST estimations. It is thus an objective of this project to study the release of gaseous iodine from multi-component iodine aerosols in accident conditions.
  - d. **Iodine oxides decomposition by carbon monoxide and/or hydrogen:** Various authors have reported the  $I_2O_5$  decomposition by carbon monoxide and other gaseous organic compounds (like  $H_2$ ,  $CH_4$ ,...) as being complete at ambient temperature. This reaction might play a significant role on iodine volatility as carbon monoxide (and hydrogen) can be present in significant amount in the containment building. However, the precise speciation of  $I_xO_y$  into the containment building remains unclear, as well as the extent of the interaction of these non- $I_2O_5$  species with CO and/or  $H_2$ . Thus, it has to be evaluated in this project, if this kind of reaction in the conditions of a severe accident can lead to a significant volatile iodine release or not.
- 2) Ruthenium topics
  - a. Based on the Ru transport experiments of STEM-1 project, a first attempt was made to integrate possible Ru source term in PSA-2 tools and it was concluded that ruthenium radiological consequences could be significant. That is why in the frame of STEM-2 it is proposed some complementary tests, mainly based on the revaporisation processes, and focused on: 1) A more representativity of the deposition surface, i.e. stainless steel (instead of glass), 2) The use of stronger oxidizing conditions, like those induced by air radiolysis products (i.e.  $O_3$ ,  $NO_x$ ,...) in order to increase the oxygen potential and thus be closer to the radiolytic conditions occurring in the RCS, and 3) The use of representative gaseous and/or aerosol "pollutants" (i.e. seed particles, silver aerosols, aerosol deposits,...) that could significantly impact the  $RuO_4(g)$  behaviour.

3) Analytical working group (AWG)

- a. An analytical working group will be set up to promote the use of these experimental results (iodine and ruthenium experiments) in some ST computations, in order to quantify the impacts as well as to discuss about a comprehensive analysis of the results obtained and extrapolation to the reactor case.

The OECD/NEA BIP-3 project composes of two main tasks; experiments on iodine chemistry and an analytical working group:

1) Experiments on iodine chemistry

- a. **Effect of paint ageing** (leaching experiments, adsorption,  $\text{CH}_3\text{I}$  production): Thermal, chemical and radiation-induced changes to paint (occurring in-service or during reactor accidents) can impact on iodine-paint interactions. In the BIP-3 project, the aim is to improve the understanding of paint aging effects on sorption behaviour and  $\text{CH}_3\text{I}$  production. Naturally-aged painted coupons and freshly coupons treated by artificial ageing techniques, such as pre-irradiation and thermal curing will be used. First, it will be determined if the amount and nature of the released organic carbon from paint depend on the ageing technique used. To that extent, if any differences are noticed, experiments will be done to assess if the adsorption/desorption rates of iodine and  $\text{CH}_3\text{I}$  production are dependent on the ageing technique used.
- b. **Adsorption/Desorption capacity as a function of total  $[\text{I}_2]$  loading:** Iodine desorption has been previously observed, in BIP and STEM tests, without irradiation and particularly at higher loadings. Question on this topic focuses on the existence of a finite number of active sites on paint and as sites become occupied; if a higher fraction of physisorbed iodine occurs. Experiments will be conducted in order to determine the relationship between loading high concentration of  $\text{I}_2$  and the fraction of iodine desorbed.
- c. **Effect of reactive containment species (sorption and  $\text{CH}_3\text{I}$  behaviour with  $\text{Cl}_2/\text{NO}_2$ ):** Some reactive gases generated during an accident may affect the iodine-paint interaction by competing with molecular iodine for adsorption sites, like  $\text{Cl}_2$  (from cable pyrolysis) and  $\text{NO}_x$  (from air radiolysis). The goal here is to evaluate the sorption and  $\text{CH}_3\text{I}$  production behaviour after exposure to competing species. The concentration of competing species will be much higher than  $\text{I}_2$  concentration (up to  $1000 \times [\text{I}_2]$ ).
- d. **Effect of Wet-dry cycling:** Higher radiolytic  $\text{CH}_3\text{I}$  production has been observed from aqueous-loaded coupons. When coupons dried after aqueous loading,  $\text{CH}_3\text{I}$  production resembles that of gas-loaded. From these observations, it was suggested either that the water facilitates the radiolytic  $\text{CH}_3\text{I}$  formation or the drying leads to iodine desorption and decreases the amount available for  $\text{CH}_3\text{I}$  formation. In these tests, the task is to evaluate the effect of water and wet/dry cycling on  $\text{CH}_3\text{I}$  production. This will improve the mechanistic understanding of  $\text{CH}_3\text{I}$  formation from paints.
- e. **Gas-phase  $\text{CH}_3\text{I}$  formation from irradiation of  $\text{CH}_4$  and  $\text{I}_2$ :** According to literature,  $\text{CH}_3\text{I}$  can be formed in the gas phase during the irradiation of  $\text{I}_2(\text{g})$  and  $\text{CH}_4(\text{g})$ . The scope of this work is to measure the  $\text{CH}_3\text{I}$  production for  $\text{I}_2$  and  $\text{CH}_4$  gas mixtures and to experimentally confirm whether the irradiation of different gas mixtures concentrations can produce  $\text{CH}_3\text{I}$ .

2) Analytical working group (AWG)

- a. An analytical working group will be set-up to promote the use of these experimental results in some ST computations, in order to quantify the impacts as well as to discuss about a comprehensive analysis of the results obtained and extrapolation to the reactor case.

## Conclusions

The main focus in the CATFIS project is study the transport and chemistry of fission products in a severe accident. The emphasis is on the phenomena, which are poorly-known internationally or not considered in the current severe accident analysis codes due to the lack of information. In 2015-2016, the effect of FP deposits chemical reactions on the primary circuit surfaces to the release of gaseous iodine from the deposits was investigated. It seemed that boron reacted with caesium iodide forming caesium-borate glass. As a result, iodine was released from the surface deposit as gas. On the other hand, additional CsOH seemed to partially bind the formed gaseous iodine. CATFIS is also currently the only project, in which the formation of air radiolysis products and their effect on the transport of FPs has been investigated. A significant increase in the fraction of gaseous  $\text{RuO}_4$  was detected due to air radiolysis product  $\text{NO}_2$ . Additionally, CsI compound seemed to react with gaseous Ru oxides and thus a remarkable transport of gaseous ruthenium compound was observed.

The recently started OECD/NEA STEM-2 and BIP-3 projects will produce new data on the chemistry of iodine and ruthenium in severe accident conditions. Part of that experimental work will complement and verify the observations made in the CATFIS project and in the previous CHEMPC and TRAFI projects of the SAFIR2010 and SAFIR2014 programs.

The experimental results produced in the CATFIS project (2015-2018) will increase the knowledge on the behaviour of fission products during a severe accident. The experimental data can be used for PSA level 2 analysis of the existing nuclear power plants.

## Acknowledgement

The financial support of VTT Technical Research Centre of Finland Ltd, The Finnish Research Programme on Nuclear Power Plant Safety (SAFIR2018), Nordic Nuclear Safety Research Programme (NKS-R) and NUClear GENeration II & III Association (NUGENIA) is acknowledged.

## References

- Gouëlle, M., Hokkinen, J. 2016a. Experimental Study on the Behaviour of CsI on Primary Circuit Surfaces: Effects of Boron and Air Ingress on Iodine Transport during a Severe Nuclear Accident, VTT report VTT-R-00046-16 (2016).
- Gouëlle, M., Hokkinen, J. 2016b. Experimental Study on the Behaviour of CsI on Primary Circuit Surfaces of a Nuclear Power Plant: Effects of Boron and Air Ingress on Iodine Transport at 400°C, VTT report VTT-R-03242-16 (2016).
- Gouëlle, M., Hokkinen, J., Kärkelä, T., Auvinen, A. 2016c. Experimental Study of the Boron and Air Effects on Iodine Transport in the Primary Circuit during Severe Nuclear Accident, International Congress on Advances in Nuclear Power Plants, San Francisco, USA, April 17-20, 2016.
- Grégoire, A.-C., Mutelle, H., Experimental study of the [Mo, Cs, I, O, H] and [B, Cs, I, O, H] systems in the primary circuit of a PWR in conditions representative of a severe accident, In the proceedings of NENE2012 conference, Ljubljana, Slovenia (2012).
- Kalilainen, J., Kärkelä, T., Rantanen, P., Forsman, J., Auvinen, A. & Tapper, U. 2011. Chapter "Primary circuit chemistry of iodine", SAFIR2010, The Finnish Research Programme on Nuclear Power Plant Safety 2007-2010, Final report, pp. 312-320.

Kajan, I., Kärkelä, T., Auvinen, A., Ekberg, C. 2017. Effect of nitrogen compounds on transport of ruthenium through the RCS, J Radioanal Nucl Chem, Published online 11<sup>th</sup> of January, 2017, DOI 10.1007/s10967-017-5172-7.

Kärkelä, T., Auvinen, A. 2009. Experimental Study on Iodine Chemistry (EXSI) - Facility for Primary Circuit experiments. Espoo, Finland, Research report VTT-R-02791-09.

Kärkelä, T., Vér, N., Haste, T., Davidovich, N., Pyykönen, J. & Cantrel, L. 2014. Transport of ruthenium in primary circuit conditions during a severe NPP accident. Ann. Nucl. En. 74, 173-183.

Kärkelä, T., Kajan, I., Tapper, U., Auvinen, A., Ekberg, C. 2017. Ruthenium transport in a RCS with airborne CsI, Submitted to Progress in Nuclear Energy.

OECD: <https://www.oecd-nea.org/jointproj/> , 2017.

Pöllänen, R., Valkama I. & Toivonen, H. 1997. Transport of radioactive particles from the Chernobyl accident. Atmospheric Environment 31(21), 3575-3590.

### 3.3 Experimental and numerical methods for external event assessment improving safety (ERNEST)

Ari Vepsä<sup>1</sup>, Kim Calonius<sup>1</sup>, Alexis Fedoroff<sup>1</sup>, Ludovic Fülöp<sup>1</sup>, Vilho Jussila<sup>1</sup>, Arja Saarenheimo<sup>1</sup>, Piritta Varis<sup>1</sup>, Billy Fälth<sup>2</sup>, Björn Lund<sup>2</sup>, Markku Tuomala<sup>3</sup>

<sup>1</sup>VTT Technical Research Centre of Finland Ltd  
P.O. Box 1000, FI-02044 Espoo

<sup>2</sup>Uppsala University  
P.O. Box 256, 751 05 Uppsala, Sweden

<sup>3</sup>Private person

#### Abstract

ERNEST project concentrates mainly on developing, validating and taking into use more reliable methods for external event assessment improving nuclear safety. The work carried out so far has included medium scale impact tests on reinforced concrete slabs for computational model validation, numerical simulations of the previously executed test, numerical simulation of a wide body passenger aircraft impact against a rigid target for impact loading model validation, extension and complementation of existing concrete material models for numerical simulations with Abaqus finite element software, numerical study of a 1/3-scale reactor containment building mock-up under pre-stressing and pressurization and comparison of the calculated results against the ones measured in the tests with the actual mock-up and model development for earthquake induced vibrations starting from the rupture of the fault.

#### Introduction

Reliable modelling methods are required for safety assessment of nuclear power plant structures, especially of the containment building, under diverse loading conditions. These loading conditions might include aircraft crashes, earthquakes, over-pressurization due to loss of cooling accidents etc. The models themselves might be fairly simple semi-empirical ones or extremely detailed and sophisticated finite element (FE) ones including complicated material models. Both types of models have in common that they have to be validated before they can be trusted. This validation in turn calls for reliable and relevant experimental data which is scarcely available publicly. All these aspects have been studied within ongoing ERNEST project. The purpose is to increase the level of confidence on the models and methods used in safety assessments.

#### Impact testing (*Vepsä, Ari*)

So far two reinforced concrete slabs have been tested in the project against shear punching. The slabs were 250 mm thick and simply supported at all four edges with the span width being 2000 mm. They were cast with high strength concrete and their only difference was the spacing of the longitudinal reinforcement. Slab E1 had  $\phi 10$  mm bars spaced 90 mm apart in both directions and on both faces. Spacing of 45 mm was used in slab E2. The impacting projectiles were stainless steel tubes with an end cap welded to the front. The one used in test E1 had an outer diameter of 219.1 mm and wall thickness of 6.35 mm. The corresponding values for projectile E2 were 260 mm and 5 mm. Both projectiles weighted roughly 50 kg and the impact velocities were 124.0 m/s in test E1 and 150.6 m/s in test E2. The response of the slabs

was measured using displacement sensors and strain gauges both on the impacted surface of the slabs as well as on the reinforcement bars. The tests were carried out using VTT's impact testing apparatus which is documented for example in the work by Vepsä (2017).

These types of impacts lead easily to both shear punching damage of the slabs, illustrated by formation and possible dislocation of a so called shear cone, as well as bending damage, illustrated by rather large displacements and strains on the reinforcement bars. To estimate the damage beforehand, the tests can be simulated numerically using finite element method. Comparison of the calculated quantities against the measured ones gives important insight on the validity of the model. As an example of the results, the displacements measured as a function of time at back side of slab E1 are shown in Figure 1 (a). The locations of the sensors relative to the centre of the slab are shown in Figure 1 (b).

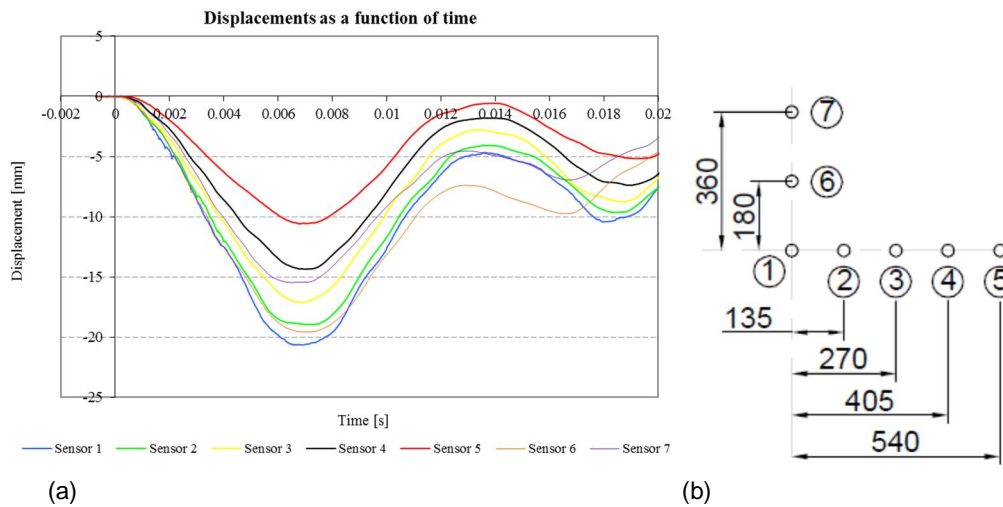


**Figure 1.** (a) Displacements measured as a function of time at the back side of slab E1 during the test  
(b) The locations of the sensors relative to the centre of the slab.

As an alternative or complementary method, the resistance of the slabs against shear punching by soft projectiles can be checked by a procedure proposed by Jowett and Kinsella (1989). The procedure compares the static punching resistance of the slab with the average impact force,  $F_a$ , created by the impacting projectile. Comparison of the safety factors against shear punching, given by this procedure, and the damage caused for the slabs in the tests gives insight on the validity of this procedure.

The result of the procedure depends heavily on the method used for computation of the average impact force. It can be computed various ways: using finite element method, using what is known as Riera formula (Riera, 1968) or assuming that

$$F_a = \frac{0.9I}{t_{0.9I}} = \frac{0.9mv}{t_{0.9I}}, \quad (1)$$

where  $I$  is the impulse generated by the projectile,  $t_{0.9I}$  is the time required for accumulation of 90% of that impulse,  $m$  is the mass of the projectile and  $v$  is the impact velocity.

Safety factors against shear punching, obtained using different ways to calculate  $F_a$ , varied between 1.70 and 0.94 for slab E1 and between 1.41 and 0.97 for slab E2. The higher values were obtained before the tests using Riera formula while the lower values were calculated after the tests assuming

$$t_{0.9I} = 0.85t, \quad (2)$$

where  $t$  is the duration of the impact, defined with the aid of high shutter speed video footage.

The lower left quartiles of the slabs were sawn off after the test and the cross-sections photographed. The vertical ones are presented in Figure 1. Test E1 resulted only mild shear punching damage as can be seen from Figure 2 (a). A shear cone formation could be detected but no shear cone dislocation was observed. A wealth of useful experimental data was collected during the test. Test E2 resulted heavy shear punching damage with a shear cone which was held in its place only with reinforcement bars and which underwent 26 mm large permanent dislocation. This is shown in Figure 2 (b).

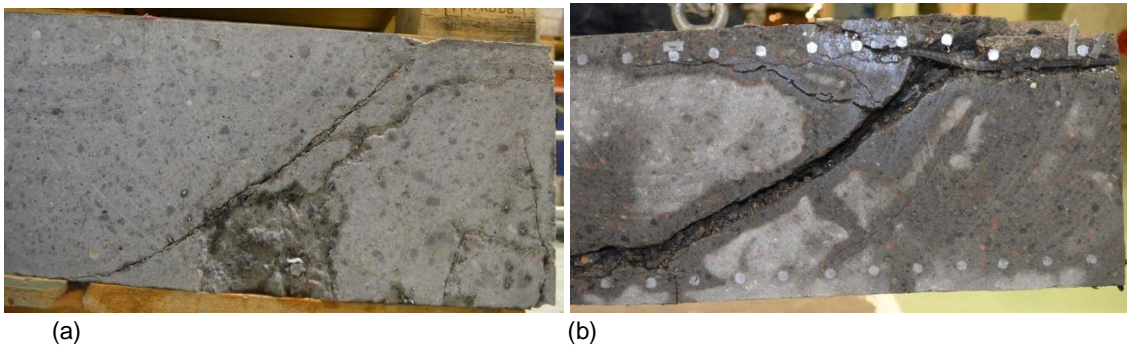


**Figure 2.** Vertical cross-sections of the lower left quartiles of the tested slabs. (a) Slab E1. (b) Slab E2.

Comparing the damage suffered by the slabs with the calculated safety factors, one can conclude that for E1, the value obtained using Riera formula to calculate  $F_a$  is closer to the truth than the one calculated after the test as shear punching failure seems to be quite far. On the other hand, for E2, it seems to be the other way around. Safety factor 1.41 is likely to be much too conservative. This illustrates the difficulties confronted when trying to realistically assess the damages caused by aircraft crash against a concrete structure.

### Continuum damage plasticity for concrete modelling (*Fedoroff, Alexis*)

The simulation of failure processes in reinforced concrete structures is a challenging task. The statement holds in particular when considering high strain rate phenomena, such as impact and blast loading, and cyclic phenomena caused by seismic loading. Numerous scientific publications, (Arros & Doumbalsky, 2007) (Rouquand et al., 2007), (Vu, 2013) as well as research reports (Saarenheimo et al., 2012) and (Fedoroff, 2016) have come, implicitly, to the common conclusion that meticulous understanding of concrete material behaviour at different scales is a pre-requisite to a successful simulation failure processes in concrete structures.

The object of this study, which has been published in the report (Fedoroff, 2017) is to provide the necessary pre-requisites in order to use and customize effectively the Concrete Damage Plasticity (CDP) material model provided in Abaqus, (DS Simulia, 2016). To fulfil this task, a thorough literature review of the main two concrete models, (Lubliner et al., 1989), (Lee, 1996), (Lee & Fenves, 1998) has been conducted and the main results have been exposed in the classical thermodynamic continuum framework.

In order to obtain reliable simulation results, the Abaqus CDP model, in particular, is difficult to handle without a proper understanding of continuum damage and continuum plasticity theories as well as some fracture mechanics concepts, (Hillerborg et al, 1979), (Hillerborg, 1985) that lie behind the mesh size sensitivity regularization. Those concepts have been discussed in the work by Fedoroff (2017). The evolution of the CDP model yield surface as a function of the isotropic hardening parameters has been studied, too, as shown in Figure 3.

Another important issue that has been discussed in the report (Fedoroff, 2017) is the confinement stress dependent character of the confined uniaxial stress test. Indeed, results from static triaxial compression tests, (Sfer et al., 2002), (Gabet, 2006), (Vu, 2013) show that there is a linear relation between the peak confined uniaxial compressive stress,  $\sigma_{c_{max}}$ , and the confinement stress,  $\varphi$ , on one hand and,

likewise, a linear relationship between the square root of the corresponding total strain,  $\varepsilon_{C_{max}}^{tot}$ , and the confinement stress. These relations have been drawn in Figure 4.

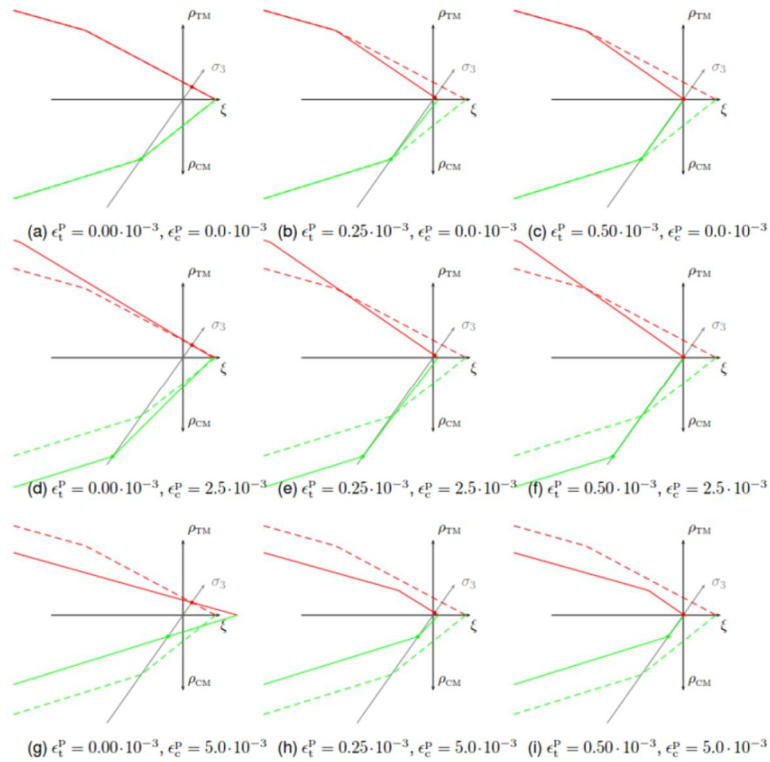


**Figure 3.** Evolution of the yield surface in the meridian plane as a function of the hardening variables in tension ( $\varepsilon_t^p$ ) and compression ( $\varepsilon_c^p$ ). The initial yield surface is represented in dashed line.

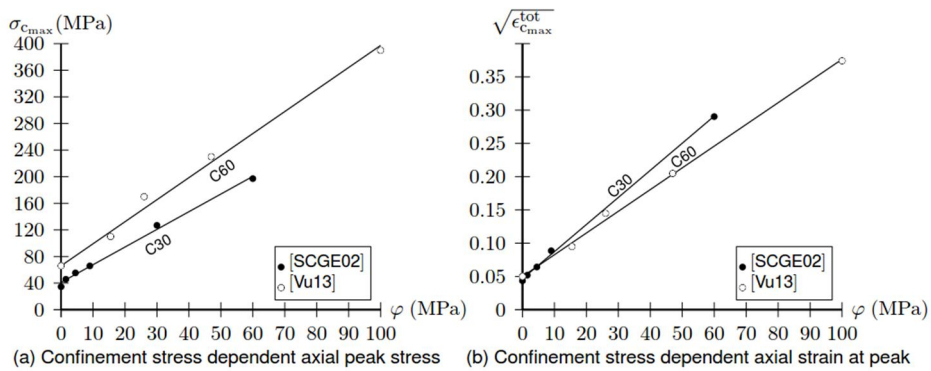


**Figure 4.** Regression curves for confined uniaxial stress tests.

It is considered that in impact simulations, inertia effects create locally highly confined triaxial stress states. The regression data from Figure 4 can be used to input a confinement dependent CDP material model in Abaqus, which response in a confined uniaxial stress state is shown in Figure 5.

Although confinement stress dependency of the CDP model alone is not sufficient for an accurate simulation of impact on concrete structures, it has, nevertheless, a major contribution to the concrete failure response. Other effects, such as strain rate sensitivity in tension need to be considered in order to obtain more realistic simulations of impacts.

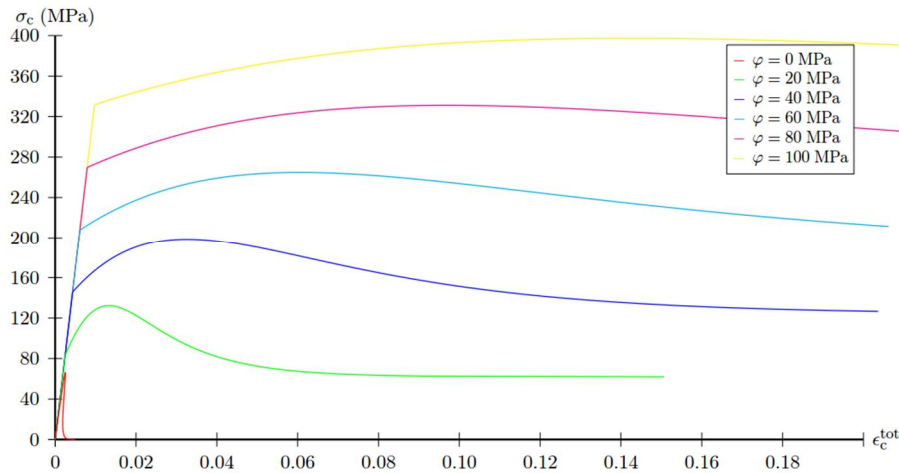


**Figure 5.** Stress-strain evolution of a confined uniaxial stress state for a C60/75 concrete.

### Impact load by a wide body passenger aircraft (*Varis, Piritta & Saarenheimo, Arja*)

A detailed finite element model of Boeing 777-300 (Continental airlines, 2002) was created for numerical simulation of the impact loads caused by a wide-body passenger aircraft crashing into a rigid target. The aircraft finite element model, shown in Figure 6, contained all primary parts of the aircraft, including engines and landing gears. The aircraft parts were meshed with 4-node reduced-integration S4R and 3-node reduced integration S3R shell elements. The target wall was an 80 x 20 m shell structure that was meshed with 4-node 3-dimensional R3D4 bilinear quadrilateral rigid elements. The model had a total of 221 563 elements and 214 961 nodes.

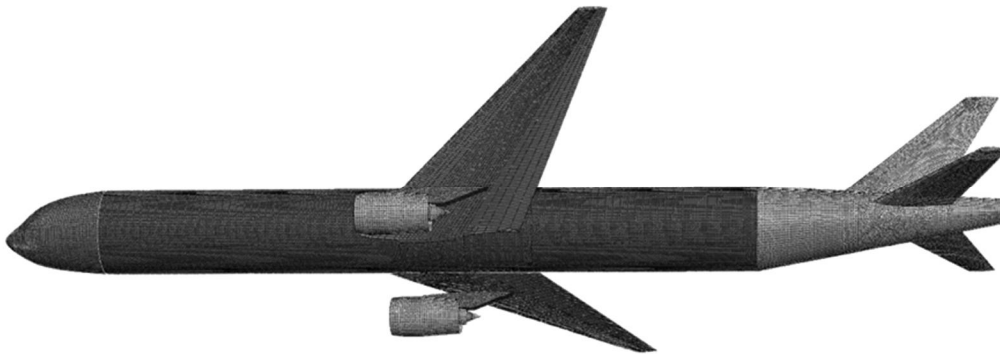


**Figure 6.** Complete Boeing 777-300 aircraft FE-model.

The impacts of the aircraft into a rigid wall were simulated with two different initial impact speeds, 110 m/s and 160 m/s, using Abaqus/Explicit (DS Simulia, 2016). For comparative reasons force-time functions were calculated also analytically by Riera approach (Riera, 1968) applying the same impact velocities as were used in the finite element calculations. The obtained force-time functions are presented in Figure 7 for impact velocity of 110 m/s. The curve in blue represents the finite element simulation results. All the other curves were obtained using Riera approach with different assumptions for the crushing force of the aircraft,  $P_c$ .

The main discrepancies between the FE and the analytical force-time functions are due to the fact the crushing forces of semi hard parts like engines and landing gear are not properly included in the crushing force assumption used in Riera approach. For this reason, mass flow and thus assumed mass distribution dominates the analytically obtained loading function. These loading functions were in agreement with the corresponding results obtained by finite element model. More detailed description of the study can be found in the work by Varis and Saarenheimo (2015).

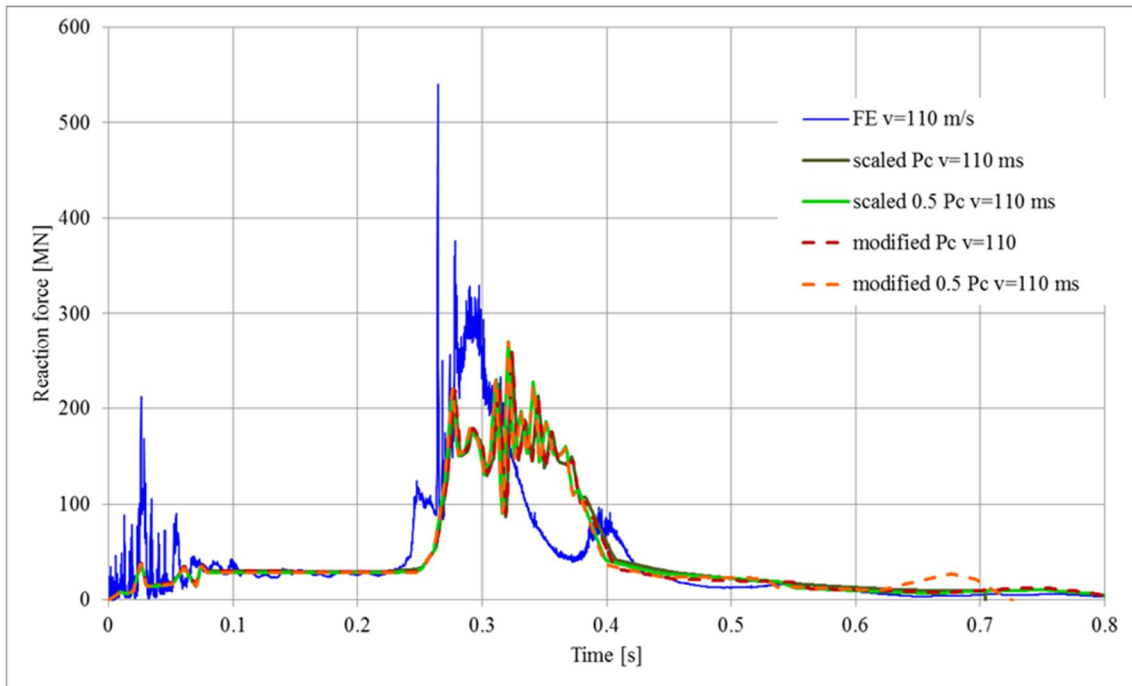


**Figure 7.** Force resultants  $F(t)$  for a Boeing 777-300,  $v_0=110$  m/s.

### Numerical studies on ageing of pre-stressed RC containment (Calonius, Kim)

An experimental mock-up of a reactor containment building at 1/3 scale shown in Figure 8 has been built by EDF near Paris (Corbin&Garcia, 2016). This programme called VeRCoRs extends the knowledge of the containment behaviour and state throughout its lifetime and helps to improve methods to assess the containment condition. It provides an opportunity to compare data from experimental testing with results from calculations using standards or computer simulations. VTT has taken part in the first international calculation benchmark called VeRCoRs 2015 and focused mainly on estimation of cracking and leakage of this building under a test pressure of 5.2 bar abs. This requires detailed modelling of tendon and concrete behaviour. All the main geometric features, such as penetrations, are included. The calculation results are also compared in close collaboration to the corresponding results by Scanscot Technology (Sweden) (referred to as SCTE hereon). The calculation and test results with conclusions are reported in a single joint report (Calonius et al., 2016).

The inner containment structure is post-tensioned with 295 bonded tendons, it does not include a liner, it has for penetrations and 500 sensors for measurements and its diameter, height and general wall thickness are 14.6 m, 25.3 m and 0.4 m, respectively. It can be divided into four main structural parts: the pedestal, the base slab, the cylindrical wall, and the dome.

The FE models created by SCTE and VTT are both three-dimensional and both created and solved with Abaqus finite element (FE) code (DS Simulia, 2014). The main difference is that SCTE uses solid elements whereas VTT uses shell elements for the concrete structure. The model of VTT is shown on the

right-hand side in Figure 8. Each tendon in the models is modelled separately using truss elements. The bending reinforcement in the SCTE model is included using embedded membrane elements with smeared rebar layers and in the VTT model as smeared layers within the shell elements. Both teams use nonlinear material models for the concrete and tendons. The aging effect on the material is taken into account on the basis of different guidelines.

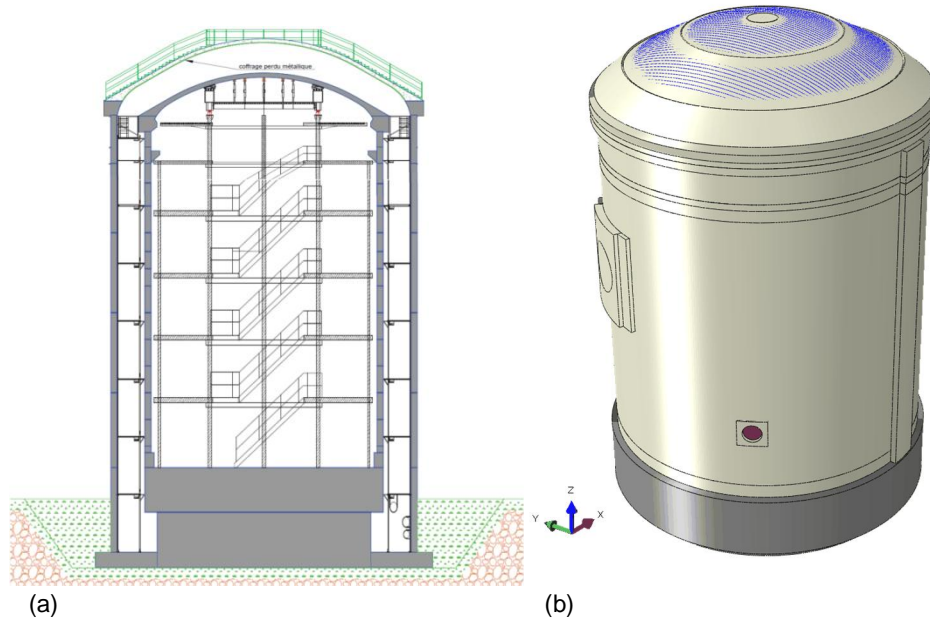


**Figure 8.** Schematic drawing (a) and FE model (b) of VerCoRs mock-up.

The main loads applied are post-tensioning and pressurization. The tendon stress decreases due to friction, seating and instantaneous deformation of the concrete. The pressurization of the containment is applied as an overpressure of 0.42 MPa on the inner surface of the FE model. Time dependent loads are evaluated using construction data provided by EDF. The pre-stress in the tendons is applied using thermal expansion analogy. The improved model by VTT simulates the tensioning and behaviour of the tendons using connector elements between the tendons and concrete.

The SCTE model uses both linear and non-linear analyses with implicit time integration. The VTT model uses only non-linear quasi-static analysis with explicit time integration. Required results in this first calculation benchmark were strain and stress at end of erection, end of post-tensioning and at 0.52 MPa abs. inner pressure. Moreover, an estimate of crack properties in the inner containment was expected to be delivered. Strain values in certain locations and directions from both SCTE and VTT analyses together with measured values are compiled in Figure 9. In this graph, only the tests results include the initial strains before the post-tensioning, which were approx. 0.01% (100  $\mu\text{m}/\text{m}$ ).

Figure 10 shows the maximum principal stress in the concrete outer surface at an overpressure of 4.2 bar in SCTE model (on the left) and in the preliminary VTT model (on the right). The colours other than black show where the material is in tension at least in some direction. It is one indication to where the cracking might occur. Red colour indicates stress level close to tensile strength. VTT later improved its model, but those results are not considered here. The cracks are mainly evaluated using cracking strain and element length as obtained in the FE analysis. The analysis results show that only minor through-thickness cracks are formed on some locations in the concrete wall.

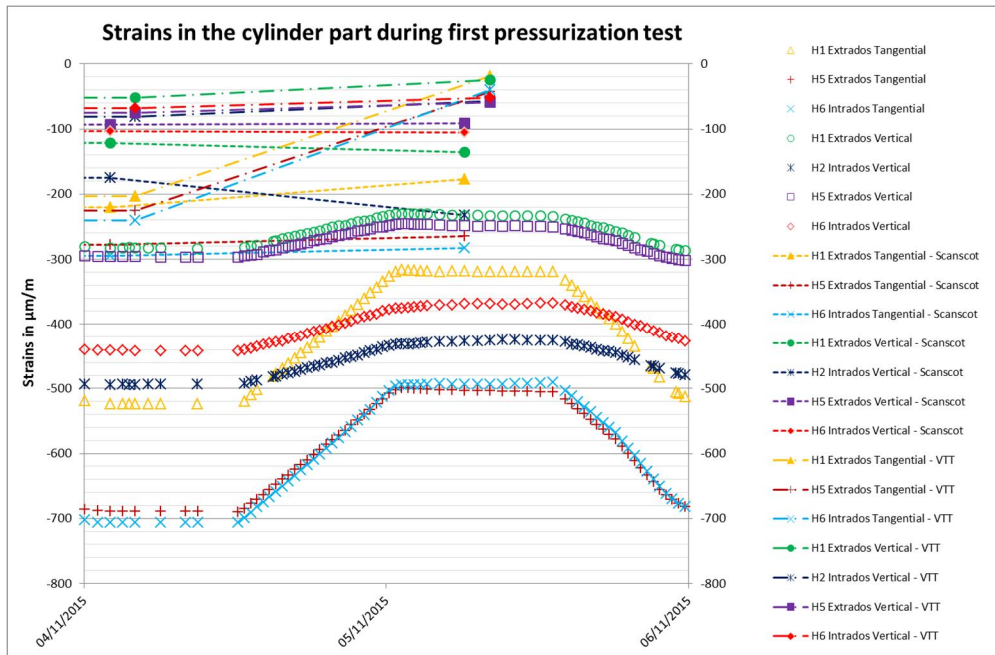


**Figure 9.** Comparison of strains in the cylinder part during the first pressurization test. The analysis results here do not realistically follow the time line. Only single values with no pressure and with 0.42 MPa over-pressure are shown and connected with dotted lines.

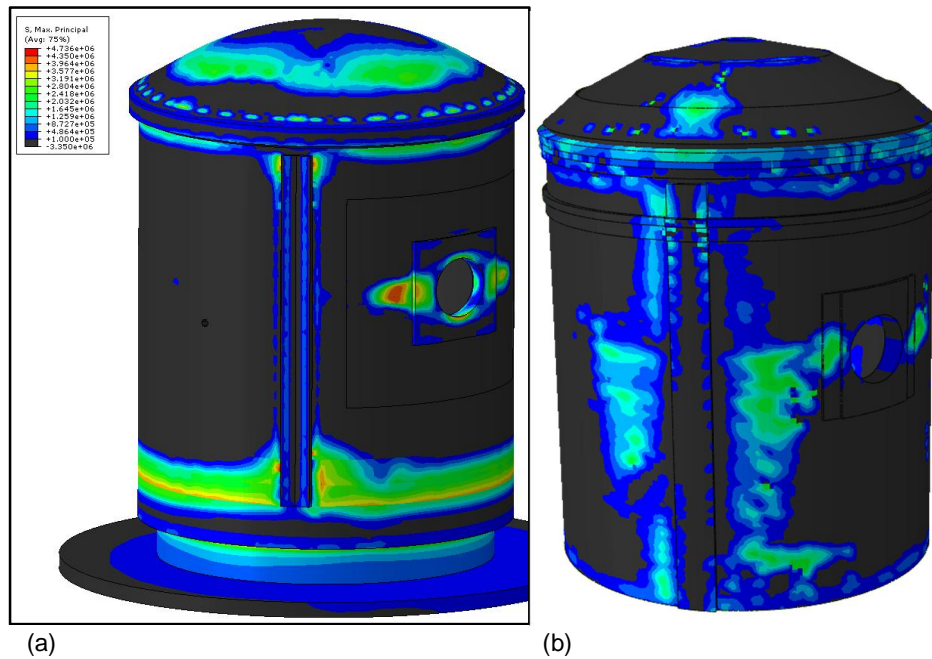


**Figure 10.** Maximum principal stress in SCTE model (a) and in VTT model (b).

The leakage through the containment has two significant mechanisms, gas flow through cracks and permeable flow through concrete. Gas flow estimation through cracks follows the assumptions according to for instance Rizkalla et al. (1984). The assumptions lead to that the mass flow rate through an idealized crack can be described by the fairly simple expression:

$$q = \sqrt{\frac{(p_1^2 - p_2^2)2w^3 B^2}{\Lambda LRT}}$$

where  $q$  is the mass flow rate,  $p_1$  and  $p_2$  are the inlet and outlet pressure respectively,  $w$  is width of the crack,  $B$  is the extent of the crack,  $\Lambda$  is a dimensionless friction coefficient between air and wall,  $L$  is the thickness of the wall,  $R$  is the specific gas constant and  $T$  is the temperature. Several models describing the friction between air and concrete are found in literature. The model employed in this study is the Badoux model (Badoux&Fellay, 2002). The permeable flow through the concrete is solved here by the work of Dullien (1992) and Abbas et al (1999). Those are not described here.

The numerical analyses by both teams, SCTE and VTT, were successful in the sense that the models worked, simulations were completed, and their behaviour seemed realistic and similar to each other on general level. The calculation model created by VTT is still under development. Compared to the test results, both models have less compression throughout the model after the post-tensioning. The effect of pressurization is more evident in the test than in the calculations, but since the real structure was so heavily in compression after post-tensioning, it is still clearly in compression during the pressurization test.

The dominating property affecting flow through the containment is the number of cracks and crack size. It appears that both VTT and SCTE overestimated those and thus also the leakage rate substantially. The exact values are not shown here, since there are still some open questions regarding the modelling and also measurements. The reason for this overestimation has to be studied in more detail in the future. Also, EDF might have further comments on their experimental results which have to be taken into account. Another uncertainty is the degree of saturation of water in the concrete containment wall. The total measured flow through the wall corresponds to a high degree of saturation.

### **Experimental and numerical vibration propagation studies (Saarenheimo, Arja & Tuomala, Markku)**

A test series called V1 considering impact induced vibration propagation and damping in a reinforced concrete structure has been carried out at VTT in an earlier impact testing project. The test target was a reinforced concrete structure with two parallel walls connected to a floor slab. The front wall was additionally supported by triangular shaped side walls which were also connected to the floor slab. The test structure was vertically supported on elastomeric bearing pads and tension bars and horizontally with steel back pipes, effective mainly in compression, and with steel bars, effective in tension. Finite element model of the structure, created with Abaqus, is shown at the left in Figure 11.

In order to obtain information on vibration propagation in damaged concrete structure at different levels of damage grades the same structure was tested six times. At each time the mass of the deformable stainless steel missile was 50 kg. The hit point was located in the middle of the front wall. The impact velocity was about 110 m/s in the first four tests (V1A-D) and about 60 m/s in the remaining two tests (V1E and F). The response of the structure was measured with strain gauges, displacement sensors and accelerometers.

Numerical studies on V1A-F tests were carried out with Abaqus/Explicit and by an in-house code (IHC). Loading transients used as an input in the calculations are presented at the right in Figure 11. Of particular interest were the so-called floor response spectra (FRS) which are calculated using either measured or simulated accelerations as an input. Acceleration FRS at the top of the rear wall, obtained using both the measured and calculated acceleration results are compared in Figure 12.

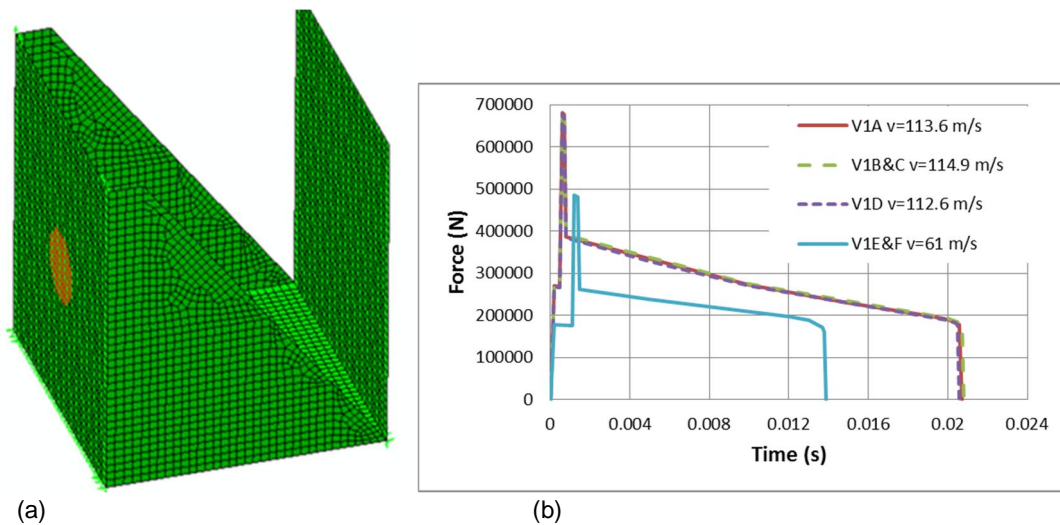


Figure 11. Finite element model (a) and impact loads (b).

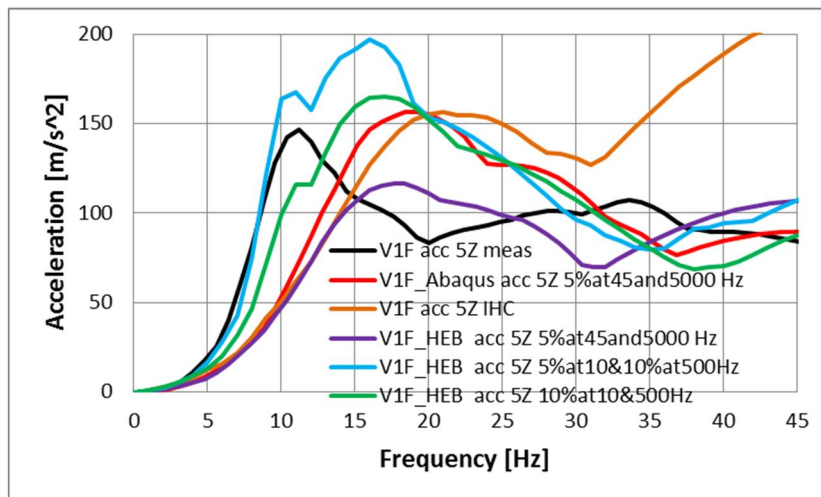


Figure 12. Acceleration floor response spectra at the top of the rear wall.

### Earthquake source modelling to support NPP safety in Finland (Jussila, Vilho; Fülöp, Ludovic; Fälth, Billy & Lund, Björn)

This section is reporting on the progress of modelling earthquake induced vibrations starting from the rupture of the fault. The purpose of this work is to contribute, together with empirical observations, to the prediction of expected vibrations from earthquake at the location of NPPs. With modelling we concentrate on larger magnitude earthquakes, where empirical observations are lacking in Fennoscandia.

It has to be mentioned that the SAFIR/NEST project made a very limited contribution to this work. Most of the results in this section are due to the financial support of the NKS project “Modelling as a tool to augment ground data in regions of diffuse seismicity/AddGROUND” (NKS-R\_2015\_113).

In the first section of this summary we highlight some characteristics of earthquakes with design significance. In the second section we present the developed modelling technique and in the last part summarise some results. The initial plan in the SAFIR2018/NEST project plan was to develop synthetic vibration databases based on broader ranges of earthquake fault rupture scenarios. Achieving this goal has not been possible within the financial confines of the program. However, the proposed modelling technique

has been benchmarked, showing good agreement with established empirical ground motion prediction equations (GMPE).

### **Hazard from earthquakes to Finnish plants**

Before advancing to the description of the work, we present a short highlight of the seismicity in Fennoscandia, and of the research direction sketched in 2015 by this research group. The main points are:

1. The magnitude distance de-aggregation of earthquake hazard for locations in Finland was reported as outcome of a previous SAFIR project in Fülöp et al., (2015). The de-aggregation for Pyhäjoki, of 5% damping average horizontal PGA with engineering significance show very significant contributions from near-field earthquakes, as follows:

- $PGA=0.05 \times g$ , means magnitude  $M=4.1$  and distance  $D=29\text{km}$ ,
- $PGA=0.1 \times g$ , mean magnitude  $M=4.3$  and distance  $D=24\text{km}$ ,

Considering also other frequencies in the spectra, we can state that most hazard to the plants and its equipment comes from distances not beyond 60-70km. This conclusion is consistent with finding from other regions of moderate seismicity e.g. Switzerland.

2. The predictions of ground motion developed using empirical data rely on very few, if any, recordings in this range of distances. For instance the GMPE calibrated to Fennoscandian data by Vuorinen (2015) has no recordings in the range of  $M>4$  and  $D<100\text{km}$ . and it has been later compared to recordings at distances  $50<D<100\text{km}$ , becoming available from the 2012, 2014 and 2016 earthquakes in Sweden

### **Developed modelling technique**

The objective of this work was to demonstrate a modelling method for the generation of near- and intermediate field synthetic ground motion data for Fennoscandian conditions, with frequencies up to 20 Hz. To simulate a dynamically rupturing fault in a model that extends several kilometres, with a discretization fine enough for such high frequencies is extremely computationally demanding. Thus, we adopted a hybrid modelling approach (Fälth et al., 2015).

Hence, the earthquake fault movement was generated using dynamic rupture modelling. The dynamic rupture was modelled using the 3DEC software, a 3D modelling tool based on the discrete element method (Itasca, 2013). The model comprised the fault plane, embedded in the finely discretized rock volume. The dimensions of the model are just large enough to prevent the boundaries from influencing the solution. The simulation time is long enough for the rupture to be just completed over the entire fault plane. An initial stress field was applied and a dynamic earthquake rupture is initiated and propagated along the fault plane. The fault slip parameters are recorded at very large (i.e. hundreds) number of points on the fault. It is desirable to have as many recording points as possible, especially to capture the fine details of a complicated rupture process affecting the higher frequencies.

A few fault and slip orientations (i.e. strike slip, reverse) and rupture scenarios corresponding to a 5.5 magnitude earthquake were studied. This magnitude correspond to the stronger earthquakes considered possible in the Fennoscandian context.

The software package used to compute the synthetic waveforms was Compsyn (Spudich & Xu, 2002), based on the discrete wavenumber element method (Olson et al., 1984). The slip on a large number of fault patches were transferred to Compsyn from the 3DEC software. The Compsyn model, embedding the fault created in this way extended to 20-70km from the epicentre.

When ground motion is simulated it is a reasonable assumption to model the crust as an elastic medium, carrying pressure (P-) and shear (S-) waves from the source to the ground surface. The earth's crust was modelled as a vertically layered medium in order to account for the significant changes in density and velocity as function of depth. Each layer boundary in the earth model is a discontinuity creating reflection,

transmission and refraction of waves. The most important discontinuity in the model is the ground surface, which produces Rayleigh and Love surface waves. All wave types propagate with different velocities and on measured ground motions one is able to pinpoint the different wave arrivals. At close vicinity to the source the waves arrive at short time intervals and overlap, while at longer distances wave arrivals separate significantly.

### Summary description of the results

Some outputs of the ground vibrations resulting from a test models of the M5.5 earthquake are given in Figure 13. The vertical fault is visible as a thick black line in the horizontal direction centered on the origin, and the epicentre as a red star. At 1.9s after rupture initiation the pressure waves emerge and at approximately 5.9s the surface waves form and start to spread.

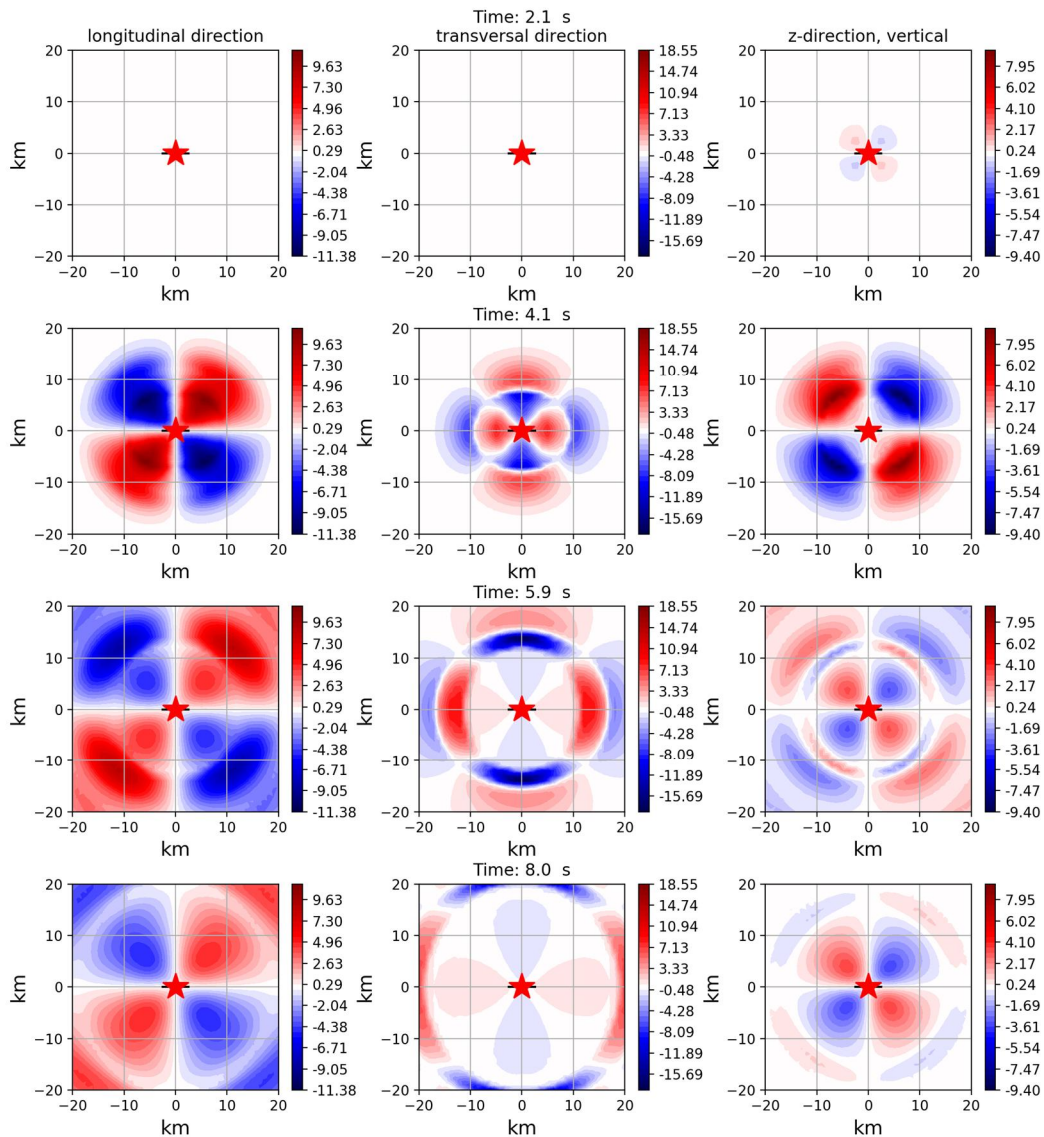


**Figure 13.** Amplitudes of ground motion displacements (mm) close to the epicentre ( $5 \times 5 \text{ km}^2$  fault rupture). Longitudinal (radial relative to epicentre), transversal and vertical components (Fülöp et al., 2017).

The ground acceleration and spectra were compared with established empirical GMPE G-16 (Graizer, 2016). Predictions up to 10km from the epicentre were processed so far, with a few examples given in Figure 14.

Comparisons between the GMPE and model results are promising, when considering the complexity of the near-field waves and the near-surface bedrock heterogeneity at the receivers. As exemplified in Figure 14, the same epicenter/hypocenter distances but different orientation relative to the fault can result in different acceleration levels. The fit of the data with the general shape of the YVL spectra (YVL B.7, 2013) is also reasonable, even if in the region of frequencies above 10Hz slightly higher amplification is observed. An analysis of the entire data-set resulting from modelling will be published in the final report of the NKS project.

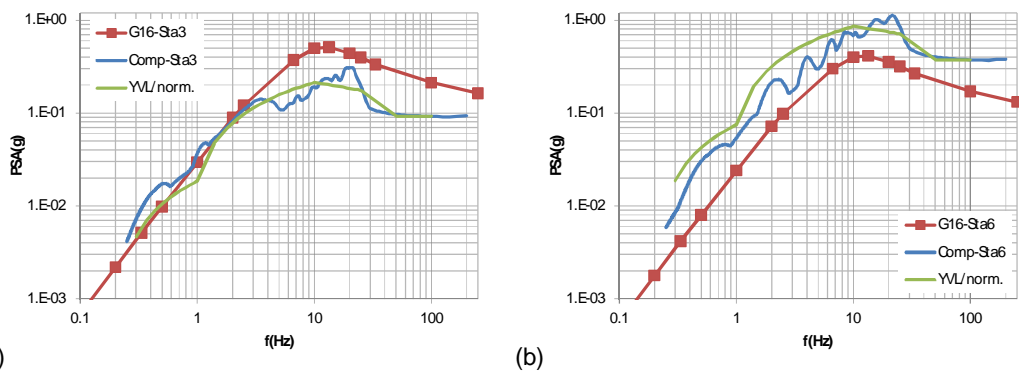


**Figure 14.** Example fit between modeling results (Comp-Sta3/Sta6), the G-16 prediction and the YVL spectra in log-log scale for an epicenter distance 10km, but different direction relative to the fault orientation (Fülöp et al., 2017).

## Acknowledgement

The authors would like to acknowledge the project funding by the National Nuclear Waste Management Fund (VYR) and VTT Technical Research Centre of Finland.

Part of this work was supported by the NKS project “*Opportunities for Source Modelling to Support the Seismic Hazard Estimation for Nuclear Power Plants*” (AddGROUND) in 2015/2016.

## References

- Abbas, A., Carcasses, M. and Ollivier, J-P. 1999. Gas permeability of concrete in relation to its degree of saturation. *Materials and structures*, vol. 32, no. 1, pp. 3-8.
- Arros, J. and Doumbalsky, N. 2007. Analysis of aircraft impact to concrete structures. *Nuclear Engineering and Design*, 1241-1249.
- Badoux, M. and Fellay, N. 2002. Swissmetro - Gas permeability of cracked concrete slabs. in *MAG-LEV'2002*, topic 5, Lausanne, Switzerland.
- Calonius, K., Nilsson, T., Elison, O. and Lehmann, S. 2016. EDF VERCORS Project – Benchmark 1: Themes 1, 2 and 3. Research Report VTT-R-00016-16.
- Continental Airlines. 2002. Boeing 777 Airplane Flight Manual.

- Corbin, M. and Garcia M. 2016. International Benchmark VeRCoRs 2015 - Overview, synthesis and lessons learnt.
- DS SIMULIA. 2014. Abaqus Analysis User's Manual Version 6.14.
- DS SIMULIA. 2016. Abaqus Manual.
- Dullien, F. A. L. 1992. Porous Media, Fluid Transport and Pore Structure, 2nd edition, San Diego, California: Academic Press, Inc.
- Fedoroff, A. 2016. Feasibility study of aircraft impact simulation on nuclear powerplant. Espoo: VTT.
- Fedoroff, A. 2017. Continuum damage plasticity for concrete modeling, VTT-R-00331-17. VTT.
- Fälth, B., Hökmark, H., Lund, B., Mai, P.M., Roberts, R. and Munier, R. 2015. Simulating Earthquake Rupture and Off-Fault Fracture Response: Application to the Safety Assessment of the Swedish Nuclear Waste Repository. Bull. Seismol. Soc. Am. 105, 134–151. doi:10.1785/0120140090
- Fülöp, L., Jussila, V., Malm, M., Tiira, T., Saari, J., Li, Y., Mäntyniemi, P., Heikkinen, P. and Puttonen, J. 2015. Seismic Safety of Nuclear Power Plants - Targets for Research and Education (SESA) - Final Report, in: SAFIR2014, The Finnish Research Programme on Nuclear Power Plant Safety 2011-2014, (Final Report), VTT Technology. VTT Technical Research Centre of Finland, Espoo, pp. 604–619.
- Fülöp, L., Jussila, V., Lund, B., Fälth, B., Voss, P., Puttonen, J. and Saari, J., 2017. Modelling as a tool to augment ground motion data in regions of diffuse seismicity - Final Report. NKS Nordic Nuclear Safety Research (draft).
- Gabet, T. 2006. Comportement triaxial du béton sous fortes contraintes: Influence du trajet de chargement. Grenoble: Université Joseph Fourier.
- Graizer, V. 2016. Ground-Motion Prediction Equations for Central and Eastern North America. Bull. Seismol. Soc. Am. 106, 1600–1612. doi:10.1785/0120150374
- Hillerborg, A. 1985. The theoretical basis of a method to determine the fracture energy  $G_f$  of concrete. Materials and structures, 291-296.
- Hillerborg, A., Modéer, M. and Petersson, P. E. 1979. Analysis of crack formation and crack growth by means of fracture mechanics and finite elements. Cement and Concrete research, 773-782.
- Itasca. 2013. 3DEC – 3-Dimensional Distinct Element Code, User's Guide. Itasca Consulting Group Inc., Minneapolis, USA.
- Jowett, J. and Kinsella, K. 1989. Soft missile perforation analysis of small and large scale concrete slabs. In: Proceedings of Structures under Shock and Impact conference 1. pp. 121-132.
- Lee, J. 1996. Theory and implementation of plastic-damage model for concrete structures under cyclic and dynamic loading. Berkley, California: PhD dissertation, University of Berkley.
- Lee, J., and Fenves, G. L. 1998. Plastic-damage model for cyclic loading of concrete structures. J. Eng. Mech., 892-900.
- Lublliner, J., Oliver, J., Oller, S. and Oñate, E. 1989. A plastic-damage model for concrete. Int. J. Solids Structures, 299-326.

- Olson, A.H., Orcutt, J.A. and Frazier, G.A. 1984. The discrete wavenumber/finite element method for synthetic seismograms. *Geophys. J. Int.* 77, 421–460. doi:10.1111/j.1365-246X.1984.tb01942.x
- Riera, J. 1968. On the stress analysis of structures subjected to aircraft impact forces. *Nuclear Engineering and Design*, Vol. 8. pp. 415-426.
- Rizkalla, S. M., Lau, B. L. and Simmonds, S. H. 1984. Air leakage characteristics in reinforced concrete. *Journal of Structural Engineering*, vol. 10, pp. 1149-1162.
- Rouquand, A., Pontiroli, C. and Mazars, J. 2007. Concrete structures under severe loading: a strategy to model the response for a large range of dynamic loads. *Fracture Mechanics for Concrete and Concrete Structures*. Catania (Italy): IA-FraMCoS.
- Saarenheimo, A., Calonius, K. and Tuomala, M. 2012. Sensitivity studies on reinforced concrete walls impacted by soft and hard missiles, VTT-R-00859-12. VTT.
- Sfer, D., Carol, I., Gettu, R. and Etse, G. 2002. Study of the behavior of concrete under triaxial. *Journal of Engineering Mechanics*.
- Spudich, P. and Xu, L. 2003. 85.14 Software for calculating earthquake ground motions from finite faults in vertically varying media, in *International Geophysics*, vol. 81, Part B, H. K. William H.K. Lee Paul C.Jennings and Carl Kisslinger, Ed. Academic Press. pp. 1633–1634.
- Varis, P. and Saarenheimo, A. 2015. Impact load by a wide body passenger aircraft, VTT-R-02907-15. VTT
- Vu, X. 2013. Vulnérabilité des ouvrages en béton sous impact: Caractérisation, modélisation et validation. Grenoble: Université Joseph Fourier.
- Vuorinen, T. 2015. New Fennoscandian Ground Motion Characterization Models (MSc thesis). University of Helsinki, Helsinki, Finland.
- YVL B.7, 2013. Provisions for internal and external hazards at a nuclear facility, Finnish Regulatory Guide on Nuclear Safety (YVL)

### 3.4 Extreme weather and nuclear power plants (EXWE)

Kirsti Jylhä, Jan-Victor Björkqvist, Carl Fortelius, Hilppa Gregow, Sebastian Heinonen, Marke Hongisto, Otto Hyvärinen, Milla Johansson, Ari Karppinen, Anniina Korpinen, Ekaterina Kurzeneva, Matti Kämäräinen, Terhi Laurila, Ilari Lehtonen, Ulpu Leijala, Antti Mäkelä, Taru Olsson, Havu Pellikka, Tuuli Perttula, Jenni Rauhala, Mikhail Sofiev, Jani Särkkä, Andrea Vajda, Ari Venäläinen, Ari Viljanen

Finnish Meteorological Institute (FMI)  
P.O. Box 503, FI-00101 Helsinki

#### Abstract

Estimates of probabilities of hazards related to external events are needed for overall safety management of nuclear power plants (NPPs). Historical time series of extreme convective weather events showed notable cross correlations between summertime 1) thunderstorm days, lightning and heavy rainfall, 2) heavy rainfall and tornadoes and 3) large hail and tornadoes. Two of four classes of synoptic-scale circulation patterns that favour significant hail (5 cm or larger) have similarities with the patterns observed in Finland in tornado situations. The record-breaking sea-effect snowfall case at Merikarvia on 8 January 2016 was well captured by the HARMONIE weather prediction model, compared to weather radar images. Even if the windstorm climate in Finland remains the same, the impacts of the storms will alter due to the ongoing change in environmental conditions. Recent studies on global sea level rise have not revealed new information that would imply major changes on the mean sea level scenarios for the Finnish coast. The local flooding risk estimates can be improved by investigating the maximum elevation of the continuous water mass on the shore by combining the effects of sea level and wind-generated waves. Rapid sea level oscillations are caused by different meteorological conditions during summer and winter seasons. Although no serious effects have occurred in Finland, large geomagnetically induced currents must be taken into account when installing new transformers or power lines affecting the operation of NPPs. High-resolution meteorological modelling has progressed to a stage where a proper assessment of coastal meteorological conditions can be fed into a dispersion modelling system.

#### Introduction

Overall safety management over the life cycle of a nuclear power plant (NPP) requires, among others, evaluation of external events triggered by exceptional geophysical conditions. Extreme weather and sea level events affect the design principles of NPPs and may pose external threats to the plants. Geomagnetic effects of extreme solar storms might reduce the reliability of the external power transmission grid. Transport and dispersion of emissions from a source located on the seashore, such as the Finnish NPPs, are subject to specific coastal atmospheric phenomena.

In 2015-2016, four themes were examined in the EXWE project: 1) extreme weather incidents, 2) extreme sea level events, 3) extreme space weather; and 4) atmospheric dispersion and dose assessment of accidental releases. The specific topics included: severe warm- and cold-season convective weather events; severe freezing rain; latest findings on strong winds; meteotsunamis and other short-period extreme-sea-level events; simultaneous occurrence of high sea level and high wind waves; solar storms and geomagnetic disturbances; and preparations needed in meteorological high-resolution modelling to be linked with a state-of-the art dispersion modelling system.

## Main objectives and challenges

In the existing Finnish NPP units, preparedness against extreme natural phenomena is continuously being improved. For example, actions have been taken to reduce the risk of heavy rainfall-induced flash floods in a NPP yard area; to avoid a blockage of air intake of emergency diesel generators as a consequence of simultaneous snowfall and wind; to prevent problems due to frazil ice formation; and to implement a supplementary cooling system of NPP reactors (Viitanen et al. 2013; Fortum 2015). Despite these already-taken measures, further research work needs to be conducted. This is because estimates of frequencies of weather-related and sea-level-related hazards are subject to considerable uncertainties.

The main source of uncertainty arises from the fact that phenomena beyond the design basis levels of nuclear power plants have a very low probability, corresponding to return periods of thousands or millions of years. Such extreme weather and sea level events occur so rarely that they are typically unprecedented anywhere in Finland and thereby missing from the relatively short time series of observations. On the other hand, as part of a continuous effort to improve the understanding of extreme weather events, it is useful also to examine moderately rare phenomena, having a return period of tens or hundreds of years.

Another challenge in producing reliable results is the fact that the probabilities of occurrence of exceptional weather, climate and sea level events are subject to the global climate change. Therefore, the patterns of extreme events, both in frequency, extremity, and magnitude, are likely to alter in the course of time. A hazard curve evaluated from time series of past measurements needs to be regularly updated. Beneficially, the updates are empowered by recent accretions of research material and developments of methods. Indeed, the study material in EXWE in 2015-2016 consisted both of instrumental records, eye-witness observations, reanalysis data, high-resolution atmospheric modelling, data assimilation and climate models' output. Besides, the research team covers a wide range of scientific expertise.

## Extreme convective weather in summer

Extreme convective weather (ECW) occurs frequently also in Finland. In the warm season, ECW is characterized by thunderstorms producing heavy rain, large hail, intensive lightning, strong wind gusts (i.e., downbursts) and tornadoes. All of these thunderstorm-related phenomena can cause impacts to infrastructure, the severity of the impacts depending on the intensity and location of occurrence of the events. Regarding the thematic of the EXWE project, the main research questions of ECW are as follows: 1) What is the probability that an ECW phenomenon of varying intensity hits a nuclear power plant site? 2) What are the uncertainties of the occurrence probabilities? 3) Are the occurrence probabilities likely to change with the changing climate? 4) What novel methods can be produced to improve the prediction of ECW phenomena?

Questions 1-3 may seem rather simple and straightforward but, unfortunately, the situation is far from simple. Firstly, to derive the occurrence probabilities, one needs observations of the phenomena. For most of the ECW phenomena to be observed (tornadoes, large hail, downburst), one needs human observation either of the phenomenon itself or its damages. This practically means that we cannot be quite sure how complete the observational time series are. Luckily, however, the more intense is the phenomenon, the more likely it is to be observed (and to have been observed also in the early years).

**Lightning** is an essential element of a thunderstorm. On the coast of the Gulf of Bothnia, the frequency of cloud-to-ground lightning typically increases from sea to land, whereas the gradient is less steep on the coast of the Gulf of Finland (Fig. 1). Because lightning can be observed nowadays in real time with high spatial accuracy, an interesting question is whether lightning location data could be used to estimate or predict the occurrence of other hazardous phenomena that are more difficult to observe, and if the observational time series of thunderstorms since 1887 could be used to estimate the distributions of other ECW phenomena as well? In the following we give some general considerations (Mäkelä et al., 2016):

- **Heavy precipitation:** Thunderstorm contains always a core of intense precipitation. Most of the lightning coincides with this core but lightning can hit also outside of it (even several kilometers). Because both heavy precipitation and lightning are governed by the intensity of the convection (the

updraft velocity), lightning and rainfall are correlated (the more lightning, the more intense the precipitation). The accumulation of precipitation at ground varies depending on the cloud movement and on the position of the new developing cells in the cloud.

- **Tornado:** Tornadoes are related to convective clouds; however, in Finland tornadoes may occur without any lightning. A key ingredient for the occurrence of a tornado is the vertical wind shear, i.e. the change of wind speed or direction with height, but this is not essential for the occurrence of lightning.
- **Large hail:** The heavy precipitation of thundercloud originates from large frozen graupels and frozen rain droplets that are forced upward inside violent updrafts. Normally, hail melts before reaching the ground. If updrafts are strong and last long enough, large hail can be observed at the ground. Therefore, lightning and the formation of large hail do have linkage in the perspective of the cloud dynamics, but whether there is a usable correlation between the two is uncertain.
- **Downbursts** (strong convective wind gusts): Essential parts of a thunderstorm are the up- and downdraft cores of air; while the updraft transports heat and moisture (i.e., energy) into the cloud, downdraft and the associated intense precipitation area and strong wind gusts finally dissipate the cloud. Therefore, heavy wind gusts are practically always involved in thunderstorms, but their intensity, extent and height of occurrence vary. It is plausible that the more lightning the storm produces, the more intense are the wind gusts; however, there are not many studies made on the subject mostly because the wind gusts, especially the most intense ones, rarely hit an observation station. It is also noteworthy that severe convective wind gusts may occur in conjunction with only sporadic lightning or even without any lightning activity before or after the wind event.

In EXWE, the warm season ECW-related work has included the systematic collection of the previous studies and time series of ECW phenomena (Mäkelä et al., 2016), the inter-comparison and cross-correlations of the different ECW time series (Laurila et al., 2016), investigating the atmospheric conditions favouring the occurrence of large hail producing thunderstorms (Rauhala et al., 2017) and investigating the improved predictability of ECW occurrence in Finland (Ukkonen et al., 2016).

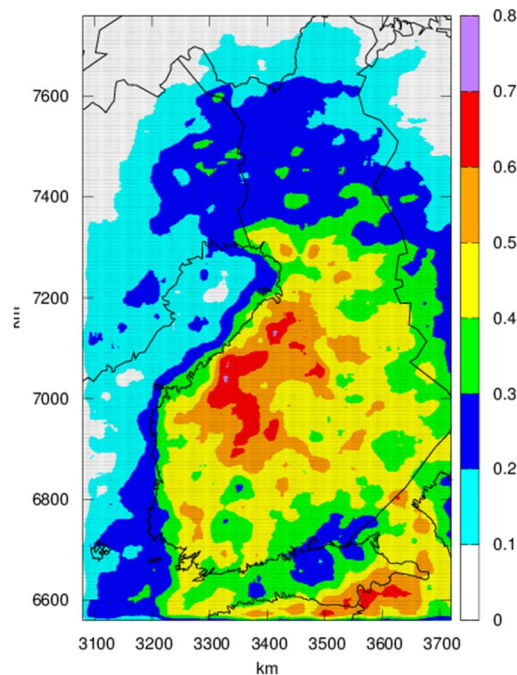


**Figure 1.** The average annual number cloud-to-ground lightning per km<sup>2</sup> in Finland 1998-2016.

When combining the annual time series of the ECW observations, it was clearly noticed that the time series of the different ECW phenomena (hail, heavy rainfall, thunderstorms, lightning and tornadoes) are likely to miss observations from the early years of the observation period. This applies especially to hail and tornado datasets; they need human observations and collecting observations has become more efficient during last years. Since 1997, the time series of all ECW phenomena are much more complete. For the spatially averaged annual number of thunderstorm days, the time series extends back in time to the 1880s (Fig. 2).

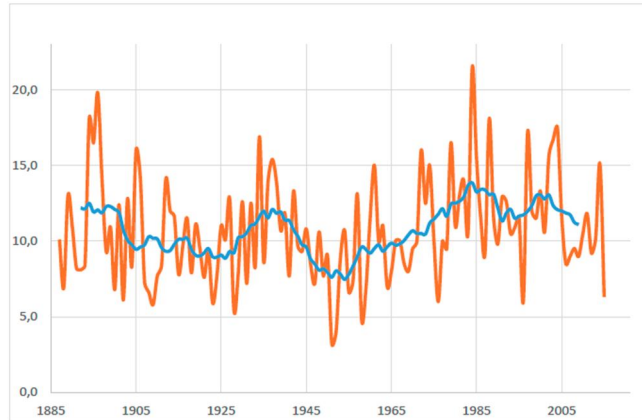


**Figure 2.** The spatially averaged annual number of thunderstorm days in Finland in 1887-2015 (orange) and a 10-year moving average (blue).

By comparing the time series of the ECW observations, it was found that:

- The annual number of heavy rainfall cases ( $\geq 30$  mm/day) was statistically significantly correlated with the annual number of thunderstorm days ( $r=0.44$ )
- The annual number of heavy rainfall cases ( $\geq 30$  mm/day) was statistically significantly correlated with the average lightning flash density ( $r =0.45$ ).
- The correlation coefficient between the annual number of thunderstorm days and average lightning flash density was 0.67.
- In about half of the years when tornadoes ( $\geq F2$ ) had been reported (23 years out of 78), there were also observations of significant hail ( $\geq 5$  cm in diameter), and vice versa.
- In about one third of the years with tornadoes ( $\geq F2$ ), very heavy rainfall cases ( $\geq 100$  mm/d) were observed. On the other hand, in about half of years with very heavy rainfall cases (13 years out of 78), there were also one or several reports of tornadoes ( $\geq F2$ ).

Atmospheric conditions and synoptic-scale circulation patterns favouring **significant hail** (diameter of 5 cm or larger) in Finland have been studied in EXWE based on 50 significant-hail reports and reanalysis data during 35 days in the period 1957–2016 (Rauhala et al., 2017). The aims are to 1) understand what types of weather patterns bring together the ingredients for significant-hail producing storms in Finland and to 2) compare typical synoptic weather patterns producing severe weather (i.e., tornadoes vs. significant hail). The methods included a) clustering of the synoptic settings into different atmospheric environments and b) production of composite synoptic maps. The clustering of synoptic settings resulted in four distinct synoptic classes (32 days) and an unclassified category with three days. Two of the classes have similarities with the patterns observed in Finland in tornado situations and severe thunderstorm patterns in the

United States, whereas the remaining classes seem more unique. Every third hail day had at least one tornado report and two of the three hail days had daily rainfall of 30 mm or more.

### Sea-effect snowfall

The year 2016 started with imposing a new national snowfall record in Finland; up to 73 cm of new snow accumulated in Merikarvia, western coast of Finland, in less than a day during 8 January. This distinctly exceeded the previous record, 50 cm, measured in a nearby coastline city, Rauma, 100 kilometers to the south on 21 November 1971.

The Merikarvia case was caused by a well-known lake-effect (here sea-effect) snow phenomenon. It is a cold-season convective situation where the cold air flows over the warmer ice-free waters. Water area acts as a source of heat and moisture. This produces an unstable boundary layer over the water body. As a result, the turbulent heat fluxes from the water surface are large and generates shallow convection that induces small and intensive convective precipitation which can drift to the coast as snowbands (Mazon et al., 2015).

Hourly radar reflectivity as well as accumulated precipitation images from the FMI weather radar network were used to identify this sea-effect snow case and to verify the weather prediction model simulation. Radar images were qualitatively compared to hourly precipitation amounts simulated by the non-hydrostatic convection-permitting HARMONIE numerical weather prediction model (Driesenaar, 2009). The preliminary results suggest that HARMONIE was able to simulate sea-effect snowfall sufficiently accurately and thus can be used to examine prominent weather situations to form snowbands (Fig. 3).

The Merikarvia case study is a continuation of a previous work in EXWE in 2015. Three past sea-effect snowfall cases (17–22 January 2006, 20–23 December 2011 and 1–4 February 2012) were then selected and examined (Luomaranta et al., 2016).

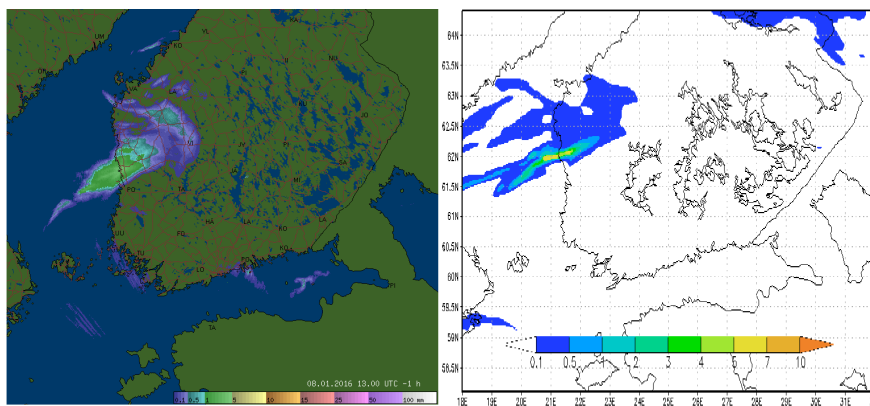


**Figure 3.** Sea-effect snowfall as observed by weather radar (left column) and simulated with the HARMONIE model (right column) at 13 UTC on 8 January 2016. The shading shows the accumulated precipitation (mm/h).

### Severe freezing rain

Climatological information about the occurrence of freezing rain (FZRA) can be produced by applying a precipitation typing algorithm that is based on vertical profiles of relative humidity and temperature. The algorithm utilizes threshold values that were first refined in EXWE in 2014 (Kämäräinen and Jokinen, 2014). Recalibrations of the algorithm were performed in 2015-2016 using an extended SYNOP weather station network in Europe. The method was then applied to the ERA-Interim reanalysis data during the period 1979-2014. The results were published as a discussion paper in Kämäräinen et al. (2016a), and in

February 2017, the manuscript was accepted to be published as a research article in *Natural Hazards and Earth System Sciences*.

Figure 4 shows the analyzed and observed empirical probabilities for duration and spatial extent of freezing rain events at weather station locations in Europe during the 1979-2014 period. Assuming that observations are correct, both the probabilities of duration and spatial extent are slightly overestimated by the analysis compared to observations in the most extreme tail of the cumulative probability distribution. In Europe the freezing rain events in coastal areas are spatially smaller compared to more continental areas so that the number of impacted stations in coastal areas is about 50% of the number of impacted stations in continental areas for all probability levels. On the other hand, the duration of the events is less dependent on the distance to the nearest coastline so that the most extreme events in all groups can last up to 40 hours.

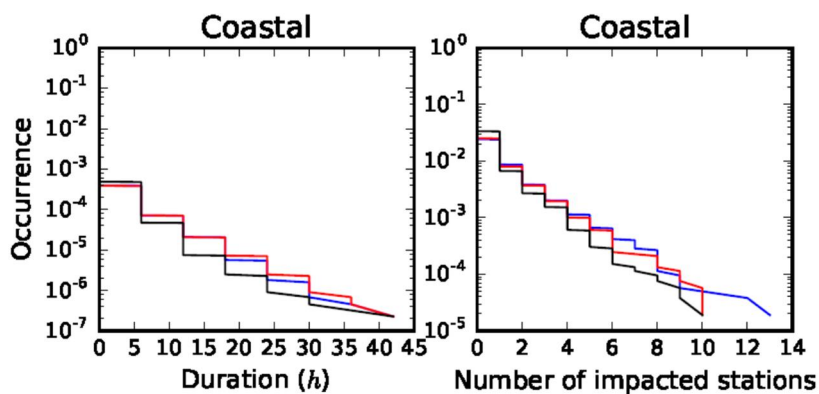


**Figure 4.** Cumulative probability distributions for duration (left column) and spatial extent (right column) of freezing rain events at coastal European weather stations in 1979-2014 according to the calibrated (blue) and uncalibrated (red) identification algorithms and observations (black). The distances of the stations (175 in total) to the nearest seashore are <140 km. Analysis is based on the ERA-Interim reanalysis data in 6-hourly time resolution. Observational data is also 6-hourly.

The recalibrated algorithm can also be applied to temporally and spatially dense regional climate model output in order to estimate changes in the occurrence and intensity of FZRA. For that purpose, Kämäräinen et al. (2016b) used different impact indicators to estimate whether the accumulated freezing rain amount exceeds certain thresholds (e.g. 0 mm, 5 mm, 25 mm) during different accumulation periods (e.g. over 6 hours, 24 hours, 72 hours). Based on the preliminary results, the previously derived results of increasing freezing rain probabilities in northern and decreasing in southern Europe can be confirmed. Nonetheless, the results were found to considerably vary between the regional models.

## Strong winds

A case study was performed about storm Mauri that hit Lapland in September 1982, resulting in two fatalities and 3 Mm<sup>3</sup> of forest damage. Mauri was found to have originated from hurricane Debby. The extratropical transition of Debby, synoptic evolution of Mauri and the large-scale circulation patterns of September 1982 were investigated using ERA-Interim reanalysis data. Unlike a typical extratropical cyclone, storm Mauri had a warm core and symmetric features (Laurila, 2016).

The most recent findings on strong winds have been summarized by Gregow et al. (2017). The findings suggest that a slight increase in the high wind speeds in Finland (sea areas and especially southern and western parts of the country) is likely, although there is variation between individual models. Climate change effects on the windstorms in Finland are more uncertain but an indication of change point regarding severe extra-tropical storms hitting Europe has evidently taken place in 1990 (highly significant result).

However, even if the windstorm climate in Finland remains the same, the impacts of the storms will alter due to the ongoing change in environmental conditions (decrease in soil frost, increase in forest growth), urbanization, and increased dependence on electricity and communication networks.

## An overview of sea level studies in EXWE

Extreme sea levels are crucial for the safety of the Finnish NPPs which are all located on coastal areas. Thus, sea level has been studied in EXWE since 2008. The different processes affecting sea levels on the Finnish coast on different timescales are illustrated in Fig. 5. The earlier studies in SAFIR2010 and SAFIR2014 focused on scenarios for the long-term mean sea level, as well as flooding risks related to short-term sea level variations at a time scale from hours to longer periods, based on conventional hourly sea level data (e.g. Johansson *et al.* 2011, Jylhä *et al.* 2015a).

In 2015-2016, we shifted the focus into even shorter-period variations. Short-period sea level oscillations, such as meteotsunamis, were studied from sea level data with sub-hourly resolution. The effect of wind waves was also included in the methods for estimating more accurately the location-specific flooding hazards related to storm surges. In addition to these new topics, a literature review on global mean sea level scenarios was performed. The purpose was to ensure whether the previously calculated local mean sea level scenarios (e.g. Kahma *et al.* 2014) are still valid or whether an update of those is needed.

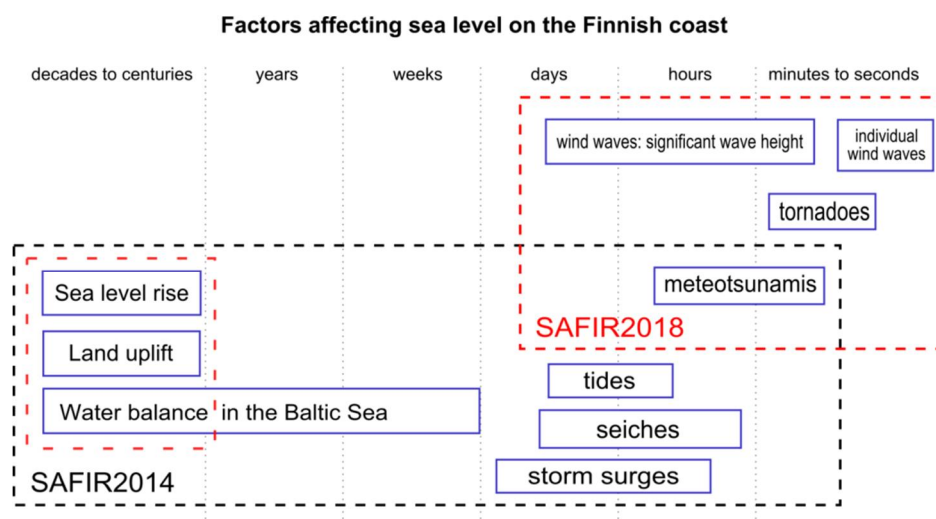


**Figure 5.** Several processes with time scales ranging from seconds to centuries affect sea level on the Finnish coast. In the SAFIR2018 programme (red), the focus of sea level research is on short-term sea level phenomena to complement previous analyses of long-term phenomena in SAFIR2014 (black). However, regular updates to long-term mean sea level scenarios are needed when new knowledge accumulates (hence, the dashed red box on left).

## Recent knowledge on global sea level rise

The long-term change of the mean sea level on the Finnish coast is affected by three factors: global sea level rise which is also reflected on the Baltic Sea, local postglacial land uplift in Scandinavia, and long-term changes in the Baltic Sea water balance. When calculating scenarios for sea level on the Finnish coast, the most relevant question is what happens with the global sea level rise in the future.

Scenarios for mean sea level on the Finnish coast were calculated by Johansson *et al.* (2014) and updated by Kahma *et al.* (2014), taking into account the Fifth Assessment Report (AR5) of the Intergovern-

mental Panel on Climate Change (IPCC, 2013). The mean sea level scenarios have been summarized e.g. in Jylhä *et al.* (2015b).

Pellikka (2016) conducted a literature review on current scenarios for the global mean sea level rise. The aim was to find out whether the recent results indicate a need to update the mean sea level scenarios for the Finnish coast. In Fig. 6, some recent predictions for the global sea level rise are presented together with those that were included in the previous scenarios for the Finnish coast (Kahma *et al.* 2014). In general, there are two methods for calculating global sea level scenarios. In process-based modelling approach, the different factors contributing to sea level rise – melting of ice sheets, glaciers and ice caps, thermal expansion, etc. – are modelled separately. In the semi-empirical approach, statistical relationship between global mean temperature (or radiative forcing) and sea level is derived from the past observations, and then applied to modelled temperature scenarios to obtain sea level predictions.

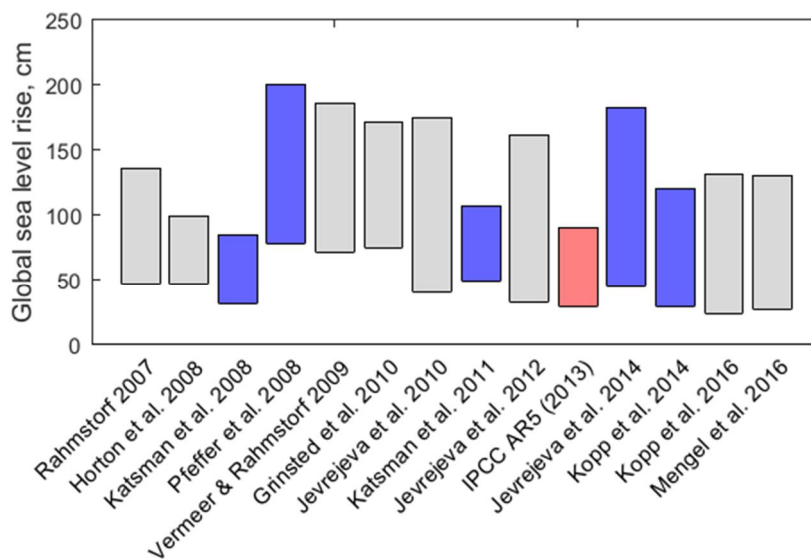


**Figure 6.** Recent sea level rise scenarios: range of predicted global mean sea level rise, normalized to the time interval 2000-2100. Blue bars represent scenarios based on process-based methods and expert assessments, gray bars are semi-empirical predictions. IPCC Fifth Assessment Report is plotted in red. (From Pellikka 2016)

Recent studies have not changed the overall uncertainty range of the global sea level rise projections for this century; they still extend from about 20 to 200 cm. The results do not imply a significant change in the previously published regional sea level scenarios for the Finnish coast. However, recent research has brought more information on the shape of the probability distribution of sea level rise, as well as on regional factors. These could be used to re-evaluate the method used to calculate the scenarios for Finland, but major changes on the scenarios are not expected.

The largest uncertainty in sea level rise predictions, especially in the northern latitudes, is the possible instability of the marine sectors of the Antarctic ice sheet. Recent observations indicate that the instability mechanism is real and already contributing to ice loss from the West Antarctic Ice Sheet. A worst-case estimate of a sea level rise contribution of more than 1 m from Antarctica was presented by DeConto and Pollard (2016), being higher than earlier estimates. This would mean a worst-case global mean sea level rise of about 2.5 m during this century, when combined with worst-case estimates for other sea level rise components: thermal expansion, melting of Greenland ice sheet, and melting of smaller glaciers and ice caps.

## Combined effect of sea level and wind waves on flooding risks

The height to which water rises in a flooding situation on a shore is affected not only by the sea level elevation, but also by the influence of waves on top of the sea level elevation. Local wave height conditions vary greatly depending on the shape of the shoreline, topography of the seabed, and archipelago shielding the coastline against largest waves. The flooding risk estimates for the Finnish coast have traditionally been based on the probability distribution of sea level extremes (e.g. Kahma *et al.* 2014), on top of which a location-specific constant value for wave action has been added.

Leijala *et al.* (2016, 2017) have started developing a new method for combining the effects of sea level extremes and wind-generated waves (wave run-up) to obtain a probability distribution representing their combined contribution to a flooding event. The height to which the continuous water mass (“the green water”) rises is calculated by combining:

- The extent of short-term sea level variability, obtained from local sea level observations.
- Scenarios for the mean sea level in the future.
- Wind-generated wave heights, obtained from local wave buoy measurements.

Probability distributions of these three variables are combined and different return periods for the joint effect are achieved for the current and future climate. Leijala *et al.* (2017) applied this method to two sites close to Helsinki, from where wave buoy measurements were available: one location close to the shore and the other location in the outer archipelago more exposed to open sea conditions. In this method the variables are treated as independent random variables, to yield the probability distribution of their sum. However, it is likely that sea level extremes and waves are not independent. Therefore, studying this dependency is a topic for further improvement of the method.

In the future, the method can be applied to NPP sites. Information on sea level variability on the entire Finnish coast is available, but to apply the method, information on the wave statistics is also needed. This can be obtained with local wave height measurements. Another option is to develop and validate a high-resolution wave model to obtain information on local wave conditions.

## Short-period sea level oscillations

Traditionally, the sea level studies and flooding risk estimates have been based on hourly or even scarcer sea level observations. These do not reveal rapid, sub-hourly oscillations, such as the several meteotsunamis observed on the Finnish coast in 2010 and 2011 (Pellikka *et al.* 2014). Pellikka *et al.* (2016, 2017) studied such rapid sea level oscillations by using sea level data with higher time resolution.

Meteotsunamis are tsunami-like waves caused by air pressure disturbances, such as thunderstorms, moving over the sea. When the speed of the disturbance coincides with the speed of a tsunami wave, the resonance between atmosphere and ocean leads to the amplification of the wave. Meteotsunami statistics for 1920s–1980s were obtained from archived tide gauge recordings from Hanko and Hamina (Pellikka *et al.* 2016): 45 events were identified from Hanko 1922–1989 (of which 27 or 60% were confirmed to be of meteorological origin from air pressure data) and 42 events from Hamina 1928–1989 (26 or 62% confirmed).

Typical meteotsunami heights recorded by the tide gauges were 10–30 cm, but the eyewitnesses have reported oscillations of even 50–100 cm. The eyewitness observations represent events in which the wave is locally amplified through resonance mechanisms related to coastal bathymetry. The meteotsunami probability distributions obtained from tide gauge data were extended towards stronger events by a simple scaling, backed with refraction model results. Fig. 7 shows the obtained meteotsunami statistics for Hanko. Such scaled distributions, however, are based on rather crude assumptions and have large uncertainties.

Sea level recordings at 1-minute time resolution are available from the Finnish tide gauges from 2004 onwards. Pellikka *et al.* (2017) analysed these data to find out what kind of meteorological conditions created the strongest events of rapid sea level oscillations. Synoptic conditions during some of the strongest events showed common patterns, but differed between the summer and winter seasons.

Summer events were generally caused by cold fronts or mesoscale convective systems, accompanied with thunder and rapid air pressure variations. The fronts were propagating over the sea with a resonant speed which matches the speed of a meteotsunami wave. Thus, these sea level oscillations were likely formed by a resonance-based mechanism of the waves. Highest recorded oscillations at the tide gauges were 15-44 cm, but locally the oscillations may be considerably stronger due to amplification by coastal topography.

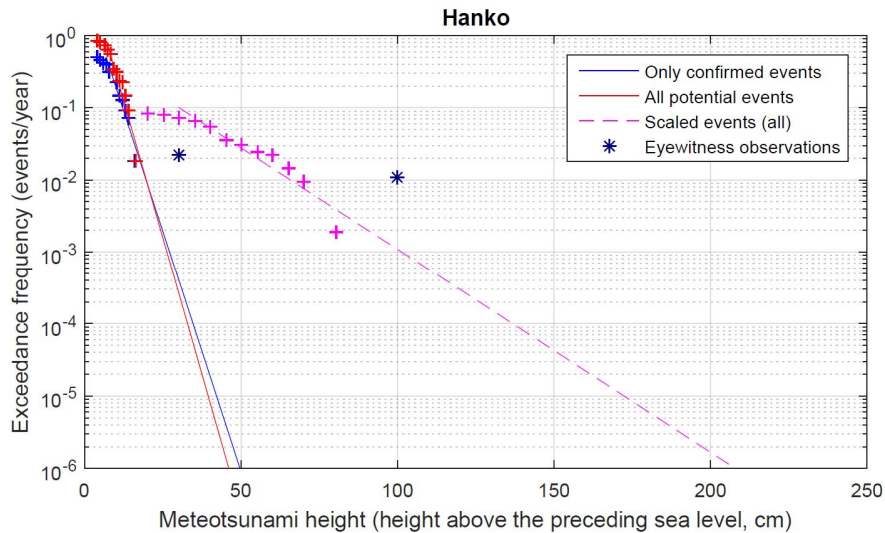


**Figure 7.** Probability distribution of the crest height of meteotsunamis recorded by the Hanko tide gauge (1922–1989). Blue crosses mark the events that have been confirmed from air pressure data, red crosses include all potential events, and crosses in magenta have been scaled with an amplification factor. Exponential distributions have been fitted to the data. Stars denote the eyewitness observations in Tvärminne in 1924 and 1927. (From Pellikka *et al.* 2016)

Winter events, on the other hand, were related to cold fronts propagating over the sea, with storm winds frequently present. Sea level oscillations were generally slower than during the summer events, indicating that the events were small storm surges rather than meteotsunamis. Highest recorded oscillations at the tide gauges were 12-38 cm, with locally stronger oscillations possible due to amplification. All of the winter events occurred in mild ice conditions. Sea ice forms annually in the Baltic Sea and may affect high-frequency sea level variations by preventing the effect of wind on sea surface and by attenuating waves.

## Extreme space weather and its effects

Normal operation of conductor systems, such as high-voltage power grids, may be disturbed by **geomagnetically induced currents** (GIC) that are quasi-DC currents compared to the AC frequency of 50 Hz (Molinski, 2002). GIC are driven by geoelectric fields at the Earth's surface that are caused by time variations of the geomagnetic field interacting with the solar wind. The solar wind is a stream of mainly protons and electrons emitted from the Sun, and it also carries a magnetic field. From the viewpoint of GIC, fast geomagnetic variations have the key role. Large magnetic storms can occur at any time during an approximately 11-year solar cycle, with the highest probability within a few years before and after the sunspot maximum. Spring and autumn are more likely seasons for enhanced activity than summer and winter. Diurnally, the probability of large GIC is related to the occurrence of auroras and is highest around the midnight (Viljanen *et al.*, 2012, 2014).

Globally, there have been only a few big events of geomagnetically induced currents per decade (Boteler *et al.*, 1998). Before 1989, GIC evidently caused only short terminations in power distribution. An exten-

sive blackout occurred in Québec, Canada, in March 1989 (Bolduc, 2002), and a transformer in New Jersey, USA, was permanently damaged (Kappenman and Albertson, 1990). In October 2003, there was a blackout in Malmö (Pulkkinen et al., 2005). One of the largest GIC events in Finland occurred on 24 March 1991, during which GIC up to 200 A were recorded at the Rauma 400 kV station (Fig. 8), however, without harmful impacts.

The number of direct observations of the geoelectric field in the Nordic countries is small. The largest values up to about 4-5 V/km are known from Sweden (Wik et al., 2009). It can be indirectly estimated that the peak maximum geoelectric fields in Finland have been at most some V/km. Besides direct observations, however, estimates for **peak geoelectric fields** can be grounded on model simulations.

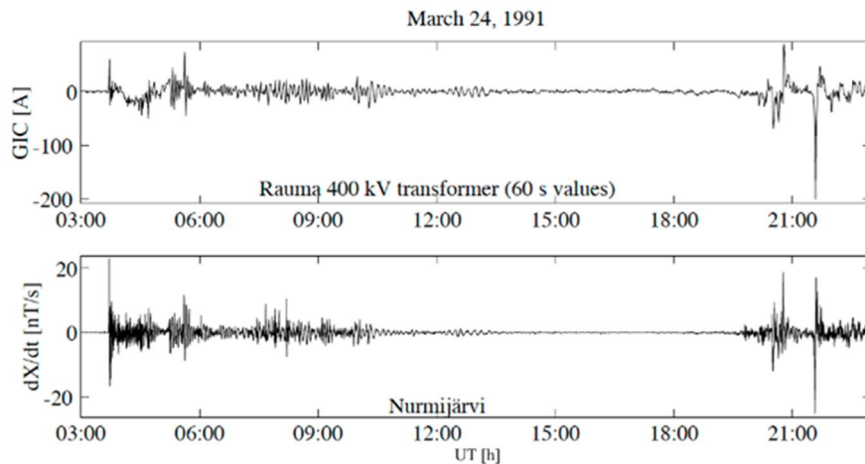


**Figure 8.** (Top) Measured geomagnetically induced currents (GIC) at the Rauma 400 kV station on 24 March 1991. (Bottom) An indicator of GIC activity, i.e. the time derivative of the northward magnetic field ( $dB/dt$ ), at the Nurmijärvi observatory during the same day.

Based on space plasma simulations, with hypothetical solar wind input, Ngwira et al. (2014) concluded that geoelectric fields larger than twice those produced by March 1989 or the October 2003 storms could occur. Ngwira et al. (2013) considered the July 2012 event when a strong solar wind burst was observed at the Earth's orbit, but aside our planet. A direct hit could have produced slightly larger electric fields than those during the March 1989 or the October 2003 storms.

Extreme geoelectric fields can also be assessed from the measured magnetic field and ground conductivity models. Viljanen et al. (2012) performed a modelling test using 1-min magnetic data from Nurmijärvi (1975-2015) and Sodankylä (1980-2010) and a simple 2-layer ground model. In that test, the largest storms appeared to be 13 July 1982 and 30 October 2003, impacts of which will be discussed below. At Nurmijärvi, the simulated July 1982 storm is about 1.5 times larger than the second largest one. The electric field reached equally large values at Nurmijärvi as at Sodankylä, under the assumption of identical ground conductivity models.

Using North European magnetometer data in 1993-2006 as input in their model of the electric field, Pulkkinen et al. (2012) found that a 1-in-100 year extreme value could be about twice the maximum in 1993-2006. Based on a similar analysis for Norway, Myllys et al. (2014) found the the 100-year maximum geoelectric field to be about twice the peak in 1994-2011 and close to the modelled electric field on 13-14 July 1982.

Wintoft et al. (2016) indicated that the largest possible electric fields might already have occurred at northern latitudes during the latest 20-30 years. However, we can still expect two times larger values within 50-150 years, or even more frequently in Central and Southern Europe. During frequently occurring moderate magnetic variations, the auroral oval stays over high latitudes where large values of an indicator of GIC activity, i.e. the time derivative of the northward magnetic field ( $dB/dt$ ) are observed. Extreme storms shift the oval southward causing large  $dB/dt$  farther south (cf. Tanskanen et al., 2002).

The longest high-resolution time series of modelled peak geoelectric fields, one for Victoria and the other for Ottawa, Canada, have been used by Nikitina et al. (2016) for extreme value analysis (Fig. 9a). The 1-in-50 years and 1-in-100 years return level estimates in Fig. 9a were normalized by Viljanen (2016a) with respect to the largest modelled geoelectric field that was calculated using the measured magnetic field at Canadian observatories. The results shown in Fig. 9b suggest that at observatories with data for at least 39 years, the extreme value is in nearly all cases only 10-20% larger than what would have been observed within the period covered by data. At other stations (17-31 years of data), a relatively larger extreme electric field is expected. So we concluded that a time series of about 40 years already contains an event close to the one expected to occur once in 100 years. On the other hand, time series of 30 years or shorter yield overestimated values for a once in 100 years event.

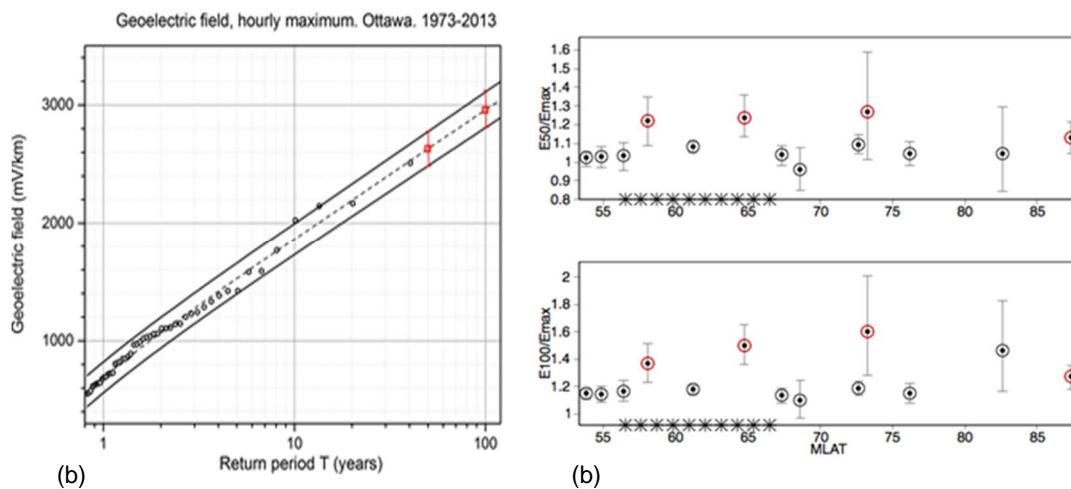


**Figure 9.** (a) Fitting of the modelled peak geoelectric fields (circles) in Ottawa to an extreme value distribution (dashed line) with 99% confidence intervals (solid lines). The predicted values once per 50 years and once per 100 years are denoted by red squares (Nikitina et al., 2016, Fig. 7). (b) Estimated 1-in-50 years (top) and 1-in-100 years (bottom) geoelectric field normalised by the maximum value modelled from magnetic data at Canadian observatories. Data coverage of 17-31 years is denoted by red and 39-42 years by black. Vertical bars indicate the 99% confidence intervals. The horizontal axis shows the geomagnetic latitude. Asterisks indicate the geomagnetic location of Finland. The plot is based on Nikitina et al. (2016, supporting information, Table S3).

Attention has concentrated on immediate impacts of GIC. However, Gaunt and Coetzee (2007) found increased levels of dissolved gases at South African high-voltage transformers after large storms in 2003, and suggested this to be the reason for that some transformers had to be removed from service after the stormiest period. Schrijver et al. (2014) analysed insurance claims for equipment losses and related business interruptions in North American commercial organizations that are associated with problems in electrical and electronic equipment. They found elevation of claim rates with increased geomagnetic activity.

GIC amplitudes as such do not provide a direct measure to assess risks, but we need to consider the tolerance of high-voltage transformers. Although currents up to 200 A have been measured in Finland (Fig. 8), and larger values have probably occurred, there have been no harmful impacts. This is due to the special design of the Finnish high-voltage power grid (Elovaara, 2007; Lahtinen and Elovaara, 2002). Lahtinen and Elovaara (2002) performed a test by feeding a large DC current through a 400 kV transformer. Based on this test and modelled GIC statistics, Lahtinen and Elovaara (2002) do not consider GIC as a significant risk in Finland. However, they note that the risk depends on the transformer design. Consequently, when installing new transformers, GIC is still one factor to be taken into account (cf. Viljanen, 2006b).

Nearly all studies of space weather effects on power grids consider only GIC. Molinski (2002) mentions that space weather affects ground-based communication systems, communication satellites and propagation of navigation signals reflected from or going through the ionosphere. He does not refer to any consequent impacts on power grids. However, Svenska Kraftnät (2012) recommends measures to be taken to ensure precise time information at substations, which could be endangered in case of GPS problems. There is an obvious need for a more extensive study on space weather effects on NPPs. Following Schrijver et al. (2014), a possible approach is to go through catalogues of all fault situations at NPPs and check whether there is correlation with space weather phenomena.

## High-resolution dispersion modelling

The dispersion calculations performed for nuclear safety assessments are typically based on Gaussian dispersion modelling. However, this assumption limits such studies to the range of 10–20 km from the site, and moreover, the Gaussian models are not well suited for simulating dispersion driven by highly dynamical and spatially complex mesoscale weather systems. Meanwhile, Lagrangian and Eulerian dispersion models, such as the FMI's SILAM model (Sofiev et al., 2006, 2015), have been developed for operational use in combination with numerical weather prediction models. Introduction of high resolution (up to 1–2 km) weather prediction systems opens up opportunities for high resolution dispersion modelling which resolves explicitly both mesoscale (convection, land-sea breezes) and large scale meteorological features. The work within this project aims to develop an integrated dispersion and dose assessment toolset based on connecting the SILAM dispersion model with state-of-the-art dose-assessment software.

The meteorological modelling, using e.g., the HARMONIE model already referred to before (Fig. 3), has progressed to a stage where a proper assessment of coastal meteorological conditions can be fed into the dispersion modelling system. Transport and dispersion of pollutants from a source located at the coast are subject to flow patterns and structures related to the contrasting aerodynamic roughness and thermal inertia of land and sea surfaces. Important coastal wind systems include the sea-breeze circulation blowing on shore at the surface and off shore aloft, and low-level jets blowing along the coastline. The atmospheric boundary layers over land and over sea are often quite different in height, stability, and turbulence; and flow across the coastline is then accompanied by a more-or-less marked internal boundary layer (IBL).

Operational weather prediction systems covering the Finnish domain employ a horizontal grid stepping of 2500 m at best, which is too coarse to be applicable in the kilometre-scale dispersion modelling targeted within EXWE. Therefore, a version of the HARMONIE numerical weather prediction system, suitable for providing input for high-resolution dispersion modelling on a kilometre-scale, was set up and executed on a domain of about 300 km x 300 km, with a grid having a spacing of only 500 m in the horizontal.

Accurate topographic data describing terrain-elevation, distribution and properties of water or land surfaces, land use, vegetation covers, built-up areas, etc. are all needed for a correct representation of the important air-surface interaction. Such data are collected from a large variety of sources, at varying spatial resolution, and have to be projected onto the computational grid of the user-model before they can be applied. Topographic data are often extremely heterogeneous or spatially discontinuous, so using adequate methods of aggregation and interpolation is essential. Currently-used methods in the HARMONIE weather prediction system are intended for a grid-spacing of several km. Modifications to the Harmonie system needed for to the high resolution runs are described in Kurzeneva et al. (2016).

The system was used to generate hind-casts for April and May 2015, when a rich set of remote-sense measurements by SODAR and LIDAR, as well as in situ data from a tower were available at Loviisa (Jurvanen, 2015). In the hind cast runs, HARMONIE was nested into operational forecasts from the European Centre for Medium Range Weather forecasts (ECMWF) providing lateral boundary conditions, as well as initial conditions for atmospheric variables every six hours. Initial conditions for surface variables were obtained by assimilating available observations. A continuous stream of output data was created, with a temporal resolution of 1 hour.

Comparing model data to observations confirms that Harmonie responds to the thermal and mechanical contrast between land and sea in a realistic manner, so that forecasts generated by the system are likely

to become a valuable data source for dispersion modelling and dispersion forecasting. A few examples of are given below. Fig. 10 shows the vertical distribution of the wind direction up to the height to 200 m, as retrieved from LIDAR and as given by HARMONIE, during three days early in May 2015. Observed variations appear to be well captured by the model. For the horizontal and vertical wind speeds, more differences were found. Variations in wind direction and speed associated with the sea-breeze circulation developing in response to differential heating over land and sea on the cloudless afternoon of 3 May, turning the low level wind from a roughly westerly direction into SW is especially well simulated by the model.

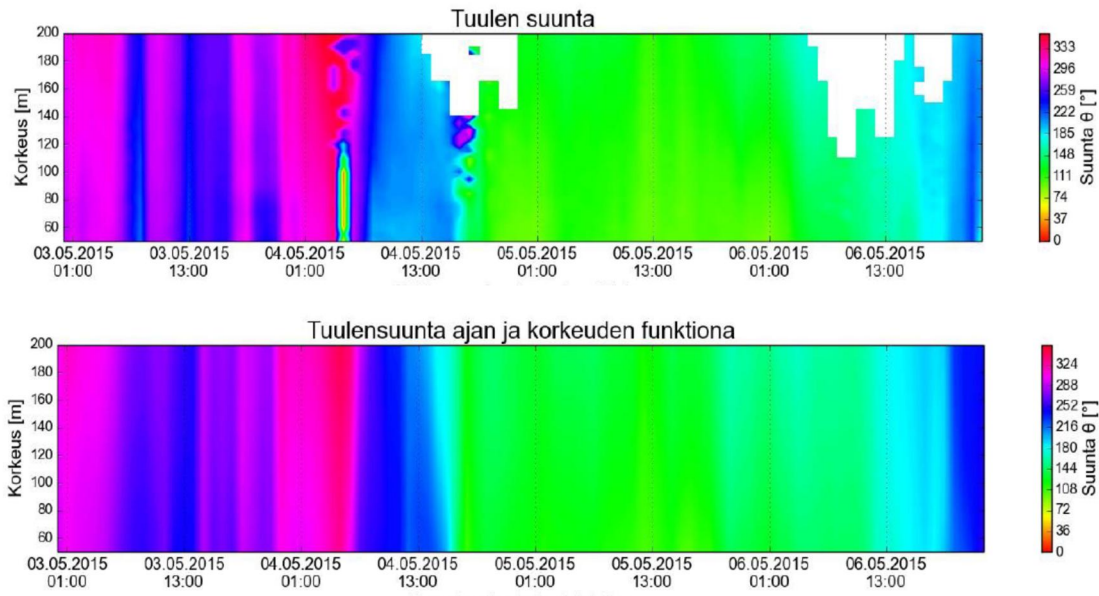


**Figure 10.** Wind direction as a function of height and time at Loviisa Hästholmen on 3-6 May 2015, as retrieved from LIDAR measurements (top) and HARMONIE model simulations (bottom).

An example of the transition from a marine boundary layer structure to a coastal one is shown in Fig. 10a, displaying profiles of potential temperature from Harmonie on 15 UTC on 4 May, extracted along a line passing Loviisa power plant from south to north. It can be clearly seen, how the cold surface temperature and stably stratified marine boundary layer found over the Gulf of Finland, gradually gives way to a heated surface and a convective well-mixed over the inland. As the distance from the coast increases, so does the temperature and the depth of the well mixed layer.

Further details of the transition are shown in Fig. 10b, showing the intrusion of the marine boundary layer structure on top of the heated surface near the coast, and the gradual increase of turbulence in the mixed layer.

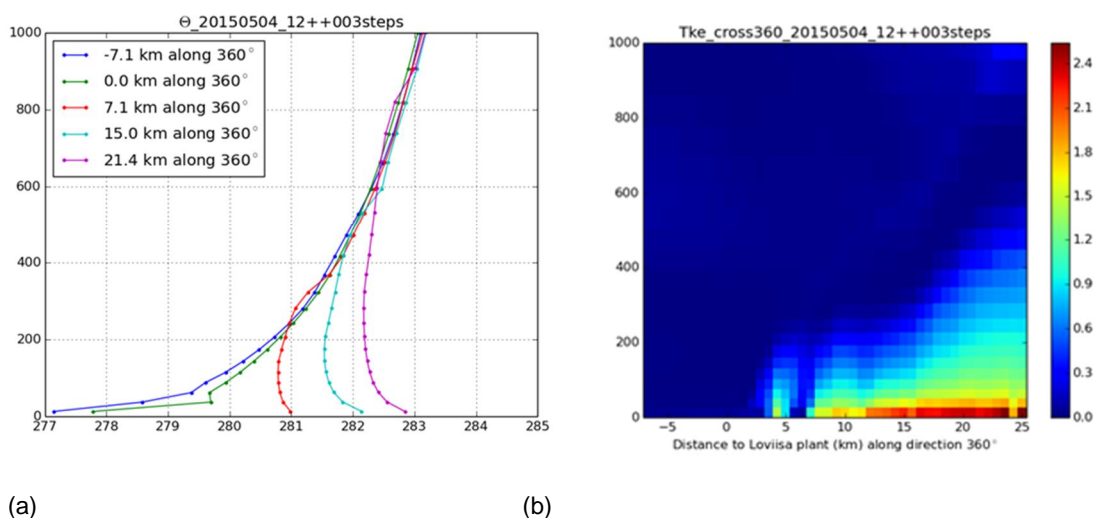


**Figure 11.** (a) Modelled potential temperature and (b) turbulent kinetic energy (right) at 15 UTC on 4 May 2015 along a line passing the Loviisa NPP from south to north, i.e. from the sea (negative distances) to the land (positive distances).

We made some preliminary test runs for connecting high-resolution (500-1000 m) HARMONIE data to SILAM during 2016. Mainly for FMI's own SILAM development but also partially for EXWE, new radioactive dose calculation models were also integrated to SILAM. Work was done on a major update of SILAM dose-module development and interface of this module with the main SILAM core. This work laid down the foundation of the SILAM interface towards the impact assessment applications Sofiev et al. (2017) documented in detail the current user interface for SILAM v5 chemical transport model.

## Conclusions

The main findings of EXWE in 2015-2016 are given below:

- The historical time series of extreme convective weather (ECW) observations for hail, heavy rainfall, thunderstorms, lightning and tornadoes are combined and analysed. A notable cross correlation exists between 1) thunderstorm days, lightning and heavy rainfall, 2) heavy rainfall and tornadoes and 3) large hail and tornadoes.
- Atmospheric conditions and synoptic-scale circulation patterns favouring significant hail (diameter of 5 cm or larger) can be clustered into four distinct synoptic classes, two of which resemble the patterns observed in tornado situations in Finland. The remaining classes seem more unique. Every third hail day had at least one tornado report and two of the three hail days had daily rainfall of 30 mm or more.
- Hourly weather radar images and simulations with the non-hydrostatic convection-permitting HARMONIE numerical weather prediction model were used to examine a record-breaking sea-effect snowfall case that took place at Merikarvia on 8 January 2016. HARMONIE was found capture the the timing and the location of the most intense snowstorm.
- After calibrations against SYNOP weather station observations in Europe, a method for estimating the occurrence of freezing rain (FZRA) in gridded atmospheric datasets was used together with re-analysis data and output from regional climate models. Freezing rain probabilities are projected to increase in northern and decrease in southern Europe, although there is a wide scatter across the regional models.

- Even if the windstorm climate in Finland remains the same, the impacts of the storms will alter due to the ongoing change in environmental conditions (decrease in soil frost, increase in forest growth), urbanization, and increased dependence on electricity and communication networks.
- Recent scenarios for the global mean sea level rise do not differ markedly from the earlier results, and thus no major changes on the mean sea level scenarios for the Finnish coast are expected. However, the calculation method could be improved by taking into account available new information on the shape of the probability distribution of sea level rise, and regional factors. The largest uncertainty in the sea level scenarios is still the response of the Antarctic ice sheets to a warming climate.
- Combining the effects of sea level and wind-generated waves yields more accurate location-specific probability estimates for the flooding risks than the sea level based estimates alone. The method for combining the probability distributions of these two factors will be developed further in the future.
- Rapid sea level oscillations of up to 100 cm have been observed on the Finnish coast. The synoptic conditions during these events differ between different seasons; the summer events are likely meteotsunamis, while the winter events are small storm surges. The occurrence frequency estimates for these rapid oscillations are still based on rather crude assumptions, and more research is needed to better assess their frequencies on the Finnish coast.
- In high-voltage power grids, geomagnetically induced currents (GIC) can cause transformer failures, malfunctioning of protection relays, and blackouts (Québec 1989, Malmö 2003). In Finland, no serious effects have occurred, thanks to the robust design of the high-voltage grid. Because large GIC events can still be expected, they must be taken into account when installing new transformers or power lines affecting the GIC distribution across the grid.
- Introduction of high resolution (up to 1–2 km) weather prediction systems opens up opportunities for high resolution dispersion modelling which resolves explicitly both mesoscale (convection, land-sea breezes) and large scale meteorological features. The work within this project aims to develop an integrated dispersion and dose assessment toolset based on connecting the SILAM dispersion model with state-of-the-art dose-assessment software.
- High-resolution meteorological modelling has progressed to a stage where a proper assessment of coastal meteorological conditions can be fed into the dispersion modelling system. Transport and dispersion of pollutants from a source located at the coast are subject to flow patterns and structures related to the contrasting aerodynamic roughness and thermal inertia of land and sea surfaces. Important coastal wind systems include the sea-breeze circulation blowing on shore at the surface and off shore aloft, and low-level jets blowing along the coastline. The atmospheric boundary layers over land and over sea are often quite different in height, stability, and turbulence; and flow across the coastline is then accompanied by a more-or-less marked internal boundary layer (IBL).

## Acknowledgement

In addition to the funding granted by the State Nuclear Waste Management Fund in Finland, this work has been partly finalized by the Swedish Radiation Safety Authority, the Finnish Meteorological Institute, the European Union's Seventh Programme for research, technological development and demonstration under the RAIN project (Risk Analysis of Infrastructure Networks in response to extreme weather; <http://rain-project.eu/>; grant agreement no. 608166) and the EU funded Copernicus Climate Changes Service Clim4Energy project (<http://clim4energy.climate.copernicus.eu/>). We acknowledge Fingrid for long-term collaboration in studies of geomagnetically induced currents in the Finnish high-voltage power grid.

## References

- Bolduc, L., 2002. GIC observations and studies in the Hydro-Québec power system. *J. Atmos. Sol.-Terr. Phys.*, 64, 1793-1802, doi:10.1016/S1364-6826(02)00128-1.
- Boteler, D.H., Pirjola, R.J. & Nevanlinna, H., 1998. The effects of geomagnetic disturbances on electrical systems at the earth's surface. *Adv. Space Res.*, 22, 17-27, doi:10.1016/S0273-1177(97)01096-X.
- Bolduc, L., 2002. GIC observations and studies in the Hydro-Québec power system. *J. Atmos. Sol.-Terr. Phys.*, 64, 1793-1802, doi:10.1016/S1364-6826(02)00128-1.
- DeConto, R.M. & Pollard, D. 2016. Contribution of Antarctica to past and future sea-level rise. *Nature* 531 (7596), 591–597.
- Driesenaar, T. (2009) General description of the HARMONIE model. Available at <http://hirlam.org/index.php/hirlam-programme-53/general-model-description/mesoscale-harmonie>
- Elovaara, J., 2007. Finnish experiences with grid effects of GIC's. In: *Space Weather - Research Towards Applications in Europe* (ed. J. Liliensten), *Astrophysics and Space Science Library*, 344, 311-326, Springer.
- Elovaara, J., Lindblad, P., Viljanen, A., Mäkinen, T., Pirjola, R., Larsson S. & Kielén, B., 1992. Geomagnetically induced currents in the Nordic power system and their effects on equipment, control, protection and operation. Paper 36-301 of the Proceedings of the CIGRE 1992 Session, 30 August - 5 September, 1992, Paris, 10 pp.
- Fortum 2015. Safety-enhancing cooling towers for Fortum's Loviisa nuclear power plant completed. Fortum Corporation Press Release 21 April 2015. <http://www.fortum.com/en/mediaroom>
- Gaunt, C.T. & Coetzee, G., 2007. Transformer failures in regions incorrectly considered to have low GIC-risk. Proceedings of the IEEE Powertech Conference, July 2007, Lausanne, Switzerland, paper 445, 6 pp, doi: 0.1109/PCT.2007.4538419.
- Gregow H., T. Laurila, A. Mäkelä, 2017. Review on strong winds in Northern Europe in the past, current and future climate. EXWE/SAFIR2018 project report 2016, FMI.
- IPCC, 2013. Summary for Policymakers. In: *Climate Change 2013: The Physical Science Basis. Contribution of Working Group I to the Fifth Assessment Report of the Intergovernmental Panel on Climate Change* [Stocker, T.F. & coauthors (eds.)]. Cambridge University Press, Cambridge, United Kingdom and New York, NY, USA.
- Johansson, M., Kahma, K., Pellikka, H., 2011. Sea level scenarios and extreme events on the Finnish coast. In: *SAFIR2010, The Finnish Research Programme on Nuclear Power Plant Safety 2007-2010, Final Report*. Puska, E.-K., Suolanen, V. (Eds.) VTT Tiedotteita – Research Notes: 2571 2011. VTT, Espoo, p. 570-578.
- Johansson, M.M., Pellikka, H., Kahma, K.K. & Ruosteenoja, K. 2014. Global sea level rise scenarios adapted to the Finnish coast. *Journal of Marine Systems* 129, 35–46.

- Jurvanen, 2015: Sekoituskerroksen korkeuden arviointi eri menetelmin Loviisan ydinvoimalaitoksen läheisyydessä. Master's thesis, University of Helsinki, Department of physics (in Finnish).
- Jylhä, K., Pellikka, H., Kämäräinen, M., Johansson, M., Saku, S., Jokinen, P., Kahma, K., Venäläinen, A., Gregow, H., 2015a. Extreme weather and nuclear power plants - EXWE summary report. In: Hämäläinen, J. and Suolonen, V. (eds.): SAFIR2014 - The Finnish Research Programme on Nuclear Power Plant Safety 2011-2014 Final Report. VTT Technology 213, Kuopio, p. 620-629.
- Jylhä K., Pellikka, H., Kämäräinen, M., Johansson, M., Saku, S., Jokinen, P., Kahma, K., Venäläinen, A. & Gregow, H (eds.) 2015b. Extreme weather and sea level events as potential external threats to nuclear power plant safety — Synthesis of the EXWE project outcomes in 2011-2014. EXWE project report, FMI.
- Kahma, K., Pellikka, H., Leinonen, K., Leijala, U. & Johansson, M., 2014. Pitkän aikavälin tulvariskit ja alimmat suositeltavat rakentamiskorkeudet Suomen rannikolla. Ilmatieteen laitos, Raportteja 2014:6. 48 p.
- Kappenman, J.G. & Albertson, V.D., 1990. Bracing for the geomagnetic storms. IEEE Spectrum, March 1990, 27-33.
- Kurzeneva, E., Fortelius, C., Karppinen A., and Sofiev, M. 2016. HARMONIE code update for preparation of high-resolution physiography data files. EXWE/SAFIR2018 project report, FMI.
- Kämäräinen, M. & Jokinen, P. 2015. Severe winter weather in Finland: Part II: Freezing rain and lake-effect snowfall. EXWE/SAFIR2014 project report 2014, Finnish Meteorological Institute.
- Kämäräinen, M., Hyvärinen, O., Jylhä, K., Vajda, A., Neiglick, S., Nuottokari, J., and Gregow, H., 2016a: A method to estimate freezing rain climatology from ERA-Interim reanalysis over Europe. Nat. Hazards Earth Syst. Sci. Discuss., doi:10.5194/nhess-2016-225, in review.
- Kämäräinen M., Vajda A., Hyvärinen O., Lehtonen I., and Jylhä K., 2016b: Future projections of freezing rain climatology in Europe. EMS Annual Meeting Abstracts, Vol. 13, EMS2016-399-1, 2016, 16th EMS/11th ECAC. <http://meetingorganizer.copernicus.org/EMS2016/EMS2016-399-1.pdf>
- Lahtinen, M. & Elovaara, J., 2002. GIC Occurrences and GIC Test for 400 kV System Transformer. IEEE Trans. Power Delivery, 17, 555-561.
- Laurila, T. 2016. Extratropical transition and characteristics of storm Mauri in September 1982. Master thesis, Univ. of Helsinki, Department of Physics, 51 p.
- Laurila T., J. Rauhala, T. Olsson, A. Mäkelä, K. Jylhä, 2016: Historical time series of extreme convective weather. EXWE/SAFIR2018 project report 2016, FMI.
- Leijala, U., Johansson, M.M., Björkqvist, J-V., Kahma, K.K. & Särkkä, J. 2016. Joint effect of high sea level and high wind waves. EXWE/SAFIR2018 project report 2015, FMI.
- Leijala, U., Björkqvist, J-V., Kahma, K.K. & Johansson, M., 2017. A probabilistic approach for combining sea level variations and wind waves. Draft, to be submitted to Coastal Engineering.

- Luomaranta, A., Kämäräinen, M., Laurila, T., and Jylhä K., 2016: Severe winter weather in Finland, Part III: Past sea-effect snowfall cases and predictors of extreme cold-season convective weather. EXWE/SAFIR2018 project report 2015, FMI.
- Mazon J., Niemelä S., Pino D., Savijärvi H., and Vihma T., 2015. Snowbands over the Gulf of Finland in wintertime. *Tellus A* 2015, 67, 25102, <http://dx.doi.org/10.3402/tellusa.v67.25102>.
- Molinski, T.S., 2002. Why utilities respect geomagnetically induced currents. *J. Atmos. Sol.-Terr. Phys.*, 64, 1765-1778, doi:10.1016/S1364-6826(02)00126-8.
- Myllys, M., Viljanen, A., Rui Ø.A. & Ohnstad, T.M., 2014. Geomagnetically induced currents in Norway: the northernmost high-voltage power grid in the world. *J. Space Weather Space Clim.*, 4, A10, doi: 10.1051/ swsc/2014007.
- Mäkelä, A., J. Rauhala, A.-J. Punkka, J. Tuovinen, K. Jylhä, 2016. Past cases of extreme warm season convective weather in Finland. EXWE/SAFIR2018 project report 2015, FMI.
- Ngwira, C.M., Pulkkinen, A., Leila Mays, M., Kuznetsova, M.M., Galvin, A.B., Simunac K., Baker, D.N., Li, X., Zheng Y. & Glocer, A., 2013. Simulation of the 23 July 2012 extreme space weather event: What if this extremely rare CME was Earth directed? *Space Weather*, 11, doi:10.1002/2013SW000990.
- Ngwira, C.M., Pulkkinen, A., Kuznetsova, M.M. & Glocer, A., 2014. Modeling extreme "Carrington-type" space weather events using three-dimensional global MHD simulations. *J. Geophys. Res. Space Physics*, 119, 4456-4474, doi:10.1002/2013JA019661.
- Nikitina, L., Trichtchenko, L. & Boteler, D.H., 2016. Assessment of extreme values in geomagnetic and geoelectric field variations for Canada. *Space Weather*, 14, doi:10.1002/2016SW001386.
- Pellikka, H., Rauhala, J., Kahma, K.K., Stipa, T., Boman, H. & Kangas, A. 2014. Recent observations of meteotsunamis on the Finnish coast. *Natural Hazards* 74, 197–215.
- Pellikka, H., Kahma, K., Karjalainen, A. & Boman, H. 2016. Meteotsunami probabilities at the Finnish NPP sites. EXWE/SAFIR2018 project report 2016, FMI..
- Pellikka, H. 2016. Recent results on future sea level rise and ice sheet instability. Literature review. EXWE/SAFIR2018 project report 2016, FMI.
- Pellikka, H., Šepić, J., Lehtonen, I. & Vilibić, I. 2017. Synoptic features of high-frequency sea level oscillations in the northern Baltic Sea. Draft, to be submitted to ...
- Pulkkinen, A., Bernabeu, E., Eichner, J., Beggan, C. & Thomson, A.W.P., 2012. Generation of 100-year geomagnetically induced current scenarios. *Space Weather*, 10, S04003, doi:10.1029/2011SW000750.
- Pulkkinen, A., Lindahl, S., Viljanen, A. & Pirjola, R., 2005. October 29-31, 2003 geomagnetic storm: geomagnetically induced currents and their relation to problems in the Swedish high-voltage power transmission system. *Space Weather*, 3, S08C03, doi: 10.1029/2004SW000123.
- Rangarayan, G.K., 1989. Indices of Geomagnetic Activity, in: *Geomagnetism*, Volume 3 (ed. J.A. Jacobs), Academic Press, 32-384.

- Rauhala J., T. Laurila, A. Mäkelä, K. Jylhä, 2017: Atmospheric conditions and circulation patterns favouring severe convective storm weather in Finland: synoptic setting of significant hail. EXWE/SAFIR2018 project report 2016, FMI.
- Schrijver, C.J., Dobbins, R., Murtagh, W. & Petrinec, S.M., 2014. Assessing the impact of space weather on the electric power grid based on insurance claims for industrial electrical equipment. *Space Weather*, 12, doi:10.1002/2014SW001066.
- Sofiev, M., Vira, J., Kouznetsov, R., Prank, M., Soares, J., Genikhovich, E., 2015. Construction of an Eulerian atmospheric dispersion model based on the advection algorithm of M.Galperin: dynamic cores v.4 and 5 of SILAM v.5.5, *Geosci.Model Developm. Discuss.*
- Sofiev, M., Vira, J., Kouznetsov, R., Prank, M., Soares, J., Genikhovich, E., 2015. Construction of the SILAM Eulerian atmospheric dispersion model based on the advection algorithm of Michael Galperin, *Geosci.Model Developm.* 8, 3497-3522, doi:10.5194/gmd-8-3497-2015.
- Svenska Kraftnät, 2012. Skydd mot geomagnetiska stormar - Elektromagnetisk påverkan på kraftsystemet (in Swedish), Dnr: 2011/805, 30 March 2012.
- Tanskanen, E., Pulkkinen, T.I., Koskinen, H.E.J. & Slavin, J.A., 2002. Substorm energy budget during low and high solar activity: 1997 and 1999 compared. *J. Geophys. Res.*, 107(A6), doi:10.1029/2001JA900153.
- Ukkonen P., Manzato A., Mäkelä, A. 2016 Evaluation of thunderstorm predictors for Finland using reanalyses and neural networks. Submitted to *Journal of Applied Meteorology and Climatology*.
- Viitanen P., R. Rantamäki, P. Alenius, H. Gregow, M. Johansson, P. Jokinen, K. Jylhä, H. Mäkelä, S. Saku and S. Syri, 2013. Adaptation measures for Finnish NPPs, case study for the OECD/NEA project. Referred to at <https://www.iea.org/media/workshops/2013/egrdrutrecht/17.Paillere.pdf>
- Viljanen, A., 2016a. Extreme space weather effects on nuclear power plants. EXWE/SAFIR2018 project report 2016, FMI.
- Viljanen, A., 2006b. Olkiluodon 400 kV muuntajan GIC-virran arviointi (in Finnish). Research report for Teollisuuden Voima Oy (not publicly available).
- Viljanen, A., Pirjola, R., Pracser, E., Katkalov, J. & Wik, M., 2014. Geomagnetically induced currents in Europe. Modelled occurrence in a continent-wide power grid. *J. Space Weather Space Clim.*, 4, A09, doi: 10.1051/ swsc/2014006.
- Viljanen, A., Pirjola R., Wik, M., Adam, A., Pracser, E., Sakharov, Ya. & Katkalov, Yu., 2012. Continental scale modelling of geomagnetically induced currents. *J. Space Weather Space Clim.*, 2, A17, doi:10.1051/ swsc/ 2012017.
- Wik, M., Pirjola, R., Lundstedt, H., Viljanen, A., Wintoft P. & Pulkkinen, A., 2009. Space weather events in July 1982 and October 2003 and the effects of geomagnetically induced currents on Swedish technical systems. *Ann. Geophys.*, 27, 1775-1787.
- Wintoft, P., Viljanen, A. & Wik, M., 2016. Extreme value analysis of the time derivative of the horizontal magnetic field and computed electric field. *Ann. Geophys.*, 34, 485-491, doi:10.5194/angeo-34-485-2016.

### 3.5 Fire risk evaluation and Defence-in-Depth (FIREd)

Anna Matala<sup>1</sup>, Topi Sikanen<sup>1</sup>, Jukka Vaari<sup>1</sup>, Antti Paaajanen<sup>1</sup>; Deepak Paudel<sup>2</sup>, Simo Hostikka<sup>2</sup>

<sup>1</sup>VTT Technical Research Centre of Finland Ltd  
P.O. Box 1000, FI-02044 Espoo

<sup>2</sup>Aalto University  
P.O. Box 12100, FI-00076 AALTO

#### Abstract

A significant proportion of the overall core damage risk in nuclear power plants (NPP) is associated with internal fires. In addition, a fire on NPP can cause large financial losses even if the risk to the reactor safety was small. Therefore the possible initiating event scenarios and the operation of defence-in-depth after ignition are important topics in the research of nuclear safety. The computational tools that are used for assessing the fire risks have developed significantly over the last ten years: The deterministic analyses are increasingly based on CFD and the probabilistic analyses using Monte Carlo simulation have been carried out. These developments have improved the reliability and accuracy of the safety analyses. In FIREd project, the research on fire risks and defence-in-depth is focused on three main topics: evaluating the fire risks of cables during plant life cycle, assessing the performance of fire-barriers, and development, maintenance and validation of fire simulation tools.

#### Introduction

The development of the computational tools have enabled more accurate and reliable deterministic analysis on fire safety of nuclear power plants. These methods need continuous effort on tool development, maintenance and increasing competence. In addition, model verification and validation are an essential part of the process.

The main objective of the FIREd project is to develop the tools for fire risk evaluation and create a new methodology for assessing the defense-in-depth in the context of fire safety. The work cannot concentrate only on the current needs or challenges, but we need to be prepared also for the future, whether it means gaining experience on the novel methodologies, or developing capabilities to assess new materials.

The project concentrates on three main topics:

1. Cable fire risks during plant life cycle,
2. Performance of the fire-barriers, and
3. Tool development, maintenance and validation.

The fire risk related to electrical cables is studied from two points of view: by investigating the possibility of simulating the flame retardants in the molecular level, and by studying experimentally the ageing effect on the fire performance of the modern flame retarded cables during the plant life cycle.

Developing capability for predicting the fire resistance of a barrier element in the fire-CFD and in other tools is the focus of the second main topic. Model uncertainty, and especially the uncertainty when two or more models are coupled, is studied statistically using Monte Carlo simulations. The wider context and implementation of fire defence-in-depth concept is also explored.

The tool development, maintenance and validation is mainly concentrated on the development of Fire Dynamics Simulator (FDS, McGrattan et al. 2014). The work of 2015-2016 has concentrated on simulating liquid pool fires. The model validation work is supported by participation to the OECD/NEA PRISME2 project, an extensive experimental program that provides good quality measurements of large scale fire scenarios.

The most important results of FIREd project from the years 2015-2016 are summarised in this report.

## Fire cable risks during plant life cycle

Multiple molecular dynamics models were used to study the decomposition of ATH, both with and without the presence of the HDPE matrix, and to quantify the specific heat contributions mentioned above. Atomistic representations of the following material components were used as a starting point (See Figure 1):

Gibbsite, the most stable polymorph of aluminium (tri)hydroxide is also the mineral form relevant for the fire retardancy application. The gibbsite structure consists of stacked sheets of linked octahedrons of aluminium hydroxide. For further information on the structure, see (Balan et al. 2006).

Corundum, the most stable polymorph of alumina, was used to model the solid residue of the ATH decomposition reaction. This is an idealization, since the residue is not expected to be perfectly crystalline in reality. For further information on the structure, see (Lewis, Schwarzenbach, and Flack 1982).

HDPE, the high-density form of polyethylene, was used as the matrix material. A perfectly crystalline form with no branching was used. This is, again, an idealization, since the degree of crystallinity of HDPE is typically much less. For further information on the structure, see (Kleis et al. 2007).

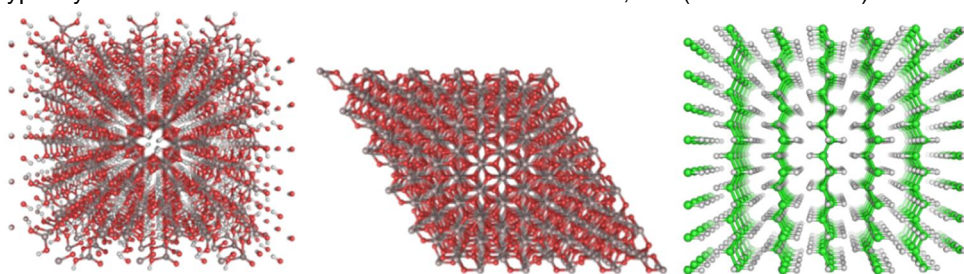


**Figure 1.** Periodic simulation box used for gibbsite (left), corundum (middle) and HDPE (right).

Decomposition simulations were performed on the different-sized versions of the gibbsite structure, as well as the HDPE-gibbsite nanocomposite (Figure 2). The high-temperature decomposition process was mimicked by a 20 ns simulation in a hybrid NVT-NVE ensemble at temperatures ranging from 1000 K to 2500 K. Each simulation was divided into 200 intervals of 100 ps. After each 100 ps interval, the molecules  $H_2$ ,  $CH_4$ ,  $H_2O$  and  $CO_2$  were removed from the system to imitate the emission of gaseous products.

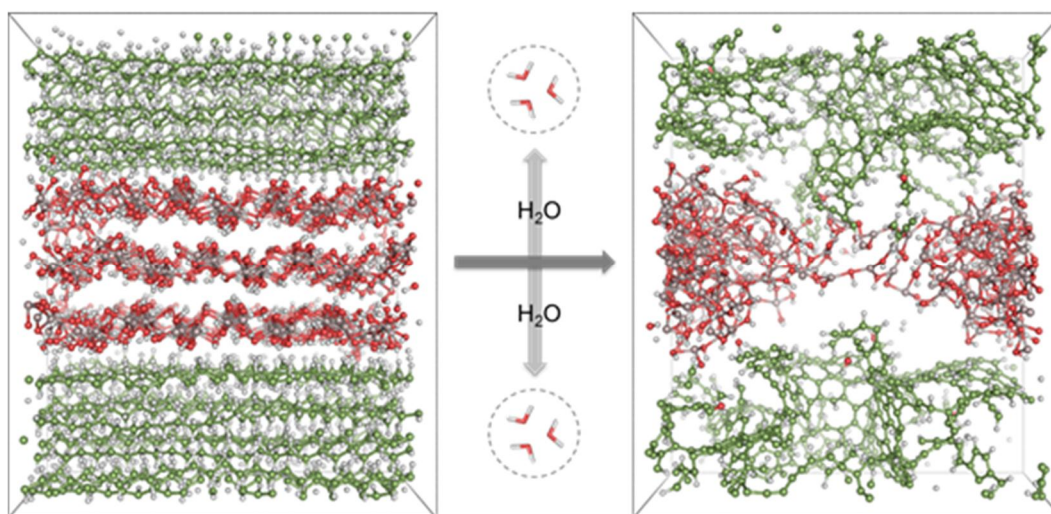


**Figure 2.** RMD decomposition model of a HDPE-gibbsite nanocomposite: (left) initial configuration and (right) final configuration after a 20 ns simulation at 2500 K with removal of water, hydrogen, methane and carbon dioxide molecules. Colour code: aluminium in dark grey, carbon in green, hydrogen in grey and oxygen in red.

We used the occurrence of water molecules in the simulations as a means to quantify the kinetics of the conversion reaction. The water production curves for pure ATH were fitted to a total of 17 different kinetics models, as given by Khawam and Flanagan (2006). Overall, the best fit to the simulated water production curves was provided by the model class based on diffusion as the rate-controlling mechanism. The results are shown in Figure 3. No fit was performed at 2000 K due to the limited amount of simulated data. The shape of the fitted curve agreed perfectly with the simulated data at  $t=2500$  K, but could not be made to conform to the curves at lower temperatures with the degrees of freedom available. In addition, fixing both A and E for all temperatures resulted in even poorer fits. Given that the ratio  $E/A$  is significant for the fits, we decided to fix A and let E vary. Letting A vary for a fixed E would have resulted in an decreasing trend for A as a function of temperature, which is not in line with the physical interpretation for A.

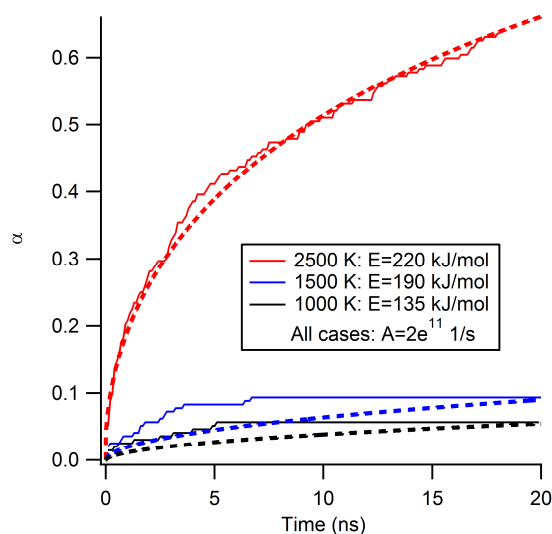


**Figure 3.** Simulated water production curves for pure ATH together with fits based on a diffusion controlled reaction model.

No kinetics analysis was performed for the ATH+HDPE system. It was found that the decomposition data for the ATH+HDPE system confirmed the presence of a chemical contribution of the base polymer to the fire retardant mechanism, providing a second reaction pathway and complicating the kinetics analysis. The water yield at high temperatures could only be explained such that hydrogen from polyethylene is present in the product molecules. This implies that ATH promotes carbonization of the base polymer, which can be considered a chemical mechanism of fire retardancy (due to the formation of an insulating char layer), demonstrating the predictive potential of the RMD method.

In addition to the decomposition kinetics, the RMD simulations provided an accurate enthalpy of decomposition for ATH, and reasonable ballpark estimates for the specific heat capacity contributions of each constituent.

*The effects of ageing of the cable materials* to the fire safety were studied experimentally. The operation conditions in a cable room include elevated temperatures (40-65 °C for I&C cables, and up to 80-90 °C for power cables including self-heating, IAEA 2012) and some radiation exposure. Naturally there is no real experimental evidence on the ageing effects on the cable materials, as it is not possible to find exactly same product with equal composition as decades old and as a brand new. Even less experience can be found concerning the novel flame retardant cables that will be installed to the new plants. Therefore, the ageing studied are often performed using accelerated ageing process. In accelerated ageing, the material sample is exposed to higher temperatures, higher radiation doses, or both, for certain length of time. In case of thermal ageing, the corresponding service temperature and service time can be calculated from the small scale experimental results (e.g., Bell & Sizmann 1966, Gillen & Clough 1997, Bystriskava et al.

2013). Higher temperatures accelerate the ageing process, but too high temperatures can lead to thermal degradation of the polymer during ageing.

In the first phase of the work, two types of FRNC cables were aged thermally (105 °C, 36-54 days) to correspond 40 and 60 years of service life in operating conditions. The fire performance of these two cable types were then compared to new, non-aged cables. The experimental work included small scale testing using microscale combustion calorimeter (MCC), and bench scale testing using cone calorimeter at two heat fluxes (30 and 50 kW/m<sup>2</sup>). The results did not show any significant differences in the fire behaviour in small or in bench scale (see Figure 4). The differences between repeated experiments were in the same order of magnitude than the differences between the new and thermally aged cables.

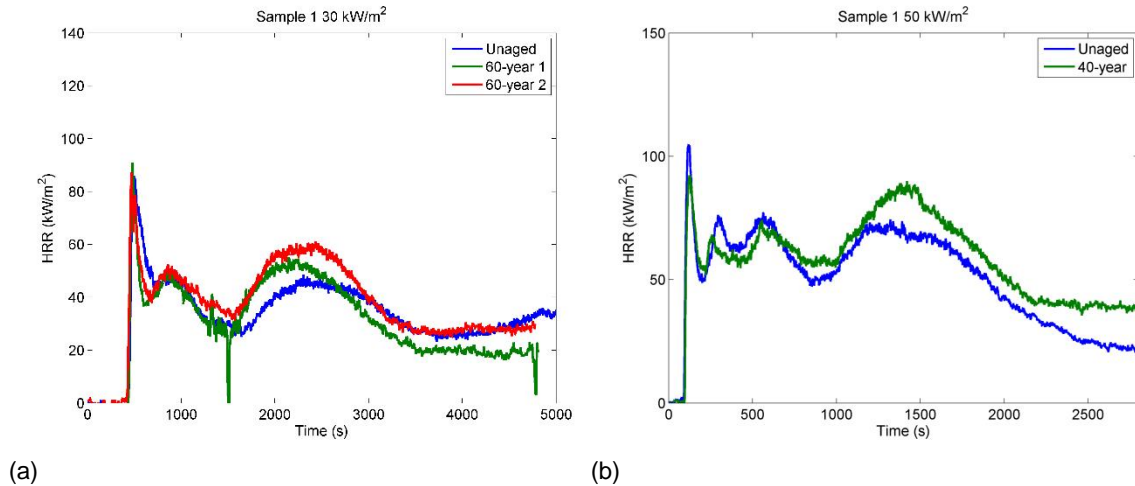


**Figure 4.** Cone calorimeter results of a cable sample 1. (a) at 30 kW/m<sup>2</sup>. (b) at 50 kW/m<sup>2</sup>.

In the second phase of the work the cable samples were exposed to a 0.3-0.4 kGy/h dose rate in 75 °C temperature (close to the operating temperature of a power cable including self-heating). The total dose was 200 kGy. This corresponds to roughly 45 years of a service life in normal conditions, or a LOCA scenario. The cables were tested in small scale using thermogravimetric analysis (TGA) and cone calorimeter at two heat fluxes (30 and 50 kW/m<sup>2</sup>). In small scale, the results between new and radiated cables were almost identical and it was concluded that the radiation did not alter the chemical composition of the cable sheath material. However, the cone calorimeter results (especially the results at 50 kW/m<sup>2</sup>) showed small, but significant changes in the fire behaviour. Some of the cone calorimeter results are shown in Figure 5. Experimental variation is known to be related to the cone calorimeter experiments to some extent. When the results were compared to the repeatability limits of the cone calorimeter method, few quantities were observed to be outside of the normal repeatability limits; the time to ignition was slightly decreased with radiated cables, and the peak heat release rate and the effective heat of combustion were slightly increased. The exact degradation mechanism is not known but it can be speculated that it may have something to do with cracking of the sample surface which would lead to the loss of thermal shielding provided by the flame retardants.

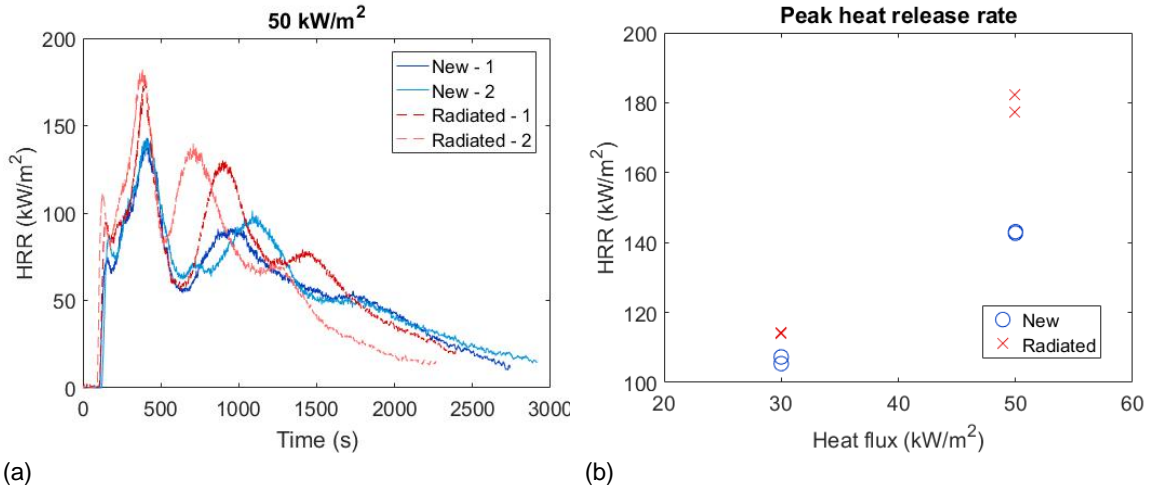


**Figure 5.** Cone calorimeter results of new and radiated cable samples. (a) Heat release rate at 50 kW/m<sup>2</sup>. (b) Peak heat release rate.

The both experimental sets include some uncertainties related to the generalisation of the results. First of all, the sample size was small, only 1-2 experiments at each conditions, due to lack of sample material. It is not possible to make definitive conclusions based on just a few tests, keeping in mind the normal experimental variation. The testing also involved only a few, quite identical types of FRNC cables. The test results could be different using cables from different manufacturers, or different materials. It is also not clear how well the accelerated ageing process relates to the real, slower ageing of a material. Still, it can be concluded that in certain conditions, the combined radiation and thermal ageing does slightly modify the fire behaviour of a flame retarded cable by weakening the protection provided by the flame retardant.

### Fire-barrier performance assessment

Accurate simulation of fire-structure response demands coupling of two or more numerical models, e.g. Computational Fluid Dynamic (CFD) model to estimate the gas temperature during fire and FEM/FDM based heat diffusion model to estimate barrier thermal response. Modelling uncertainty of each model affects the uncertainty measure of the output quantity on a different scale. A simple statistical relationship has been formulated with a aim to bypass the modelling errors associated with each link leading to the estimation of true output uncertainty,

$$\sigma_{\hat{Y}}^2 = \delta^2 \sigma_Y^2 + \sigma_{\epsilon}^2 \quad (1)$$

Where  $\sigma_Y$  and  $\sigma_{\hat{Y}}$  are the measure of true and observed output uncertainty,  $\delta$  and  $\sigma_{\epsilon}$  are the quantitative measure of total modelling error. In this regard the output uncertainty is assumed to be affected by two distinct sources of uncertainties; i) Uncertain input parameters ii) Modelling uncertainty associated with physical assumption, model structure and simplification. Uncertainty in input and output parameter can be expressed as squareroot of second central moment, i.e, Standard deviation. Explanation of modelling uncertainty however requires two different error parameters i) Systematic bias ( $\delta$ ): a measure of the factor by which the model output falls above or below the true value. ii) Random error ( $\epsilon$ ): inherent unpredictable error in the model; quantitatively a particular value of standard deviation about zero mean. Systematic bias and random error of a model are estimated by comparing model outputs with experimental measurements. To develop a method to estimate the combined error, we had to assume a scenario: A fire barrier, represented by a concrete slab, is exposed to hot gas (constant temperature), and the heat conduction is simulated using a 1D Finite Element Method (FEM). The model calculates the barrier's cold side temperature based on the gas temperature, ambient temperature, wall thickness and material parameters. Gas tem-

perature and its associated uncertainty values are boundary conditions to the 1D heat conduction model. Concrete material properties are considered as uncertain input parameters for the stochastic analysis. The adopted stochastic method for the estimation of true and the simulated output quantity is Monte-Carlo simulation with Latin Hypercube Sampling (LHS). Modelling errors were arbitrary but selected according to the ones reported for the FDS fire simulation software (McGrattan et al. 2013).

Figure 6a shows the distribution of gas temperature and Figure 6b shows an example of the true, observed and estimated output distributions, in a case where there is systematic bias and the random error in both gas temperature and heat conduction model {Gas, Wall}. The errors are imposed at each iteration of MC simulation. FEM model takes into account both radiative and convective heat fluxes ("both") and the distribution type selected for both, the input gas temperature and the wall material properties is normal distribution ("n.n").

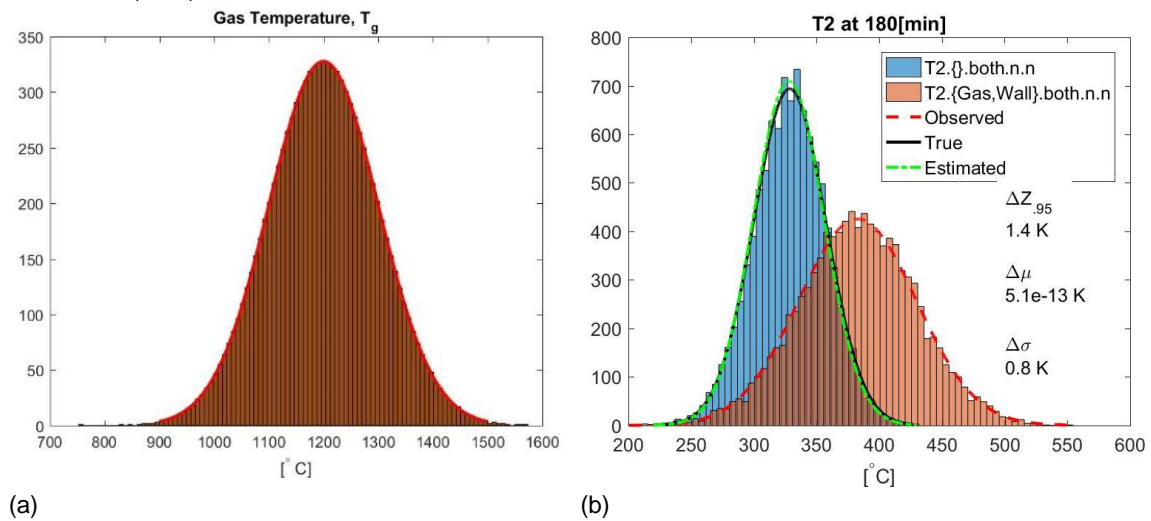


**Figure 6.** (a) Gaussian profile of Gas temperature, a input parameter for stochastic analysis. (b) True, observed and estimated distribution of cold side temperature, T2 at = 180 [min].

From the **Figure 6b** one can notice that the estimated output distribution closely matches the true output distribution. This indicates that the true distribution of the output can be estimated using a simple statistical relationship (Eq. (1)) provided that the quantitative measure of total modelling error is available.

A separate stochastic analysis was carried in order to create a plot that shows the modelling accuracy requirement for heat diffusion model such that the uncertainty in the prediction of wall temperature do not exceed the acceptable uncertainty range. Figure 7a shows the uncertainty in the prediction of cold side temperature with respect to the relative standard deviation in random errors of heat diffusion model. A line residing at the upper edge of the band correspond to systematic bias value of 1.5 and the one on the lower edge correspond to 0.5. Similarly, Figure 7b plots the probability that the cold surface of wall to reaches 312 °C within 24 hours. The systematic bias and relative standard deviation of random errors in gas temperature estimation for FDS model are neary 1.1 and 0.1 respectively (McGrattan et. al. 2013).

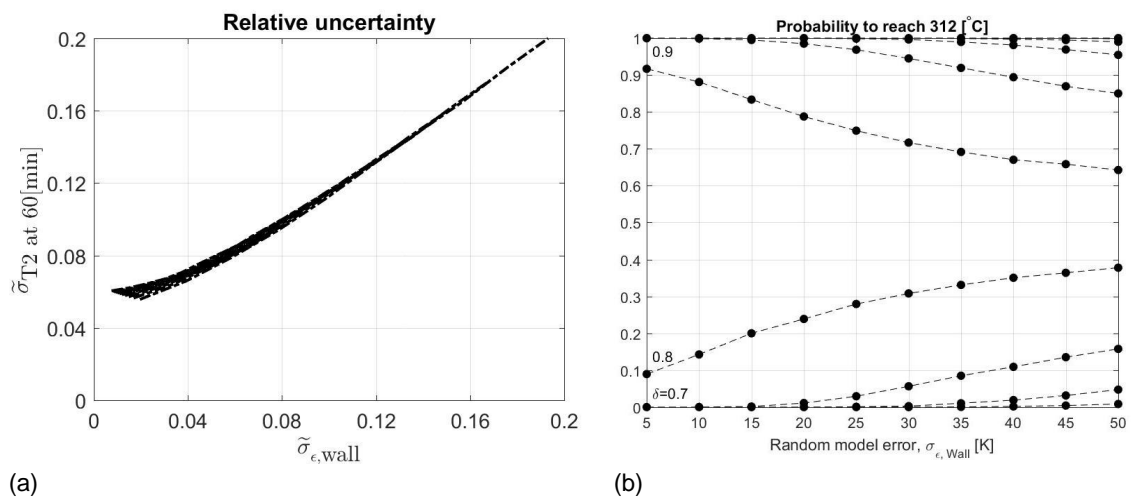


**Figure 7.** (a) Relative uncertainty in the estimation of cold side temperature. (b) Probability for the cold side temperature to reach 312 °C.

From Figure 7a, we can read the required wall model accuracy (horizontal axis) given the expected uncertainty of the cold side temperature (vertical axis). For example, in order to obtain a relative uncertainty in the cold side temperature less than 0.1, we must make sure that the the relative standard deviation of wall model's random errors is less than about 0.08. Figure 7b shows that the bias error in the heat diffusion model can effect the measure of barrier failure probability significantly.

### Fire simulation development, maintenance and validation

In 2015 methodology for predicting the spreading and combustion of liquid fuel released from an aircraft impact was validated and a journal manuscript was written of the results. Calculations were done with Fire Dynamics Simulator, and the aircraft impact was modeled as a spray boundary condition. The spray boundary condition was developed and validated using data from the IMPACT experiments using water-filled missiles. The predicted liquid front speeds were compared with water spray front propagation data (see Figure 8). The predicted lifetimes and diameters of fireballs were compared with experimental correlations (see Figure 9). A full-scale simulation of the aircraft impact on a nuclear island was performed. The simulation results were used to assess the adequacy of physical separation in the case of aircraft impact. We concluded that 10–20% of the fuel involved in the crash will accumulate in pools around the building.

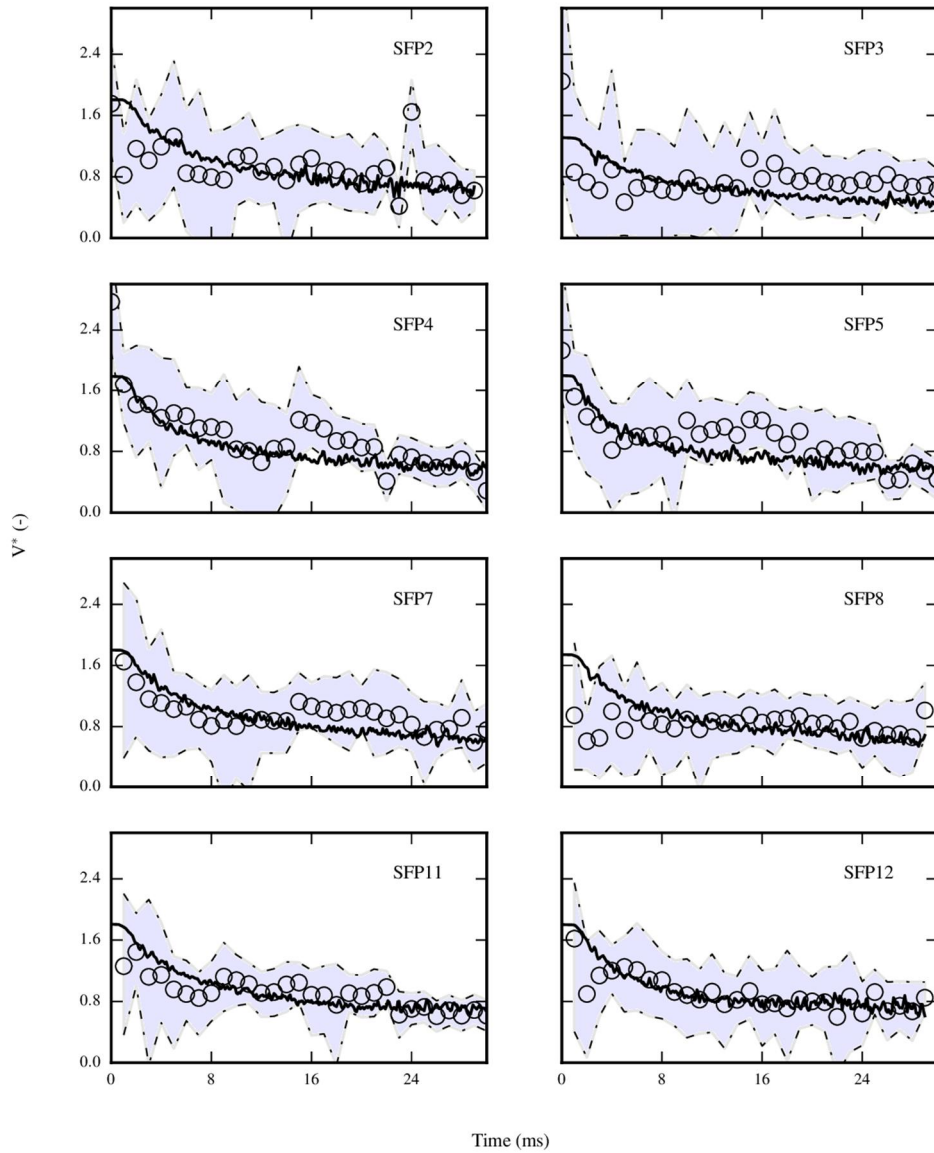


**Figure 8.** Validation of FDS spray model using the IMPACT experiment series. On the y-axis, spray front propagation velocity nondimensionalized by impact velocity. The shaded area shows variation in experimental measurements. The open circles show the median of the experimental data. Black line shows FDS predictions.

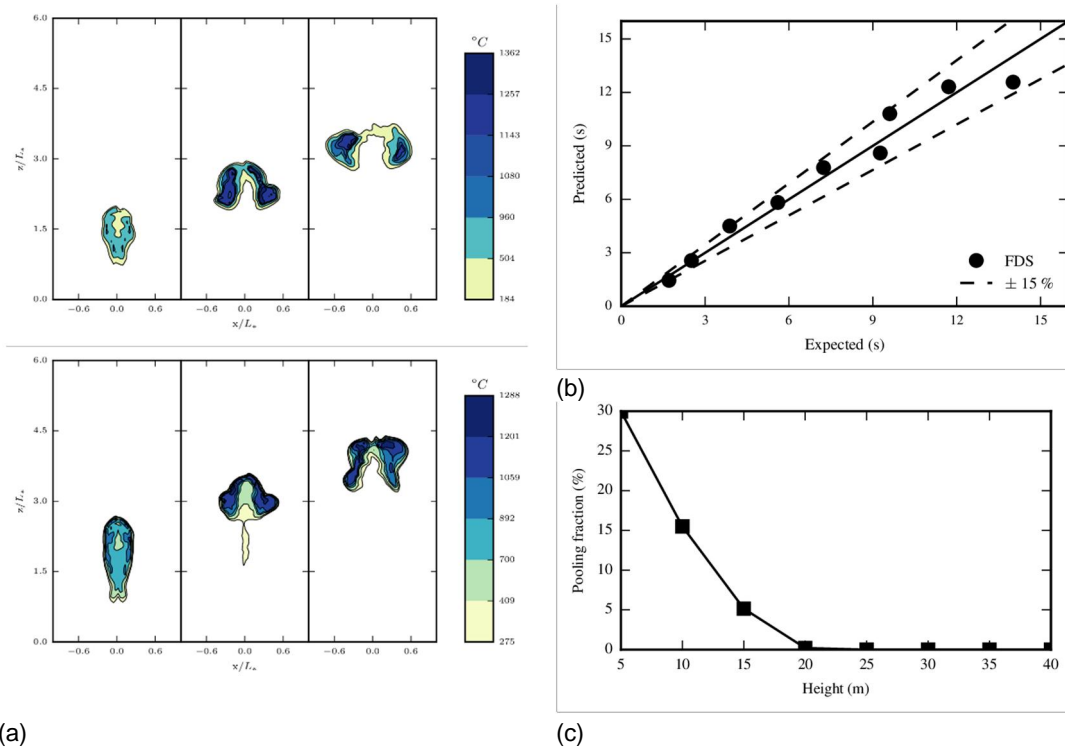


**Figure 9.** (a) Instantaneous shapes of fireballs resulting from vertical releases of fuel. (b) Predicted fireball lifetimes compared with correlation. (c) Pooling fraction as function of impact height from ground.

In 2016 predictive simulations of liquid pool fires in mechanically ventilated compartments were conducted. The results showed that code is capable of predicting the steady state burning rates of the TPH pool fires in in compartments within 15% of the experimental value. The effect of lowered oxygen vitiation on the burning rate of pool fires was correctly captured. Simulations were done using the Fire Dynamics Simulator and the experiments considered were conducted in the OECD PRISME project. The main difference between the conducted study and previous simulation studies is the use of a detailed liquid evaporation model and the direct calculation of the vitiation and thermal environment interactions through the CFD solver.

In some simulations, the predicted burning rate showed strong oscillations that were not observed in the experiments. Similar oscillations have been observed in other experiments conducted in the same enclosure, though. The appearance of the oscillations was found to depend on the details of the geometry, grid resolution and the combustion modelling options.

It was also found that the 1-d heat transfer model employed in this work could not reproduce the temperature gradient in the liquid phase. It is possible, that the gradual rise seen in burning rates of open atmosphere pool fires could be explained by enhanced heat transfer within the liquid phase by , e.g., lateral convection. The effect of non-gray radiation transport should also be investigated in the future.

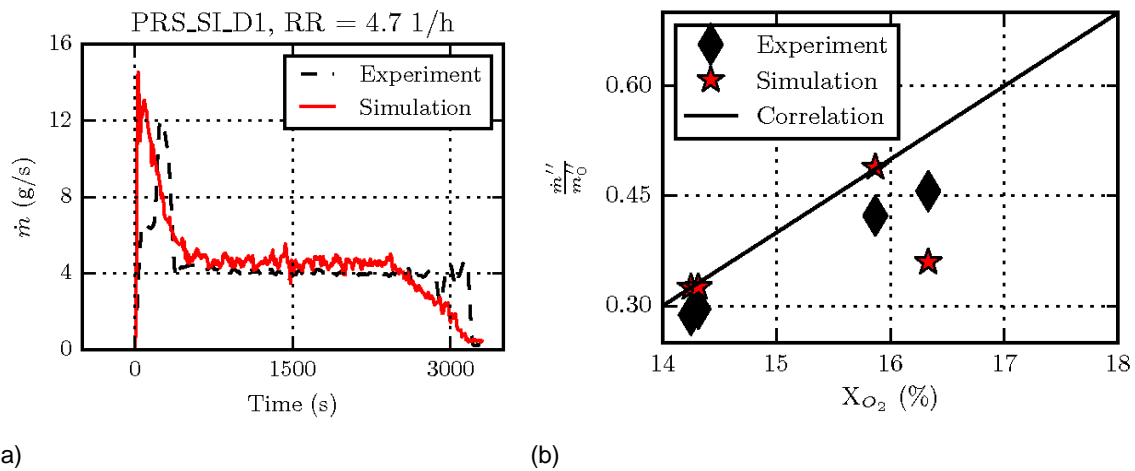


**Figure 10.** (a) Comparison of predicted and experimental burning rates for a liquid pool fire in a mechanically ventilated room (PRISME Source PRS\_Sl\_D1). (b) Burning rates as a function of oxygen concentration near the pool floor for the PRISME Source tests.

## Acknowledgement

Antti Pasanen from VTT is acknowledged for carrying out the thermogravimetric experiments.

## References

- Balan, E. Lazzeri, M. Morin, G. and Mauri, F.. 2006. "First-Principles Study of the OH-Stretching Modes of Gibbsite." *American Mineralogist* 91 (1): 115–19. doi:10.2138/am.2006.1922.
- Bell, F. and Sizmann, R. 1966. Determination of Activation Energy from Step Annealing. *Phys. stat. sol.* 15, pp.369.
- Bystritskaya, E.V., Monakhova, T.V. and Ivanov, V.B. 2013. TGA application for optimising the accelerated aging conditions and predictions of thermal aging of rubber. *Polymer Testing* 32, pp.197-201.
- Gillen, J.T. and Clough, R.L. 1997. Prediction of Elastomer Lifetimes from Accelerated Thermal-Ageing Experiments. *Proceedings of Elastomer-service life prediction symposium, Ohio, USA.*
- IAEA. 2012. *Assessing and Managing Cable Ageing in Nuclear Power Plants.* IAEA nuclear energy series No. NP-T-3.6, 111 p.
- Khawam A., Flanagan DR. 2006. Solid-State Kinetic Models: Basics and Mathematical Fundamentals. *J Phys Chem B* 110(35):17315–17328
- Kleis, J., Lundqvist, B.I., Langreth, D.C. and Schröder, E.. 2007. "Towards a Working Density-Functional Theory for Polymers: First-Principles Determination of the Polyethylene Crystal Structure." *Physical Review B - Condensed Matter and Materials Physics* 76 (10): 2–5. doi:10.1103/PhysRevB.76.100201.

Lewis, J., Schwarzenbach, D. and Flack, H.D. 1982. "Electric Field Gradients and Charge Density in Corundum,  $\alpha$ -Al<sub>2</sub>O<sub>3</sub>." Acta Crystallographica Section A 38 (5): 733–39. doi:10.1107/S0567739482001478.

McGrattan, K., Hostikka, S., McDermott, R., Floyd, J., Weinschenk, C. and Overholt, K. 2013. Fire Dynamic Simulator Technical Reference Guide Volume 3: Validation, NIST Special Publication 1018-3.

McGrattan, K., Hostikka, S., Floyd, J., McDermott, R., Weinschenk, C. and Overholt, K. (2014) Fire Dynamics Simulator Technical Reference Guide. Volume 1: Mathematical Model. NIST Special Publication 1018, Sixth Edition.

### 3.6 Safety of new reactor technologies (GENXFIN)

Sami Penttilä<sup>1</sup>, Jarno Kolehmainen<sup>1</sup>, Aki Toivonen<sup>1</sup>, Tarja Jäppinen<sup>1</sup>, Pekka Nevasmaa<sup>1</sup>, Ville Tulkki<sup>1</sup>, Antti Rantakaulio<sup>2</sup>, Mikko Niemi<sup>2</sup>

<sup>1</sup>VTT Technical Research Centre of Finland Ltd  
P.O. Box 1000, FI-02044 Espoo

<sup>2</sup>Fortum Power and Heat Oy  
P.O. Box 100, FI-00048 FORTUM

#### Abstract

The main mission of the GENXFIN project is to improve scientific and technologic expertise in the field of new nuclear energy technologies and related processes through international collaboration. The main objective is to coordinate participation in various international working groups and information dissemination on interested parties. Essential part of the project was to get familiar with the licensing of innovative Small Modular Reactor (SMR) concepts which is interesting from a national perspective. Material Research on new reactor technologies has an educational role in Finland but it is also a platform for technology development. In order to mitigate the worst effects of climate change the whole energy sector needs to be decarbonized.

#### Introduction

Finland has limited resources to follow the developments in reactor technology, let alone make significant developments of our own. In the current world, however, the operating environment is changing at such a pace that it is imperative to systematically follow this development in order to run the current NPP's and those under construction both safely and economically. Among the known changes are the German "Energiewende", the French strategy for maximum 50% nuclear by 2025 and the decisions to advance shut-downs of certain NPPs, and plans for future reactors in Europe. However, the implications are not as well known.

For the past ten years, a networking project called GEN4FIN (<http://gen4fin.vtt.fi>) has been active in keeping abreast of Generation IV (Gen4) reactor technology. Recently Small Modular Reactors (SMR) have been added to the agenda of GEN4FIN. As many of the research issues are cross-cutting across reactor types and generations, the best way to disseminate the information collected in this effort is the SAFIR2018 programme.

In this new mode of operation, the networking project GENXFIN was established to follow developments and coordinate national projects related with new reactor technologies, including Gen4, SMR and CHP (Combined Heat & Power). Additionally, combined technical-economic issues will be covered, for example load following and grid developments related with new kinds of electricity generating systems, as well as advanced fuel cycles. The objective of the GEN4FIN project has been to enhance national expertise in science and technology of nuclear reactors. The project has international cooperation within GIF (Generation IV International Forum), EERA (European Energy Research Alliance) and Nordic-Gen4 network project, as well as in some Coordinated Research Projects (CRP) of the IAEA and in ESNII (European Sustainable Nuclear Industrial Initiative). This type of international cooperation will continue within GENXFIN project.

In the long term, the goal in GENXFIN is to create new expertise on nuclear energy and business opportunities for the Finnish industry by promoting technology transfer, innovative industrial processes and materials technology. The GEN4FIN network created a national roadmap on Generation IV (Kyrki-

Rajamäki et al. 2008) where the Finnish participation of Gen4 research and development was planned. The network participated actively in the national research strategy project (YES) under the MEE in 2013 - 2014. In 2015, the GEN4FIN network has continued its activities in the traditional mode of operation and made plans for the coming years in the current operating environment that has changed since the start. This planning phase led to a decision to initiate the GENXFİN.

Research on future reactor technologies has an educational role in Finland but it is also a platform for technology development. Licensing of innovative reactor concepts like SMRs is interesting from a national perspective, and the network has added now SMR's on its research agenda. It is important to consider the feasibility of new technologies including scientific, technical, economic and political aspects.

### **Safety features and licensing issues of integral pressurized water small and modular reactors**

The Finnish regulatory guides on nuclear safety define the main requirements that a new nuclear power plant must fulfil to be able to be licensed in Finland. In GENXFİN project the main safety features of selected SMR designs were described and obstacles seen in the licensing process investigated. Also special attention was paid to the treatment of passive safety systems. The scope of this investigation was limited to light water reactors because the currently operated reactors in Finland are LWRs in which the regulations are based on.

The interest in SMRs has been recently growing internationally because their potential for climate change mitigation has been realized. The small reactor size of SMRs may make it possible e.g. to replace old coal-fired power plants at existing sites (OECD, 2011). Other common reasons for deployment of SMRs are desalination of seawater, combined power and heat (CPH) production, grid balancing and production of process heat.

Integrated pressurized water reactor (IPWR) SMRs (NuScale and SMART) were the main designs studied, because the licensing process of these kinds of reactors is in very advanced stage. The research has been carried out in cooperation between VTT and Fortum. The fundamental safety functions of SMART and NuScale reactor are evaluated more precisely. The examination of the NuScale reactor is done by Fortum and SMART is done by VTT. However, there was not enough public information considering all of the safety systems used, the new and innovative safety features was focused on. The investigation was fixed to the safety systems of one reactor module and the possibility of multiple module accident was not taken into account.

Korea Atomic Energy Research Institute (KAERI) is the designer of the SMART reactor. The aim of the SMART design is to enhance safety and economics. Inherent safety features and passive safety systems are incorporated to the design, system simplification, component modularity and reduction of construction time will improve the economics (IAEA, 2012). The steam generators, pressurizer and the coolant pumps are installed inside the reactor vessel. The designed thermal power of SMART is 330 MW. (Bae et al., 2015) The standard design of SMART was approved in July 2012 by the Korean Nuclear Safety and security Commission (IAEA, 2012).

The SMARTs safety systems consist of passive and active systems. The basic safety concept of SMART consists of a reactor shutdown system (RSS), a safety injection system (SIS), a passive residual heat removal system (PRHRS), a shutdown cooling system(SCS), containment spray system (CSS), reactor overpressure protection system (ROPS) and severe accident mitigation system (SAMS). (IAEA, 2011)

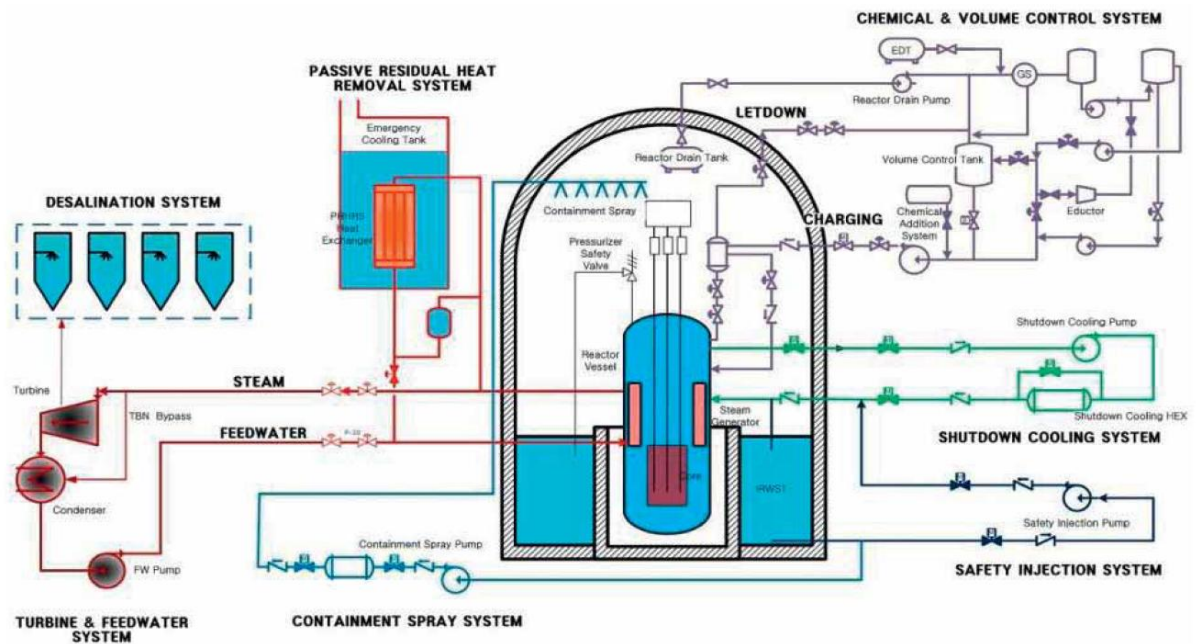


**Figure 1.** Engineered safety systems of SMART (IAEA, 2012)

The NuScale reactor is expected to apply for the design certification from NRC by the end of 2016 (NRC, 2016). NuScale power plant consists of 12 power modules and each own module has its own dedicated steam turbine-generator. Modules are placed in reactor pool which is common for all the modules. Each module produce power of 160MWth and 45 MWe. Each module consists of integrated reactor vessel which is enclosed by high pressure containment vessel. NuScale power module has a few very distinctive feature such as a reactor pool and the passive safety systems related to it and the steam generators. The reactor pressure vessel includes two helicoil steam generators where secondary side water flows inside of the tubes and primary coolant is outside, which is vice versa compared to steam generators of current pressurized water reactors. (NuScale, 2011)

The NuScale power module's safety systems consists also of small number of active and passive systems. Active systems consist of reactor trip system. Passive systems are passive decay heat removal system (DHRS), emergency core cooling system and containment heat removal system.

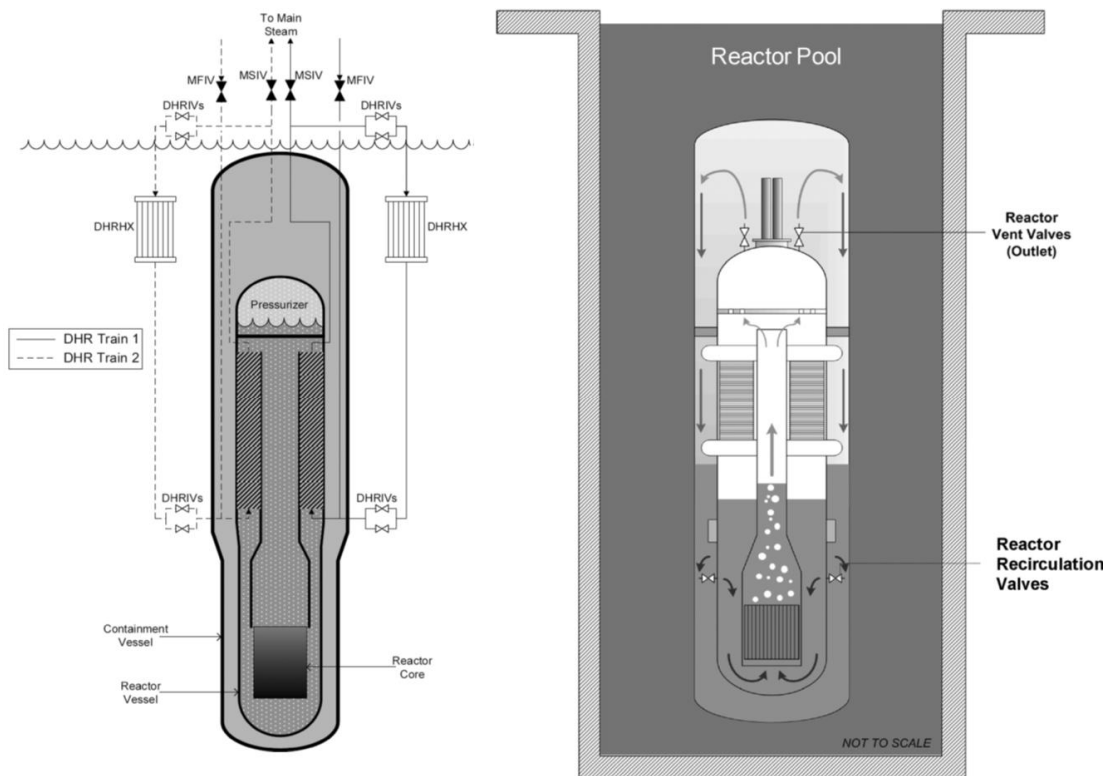


**Figure 2.** Decay heat removal system (left) and Emergency core cooling system and containment heat removal system (right) of NuScale power module (NuScale, 2011)

The Finnish licensing process has been designed with large LWR's in mind. This makes the licensing process quite rigid and does not take into account the different design features of SMRs like modularity and multi reactor installations. This being said, no reason why SMRs could not be licensed to Finland, if the Finnish regulatory demands are met, has been identified. The lack of detailed publicly-available information on the SMR designs makes it so, that nothing sure can be said on the licensability of particular SMR concepts.

The DiD principle is the basis of the safety design of the reviewed SMRs and also the foundation of the Finnish regulatory guidelines of nuclear safety. The passive decay heat removal safety systems, featured in many SMRs, are taken into account in Finnish regulations by giving them a reduced failure criterion (N+1) compared to (N+2) for active systems.

The main hurdle seen in the licensing of IPWR SMRs is the independency of DiD levels. Also the Finnish regulations demand that there are independent safety systems against severe accidents. The actual licensing process is very time consuming and the public information is in no way detailed enough to truly give a definitive statement on the issue.

### SMR material issues

Coolants of different small modular reactor (SMR) concepts include effectively all the same coolants as large advanced energy production reactors, i.e., light water, heavy water, gas, sodium, lead or lead-bismut, and molten salt. Small reactors that are already operating, are under construction, or are in advanced development stage are shown in Table 1.

The trend of development has been towards advanced reactors that produce less than 300 MWe, and are designed to be built in factories and shipped to construction sites as more or less complete assemblies. One of the design philosophies is modularization, by which the structures, systems and components are shop-fabricated then shipped and assembled onsite when plant extension is desired. This way initial investment costs and construction times can be reduced. (World Nuclear Association, 2017)

The target of this sub task was to take a look into materials selection of light water cooled SMRs, challenges caused to joining techniques and non-destructive inspection by the integral nature of the SMRs, and issues related to the acceptance of new materials to nuclear power plant applications.

**Table 1.** Small reactors from advanced design stage to reactors already operating. (World Nuclear Association, 2017)

	Name	Capacity	Type	Developer
Operating	CNP-300	300 MWe	PWR	CNNC, operational in Pakistan & China
	PHWR-220	220 MWe	PHWR	NPCIL, India
	EGP-6	11 MWe	LWGR	at Bilibino, Siberia (cogen)
Under construction	KLT-40S	35 MWe	PWR	OKBM, Russia
	CAREM-25	27 MWe	integral PWR	CNEA & INVAP, Argentina
	HTR-PM, HTR-200	2x105 MWe	HTR	INET, CNEC & Huaneng, China
Advanced development stage	VBER-300	300 MWe	PWR	OKBM, Russia
	NuScale	50 MWe	integral PWR	NuScale Power + Fluor, USA
	Westinghouse SMR	225 MWe	integral PWR	Westinghouse, USA*
	mPower	180 MWe	integral PWR	Bechtel + BWXT, USA
	SMR-160	160 MWe	PWR	Holtec, USA
	ACP100	100 MWe	integral PWR	NPIC/CNNC, China
	SMART	100 MWe	integral PWR	KAERI, South Korea
	Prism	311 MWe	sodium FNR	GE-Hitachi, USA
BREST	300 MWe	lead FNR	RDIPE, Russia	

The materials used in some light water cooled SMRs, challenges caused to joining techniques and non-destructive inspection by the integral nature of the SMRs, and issues related to the acceptance of new materials to nuclear power plant applications are described here. At present, very little information is publicly available concerning the specific materials used in different LWR SMRs, but in general everything implies that the main materials are austenitic stainless steels 304L, 316L, 347, nickel base or high nickel alloys 690, 800, pressure vessel steels and zirconium based alloys, i.e., the same that are used in present day large LWRs.

Due to the tight spaces resulting from the integral construction on-site welding may be difficult, which emphasizes the need for high reliability of the applied welding process. Along with this, ensuring higher weld quality concomitantly calls for the development and implementation of advanced NDE methods, as well. This can be accomplished, e.g., by robotization of welding fabrication and/or using automated welding processes coupled with in-situ monitoring of welding.

The close-packed structures very likely result in a need to develop new or improved NDE methods. A number of questions concerning the in-service inspections were left open due to the lack of detailed information of the components and the access into them.

In the present review, no implications of the application of new materials were found. However, if new materials are used, they should be included in ASME boiler and pressure vessel or other corresponding code. The acceptance process is not simple and strong co-operation between national/international recognized organizations and ASME or corresponding code administrative committee is needed.

## **International co-operation**

One of the objectives in GENXFİN project is to participate in the international networks and working groups and increase the interdisciplinary research activities and knowledge transfer within Finland in future reactor technology areas. It is important to participate in development of future reactors in Europe from the start as joining later has smaller prospective. Active following of the European Sustainable Nuclear Industrial Initiative (ESNII) Task Force (TF) enables participation in the coming industrial projects. Participation in the IAEA activities, GIF working groups and European Energy Research Alliance (EERA) Joint Programme Nuclear Materials (JPNM) has enabled VTT to remain in active role in the global nuclear field especially in materials and manufacturing technology of new reactor concepts.

The lifetime of currently operated LWRs are being extended to 60 years, and further research concentrates on investigation of possible extension to 80 years or more. It is anticipated that significantly greater amounts of degradation could occur with the current materials if they are kept in operation for extended lifetime. Therefore, it is important to identify and qualify new materials for the most affected components and identify technologies such as surface engineering leading to decreased rate of degradation in current and future LWRs.

The Supercritical Water-cooled Reactor (SCWR) is an innovative light water cooled reactor (LWR) concept mainly for large scale production of electricity. Because of core outlet coolant temperatures, in the range of 500–625°C, the SCWR is expected to achieve much higher thermal efficiencies (43–48%) than those of currently operating LWRs (33–35%), and thereby offering improved economic competitiveness. Because SCWRs operate at temperatures exceeding the ones of currently operating LWRs and because of unique properties of supercritical water the development of a viable core design possesses some challenges. Material selection for in-core components is a key challenge. Thin-walled fuel cladding faces many requirements in SCWR so that commercially available low Ni alloys cannot be utilized especially at temperatures higher than 600°C. At the moment, material choices are based mainly on advanced alloys, like ODS alloys etc. or coatings as a long-term solution. In short term, surface engineering solution on austenitic alloys could be an option.

One objective of international collaboration is to develop new reactor materials and to investigate the suitability of common reactor materials of existing LWRs for their deployment in SCWRs. This requires investigating the corrosion and environmentally assisted cracking behaviour of candidate reactor materials in SCW and how they are influenced by water chemistry (e.g. hydrogen), thermal ageing and surface quality/finish. Another objective is to investigate water chemistry issues of SCW like water radiolysis, corrosion product transport and corrosion kinetics and the development of corresponding water chemistry measurement instrumentation. Also one essential topic is to explore the potential of joining technologies for use in SCWRs (e. g. welding) and coatings & insulation to create the required corrosion resistance.

In GIF SCWR M&C PMB, VTT has been responsible of the Chair duties since 2013. Before 2016, the contributions needed for this were covered by GEN4FIN network project. In 2016, this task was continued through GENXFİN project. SCWR concept was included in NUGENIA Technical Area 6 “Innovative LWR Design & Technology” as a new topic in 2015. Through this collaboration, R&D on the SCWR concept is beneficial for the further development of innovative Gen III / III+ reactor concepts. Results of the GIF projects and IAEA activities are also beneficial for new-build GenIII reactors as well as R&D of innovative water-cooled small-modular reactors e.g. instrumentation and new joining technologies.

## **The vision: Nuclear power will be the key to prosperous zero-carbon future**

In order for the nuclear power to be a key player in the future, it will need to be able to provide energy safely, sustainably, reliably and economically in a wide range of applications, while at the same time leveraging its unique strengths among low-carbon technologies. Nuclear power plants can provide baseload electricity reliably, but the future applications will be more diverse, also including items such as grid service, co-generated heat and electricity as well as dedicated high temperature heat for industrial processes.

The whole energy sector needs to be decarbonized in order to mitigate the worst effects of climate change. While to date most of the visible efforts have focused on the electricity sector, the whole energy production must be decoupled from the fossil fuels. This includes the industry, transportation and agriculture. The options to produce low-carbon energy include biomass, hydro, solar, wind and nuclear power. Among these options, nuclear power uniquely offers scalable dispatchable electricity and a potential to produce high temperature heat while requiring a small environmental footprint.

### **Highlights**

- Safe and sustainable nuclear energy is an essential component of the zero-carbon future.
- Advanced reactors increase the potential of nuclear energy; future applications include electricity, district heating as well as heat for industrial processes.
- Spearheading the new applications with domestic projects will aid in decarbonization of Finnish society, ensure the talented workforce and provide opportunities to Finnish technology export sector.
- Understanding of the potential of the use of the nuclear power in the zero-carbon future will be essential in obtaining societal acceptance for the industry.

### **Case Finland**

While Finnish electricity is fairly low carbon to begin with, the long distances, heavy industry and northern location offers unique challenges to clean energy production.

The current lack of expandable cheap storage of electricity makes the so called baseload electricity production a required part of electricity system. This role is currently performed by nuclear power plants, and given the slow development of storage technologies it should not be dismissed in the future either. Load following is an option for nuclear power plants, and some SMR designs are purposely designed to accommodate it, increasing nuclear power's role in the electricity system.

Currently a large fraction of the residential heating is done with the coal and biomass, and these could be well switched to nuclear district heating. While the available biomass reserves are large they are still limited. The transportation sector will partially switch to electricity, the inertia and the limitations of electric vehicles ensure that the liquid fuels will be needed for a long time.

The heavy process industry in Finland utilizes industrial heat in various applications. For large scale (tens or hundreds of megawatts of heat) a SMR, potentially utilizing gas as a coolant, could replace the use of burning hydrocarbons in the creation of the heat. The low-carbon industrial production of substances such as hydrogen or nitrogen could also be achieved with advanced nuclear reactors.

SMRs being modular and multi-unit by design offer unique opportunities for Finnish technology and manufacturing industry. By utilizing domestic supply chains new expertise can be grown which would have a large export potential.

The expansion of nuclear power use will benefit the Finnish society by providing sustainable low-carbon energy to various uses with minimal environmental effects. The expertise gained during the build-up and utilization of the new facilities can be utilized by the Finnish technology sector for export, such as equipment manufacturing, design and consultation of foreign projects.

The visible role of nuclear power in the climate mitigation promotes the societal acceptance of nuclear power. In a converse case, where nuclear power provides ever diminishing part of the low-carbon energy, the use of nuclear power and funding of its research would become harder and harder to justify to the general populace and the policy makers. As it is, the increased role of nuclear power will benefit the current nuclear actors by aiding in the justification of their work.

New high profile projects will provide incentive for young people to enter the nuclear field and will yield interesting career options to them. New research project would be easier to justify to the national funding bodies. The Finnish tradition for being on the cutting edge of nuclear technology will be maintained by the new projects. As many of the possible applications of the new nuclear power plants are in conjunction with non-nuclear processes, it would be pertinent for the current nuclear utilities to act in an advisory capability while the new nuclear users build up their competence. This would bring new business opportunities also to the current utilities. In addition, the increased national know-how is needed to support the safety authority in its work when novel nuclear technologies are deployed in Finland and its vicinity.

The implementation of this vision will require societal acceptance in the expansion of the use of the nuclear power, the commitment of national actors towards the long term goal of sustainable zero-carbon future, adoption of innovative solutions by new end-users and the successful collaboration between international advanced reactor developers and the domestic actors.

## References

- Bae, H., Ryu, S., Yi, S., Park, H., Cho, Y., Suh, J. 2015. An SBLOCA test of pressurizer safety valve line break with the SMART-ITL facility and its MARS-KS code simulation. NURETH-16, Chicago, IL, August 30-September 4, 2015.
- IAEA. 2011. Status report 77 - System-Integrated Modular Advanced Reactor (SMART). 2011.
- IAEA. 2012. Status of Small and Medium Sized Reactor Designs, Supplement to the IAEA Advanced Reactors Information System (ARIS), <http://aris.iaea.org>. 2012.
- Kyrki-Rajamäki, R. et al. Finnish research network for generation four nuclear energy systems, VTT working papers 90, 1/2008, 978-951-38-7149-9, <http://www.vtt.fi/publications/index.jsp>
- NRC. 2016. Pre-Application Review of the NuScale Design. [Ref. 3.1.2017] <https://www.nrc.gov/reactors/advanced/nuscale/review.html>
- NuScale, 2011. NuScale Plant Safety in Response To Extreme Events. Nucl Tech, 128, 153-163 (May 2012). [http://www.nuscalepower.com/images/our\\_technology/NuScale-Safety-Nucl-Tech-May12-pre.pdf](http://www.nuscalepower.com/images/our_technology/NuScale-Safety-Nucl-Tech-May12-pre.pdf)
- OECD. 2011. Current status, technical feasibility and economics of small Nuclear Reactors.
- World Nuclear Association. 2016. Small Nuclear Power Reactors. [Ref. 29.12.2016] <http://www.world-nuclear.org/informationlibrary/nuclear-fuel-cycle/nuclear-power-reactors/small-nuclear-power-reactors.aspx>

### 3.7 Probabilistic risk assessment method development and applications (PRAMEA)

Kim Björkman<sup>1</sup>, Jan-Erik Holmberg<sup>2</sup>, Ilkka Karanta<sup>1</sup>, Terhi Kling<sup>1</sup>, Marja Liinasuo<sup>1</sup>, Alessandro Mancuso<sup>3</sup>, Teemu Mätäsniemi<sup>1</sup>, Markus Porthin<sup>1</sup>, Ahti Salo<sup>3</sup>, Tero Tyrväinen<sup>1</sup>

<sup>1</sup>VTT Technical Research Centre of Finland Ltd  
P.O. Box 1000, FI-02044 Espoo

<sup>2</sup>Risk Pilot Ab Suomen sivuliike  
P.O. Box 72, FI-02101 Espoo

<sup>3</sup>Aalto University  
P.O. Box 14100, FI-00076 Aalto

#### Abstract

PRAMEA aims to generate new knowledge in probabilistic risk assessment (PRA), covering most research related to it in the SAFIR2018 program. In human reliability assessment (HRA), research has concentrated mostly on the development of a framework for conducting HRA in the context of advanced (digitalized) control rooms in nuclear power plants. Research on multi-unit PRA has produced information on state of the art in the field, and a proposed framework for carrying out multi-unit PRA analyses. Research on dynamic PRA has produced information about the applications of dynamic flowgraph methodology, a method for conducting dynamic PRA modelling and analyses. Research on level 2 PRA has created a summary of VTT's recent research on the topic, and assessment of factors affecting release height and temperature in severe accidents of nuclear power plants, together with methods for estimating these. Research on level 2 PRA has been carried out on two fronts. Methods and implementation of integrating risks, conducting statistical analyses in level 2, and integrating level 1 and level 2 analyses to provide a richer picture of the effect of factors from level 1 to level 2 results, have been developed. In the PRAMEA part of a Nordic co-operation project, methods for conducting level 3 analyses by integrating level 2 and level 3 methods, and probabilistic and deterministic analyses have been studied and developed, producing a pilot study on the Fukushima accident. Also a guideline document for conducting level 3 analyses has been produced in the Nordic project. Recently used methods for population dose assessment have been reviewed.

#### Introduction

Probabilistic risk assessment (PRA) is the field of quantifying risks in terms of probabilities, evaluating the contribution of different subsystems, processes etc. to total system risk, and assessing the uncertainty related to the analyses. Modernisation taking place in the nuclear energy domain raises the need to renew the practices and perhaps also the principles of PRA used in the nuclear field. PRAMEA project aims to answer that need. The objectives of the project are to

- Improve and develop methods for risk-informed decision making to support strategic and operative plant management
- Improve and develop PRA methods in terms of uncertainties and critical areas
- Develop PRA knowledge and expertise in Finland
- Foster international co-operation and import the best practices of the field to Finland

In the project, research on human reliability analysis, dynamic reliability analysis, multi-unit PRA, level 2 PRA, PRA computational methods, level 3 PRA, and the risk analysis of organizations and operations has been conducted. The remaining sections describe these developments.

The project is cooperation between VTT, Risk Pilot consulting company, and Aalto University. It has versatile cooperation both domestically and internationally, including participation in Nordic cooperation projects together with Swedish partners (Kungliga Tekniska Högskolan, Lloyd's Register Consulting, Risk Pilot Ab, ÅF Consult, Vattenfall), and in international activities (the WGRISK group of OECD/NEA, and ETSON).

## Human reliability analysis

### Framework for human reliability analysis in advanced control rooms

Digital human-system interfaces (HSIs) are becoming common in nuclear power plants (NPPs) through modernisations and new-builds. NPP control rooms with modern digital HSI are commonly referred to as advanced control rooms (ACRs). The use of digital HSI changes the working environment of the operator, induces new tasks and modifies the group dynamics and communication. The effect of digital HSI in the nuclear domain is not entirely known but some conclusions or assumptions have been made. It is suggested that it improves crew performance and reduces workload [Roth and O'Hara 2001]. Negative effects are assumed to include declined primary task performance due to attention shift to interface management, and sub-optimal use of the HSI in high workload situations due to minimized capability to focus on interface management tasks [O'Hara et al. 2002].

Human error probability is very context-sensitive [Lee et al. 2011b]; when circumstances change, there is a need for re-examination, and possibly revision, of existing human reliability analysis (HRA) methods and work practices. Most of the HRA methods commonly used today were developed before the introduction of advanced control rooms and digital HSI and thus do not properly account for the changes in the work of the operator induced by them. Traditional HRA methods cannot properly address the new aspects introduced by digital HSI. While their shortcomings in modelling the operator performance in advanced control rooms have been recognised (e.g., OECD [2008]), the development of new methods, or updating of old ones, has started during recent years.

The report of Porthin et al. [2016] reviews recent development related to HRA in NPPs using digital HSI. One of the most mature developments in this area is the Korean HuRECA method, which extends the K-HRA (the Korean application of THERP and ASEP) method with digital HSI aspects. Still, up to 2015 it has not been applied in practice. In addition to HuRECA, the methodological progress during recent years has been performed mainly by Korean and Chinese researchers, including proposals for new PSFs and typical error types when using soft controls. Also the EPRI user group recognises the new methodologic HRA challenges introduced by the use of digital HSI, but so far the updates to EPRI HRA Calculator have been very minor.

A central goal for the HRA is to ensure that operator performance using the newer technology is at least as reliable as performance using the older technology. While the need for method development has been recognised and some progress is under way, further work in the field is needed to properly take the new aspects introduced by digital HSI into account in HRA. This includes e.g. the reviewing of human errors in interacting with digital HSIs in non-nuclear industries, further exploring the human failure events using digital HSI, identifying and establishing empirical basis for quantification of PSFs suitable for digital HSI, validation studies using research simulators, and development of guidance for including and quantifying these human failure events in the HRA and PRA [Boring, 2014].

The report of Porthin et al. [2017] examined the use of PSFs in HRA methods when assessing the HEP in post-initiator situations in the main control room, with focus on advanced control rooms. The PSFs of commonly used traditional HRA methods were reviewed. Although each HRA method has its own set of PSFs, they can in general be summarized into nine categories: stress level, action type, experience, time

constraints, places where operator actions are taken, procedures, training, HSI and team factor. In general, first generation HRA methods do typically not address all these PSF categories, whereas many second generation methods address all, or most of, the categories in one way or another.

The differences in the work of an operator in advanced vs. analogue control rooms were discussed by Porthin et al. [2017] from a cognitive point of view. It is evident that a new concept of working in combination with the use of integrated information systems, soft controls and computer-based procedures challenges the operator in her work in another way than analogue control rooms. Some challenges from analogue control rooms are no longer an issue, whereas also new challenges emerge. The flexibility and versatility of the computerized systems enable both improved support and possibilities for task tailored information to the operator, but in the same time bring increased complexity to the user interface and possibilities for new types of errors. It can be concluded that even if the main categories for PSFs for analogue control rooms are still valid in digital settings, their interpretation and detailed definitions as well as effects on the HEP may be different.

Porthin et al. [2017] presents also different approaches to estimate the effects of PSFs on human performance. Lee et al. [2011a] developed a qualitative evaluation framework for PSFs by identifying a list of human factors issues and checking them against PSF categories. It resulted in qualitative evaluation questions regarding the PSFs by considering the human factors issues deemed relevant for each PSF. The quantitative effect of PSFs can be estimated using data from actual historical measurements, expert judgement or data from simulator studies and experimental research. As an example, Kim et al. [2015] propose a logistic regression to model the relationship between PSFs and the HEP. Although their analyses are based on laboratory experiments with limited real world validity, they demonstrate a theoretically sound data driven approach to estimating PSF effect to the HEP values, reducing the need for subjective analyses.

## Dependences in human reliability analysis

Despite 30 years of development and experience with human reliability analysis (HRA) for PRA, there are weaknesses in the methods, which unnecessarily decrease the credibility of HRA. How to account for dependencies has been identified as a problem area for HRA. Dependencies in HRA generally refer to the probabilistic relationship between two or more human interactions analysed and modelled in PRA

There are several types of dependencies that may need to be accounted in HRA:

- Dependencies between category A human errors, i.e., errors made before an initiating event causing latent unavailabilities in safety systems. For instance, alignment errors in redundant system trains are a critical issue. Also inter-system and procedural dependencies, which are often ignored, may be important.
- Dependencies between category B human errors, i.e. errors causing an initiating event and its recovery. In this category, treatment of dependencies is heavily dependent on the level of details of the analysis and the meaning of recovery.
- Dependencies between category C human actions, i.e., actions made after an initiating event. This includes a large range of dependencies, e.g.,
  - Context dependency
  - Dependencies between level 1 and 2 PSA actions.
  - Time-constrained actions with limited resources. The more time is spent in one action, the less time there is for the following action.
  - Dependencies between distributed actions, coordination between control room actions and local actions (e.g. fire scenarios)
  - Dependencies in multi-unit scenarios.

We performed two case studies is to evaluate existing methods and develop supplementary guidance for a new method for the assessment of dependencies in HRA and the need for additional method development.

In the first case study on category A action dependences [Porthin 2015], we examined the probabilistic assessments of dependency between multiple pre-initiator actions in Fortum's HRA as part of Loviisa 1 and 2 Probabilistic Safety Assessment (PSA). The chosen case example was the calibration error of two redundant thermostats due to a common cause failure (CCF) leading to loss of certain cooling systems in emergency situations due to no actuation of auxiliary air conditioning. Fortum's dependency model has been developed based on the Technique for Human Error Rate Prediction (THERP) method, from which it has been somewhat modified to better meet Fortum's needs. It can be concluded that the model gives similar results as THERP, seems reasonable and differentiates between different situations. The clearly defined questionnaire for determining the dependency level adds transparency and reproducibility to the method. It is also in reasonable agreement with NUREG-1792 Good Practices for Implementing HRA.

In the second case, the analysis of dependences of post initiating event operator actions was demonstrated (Holmberg & Jacobsson 2015). Loss of coolant accident (LOCA) during shutdown in a boiling water reactor is used as an example of a complex scenario. The main focus is in the qualitative analysis of the scenario where the relevant operator actions and their interdependences are identified. Quantification of dependences is demonstrated using one commonly applied method.

The main challenge in the analysis of complex sequences is to identify and define operator actions in a meaningful way which fits in the PSA model environment. The proposed analysis approach has main focus in the qualitative analysis and it is structured into the following steps:

1. Analysis of main safety objectives.
2. Analysis of tasks related to the main safety objectives. (task analysis)
3. Sequence analysis
4. Quantification of the basic events (human failure events).

In the dependency assessment the attention is paid to the cases where judgement between no and fully dependency is needed. It should be noted that there are also many evident dependences implied by the sequence, where there is no need to make judgements since in these cases the latter (dependent) action is needed only because the preceding action has either failed or succeeded. As an example the action "immediate isolation of the LOCA" divides the LOCA scenarios into two different branches. The following actions are obviously dependent on the success isolation action, but the outcome from the isolation effort can be included in the definition of the context of the following human failure event (HFE).

In the example, the interesting cases are related to the various methods to recover residual heat removal from the reactor core. In top-LOCA, there is a several hour time window to establish a cooling method. However, the actions are presumably performed by the same crew and guided by the same emergency operating procedure and have common cues. If a method like SPAR-H is followed, the dependency category will be full or high/moderate between the use of different system alternatives (Gertman et al. 2005).

Quantification example shows that high/moderate dependency instead of full dependency can reduce the core damage frequency for this initiating event by a factor 7, which is considerable difference. It can be hard to justify whether full dependency is a conservative assumption or high/medium dependency is an optimistic assumption. If shutdown top-LOCA is a significant initiating event, a sensitivity analysis of the case should be included in PRA. It is also important to include a systematic qualitative analysis of possible actions related to the scenario.

## Non-PRA applications of HRA

HRA is a tool for assessing the human contribution to failures, usually as part of PRA. The PRA typically only makes use of the quantitative Human Error Probability (HEP) that is produced by the HRA, meaning that the detailed qualitative analyses that underpin this calculation and the knowledge that is produced in the activity are not utilised outside of the HRA. However, qualitative HRA can provide valuable insights into the individual, workplace and organisational factors that drive human performance and errors, and may be useful for a range of risk-informed applications beyond the PRA.

A questionnaire was carried to how HRA has been used outside PRA and what potential HRA has to widen its scope in the nuclear domain (Holmberg & Liinasuo 2017). This questionnaire was distributed to Nordic PRA/HRA organisations. In Finland and Sweden, HRA is used in great majority of cases for PRA purposes only. The lack of broader experience of the area seems to be one reason for that as in the survey, the need for guidance was emphasised. The counterpart for this lack of expertise is the lack of respect towards HRA from the part of organisations which are to utilise the HRA originating results. These forces strengthen each other: without understanding the value of HRA, resources are not distributed to develop HRA and HRA expertise, and without proper resources, less HRA can be done.

A reasonable way to solve this problem would be to strengthen HRA from the inside of the HRA community. That can be done in PRA and non-PRA context. Regarding the usage of HRA in non-PRA purposes, lot of possibilities can be identified. Part of them are realised but a lot can still be done. SAFIR programme provides one possibility to strengthen HRA from various perspectives.

## **PRA level 1 method development**

### **Multi-unit PRA modelling**

The Fukushima Daiichi accident in March 2011 pointed out that the risk of external events affecting multiple nuclear power plant (NPP) units is significant. Consequently, interest in multi-unit probabilistic risk assessment has also increased. A large part of the nuclear power sites houses more than one NPP and/or other nuclear facility such as a spent fuel pool storage.

Currently, multi-unit risks have not typically been adequately accounted for in risk assessments. Due to possible dependencies between the units at a site the question of several simultaneous reactor accidents is not one of possibility but rather one of probability (Fleming 2005). Based on the literature study (Björkman & Tyrväinen 2015), a large part of the research seems to focus on identifying and accounting for different kinds of dependencies and on external hazards.

In (Tyrväinen et al. 2017), we outlined a methodology for preliminary multi-unit PRA. The methodology aims to estimate multi-unit core damage frequencies (or large early release frequencies) related to different multi-unit dependencies. The idea is to utilize existing PRA models of individual units as much as possible. The methodology contains ten steps:

1. Identification and classification of multi-unit dependencies
2. Analysis of identified dependencies
3. Probability estimation
4. Extension of unit PRA models
5. Screening of events and event combinations
6. Computation of conditional accident probabilities
7. Computation of risk metrics of multi-unit event combinations
8. Construction of new multi-unit model
9. Computation with the new multi-unit model
10. Computation of multi-unit accident frequency and event importance

In steps 1-3, multi-unit dependencies are identified, analysed and modelled, and probabilities are estimated for them. Existing PRA models of individual units can be extended in step 4 to include those multi-unit dependencies that have not been taken into account in the models previously. In step 5, multi-unit dependencies are screened based on their probabilities and PRA models so that significant multi-unit event combinations can be identified for further quantitative analysis. In steps 6-7, the risk related to a multi-unit event combination is estimated by calculating the conditional core damage (or large early release) probability of the event combination in the PRA model of each considered reactor unit. If some dependencies cannot be analysed using single unit models, they are analysed using a new multi-unit

model in steps 8-9. Finally, total multi-unit accident frequency and importances of different multi-unit dependencies are calculated in step 10.

During 2017–2018, the goal is to study risk metrics, safety goals and results presentation for site risk analysis. Another major objective is to develop methods to assess risk for multi-unit scenarios. In this respect, the project will go in details of the approach outlined in (Tyrväinen et al. 2017) and test the approach through pilot studies.

## Dynamic flowgraph methodology

Dynamic flowgraph methodology (DFM) (Garrett et al. 1995) is method for the reliability analysis of dynamic systems with time-dependencies and feedback loops. As in fault tree analysis, the aim of DFM is to identify which conditions can cause a top event, which can be, for example, the system's failure. DFM has most often been applied to different digital control systems. One reason for this is that a DFM model can represent the interactions between a control system and the controlled process. Components of DFM models are analysed at discrete time points and they can have multiple states. The reason for the development of DFM is that traditional methods, such as fault tree analysis, can describe the system's dynamic behaviour only in a limited manner. DFM can more accurately represent system's evolution in time.

In (Tyrväinen 2017), we performed a literature survey that focused on applications of DFM. The application areas include digital control and safety systems in nuclear power plants, space systems, hydrogen production plants, human performance, networked control systems and field programmable gate arrays. In most of the applications, DFM has been used to analyse how control system failures can cause some physical variable, e.g. water level or pressure, to have too low or high value. Generally, DFM has been found useful within the application areas. Most of the presented models have been quite moderately sized, though larger models exist too.

## Level 2 PRA

Level 2 probabilistic risk analysis (PRA) studies how a nuclear power plant accident progresses after core damage and how frequent and large radioactive releases are (IAEA 2010). FinPSA is a PRA software tool (VTT 2016), which was originally developed by STUK, and which is currently maintained and developed by VTT. New development includes the level 2 modelling which is based on containment event trees (CETs) and parametric model behind of them. The parametric model is specified by containment event tree programming language (CETL). The language is used to define functions to calculate conditional probabilities of CET branches, timings of the accident progression and amounts of releases. A CETL function is defined for each branch of a containment event tree, and the parametric model also contains initial conditions, where e.g. global probability and process variables can be defined. In addition, the model has a global “common section”, where e.g. global variables and functions that are common to all CETs in the model can be defined. The CETL programming is very flexible. At any branch, new value can be set or calculated for any global variable, and that way accident progression can be modelled dynamically. The parametric modelling also makes it possible to incorporate information from deterministic safety analyses into the model or to implement some deterministic computation inside the level 2 PRA model. Binning rules can also be defined to divide severe accident end states in the end points of the CETs into release categories.

To account for uncertainties related to variable values, it is possible to define value distributions and perform Monte Carlo simulations. At each simulation run, a value is sampled from each defined distribution, and based on that, conditional probabilities are calculated for all the branches, and values are calculated for all variables of the parametric model while resolving accident progression from the plant damage state (PDS) to each end point of the CET. After the simulations, statistical analyses are performed to calculate frequency and variable value distributions for each level 2 sequence and release category among other statistical results and correlation analyses. It is also possible to just resolve point values for the vari-

ables in the level 2 model based on the mean values of distributions, which can be used e.g. to obtain preliminary results fast and test newly developed model.

## Integrated deterministic and probabilistic safety assessment

Integrated deterministic and probabilistic safety assessment (IDPSA) combines two approaches to safety analysis of nuclear power plant, deterministic and stochastic, to support risk-informed decision making. IDPSA takes both stochastic disturbances and deterministic response of a nuclear power plant, and especially their mutual interactions, into account in safety justifications. The methodology can also reveal new plant weaknesses and reduce conservatism in the analysis. We have applied IDPSA to the analysis of severe nuclear power plant accidents and level 2 PRA. Severe accidents involve complex physical phenomena of which information can be best gathered by performing deterministic analyses.

In (Tyrväinen & Silvonen 2015), we prepared a summary on previous IDPSA research at VTT. It covered case studies on steam explosions, passive autocatalytic hydrogen recombinators, passive containment cooling system and ex-vessel coolability. In the studies, both probabilistic and deterministic analyses were performed. Especially, it was demonstrated how the results of deterministic simulations can be incorporated into a containment event tree model. Knowledge on severe accident phenomena and modelling capabilities were gathered. The analysis procedures of these case studies can be followed in forthcoming case studies, because the analysis and modelling principles are quite similar regardless of which phenomenon and plant type is analysed.

In (Tyrväinen & Karanta 2017), we studied factors that affect the height and temperature of radioactive releases. The height and temperature have typically not been included in level 2 PRA, even though they are needed as inputs for level 3 PRA. Release height is usually the height of the location where the reactor building leaks (which depends on the containment failure mode), or the height of the chimney if the release is controlled. In an uncontrolled accident case, both the containment failure location and the flow path of radionuclides in the reactor building need to be analysed to determine the release height. The temperature of release from containment is in most cases close to 100°C, but the temperature of radionuclides can potentially change during their migration in the reactor building. Higher temperatures can be caused by fires and explosions. There are computer codes that can be used to analyse radionuclide flows in reactor building and determine the release heights and temperatures.

We have also started studying hydrogen explosions in boiling water reactor (BWR) nuclear power plant (Tyrväinen & Karanta 2017). Hydrogen explosions can occur in nuclear power plant containment if heated zirconium reacts with steam producing significant amount of hydrogen during severe accidents. These explosions have the potential to be powerful enough to break the containment and cause a large early release. Hydrogen explosions in BWR plants have been studied little because inerting of containment - filling the containment with a non-flammable gas (usually nitrogen) - prevents explosions with certainty. However, an accident can also occur when the containment is not inert, e.g. during start-up or shut-down. Hydrogen explosions outside containment are considered more likely, but they have usually not been modelled in PRA because they presumably would not break the containment and cause radioactive release. However, those hydrogen explosions can break the reactor building and increase the releases to environment, like in Fukushima. Therefore, hydrogen explosions outside containment are identified as a potential PRA research topic.

We have developed a simplified CET model of a BWR plant, which was originally constructed in (Silvonen 2013). We identified that there were no uncertainty distributions specified for probability parameters in the original model. Therefore, we developed complete uncertainty analysis for the model in (Tyrväinen & Karanta 2017). In the process, we identified problematic issues and good practises for performing uncertainty analysis in FinPSA level 2. The original model was heavily based on computation with physical parameters, whereas in the new version, the focus is on probabilistic modelling. The mean values of the probability distributions used in the new model were derived from the original model and its results. If there had not been the original model, other supporting analyses to estimate those mean values of probability parameters would have been needed instead. It can actually be a good idea to perform the modelling in

two phases like this: first focusing on physical modelling to obtain preliminary results and implementing the uncertainty analysis later. The latest version of the CET model is partially presented in Figure 1.

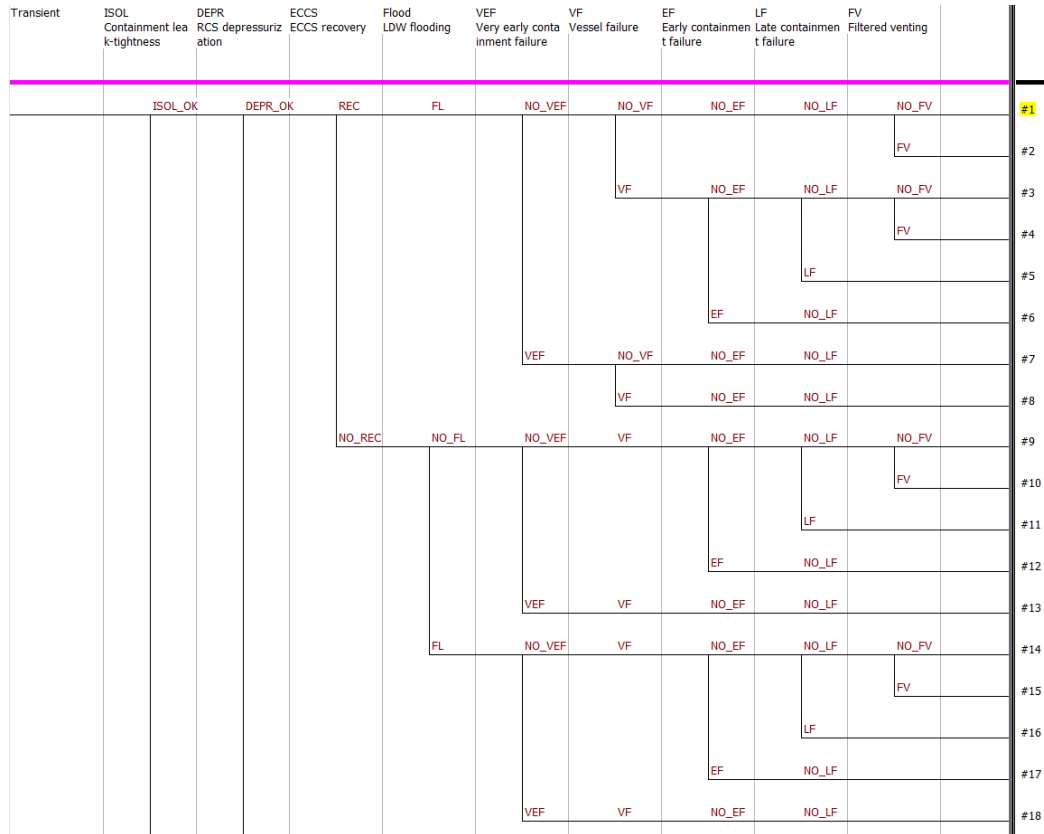


**Figure 1.** A simplified CET model for BWR plant.

### Method support for level 2 PRA

Level 2 PRA modelling in FinPSA is based on containment event trees (CETs) and a parametric model behind of them. Values of parametric model variables are collected while resolving accident progression scenarios. Monte Carlo simulations of the level 2 model take into account variable value uncertainties and produce a huge amount of data from different CETs. To combine the collected analysis data and to form more informative computation results we have implemented a risk integrator component (Figure 2) and updated FinPSA user guide. All these additions needed also comprehensive testing to ensure the software quality.

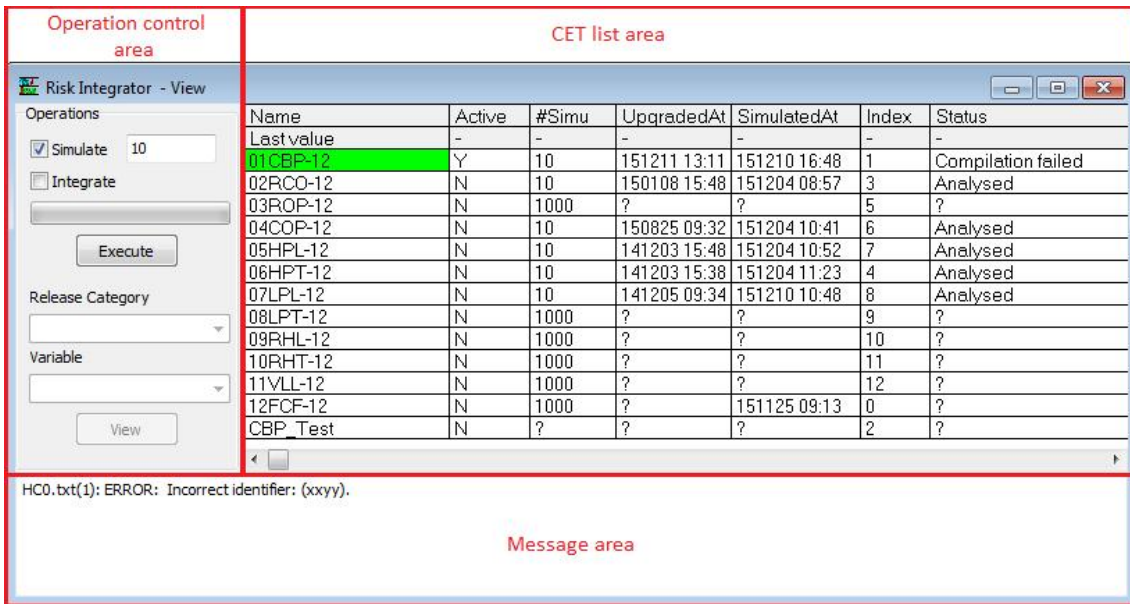


Figure 2. Risk integrator user interface.

The risk integrator user interface consists of three parts (VTT 2016b). The upper left part is an operation control area, the upper right part shows a list of containment event trees and a message area is in the bottom. The operation control area is used to give commands to the risk integrator and to set up command options. The risk integrator can perform simulation for all active CETs in co-ordinated manner. Number of simulation cycles from 1 to 10 000 is defined by user. Main function of the risk integrator after simulations is to create total PRA results by combining the individual results of active CETs. The result integration can also be done without simulations if sufficient simulation results already exist for individual CETs. In addition, the operation control area provides functions to view the total result. The result can be visualised according to selected release category and selected variable. The CET list area shows main information for CET management. Provided information includes properties such as name, active, number of simulation cycles, upgraded at, simulated at and status. CET participation to simulation is defined by value of the active property. Number of simulated cycles visualise how many result values are available for integration and SimulatedAt property shows the moment of CET resolving. UpgradedAt property stores a timestamp when a graphical CET or related parametric model files have been modified. Index maps CET data to a disc folder. After all, the status property visualise actively the progress of CET solving. The message area lists detail information related to the status of CET in the bottom of risk integrator user interface.

The risk integrator performs a lot of calculations behind the user interface. For each variable in each release category defined in the binning rules, it computes the contributions of different CETs, variable value distribution, basic statistical indicators (Figure 3) and complementary cumulative distribution (Figure 4). Also, correlation analyses (Figure 5) between the frequency of the release category and the selected variable are performed.

s\_cs statistical numbers:

Mean: 1.94E-01  
 St. dev.: 2.00E-01  
 Min: 7.85E-05  
 Max: 9.86E-01

s\_cs percentiles:

0.1	7.85E-05
1.0	9.90E-04
2.5	2.24E-03
5.0	5.73E-03
10.0	1.34E-02
20.0	2.99E-02
30.0	5.56E-02
40.0	8.86E-02
50.0	1.27E-01
60.0	1.70E-01
70.0	2.40E-01
80.0	3.31E-01
90.0	4.87E-01
95.0	6.33E-01
97.5	7.63E-01
99.0	8.54E-01
99.9	9.54E-01

Figure 3. Basic statistical indicators

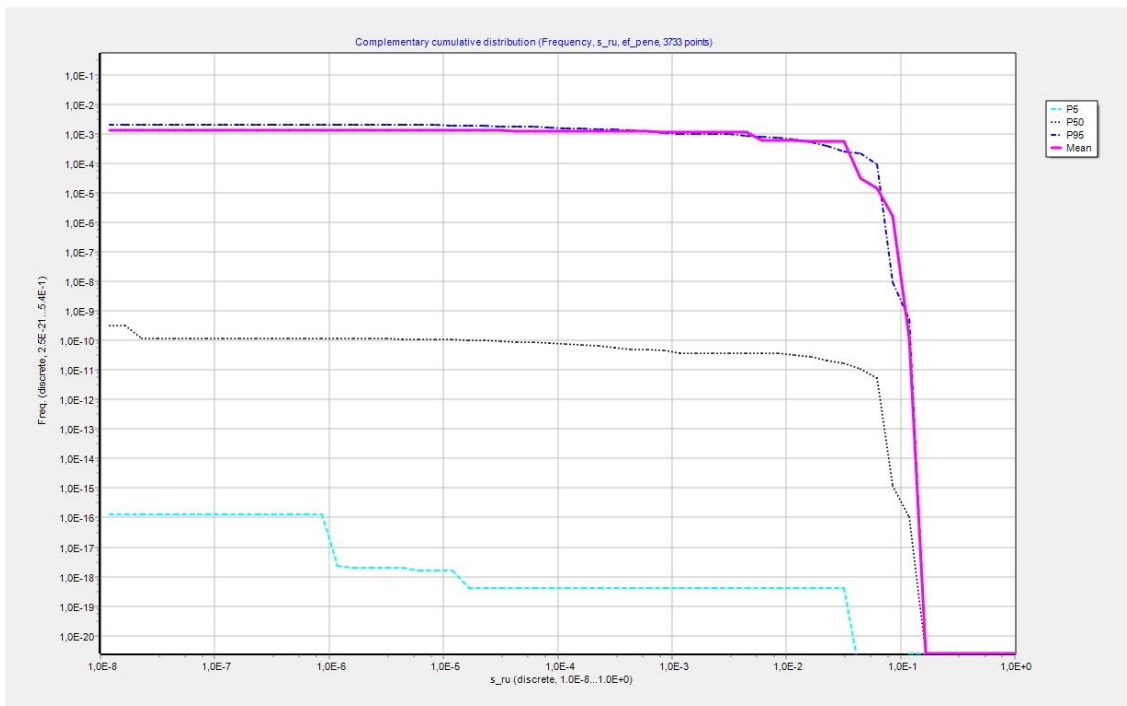
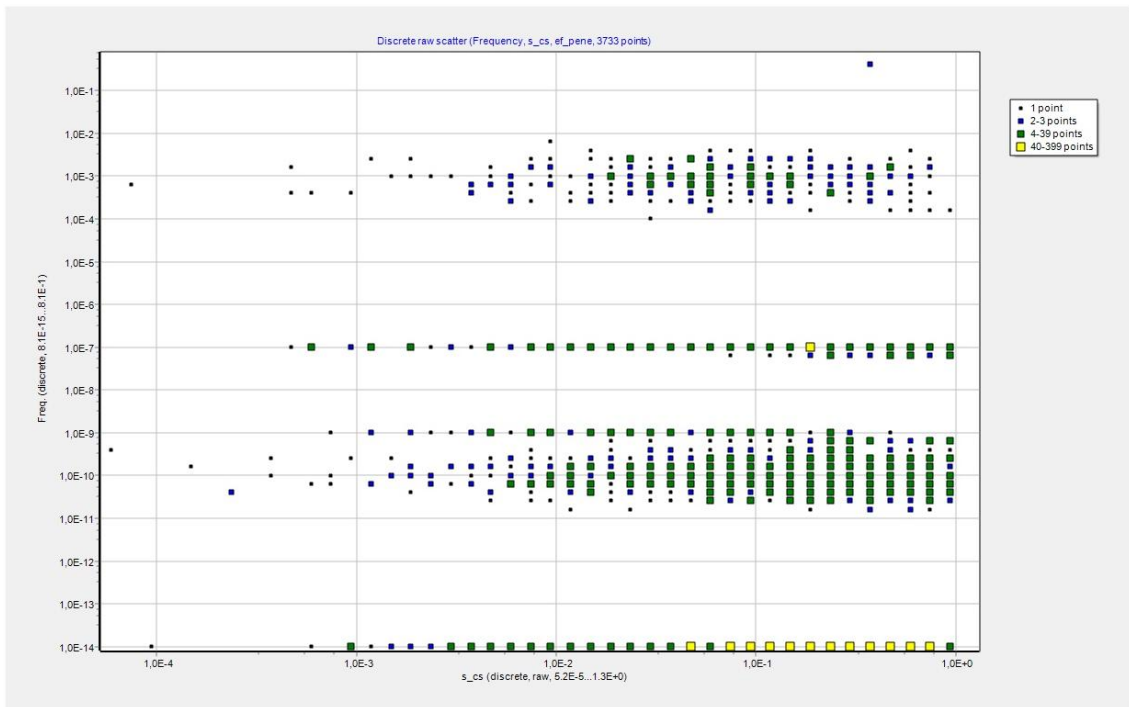


Figure 4. Complementary cumulative distribution.



**Figure 5.** Scatter plot between the cesium release fraction and conditional probability of the release category.

### Method support for levels 1 and 2 tight integration

PRA is most accurate when dependencies between levels 1 and 2 are modelled, and all the relevant information is passed from level 1 to level 2. In FinPSA, analyses of levels 1 and 2 are performed using different methods, which complicates the integration. Figure 6 presents different phases of FinPSA analysis including both levels 1 and 2.

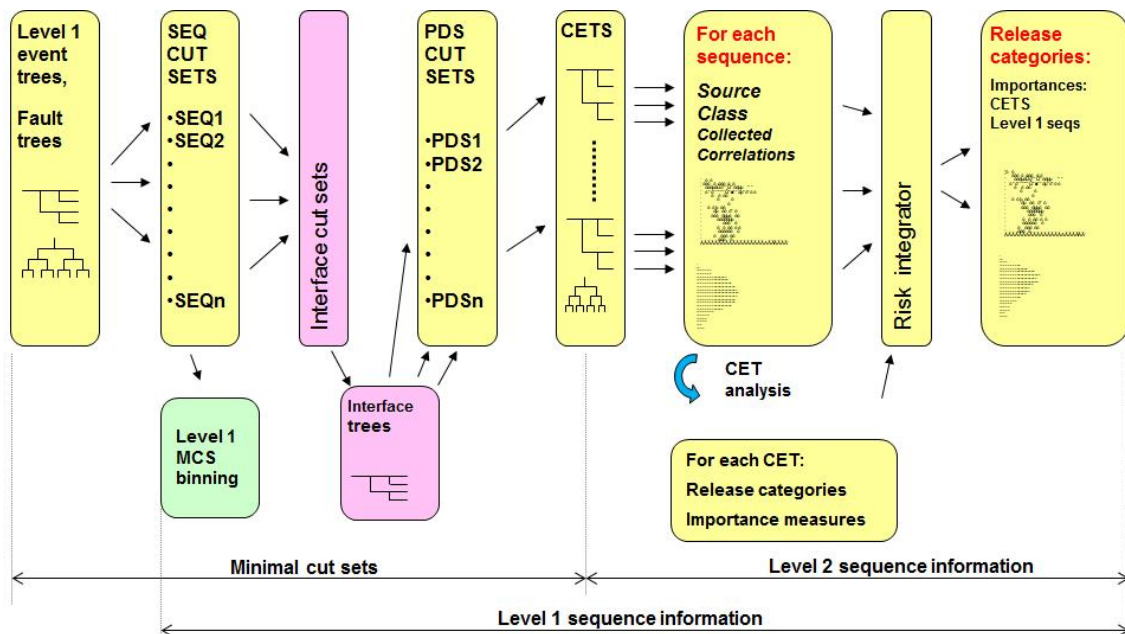


Figure 6. FinPSA analysis phases.

We have developed tight integration of PRA levels 1 and 2 in FinPSA (Björkman 2017). There are two main areas in tight integration (Tyrväinen 2016):

1. How level 1 information is incorporated and utilised in level 2 models
2. How level 1 accident sequences and basic events are seen in level 2 results

There are typically many level 1 accident sequences leading to the same plant damage state (PDS). Different accident sequences can affect later severe accident progression differently. Therefore, it is possible to define categories for level 1 sequences inside a PDS in the corresponding CET model. In the CET, it is then possible to calculate the conditional probability of a level 1 sequence category, e.g. in order to calculate the probability of a CET branch. It is also possible to reduce the level 1 sequence list of the PDS so that only specific sequences contribute to specific level 2 sequences. In addition, it is possible to calculate the conditional probability, i.e. Fussell-Vesely value, of a level 1 basic event in level 2.

It can be calculated how level 1 sequences, basic events and initiating events contribute to the values of level 2 variables, namely frequencies of level 2 sequences and release categories, and values of source variables. These contributions represent the importances of level 1 events with regard to level 2 results. This way level 2 results can be traced back to level 1.

We have implemented all the features presented in the user guide (Tyrväinen 2016) into FinPSA. The implementation required updating all modules of the level 2 part of FinPSA.

## Verification and validation

Because of FinPSA's complexity and importance to nuclear safety and to maintain and assure high quality of FinPSA also after the tool updates comprehensive testing is required for the previous topics. To cover the developed features, test plans were updated, the tests executed and the results reported. The main features that were tested included the risk integrator and tight integration of levels 1 and 2. Also the enhanced error reporting features were tested.

Regarding risk integration and error reporting tests were planned and specified for 34 properties (Björkman 2016). Regarding tight integration the tests covered 10 new properties (Mätäsniemi 2017). The tests were divided into priority classes. For each test, coverage and evidence value were considered.

### **Level 3 PRA**

Level 3 PRA concerns assessing in a probabilistic framework the health, environmental and economic consequences of a nuclear power plant accident. Level 3 PRA research has proceeded on two fronts.

We have participated in a Nordic project that has aimed at developing guidance on conducting level 3 PRA analyses in the Nordic context. The guidance document (Caldwell et al. 2017) has been finalized. It contains information on the Nordic and international regulatory framework affecting level 3 analyses, available international guides and standards relevant to level 3 analyses, and available software. The benefits, challenges and limitations of level 3 analyses are considered. Elements of the analysis are described as a part of level 3 analysis process. Also recommendations are made.

PRAMEA project has also conducted a pilot study (Karanta et al. 2016, Tyrväinen et al. 2016) that has supported the development of the guidance document. The subject of the study was an alternative version of the Fukushima accident, where the source term used was the same as in the real Fukushima accident, but the population was located where they had been before the tsunami of March 2011. The radiological consequences (number of cancer deaths) were analysed in a systematic probabilistic framework. The case study consisted of method development, and application of the method to the selected case. The method consisted of modelling level 3 PRA computation cases in a dynamic event tree (FinPSA level 2, see the previous chapter) and incorporating deterministically calculated population doses into the event tree model.

The developed event tree model is presented in Figure 7. Weather was treated probabilistically instead of using the actual weather from the time of the accident. The event tree contains branches for different wind directions and precipitation cases. Wind speed was however treated as a continuous variable in the parametric model. We performed atmospheric dispersion and dose calculations using VTT's ARANO software (Savolainen & Vuori 1977) for each weather case. Population sheltering and evacuation were also modelled in the event tree.

Fukushima	WDIR Wind direction	PRECIP Precipitation	WSPEED Wind speed	Shelter Population shel tering	EVAC Evacuation	
	OTHER					#1
	NWEST	NO	WS	NO_PS	EV	#2
				PS	EV	#3
		PR	WS	NO_PS	EV	#4
				PS	EV	#5
	WEST	NO	WS	NO_PS	EV	#6
				PS	EV	#7
		PR	WS	NO_PS	EV	#8
				PS	EV	#9
	NORTH	NO	WS	NO_PS	EV	#10
				PS	EV	#11
		PR	WS	NO_PS	EV	#12
				PS	EV	#13
	SWSOUTH	NO	WS	NO_PS	EV	#14
				PS	EV	#15
		PR	WS	NO_PS	EV	#16
				PS	EV	#17

**Figure 7.** Event tree model for the consequence analysis of the modified Fukushima accident.

The main research result is the developed method, but as a side effect, some information was obtained concerning the Fukushima nuclear accident in March 2011. The results indicate that the very small radiological consequences of the accident (no projected deaths) were not the result of good luck, but rather the result of general weather conditions in Japan at that time of year, and the efficiency of the Japanese countermeasures implementation (especially evacuation) that the Fukushima nuclear accident demonstrated.

The expected number of cancer deaths was 3.6. Figure 8 presents the complementary cumulative distribution of the number of cancer deaths.

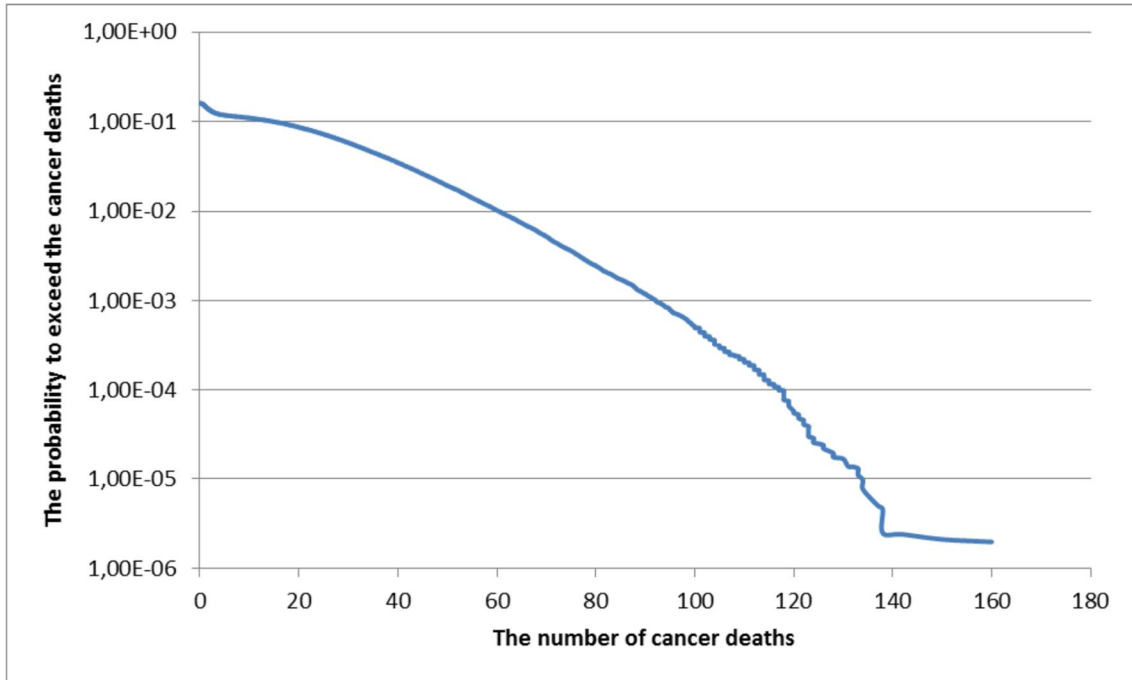


**Figure 8.** Complementary cumulative distribution of the number of cancer deaths.

Methods used in population dose assessment have been reviewed (Karanta 2017). Population dose assessment considers the dose of ionizing radiation resulting to humans as a result of a nuclear accident. The review considers methods used recently either in modern level 3 analysis software (VALMA, SILAM, RODOS/JRODOS) or as part of recent major studies (SOARCA study by the Nuclear Regulatory Commission, Fukushima study by UNSCEAR). There has been relatively little progress in population dose assessment in the last 20 years. Some problems remain in assessment, resulting in uncertainty in dose assessment results, and therefore some recommendations for future research were made.

## Risk analysis of organizations and operations

In the framework of Probabilistic Risk Assessment (PRA, Zio 2007), we have developed a method to support the selection of cost-efficient portfolios of safety actions. Instead of the traditional Fault Trees (Zio 2011), we have represented the combinations of events leading to system failure with Bayesian Belief Networks (BBNs, Jensen 20010, Weber et al. 2012) in which also event dependencies and multi-state failure behaviours can be encoded. We have developed a computationally efficient enumeration algorithm to evaluate all possible combinations (portfolios, Salo et al. 2011) of safety actions and to identify those that minimize the risk of failure at different cost levels of implementing actions. This provides a systemic approach, so that instead of relying on risk importance measures (Kuo Zhu 2012) to apply safety actions on individual events, we determine the optimal portfolio of safety actions which minimizes the risk of the top event. The method has been applied studied by revisiting a case study concerning the airlock system failure in a CANDU Nuclear Power Plant (Di Maio et al. 2014). The results have been compared with those of choosing actions according to the risk importance measures, and they have . The current research has been presented at EURO 2016 conference and at ESREL 2016 conference (Mancuso et al. 2016). The

journal paper (Mancuso et al. 2017) has been submitted to the peer-reviewed journal *Reliability Engineering and System Safety* for peer-review.

Beside that, in 2015 the research team worked on the development of a novel risk-based methodology for optimizing the inspections of large underground infrastructure networks in the presence of imprecise information about the network features and parameters. The methodology employs Multi Attribute Value Theory (French 1988, Keeney Raiffa 1976) to assess the risk of each pipe in the network, whereafter the optimal inspection campaign is built with Portfolio Decision Analysis (PDA, Salo et al. 2011). Specifically, Robust Portfolio Modeling (RPM, Liesiö et al. 2008) is employed to identify Pareto-optimal portfolios of pipe inspections. The proposed methodology has illustrated by reporting a real case study on the large-scale maintenance optimization of the sewerage network in Espoo, Finland. This research has been presented at ESREL 2015 conference (Compare et al. 2015) and published in *Reliability Engineering and System Safety* (Mancuso et al. 2016).

## References

- Björkman, K. 2016. FinPSA – Software testing – Verification and validation results for level 2: Risk integrator & error reporting. Espoo: VTT. VTT-R-00164-16. 24 p,
- Björkman, K. 2017. FinPSA – Software design –Tight integration of levels 1 & 2. Espoo: VTT. VTT-R-04831-16. 13 p.
- Björkman, K. & Tyrväinen, T. 2015. Multi-Unit PRA — Literature Review. Espoo: VTT. VTT Technology VTT-R-04580-15. 11 p.
- Boring, R. L. 2014. Human Reliability Analysis for Digital Human-Machine Interfaces: A Wish List for Future Research. PSAM12, Probabilistic Safety Assessment and Management Conference, 22–27 June 2014, Sheraton Waikiki, Honolulu, Hawaii, USA.
- Caldwell, A.M., A. Olsson, A. Georgiadis, R. Josek, G. Johanson, J.-E. Holmberg, I. Karanta, K. Fritioff. Level 3 PSA guidance for Nordic conditions. Not yet published, 59 pages.
- Compare, M., Mancuso, A., Laakso, T., Salo, A. & Zio, E. 2015. Identification of the most critical pipes in the presence of imprecise information, *Safety and Reliability of Complex Engineered Systems*, pp. 2717-2722, Taylor & Francis Group, London.
- Di Maio, F., Baronchelli, S. & Zio, E. 2014. Hierarchical differential for minimal cut sets identification: Application to nuclear safety system, *European Journal of Operational Research* 238, pp. 645-652.
- Fleming, K. 2005. On the Issue of Integrated Risk – A PRA Practitioners Perspective. San Francisco, CA: Proceedings of International topical meeting on Probabilistic Safety Analysis, (PSA2005). 9 p.
- French, S. 1988. *Decision theory: an introduction to the mathematics of rationality*, John Wiley & Sons, New York.
- Garrett, C.J., Guarro, S.B. & Apostolakis, G.E. 1995. The dynamic flowgraph methodology for assessing the dependability of embedded software systems. *IEEE Transactions on Systems, Man and Cybernetics* 25, 824-840.
- Gertman, D., Blackman, H., Marble, J., Byers, J. & Smith, C. 2005. The SPAR-H Human Reliability Analysis Method, NUREG/CR-6883, U.S. Nuclear Regulatory Commission, Washington D.C.

- Holmberg, J.-E. & Jacobsson, M. 2016. Dependencies in human reliability analysis — case study on shut-down LOCA, Report 14124\_R001, Risk Pilot Ab, Espoo, 34 p.
- Holmberg, J.-E. & Liinasuo, M. 2016. Non-PSA applications of HRA, Report 14124\_R003, Risk Pilot Ab, Espoo, 25 p.
- International Atomic Energy Agency, IAEA. 2010. Development and application of level 2 probabilistic safety assessment for nuclear power plants: Specific safety guide No: SSG-4. Vienna. 66 p. + app. 20 p.
- Jensen, F. 2001. Bayesian Networks and Decision Graphs. Springer-Verlag, New York.
- Karanta, I. Dose assessment in level 3 PRA - a review of recently used methods. Espoo: VTT, VTT Technology VTT-R-00738-17, 14 p.
- Karanta, I., Tyrväinen, T. & Rossi, J. 2016. Improvements to a level 3 PSA event tree model and case study. Espoo: VTT. VTT Technology VTT-R-05819-15. 21 p. + app. 10 p.
- Keeney, R.L. & Raiffa, H. 1976. Decisions with multiple objectives: preference and value trade-offs, John Wiley & Sons, New York.
- Kim, Y., Park, J., Jung, W., Jang, I. and Seong, P.H., 2015. A statistical approach to estimating effects of performance shaping factors on human error probabilities of soft controls. *Reliab Eng Syst Saf* 2014; 142: 378-387.
- Kuo, W. & Zhu, X. 2012. Importance Measures in Reliability, Risk and Optimization: Principles and Applications, John Wiley & Sons.
- Lee, S. W., Kim, A. R., Ha, J. S. and Seong, P. H., 2011a. Development of a qualitative evaluation framework for performance shaping factors (PSFs) in advanced MCR HRA. *Annals of Nuclear Energy*, 38, 1751 – 1759.
- Lee, S.J., Kim, J., Jang, S-C. 2011b. Human Error Mode Identification for NPP Main Control Room Operations Using Soft Controls. *Journal of Nuclear Science and Technology* 48(6), pp. 902-910.
- Liesiö, J., Mild, P. & Salo, A. 2008. Robust portfolio modeling with incomplete cost information and project interdependencies, *European Journal of Operational Research* 190 (3), pp. 679-695.
- Mancuso, A., Compare, M., Salo, A. & Zio, E. 2016. Bayesian approach for safety barrier portfolio optimization. *Risk, Reliability and Safety: Innovating Theory and Practice*, pp. 1765-1772, Taylor & Francis Group, London.
- Mancuso, A., Compare, M., Salo, A. & Zio, E. 2017. Portfolio optimization of safety actions for reducing risks in nuclear systems, submitted to *Reliability Engineering and System Safety*.
- Mätäsniemi, T. 2017. FinPSA – Software testing – Verification and validation plan and results for tight integration. Espoo: VTT. VTT-R-00552-17. 79 p + app. 7 p,
- OECD, 2008. HRA Data and Recommended Actions to Support the Collection and Exchange of HRA Data. OECD NEA CSNI WGRISK Report, NEA/CSNI/R(2008)9.
- O'Hara, J. M., Brown, W. S., Lewis, P. M. and Persensky, J. J. 2002. The Effects of Interface Management Tasks on Crew Performance and Safety in Complex, Computer-Based Systems: Overview and Main Findings (NUREG/CR-6690, BNL-NUREG-52656), Washington, DC.

- Porthin, M. 2015. Methods for handling of dependencies in HRA: Fortum case study, VTT-R-05397-15, Espoo.
- Porthin, M., Liinasuo, M. and Kling, T., 2016. HRA of digital control rooms: Literature review. Research Report VTT-R-00434-16.
- Porthin, M., Liinasuo, M. and Kling, T., 2017. Performance shaping factors for advanced control room HRA. Research Report VTT-R-00905-17.
- Roth, E. and J. M. O'Hara, M. J. 2001. Integrating Digital and Conventional Human-System Interfaces: Lessons Learned from a Control Room Modernization Program (NUREG/CR-6749), Washington, DC.
- Salo, A., Keisler, J. & Morton, A. 2011. Portfolio Decision Analysis – Improved Methods for Resource Allocation, International Series In Operations Research & Management Science, Vol. 162, Springer-Verlag.
- Savolainen, I. & Vuori, S. 1977. Assessment of risks of accidents and normal operation at nuclear power plants. Espoo: VTT.
- Silvonen, T. 2013. Steam explosion case study using IDPSA methodology. Espoo: VTT. VTT Technology VTT-R-05974-13. 33 p. + app. 19 p.
- Tyrväinen, T., Häggström, A., Bäckström, O. & Björkman, K. 2017. A methodology for preliminary probabilistic multi-unit risk assessment. Espoo: VTT. VTT Technology VTT-R-00086-17. 20 p. + app. 9 p.
- Tyrväinen, T., Karanta, I. & Rossi, J. 2016. Finnish experiments on level 3 PRA. Seoul, Korea: 13th International Conference on Probabilistic Safety Assessment and Management, (PSAM 13). 10 p.
- Tyrväinen, T. & Karanta, I. 2017. Level 2 PRA studies – Source term characteristics and hydrogen explosions. Espoo: VTT. VTT Technology VTT-R-00354-17. 19 p. + app. 2 p.
- Tyrväinen, T. & Silvonen, T. 2015. Summary on integrated deterministic and probabilistic safety assessment development and case studies. Espoo: VTT. VTT Technology VTT-R-04473-15. 31 p.
- Tyrväinen, T. 2016. FinPSA – User guide – Tight integration of PRA levels 1 and 2. Espoo: VTT. VTT Technology VTT-R-03893. 11 p. + app. 1 p.
- Tyrväinen, T. 2017. Dynamic flowgraph methodology and its applications. Espoo: VTT. VTT Technology VTT-R-03364-16. 18 p.
- Vesely, W.E., Goldberg, F.F., Roberts, N.H. & Haasl, D.F. 1981. Fault tree handbook. Washington D.C.: U.S. Nuclear Regulatory Commission. NUREG-0492. 202 p.
- VTT Technical Research Centre of Finland Ltd. 2016. FinPSA – Tool for promoting safety and reliability. <https://www.simulationstore.com/finpsa>.
- VTT Technical Research Centre of Finland Ltd. 2016b. Level 2 tool user's guide for FINPSA 2.0 and other users.
- Weber, P., Median-Oliva, G. & lung, B. 2012. Overview on Bayesian networks application for dependability, risk analysis and maintenance areas, Engineering Applications of Artificial Intelligence 25 (4), pp. 671-682.

Zio, E. 2007. An Introduction to the Basics of Reliability and Risk Analysis. World Scientific Publishing, Singapore.

Zio, E. 2011. Computational Methods for Reliability and Risk Analysis. World Scientific Publishing, Singapore.

## 4. Reactor and fuel

### 4.1 Nuclear criticality and safety analyses preparedness at VTT (KATVE)

Pauli Juutilainen<sup>1</sup>, Eric Dorval<sup>1</sup>, Risto Huhtanen<sup>1</sup>, Jaakko Leppänen<sup>1</sup>, Antti Rätty<sup>1</sup>, Silja Häkkinen<sup>1</sup>, Toni Kaltiaisenaho<sup>1</sup>, Petri Kotiluoto<sup>1</sup>, Juho Peltola<sup>1</sup>, Karin Rantamäki<sup>2</sup>, Ville Valtavirta<sup>1</sup>, Riku Tuominen<sup>1</sup>,  
Tuomas Viitanen<sup>2</sup>

<sup>1</sup>VTT Technical Research Centre of Finland Ltd  
P.O. Box 1000, FI-02044 Espoo

<sup>2</sup>VTT at the moment of contribution

#### Abstract

Developing the capabilities in criticality safety, radiation shielding, activation analysis, dosimetry and dry storage modelling has been the main objective in the KATVE project. The development consists of both code and method development as well as educating new experts. The work on criticality safety has mostly consisted of assembling the validation package for fresh fuel criticality analysis and creating competence to utilize burnup credit in the spent fuel criticality safety studies. Photon transport routines have been developed to the Serpent Monte Carlo code in order to expand its applicability from reactor physics and burnup calculation to various radiation shielding applications. Dry storage cask has been a new research subject in the Finnish scope. The heat transfer in such a cask has been computed to determine the peak cladding temperature of the stored fuel pins as a function of time. It was found that the temperature is kept below the given limit of 400 °C three and half years after discharging from the core. The activation analysis and dosimetry capabilities have been maintained: the MAVRIC code has been taken into use and new experts have been educated to use the dosimetry calculation chain.

#### Introduction

The KATVE project covers a group of research themes that are at least loosely connected to reactor physics, in addition to which a new research subject, dry storage facility, has been part of the project. The project aims at improving the analysis preparedness in the selected fields, which requires both code development and educating new experts. Criticality safety is one of the subjects that has been neglected at VTT in the recent history, but during the SAFIR2014 programme it was addressed more strongly than earlier. For example, the work to construct a proper validation package restarted after a hiatus of more than a decade. It is, however, a long-lasting process and will continue for some time, but eventually the package should provide the correct bias of the computational system and thus enable the criticality safety analysis fulfilling the international standards.

Radiation shielding is another major KATVE topic that has not received as much attention as it should have over the recent years. In order to improve the computational tools, photon transport functionalities

have been developed to the Serpent Monte Carlo code. The feature enables radiation shielding calculations, but expanding the code outside of its original field of reactor physics has raised new challenges that require special attention, such as implementing variance reduction techniques.

The safety of dry storage casks was chosen to be a part of the studies in KATVE. Used fuel rods from nuclear power plants have to be contained in interim storage facilities for approximately 40 years before the final disposal. Even longer time up to 100 years have been suggested. Storage pools have been the established solution to the problem in Finland, but the idea of dry storage has also raised some interest. The safety aspects for such storage include radiation shielding, criticality safety, containment and structural safety and heat removal capacity. The present project focuses on heat removal capacity and the long term fuel behaviour during interim storage. The whole chain includes analysis of heat decay rate of used fuel, heat transfer and temperature estimate of the cask and fuel at selected time and analysis of integrity of fuel rods under these conditions over the whole storage history.

It had been noticed that in both activation analysis and neutron dosimetry needs to update and modernise the calculation system had become necessary. The codes previously used at VTT had become outdated in several ways. In order to ensure that VTT's typical calculation cases can be reliably tackled, the MAVRIC code was taken into use to replace the older codes. As the first steps, two cases were calculated with it for training purposes as a part of the KATVE project.

The neutron irradiation affects the structural integrity of many critical components within nuclear reactors. Neutron dosimetry is used to estimate the neutron doses of these components by combining measurement data with computational results. Recently, the competence of VTT in this field has significantly reduced along with the retirement of well-established experts. Thus, the focus of the project in this topic has been in educating new experts.

## Criticality Safety

The work of improving criticality safety analysis capabilities has consisted of developing the criticality safety validation package and acquiring general understanding about the requirements and international practicalities related to the usage of burnup credit in spent fuel storage configurations. The criticality safety analyses in general is preferably performed with continuous-energy Monte Carlo codes. The bias of the computing platform that consists of the software, cross-section library, operating system and hardware needs to be carefully defined through calculations against well-documented, high-quality critical experiments. The defined bias is used in the criticality safety analyses as an extra safety margin in addition to the standard subcriticality margin set by the regulator. The progress has been annually reported as VTT reports, meaning two reports during SAFIR2018 (Valtavirta, 2016) (Tuominen, 2017)

The validation package has been assembled for the MCNP (Goorley, 2012) and Serpent (Leppänen, 2015a) Monte Carlo codes at VTT over the recent years. The process originally started for MCNP a long time ago, but was almost immediately halted due to change in personnel. The work continued in the beginning of the SAFIR2014 programme and was soon extended to Serpent. At the mid-SAFIR2018, or early 2017, the package contains 72 critical experiments for MCNP and 234 for Serpent, all picked-up from the ICSBEP Handbook. A proper validation package consists of a large number of independent critical experiments modelled with the code that is to be validated. At least more than 100 cases should be included, but in addition to the number of cases, also the independency between them should be considered. For example, almost two thirds of the Serpent inputs are based on the variations of the Hungarian ZR-6 reactor, because of which many of them have to be excluded from the final package. Thus the work to add more critical experiments for both codes has to continue.

The first sets of experimental series added to the package have been VVER-440 and VVER-1000 type configurations, whose most distinct feature is the core consisting of hexagonal fuel assemblies. In addition to the above-mentioned ZR-6 reactor, these modelled experiments have been performed in Czech LR-0 (two sets, 25 + 10 cases) and Russian SF-9 (14 cases). The package for Serpent was also expanded with two sets of experiments (24 + 10 cases) performed in a square lattice core at the Valduc facility of CEA in France.

The large number of inputs has to be run and analysed automatically, for which a validation script has been and is continuously developed. Running the calculations and performing the statistical analyses based on the calculated  $k_{\text{eff}}$  values and the related computational as well as experimental uncertainties are the key functions of the script to determine the computational bias. However, in order to make the whole process run smoothly, several details need to be considered and programmed into the script. A major usability issue is the selection of the desired cross-section library with which the system is to be validated. With this kind of an approach it is likely that cross-section data is obtained from several different library versions in a single calculation. This is due to the fact that in case of a few elements, usually encountered in structural materials, some library versions provide the cross-section data for the element only, whereas some other libraries provide the data separately for the isotopes of the same element. The easy way to work around this feature is to set a priority order of library versions to be used, which is possible in the validation script for both MCNP and Serpent.

The user may also want to constrain the calculations to be run with a single cross-section library. In this case it is typical that the material definitions in MCNP and Serpent have to be modified such that they contain only nuclides that are included in the desired library version. The function performing such a modification was added to the script running the Serpent validation, but needs to be implemented for MCNP run in the future. The codes somewhat differ in the input syntax regarding the library definitions, so the improved script cannot be directly extended to handle the MCNP inputs in this case.

The script currently calculates the bias for both MCNP and Serpent, but for a proper validation report it is also important to include trend analysis of various parameters affecting the neutronics, such as uranium-235 enrichment, boron concentration in the moderator, lattice pitch and fuel-to-moderator ratio. The required function has been implemented to the script, but it can work only if the parameters are given in a standardised manner, either in the code input or in separate file. For Serpent, the data exists to some extent, but the MCNP inputs do not contain any parameters yet.

As a summary, the work on the criticality safety validation package has taken major steps forward over the recent years, but the work will continue. Larger number of critical experiments are needed and the script has to be improved. Some of the required improvements to the script are known and on the to-do-list, but it is probable that more of such issues will emerge later. It is also important to keep the script documentation up-to-date when new functionalities are created.

For parametric storage pool criticality safety studies, a calculation package called LoKriTu has been constructed in order to enable  $k_{\text{eff}}$  calculations in case that a pool loses its heat removal and the coolant begins to boil. The consideration of such a situation became interesting after the events in Fukushima. Meanwhile the LoKriTu package has mostly been developed as a contract assignment, the package and some example calculations were presented in ICNC 2015 (International Conference on Nuclear Criticality Safety) (Rantamäki, 2015). With the automated package it is possible to calculate the pool  $k_{\text{eff}}$  at several different combinations of material densities and storage geometry models. The package consists of MCNP input templates filled with keywords that are to be replaced by desired input values by the script. The desired values are given to the script as separate input and data files. The script also produces a report where the source information and results are presented. For the ICNC 2015 paper, the pool  $k_{\text{eff}}$  was calculated in two various geometries as a function of various values of moderator density, steam density and the steam layer thickness. The moderator density proved to have the most significant reactivity effect.

## **Photon transport and variance reduction in Serpent**

The implementation of a photon transport mode in the Serpent code started outside the KATVE project, originally for the purpose of accounting for gamma heating in coupled multi-physics simulations (Leppänen, 2015b). The photon physics routines were completed in 2015 (Kaltiaisenaho, 2015). The capability to model photons in addition to neutrons, however, enabled broadening the scope of Serpent applications beyond reactor physics. The focus in the KATVE project is in radiation shielding and transport applications, but the methodology can be applied to other fields as well, such as fusion research. In addition to implementing the physics routines for photon transport, the KATVE project has involved work relat-

ed to the production of radioactive source terms and variance reduction. The work has also involved implementing special detector types for photon transport calculations.

The physics model in the photon transport mode covers the four basic photo-atomic interactions: Rayleigh scattering, Compton scattering, photoelectric absorption and pair production for particle energies ranging from 1 keV to 100 MeV. The interactions are treated using detailed physics models which are covered in (Kaltiaisenaho, 2016). The production of secondary particles includes fluorescence photons from atomic relaxation, and bremsstrahlung modelled using the thick-target bremsstrahlung approximation (TTB). The TTB approximation is used to replace an explicit transport mode for secondary photon and electrons. The photon cross sections are read from ACE format libraries, whereas all the additional data is obtained from auxiliary files.

The photon physics routines were accompanied by a radioactive decay source mode. In this calculation mode Serpent reads radioactive decay data from ENDF format data libraries, and forms the source term by combining the compositions of radioactive materials to nuclide-wise emission spectra. This way the photon source can be provided by simply defining the composition of the radioactive material. The source term generation can be combined to a neutron activation or burnup calculation, in which case the compositions are read from a binary restart file produced by another Serpent run. Normalization is done automatically, and the same input files can be used for both neutron and photon transport calculations with minimal modifications. The most relevant application for the radioactive decay source mode in KATVE is a shielding calculation performed for a spent fuel transport or storage cask, in which the irradiated material compositions are obtained from Serpent burnup calculations. The methodology has also been applied for the calculation of shut-down dose rates in a fusion reactor (Sirén, 2016; Leppänen, 2016). Even though this study was part of an effort to broaden the scope of Serpent applications to new fields, the challenging test case made it very relevant considering methods developed within the KATVE project.

Radiation shielding applications involve calculation of dose rates in locations isolated from the source by physical barriers. This type of geometry is challenging for the Monte Carlo method, and in practice requires efficient use of variance reduction techniques. Serpent was originally developed as a reactor physics code, and variance reduction for shielding applications is therefore a new topic and challenge. The implemented approach is based on the use of weight-windows on a super-imposed Cartesian or cylindrical mesh (Leppänen, 2017). The importance map can be read from standard WWINP format files used by the MCNP code (Pelowitz, 2013). This enables the use of state-of-the-art variance reduction tools, such as ADVANTG (Mosher, 2013) or MAVRIC (Peplow, 2011). An alternative approach is to calculate the importances using a light-weight built-in solver based on the response-matrix method. The development of the internal solver is still under way.

## **Neutron dosimetry and activation analysis**

In-core neutron flux calculations are required at VTT mainly as input quantities for dosimetric calculations to study the effect of neutron irradiation on material properties. The calculations cases are often so complicated that deterministic codes are preferred to heavier Monte Carlo methods.

Discrete ordinates codes DORT and TORT (DOORS, 2017) (Rhoades, 1997) have been used earlier, but they are no longer developed or updated and contain some outdated features. Therefore the MAVRIC (Monaco with Automated Variance Reduction using Importance Calculations) code (Peplow, 2011) has been chosen to possibly replace these codes gradually. MAVRIC is under constant active development and is also integrated into the SCALE code package (ORNL, 2017) that has been used in VTT for a long time. It combines deterministic and Monte Carlo in order to utilize the strengths of both methods, that is, to provide a coarse solution with fast deterministic calculation and use the data in a more detailed Monte Carlo calculation. MAVRIC has been introduced at VTT through training and testing it with two separate calculation cases: the Kobayashi benchmark and dosimeter samples irradiated at Loviisa power plant (Räty, 2015; Räty 2017).

## Kobayashi Benchmark with MAVRIC

The purpose of the work was to model three simple benchmark cases (Kobayashi, 2000) determined by OECD/NEA in 1996. These are generally known as Kobayashi benchmarks. The calculation cases are designed especially to estimate fluxes at strongly heterogeneous material configurations. This is especially important in methods based on discrete ordinates, because used angle distributions may result in strong computational perturbations or ray-effects.

Moreover, discrete virtual cross sections for these materials are also determined. During the work it was noticed that the user cannot input virtual cross sections to MAVRIC. It is designed only for real world problems and materials. This came as a surprise, because Kobayashi benchmark had been modelled earlier with MAVRIC by Oak Ridge National Laboratories (Evans, 2010). However, it is possible only in code developer version, which is not available for VTT. Consequently, this study was carried out by choosing real world materials such that the fractions of their cross sections are relatively close to those determined in the benchmark. This meant uranium, aluminium and void. However, the final results are not directly compatible with official benchmark solutions, but give qualitative data on code behaviour.

All the three calculation cases were modelled using ENDF/B-VII based cross section libraries. The third degree of Legendre polynomials and 12 degree of discrete ordinates were, as suggested in the code manual (Peplow, 2011) for cases with strong heterogeneity. Neutron source was normalised with the solution reported in Reference [Kobayashi, 2000]. Comparing the fractions of calculated fluxes along different materials regions showed less than 10 percent differences between MAVRIC calculations and results calculated with GMVP code in Reference (Kobayashi, 2000).

Ray effects were studied only qualitatively, and fluxes behaved reasonably well at material interfaces. Moreover, using smaller degree of discrete ordinates was also tested. This resulted in much worse ray effects. An example of calculated fluxes from calculation case 3 is illustrated in Figure 1.

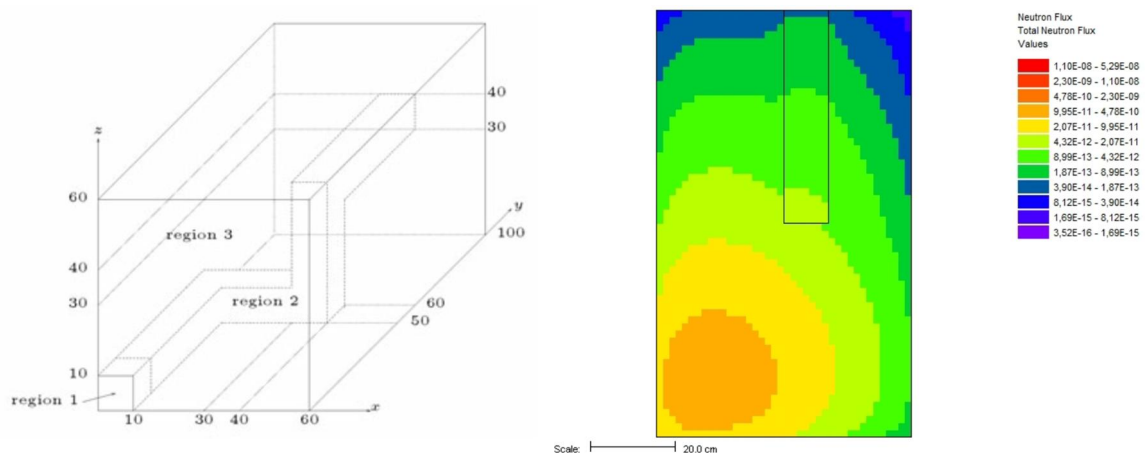


**Figure 1.** Geometry in Kobayashi calculation case 3 and calculated neutron flux in the upper void dog leg. Cross section is at the height of  $z=35$ .

## VVER-440 dosimeters with MAVRIC

The second work with MAVRIC studied the irradiated specimens of RVP material at the reactor periphery. The aim was to calculate the cumulative neutron fluxes for certain dosimeter samples at Loviisa power plant (Räty, 2017). Dosimeter samples are irradiated inside Loviisa RVP at downcomer side relatively close to the core.

All the bundles and pressure vessel internals were included in the model. Reactor upper and lower parts were omitted. Public data on VVER-440 core and fuel was used to model the geometry and fuel

bundles, but actual fuel enrichment, burnup and power density data were obtained from Fortum power company.

Surveillance chains have been irradiated over several power cycles. Total cumulate fluxes for dosimeters were calculated by modelling the core for each of these cycles separately and summing up the results taking into account the length of each cycle. In the end, results were compared with results from earlier studies that had also been verified with measurements.

Due to confidentiality reasons, only relative values were listed in the final results. Cumulative total fluxes calculated with these two codes showed around 10...15 percent differences. The calculation model included several simplifications and some parameters were based on public data only, so the error is reasonable for dosimetric calculations. Modelled geometry and comparison of flux spectra is presented in Figure 2.

### VVER-440 dosimeters with Serpent

Earlier versions of VTT's own Monte Carlo code Serpent did not include variance reduction techniques for complicated geometries. This is a new feature that was introduced to the developer version of Serpent in 2016 (Leppänen, 2017). As part of code development work, variance reduction feature was tested (Viitanen, 2016) with the same flux calculations as in Reference (Räty, 2017).

The variance reduction technique decreased the calculation time requirement by factor 100–700, depending on the reaction response. Used importance is illustrated in Figure 3.

Due to confidentiality reasons, only relative values between calculations and measurements were reported as a conference paper in AER VVER reactor physics conference in October 2016 (Viitanen, 2016). The calculated activities were in relatively good agreement with the measurements, taking into account that the calculation model included many simplifications. The C/E values for fast neutron activation were between 0.95–1.27, and for thermal activation the values were between 1.06–1.99.

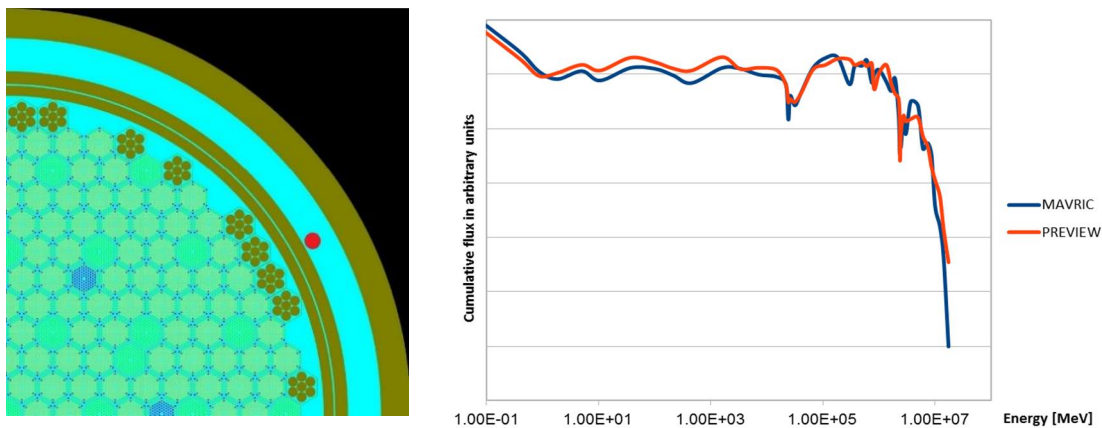


**Figure 2.** Figure from the calculation model and qualitative comparison of fluxes for dosimeters 1 and 2.

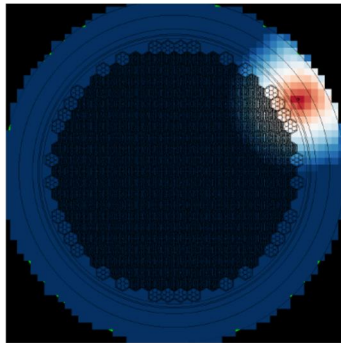


**Figure 3.** Importance map used in the Serpent variance reduction calculation.

### FiR1 activity inventories

FiR1 TRIGA research reactor in Finland was shut down in 2015. It is the first nuclear facility to be decommissioned in Finland, so the project poses interest in new kinds of studies. One of such efforts was published in Nuclear Technology in April 2016 (Räty, 2016), describing the calculations of activity inventories in TRIGA.

The objective of the article was to estimate the residual activity in the decommissioning waste of the TRIGA Mark II-type research reactor FiR 1 in Finland. Neutron flux distributions were calculated with the Monte Carlo code MCNP and these were used in the ORIGEN-S point-depletion code to calculate the neutron-induced activity of materials at different time points by modeling irradiation history and radioactive decay. An illustration of the neutron fluxes at different configuration in the reactor history is presented in Figure 4.

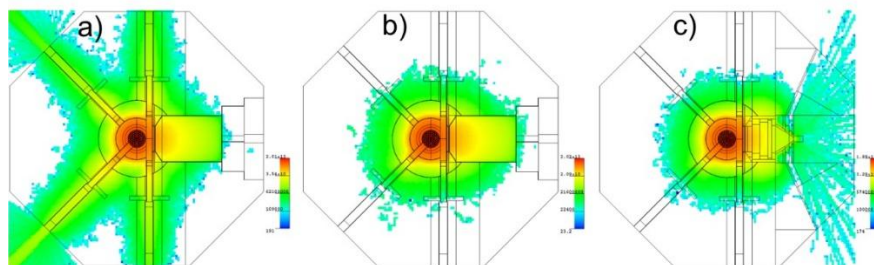


**Figure 4.** Calculated neutron fluxes in the reactor structures at different operation periods of FiR1 research reactor history.

Calculated activities were compared with the inventory estimates of two other decommissioned research reactors. Reasonable results were obtained, taking into account their different operating history. Results of this calculation are used important in the planning of future the decommissioning activities, especially for predicting the radiological impact to personnel and the environment.

### LSL-M2 code in neutron dosimetry

The neutron adjustment program LSL-M2 (Stallman, 1986) has been used in dosimetry work at VTT for several years. Along the history of use of this program, several users have been responsible for dosimetry work, in addition to numerous changes in the computer architecture and operating systems used. These changes pose challenges from the point of view of knowledge retention; use of best practices; and software portability.

Research report (Viitanen, 2015) provides a concise hands-on guide for the use of LSL-M2 with particular emphasis on the processing of input data for the code, which is an aspect not readily available in the program documentation. The processing of data is clearly divided into two parts: the generation and migration of multi-group cross section data among different group structures, and the estimation of covariances. The results of this exercise provide valuable information about which set of processing tools should be preferred depending on the basic nuclear data format available, since many combinations of data library and processing code proved to be incompatible.

With regard to covariances, the report documents a new Matlab script to be used in the calculation of activity covariances of activities. As for the estimation of covariances in group fuences originated in the basic nuclear data proved to be much more challenging. Instead, a simpler, conservative method is proposed, where correlations are related by the logarithmic distance of their weighted energies per energy group.

Finally, the exercise puts to the test the LSL-M2 program on activation measurements performed at the FiR 1 reactor. Overall, the report gathers and formalizes a number of best practices that were scattered in a variety of internal notes, and were at risk of being lost due to VTT personnel and computer architecture changes.

## **CFD analysis of varying cooling times for spent fuel in dry storage cask**

Air-cooled dry storage for spent nuclear fuel has been used abroad, but not in Finland. No experience on the thermal hydraulic analysis of the cooling of such facilities exists in Finland, but the concept has raised some interest recently. As the first step of the project, the heat transfer and peak cladding temperature of the spent fuel pins were investigated in a single cask (Huhtanen et al. 2016a) for fuel after seven year cooling time in water pool. The method was found to be consistent with the experimental results, although the experiment setup was not exactly the same as simulated in the task. At the next phase (Huhtanen, 2016b), the model was slightly improved and the calculations extended to cover a longer period up to 300 years.

The Peak Cladding Temperature (PCT) of the fuel pins is obtained as a result of the CFD analysis of heat transfer from the dry cask storage facility. The temperature history is used for studying the integrity of the fuel cladding during the years of interim storage as a later part of the KATVE-project.

Nuclide inventories and decay heat source terms were calculated using the Serpent Monte Carlo code according to the instructions of the BEAVRS benchmark (Horelik, 2013). Some simplifications were made in the burnup calculation, but the model can be considered representative of the irradiation of an average assembly in the reactor core. The heat transfer calculations were performed with OpenFOAM version 3 (OpenFOAM, 2015). The spent fuel was assumed to be stored in the Castor-V/21 cask (Dziodosz, 1986).

Total heat rate depends on fuel history in the reactor and storage time after the reactor. Fuel rods are kept in storage pools for several years. Activity is reduced exponentially during the storage time. The sources for one rod after different cooling times from 3 to 100 years are shown in Figure 5a. The number of all rods in a bundle is  $17 \times 17 = 289$ . There are 24 empty guide tubes and one instrument tube in a bundle. Thus the number of active rods is 264. The total heat of cask with 21 bundles up to 300 years is shown in Figure 5b.

The cask is filled with helium due to its good heat conductivity. The pressure inside the cask depends on temperature, when a certain amount of gas is sealed into the cask. In the simulation it is assumed that pressure inside the cask is approximately 1.0 bar.

The atmosphere outside the cask is normal air, defined as ideal gas. The heat transfer mechanisms from the cask are natural convection and radiation to the environment. The definition of free stream flow at the outer boundary is quite tricky to set properly. Free stream definition was used first, but then it was decided to set a mild inflow from the outer cylindrical surface. This makes solution more stable without affecting the flow too much. The top surface is defined as free stream boundary. Temperature on all boundaries is assumed to be 300 K. Floor level is solid with constant temperature 300 K.

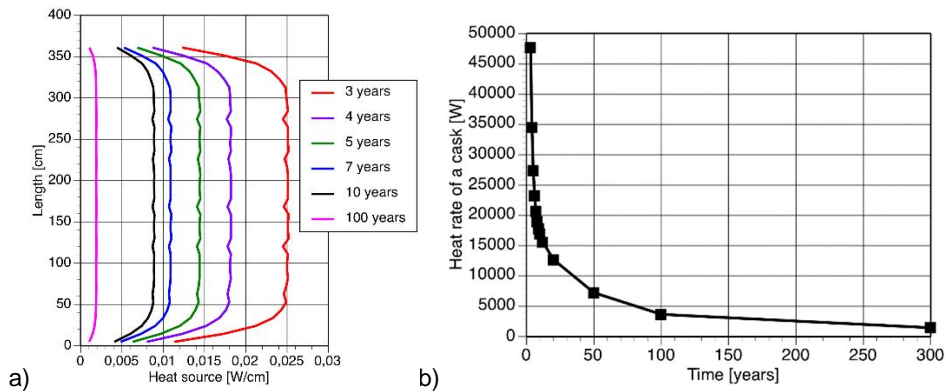


**Figure 5.** a) Heat release rate along a single rod fuel material as calculated with the Serpent code. b) The total heat rate in a cask with 21 fuel rod assemblies over time.

## Results

The simulation was performed as a steady state analysis for each time value having its own heat load. The heat load changes so slowly that the flow at each time instant can be considered as quasi-steady.

The heat and fluid flow simulations were performed using the methods presented in (Huhtanen, 2016a). The results show that the case with 4 year old rods gives peak cladding temperature 351 °C, well below the defined limit of 400 °C given in (U.S.NRC, 2010). Results for 3 year old rod give a maximum temperature 432 °C, which exceeds the limit value. We tried to interpolate the heat rate giving the limit value by increasing the heat rate profile at 4 years by 20%. The result represents the situation approximately at 3.4 years. The peak cladding temperature with this rate is 394 °C, slightly below the limit.

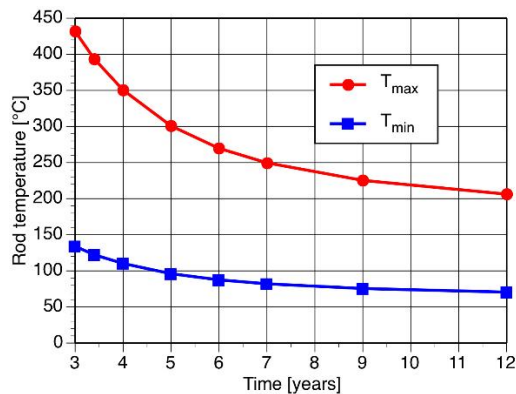


**Figure 6.** Maximum and minimum cladding temperature after different cooling times during the first 12 years.

The calculated cladding temperature values at different cooling times are shown in Figure 6. The time history has been calculated up to 300 years, but the first years are the most important in estimating the integrity of fuel cladding during the interim storage period.

The general temperature field at 4 years is shown in Figure 7. The maximum temperature in almost all simulations is on level 3.60 m, except at 300 years it is on level 3.39 m. The highest temperature is found in the second assembly. The convective heat transfer in the wider open channels around the middle assembly keep the rod temperatures on slightly lower level.

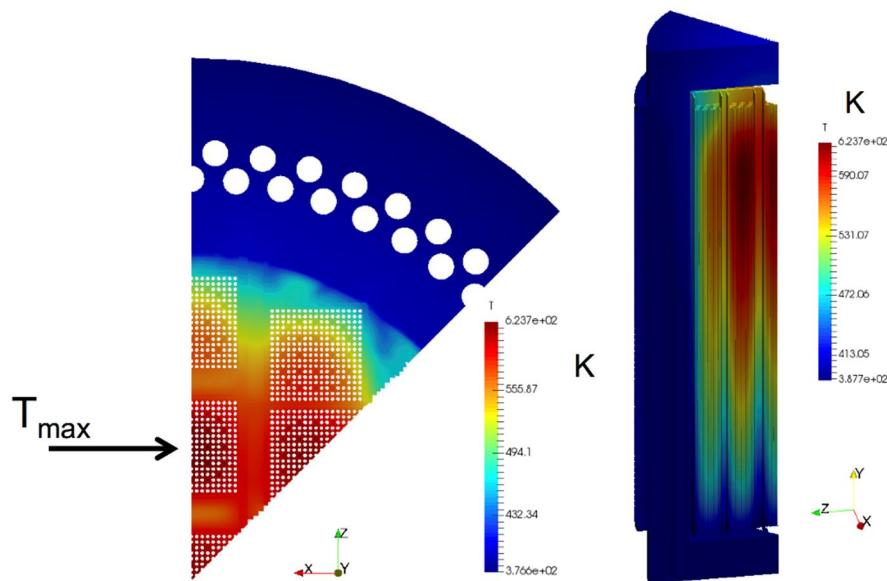


**Figure 7.** Temperature field and location of maximum temperature at 4 years. Cross section is taken from level 3.6 m. Temperature range is 388K (115°C) ... 624K (351°C). Height of the cask is 4.9 m.

Temperature profiles at the location of maximum temperature are shown in Figure 8. Location of maximum temperature is kept practically in the same rod and height up to 100 years. At 300 years the location of maximum temperature is moved to the middle assembly, but the temperature difference between the locations is very small. The graph gives the temperature profile at 300 years at the original 'hot spot'.

The minimum temperature values of the rods are found at the bottom of rods as expected. The cooling air flows upwards of the assemblies and cooling rate is best at the bottom of the assembly. Flow and temperature field in a cross section near the symmetry axis is shown in Figure 9. The plane is between the first two rows of the fuel rods. Velocity magnitude is very low in the rod bundle due to tight packing of rods and friction resistance. In the open channels of the basket flow velocity is much higher. The influence of this to the cooling efficiency is clearly seen in the temperature field. The more detailed description of the simulation and results is given in (Huhtanen, 2016b).

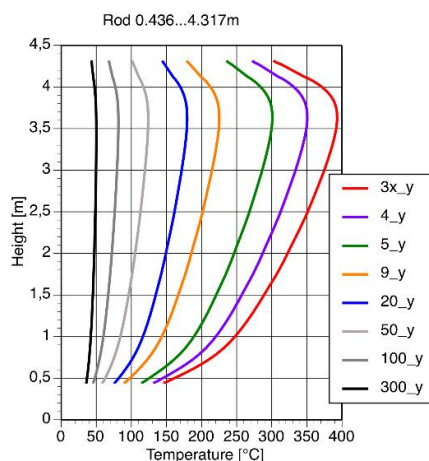


**Figure 8.** Temperature profile of the rod at maximum temperature at different time steps. Location of maximum temperature is kept in the same rod up to 100 years. At 300 years it is located in the middle assembly. However, at that time the temperature difference between the locations is very small.

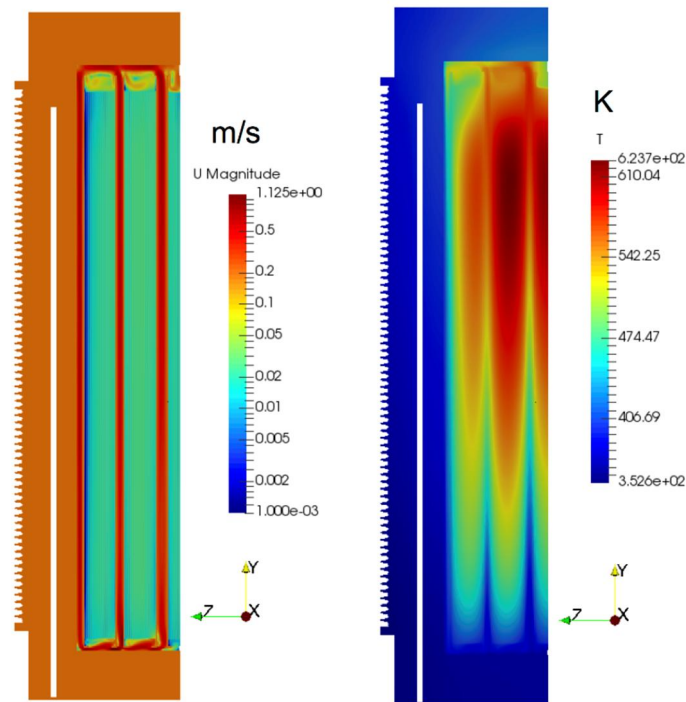


**Figure 9.** Velocity magnitude (left) and temperature (right) on plane 0.02 m from the symmetry plane, between the first rows of fuel rods.

## References

- DOORS 2017. One, Two- and Three-Dimensional Discrete Ordinates Neutron/Photon Transport Code System, RSICC web page, <http://www-rsicc.ornl.gov/codes/ccc/ccc6/ccc-650.html>
- Dziadosz, D. & Moore, E. V. 1986. The Castor-V/21 PWR Spent-Fuel Storage Cask: Testing and Analyses. EPRI NP-4887. November 1986. 262 p.
- Evans T. M. 2010. DENOVO: A New Three-Dimensional Parallel Discrete Ordinates Code in Scale, Nuclear Technology 171 (2010), pp. 171–200
- Goorley, T. et al. 2012. Initial MCNP6 Release Overview. Nuclear Technology, 180 (2012) 298–315.
- Horelik, N. & Herman, B. 2013. BEAVRS. Benchmark for Evaluation And Validation of Reactor Simulations. Release rev. 1.1.1. MIT Computational Reactor Physics Group. October 30, 2013. 163 p.
- Huhtanen, R., Peltola, J. & Leppänen, J. 2016a. Heat transfer in dry storage cask. VTT Research report, VTT-R-00810-16. 26p.
- Huhtanen, R., Peltola, J. & Leppänen, J. 2016b. CFD analysis of varying cooling times for the fuel. VTT Research report VTT-R-05236-16. 22p

- Kobayashi, K., Sugimura, N. & Nagayay, Y. 2000. 3-D Radiation Transport Benchmark Problems and Results for Simple Geometries with Void Regions, Organisation for Economic Co-operation and Development Nuclear Energy Agency
- Mosher, S. et al. 2013. ADVANTG – An Automated Variance Reduction Parameter Generator. ORNL/TM-2013/416, Oak Ridge National Laboratory (2013).
- Leppänen, J., Pusa, M., Viitanen, T., Valtavirta, V. & Kaltiaisenaho, T. 2015a. The Serpent Monte Carlo code: Status, development and applications in 2013. *Annals of Nuclear Energy*, 82 (2015) 142–150
- Leppänen, J., Hovi, V., Ikonen, T., Kurki, J., Pusa, M., Valtavirta, V. and Viitanen, T. 2015b. The Numerical Multi-Physics project (NUMPS) at VTT Technical Research Centre of Finland. *Ann. Nucl. Energy*, 84 (2015) 55-62.
- Leppänen, J. and Kaltiaisenaho, T. 2016. Expanding the Use of Serpent 2 to Fusion Applications: Shutdown Dose Rate Calculations. In proc. PHYSOR 2016, Sun Valley, ID, May 1-6, 2016.
- Leppänen J., Viitanen T., Hyvönen O. 2017. Development of a Variance Reduction Scheme in the Serpent 2 Monte Carlo Code, M&C 2017 - International Conference on Mathematics & Computational Methods Applied to Nuclear Science & Engineering, Jeju, Korea, April 16–20, 2017
- NJOY 2013. The NJOY Nuclear Data Processing System, Version 2012. Los Alamos National Laboratory, LA-UR-12-27079 Rev, 2013.
- OpenFOAM 2015. OpenFOAM 3.0.1, <http://www.openfoam.org>, OpenFOAM Foundation, 2015.
- ORNL 2017. Oak Ridge National Laboratories, SCALE – A Comprehensive Modelling and Simulation Suite for Nuclear Safety Analysis and Design, <http://scale.ornl.gov/>
- Pelowitz, D. (editor). 2013. MCNP6 User's Manual: Appendix C Mesh-Based WWINP, WWOUT, and WWONE File Format. LA-CP-13-00634, Los Alamos National Laboratory (2013).
- Peplow, D. E. 2011. MAVRIC: Monaco with Automated Variance Reduction Using Importance Calculations, Oak Ridge National Laboratories ORNL/TM-2005/39, version 6.1
- Rantamäki, K. 2015. Criticality Calculation Package and Its Use for a Spent Fuel Storage Pool with Steam Layer. In proceedings of ICNC 2015, Charlotte, NC, USA, September 13–17, 2015
- Rhoades, W.A. 1997. The TORT Three-Dimensional Discrete Ordinates Neutron/PhotonTransport Code. Oak Ridge National Laboratories, ORNL/TM-13221, 1997
- Räty, A. 2015. Kobayashi benchmark MAVRIC-ohjelmalla, VTT tutkimusraportti VTT-R-06333-15. 2015. 20 p. + app. 2 p. (in Finnish)
- Räty, A, Kotiluoto P, 2016. FIR1 TRIGA activity inventories for decommissioning planning. *Nuclear Technology* 194 (2016) pp. 28–38
- Räty, A., 2017. Calculating the cumulative flux of VVER-440 dosimeters with MAVRIC and KENO, VTT Research Report VTT-R-00380-17
- Sirén, P. and Leppänen, J. 2016. Expanding the use of Serpent 2 to Fusion Applications: Development of a Plasma Neutron Source. In proc. PHYSOR 2016, Sun Valley, ID, May 1-6, 2016.

- Stallman, F. W. 1986. LSL-M2: A Computer Program for Least-Squares Logarithmic Adjustment of Neutron Spectra, NUREG/CR-4349, Oak Ridge National Laboratory. 1986. (Additional unpublished manual provided with version 2.0)
- Tuominen, R., Valtavirta, V. & Juutilainen, P. 2017. Kriittisyysturvallisuuden validointipaketin tilanne 2016. VTT Tutkimusraportti VTT-R-00749-17 2017. 19 p. (in Finnish)
- U.S.NRC 2010. Standard review plan for spent fuel dry storage systems at a general licence facility. NU-REG-1536, revision 1. U.S.NRC Final report. July 2010. 424p
- Valtavirta, V. Juutilainen, P. 2016. Kriittisyysturvallisuuden validointipaketin tilanne 2015. VTT Tutkimusraportti VTT-R-00301-16. 2016. 15 p. + app. 15 p. (in Finnish)
- Viitanen, T. 2015. On adjustment of neutron spectra using LSL-M2 program. VTT Research report VTT-R-06065-15. 2015. 39 p.
- Viitanen T, Leppänen J. 2016. Calculating neutron dosimeter activation in VVER-440 surveillance chains with Serpent, 27th Symposium of AER on VVER Reactor Physics and Reactor Safety, November 2016, Helsinki, Finland

## 4.2 Development of a Monte Carlo based calculation sequence for reactor core safety analyses (MONSOON)

Jaakko Leppänen

VTT Technical Research Centre of Finland Ltd  
P.O. Box 1000, FI-02044 Espoo

### Abstract

The MONSOON project continues the development of the Serpent Monte Carlo code, with the specific goal of establishing a complete and independent calculation sequence for the safety analyses of Finnish power reactors. The work consists of developing methodologies for spatial homogenization, which forms the first part of the traditional multi-stage calculation scheme applied for core physics calculations. The work was started already in the KÄÄRME project of SAFIR2014, which provided a proof-of-concept type demonstration for the use of the continuous-energy Monte Carlo method for spatial homogenization. The MONSOON project aims to proceed from feasibility studies to practical applications and routine full-scale safety analyses. Serpent development is carried out in close collaboration with a large international user community. The code is currently used in more than 170 organizations in 37 countries around the world.

### Introduction

Nuclear reactor safety analyses involving coupled full-scale fuel cycle and transient calculations currently rely on a two-stage calculation scheme, in which the neutron transport physics at the fuel assembly level is first condensed into a set of representative group constants, which are then used as the input data for a reduced-order steady-state or dynamic full-core calculation. Group constant generation involves a procedure called spatial homogenization, which essentially implies the solution of the heterogeneous transport problem at the local fuel assembly level. The procedure is repeated for different assembly types, burnups and reactor operating conditions, and the result is a complete data library, providing the sufficient building blocks for the coupled full-scale calculation.

Managing this calculation scheme as a whole is an important part of reactor core analysis, and profound understanding of the methods, theory and underlying physics is absolutely essential for the safe and reliable utilization of nuclear energy. The MONSOON project aims to enhance the knowledge basis needed for performing independent safety analyses for Finnish power reactors, relying on a novel approach using the continuous-energy Monte Carlo method for spatial homogenization. The work extends the methodologies applied in the calculation scheme to state-of-the-art and beyond. The primary calculation tool is the Serpent Monte Carlo code (Leppänen, 2015a), which has been developed for reactor physics applications at VTT since 2004 (Leppänen, 2007).

The MONSOON project essentially continues the work started in the KÄÄRME project of SAFIR2014. The success of the previous work was recognized in the SAFIR2018 Framework Plan (SAFIR2018), where it was explicitly stated that the Serpent code has proven to be an international success, and that its development should be continued and the range of application targets broadened. It was also pointed out that the work connects to a broader goal of developing a fully independent reactor physics calculation system, accompanied by fundamental, source-code level understanding of the underlying computational methodology. Encouraged by the recognition and positive feedback, the original project plan for the MONSOON project was drafted with ambitious goals. The primary objective was to develop the methodology for Monte Carlo based spatial homogenization into a practical computational framework for routine nuclear reactor

safety analyses. In other words, to proceed from proof-of-concept type studies to practical applications. The major tasks and goals included in the original project plan can be summarized as follows:

1. Complete the methodological development in the Serpent code that was started in SAFIR2014
2. Establish the systematic procedures required for producing the full set of homogenized group constants for different reactor types (VVER, PWR, BWR) and applications (fuel cycle simulations and transient analyses)
3. Perform extensive validation for the developed computational methodology involving the most relevant calculation codes used at VTT (ARES, TRAB3D, HEXBU-3D, HEXTRAN, Apros, PARCS, Simulate, DYN3D, etc.)
4. Study new approaches and methodologies for Monte Carlo based spatial homogenization and nodal diffusion calculations (3D methods, coupled calculations, etc.)
5. Maintain contacts and enhance collaboration with Serpent users and the international reactor physics community

Unfortunately, the planned project volume was considerably reduced in 2015 and 2016. The applied volume in 2015 was 23.5 person-months and 275 k€. The realized volume was 12.7 pm and 148 k€. In 2016 the volume was further reduced to only 7.8 pm and 100 k€. With one third of the original funding it became apparent that accomplishing the planned tasks would not be possible, and most of the ambitious goals had to be dropped early on. Another major drawback was that two key members of the project group and Serpent developer team left VTT to pursue a career outside the nuclear field in 2016.

The project was essentially reduced to completing the work carried over from SAFIR2014. This involved some methodological development in the Serpent code and validation of the Serpent-ARES code sequence for PWR fuel cycle simulations. These tasks were completed by the end of 2016. Some development and validation tasks were also carried out in collaboration with the KATVE, SADE and PANHCO projects. Additional funding from Fennovoima in 2016 enabled running preliminary validation studies for a Serpent-HEXBU steady-state VVER-1000 benchmark calculation.

The following sections focus on international collaborations and the Serpent-ARES calculations. Other accomplishments, including education of new experts are covered by a brief summary

## International collaboration

The Serpent code has been in public distribution since 2009. When the MONSOON project started in 2015, the number of users was around 380. At the time of this writing the user community had grown to 650 users in 172 organizations around the world. Serpent is most commonly used by university students for academic research and thesis work, but the code has an extensive user basis in various research organizations as well. In recent years Serpent has also been adopted by the nuclear industry and small businesses working on innovative reactor designs. The strong emphasis in academic research is reflected in the number of publications. A total of 440 peer-reviewed scientific journal articles and conference papers and 120 theses have been published on Serpent-related topics since the beginning of code development in 2004. In Finland, Serpent development and applications have provided topics for five doctoral and 26 M.Sc. and B.Sc. theses and special assignments at Aalto University and Lappeenranta University of Technology. Two more doctoral theses at Aalto are to be completed by mid-2017. The number of Serpent users and publications since 2005 is presented in Figures 1 and 2.

Active communication with Serpent users is maintained in various ways. Serpent has an official website<sup>1</sup>, and an interactive discussion forum.<sup>2</sup> A Wiki-based on-line User Manual was established in November 2015,<sup>3</sup> as a replacement for an old pdf-manual that was missing most of the new features implemented in the code in recent years. Annual international user group meetings have been hosted together with

---

<sup>1</sup> <http://montecarlo.vtt.fi>

<sup>2</sup> <http://ttuki.vtt.fi/serpent>

<sup>3</sup> <http://serpent.vtt.fi/mediawiki>

Serpent user organizations since 2011. The 2015 UGM was hosted by the University of Tennessee in Knoxville, USA, and in 2016 the meeting was held in Milan, Italy. Both events covered 3 full days of Serpent-related presentations by some 40 participants.

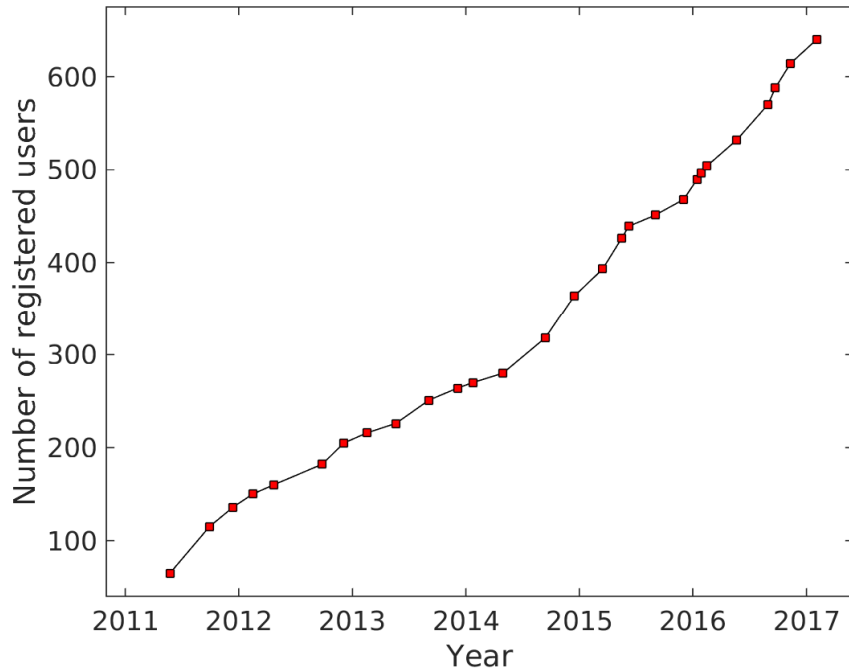


**Figure 1.** Number of registered Serpent users since 2011.

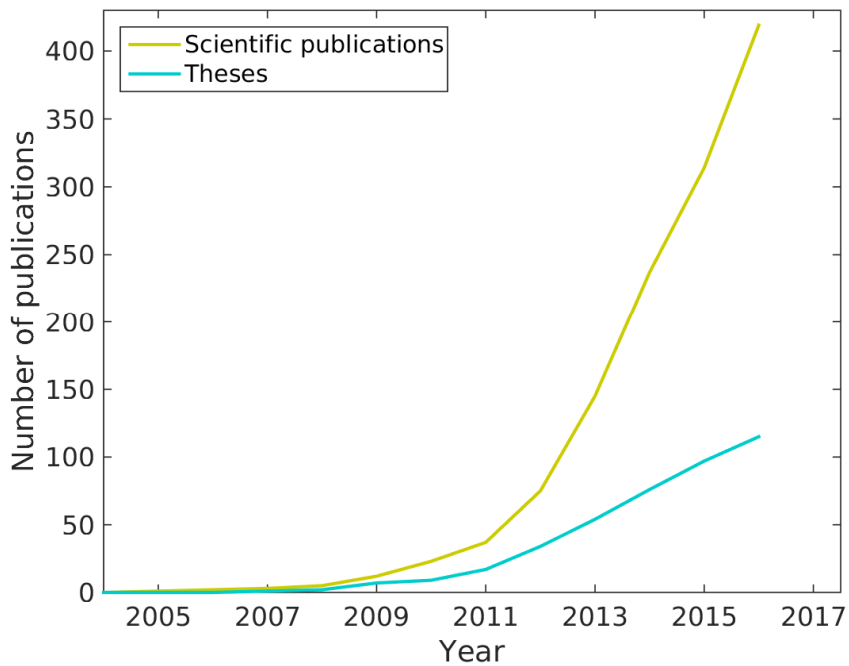


**Figure 2.** Number of Serpent-related publications and theses since 2005.

The Serpent developer team has actively organized half-day workshops at international conferences and meetings. Such events in 2015-2016 include the international reactor physics conference PHY-SOR2016 in Sun Valley, Idaho, the Canadian Nuclear Society 7th International Conference on Modeling and Simulation in Nuclear Science and Engineering in Ottawa, and the 26th Symposium of AER on VVER Reactor Physics and Reactor Safety in Helsinki. Other forms of international collaboration include participation in the American Nuclear Society Reactor Physics Division Executive Committee in 2013-2016, and invited talks at various universities, most recently at Massachusetts Institute of Technology (MIT) in December 2015.

The international collaboration has proven extremely valuable, as several user organizations have provided major contributions to the development and validation efforts. Methodology for spatial homogenization has been developed in close collaboration with the Helmholtz-Zentrum Dresden-Rossendorf (HZDR) in Germany. HZDR is using Serpent extensively for producing cross sections for their DYN3D code. Serpent-generated group constants have also been used with the PARCS nodal diffusion code, which has a large user community especially in the US. Typical validation studies involve comparisons between Serpent and another reactor physics codes such as CASMO or HELIOS. Validation can also be extended to cover the full computational sequence by comparing the results from nodal diffusion calculations using Serpent-generated cross sections to a reference 3D Serpent solution. Most of these studies have been performed for steady-state zero-power initial cores, but some users have also modeled transients (Knebel, 2016). The validation studies performed by Serpent users complement the work that had to be dropped from the original MONSOON project plan due to reductions in project volume. Without these invaluable contributions it would be practically impossible to keep up the current pace of code development.

Other forms of international collaboration include hosting visiting scientists and students. A doctoral student from Jozef Stefan Institute (JSI) visited VTT for a period of one week in September. The purpose of the visit was to exchange information on methods applied for spatial homogenization and to familiarize JSI in the use of the Serpent-based calculation sequence. Westinghouse, Sweden has followed the development of Serpent closely for several years, and in 2015 an M.Sc. student was hired for validating and benchmarking their lattice physics code system against Serpent. The current plan for Westinghouse is to sponsor another M.Sc. thesis work related to the use of Serpent as part of their reactor analysis calculation sequence. The possibility of VTT hosting the student is being discussed. Ukrainian expert organization RPA Impulse has expressed interest in validating Serpent for reactor physical safety analyses using operating data from 12 VVER-1000 reactor units collected over the past 12 years. Discussions on possible forms of collaboration have been started.

## **Validation of the Serpent-ARES code sequence**

Even though the original plan was to develop the Serpent-based code sequence for spatial homogenization into a practical computational framework for routine nuclear reactor safety analyses during the four years of the MONSOON project, the considerable reduction in project budget meant that many of the original goals had to be dropped. The reductions affected most severely the validation task. Instead of covering steady-state fuel cycle simulation and dynamic transient calculations for VVER, PWR and BWR reactor types, the work was focused on a single code sequence (Serpent-ARES) and a calculation case for which some preliminary studies were carried out already in SAFIR2014. This type of approach can be considered sufficient when it accompanies the development of new computational methods, but moving from proof-of-concept type studies to practical applications clearly requires more extensive validation effort.

ARES is BWR/PWR core simulator, developed at the Finnish Radiation and Nuclear Safety Authority (STUK), and used at VTT mostly for research purposes. The neutronics model in ARES solves the two-group steady-state diffusion equations in rectangular geometry, using the analytical function expansion nodal model (AFEN). This neutronics model represents a more advanced approach to the nodal diffusion problem compared to the methods used in VTT's in-house nodal codes. The results are therefore interesting also for the purpose of evaluating the accuracy and development potential of reduced-order methods for core analysis. The homogenized group constants for ARES were produced using the standard meth-

odology available in Serpent 2 (Leppänen, 2016a). One of the major challenges was managing the very large number of assembly-level calculations required for covering all operating states in the reactor core. Historically the Monte Carlo method has been considered computationally too expensive for this task, so one of the major goals of the study was a demonstration of practical feasibility using today's computational resources.

The test case for the Serpent-ARES code sequence was the MIT BEAVRS benchmark (Horelik and Herman, 2013), which was originally established for the purpose of validating high-fidelity core analysis methods against experimental reactor physics measurements. The benchmark model consists of a detailed description of a commercial 1000 MW Westinghouse PWR core, with assembly loading patterns and operating histories covering the first two core cycles. Experimental data includes control rod bank worths, power distributions and boron let-down curves. The detailed geometry and material data provided in the benchmark specification allowed constructing a very precise 3D model of the core for reference Serpent calculations. This way the Serpent-ARES results could be compared not only to experimental data, but also to a high-fidelity Monte Carlo solution. This type of comparison is extremely valuable for the validation of reduced-order methodologies, since all uncertainties from nuclear interaction data and experimental measurements are reduced to zero, and the comparison truly reflects how well the computational sequence preserves the physics of the heterogeneous transport solution.

The first part of the study was completed in the KÄÄRME project of SAFIR2014 (Leppänen, 2014). This study covered the hot zero-power (HZP) state of the PWR core. The omission of fuel burnup and the uniform distribution of material temperatures and densities allowed generating homogenized group constants corresponding to the exact operating state, which considerably simplified the overall procedure. The same conditions were easily replicated in a heterogeneous core model, which allowed using full-scale Serpent simulations as the reference result for comparison. The differences between the Serpent-ARES code sequence and the reference Serpent 3D calculation turned out to be small, although reaching the maximum level of accuracy required using colorset configurations to account for the effects of surrounding assemblies in spatial homogenization.

In the second part of the study (Leppänen, 2016b) the calculations were extended to hot full-power (HFP) state and fuel cycle simulations. Producing the full set of group constants for ARES required a very large number of calculations, taking into account the variation in fuel temperature, moderator temperature and density, coolant boron concentration and insertion of control rods. The cross section model in ARES is based on the combination of tabular interpolation and polynomial expansions. History effects were included for water density and boron concentration. The calculations were repeated for 9 different assembly types irradiated up to 50 MWd/kgU burnup. Covering all assembly types and reactor operating conditions required running the Monte Carlo transport simulation 11,868 times, not counting the transport solutions run during fuel depletion. Each simulation involved 10 million neutron histories. The branch variations were invoked using a built-in automated calculation sequence in the Serpent code (Leppänen, 2016a), and the manual effort required for preparing the input files remained moderate.

The calculations were run in VTT's computer cluster, "The Doctor", which consists of a heterogeneous configuration of 14 nodes with 16 cores, 45 nodes with 20 cores, 8 nodes with 32 cores, 10 nodes with 36 cores and 1 node with 60 cores. At the time of the study the capacity of the cluster was somewhat insufficient for the number of its users, and the average load especially in the most high-performing nodes was constantly high. Since the overall computational cost of group constant generation was divided between 81 separate history cases, it was decided that the most efficient way to utilize the available computer capacity was to run simultaneously as many cases as possible. The number of cores assigned to each case was kept relatively low, in order to fit the jobs in the 20-core nodes in which the average load was not prohibitively high.

The history cases with the largest number of branches were submitted with 20 parallel OpenMP threads and the remaining cases with 10 threads. This way it was possible to start all long runs immediately, while most of the shorter ones remained in queue waiting for more nodes to become available. The running times are plotted in Fig. 3. Some of the histories stand out with considerably longer running times compared to the rest. This was caused by the overloading of the nodes with jobs started by other users who

by-passed the queuing system of the grid engine. These became the limiting cases for the overall running time. The longest running history was started soon after the jobs were submitted, and it was the last one completed, 46 h later. Since the procedure of group constant generation has to be performed only once, this test case can be taken as a practical demonstration that the continuous-energy Monte Carlo method can be used for spatial homogenization at an acceptable computational cost.

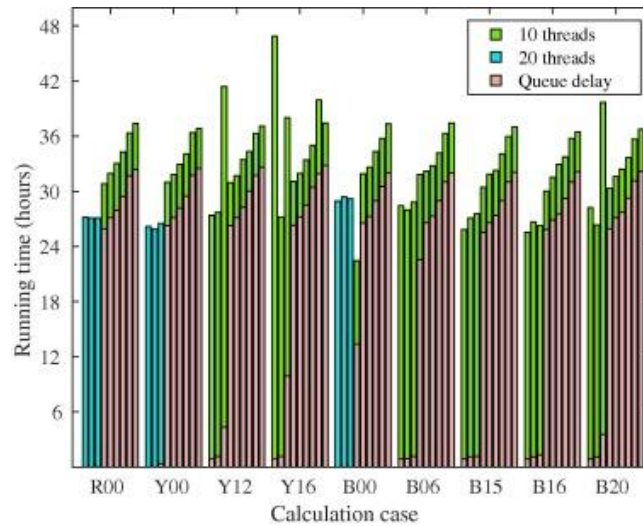


**Figure 3.** Wall-clock running times of the 9 history cases. The longest histories were submitted first and therefore started immediately, while the remaining cases were left in the queue waiting for more computer nodes to become available. Cases with the largest number of branches (all state-point variations + control rod insertion) were run with 20 and the remaining cases with 10 CPU cores.

The calculations performed in the study involved the evaluation of critical boron concentrations and control rod bank worths for various configurations, comparison of HFP core power distributions to reference Serpent 3D results and calculation of boron dilution curve for the first core cycle. The results of the control rod calculations are presented in Tables 1 and 2. The labeling corresponds to that used in Table 19 of (Horelik and Herman, 2013). Both the critical boron concentrations and control rod bank worths show good agreement with the experimental reference results.

Hot full-power calculations were performed for the fresh core at 3411 MW fission power, assuming zero concentrations for fission product poisons. The resulting node-wise coolant density and fuel and coolant temperature distributions from the ARES calculation were passed into the corresponding Serpent 3D reference model via a data interface specifically developed for coupled multi-physics calculations (Leppänen, 2015b). The reference calculation was run with 65 billion neutron histories. The results are plotted and compared in Figures. 4, 5 and 6. The differences in radial power distribution peak at 3.5% in assemblies with 15 asymmetrically positioned burnable absorber pins. There is also a noticeable radial tilt in the flux distribution, leading to a systematic under-prediction of assembly powers at the core center. The errors in the outer rings generally remain below 1%. The comparison of axial power profiles in Fig. 6 shows a good agreement.

Fuel cycle simulations for core cycle 1 were run with ARES. Reactor power was kept constant at 3411 MW, and the cycle length was set to 326 days with 30 intermediate steps as listed in Table 21 of (Horelik and Herman, 2013). All control rods were withdrawn from the core, and equilibrium iteration was applied for fission product poisons Xe-135 and Sm-149. It should be noted that this operating history does not correspond to actual reactor operation during cycle 1, but rather the boron let-down curve provided in units of effective full-power days (EFPD) in the benchmark specification.

**Table 1.** Critical boron concentrations (in ppm) for the different control rod bank configurations. Comparison between Serpent-ARES and experimental reference results.

Configuration	ARES	Ref.	Diff.
ARO	972	975	-3
D	910	902	8
C, D	812	810	2
A, B, C, D	677	686	-9
A, B, C, D, SE, SD, SC	488	508	-20

**Table 2.** Control rod bank worths (in pcm). Comparison between Serpent-ARES and experimental reference results.

Configuration	ARES	Ref.	Diff.
D	794	788	6
C	1232	1203	29
B	1206	1171	35
A	563	548	15
SE	473	461	12
SD	786	772	14
SC	1109	1099	10

The measured and simulated boron let-down curves are compared in Fig. 7. The results are in good agreement. The critical concentration is systematically under-predicted by ARES, but the differences remain below 25 ppm. The simulation is terminated when the boron concentration reaches zero at 324.8 days, which means that the overall cycle length falls short by only 29 hours.

## Other results

One of the novel research topics kept in the project plan was the application of fuel performance code coupling to burnup calculations performed for the purpose of spatial homogenization. The methodology for running the coupled simulation was established earlier (Leppänen, 2015b), and the motivation for the study was to see whether incorporating a detailed temperature feedback model in the neutronics simulation would affect the results of group constant generation. The underlying physical assumption was that the conventional approach applied in spatial homogenization in which all fuel materials are modeled at a single effective temperature overlooks certain heterogeneous effects, in particular the reduced power level in burnable absorber bearing fuel pins and the radial temperature gradient over the uranium pellet. The results are reported in a scientific journal article (Valtavirta, 2017a), and the study is a part of a doctoral thesis, to be completed by mid-2017 (Valtavirta, 2017b). The work was carried out in collaboration with the PANCHO project.

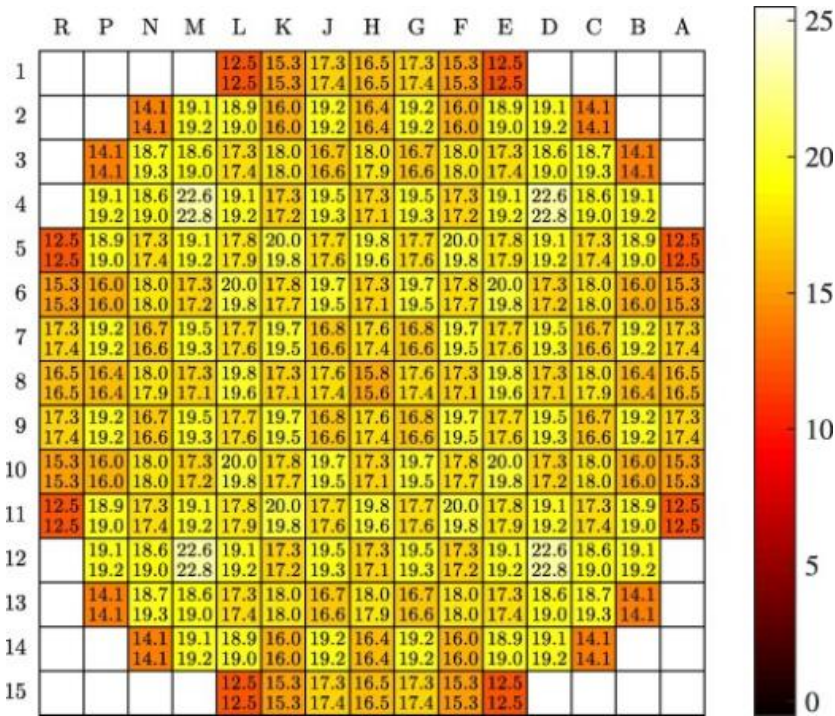


**Figure 4.** Radial power distribution in the hot full-power state of the initial core (assembly powers in MW). Top value shows the reference Serpent 3D result and bottom value the Serpent-ARES result.

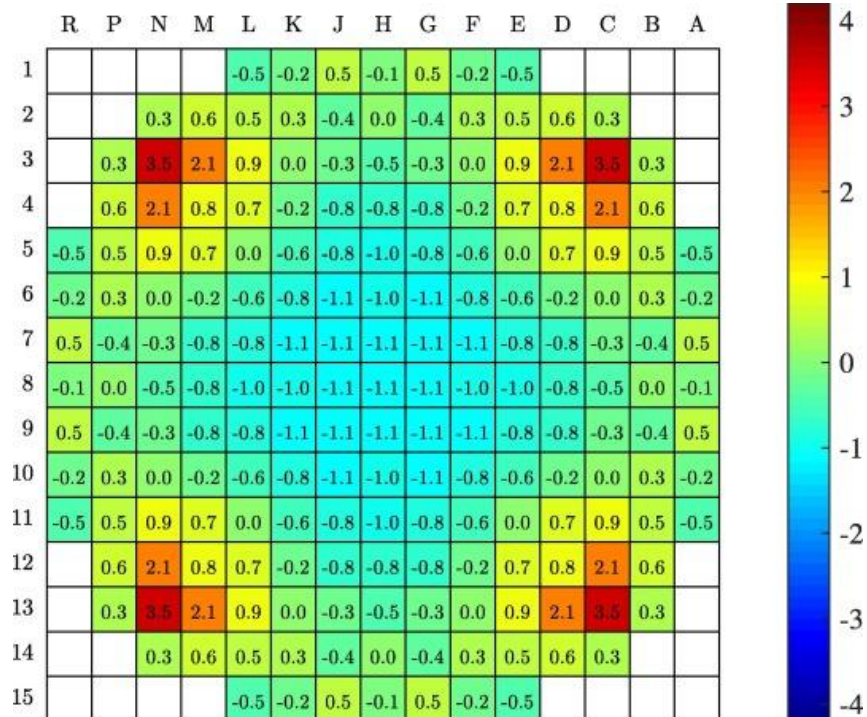


**Figure 5.** Relative differences in the radial power distribution between Serpent-ARES and the reference Serpent 3D result (in percent).

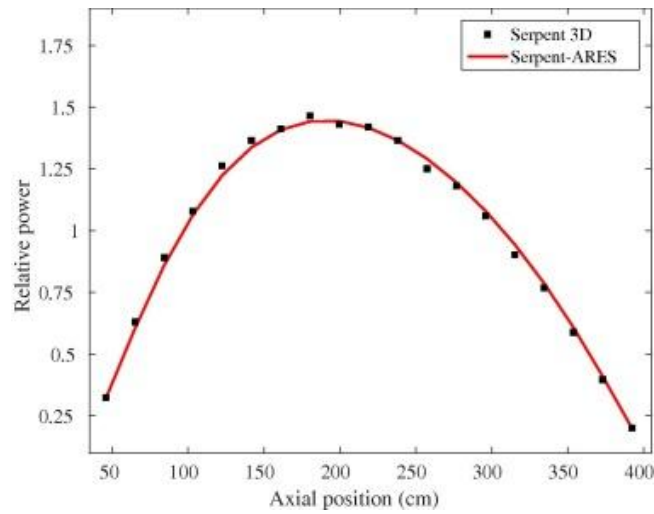


**Figure 6.** Axial power profiles averaged over all radial nodes. Serpent-ARES compared to the reference Serpent 3D result. The small dips in the Serpent 3D result are caused by fuel spacers, which are omitted in the ARES core model.

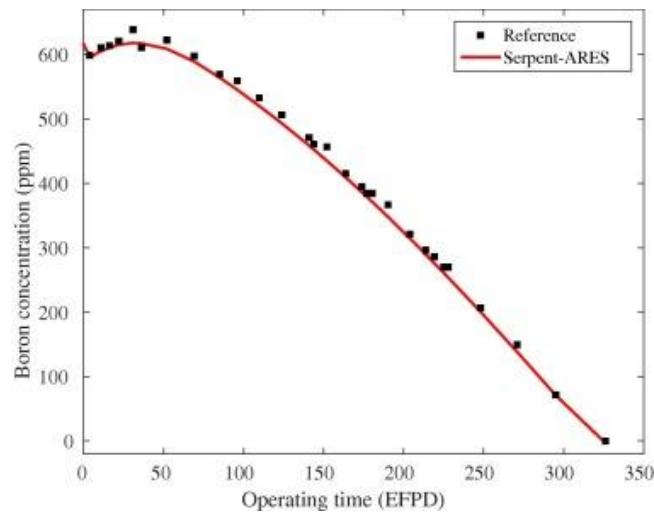


**Figure 7.** Boron let-down curve for cycle 1 calculated by Serpent-ARES compared to experimental reference data.

Even though the practical feasibility of using the Monte Carlo method for spatial homogenization was demonstrated using the Serpent-ARES code sequence, the MONSOON project in 2015-2016 also included a number of studies with other codes. Various calculations involving the Serpent-TRAB3D code sequence were carried out in collaboration with the SADE project. The pin-power reconstruction model in TRAB3D was modified and improved, and applied to an EPR HZP core calculation. (Sahlberg, 2015). The effect of axial heterogeneities in the EPR core was studied in an M.Sc. thesis project (Sahlberg, 2016a). Serpent was used in both studies for producing group constant data for TRAB3D, as well as for providing the reference 3D solution.

Calculations were also performed for hexagonal cores. Serpent was used for modeling the V-1000 zero-power critical facility at Kurchatov Institute. The same core was modeled with HEXTRAN, using Serpent-

generated group constants (Sahlberg, 2016b). Fennovoima provided additional funding in late 2016 for the validation of the Serpent-HEXB3D calculation sequence. The test case was a VVER-1000 full-core benchmark problem, in which the results from HEXB3D were compared to a reference Serpent calculation (Rintala, 2017).

The MONSOON project in 2015-2016 has involved the work of five young professionals under the age of 35. One doctoral thesis on Serpent development was completed in 2015 (Viitanen, 2015) and one M.Sc. thesis on the Serpent-TRAB3D code sequence in 2016. One more doctoral thesis is to be completed later this year (Valtavirta, 2017), and two recently graduated project group members have started their doctoral studies.

## Discussion and future plans

Despite the major reductions in the project volume, many of the planned tasks were accomplished by the end of 2016. The calculation routines implemented in the Serpent code for group constant generation can be considered practically ready for routine use. The methodology was put to test in a PWR fuel cycle simulation using the ARES nodal diffusion code, and the calculations demonstrated that the high computational cost of the Monte Carlo method is no longer a practical limitation. The work left for the remaining two years extends the validation calculations to BWR's and transient analysis. Even though the procedures applied for group constant generation are similar to the previous studies, there are significant new challenges.

The validation studies using various nodal diffusion codes and comparison of results to reference 3D Serpent calculations have for the first time provided insight into the accuracy of the two-stage calculation sequence based on spatial homogenization and reduced-order methods for core calculations, without significant uncertainties resulting from external factors. One of the major findings is that the AFEN method used in the ARES code can be considered vastly superior compared to the other nodal diffusion solutions. It has also become apparent that the current heterogeneous core designs are pushing the boundaries of methods developed with the assumption of much more homogeneous configurations.

Based on these observations it has been concluded that drastic measures are needed in order to keep up with the development. These observations, together with other factors related to the education of a new generation of reactor physics experts, have prompted the idea of renewing the calculation system used at VTT for reactor core safety analyses (Leppänen, 2017). The development of new methodologies for core calculations is a formidable task, extending well beyond the scope of the on-going SAFIR2018 programme. As part of this effort, some preliminary studies on the development of a new modern nodal diffusion solver are included in the MONSOON2017 project plan. The main goal of this task is to further demonstrate the need for a more accurate reduced-order solver for reactor core calculations, and that such solver can be developed over a period of several years with reasonable effort.

## References

- Horelik, N. and Herman B. 2013. Benchmark for Evaluation and Validation of Reactor Simulations rev. 1.1.1 MIT Computational Reactor Physics Group (2013).
- Knebel, M., Mercatali, L., Sanchez, V., Stieglitz, R. and Macian-Juan, R. 2016. Validation of the Serpent 2-DYNSUB code sequence using the Special Power Excursion Reactor Test III (SPERT III). *Ann. Nucl. Energy*, 91 (2016) 79-91.
- Leppänen, J. 2007. Development of a new Monte Carlo reactor physics code. D.Sc. Thesis, Helsinki University of Technology, 2007.

- Leppänen, J., Mattila, R. and Pusa, M. 2014. Validation of the Serpent-ARES code sequence using the MIT BEAVRS benchmark - initial core at HZP conditions. *Ann. Nucl. Energy*, 69 (2014), pp. 212–225.
- Leppänen, J., et al. 2015a. The Serpent Monte Carlo code: Status, development and applications in 2013. *Ann. Nucl. Energy*, 82 (2015) 142-150.
- Leppänen, J., et al. T. 2015b. The Numerical Multi-Physics project (NUMPS) at VTT technical research centre of Finland *Ann. Nucl. Energy*, 84 (2015), pp. 55–62.
- Leppänen, J., Pusa, M. and Fridman, E. 2016a. Overview of methodology for spatial homogenization in the Serpent 2 Monte Carlo code. *Ann. Nucl. Energy*, 96 (2016) 126-136.
- Leppänen, J. and Mattila, R. 2016b. Validation of the Serpent-ARES code sequence using the MIT BEAVRS benchmark – HFP conditions and fuel cycle 1 simulations. *Ann. Nucl. Energy*, 96 (2016) 324-331.
- Leppänen, J. et al. 2017. Renewal of VTT's calculation system for nuclear reactor core physics analyses. VTT-R-00707-17. VTT Technical Research Centre of Finland, 2017. (confidential)
- Rintala, A. 2017. Serpent – HEXBU-3D calculation chain in case of a hot zero power VVER-1000 initial core." VTT-R-00580-17, VTT Technical Research Centre of Finland, 2017.
- SAFIR2018 Planning group. National Nuclear Power Plant Safety Research 2015-2018, SAFIR2018 Framework Plan.
- Sahlberg, V. 2015. Validating Pin Power Reconstruction Module with Serpent 2 – TRAB3D Code Sequence. Special assignment, Aalto University, 2015.
- Sahlberg, V. 2016a. Modelling of axial discontinuities in reactor cores with Serpent 2 - TRAB3D code sequence. M.Sc. Thesis, Aalto University, 2016.
- Sahlberg, V. 2016b. Recalculating the steady state conditions of the V-1000 zero-power critical facility at Kurchatov Institute using Monte Carlo and nodal diffusion." In proc. 26th Symposium of AER, Helsinki, Finland, Oct. 10-14, 2016.
- Valtavirta, V. and Leppänen, J. 2017a. Coupled Neutronics–Fuel Behavior Burnup Calculations Using the Serpent 2 Monte Carlo Code. *Ann. Nucl. Energy* (in review).
- Valtavirta, V. 2017b. Development and applications of multi-physics capabilities in a continuous energy Monte Carlo neutron transport code." D.Sc. Thesis, Aalto University, 2017. (in pre-examination).
- Viitanen, T. 2015. Development of a stochastic temperature treatment technique for Monte Carlo neutron tracking. D.Sc. Thesis, Aalto University, 2015

### 4.3 Neutronics, burnup and nuclear fuel (NEPAL15)

Pertti Aarnio<sup>1</sup>, Jarmo Ala-Heikkilä<sup>1</sup>, Olli Hyvönen<sup>1</sup>, Aarno Isotalo<sup>1,2</sup>, Markus Ovaska<sup>1</sup>

<sup>1</sup>Aalto University School of Science, Dept. of Applied Physics  
P.O. Box 15100, FI-00076 Aalto

<sup>2</sup>Current affiliation: Teollisuuden Voima Oyj

#### Abstract

This project was a direct one-year continuation of the NEPAL project of the SAFIR2014 programme. Our main focus area has been accurate burnup calculations that aim at finding rare but potentially problematic nuclides like strong absorbers or other reactor-physically important nuclides. New burnup calculation methods have been developed, implemented mainly in the Serpent code, and thoroughly evaluated. Evaluations show significant improvements in accuracy without additional computational resources. The work has been published in open scientific literature and at conferences. In these projects, we have also developed a novel mesoscopic model of the thermal creep failure of fuel pellets. The model includes damage accumulation from radiation-induced fission gas buildup and the behaviour of the gases themselves. Additionally, optimal reconstruction parameters for cross section libraries of Serpent have been investigated.

#### Introduction

The Fission and Radiation Physics Group at Aalto University School of Science has concentrated on developing calculation methods for reactor physics, modeling basic physical and chemical phenomena in nuclear fuel, and researching new fuel cycles and next generation nuclear reactors. The activities seamlessly combine education and research of nuclear engineering. The essential field of know-how of the group covers physics-based analyses and numerical computation, especially development of Monte Carlo codes.

The objective of NEPAL15, a direct continuation of the NEPAL project in the SAFIR2014 programme, was to increase our knowledge on burnup calculations on one hand and nuclear fuel behaviour on the other hand. We explored new methods in an academic manner, but we have practical applications in sight for the longer term.

A central goal of NEPAL15 was education of new experts in the field. In the preceding NEPAL project, one DSc thesis, one MSc thesis and one BSc thesis were produced, and all by different authors. In NEPAL15, one of the deliverables was a BSc thesis.

#### Objectives

The contents and results of the NEPAL project have been summarized in the SAFIR2014 final report available at <http://safir2014.vtt.fi/>. In the burnup calculation task, we sent our postdoc Aarno Isotalo to work at Oak Ridge National Laboratory (ORNL) in June 2014 to develop various methods of mutual interest. These included the advanced depletion coupling schemes developed by us and the CRAM solver developed at VTT. Additionally, runtime and memory enhancements were investigated and implemented in various codes. This visit lasted until December 2015, a total of 19 months, and produced a number of scientific publications listed in the References.

In the task on mesoscopic fuel model, the objective was to further increase the realism in our thermo-mechanical model. In order to produce quantitative predictions more information and models were needed on the percolation threshold, growth rate of damages and thermal creep failure. The simulation results were to be compared to empirical measurements. This work was planned as a Bachelor's thesis or special assignment, but we did not manage to recruit a summer student for the task.

In RG meeting 1/2015 it was agreed that NEPAL15 funding would be used for another Bachelor's thesis where a BSc student optimized cross section libraries for Serpent 2 under the supervision of DSc Tuomas Viitanen (VTT). It had been observed that the cross section libraries in Serpent 1 were not accurate enough for all reactor systems. On the other hand, the memory consumption had to be kept under control, so the accuracy should be increased sensibly. This optimization was done in a BSc thesis under NEPAL15.

## Burnup calculation methodology

In the first part of DSc A. Isotalo's work at ORNL (see References), he implemented a CRAM depletion solver to the ORIGEN module of SCALE. The new CRAM solver is superior to the old solver of ORIGEN in every way, and should eventually replace the old solver in all applications.

In addition to implementing CRAM, A. Isotalo developed three new capabilities for it. The first of these is a way to include a source term in the calculations, which has previously not been possible with CRAM. This allows CRAM to be used for modeling systems, such as molten salt reactors and reprocessing facilities, with material flows. The new method can even handle source terms with general polynomial time-dependence. Using a time dependent source term of any kind has previously not been possible with any depletion algorithm capable of handling the full system of nuclides.

The second new capability is internal substepping which further improves the already remarkable accuracy of CRAM with only a modest effect on running times. Even decay problems, where there have previously been concerns about the accuracy and reliability of CRAM, can now be solved with ten correct digits for all nuclides with atomic fraction above an arbitrary limit.

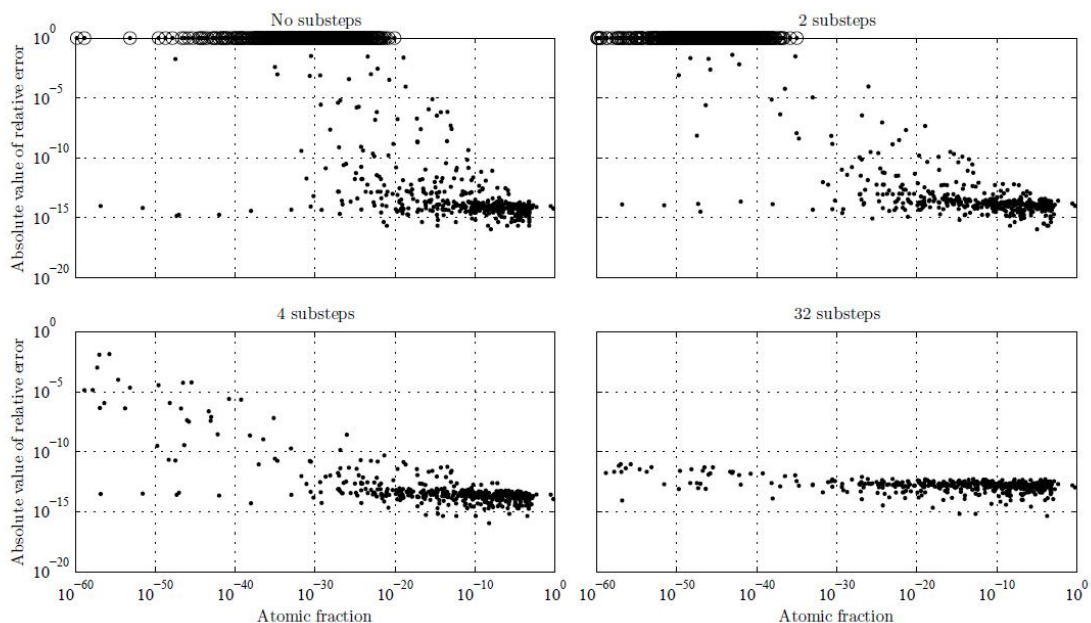


**Figure 1.** Relative errors with different numbers of internal substeps when old fuel is decayed for 365 days. Circles indicate errors that have been reduced to 1 for plotting. [Isotalo, Pusa 2016]

Finally, A. Isotalo developed a new method for calculating the time-integrals or averages of any and all quantity that are weighted sums of the atomic densities as a part of a single depletion solution with CRAM. Examples of such quantities are time-average atomic densities, the number of fissions, and the amount of energy released during a depletion step. The new method is fast and extremely accurate, which enables these quantities to be used in ways that have not previously been realistic.

A. Isotalo also participated in developing and implementing an internal burnup calculation capability for the new high performance Monte Carlo transport code called Shift. In particular, he implemented the higher order neutronics-depletion coupling schemes developed as a part of his PhD research. The capability has been completed and is being tested. A conference paper was written that describes the implemented burnup calculation capabilities.

In addition to regular code development activities, A. Isotalo used Shift to study the use of flux renormalization in constant power burnup calculations to further improve the implemented burnup calculation methodology. This includes developing a new renormalization method that leverages the new CRAM capabilities, a comparison of different renormalization strategies, and scoping on how much of a difference renormalization actually makes.

## Mesoscopic modelling of nuclear fuel

During the four-year NEPAL project in the SAFIR2014 programme, M. Ovaska developed a computational model for simulating the microstructural evolution of nuclear fuel [Ovaska, Alava 2015]. The model includes damage accumulation from thermal creep deformation and from fission gas buildup within the pellet. Damage accumulation is linked with increasing porosity of the fuel, as microcracks and gas bubbles are formed. Diffusion of fission gases is simulated from the viewpoint of percolation theory: gas flows through interlinked pores, and can only reach the surface of the pellet through continuous pore pathways.

In NEPAL15, it was our plan to continue this modeling as a Bachelor's thesis or special assignment under supervision of M. Ovaska. Due to manpower limitations, this plan was not realized.

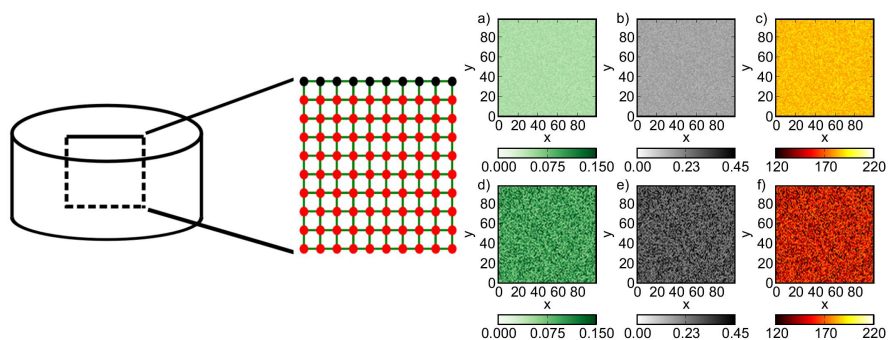


**Figure 2.** On the left: Schematic of the simulation system: A rectangular cross-section from a pellet. Gas nodes (red) are interconnected through bonds (green). Fission gas is released through the top boundary (black nodes). On the right: Example snapshots of porosity (a & d), damage (b & e) and Young's modulus in GPa (c & f). The top row (a-c) corresponds to the initial state, and the bottom row (d-f) shows a later stage when creep and radiation damage have weakened the pellet. [Ovaska, Alava 2015]

## Processing cross section libraries for Serpent 2

In O. Hyvönen's BSc thesis, optimal reconstruction parameters for cross section libraries used with neutron transport calculation code Serpent 2 were sought. The nuclear data processing system NJOY, operated with a wrapper code SFFER by DSc Tuomas Viitanen, was used to generate the cross section libraries. The essential reconstruction parameters in question were *err*, *errint* and *errmax* of NJOY's *RECONR* module.

Accuracy of the generated libraries was tested with Serpent 2 using simplified models of two thermal (HTGR, PWR) and one fast reactor (LFR). Fresh fuel calculations were used to establish a fundamental baseline for accuracy, and depleted fuel calculations were performed to examine if the presence of hundreds of different nuclides in the fuel affects how the reconstruction parameters should be chosen. Results of a simulation were compared to the reference result of the same simulation, calculated with highly accurate libraries.

As a result, the suggested reconstruction parameters for optimal thermal libraries are  $err = 0.005$ ,  $errint = 2.5 \cdot 10^{-7}$  and  $errmax = 0.05$ . However, a library used for fast reactor simulations should not be generated with these values, as the integral thinning property they enable in the *RECONR* module impairs the accuracy of the library with fast reactors. However, it seems that the Serpent default library reconstructed with  $err = 0.01$  and with integral thinning disabled by choosing  $errmax = err$  is accurate enough.

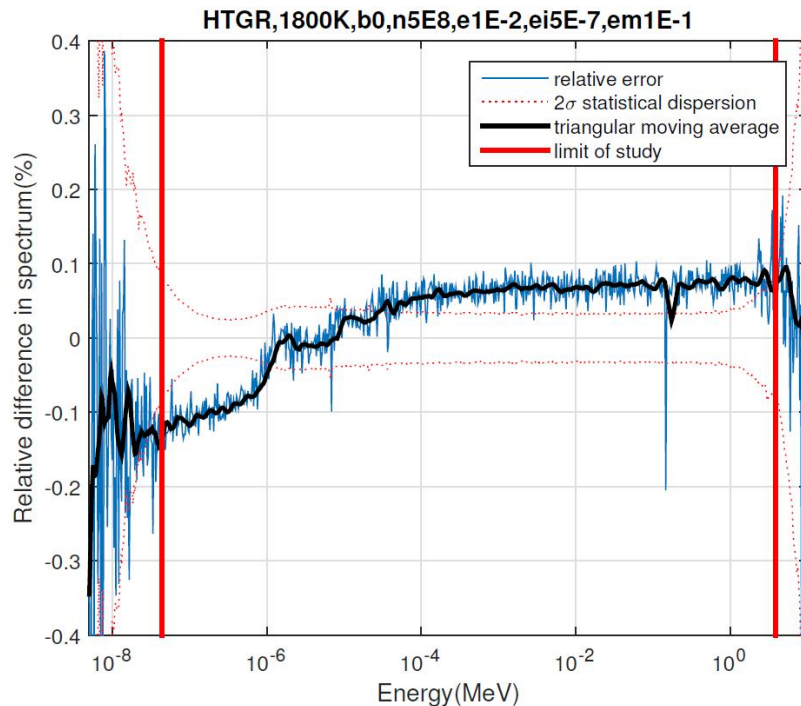


**Figure 3.** A relative difference neutron spectrum utilized in the parameter optimization. The title contains all relevant information about the simulation: case (HTGR), temperature (1800 K), fuel burnup ( $b_0 = 0$  MWd/kgU), number of neutron histories ( $n5E8 = 5 \cdot 10^8$ ), *err* ( $e1E-2 = 0.01$ ), *errint* ( $ei5E-7 = 5 \cdot 10^{-7}$ ) and *errmax* ( $em1E-1 = 0.1$ ). [Hyvönen 2015]

## **Conclusions**

The objectives of the NEPAL and NEPAL15 projects can be defined primarily as new calculation methods and scientific publications documenting them. Moreover, the new expertise in the field and the new experts themselves are important deliverables of the project. One DSc thesis, one MSc thesis and two BSc theses were produced in these projects, and all by different authors, so we can conclude that the projects have reached their main objective. As of this writing, these young experts have continued their careers in other organizations in the nuclear field, thus completing the delivery.

These projects show that it is possible to contribute to the publicly-funded nuclear safety research in a university environment. Our scientifically oriented basic research is not necessarily applicable at the regulator and utilities in the short term, but it is instrumental in keeping the research at a high level and educating new experts to the field.

## **Acknowledgement**

We acknowledge the fruitful collaboration of VTT and Oak Ridge National Laboratory. We also acknowledge the computational resources provided by the Aalto Science-IT project.

## References

- Isotalo, A.E., Davidson, G.G., Pandya, T.M., Wieselquist, W.A., Johnson, S.R., Flux renormalization in constant power burnup calculations, *Annals of Nuclear Energy* 96 (2016) 148-157. <http://dx.doi.org/10.1016/j.anucene.2016.05.031>
- Isotalo, A.E., and Pusa, M., Improving the Accuracy of the Chebyshev Rational Approximation Method by Using Substeps. *Nuclear Science and Engineering* 183 (2016) 65-77. <http://dx.doi.org/10.13182/NSE15-67>
- Isotalo, A.E., Calculating Time-Integral Quantities in Depletion Calculations. *Nuclear Science and Engineering* 183/3 (2016) 421-429. <http://dx.doi.org/10.13182/NSE15-119>
- Davidson, G.G., Pandya, T.M., Isotalo, A.E., Johnson, S.R., Evans, T.M., Wieselquist, W.A, Nuclide depletion capabilities in the Shift Monte Carlo code, *Proceedings of Physics of Reactors 2016, PHY-SOR 2016: Unifying Theory and Experiments in the 21st Century, Sun Valley 1-5 May 2016*.
- Isotalo, A.E., Sahlberg, V., Comparison of Neutronics-Depletion Coupling Schemes for Burnup Calculations. *Nuclear Science and Engineering* 179/4 (2015) 434-459. <http://dx.doi.org/10.13182/NSE14-35>
- Isotalo, A.E., Comparison of Neutronics-Depletion Coupling Schemes for Burnup Calculations 2. *Nuclear Science and Engineering* 180/3 (2015) 286-300. <http://dx.doi.org/10.13182/NSE14-92>
- Isotalo, A.E., Wieselquist, W.A., Method for Including External Feed in Depletion Calculations with CRAM and Implementation to ORIGEN. *Annals of Nuclear Energy* 85 (2015) 68-77. <http://dx.doi.org/10.1016/j.anucene.2015.04.037>
- Ovaska, M., Alava, M.J., Joint modeling of thermal creep and radiation damage interaction with gas permeability and release dynamics: the role of percolation. *Physica A* 436 (2015) 538-546. <http://dx.doi.org/10.1016/j.physa.2015.05.068>
- Hyvönen, O., Finding optimal reconstruction parameters for cross section libraries used with Serpent 2, Bachelor's thesis, Aalto University School of Science, Sep 13, 2015.

#### 4.4 Physics and chemistry of nuclear fuel (PANCHO)

Asko Arkoma, Timo Ikonen, Joonas Kättö, Henri Loukusa, Emmi Myllykylä, Rami Pohja, Ville Tulkki, Ville Valtavirta

VTT Technical Research Centre of Finland Ltd  
P.O. Box 1000, FI-02044 Espoo

##### Abstract

PANCHO has been the essential platform for the ongoing development of FINIX fuel behaviour module and its accompanying automatic validation system. The studies on fuel behaviour in accident conditions have been framed within the international projects, where the accident simulation codes have been tested and validated. Also a coupling between SCANAIR and GENFLO codes has been developed in the project.

The chemistry experiments aimed to investigate characteristics of initial dissolution of crystalline ThO<sub>2</sub> by adding <sup>229</sup>Th tracer into the aqueous phase. The experiments were conducted for total 534 days and are to be complemented by modelling approach. The experimental campaign on cladding creep demonstrates that the VTT equipment is capable of performing suitable transient tests which support the modelling activities. One DSc thesis has been finalized based on the ongoing cladding creep modelling work.

##### Introduction

The project PANCHO – Physics and Chemistry of nuclear fuels investigates the integral fuel behaviour as well as combines the experimental and the modelling approaches in studying several topical features of nuclear fuel behaviour. These topics are the the chemistry of the fuel pellet and the mechanical response of the cladding.

Nuclear fuel both produces the energy in nuclear power plants and acts as the first two barriers to the spread of radioactive fission products. The UO<sub>2</sub> matrix of the fuel pellets contains approximately 99% of the born radionuclides, while the cladding tube contains the rest. Therefore the integrity of the fuel during normal operation and accidents is of utmost importance. Traditionally fuel performance has been analysed with integral fuel codes that contain semi-empirical correlations deduced from experiments. These correlations and models become more and more mechanistic as the understanding and the demands increase.

These models are often empirical, and therefore understanding the domain of validity of the codes is of great importance. The models are often validated for a certain set of conditions, with different models used for describing behaviour at different conditions. The code validation is performed against large databases of experimental data. The experiments on nuclear fuel are complex and expensive. Therefore they require international consortiums which are vital for the transfer of information and expertise. The current European experimental facilities include Halden Reactor in Norway and Osiris in France. The CABRI reactor has been reworked to facilitate experiments in a water loop and is nearing operational condition, while the future Jules Horowitz Reactor is being built in France. PANCHO has served as a framework for Finnish collaboration with the Halden Reactor as well as the CABRI TAG project.

In PANCHO, the Finnish fuel code FINIX is developed and validated for simulations of the fuel behaviour across a wide range of scenarios, such as loss of coolant accidents and reactivity insertions. FINIX can be then implemented in a wide range of codes to provide systematic description of fuel behaviour. This simplified approach to multiphysics is unique in the world. The tools and expertise to analyse reactor safety during loss of coolant and reactivity initiated accidents in Finnish reactors are improved via strong international co-operation. Phenomena pertaining to LOCA and RIA are studied and the understanding is transferred to Finnish experts and tools.

In PANCHO the fuel pellet chemistry investigations concentrate on the leaching behaviour of fuel materials in the storage conditions of defective fuel rod. As for the cladding investigations the issue of transient creep is studied both theoretically and experimentally. The produced data combined with the more accurate creep strain models can be utilized to improve the tools used in the estimation of fuel cladding tube behaviour and lifetime.

## FINIX development

In SAFIR2014, the FINIX fuel behaviour module was developed within the PALAMA project. FINIX is a general purpose fuel behaviour module for thermal and mechanical fuel behaviour in multi-physics simulations, and has been integrated into VTT's Serpent 2 reactor physics code and reactor dynamics codes. In PANCHO, further development and validation of the FINIX fuel behaviour module is a major goal during 2015-2018.

As FINIX is intended for multiphysics simulations, it is important that the code is easy to couple with other simulation programs. Therefore a new version of the code, FINIX 0.15.6, was released with redesigned data structures and an improved interface for coupled simulations. In addition, version 0.15.6 introduced the ability to read FINIX and FRAPTRAN input files and to print node specific output files, a summary file, and a file showing the contents of all FINIX data structures.

In 2015, a time-independent plastic deformation model was implemented in FINIX. Previously, only elastic deformation of the cladding was modelled. Time-independent plastic deformation is very important when describing the behaviour of fuel under reactivity-initiated accident (RIA) conditions. In a RIA, the fuel expands rapidly, pushes against the cladding and plastic deformation occurs if the yield stress of the cladding is exceeded. The PNNL yield stress correlation was implemented in FINIX, with the plastic deformation being calculated with the widely used radial return algorithm. In Figure 1, the cladding outer radius over the length of the fuel rod is shown during a RIA event. The pellet-cladding gap would not open again during the transient if only elastic deformation were modelled. This is because the initial thermal expansion of the fuel would not result in permanent deformation in the cladding, and the cladding would return to its original state after the fuel shrinks with decreasing temperature.

One further development in 2016 was the implementation of a steady state (or time-independent) temperature solver for FINIX. Previously FINIX relied on a time-dependent solution for the radial one dimensional heat equation also when the time-independent solution was required. The steady state temperature solution was obtained by using the time dependent temperature solver with a very long timestep.

The steady state fuel behaviour solution is naturally required if the coupled problem being solved is a time-independent one, but it also provides the initial conditions for transient simulations. As the use of a time-dependent solver with a very large timestep to obtain the steady state solution was seen to be both computationally wasteful and a possible source for convergence difficulties a separate steady state solver was implemented.

The new steady state solver used a similar linearization of the material heat conductivities and power density as the time-dependent solver in order to produce a temperature solution very close to the one given by the transient solver. The implementation of the steady state solver was successful, with verification conducted against the transient solver. The agreement between the two solvers was seen to be very good with the steady state temperature solver saving approximately 15 percent of the computation time.

Publicly available material property correlations for VVER fuel cladding (E110) were implemented in FINIX. With these correlations, FINIX is now able to model VVER fuel more accurately.

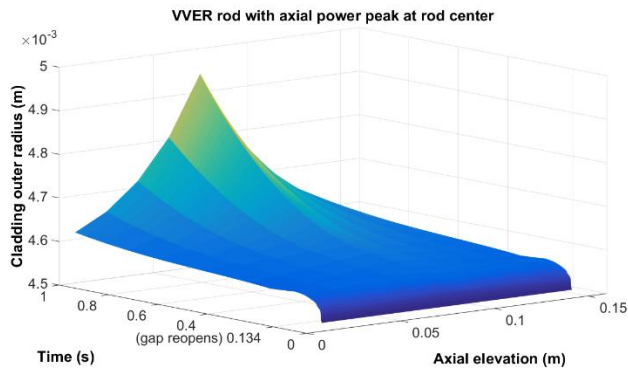


**Figure 1.** Cladding outer radius as calculated by FINIX with plastic deformation modelling capability for a VVER rod with axial power peak at rod center.

## Validation system

Validation is an important step in software and model development. When nuclear fuel performance codes are developed and updated, their simulation results are compared against experimental data or reference program simulation data. In a proper validation process a large number of simulations are performed, and the results from each simulation run are compared to a large amount of data. This kind of validation is time-consuming and error-prone when performed manually. The SPACE validation tool is a program that automates the validation process and makes the validation of fuel performance codes easier, more reliable and more efficient.

In 2016 the SPACE validation tool was completely rewritten based on the software development plan that was created in 2015. The new validation tool is composed of a relational database and a piece of software for simulation program validation. The redesigned database, shown in Figure 2, contains all the data that are needed to construct the simulation program input files. It also contains the experimental data to which the simulation results can be compared. As the data is stored in a relational database, it is possible to run SQL queries against the data. This has several advantages, such as finding the fuel rods that meet the certain criteria and running the validation by using these rods only. It is also easier to manage a relational database than a flat-file database that was the database solution in the earlier SPACE versions.

SPACE allows the user to compare the simulation results of one or two simulation programs against the reference data. The reference data can be either experimental data or simulation data produced by a validated simulation program. As the validation tool runs a large number of simulations and compares the simulation results against the reference data, it will be easy to assess the validity of the simulation program or a single model of the program. The new version of the SPACE validation tool has been designed to be a general-purpose tool for fuel performance code validation, which means that the system is not tailored for any single simulation program. The current version supports FINIX and FRAPTRAN, but adding a support for a new simulation program is straightforward.

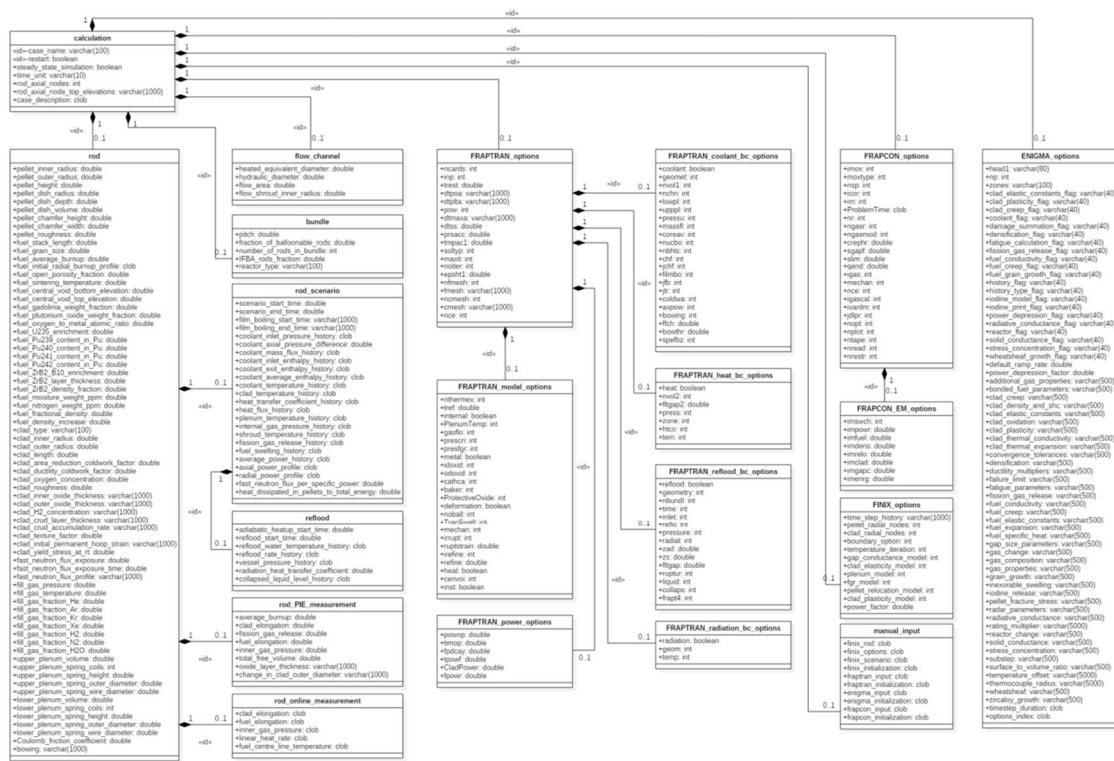


Figure 2. SPACE database.

## Fuel behaviour during loss of coolant accidents

The goal of the LOCA research in 2015–2018 is to gain a comprehensive and profound picture of nuclear fuel behaviour under LOCA conditions. Of high importance is taking part in international efforts to better model fuel behaviour under LOCA conditions, and to share good principles, data and information on the subject. These activities will support VTT's in-house model development, verification and validation.

To meet these goals, VTT participated in an IAEA Coordinated Research Project called Fuel Modelling in Accident Conditions (FUMAC) that was launched in 2014. The aim of the project is to support the participants from different countries in their efforts to develop reliable tools for modelling of fuel behaviour during accidents. This task will be tackled by simulating predetermined experiments and by comparing the simulation results between the participants. VTT's contribution in the first phase of the project was to calculate a set of AEKI separate effect tests and an integral VVER LOCA test IFA-650.11 performed at the Halden reactor. The code used in the calculations was FRAPTRAN-GENFLO.

It was concluded that the behaviour of the cladding tubes in the AEKI ballooning tests could not be predicted reliably with FRAPTRAN. The calculated tube burst time was significantly affected by the size of the time step, possibly because of a bug in the ballooning model that is used together with the FRACAS-I mechanical model. On the other hand, the overall behaviour of a segmented fuel rod in the Halden LOCA experiment was simulated relatively accurately with FRAPTRAN-GENFLO. The calculated deformation and burst time were very close to the measured values. However, there were some lag in the calculated plenum temperature rise after blowdown, and therefore the calculated internal pressure in the rod during the ballooning phase was lower than the measured.

The preliminary results calculated in the first phase of the FUMAC project guided the discussion in the second research coordination meeting that was held in May 2016. The meeting allowed the participants to share information and to plan the final phase of the project. The data, information and expertise that will be gained during the FUMAC project will be essential in developing and validating the VTT's in-house fuel behaviour module FINIX.

## Fuel behaviour during reactivity initiated accidents

During the first two years of PANCHO, the fuel modelling in reactivity initiated accident (RIA) conditions has been focused on studies of uncertainties and sensitivities in modelling, and on BWR thermal hydraulics (TH) modelling. In this context, VTT participates to the OECD/NEA RIA fuel codes benchmark Phase II with the SCANAIR code developed by IRSN. SCANAIR's TH model is not able to take bulk boiling of BWR into account, and therefore an interface between SCANAIR and a TH code was defined in 2014. The work has continued in 2015 and 2016 with verification and validation of the coupling between SCANAIR and VTT's GENFLO TH code.

### OECD/NEA RIA fuel codes benchmark Phase-II

Phase II of the RIA modelling codes benchmark is divided into two Activities. In the 1<sup>st</sup> Activity (years 2014-2015), 10 simplified RIA cases were simulated (OECD/NEA, 2015). In the 2<sup>nd</sup> Activity (2015-2016), uncertainty and sensitivity analysis was done for a selected case from Activity 1. The number of uncertainty runs was 200. VTT participated to both activities with SCANAIR V\_7\_4 and V\_7\_5 by simulating all the specified simplified cases and uncertainty runs, and by performing the sensitivity analysis.

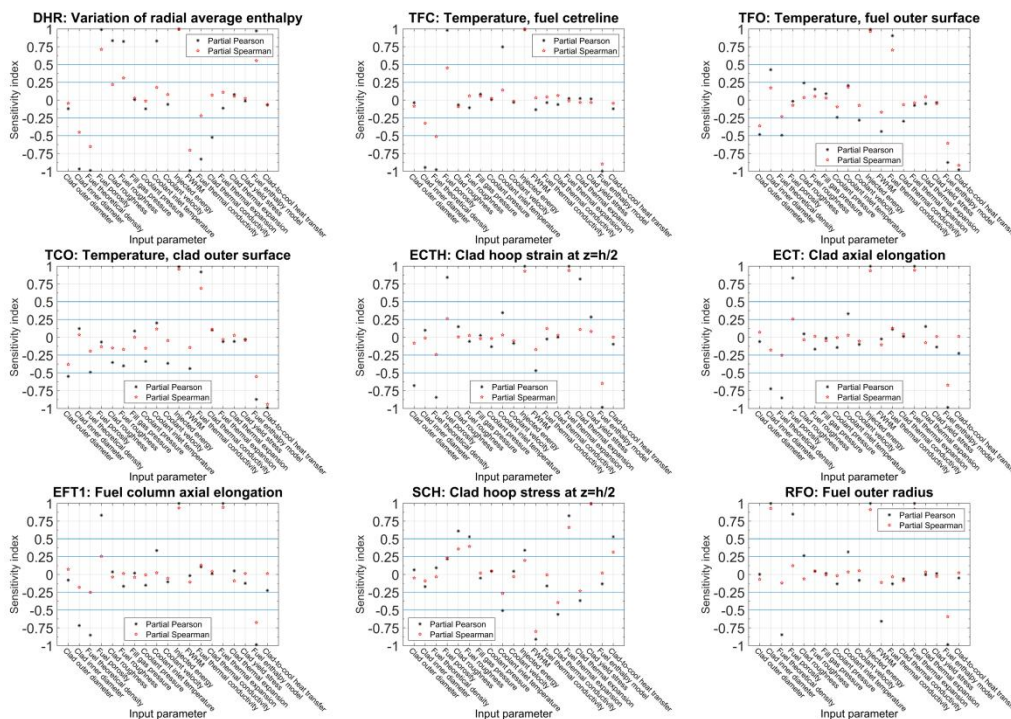


**Figure 3.** Sensitivity study made in the RIA benchmark by calculating the correlation coefficients.

## SCANAIR GENFLO coupling

Verification of the coupled code has been done (Arkoma, 2016a), and the coupling is now in the validation stage (Arkoma, 2016b). First validation cases have been calculated; two pool tests on BWR fuel in ambient temperature and pressure, and two RIA benchmark cases from Phase II, on PWR fuel with and without boiling. The first results seem reasonable. Validation should be continued within the proposed RIA benchmark Phase III. A journal manuscript has been prepared on SCANAIR-GENFLO coupling, complemented with updated results on BWR cladding low temperature failure analysis made in 2012.

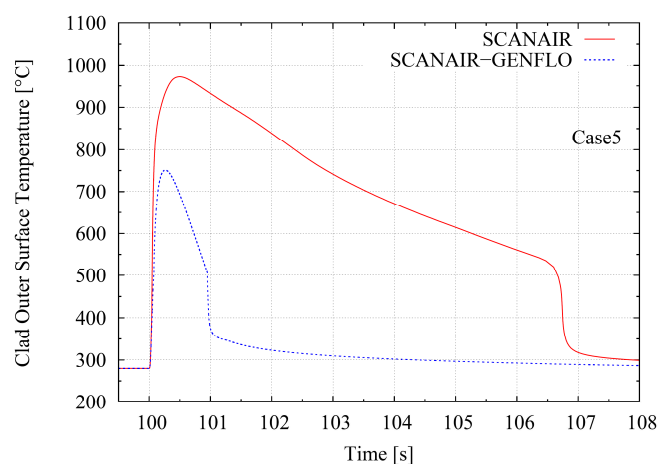


**Figure 4.** Cladding outer surface temperature in SCANAIR-GENFLO vs. stand-alone SCANAIR in RIA benchmark PWR case with boiling.

## Leaching of thorium fuel

The experimental section of chemistry investigations concentrate on the leaching behaviour of fuel materials in the storage conditions of defective fuel rod. The aim is to produce data for validation of models. The experiments were started in 2015 with the dissolution studies with crystalline  $\text{ThO}_2$  with similar microstructure to  $\text{UO}_2$  fuel matrix which continued the work performed in EURATOM FP7 project REDUPP (Reducing Uncertainty in Performance Prediction). Originally a modelling task was also included, however, due to the cuts in the funding this work was left out from PANCHO.

The experiments, aiming to investigate characteristics of initial dissolution of crystalline  $\text{ThO}_2$  by adding  $^{229}\text{Th}$  tracer into the aqueous phase, were started during the REDUPP and continued within the first year of the PANCHO for total 534 days. In addition, leached pellets were analysed with alpha spectrometry to study layer precipitated on the surface of  $\text{ThO}_2$  pellets during the leaching period. The experiments showed that  $^{232}\text{Th}$  was released from the solid  $^{232}\text{ThO}_2$  samples into the aqueous phase, even though the solution contained excess of  $^{229}\text{Th}$  compared to the solubility limit of thorium. This indicated that early stage of the dissolution was rather controlled by the stability of surfaces than by the chemical equilibrium. Previous results [Corkhill et al] showed that during the early stage, the dissolution took most probably place on grain boundaries and crystallographic defects, which can be defined as "high energy surface sites". As the leaching proceeds the thorium concentration level down, but the isotopic ratio continues to decrease, which shows that the dissolution/precipitation reactions continue at the surfaces even though the chemical equilibrium is achieved, as can be seen from Figure 5. The  $^{229}\text{Th}$  tracer experiments and their results are reported more detail in elsewhere [Myllykylä et al. 2017]

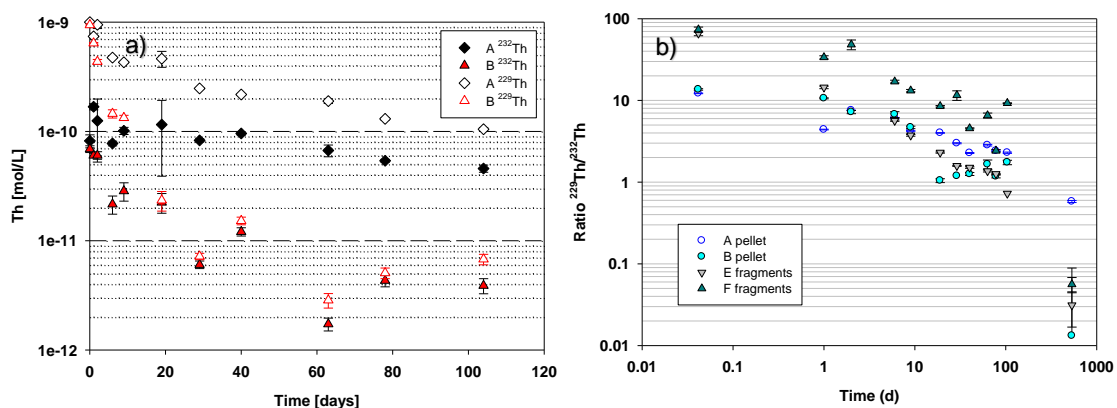


**Figure 5.** Evolution of thorium concentrations (a) and isotopic ratio  $^{229}\text{Th}/^{232}\text{Th}$  (b) (measured with sector field ICP-MS) in dissolution experiments conducted with  $\text{ThO}_2$  pellets (A and B) and fragments (E and F) in 0.01 M NaCl under anaerobic conditions.

The direct alpha spectrometric measurements of leached  $\text{ThO}_2$  pellets accompanied with Advanced Alpha Spectrometric Simulation (AASI) suggested a formation of thin layer ( $< 0.1 \mu\text{m}$ ) onto the  $^{232}\text{ThO}_2$  pellet. According to the measured spectrum (see Fig. 6) the layer contained increased amount of  $^{229}\text{Th}$  and daughter nuclides from both  $^{232}\text{Th}$  and  $^{229}\text{Th}$  decay series. The existence of step like characteristics of  $^{229}\text{Th}$  and its daughters in the spectrum indicate their intrusion also below the thin surface layer into the bulk  $^{232}\text{ThO}_2$ . Due to energetically less stable nature of the grain boundaries, they are most probable intrusion route into the bulk pellet. [Mylykylä et al. submitted 12/2016]

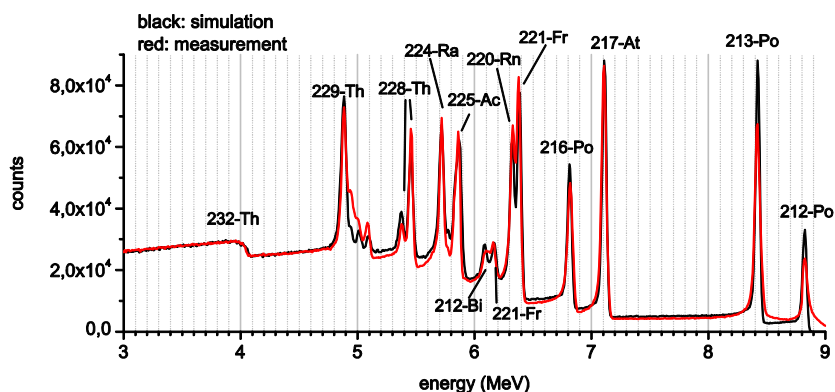


**Figure 6.** Measured (red) and simulated (black) spectra of the  $^{232}\text{ThO}_2$  pellet A with the concentrated layer of  $^{229}\text{Th}$  on top of the pellet.

During PANCHO project, new dissolution experiment of  $\text{ThO}_2$  pellets were conducted in clear MilliQ-water at  $80^\circ\text{C}$  under anaerobic conditions to simulate the storage conditions of detective fuel rod. The higher temperature did not have increasing effect to the solubility of thorium pellets under used conditions. The chemical history indicated to have more effect on solubility than the temperature, as the “fresh” intact pellets released more thorium into solution than those already leached in previous experiments. This supports the hypothesis of the relatively rapid initial dissolution, which occurs at “the high energy surface sites”, like the crystallographic defects and grainboundaries.

## Cladding creep

The cladding creep task builds on the previous modelling work on the creep phenomena, the LCSP model and the viscoelastic model that have been developed in past SAFIR projects and in the IDEA project funded by the Academy of Finland. In 2015 and 2016 the LCSP model was further developed and a possibility to apply the LCSP modelling approach for creep transient response was investigated. Furthermore, a doctoral thesis "Modelling nuclear fuel behaviour and cladding viscoelastic response" was prepared and defended.

The development of creep modelling of cladding materials benefits from experimental transient creep data at both in-reactor and ex-reactor conditions. Certain amount of transient creep data is available, but especially data including temperature and/or load drops, which is valuable for building the understanding of recovery phenomena in zirconium alloys during creep, is scarce in open literature. To gain additional transient creep data at ex-reactor conditions, which can be produced by using the VTT biaxial creep testing facilities, an experimental campaign to support the aforementioned modelling activities was planned.

To study the capabilities of VTT's equipment for transient experiments, an experimental campaign using available materials and experimental facilities was initiated in 2015. At first stage, a temperature transient test with internal pressure and additional axial load was performed for a cold worked E110 zirconium alloy specimen. The internal pressure of the specimen and the additional axial pull load was applied to the specimen so that the axial to hoop stress ratio equaled 1 ( $\alpha = 1$ ). The stress level remained the same throughout the test, but a temperature transient (from 360°C to 400°C) was introduced after 500 hours. At the second qualification test, an E110 specimen was exposed to several stress transients (load increases and drops) and the hoop to axial stress ratio was altered during the test. Based on the results of these tests, the VTT equipment is capable of performing suitable transient tests which support the modelling activities, but the performance of certain measurement units should be further improved to maximally utilize the results of test planned for Zircaloy-4 alloy.

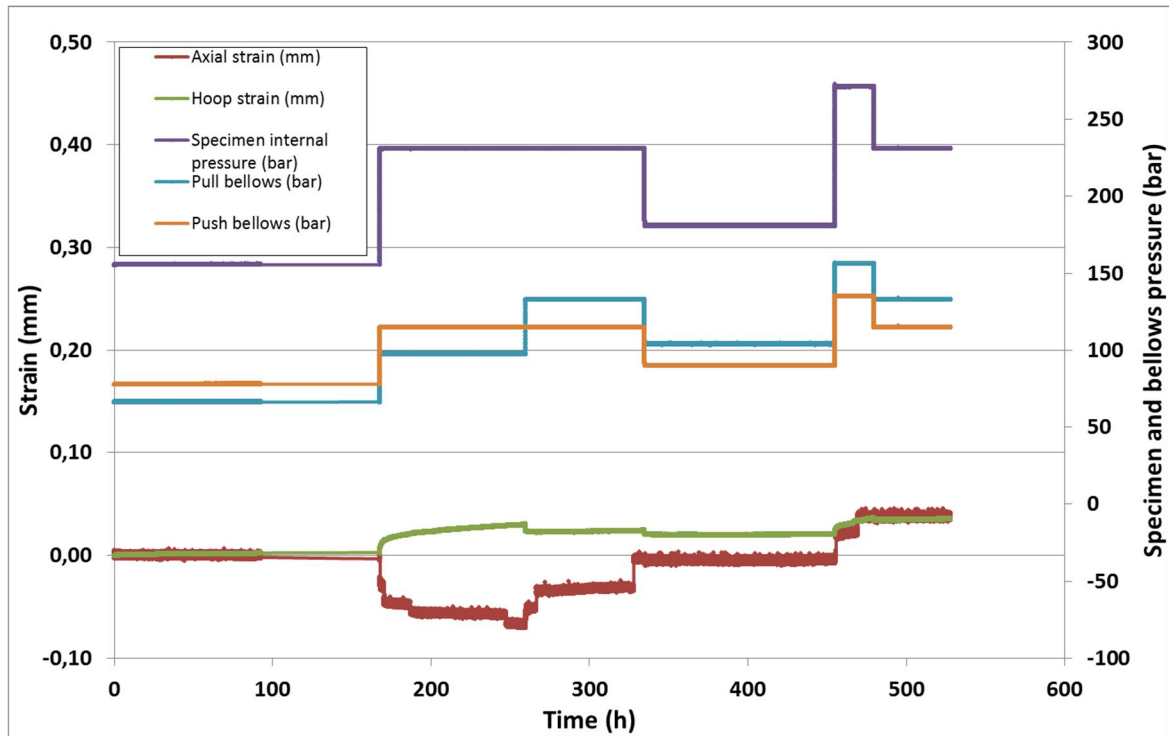


**Figure 7.** The curves for axial strain, hoop strain, specimen internal pressure, pull bellows and push bellows in a transient creep test.

The doctoral thesis “Modelling nuclear fuel behaviour and cladding viscoelastic response” was prepared and defended. The scope of the thesis consisted of two main themes. The first was the uncertainty and sensitivity in fuel behaviour modelling and the tools required for its propagation to the rest of the nuclear reactor calculation chain. The second was the analysis and modelling of cladding response to transient stresses. Propagation of uncertainties through the nuclear reactor calculation chain is an international ongoing effort, and the complex interactions in the fuel rods make them challenging to analyze. In the thesis uncertainty and sensitivity of fuel behaviour codes was investigated and the development of a fuel module suitable for propagation of the uncertainties was detailed. In the thesis a simple methodology for predicting fuel cladding macroscopic response to stresses and imposed strains was developed by taking anelastic behaviour into account. The model was shown to perform well in describing both creep and stress relaxation experiments.

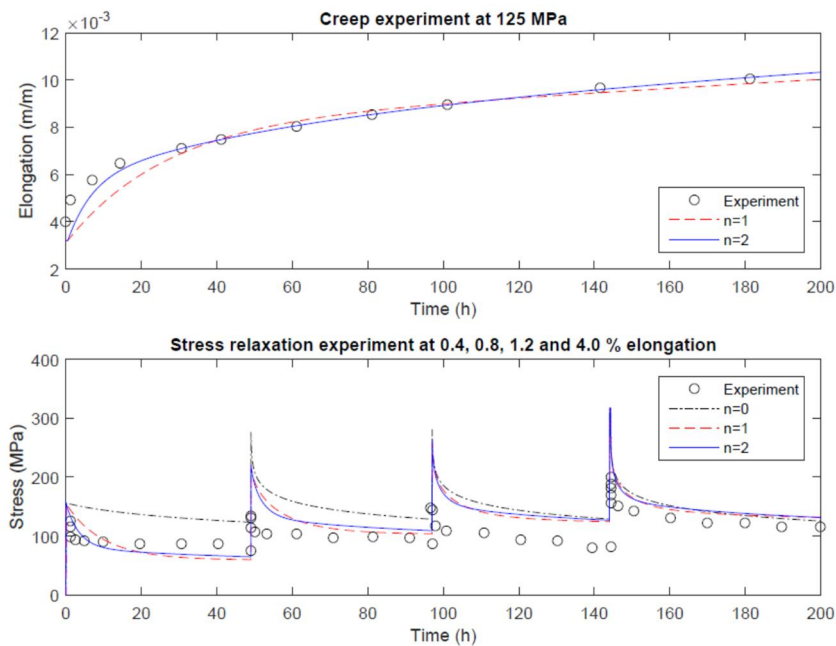


**Figure 8.** Demonstration of spring-dashpot model in modelling creep and stress relaxation experiments.

## References

- Arkoma, A. 2016a. Verification of the SCANAIR-GENFLO coupling. VTT Research Report, 31.1.2016, VTT-R-00777-16
- Arkoma, A. 2016b. Validation status of SCANAIR-GENFLO coupling. VTT Research Report, 13.10.2016, VTT-R-04351-16
- Corkhill, C.L., Myllykylä, E., Bailey, D.J., Thornber, S.M., Qi, J., Maldonado, P., Stennett, M.C., Hamilton, A. and Hyatt, N.C. 2014. Contribution of Energetically Reactive Surface Features to the Dissolution of CeO<sub>2</sub> and ThO<sub>2</sub> Analogues for Spent Nuclear Fuel Microstructures, *ACS Applied Materials & Interfaces*, 2014, 6, 12279–12289
- Ikonen, T., Syrjälähti, E., Valtavirta, V., Loukusa, H., Leppänen, J. and Tulkki, V. 2015. Multiphysics Simulation of Fast Transients with the FINIX Fuel Behaviour Module, *Topfuel 2015*, 13-17 September 2015, Zurich, Switzerland.
- Ikonen, T., Kättö, J. and Loukusa, H. 2015. FINIX - Fuel behavior model and interface for Multiphysics applications - Code documentation for version 0.15.12, VTT Research Report VTT-R-05887-15, 2015.
- Ikonen, T., Syrjälähti, E., Valtavirta, V., Loukusa, H., Leppänen, J. and Tulkki, V. 2016. Multiphysics simulation of fast transients with the FINIX fuel behaviour module, *Special TopFuel2015 issue of EPJ-N* in September 2016. <http://dx.doi.org/10.1051/epjn/2016032>
- Ikonen, T. VTT's modifications to the FRAPCON-4.0 code, VTT Research report, VTT-R-0119-17.

- Kättö, J., Ikonen, T., Syrjälahti, E., Valtavirta, V., Loukusa, H., Leppänen, J. and Tulkki, V. Multiphysics simulations of fast transients in VVER-1000 and VVER-440 reactors, 11th INTERNATIONAL CONFERENCE ON WWER FUEL PERFORMANCE, MODELLING AND EXPERIMENTAL SUPPORT, Bulgaria.
- Kättö, J. 2016. Fuel Rod Experiments Simulated within the FUMAC Project, VTT Research Report, VTT-R-00445-16.
- Kättö, J. 2017. SPACE - Validation tool for simulation software - User's guide for version 2.0.0, VTT Research Report, VTT-R.00204-17.
- Loukusa, H., Ikonen, T., Rätty, A. and Tulkki, V. 2015. Thermochemical Modelling of the Oxygen Potential of Uranium Oxide Fuel Pellets Under Irradiation, Topfuel 2015, 13-17 September 2015, Zurich, Switzerland.
- Loukusa, H., Ikonen, T., Valtavirta, V. and Tulkki, V. 2016. Thermochemical modeling of nuclear fuel and the effects of oxygen potential buffers, Journal of Nuclear Materials, 2016, accepted manuscript.
- Myllykylä, E., Lavonen, T., Koivula, L., Ollila, K. and Siitari-Kauppi, M. 2017. Dissolution of Crystalline ThO<sub>2</sub>: study of dissolution process with initial <sup>229</sup>Th spike, Journal of Radioanalytical & Nuclear Chemistry, 2017, 311(1): 225-235.
- Myllykylä, E., Koivula, L., Tanhua-Tyrkkö, M., Helariutta, K., Lavonen, T., Ollila, K. and Siitari-Kauppi, M. 2016. Direct alpha spectrometry for analysing the leached ThO<sub>2</sub> pellets, Journal of Nuclear Materials (submitted 28th December 2016).
- OECD/NEA, Working Group on Fuel Safety (WGFS). 2015. WGFS RIA fuel codes benchmark Phase-II, Report - Volume 1, Simplified Cases Results, Summary and Analysis, November 2015
- Pohja, R. 2015. LCSP creep strain model performance of zirconium based fuel cladding materials in steady state and transient creep conditions, VTT Research Report VTT-R-06036-15.
- Pohja, R. and Huutilainen, S. Report on an experimental campaign on cladding transient behaviour, VTT Research Report VTT-R-XXXXX-17.
- Pohja, R., Tulkki, V., Ikonen, T., Moilanen, P., Rantala, J., Huutilainen, S. and Ehrnstén, U. 2016. Creep performance of fuel cladding, Proceedings of Baltica X conference. VTT Technology 261.
- Tulkki, V. 2015. Modelling nuclear fuel behaviour and cladding viscoelastic response, D.Sc. (Tech) thesis, Aalto University School of Science.
- Tulkki, V. 2015. Analysis and modelling of Halden cladding creep experiments, HWR-1189.
- Tulkki, V. and Ikonen, T. 2015. Modelling anelastic contribution to nuclear fuel cladding creep and stress relaxation, Journal of Nuclear Materials, 465, 34-41.
- Tulkki, V. and Ikonen, T. 2015. Modelling cladding response to changing conditions, Topfuel 2015, 13-17 September 2015, Zurich, Switzerland.
- Valtavirta, V. 2017. Implementing a steady state temperature solver for FINIX, VTT Research Report VTT-R-00518-17.

## 4.5 Safety analyses for dynamical events (SADE)

Ville Sahlberg, Hanna Rätty, Ville Hovi, Anitta Hämäläinen, Mikko Ilvonen, Elina Syrjälähti, Veikko Taivassalo

VTT Technical Research Centre of Finland Ltd  
P.O. Box 1000, FI-02044 Espoo

### Abstract

In 2015, a pin power reconstruction module was implemented to the transient analysis code TRAB3D and its results were compared to the reactor physics code Serpent 2. The comparison led to the discovery of a need to improve the capabilities to model axial heterogeneities in reactor cores. Master's thesis on the subject was completed in 2016 and differences between TRAB3D and Serpent 2 predictions were halved. Serpent 2 was used to generate group constants for both TRAB3D and the transient analysis code HEXTRAN.

HEXTRAN and the systems code SMABRE were successfully coupled internally and moved to the Linux computing environment. In addition, the porous-CFD code PORFLO was coupled with HEXTRAN and SMABRE. The fully coupled HEXTRAN-SMABRE-PORFLO simulation framework was established and demonstrated by calculating VVER-440 and VVER-1000 transients.. The results demonstrated the feasibility and advantages of coupling 3D thermal hydraulics with 3D neutronics and system codes .

### Introduction

The objective of the project is to enhance the capability for independent transient analysis calculations. This can be utilized by the safety authority and other end-users for safety analyses independent from those of power plant designers and fuel vendors. The main outline is to improve VTT's modelling capabilities by routine coupled use of the CFD-type thermal hydraulics solver PORFLO and the reactor dynamics codes HEXTRAN and TRAB3D. To utilise the full potential of the new thermal hydraulics modelling, the neutronics modelling needs to be detailed. To ensure the improvements in accuracy have the most impact, the whole safety analysis methodology should be revised. The goal is to have a tool which is more accurate and still fast and robust enough for practical safety analyses. The developed computational tool set of coupled neutronics, system codes and 3D thermal hydraulics have been and will be tested and demonstrated in cases relevant from the safety analysis point of view. The objective is that by the end of the project we will have calculated several transients and accidents of real interest. Developing and maintaining our own independent codes enables the best possible expertise on safety analyses through in-depth understanding of the tools.

### Neutronics and reactor core

#### Development of neutronics models

The transient behaviour of quadratic assembly PWRs and BWRs are modelled at VTT by the reactor analysis code TRAB3D [1]. To improve the resolution at which power distribution can be analysed, a pin power reconstruction module has been implemented to TRAB3D [1]. During the implementation, the previous

work on the reconstruction module was expanded to take into account the fuel and moderator temperature as well as soluble boron content. The reconstruction module utilizes the full core solution from TRAB3D and an additional pre-calculated assembly-wise input from the reactor physics code Serpent 2 [3]. The reconstructed pin powers of an EPR core with a zero burnup startup load in Hot Zero Power (HZP) conditions were compared to the results of a 3D full core Serpent 2 reference calculation. For the purposes of analysing neutronics models, the Serpent 2 results can be perceived as the correct solutions to the problems. The reconstructed values were within -10.79% and +10.29% of the Serpent 2 results. One reason for the differences is that the global radial shape of the TRAB3D solution affects the reconstruction and the radial power distributions of TRAB3D and Serpent 2 are not identical. The pin powers from Serpent 2 and TRAB3D in one node of the EPR calculation case are presented in Figure 1. In addition, albedo generation with Serpent 2 for TRAB3D was developed during the work, which reduced the total difference between the two codes by roughly one third.

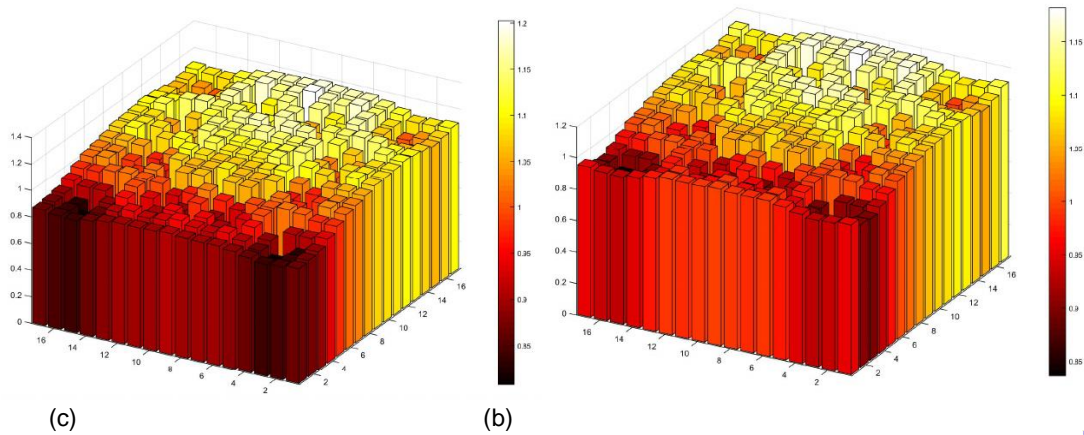


**Figure 1.** The relative pin powers of the center node of the EPR core reconstructed by TRAB3D (a) and calculated by Serpent 2 (b)

The analyses performed during the implementation of the pin power module to TRAB3D revealed a need for improved modelling of axial heterogeneities in modern reactor designs such as EPRs. A Master's thesis on the subject was begun in 2015 and finished during 2016 [4]. The case examined in the Master's thesis was an EPR core with a zero burnup startup load in hot zero power conditions. Axial discontinuity factors were generated for TRAB3D using 3D single assembly Serpent 2 calculations and a reproduction of TRAB3D's neutronics model.

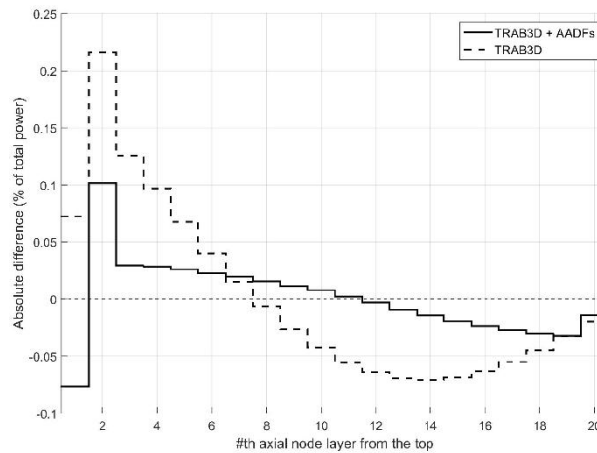


**Figure 2.** The relative differences between the relative axial powers of TRAB3D and Serpent 2 for a HZP EPR core for TRAB3D calculations with and without axial discontinuity factors (middle). A 2D



slice of one of the 3D assembly geometries used for the generation of the axial discontinuity factors (right). In addition, TRAB3D was modified to enable the use of axial discontinuity factors. For the HZP EPR core case, the use of axial discontinuity factors reduced the maximum difference between the axial relative powers of TRAB3D and Serpent 2 by 52.9% and the total integrated difference in the axial relative powers by 58.9%

However, notable differences between TRAB3D and Serpent 2 remain. Comparison of the intra-nodal flux solution from TRAB3D's model to an intra-nodal flux solution obtained by AFEN (Analytic Function Expansion Nodal) methodology indicate that with a sufficiently sophisticated neutronics model there is no need for axial discontinuity factors, as such a model would adapt to axial heterogeneities automatically. The high values for the leakage-corrected axial discontinuity factors for TRAB3D (up to 1.8, while traditional radial discontinuity factors are usually in the range of 0.98 to 1.02) support the conclusion.

The generation and use of the axial discontinuity factors proceeds in several steps:

- 1) Generation of traditional 2D assembly-wise group constants with Serpent 2
- 2) Generation of radial and axial albedos with Serpent 2
- 3) 3D Serpent 2 calculation of each assembly type in the core
- 4) Axial single-assembly calculations of each assembly type in the core using TRAB3D's calculation model and the group constants from step 2
- 5) Leakage-corrected axial discontinuity factors are the ratios of surface flux solutions from steps 3 and 4

Of these steps, the steps 1 and 2 constitute the generation of the traditional group constant inputs for TRAB3D. Step 3 is used to extract the heterogeneous solution of the system with an acceptable computational cost and step 4 is to extract the homogeneous solution of the system. The axial discontinuity factors are the ratios of the heterogeneous and homogeneous surface fluxes, and these leakage-corrected discontinuity factors can be used together with the traditional group constants.

### Utilization of Serpent 2 for group constant generation

The work on pin power reconstruction and axial discontinuity factors involved developing a framework for the generation and use of group constants from Serpent 2 in the reactor analysis code TRAB3D. The work involved generating group constants for the hot zero power conditions as well as the calculation of albedo boundary conditions for TRAB3D. The work did not extend to the generation of group constants for hot full power (HFP) or transient calculations.

In addition, the foundation for the use and generation of group constants and albedos for the reactor analysis code HEXTRAN for VVER-type reactors has been developed in the SADE project. The steady state condition at the V-1000 zero power facility at Kurchatov Institute was calculated using both Serpent 2 and HEXTRAN [5]. The group constants for HEXTRAN were generated with Serpent 2. The geometry of one of the 2D single assembly calculation cases for the group constant calculations is presented in Figure 3.

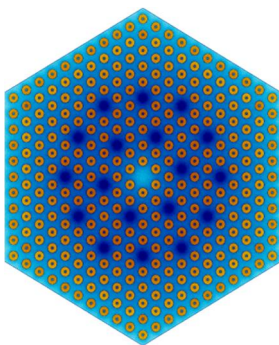


**Figure 3.** The mesh plot of one of the 2D single assembly geometries used for group constant generation for the V-1000 core by Serpent 2. The cool colors represent thermal flux magnitude and the warm colors represent fission power density.

Experimental results of the steady state obtained at Kurchatov Institute in 1990-1992 were available for the calculation case. The results of a 3D Serpent 2 full core calculation were compared to the measurements. In addition, the 3D Serpent 2 full core calculation was compared to the HEXTRAN results, and the HEXTRAN results were compared to the measurements.

The root-mean-square difference (RMS) between Serpent 2 results and the measurements was 5.19% and in 129 assemblies out of the 163 (79.1%), the differences between Serpent 2 and the measurements were within the sum of the experimental accuracy of the measurements and the relative statistical accuracy of Serpent 2. The Serpent 2 calculation produced an effective multiplication factor of  $k_{\text{eff}} = 1.01554$  for the critical steady state. The HEXTRAN and Serpent 2 results agreed as well as was expected and the RMS between the two was 3.83%. The HEXTRAN calculation produced an effective multiplication factor of  $k_{\text{eff}} = 1.018493$ , within 300 pcm of the Serpent 2 result. From the comparison of Serpent 2 and HEXTRAN results, it can be concluded that the Serpent 2 - HEXTRAN calculation chain has been established successfully.

The comparison between HEXTRAN and the measurements was not deemed meaningful, as the measurement results are relative powers of single fuel rods and HEXTRAN does not have an internal pin power reconstruction module. The results of the V-1000 calculation case were presented at the AER 2016 conference held in Helsinki, Finland [5], and they were chosen for publication in the KERNTECHNIK journal [6]. The relative differences between the measurements and the 3D full core Serpent 2 calculation are shown in Figure 4.

As both the Serpent 2 and HEXTRAN calculations overestimated the effective multiplication factor significantly, the case was investigated further. It was found that modelling the spacer grids of the core explicitly in the Serpent 2 calculation geometry significantly improved the estimation of the effective multiplication factor. In addition, it was found that the experimental accuracy of the soluble boron concentration was such that it allowed significant differences in the neutronics solution within its allowable limits. Adding the spacer grids to the Serpent 2 model reduced the effective multiplication factor by 660 pcm and adjusting the soluble boron concentration to the highest allowed value within the experimental accuracy reduced the effective multiplication factor by 577 pcm. The final Serpent 2 model of the V-1000 core produced an effective multiplication factor of  $k_{\text{eff}} = 1.00243$ , which is in excellent agreement with the measured critical steady state of the system. The results of this refinement of the V-1000 case have been accepted for publication and presentation at M&C conference and will be presented in April 2017 [7].

### Reactor dynamics

The results of a TRAB3D simulation of the O2 benchmark were presented at the O2 4<sup>th</sup> workshop in 2015 [8]. The TRAB3D model for Oskarshamn-2 was created, tested and used for the simulation of the benchmark. The model was constructed from scratch to provide an additional experience in BWR modelling. The control rod worths of the benchmark were modified slightly to produce a partial scram that is efficient enough for the case.

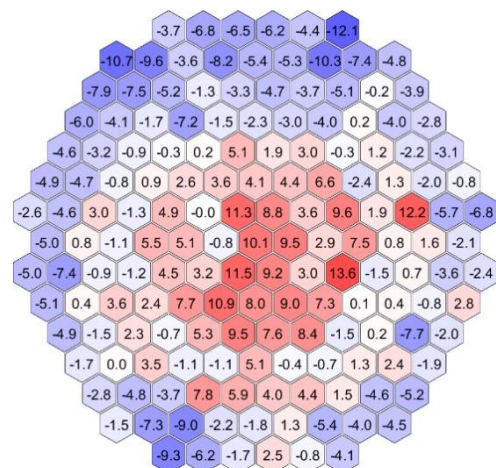


**Figure 4.** The relative differences in percents between the measurements and the results of the 3D Serpent 2 full core calculation of the V-1000 core.

The development of the reactor power through the transient is presented in Figure 5. The TRAB3D calculations re-produced both the initial power fluctuations as well as the power oscillations. In addition, the TRAB3D simulation was terminated before scram due to local dryout. This is a known limitation in TRAB3D. However, this limitation did not hinder the simulation and modelling of the oscillations after the scram. It was found that the initiation of the oscillations is very sensitive to modelling details and the prevailing operational conditions.

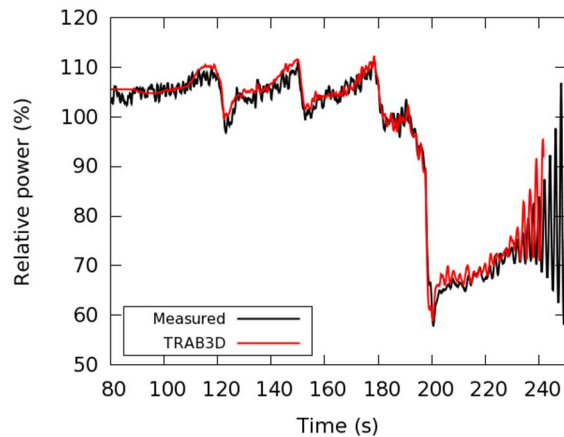


**Figure 5.** The measured and simulated relative reactor power through the O2 benchmark transient.

### Cooperation with PANCHO: fuel behaviour modelling

The light-weight fuel behaviour module FINIX was coupled with both TRAB3D and HEXTRAN, and the success of the couplings were confirmed by calculating several transient calculation cases in cooperation with the PANCHO project. Results of FINIX-HEXTRAN coupling were presented in a conference paper at Topfuel conference. The AER 3<sup>rd</sup> benchmark was calculated with HEXTRAN and FINIX [9]. These results were also presented at the 11<sup>th</sup> International Conference on WWER Fuel Performance, Modelling and Experimental support [10]. Additionally a control rod ejection transient in a VVER-440 reactor was modelled with coupled FINIX-HEXTRAN and the results were published in EPJ Nuclear Sciences & Technologies [11].

The performance of FINIX-TRAB3D coupling was confirmed by calculating a main steam line break benchmark transient CITE. In the calculation the coupling between FINIX and TRAB3D was tested and analysed. FINIX has significant impact on the average fuel temperature during the transient. The results of this calculation were published in cooperation with PANCHO as a part of a paper in the Annals of Nuclear Energy [12].

### Open core geometry and RPV

The whole core transient analyses are emphasised especially in cases where mixing in a Reactor Pressure Vessel (RPV) and open core geometry play an essential role. Computational tools enabling more realistic modelling of transients were further developed and validated. A reactor dynamics code was coupled with fully three-dimensional thermal-hydraulics. The goal is to have a computational tool, which is more accurate with known uncertainties and still fast and robust enough for practical safety analyses.

### Internal coupling between the HEXTRAN and SMABRE codes

The primary solution to the analysis needs that arise from open core geometry was the internally coupled HEXTRAN-SMABRE. The original parallel coupling between the reactor dynamics code HEXTRAN and the system code SMABRE is designed for cases in which flow in a reactor core propagates in separate flow channels. Implementation of a new internal coupling method between HEXTRAN and SMABRE was completed in 2015 [13]. At the same time, a new computing surrounding was taken into use and the codes were moved from the 35-years used UNIX computers to the Linux ones. With the new coupled HEXTRAN-SMABRE code, either the extensively used parallel coupling method or the new internal coupling method

is selected. With the parallel coupling, HEXTRAN solves neutronics, heat transfer and thermal hydraulics in a core. When the internal coupling is chosen, HEXTRAN computes only the core neutronics and heat transfer inside fuel rods. With both options, SMABRE solves thermal hydraulics of the whole circuit.

The new coupled HEXTRAN-SMABRE code was tested with different kinds of transients of the VVER-440 and VVER-1000 plants [13]. Figure 6 shows selected results for a control rod ejection transient in a VVER-440 reactor. The location of an ejected control rod typical in a safety analysis is assumed in the edge area in the core. The evolutions of the relative fission power for the internal and parallel couplings, on the left in the figure, are in close agreement with each other. This indicates that the internal coupling of HEXTRAN and SMABRE in the new computing surrounding is performing correctly. The power distribution in a crosscutting of the core, on the right in the figure, reflects the main result of the control rod ejection transient, a very peaked fission power in the radial, but also in the axial direction.

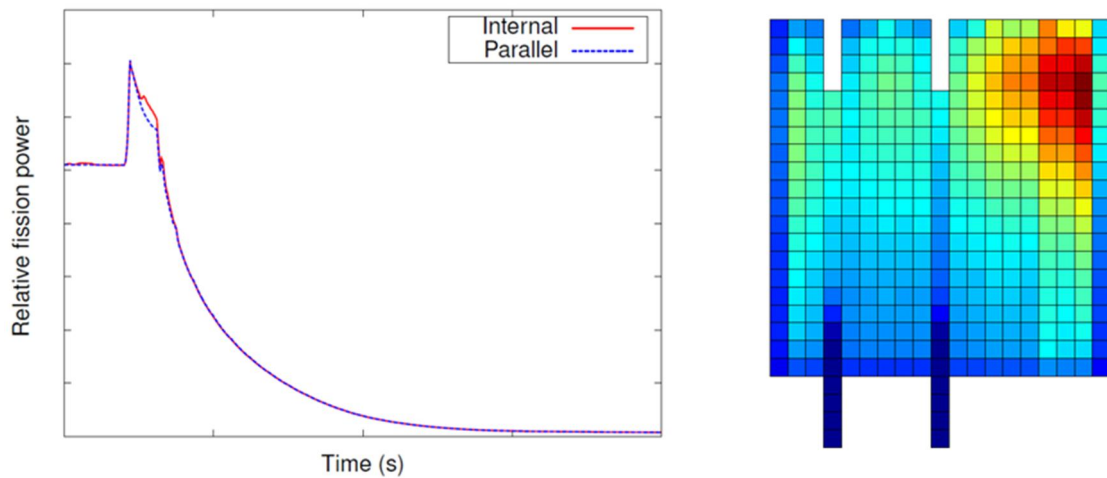


**Figure 6.** In a control rod ejection transient for a VVER-440 reactor, the evolution of the relative fission power (left) and power distribution in a core crosscutting at the time of the maximum total fission power with the internally coupled HEXTRAN-SMABRE (right).

### One-way coupling of the HEXTRAN and PORFLO codes

The VTT-developed porous-CFD code PORFLO was one-way coupled with the core neutronics code HEXTRAN. A time-dependent node-wise 3D heating power field pre-computed with HEXTRAN can be applied in PORFLO simulations for thermal-hydraulics. The one-way coupling of HEXTRAN and PORFLO was tested in computations for a VVER-1000 transient benchmark (OECD/NEA benchmark V1000CT-2), in which a large break in the main steam line between the steam generator and steam isolation valve is assumed. In the analysed case, Exercise 2, boundary conditions for the cold and hot legs are specified and the influence of the coupling of 3D neutronics and hydraulics in the pressure vessel is examined. The one-way coupled HEXTRAN-PORFLO simulations were performed for a realistic scenario with a trip of the main cooling pump in Loop 4 (Scenario 1) as well as for a pessimistic scenario with the assumption that all pumps continue in operation (Scenario 2). In addition, both scenarios comprise two variants with stuck control rods in one or two fuel assemblies.

Two meshes were created for the pressure vessel. The coarse mesh comprises approx. 280 000 cells and the less-coarse mesh approx. 570 000 cells. The block structured meshes consist of mostly hexahedral and prism blocks, which are connected together with a small number of tetrahedral and pyramid elements.

Figure 7 exemplifies computational results in the one-way coupled HEXTRAN-PORFLO simulation for Scenario 2 (Variant b) with the coarse mesh. The deviation of the evolution of the coolant temperature in

the interesting hot leg 4 from the results of the codes with coarser spatial discretizations results mainly from the smaller dispersion in the CFD-based analysis.

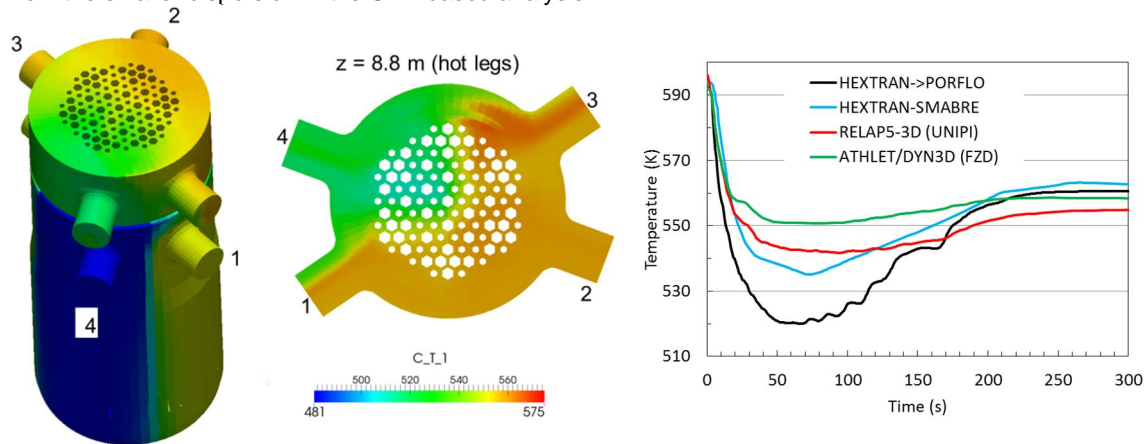


**Figure 7.** Coolant temperature (K) on the outer surface of the CFD domain (left) and on a horizontal cross section (middle) at the time of 71 s as well as the coolant temperature in the hot leg 4 as a function of time for the one-way coupled HEXTRAN-PORFLO simulation of a VVER-1000 transient (OECD/NEA benchmark V1000CT-2-Exercise 2) with the results of other codes (right). The coarse CFD mesh was used.

#### Full 2-way coupling of PORFLO with the HEXTRAN and SMABRE codes

Full couplings of the codes HEXTRAN and SMABRE with the PORFLO code were implemented. 2-way coupling routines were developed for information exchange between the codes. Some significant modifications were also necessary in the coupled codes. In addition, new parameters controlling the coupling were added in the inputs. The main communications between the codes are visualized in Figure 8 with the primary quantities transferred. Typically a CFD mesh covers a pressure vessel or part of it and a SMABRE nodalization the rest of a plant (Figure 9). HEXTRAN communicates with PORFLO but not with SMABRE. Data transfer between PORFLO and HEXTRAN or SMABRE is handled through the TCP/IP sockets.

The 2-way coupling of HEXTRAN and PORFLO provides more realistic thermodynamic data for 3D neutronics calculations. 3D neutronics computation in HEXTRAN is based on 3D core thermodynamic data sent by PORFLO. After receiving a new 3D field for the coolant heating power, PORFLO updates thermodynamic data and returns it to HEXTRAN. Converged solution is thus obtained by iteration within a time step. Furthermore, the VTT-developed fuel behaviour module FINIX can optionally be used with HEXTRAN and/or PORFLO.

The PORFLO code is also fully coupled with the system code SMABRE. The main quantities transferred between the codes are given in Figure 8. In the coupled SMABRE-PORFLO simulations, a converged and consistent solution is also obtained by iteration within a time step.

Due to the very limited project funding, the SMABRE-PORFLO and HEXTRAN-PORFLO couplings were finalized and test simulations were also carried out outside the project. On the other hand, the developed approach of coupling codes could also relatively easily be applied in coupling other codes.

The applicability of the new coupled HEXTRAN-SMABRE-PORFLO simulation framework for nuclear power plants was tested in two transients. A VVER-1000 main-steam-line-break transient benchmark (OECD/NEA benchmark V1000CT-2 - Exercise 3) and the 7<sup>th</sup> dynamic AER benchmark for the start-up of an inoperable cold loop in VVER-440 were successfully computed with the CFD-coupled code system.

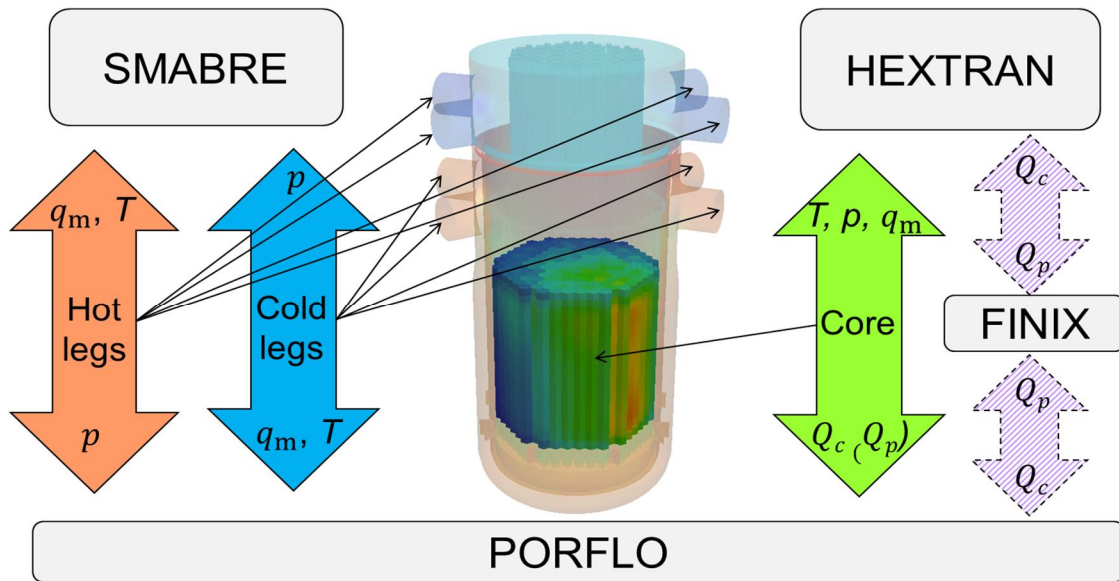


**Figure 8.** Visualization of the couplings and data transfer between HEXTRAN, FINIX, SMABRE and PORFLO with the CFD modelling domain in a coupled VVER-1000 simulation.

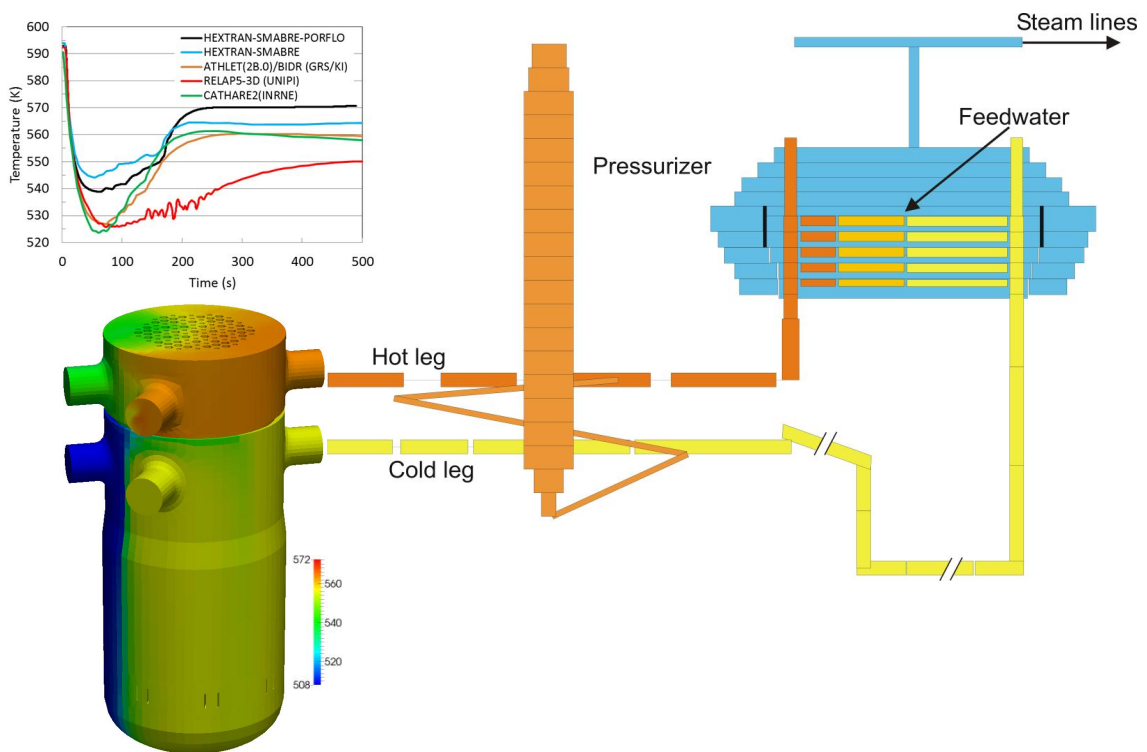


**Figure 9.** Schematic representation of coupling the CFD modelling domain for the pressure vessel (coloured by the coolant temperature) with the SMABRE nodalization (nodes shown only for one loop) in a coupled simulation of a VVER-1000 plant. Top left corner: Coolant temperature in the hot leg 4 in a fully coupled HEXTRAN-SMABRE-PORFLO simulation for a VVER-1000 transient with the results of other codes (OECD/NEA benchmark V1000CT-2 - Exercise 3).

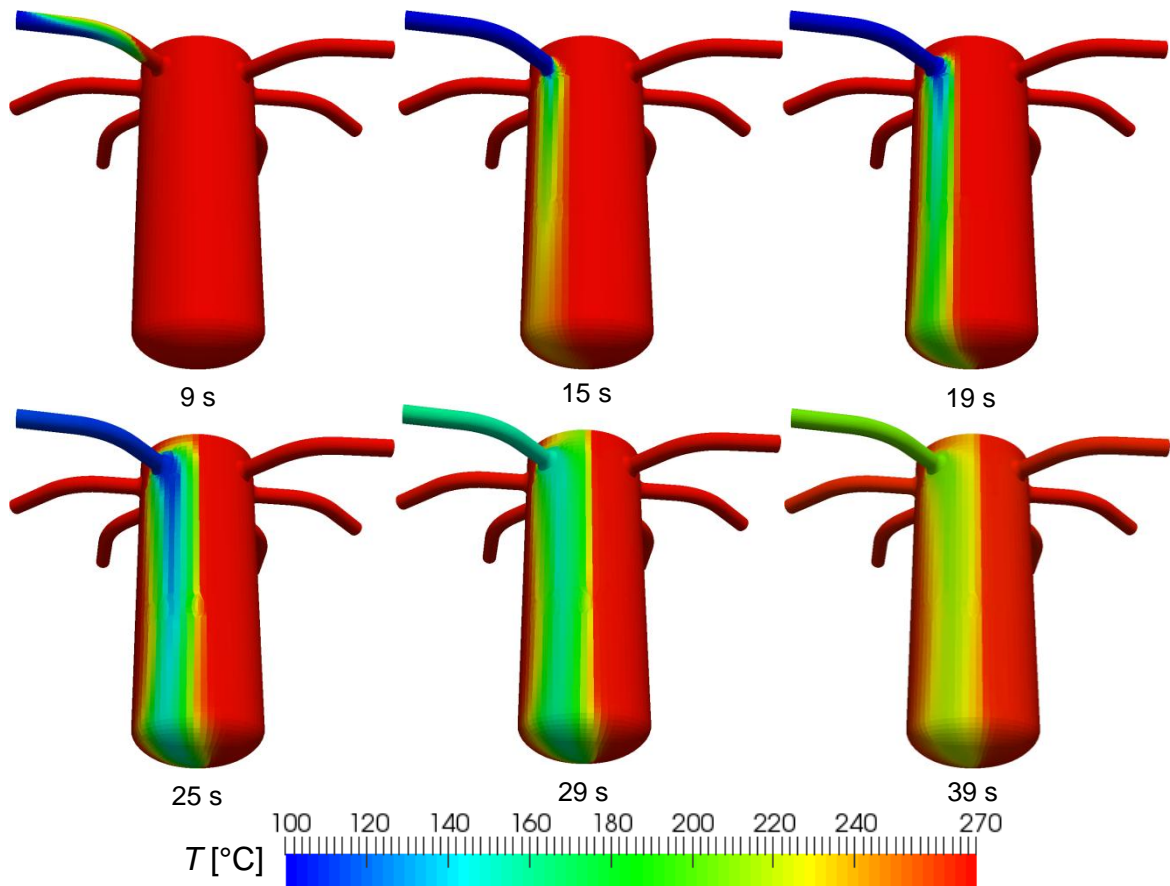


**Figure 10.** Temperature [°C] at the outer surface at selected time steps in the coupled SMABRE-PORFLO simulation for the 7<sup>th</sup> dynamic AER benchmark for the start-up of an inoperable cold loop in VVER-440.

In the simulation for VVER-440, the computational domain in CFD modelling consists of a part of the primary circuit from the cold leg MIVs to the lower end of the core [14,15]. The mesh comprises 165 000 cells, most of which are hexahedra and prisms. The SMABRE model covers the rest of the plant. Only the coupling of SMABRE and PORFLO is thus needed. General progression of the transient is depicted in Figure 10, where the coolant temperature distribution is plotted on the outer surface of the CFD domain.

The VVER-1000 analyses were carried out for Exercise 3 of the same main-steam-line-break VVER-1000 transient benchmark discussed with the one-way coupled HEXTRAN-PORFLO simulations above (OECD/NEA benchmark V1000CT-2). In Exercise 3, the behaviour of the whole plant is simulated. Fully CFD-coupled HEXTRAN-SMABRE-PORFLO computations were performed for a variant of the pessimistic scenario. The CFD modelling domain covers most of the pressure vessel (Figure 9). The same coarse and less-coarse meshes were used as in the one-way coupled HEXTRAN-PORFLO simulations introduced above. The CFD domain is connected to the SMABRE system description for the rest of the plant at the four cold and hot legs (Figures 8 and 9).

Figure 9 shows the computed coolant temperature in the hot leg 4 as a function of time with the results of other modelling tools. The deviation from the HEXTRAN-SMABRE curve results from smaller dispersion. The temporal core inlet temperature and assembly-wise fission power for the simulations with and without CFD couplings are compared in Figure 11. With CFD-coupling, the distribution of the core inlet temperature is clearly more realistic and the peak power is higher than in the HEXTRAN-SMABRE results.

Already the first two coupled simulations demonstrated the feasibility and advantages of coupling 3D thermal hydraulics with 3D neutronics and system codes. The results emphasise the importance of realistic 3D thermal hydraulics modelling of the pressure vessel providing more realistic and reliable computational results for nuclear power plants. Coupled simulations with 3D neutronics and CFD-level representations for pressure vessels will likely bring out new information on the behaviour of the reactors during transients. Furthermore, the simulations provided more realistic novel reference results for the benchmarks.

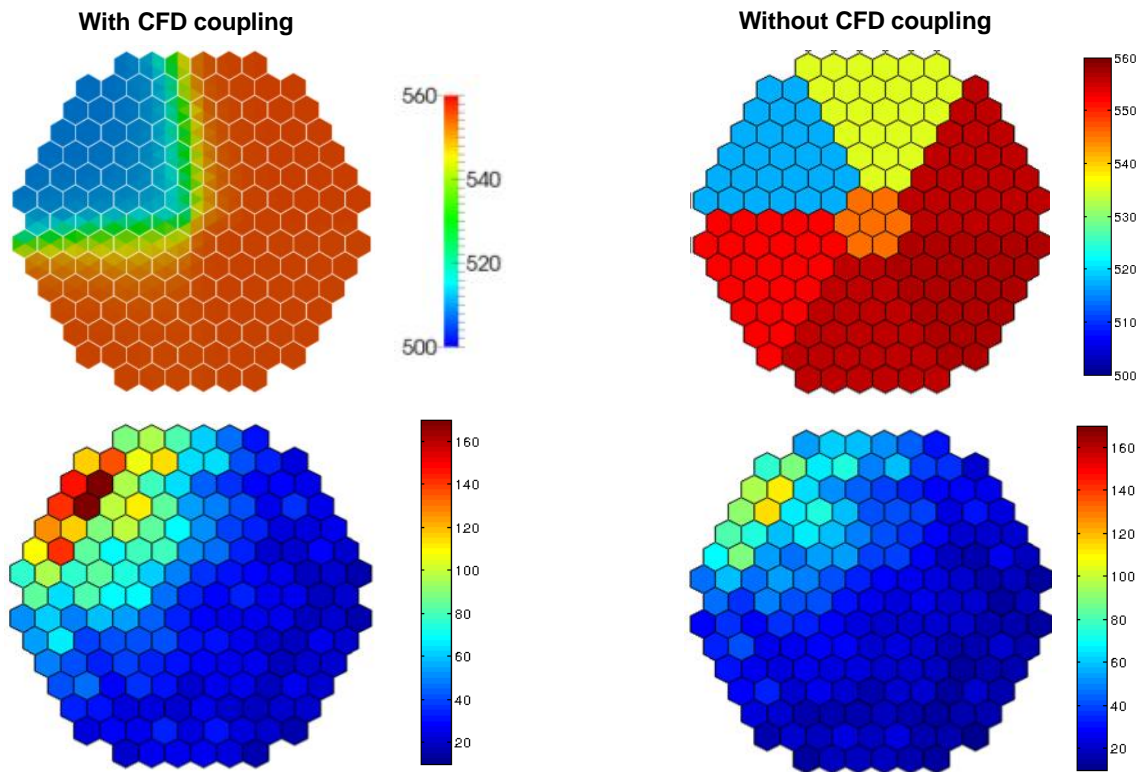


**Figure 11.** Temporal (60 s after the break) core inlet temperature (top) and assembly-wise fission power (bottom) in the CFD-coupled HEXTRAN-SMABRE-PORFLO (left) and HEXTRAN-SMABRE (right) simulations for a VVER-1000 transient (OECD/NEA benchmark V1000CT-2 - Eercise 3).

## International co-operation and QA

The cooperation and information exchange on VVER safety within the AER framework together with other countries which use VVER reactors comprise an important part of the international co-operation in the SADE project and has been continued. In 2016 the AER Symposium was held in Helsinki, Finland, and VTT participated in organising the symposium, while Fortum had the main organising responsibility. Two SADE papers were presented in the symposium. The cooperation within AER includes participation in the AER working group D on VVER safety analysis and in the AER scientific council. For 2016, attending the scientific council was cancelled for SADE project. In 2016, Anitta Hämäläinen participated in the AER Working Group 6 at Villingen, Switzerland [16]. In addition, participation in the OECD Nuclear Energy Agency (NEA) working groups and benchmarks is an important way of validating the methods and codes used in reactor analysis. SADE includes the participation in the meetings of the NEA Working Party on the Scientific Issues of Reactor Systems (WPRS), which is responsible for the organization of the reactor dynamics benchmarks among other activities. In 2015, Elina Syrjälähti participated in a WPRS meeting

[17] and in addition VTT has participated in the OECD/NEA BWR stability benchmark (O2) [8] and in the AER working group D meeting [18] in the SADE project.

## References

- 1 Kaloinen, E., Kyrki-Rajamäki, R., TRAB3D, a new code for three-dimensional reactor dynamics. In Proceedings of ICON-5, Nice, France, May 26-30, 1997.
- 2 Sahlberg, V., Validating Pin Power Reconstruction Module with Serpent 2 – TRAB3D Code Sequence”, special assignment, Research report VTT-R-04065-15
- 3 Leppänen, J., Pusa, M., Viitanen, T., Valtavirta, V., Kaltiaisenaho, T., The Serpent Monte Carlo Code: Status, development and applications in 2013. *Annals of Nuclear Energy* 82 (2015) p. 142 <http://dx.doi.org/10.1016/j.anucene.2014.08.024>
- 4 Sahlberg, V., Modelling of axial discontinuities in reactor cores with Serpent 2 - TRAB3D code sequence, Master's Thesis, Aalto University. 59+6 p. <http://urn.fi/URN:NBN:fi:aalto-201608263123>
- 5 Sahlberg, V., Recalculating the steady state conditions of the V1000 zero power facility at Kurchatov Institute using Monte Carlo and nodal diffusion. Conference proceedings. Atomic Energy Research (AER), pp. 485-497. 26<sup>th</sup> Symposium on VVER reactor physics and reactor safety, October 10-14, 2016, Helsinki, Finland. ISBN 978-963-7351-26-6, ISBN 978-963-7351-27-3.
- 6 Sahlberg, V., Recalculating the steady state conditions of the V1000 zero power facility at Kurchatov Institute using Monte Carlo and nodal diffusion, KERNTÉCHNIK special AER issue, 8/2017. Submitted for publication.
- 7 Sahlberg, V., Calculating V-1000 Core Model with Serpent 2 - HEXTRAN Code Sequence. Conference proceedings, M&C 2017 - International Conference on Mathematics and Computational Methods Applied to Nuclear Science & Engineering, April 16-20, 2017, Jeju, Korea. Submitted for publication.
- 8 Syrjälähti E. TRAB3D simulation of O2 benchmark. OECD/NEA O2-4 workshop, May 18-19, 2015, Madrid, Spain. (contributed talk)
- 9 Ikonen, T., Syrjälähti, E., Valtavirta, V., Loukusa H., Leppänen, J. & Tulkki, V. Multiphysics simulation of fast transients with the FINIX fuel behaviour module In: TopFuel 2015, 13-17 September 2015, Zurich, Switzerland, paper A0110, p. 572-581. <https://www.euronuclear.org/events/topfuel/topfuel2015/transactions/topfuel2015-transactions-oral-1.pdf>. ISBN 978-92-95064-23-2.
- 10 Syrjälähti E., Valtavirta V., Kättö J., Loukusa H., Ikonen T., Leppänen J. and Tulkki V. Multiphysics simulations of fast transients in VVER-1000 and VVER-440 reactors. In: 11<sup>th</sup> International Conference on WWER fuel performance, modelling and experimental support. 26 September – 03 October 2015, Golden Sands Resort, Bulgaria

- 11 Ikonen, T., Syrjälähti, E., Valtavirta, V., Loukusa H., Leppänen, J. & Tulkki, V. Multiphysics simulation of fast transients with the FINIX fuel behaviour module. EPJ Nuclear Sci. Technol. 2, 37 (2016). <http://dx.doi.org/10.1051/epjn/2016032>
- 12 Ikonen, T., Loukusa H., Syrjälähti E., Valtavirta V., Leppänen J., Tulkki V. Module for thermomechanical modeling of LWR fuel in multiphysics simulations. Annals of Nuclear Energy 84 (2015) 111–121. doi:10.1016/j.anucene.2014.11.004. <http://www.sciencedirect.com/science/article/pii/S0306454914005842>
- 13 Syrjälähti, E., HEXTRAN-SMABRE version 4060 with internal coupling between the HEXTRAN and SMABRE codes, Research report VTT-R-00457-16.
- 14 Hovi, V., Taivassalo, V., Hämäläinen, A., Syrjälähti, E., Rätty, H. Startup of a cold loop in a VVER-440, the 7th AER benchmark calculation with HEXTRAN-SMABRE coupled with porous CFD code PORFLO. Conference proceedings. Atomic energy Research (AER), pp. 369-389. 26<sup>th</sup> Symposium on VVER reactor physics and reactor safety, October 10-14, 2016, Helsinki, Finland. ISBN 978-963-7351-26-6, ISBN 978-963-7351-27-3.
- 15 Hovi, V., Taivassalo, V., Hämäläinen, A., Rätty, H., Syrjälähti, E. Start-up of a cold loop in a VVER-440, the 7th AER benchmark calculation with HEXTRAN-SMABRE-PORFLO. KERNTECHNIK special AER issue 8/2017. Submitted for publication.
- 16 Hämäläinen, A. Simulation of the AER 7th benchmark with HEXTRAN-SMABRE-PORFLO, preliminary results. AER working group D meeting, May 30-31, 2016, Villingen, Switzerland. (contributed talk).
- 17 Syrjälähti E. Travel report OECD/NEA WPRS meeting.
- 18 Hovi, V., Taivassalo, V., Ilvonen, M., Hämäläinen, A. and Syrjälähti, E. Simulation of the AER 7th benchmark with PORFLO and HEXTRAN-SMABRE. AER working group D meeting, May 18-19, 2015, Madrid, Spain. (contributed talk).

## **5. Thermal hydraulics**

### **5.1 Comprehensive and systematic validation of independent safety analysis tools (COVA)**

Seppo Hillberg, Ismo Karppinen, Ari Silde, Jarno Kolehmainen, Eric Dorval, Joona Leskinen, Joona Kurki, Torsti Alku, Sampsa Lauerma, Dmitri Skripnikov, Tatu Hovi

VTT Technical Research Centre of Finland Ltd  
P.O. Box 1000, FI-02044 Espoo

#### **Abstract**

Apros is a system-scale safety analysis tool developed at VTT in cooperation with Fortum since 1986. Apros is used for safety analyses of light water reactors, and thanks to addition of new advanced features in the recent years, it can also be utilized in analysing generation IV nuclear reactors. As a commercial code Apros has a rigorous and extensive version-validation process whose purpose is to ensure that no unwanted changes or error have been introduced in any of the application areas while introducing the new features or changes of existing features and corrections of detected errors into the new released version.

The overall objective of the COVA project is to improve the state of Apros' validation through a systematic and rigorous approach to the validation process, and also to promote this kind of approach to the validation process. The process enhances the expertise in thermal hydraulic area of Generation II and III LWR reactors and includes as an essential part training of new experts to this relevant area of reactor safety. While the main effort is being carried out using Apros, as it has higher national interest as a self-developed independent and versatile safety analysis tool, U.S. NRC's TRACE is also used in analyses of new experiments and in code-to-code comparisons with Apros.

#### **Critical assessment of thermal-hydraulic and containment models' validation**

The project started in 2015 with an assessment of Apros's thermal-hydraulic and containment models' validation by compiling databases of the calculated validation cases and then by comparing them to the OECD/NEA's separate effect test [1,2] and containment [3] validation matrices. This work formed a foundation [4,5] on which much of the work done in COVA during its four-year period is based.

## Validation assessment of Apros' thermal-hydraulic model

Assessment of Apros' TH model was commenced by gathering a list of all validation cases calculated with Apros throughout its development history, including information on what code version was used for each analysis and what kind of results was obtained. All available analysis reports on these calculations were gathered so that new simulation results could be later compared to earlier results if the same cases are chosen for recalculation. In the next stage OECD NEA's thermal hydraulic validation separate effects test matrix [1,2] (a part of the table is presented in Figure 1) was used to craft a comprehensive set of validation cases that, when analysed, would ensure the best possible validation of the code for all safety relevant nuclear power plant scenarios.

0. Basic Phenomena	<ol style="list-style-type: none"> <li>1. Evaporation due to Depressurisation</li> <li>2. Evaporation due to Heat Input</li> <li>3. Condensation due to Pressurisation</li> <li>4. Condensation due to Heat Removal</li> <li>5. Interfacial Friction in Vertical Flow</li> <li>6. Interfacial Friction in Horizontal Flow</li> <li>7. Wall to Fluid Friction</li> <li>8. Pressure Drop at Geometric Discontinuities</li> <li>9. Pressure Wave Propagation</li> </ol>
1. Critical Flow	<ol style="list-style-type: none"> <li>1. Breaks</li> <li>2. Valves</li> <li>3. Pipes</li> </ol>
2. Phase Separation / Vertical Flow with and without Mixture Level	<ol style="list-style-type: none"> <li>1. Pipes / Plena</li> <li>2. Core</li> <li>3. Downcomer</li> </ol>

**Figure 1.** Phenomena identified in the OECD SET –matrix [1,2] were used in categorizing the current Apros validation base (only part of the table is shown).

Recommendations for code assessment in each phenomenon were listed and recommendation was given that further validation work should be started with filling the gaps and extending the validation base in assessment of the basic phenomena. Among those, the interfacial friction in vertical flow was identified as one of the most important ones, since it affects other phenomena, like heat transfer in two phase flow (e.g. core cooling in accident conditions).

Apros' validation of separate effect phenomena was found to be quite comprehensive and most of the phenomena being covered. However, room for improvement was still found as some of the phenomena are assessed with only a single experiment in one test facility. Assessment of some combined phenomena would benefit from dedicated validation and the assessment base of the code should be extended.

## Validation assessment of Apros' containment model

Validation assessment of Apros' containment package [5] covered a total of 43 tests, of which 21 were separate effect tests. In addition, 7 benchmark exercises were assessed. The validation cases covered the most common light water reactor containment types, such as BWR suppression pool containment, PWR large dry containment, PWR ice condenser containment, eastern type PWR bubble condenser containment, BWR containment with internal or external passive cooler, and German 1300 PWR containment. The range of pressure, gas and liquid water temperature and steam/light gas concentrations in the calculated experiments covered acceptably the typical containment conditions in design basis accidents (DBAs).

The assessment showed that Apros is capable in calculating the general containment behaviour (such as pressure, gas temperatures, steam-gas –mixture composition, flow paths etc.) in DBAs and did not reveal any severe deficiencies that could prevent from using Apros for DBA analyses. However, further

validation, especially against separate effect tests, was recommended. Some important separate effects topics that would need further validation were identified as: condensation on wall surface, condensate film flow on the walls and its effects on heat transfer, convection heat transfer between atmosphere and structures, pool surface evaporation and condensation, surface temperature of water pool, spray modelling in specific situations, clearing time of suppression pool vents, heat transfer between liquid water and structure, ice melting rate, and hydrogen deflagration (Figure 2).

EXPERIMENT	STUDIED PHENOMENON	REMARKS
TOSQAN ISP-47 or TOSQAN condensation tests	- Condensation rate on wall condenser - Pressure - Gas temperatures - Steam and helium concentrations - Stratification	Main focus is on condensation calculation. The gas stratification field should be calculated (adjusted) sufficiently well to enable the validation of condensation calculation.
Some separate effect test for convection heat transfer	- Convection heat transfer	No suitable test found yet.
TOSQAN sump test	- Pool surface evaporation and condensation	
Test on surface pool temperature	- Pool surface temperature in condensation and evaporation cases.	No suitable test found yet.
AECL-SP Dousing test no 1	- Heat removal by dousing (spray)	

**Figure 2.** 22 cases were recommended for further validation [5] (only part of the table is shown).

### Validation analyses based on the assessment reports

Several experiments have been calculated based on the findings of validation assessment reports described previously and these are listed in Table 1.

**Table 1.** Separate effect tests calculated in 2015-2016.

Experiment or case	Phenomena or scenario	Used code
19-rod bundle experiments [6]	bundle heat transfer and friction	Apros
ACHILLES ISP-25 [7]	core reflood	Apros
ERSEC ISP-7 [8]	core reflood	Apros
FLECHT SEASET test 31302 [9] FLECHT SEASET test 32013 [9,10]	core reflood	Apros
LOTUS [6]	friction and phase separation in annular flow	Apros
TOSQAN test T201 [11]	wall condensation, sump evaporation	Apros containment

One of the simulated cases was the ISP-7 case of the tubular ERSEC reflooding experiments [8] (Figure 3). The phenomena related to core reflooding were identified as high priority a couple of years back at VTT and a development project was started in order to improve the code capability. In this development project a mechanism for an automatically adapting nodalisation of the channel wall heat structures was created. The new adapting nodalisation mechanism refines the calculation grid in the vicinity of the quench front in reflooding scenarios, so that the very steep axial temperature gradients in the wall can be captured. This is essential in order to be able to accurately simulate the progression of the quench front, as the heat conduction in the channel wall as well as a reflooding-specific heat flux model are dependent on the axial wall temperature gradient. In addition to the adapting nodalisation mechanism, a few smaller improvements were implemented into the reflooding models of Apros, which should improve Apros' predictive capability to some extent.

In order to verify the functionality of the adapting nodalisation scheme, assess the effect of other improvements made into the code, and to help identifying aspects in the code that would still need improvement, the ISP-7 case was recalculated with the current development version of Apros. As the improvement is still on-going, the results gained only reflect the current unfinished status of the work.

The simulations mainly confirmed the need to use a very fine nodalisation for the channel wall heat structures in the case of re-flooding simulations. The adapting nodalisation mechanism was verified to work as expected and give results very close to a fixed fine nodalisation. Consequently, it was recommended to carry out any future validation simulations related to reflooding scenarios by using the adapting nodalisation together with a coarse thermal-hydraulic nodalisation. Similar nodalisation strategy was then recommended to be applied also in real life safety analysis simulations. Despite the improvements, it was still seen that the results demonstrated a need to further improve the physical models affecting the outcome of reflooding situations.

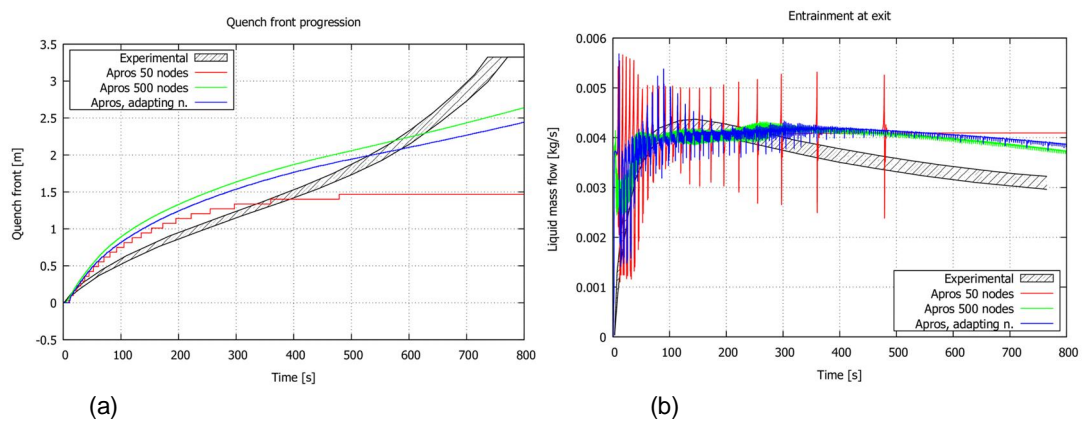


**Figure 3.** (a) Quench front progression and (b) entrainment at heated channel exit in ISP-7 calculation [8].

### Simulation of new experiments

Apart from the work governed mainly by the validation matrix assessment work, an integral part of COVA are also the analyses of new experiments and benchmark exercises. In years 2015 and 2016 such cases included for example the OECD/NEA's ATLAS SBLOCA and FONESYS critical flow benchmarks and simulation of OECD/NEA HYMERES experiments. The calculated cases are listed in Table 2.

**Table 2.** Benchmarks and new experiments calculated in 2015-2016.

Experiment or case	Used code
ATLAS A5.1 benchmark [12]	Apros
ATLAS A5.1 post-test calculation [13]	Apros
ATLAS A5.2 pre-test calculation [14]	Apros
FONESYS critical flow benchmark [15]	Apros
FONESYS extended critical flow benchmark [16]	Apros
HYMERES HM 2-1 and 3-2 calculations [17]	Apros containment
HYMERES HP6 scoping calculations [18]	Apros containment

Two of the calculated cases were the HM2-1 and HM3-2 HYMERES MISTRA experiments, calculated with Apros containment. MISTRA is a large experimental facility belonging to the CEA and located at Sac-lay nuclear research centre, devoted to containment thermal-hydraulics and hydrogen risk. The containment is a stainless-steel cylindrical vessel with an internal volume of 97.6 m<sup>3</sup> and comprises two shells, a flat cap and a bottom, which are joined by twin flanges. The outer dimensions of the facility correspond to a linear length scale ratio of 0.1 in relation to a typical French PWR containment. Three so-called condensers are inserted into the MISTRA vessel along the vertical walls. The inner compartment consists of a vertical cylinder, which is closed at the bottom, and is fitted with a ring plate [19]. The facility is shown in Figure 4.

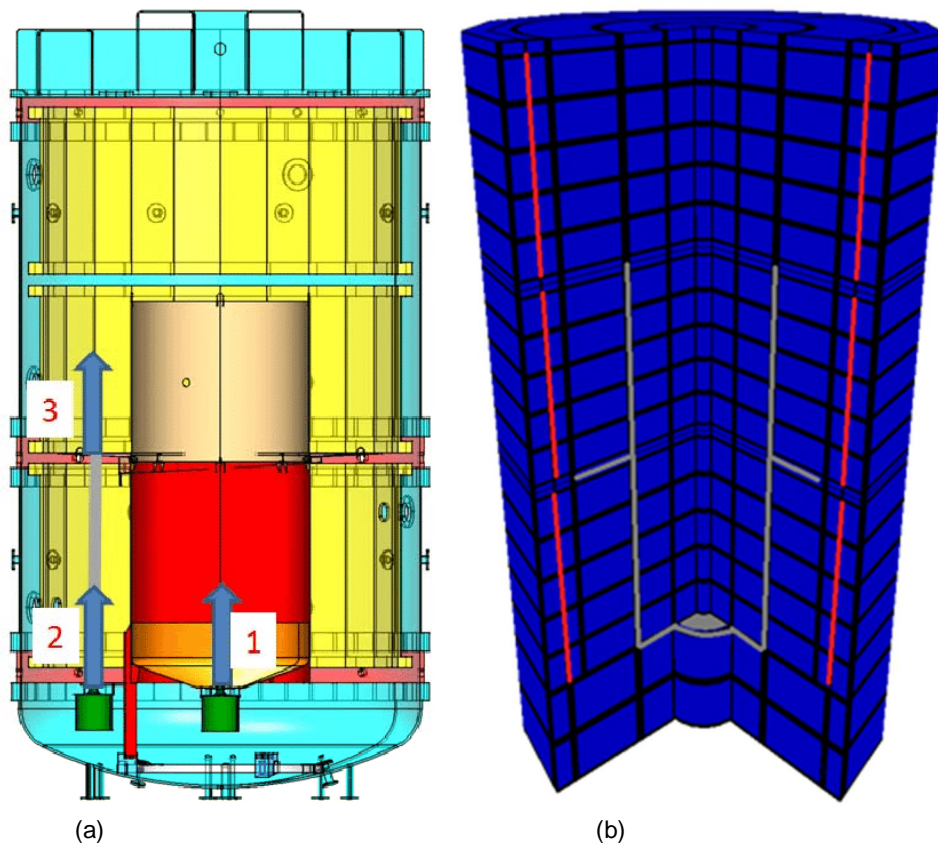


**Figure 4.** (a) MISTRA facility [20] and (b) Apros containment nodalization [17].

HM2-1 and HM3-2 experiments study helium distribution in the compartmented volume of the MISTRA facility. In the experiments a stratified dry atmosphere is first created and then helium injection is started to the inner compartment. After this, depending on the test, one or two heat sources that simulate passive autocatalytic recombiners (PARs) are introduced to the upper part of the facility.

The Apros containment model of the MISTRA facility is divided into 22 vertical levels to make it possible to capture the stratification of the gases. The model has 208 containment nodes. The two bottom levels are divided into 6 horizontal nodes, the levels 3-20 are divided into 10 horizontal nodes and the two top levels are divided into 8 horizontal nodes. The outer shell of the MISTRA facility is modelled with 34 heat structures, the inner cylinder with 57 heat structures and the condenser plates are modelled with 5 heat structures each. The model doesn't contain water sumps because the experiments were done in a dry air-helium gas atmosphere.

The heaters used in the experiments (PARs) are modelled with two nodes each. The area of the heater module is modelled with a node that represents the total volume of gas space between the heater plates of the mock-up PAR. The rest of the heater was modelled with the second node. The housing of the heater was not modelled. [17]

Previous analysis of the HM2-1 experiment at VTT [21] had showed that the model under predicted temperatures in the bottom part of the inner compartment during the whole experiment. This was believed to be caused by the lack of radiation heat transfer and heat conduction in the vertical direction of the inner compartment wall.

For the new simulations the model was improved. This was done by adding radiation heat transfer between the outer wall of the inner compartment and the middle and bottom condenser plates. Also radiation heat transfer was taken into account inside the inner compartment and vertical heat conduction was added to the heat structures. The HM2-1 and HM3-2 experiments were then calculated using this improved model. The new results were significantly better than the old ones. Improvement was especially seen in gas temperatures near the bottom of the facility (Figure 5).

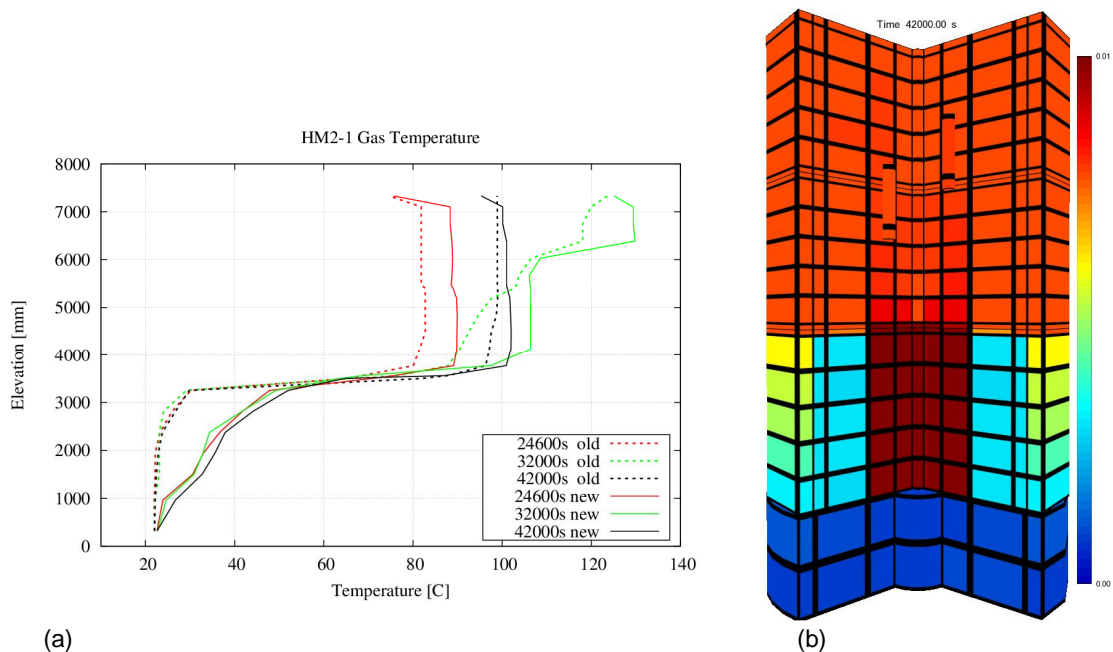


**Figure 5.** (a) HM2-1 calculated gas temperatures and (b) HM3-2 helium fraction at the end of simulation.

## International cooperation

Participation in international research projects related to nuclear safety research in the field of thermal hydraulics forms an essential part of the project: experimental data produced in these activities is directly utilized in the validation work carried out within COVA, and on the other hand, these validation activities support conduction of the experiments, in addition to promoting international cooperation and networking in the field of nuclear safety research. Additionally participation fees of some of these programmes are being channeled through COVA. In years 2015-2016 the following research programs have been participated:

- The OECD/NEA PKL-Phase 3 (primary coolant loop test facility) project continued until December 2015. The programme was investigating safety issues relevant for current pressurized water plants as well as new PWR concepts. Mr. Ismo Karppinen from VTT was appointed as a member of the project review group by the SAFIR2014 steering group.
- OECD/NEA HYMERES (Hydrogen Mitigation Experiments for Reactor Safety), which ended in December 2016, aimed to improve the understanding of the hydrogen risk phenomenology in containment in order to enhance its modelling in safety assessments. Mr. Ismo Karppinen from VTT was a member of the program review group (PRG). Extension to the programme is being prepared.
- OECD/NEA ATLAS (Advanced Thermal-hydraulic test Loop for Accident Simulation) project continues until March 2017. The project is aimed at topics of high safety relevance for both current and future power plants. Mr. Joonas Kurki from VTT has been appointed as a member of the project review group by the SAFIR2014 steering group.
- OECD/NEA CSNI WGAMA (Working Group on Analysis and Management of Accidents) aims to advance the current understanding of the physical processes related to reactor safety. Mr. Ismo Karppinen from VTT has been appointed as one of the two country representatives of Finland in the task group.
- U.S. NRC CAMP (Code Application and Maintenance Program) is formed to exchange information on thermal-hydraulic safety related issues between U.S. NRC and its international partners. TRACE, PARCS, RELAP5 codes and graphical interface SNAP are made available through this program. Finland is represented in the program by Mr. Seppo Hillberg from VTT.
- FONESYS Network (Forum & Network of System Thermal-Hydraulics Codes in Nuclear Reactor Thermal-Hydraulics) is an international network of system-thermal hydraulic code developers. It has been created to promote the use of system thermal-hydraulic codes and application of Best estimate plus uncertainty approaches, to establish acceptable and recognized procedures and thresholds for verification and validation, and to create a common ground for discussing envisaged improvements in system codes. Among its activities, FONESYS arranges benchmarks for code comparison and verification and provides a channel of discussion for top level experts of the system thermal hydraulic field. VTT has participated in FONESYS since its formation in 2010 as developer of the Apros simulation code.

## References

1. N. Aksan, F. D'Auria, H. Glaeser, R. Pochard, C. Richards and A. Sjöberg. 1993. Separate Effect Test Matrix for Thermal-hydraulic Code Validation, Volume 1, Phenomena Characterisation and Selection of Facilities and Tests. NEA/CSNI/R(93)14/Part.1/Rev., OECD/GD(94)82.
2. N. Aksan, F. D'Auria, H. Glaeser, R. Pochard, C. Richards and A. Sjöberg. 1993. Separate Effect Test Matrix for Thermal-hydraulic Code Validation, Volume 2, Facility and Experiment Characteristics. NEA/CSNI/R(93)14/Part.2/Rev., OECD/GD(94)83.
3. OECD/NEA CSNI. 2014. Containment Code Validation Matrix. NEA/CSNI/R(2014)3.
4. Karppinen, I. 2016. Assessment of Apros thermal hydraulic models with separate effect tests. VTT, Espoo. VTT-R-06020-15
5. Silde, A. 2016. Assessment of Apros containment software. VTT, Espoo. VTT-R-04560-15.

6. Lauerma, S., Skripnikov, D., Hovi, T. 2016. Friction and heat transfer experiment simulations with Apros. VTT, Espoo. VTT-R-06266-15.
7. Leskinen, J. 2017. Assessment of Apros reflow models against the ACHILLES natural reflow experiment. VTT, Espoo. VTT-R-00138-17.
8. Kurki, J. 2017. Simulation of the ISP-7 reflooding experiment with Apros. VTT, Espoo. VTT-R-00359-17.
9. Dorval, E. 2017. A re-evaluation of FLECHT SEASET test 32013 with Apros. VTT-R-03993-16.
10. Karppinen, I., Hillberg, S. 2013. Validation of Apros and TRACE with FLECHT SEASET reflooding experiment. VTT, Espoo. VTT-R-09202-13.
11. Silde, A. 2017. Simulations of wall condensation and sump evaporation TOSQAN test T201 using the Apros containment code. VTT, Espoo. VTT-R-05557-16.
12. Hillberg, S. 2016. Simulation of the ATLAS A5.1 benchmark in blind phase with Apros. VTT, Espoo. VTT-R-06347-15.
13. Hillberg, S. 2016. Simulation of the ATLAS A5.1 SBLOCA benchmark in post-test phase with Apros. VTT, Espoo. VTT-R-02390-16.
14. Hillberg, S. 2016. ATLAS A5.2 IBLOCA pre-test calculation with Apros. VTT, Espoo. VTT-R-03700-16.
15. Kurki, J., Alku, T., Karppinen, I. 2016. Simulation of the FONESYS FO-02 Critical flow benchmark with Apros. VTT, Espoo. VTT-R-06071-15.
16. Hillberg, S. 2017. Simulation of the extended FONESYS FO-02 critical flow benchmark with Apros. VTT, Espoo. VTT-R-00034-17
17. Kolehmainen, J. 2015. Simulation of the HYMERES MISTRA HM 2-1 and HM 3-2 experiments with containment package of Apros 5.14.09. VTT, Espoo. VTT-R-05463-15.
18. Kolehmainen, J. HYMERES HP6 scoping calculations with Apros 6.05. VTT, Espoo. VTT-R-04125-16.
19. OECD/NEA. 2016. NEA Hydrogen Mitigation Experiments for Reactor Safety (HYMERES) Project. Retrieved from <https://www.oecd-nea.org/jointproj/hymeres.html>.
20. Paladino, D., Mignot, G., Kapulla, R., Parenjape, S., Andreani, M., Studer, E., Brinster, J., Dabbene, F. OECD/NEA HYMERES Project: For the Analysis and Mitigation of a Severe Accident Leading to Hydrogen Release Into a Nuclear Plant Containment. Proceedings of ICAPP 2014, paper 14322.
21. Kolehmainen, J. 2015. Simulation of the Hymeres MISTRA HM2-1 experiment with containment package of Apros. VTT, Espoo. VTT-R-00404-15.

## 5.2 Couplings and instabilities in reactor systems (INSTAB)

Markku Puustinen, Jani Laine, Antti Räsänen, Lauri Pyy, Vesa Tanskanen, Elina Hujala, Eetu Kotro, Giteshkumar Patel

Lappeenranta University of Technology  
School of Energy Systems  
Nuclear Engineering  
P.O. Box 20, FI-53851 Lappeenranta

### Abstract

In the INSTAB project, mechanisms and efficiency of mixing with different subsystems in the suppression pool have been investigated experimentally in the PPOOLEX facility. Tests with a model of a safety relief valve sparger verified that mixing of a thermally stratified water pool can happen also through an erosion process in addition to internal circulation, if suitable flow conditions prevail. Tests with a model of a residual heat removal system nozzle indicated that orientation of the nozzle plays an important role in the success of the mixing process of a thermally stratified pool. The nozzle injection flow rate, injection water temperature and  $\Delta T$  in the pool have an effect on the mixing process but that effect is not as dominant as of the nozzle orientation. Preliminary wetwell spray tests in PPOOLEX revealed that mixing of a thermally stratified pool with the help of spray injection from above could be possible. The Effective Momentum Source and Effective Heat Source models, developed and implemented to the GOTHIC code by KTH, have been validated for blowdown pipes, SRV spargers and RHR nozzles largely on the basis of the experiment results obtained in the INSTAB project at LUT. In the CFD simulation exercises of steam injection through a blowdown pipe into a suppression pool, done in the INSTAB project, it has been found out that CFD modelling of a pressurizing two-compartment suppression pool requires that the interfacial area density between the liquid and vapour phases is resolved either by using a very dense computational grid or by applying a special interfacial instability model. In addition, OpenFOAM models for the simulation of direct contact condensation phenomenon have been developed and validated against the INSTAB experiment results at LUT and VTT.

### Introduction

BWR containment is a complex system that includes such typical elements as a pressure suppression pool (PSP), spray and containment venting systems for containment pressure control, blowdown pipes for rapid steam condensation in case of LOCA, spargers for the pressure vessel safety relief valves (SRV), strainers for water supply to emergency core cooling (ECC) and spray systems, nozzles and strainers of the residual heat removal (RHR) system, vacuum breakers, etc. There are several scenarios of safety importance where containment pressure suppression function and pressure suppression pool operation are affected by (i) stratification and mixing phenomena, (ii) interactions with emergency core cooling system, spray, residual heat removal and filtered containment venting (FCV) systems, (iii) overall water balance in the containment compartments, and (iv) interplay between pool behaviour, diagnostics and procedures. Those scenarios include, for example, different LOCAs (steam line break inside the radiation shield, broken blowdown pipes, leaking safety relief valves), station blackouts and severe accidents. There is a need for validated tools for simulation of realistic accident scenarios with interplay between phenomena, safety systems, operational procedures, and overall containment performance.

The INSTAB project aims to increase understanding of the phenomena related to BWR pressure suppression function to enhance capabilities to analyse Nordic BWR containments under transient and acci-

dent conditions. Information is gathered particularly on the effects of the SRV spargers, RHR nozzles and blowdown pipes on mixing and stratification of the wetwell pool as well as on feedbacks between the wetwell water pool and spray operation.

To achieve the objectives a combined experimental/analytical/computational program is being carried out. With experiments on pool operation related phenomena in the PPOOLEX test facility a database for the development, improvement and validation of numerical simulation models will be generated. Sophisticated, high frequency measurement instrumentation, high-speed video cameras and a PIV system are used in order to get detailed enough data from the experiments.

The Effective Heat Source (EHS) and Effective Momentum Source (EMS) models for steam injection through blowdown pipes have been successfully developed, validated and implemented to the GOTHIC code by KTH with the help of the experiment results of the previous SAFIR and NKS projects [Li et al., Villanueva et al.]. The experiments being carried out in the INSTAB project and complementary CFD simulations at VTT in the NURESA project will help further extend the concepts of the EHS and EMS models to spargers, RHR system nozzles and containment sprays.

Recent and ongoing work on CFD code and model development and increased computational capacity make the simulations of earlier direct contact condensation (DCC) experiments in the PPOOLEX facility appealing i.e. expected simulation results would at least qualitatively mimic the experimental reality [Tanskanen et al., 2014]. CFD simulations and other emerged analysis methods, such as utilization of pattern recognition algorithms, can also help to understand the experimental results more profoundly. The extensive database gathered in the previous PPOOLEX studies of steam discharge into a pool of sub-cooled water is therefore exploited in the assessment of the capability of CFD codes to simulate direct contact condensation situations.

Networking among international research organizations has been enhanced via participation in the NORTHNET framework and the NKS/COPSAR project. Analytical and numerical work at KTH is combined to the INSTAB and NURESA projects of SAFIR2018. Furthermore, PPOOLEX data on DCC from the INSTAB project is used in the validation of an OpenFOAM-solver at VTT.

## **PPOOLEX test facility**

The PPOOLEX facility, a model of BWR containment, is used in most of the thermal hydraulic experiments carried out in the INSTAB project [Puustinen et al. 2006]. The facility consists of a wetwell compartment (condensation pool), drywell compartment, inlet plenum and steam line piping. An intermediate floor separates the compartments from each other but a route for gas/steam flow from the drywell to the wetwell is created by a vertical blowdown pipe attached underneath the floor. In recent experiments with the sparger pipe the drywell compartment has been bypassed by connecting the steam line directly to the upper end of the sparger pipe.

The main component of the facility is the ~31 m<sup>3</sup> cylindrical test vessel, 7.45 m in height and 2.4 m in diameter. The test facility is able to withstand considerable structural loads caused by rapid condensation of steam. The removable vessel head and a man hole in the wetwell compartment wall provide access to the interior of the vessel for maintenance and modifications of internals and instrumentation. The drywell is thermally insulated. A sketch of the test vessel is shown in Figure 1. Steam needed in the experiments is produced with the nearby PACTEL test facility, which has a core section with 1 MW heating power and three horizontal steam generators [Tuunanen et al.]. Steam is led through a thermally insulated steam line from the PACTEL steam generators to the PPOOLEX test vessel.

The applied instrumentation depends on the experiments in question. Normally, the test facility is equipped with several thermocouples for measuring steam, pool water and structural temperatures and with pressure transducers for observing pressures in the drywell, inside the blowdown pipes, at the condensation pool bottom and in the gas phase of the wetwell. Steam flow rate is measured with a vortex flow meter in the steam line. Additional instrumentation includes, for example, strain gauges on the pool outer wall and valve position sensors. A Particle Image Velocimetry system and up-to-date high speed cameras

also belong to the set-up. National Instruments PXIe PC-driven measurement system is used for data acquisition. The system enables high-speed multi-channel measurements.

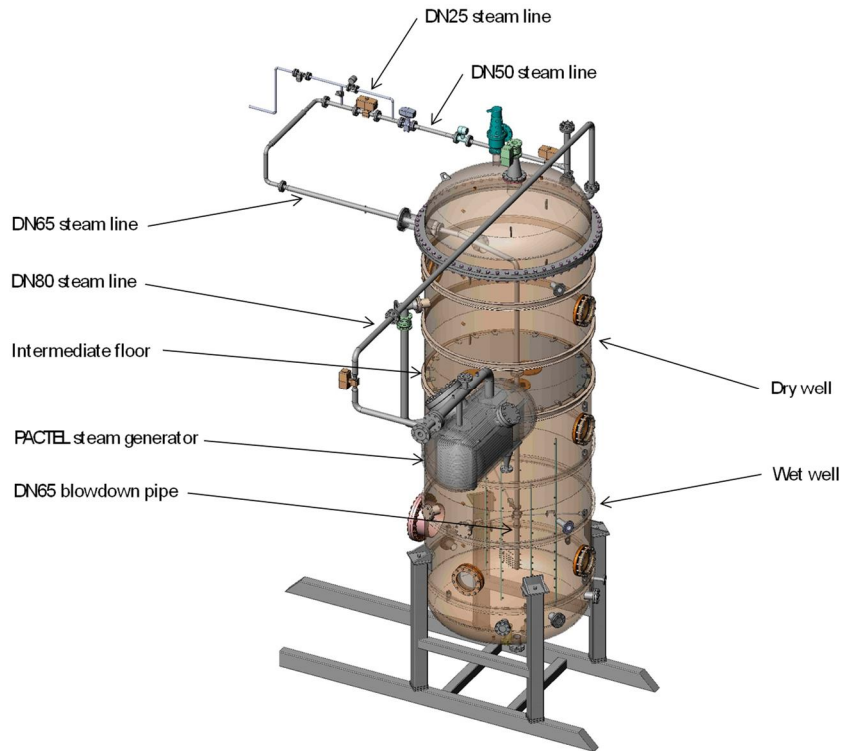


**Figure 1.** PPOOLEX test facility.

## Tests with SRV sparger on mixing and behaviour of thermocline

SRV sparger tests on the mixing phenomenon and on the behaviour of a thermocline were carried out in the PPOOLEX test facility in 2015 and 2016 to obtain additional data for the development of the Effective Momentum Source and Effective Heat Source models to be implemented in the GOTHIC code by KTH which plans to extend the models to cover also situations where steam injection into the pool is via a sparger pipe [Puustinen et al.2016, Puustinen et al.2017a]. The test parameters were selected by KTH on the basis of pre-test simulations and analysis of the results of the earlier SRV sparger tests in PPOOLEX.

As opposed to the earlier tests with the sparger pipe in PPOOLEX only one row of horizontally oriented injection holes at the sparger head or the eight vertically downwards oriented holes of the load reduction ring (LRR) were used for steam injection in the 2015 tests. The used steam mass flow rates were such that steam flowed through the injection holes as small jets and condensed mainly outside the sparger pipe. Because no chugging kind of phenomenon existed and the steam jets were too weak to create much turbulence in the pool, suitable conditions for thermal stratification to occur prevailed. The transition region, where the shift from cold to warm pool water occurred, was practically just below the sparger elevation when steam injection was through the sparger head. When the steam injection was vertically downwards from the load reduction ring the transition region was deeper in the pool.

Complete mixing was achieved with both tested cases. Figure 2 shows the progression of mixing in the pool water when injection direction was downwards from the load reduction ring of the sparger. In the earlier tests with all the 32 injection holes of the sparger head unblocked a considerably larger steam flow rate was not enough to mix the pool. Then the flow mode was different and not enough momentum and internal circulation were created for complete mixing to happen. Mixing was observed only above and a short distance below the sparger head outlet elevation.

These additional sparger tests in the PPOOLEX facility verified that the existing flow mode of injected steam is a crucial factor in the success of the mixing process of a thermally stratified water pool. Mixing with a larger absolute flow rate can be less successful than with a smaller flow rate if the flow mode after dividing the flow to smaller jets in a sparger head holes is such that not enough momentum and internal circulation is created in the pool for complete mixing to take place.

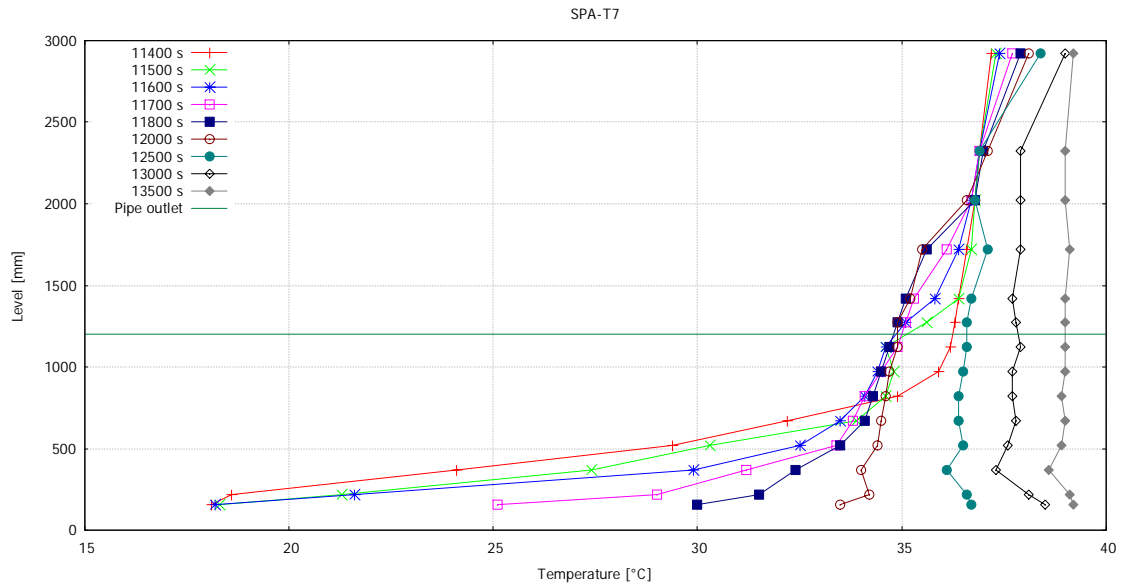


**Figure 2.** Progression of mixing in pool water when injection direction is downwards from the load reduction ring of the sparger.

In the 2016 experiment series, the first test was done with all the 32 injection holes at the sparger head open whereas the second one was done with only the eight holes in the bottom row open. Particularly the behaviour of the thermocline between the cold and warm water volumes and the progression of the erosion process was of interest. For this purpose also PIV measurements were tried during the tests.

In both tests the initial uniform temperature profile first changed to a stratified situation and eventually back to a uniform and mixed situation. Along the tests the thermocline moved downwards. Elevation of the thermocline at the end of the stratification phase was predicted well in the pre-test simulations with GOTHIC by KTH when all the injection holes of the sparger head were open. However, the thickness of the thermocline was larger than expected. Complete mixing of the water pool through an erosion process was achieved with quite a small steam mass flow rate in the test with most of the injection holes blocked (Figure 3).

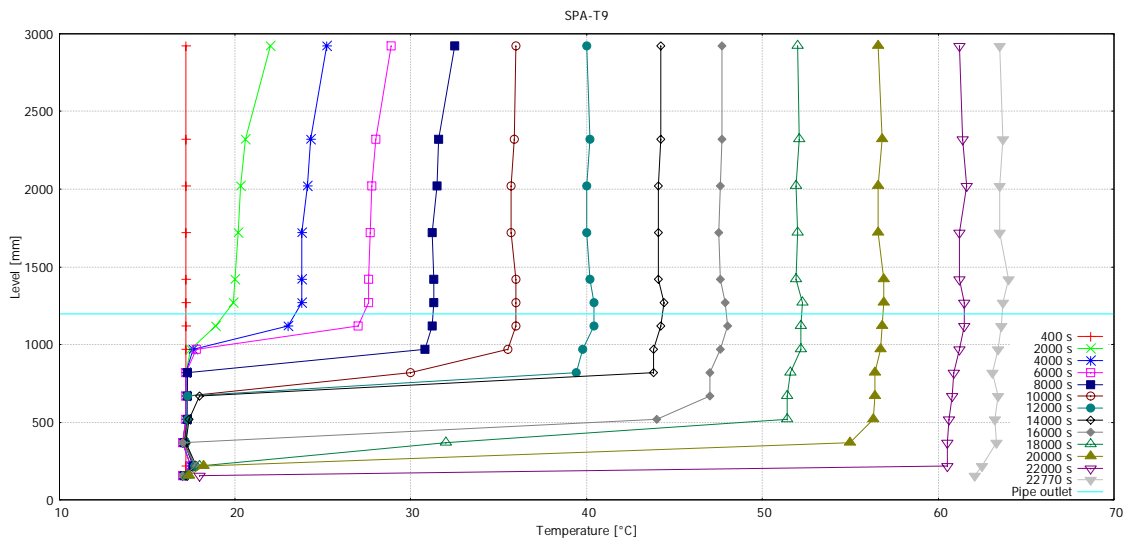


**Figure 3.** Development of vertical temperature profile of pool water in a test with part of the injection holes blocked.

The few sequences with recognized flow patterns from the PIV measurements of the 2016 tests with the SRV sparger indicate that some kind of swirls could exist around the elevation of the thermocline. The flow direction just under the thermocline can also be opposite to that just above the thermocline. Figure 4 shows a velocity vector field averaged over such a 5.7 second time period where the flow patterns were constant enough for the PIV measurement to succeed. Generally, the somewhat chaotic nature of the investigated phenomenon created problems when measuring with a slow-speed PIV system and therefore definitive conclusions on the detailed behaviour of the flow fields in the vicinity of the thermocline can't be made.

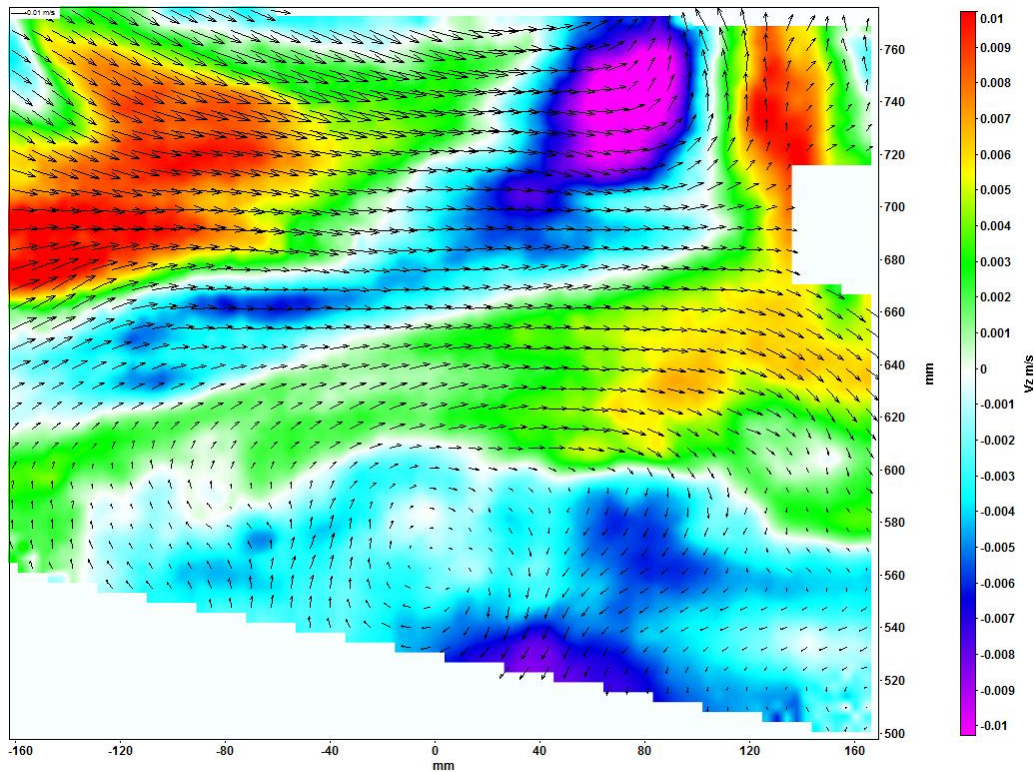


**Figure 4.** Averaged velocity vector field over a 5.7 second time period from the vicinity of the thermocline.

The mixing mechanism in the SRV sparger tests in 2016 was somewhat different than in many previous tests done in the PPOOLEX facility either with a straight blowdown pipe or with a sparger pipe. Now, the layers of cold water slowly eroded rather than mixed through internal circulation as has been the case in most of the tests carried out before. As a result, the thermocline region shifted slowly downwards as the mixing process proceeded. These tests in PPOOLEX verified that mixing of a thermally stratified water pool can happen through an erosion process instead of internal circulation if suitable flow conditions in the pool created by steam jets at the injection holes of the sparger prevail.

### Mixing tests with a RHR nozzle

A series of residual heat removal system nozzle tests were carried out in the PPOOLEX facility at LUT in 2016 [Puustinen et al. 2017b]. For the tests the PPOOLEX facility was equipped with a model of a RHR nozzle on the basis of suggestions from KTH. To keep the manufacturing process as simple as possible it was decided that standard pipe parts will be used. Therefore the RHR nozzle in PPOOLEX differs somewhat from the original proposal. Figure 5 presents the proposal from KTH and the final construction of the nozzle installed to PPOOLEX in its vertical position. Both vertical and horizontal position of the nozzle were used in the RHR nozzle tests in PPOOLEX.

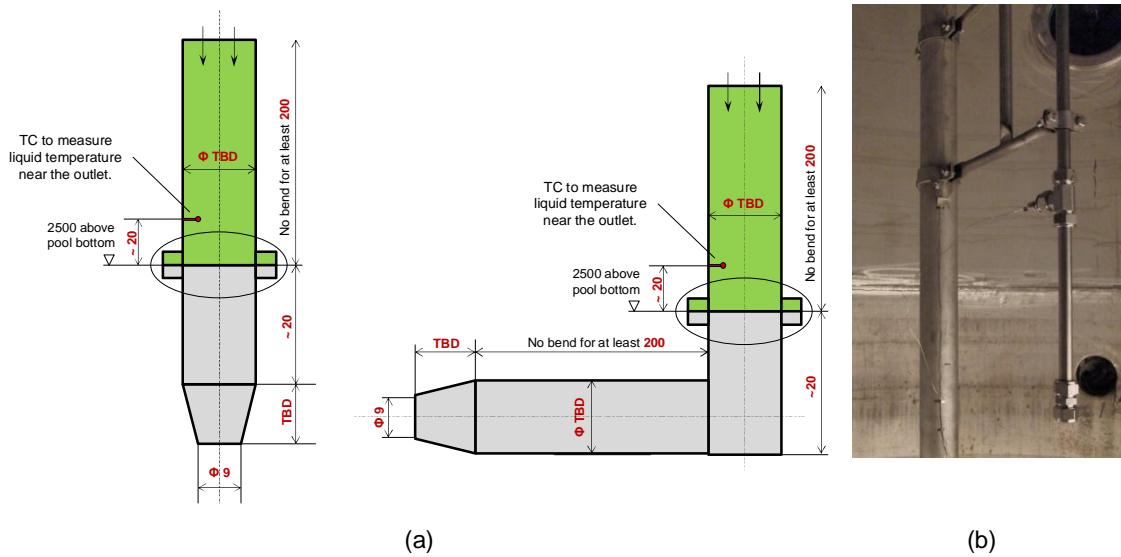


**Figure 5.** (a) Proposal for a RHR nozzle from KTH. (b) Final construction of the nozzle.

The main purpose of the tests was to obtain additional data for extending the EMS and EHS models to RHR system nozzles. Mixing of a thermally stratified pool with the help of water injection through a RHR nozzle was of special interest. Particularly the effects of nozzle orientation,  $\Delta T$  in the pool, injection water temperature and injection water mass flow rate were studied.

The detailed test specifications were put together and the test parameters were selected on the basis of pre-test simulations with GOTHIC code by KTH. Two stratification and two mixing phases were included. Thermally stratified condition was created by injecting steam into the pool water via the sparger pipe.

During the stratification phases two regions with clearly different water temperatures and a narrow thermocline region between them developed in the pool. The mixing process was initiated when the target temperature difference between the bottom and the top layer of the pool had been reached.

With the vertical orientation of the RHR nozzle mixing was otherwise successful but incomplete above the nozzle elevation (Figure 6). Complete mixing was achieved with the horizontal orientation of the RHR nozzle.

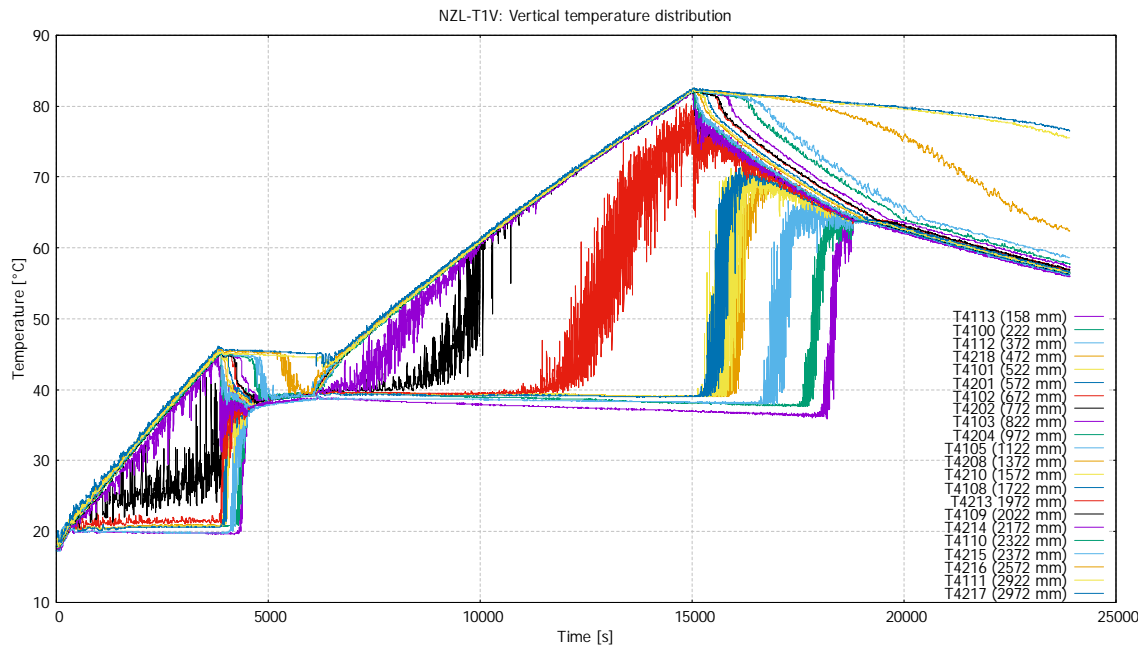


**Figure 6.** Incomplete mixing in wetwell pool above RHR nozzle elevation with nozzle in vertical position.

### Spray tests

The shadowgraphy application of the PIV measurement system was used to test single spray nozzles in a testing station specifically built for this purpose at LUT [Pyy 2016]. The main objective was to get experience from the use of the shadowgraphy application in order to be able to evaluate its suitability for demanding measurements of different characteristics of spray nozzles.

Five different measurement positions were selected underneath of the spray jet to be used in the tests. The interest was to find out if it has any effect on the droplet size distribution when the measurement area is shifted vertically and horizontally. In the three centreline positions the droplet size distributions looked alike. The majority of the droplets were in the size range of 0.2-0.8 mm whereas the droplet distribution was broader in the two other positions, which were 300 mm away of the centreline axis. Figure 7 shows the droplet size distributions in all measurement positions in the single spray nozzle tests.

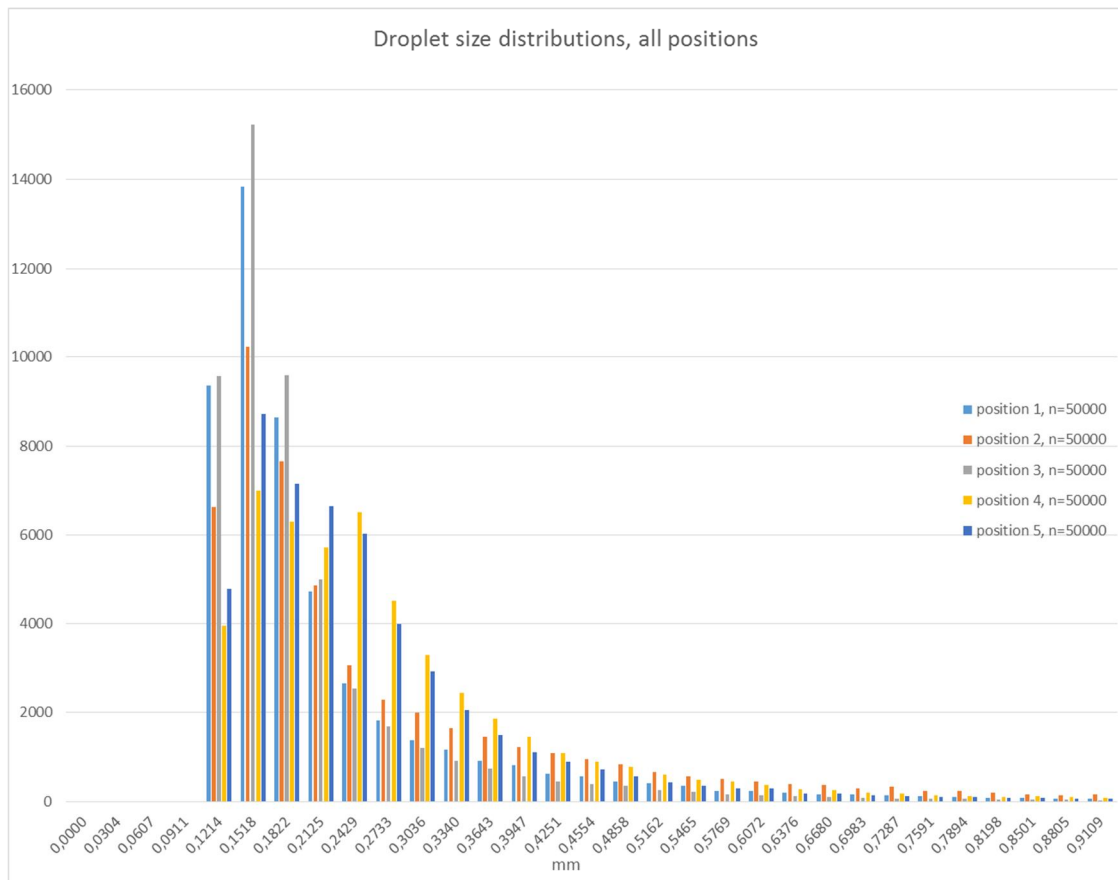


**Figure 7.** Droplet size distributions in all measurement positions in the single spray nozzle tests.

There are many user-defined parameters in the shadowgraphy application which are used for processing of the particle images. The selection of these parameters has a strong effect on the measurement results and therefore emphasis should be put to making the experimental arrangement as simple as possible.

The measured droplet size distributions revealed that the scaling factor of the used application was too large for these tests in order to get a full range of different droplet sizes. In future spray nozzle tests the camera of the PIV system should always be placed as close to the measurement area as possible in order to get the scaling factor to be as small as possible.

A four nozzle spray system was installed to the PPOOLEX facility and three preliminary spray injection tests, where mixing of a stratified pool by spray injection from above was studied, were carried out [Puustinen et al. 2017c]. It has been suggested that mixing induced by spray had a role in the pressure drop in Fukushima Unit 3 where pressure build-up in the containment during the first 20 hours after station blackout was attributed to stratification in the pool. Furthermore, the results of these preliminary and forthcoming spray tests in PPOOLEX are aimed to be used for improving simulation models in CFD and system codes.

The same kind of full cone spray nozzles, which were tested in a separate testing station with the shadowgraphy application, were used in the PPOOLEX spray tests. These preliminary spray tests indicate that it might be possible to mix a stratified pool with the help of spray injection from above. If spray injection was continued long enough internal circulation developed and finally mixed the pool. Figure 8 shows the development of the stratified situation until 13400 s into the experiment and then the mixing period until complete mixing. The used spray flow rate was about 32 l/min for each spray nozzle and the temperature of spray water about 10 °C.

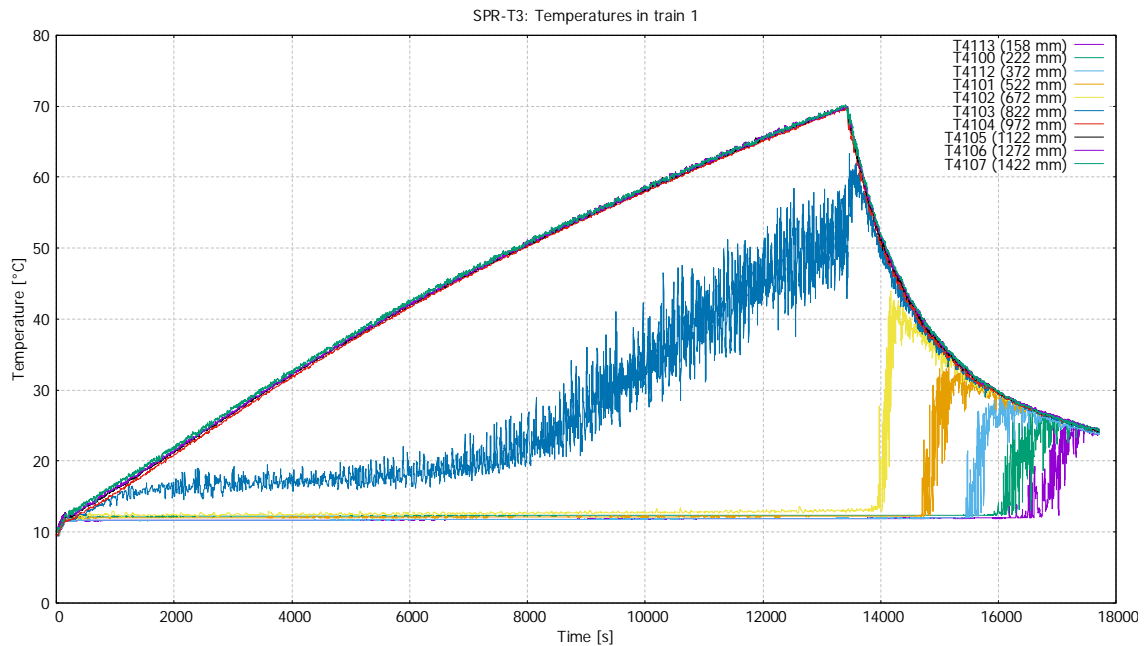


**Figure 8.** Mixing of a thermally stratified pool with the help of spray injection from above.

### CFD calculations of earlier tests

CFD modelling of pressurizing two-compartment suppression pool requires that the interfacial area density between the liquid and vapour phases is resolved either by using a very dense computational grid or by applying a special interfacial instability model. To solve the problem interfacial area density modelling has been addressed by including the effect of interfacial instabilities e.g. Rayleigh-Taylor instability to the NEPTUNE\_CFD code. A plausible and simple solution for addressing interfacial area density modelling was introduced in the NURETH-16 conference by Pellegrini et al. Implementation of the model to the NEPTUNE\_CFD code has been done and it seems to perform qualitatively well enough [Tanskanen et al. 2016, Patel et al. 2016].

Simulations of a plexiglass blowdown pipe case in PPOOLEX have been done in order to investigate the effect of the RTI model on calculation results of direct contact condensation [Tanskanen 2017]. The transparent plexiglass blowdown pipes allowed the visual observation of chugging inside the blowdown pipes. Low thermal conductivity of plexiglass made it possible to exclude the effect of wall condensation as well. The condensation rate was lower and qualitative characteristics of condensing bubbles were different in the case without the Rayleigh-Taylor instability model compared to the case with it (Figure 9).

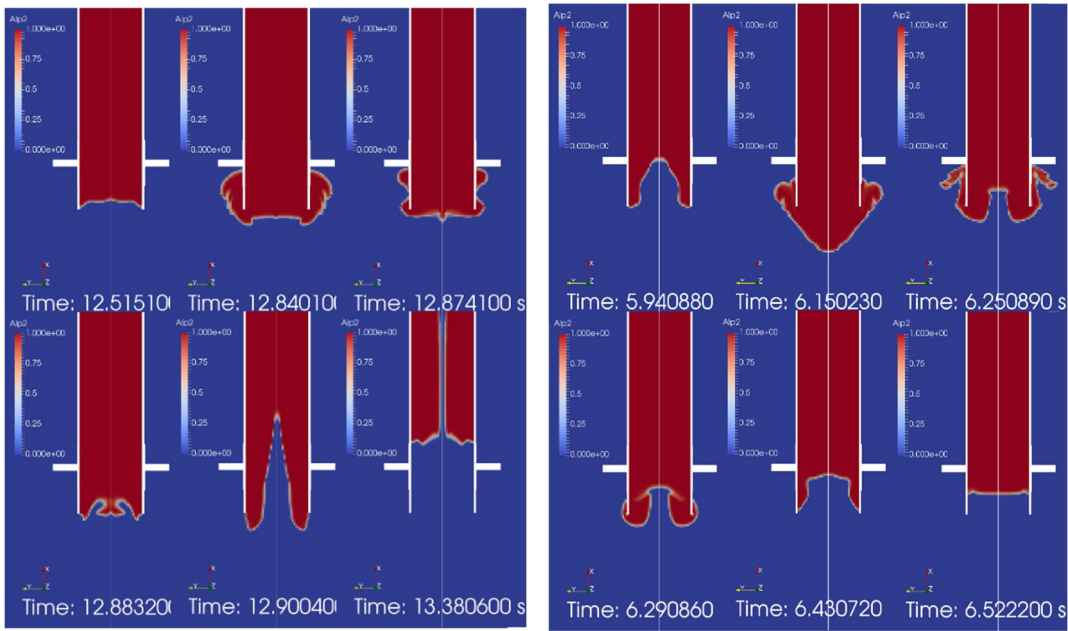


**Figure 9.** Volume fraction fields from NEPTUNE\_CFD simulation of the transparent pipe test with the Rayleigh-Taylor instability model on (left) and off (right).

The pressure data from selected earlier PPOOLEX tests have been analysed [Tanskanen 2017]. The chugging frequencies from different pressure transducers were evaluated by using fast Fourier transform (FFT) and compared to the bubble oscillation results of the NEPTUNE\_CFD simulations. It is possible to sort out different frequencies caused by the blowdown pipe, test vessel and bubbles from the FFTs. Figure 10 shows the results of FFT from the pressure transducer close to the blowdown pipe outlet. The most probably frequencies and corresponding sources are presented in Table 1.

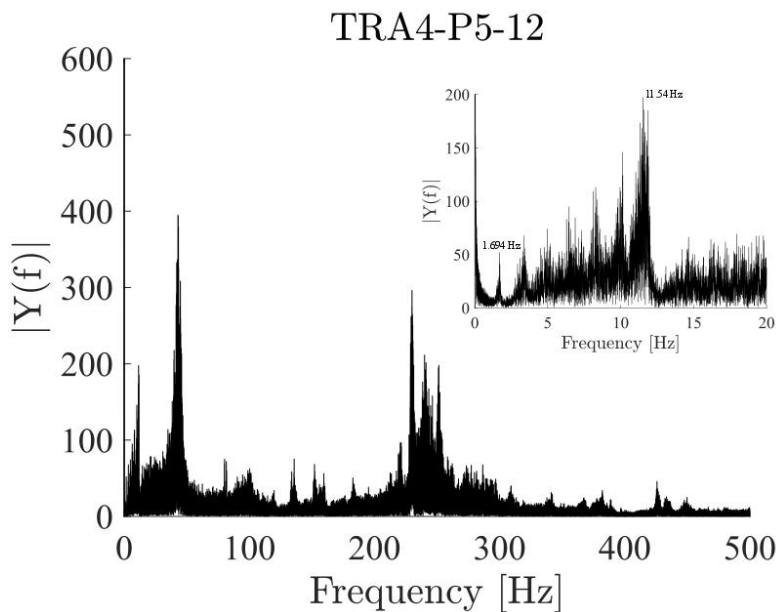


**Figure 10.** FFT of pressure transducer at the blowdown pipe outlet from a PPOOLEX test with a transparent blowdown pipe.

**Table 1.** Frequencies in FFT of a PPOOLEX test with a transparent blowdown pipe and their probable sources

Frequency in FFT [Hz]	Possible source of frequency
0.5–3.5	chugging frequency
11–12	vessel
41–45	natural frequency of the bubble
80–83	vessel
150	vessel
250–300	bubble/blowdown pipe

## Conclusions

Thermal hydraulic tests in the INSTAB project have focused on generating a large database on suppression pool phenomena to be used for the validation of CFD and system codes used for safety analysis of nuclear power plants. The results of the tests on the efficiency of mixing of a thermally stratified pool have been utilized particularly in the development work of the EMS and EHS models for blowdown pipes, SRV spargers and RHR nozzles by KTH. These models are being implemented to the GOTHIC code but they will be available to users of other codes as well. The tests with a model of a SRV sparger in the PPOOLEX facility verified that mixing of a thermally stratified water pool can happen also through an erosion process in addition to internal circulation, if suitable flow conditions prevail. Additional tests, particularly with a planned separate effects test facility on sparger behaviour, are needed to provide closures for the EMS/EHS model development work for spargers. The tests with a model of a RHR system nozzle indicated that orientation of the nozzle plays an important role in the success of the mixing process of a thermally stratified pool. Preliminary wetwell spray tests in the PPOOLEX facility revealed that mixing of a thermally stratified pool with the help of spray injection from above could be possible. In future spray tests in PPOOLEX the validity of this finding will be checked in more detail.

In the CFD simulation exercises of steam injection through a blowdown pipe into a suppression pool it has been found out that CFD modelling of a pressurizing two-compartment suppression pool requires that the interfacial area density between the liquid and vapour phases is resolved either by using a very dense computational grid or by applying a special interfacial instability model. The problem with interfacial area density modelling was addressed by including the effect of interfacial instabilities e.g. Rayleigh-Taylor instability to the NEPTUNE\_CFD code. Simulations of a plexiglass blowdown pipe case indicated that the condensation rate was lower and qualitative characteristics of condensing bubbles were different in the case without the Rayleigh-Taylor instability model compared to the case with it. In addition, OpenFOAM models for the simulation of direct contact condensation phenomenon have been developed and validated against the INSTAB experiment results at LUT and VTT.

Recent and ongoing work on CFD code and model development and increased computational capacity make the simulations of earlier DCC experiments in the PPOOLEX facility appealing. CFD simulations and other emerged analysis methods, such as utilization of pattern recognition algorithms, could also help to understand the experimental results more profoundly. The goal is to exploit the extensive database gathered in the previous PPOOLEX studies of steam discharge into a pool of sub-cooled water in the assessment of the capability of CFD codes to simulate direct contact condensation situations.

## References

- Li, H., Villanueva, W., Puustinen, M., Laine, J., Kudinov, P. 2014. Validation of effective models for simulation of thermal stratification and mixing induced by steam injection into a large pool of water. *Science and Technology of Nuclear Installations* (Volume 2014), Article ID 752597.
- Patel, G., Tanskanen, V., Hujala, E., Hyvärinen, J. 2016. Direct contact condensation modeling in pressure suppression system. *Nuclear Engineering and Design*. Available online 13 September 2016. <http://dx.doi.org/10.1016/j.nucengdes.2016.08.026>.
- Puustinen, M., Partanen, H., Räsänen, A., Purhonen, H. 2007. PPOOLEX Facility Description. Lappeenranta: Lappeenranta University of Technology. Technical Report PPOOLEX 3/2006.
- Puustinen, M., Laine, J., Räsänen, A. 2016. Additional Sparger Tests in PPOOLEX with Reduced Number of Injection Holes. Lappeenranta: Lappeenranta University of Technology. School of Energy Systems. Nuclear Engineering. Research Report INSTAB 1/2015.
- Puustinen, M., Pyy, L., Laine, J., Räsänen, A. 2017a. Sparger Tests in PPOOLEX on the Behaviour of Thermocline. Lappeenranta: Lappeenranta University of Technology. School of Energy Systems. Nuclear Engineering. Research Report INSTAB 1/2016.
- Puustinen, M., Laine, J., Räsänen, A., Kotro, E. 2017b. Mixing Tests with a RHR Nozzle in PPOOLEX. Lappeenranta: Lappeenranta University of Technology. School of Energy Systems. Nuclear Engineering. Research Report INSTAB 2/2016.
- Puustinen, M., Laine, J., Räsänen, A., Kotro, E. 2017c. Preliminary Spray Tests in PPOOLEX. Lappeenranta: Lappeenranta University of Technology. School of Energy Systems. Nuclear Engineering. Research Report INSTAB 3/2016.
- Pyy, L. 2016. Single Nozzle Spray Tests. Lappeenranta: Lappeenranta University of Technology. School of Energy Systems. Nuclear Engineering. Research Report INSTAB 2/2015.
- Tanskanen, V., Jordan A., Puustinen M., Kyrki-Rajamäki R. 2014. CFD simulation and pattern recognition analysis of the chugging condensation regime. *Annals of Nuclear Energy* Vol. 66 (2014), pp. 133-143. <http://dx.doi.org/10.1016/j.anucene.2013.12.007>.
- Tanskanen, V., Hujala, E., Puustinen, M. 2016. Numerical Simulation of a PPOOLEX Chugging Case with a Rayleigh-Taylor Instability Model for Interfacial Area. Lappeenranta: Lappeenranta University of Technology. School of Energy Systems. Nuclear Engineering. Research Report INSTAB 4/2015.
- Tanskanen, V., Hujala, E., Patel, G. 2017. Simulation and Analysis of PPOOLEX Chugging Cases: Plexiglass Blowdown Pipe. Lappeenranta: Lappeenranta University of Technology. School of Energy Systems. Nuclear Engineering. Research Report INSTAB 4/2016.
- Tuunanen, J., Kouhia, J., Purhonen, H., Riikonen, V., Puustinen, M., Semken, R. S., Partanen, H., Saure, I. & Pylkkö, H. 1998. General Description of the PACTEL Test Facility. Espoo: VTT. VTT Research Notes 1929. ISBN 951-38-5338-1.
- Villanueva, W., Li, H., Puustinen, M., Kudinov, P. 2015. Generalization of experimental data on amplitude and frequency of oscillations induced by steam injection into a subcooled pool. *Nuclear Engineering and Design* 295 (2015), pp. 155-161. <http://dx.doi.org/10.1016/j.nucengdes.2015.08.031>.

### 5.3 Integral and separate effects tests on thermal-hydraulic problems in reactors (INTEGRA)

Vesa Riikonen, Virpi Kouhia, Otso-Pekka Kauppinen, Joonas Telkkä

Lappeenranta University of Technology  
P.O. Box 20, FI-53851 Lappeenranta, Finland

#### Abstract

The objective of the project is to improve the understanding of thermal-hydraulic system behaviour by performing integral and separate effects tests, in particular regarding the impact of non-condensable gases on core cooling /1/ and reliability of natural circulation loop decay heat removal. Carefully designed experiments are the most reliable way to obtain fundamental understanding and reliable data of the phenomena. This data will be used in the development and validation of computer codes for the safety analyses of nuclear power plants. Performing experiments not only requires the hardware and programs controlling the devices and gathering data, but also the knowledge of the system behaviour. Computer analyses with system and CFD codes are needed in the planning of the experiments as well as in post analyses to help understanding the physics in the experiments /2/, /3/, /4/.

#### Introduction

A part of the international efforts in enhancing the reactor safety is the OECD projects. Finland participates in several of such projects and has also provided test data to the OECD/NEA PKL Phase 3 project (PKL-3) /5/, /6/, /7/, /8/. The most of the OECD countries using nuclear power were participating the project, which was set to investigate safety issues related to beyond design basis accident transients with significant core heat-up, i.e. station blackout scenarios or loss-of-coolant accidents (LOCA) in connection with a failure of safety systems. The OECD/NEA PKL Phase 3 project ended in April 2016. The new OECD/NEA PKL Phase 4 project began in 2016 and Finland is also participating it with two PWR PACTEL /9/ experiments.

Non-condensable gases, if present in the reactor cooling system, affect the functioning of many safety systems in a nuclear power plant. Nitrogen can temporarily increase the water level in the core by a piston effect. The piston effect has been studied with the UPTF and BETHSY test facilities. In UPTF the pressure rise in the loop was observed, but the impact on the core cooling could not be assessed due to the restrictions of the facility. Tests with the BETHSY facility confirmed the potentially significant impact of nitrogen gas injection from the accumulators on the core cooling in a large break LOCA. In the INTEGRA project the effect of nitrogen in LOCA situations was studied experimentally with the PWR PACTEL facility /1/. In these tests with PWR PACTEL the safety functions were the accumulator injection, secondary side depressurization, and core power reduction. Four of these tests included the accumulator injection to a cold leg like in the EPR and two to the upper plenum as in the VVER and AES type power plants. The experiments complement needs to have experiment data for code validation.

Many currently marketed LWR designs feature varying numbers of naturally circulating decay heat removal loops. Large diversity of design configurations is available. A review on passive heat removal system characteristics was written in LUT /10/. An open natural circulation type heat removal system was selected to be studied experimentally with a new facility that is now under a design phase /11/. The reference system for this facility is the containment passive heat removal system designed for the AES-2006 type power plant.

## PWR PACTEL nitrogen experiments

Non-condensable gases, if present in the reactor cooling system, affect the functioning of many safety systems in a nuclear power plant. The driving force of the accumulator injection is the pressurized nitrogen volume at the top of the accumulator tanks. The release of nitrogen to the primary side is either prevented with some system or nitrogen is let to flow to the reactor cooling system when the accumulators are empty of water. Nitrogen can temporarily increase the water level in the core by the piston effect (Figure 1).

The effect of nitrogen in LOCA situations was studied experimentally /1/ with the PWR PACTEL facility. The main goal was to independently verify whether the claimed positive effect of nitrogen on the core cooling can be reproduced and to generate data for the development and validation of thermal-hydraulic system codes.

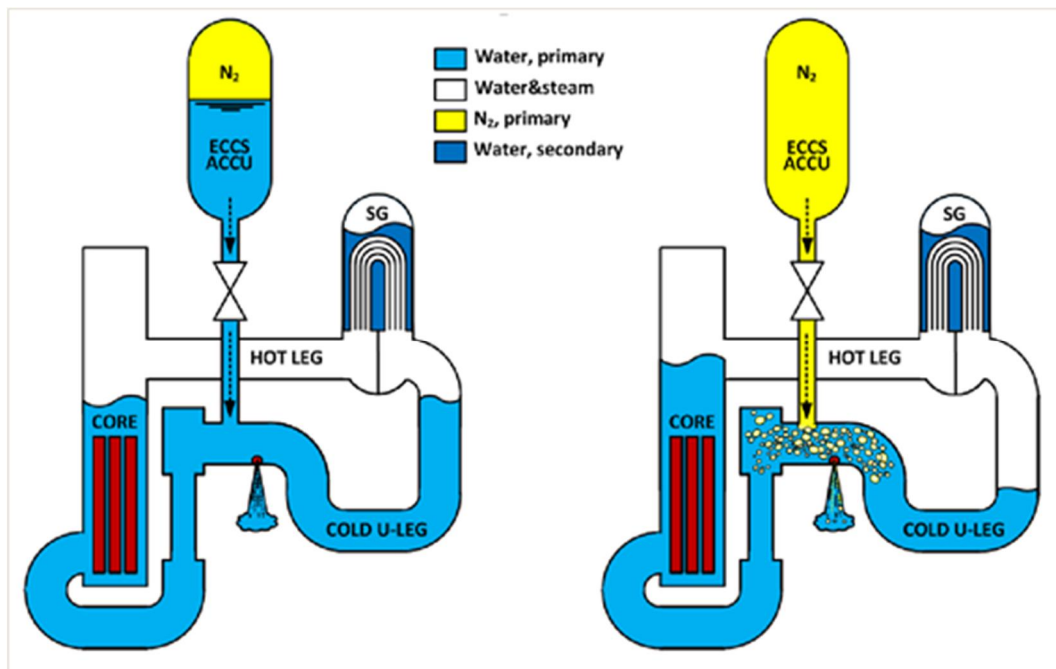


**Figure 1.** Anticipated behaviour of the reactor cooling system during LOCA when nitrogen injection from the accumulator is possible.

The series of the nitrogen experiments (NCG) included six experiments. Three of them were reference experiments where nitrogen was not released to the primary system. In four experiments the accumulator injection was located in a cold leg as in the EPR power plant. In two of those four experiments, the break location was in a cold leg and in the others in a hot leg. In the last two experiments the accumulator injection location was in the upper plenum like in VVER and AES type power plants and the break location was in a cold leg. Table 1 presents the characteristics in each experiment.

**Table 1.** The experiment characteristics in the PWR PACTEL nitrogen experiments.

EXPERIMENT	NCG-10	NCG-11	NCG-12	NCG-13	NCG-14	NCG-15
Accumulator injection	CL1	CL1	CL1	CL1	UP	UP
Break location	CL2	CL2	HL2	HL2	CL2	CL2
Reference experiment - no nitrogen injection	X		X		X	

A connection line between the downcomer top part and the upper plenum was constructed into the PWR PACTEL facility to present the bypass line available in the EPR type power plant. This connection line was set open in the first four experiments. As this type connection line is not present in a VVER type power plant, the bypass line valve was set closed in the last two experiments.

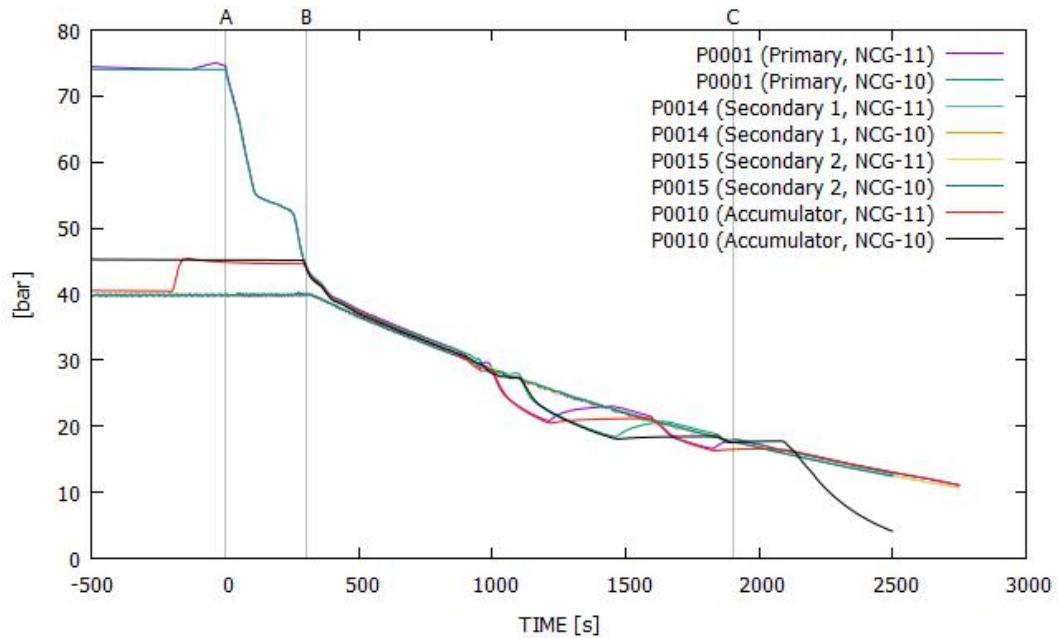


**Figure 2.** Primary and secondary side pressures in the NCG-10 and NCG-11 experiments. In the NCG-10 experiment the accumulator pressure was released to the atmosphere after the water injection ended.<sup>4</sup>

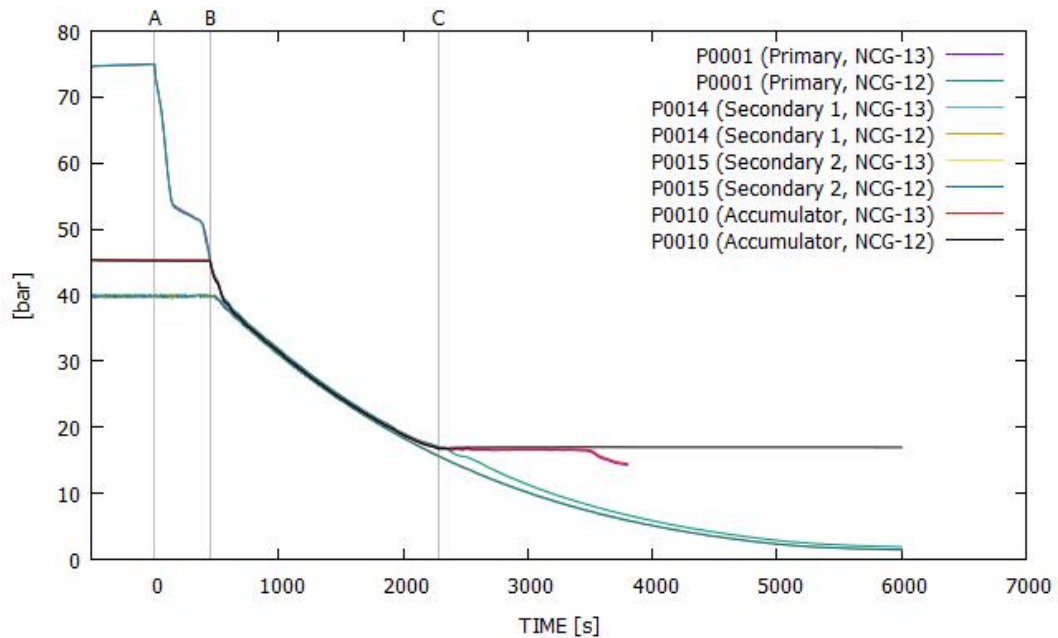


**Figure 3.** Primary and secondary side pressures in the NCG-12 and NCG-13 experiments.<sup>1</sup>

<sup>4</sup> A: break opens, B: accumulator water injection begins, C: accumulator water injection ends.

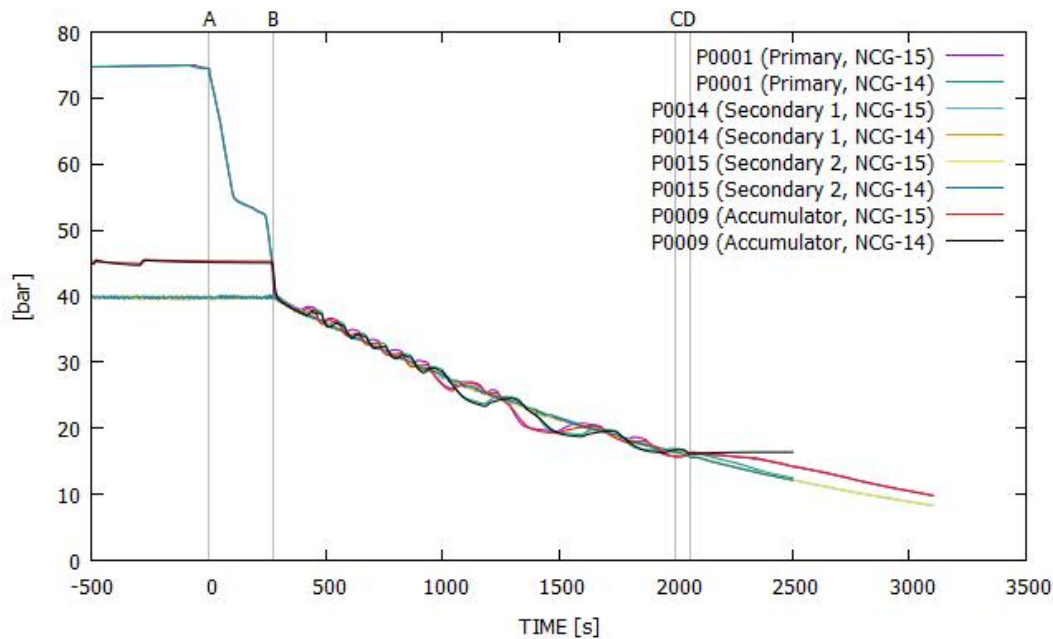


**Figure 4.** Primary and secondary side pressures in the NCG-14 and NCG-15 experiments.<sup>5</sup>

The transients started when the break valve was opened and the leak from the primary system began. Then the primary side pressure dropped sharply (Figure 2 – Figure 4) until the saturation temperature reached the core outlet temperature. This pressure decrease caused water in the core region to boil and water in the upper plenum to flash to steam and slowed down primary side pressure drop rate. When the water level in the upper plenum decreased below the hot leg elevation, steam began to flow through the hot legs into the steam generators and out of the break. This steam flow caused the primary side pressure to drop near the level of the secondary side pressure. The accumulator water injection began when the primary side pressure dropped to the accumulator pressure of 45 bar. The secondary side depressurization with the cooldown rate of 100 °C/h began when the primary side pressure decreased to the pressure level of 43 bar.

With the cold leg break (NCG-10, NCG-11) the loss of primary coolant and the depressurization of the primary side led finally to a core heat up (Figure 5). The water level in the core decreased until the loop seal clearing (Figure 6) of at least one U-leg occurred. Once the U-leg draining occurred steam could flow through the U-legs and exit the primary side through the break restoring a normal water distribution in the primary side. The loop seal clearing induced the recovery of core cooling and the core temperatures dropped. After the U-leg draining a part of water from the accumulator escaped from the system directly through the break. When the accumulator water injection ended also nitrogen from the accumulator could escape directly through the break.

The cold leg break experiments with the cold leg accumulator injection confirmed the potentially significant impact of the nitrogen gas injection from the accumulators on the core cooling. The injection of the accumulator nitrogen blanket into the primary side did not cause a pressure rise in the cold leg and the downcomer with respect to the upper plenum. Because of that there was not the expected piston effect driving water into the core and temporarily increasing the water level in the core. However, there was a clear time difference between the experiments with and without nitrogen when the second core heat up occurred. The break location in the cold leg was quite close to the downcomer and allowed the accumulator injection water and nitrogen to escape easily from the system. The results might be different if the break location was at the bottom of the loop seal or near the steam generator. However, the nitrogen injec-

<sup>5</sup> A: break opens, B: accumulator water injection begins, C: accumulator water injection ends in the NCG-15 experiment, D: accumulator water injection ends in the NCG-14 experiment.

tion had a positive impact on the core cooling, but not by momentarily redistributing water masses in the vessel as expected.

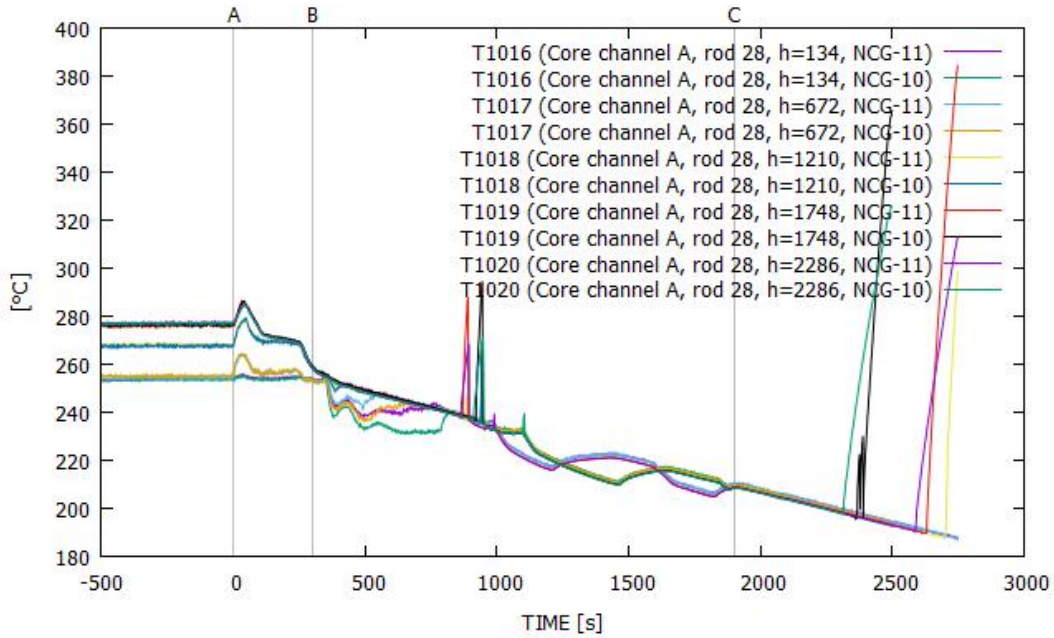


Figure 5. Core temperatures in the NCG-10 and NCG-11 experiments.<sup>6</sup>

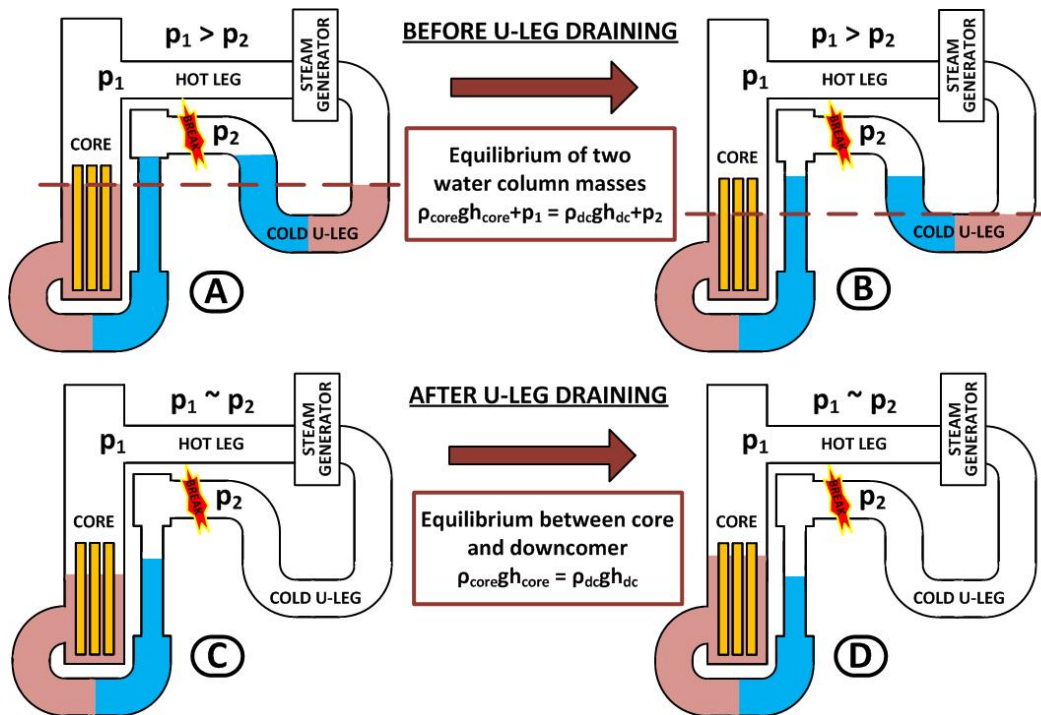
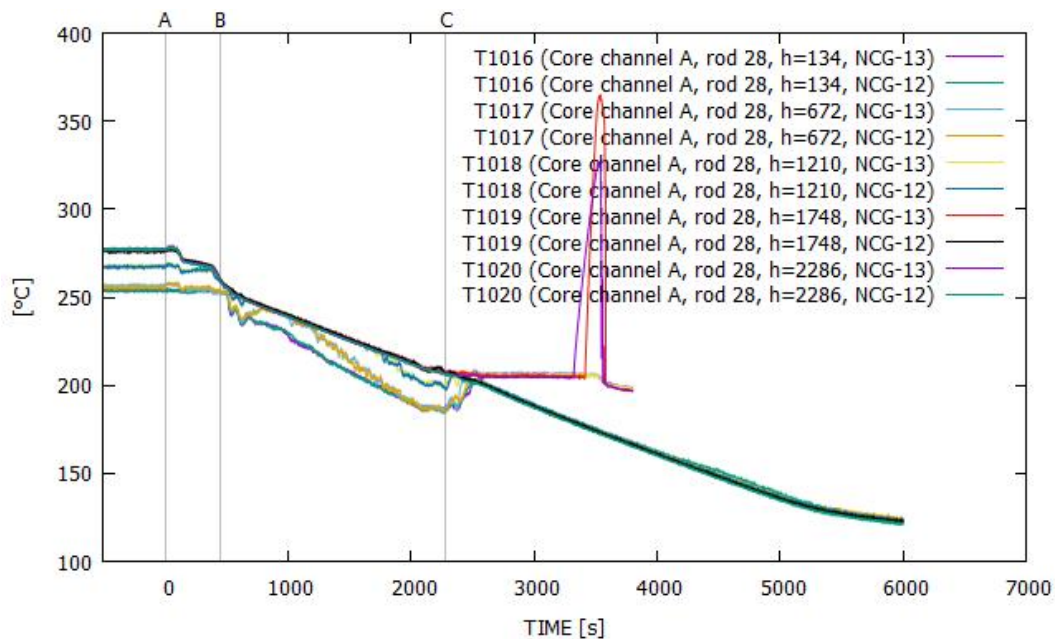


Figure 6. Illustration of the loop seal clearing phenomena (A => B => C => D).

<sup>6</sup> A: break opens, B: accumulator water injection begins, C: accumulator water injection ends.

With the hot leg break the system behaviour in the beginning of the experiments (NCG-12, NCG-13) until the accumulator injection to the cold leg began was similar to the cold leg break experiments. After the water level in the core was determined by the manometric effect. Water in the core and downcomer was in hydrostatic equilibrium. Unlike in the cold leg break experiments steam produced in the core could escape from the primary side through the break since the break location was in the hot leg.

After the accumulator water injection and the secondary side depressurisation was started, the heat from the primary side was removed through the break and through the steam generators to the secondary side. With the nitrogen injection the accumulator and primary side pressures stayed fairly constant (Figure 3) until the temperature of the core started to increase (Figure 7) and the core power was decreased by the core protection system. Without the nitrogen injection the primary side and accumulator pressures followed the secondary side pressure and no core temperature increase was observed. With the hot leg break the injection of the accumulator nitrogen blanket into the primary side had a negative impact on the core cooling.



**Figure 7.** Core temperatures in the NCG-12 and NCG-13 experiments.<sup>7</sup>

In the upper plenum injection experiments (NCG-14, NCG-15) the effect of non-condensable gases on natural circulation during a SBLOCA was studied and experiment data especially for the APROS validation was generated. In these experiments the connection line between the upper plenum and the downcomer was closed.

The system behaviour in the beginning of the experiments until the accumulator injection began was similar to the cold leg injection experiments. During the accumulator water injection period the secondary side depressurization steadily decreased the primary side pressure and cooled down the system. In this period the system behaviour was cyclic (Figure 4). The cold accumulator injection water condensed steam in the upper plenum and dropped the primary side pressure and increased the steam generation rate in the core. The steam created in the core stopped the primary side pressure decrease and paused the accumulator injection. As the accumulator injection was paused the condensed water flashed into steam again increasing the primary side pressure and a new cycle began. This cyclic behaviour continued the whole accumulator water injection period. After the accumulator nitrogen injection started the primary pressure increased slightly above the secondary side pressure and decreased steadily.

<sup>7</sup> A: break opens, B: accumulator water injection begins, C: accumulator water injection ends.

During the accumulator water injection period the water level in the core was determined by manometric effect. Steam produced in the core could not escape from the primary side through the break since the primary side water was stratified in the U-legs and the connection line between the upper plenum and the downcomer was closed. There was a small core heat up (Figure 8) before the accumulator water injection ended. The core heat up was halted presumably by the accumulator water injection. After the accumulator water injection ended the water level in the core decreased and led to a core heat up again.

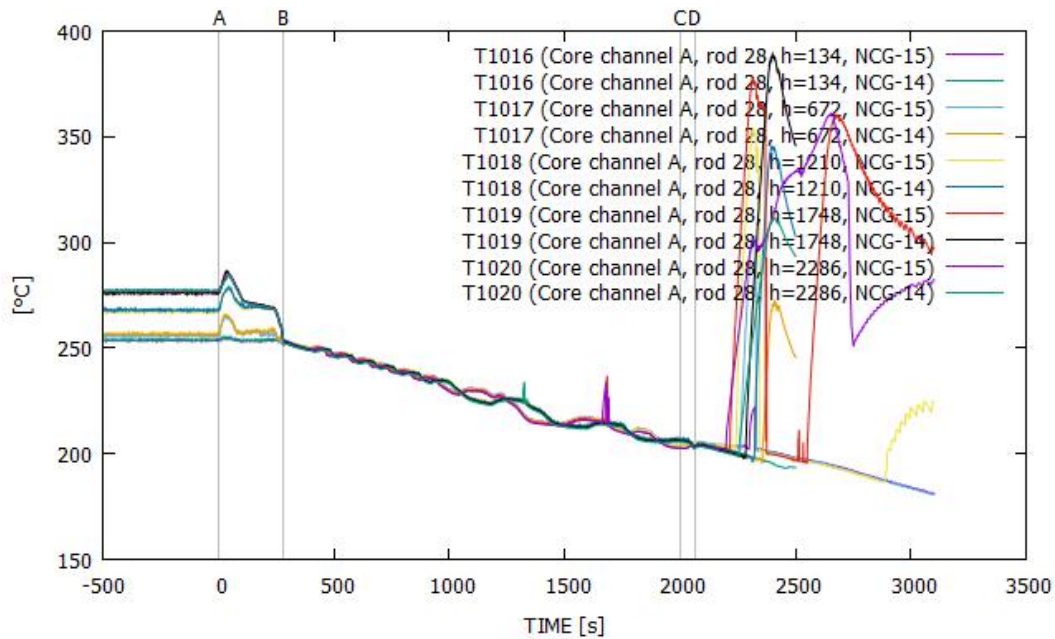


**Figure 8.** Core temperatures in the NCG-14 and NCG-15 experiments.<sup>8</sup>

In the upper plenum injection experiments the goal to study the effect of non-condensable gases on natural circulation during a SBLOCA was not achieved. That would require at the same time measurable flow rates in the loops, the water level in the core below the hot leg entrance, adequate core cooling to prevent the core heat up, and enough nitrogen in the loops to stop the loop flow. It is not possible to achieve all the required conditions at the same time. As these experiments showed the core will easily heat up if the cold leg loop seals are blocked with water. When the loop seals open nitrogen in the primary side can escape the system through the break. Nevertheless, these experiments gave useful data for the code validation especially because there are only few experiments available where the accumulator injects to the upper plenum which is a special feature of the VVER and AES type reactors.

### Simulations of PWR PACTEL nitrogen experiments

The APROS and TRACE system codes are utilized within the SAFIR2018 INTEGRA project to support the planning of the PWR PACTEL facility experiments in Lappeenranta University of Technology (LUT). The codes have been used in pre-test and post-test analyses. The main purpose of the pre-test simulations in the project is to assist in defining test parameters, to obtain a tentative insight on possible conditions to be expected during the actual experiments, and observe beforehand possible issues compromising the safe

<sup>8</sup> A: break opens, B: accumulator water injection begins, C: accumulator water injection ends in the NCG-15 experiment, D: accumulator water injection ends in the NCG-14 experiment.

operation of the facility. Hence, typically parameters and geometrical issues used in the pre-test analyses have been somewhat different from the final conditions in the experiments. If feasible, to improve the performance of the simulation models the models are tested with post-test cases, using the final experiment conditions and parameters. Two nitrogen experiments (NCG-13 and NCG-15) performed with the PWR PACTEL facility were chosen for the post-test simulations /4/.

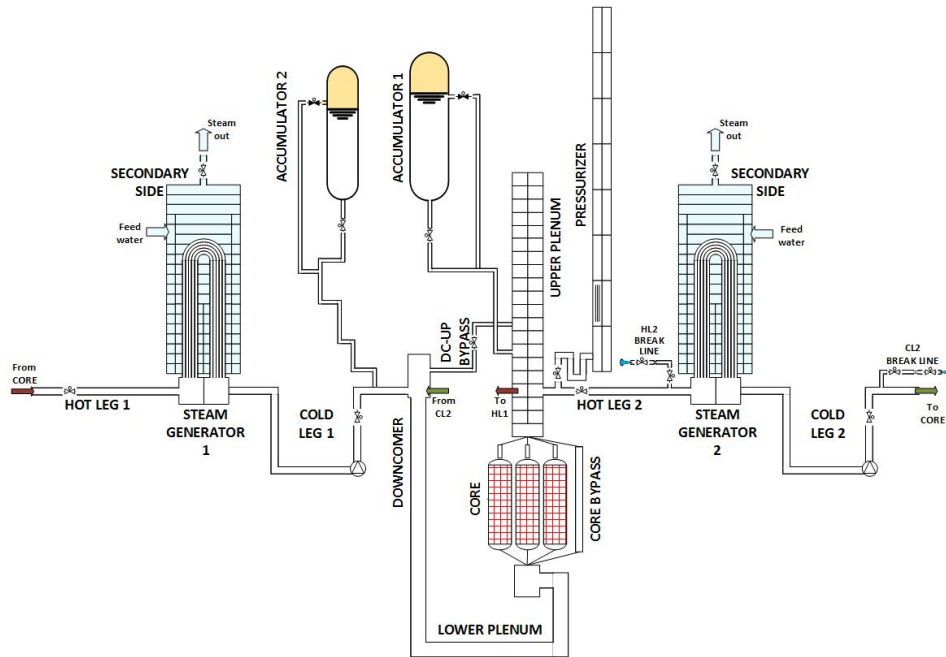


Figure 9. Schematic view of the PWR PACTEL simulation model for the APROS code.

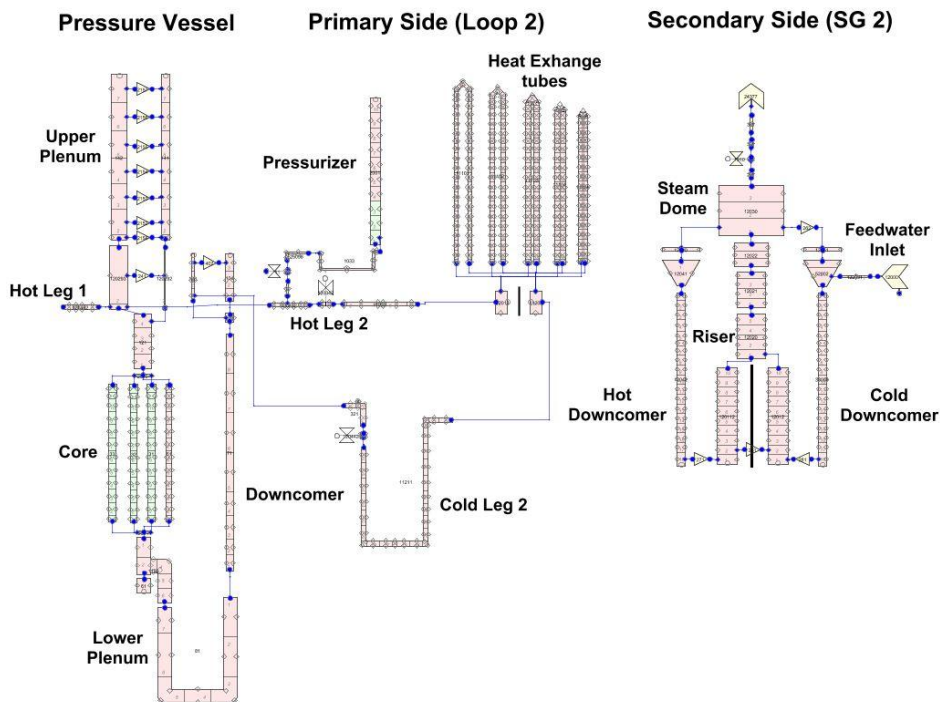
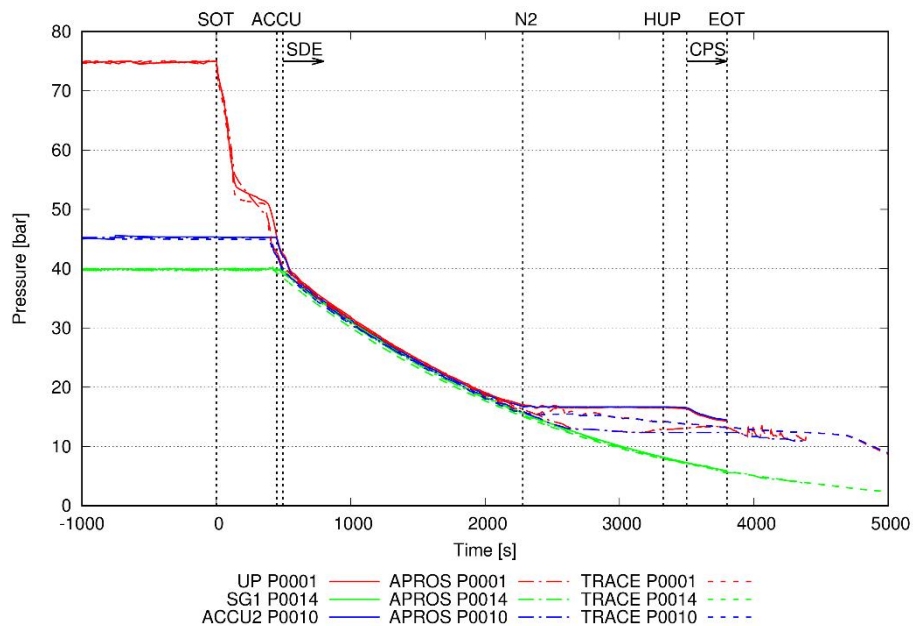


Figure 10. The PWR PACTEL simulation model for the TRACE code.

Both simulation models, i.e. the PWR PACTEL facility models with the APROS (version 5.15.06) and TRACE (version of 5.0 patch 4) codes, have been built with similar principals. The facility is modelled in details, including the whole primary side, the secondary sides of the steam generators and the ECCS as needed. The geometry is modelled fairly detailed and the measurement elevations of the facility are taken into account in the nodalizations. In both simulation models the 51 heat exchange U-tubes of the PWR PACTEL steam generators are lumped together into 5 parallel pipe components according to the different main lengths of the U-tubes. The general scheme of simulation models are presented in Figure 9 and Figure 10.

In the TRACE simulation of the NCG-13 experiment the hot leg break flow rate and the accumulator water reduction followed the experiment references during the accumulator water injection period exemplary. In the APROS simulation the accumulator water injection period continued longer compared to experiment. During the nitrogen injection period in the experiment the primary side pressure were stabilized to the constant level. The reason for this is unclear. It is possible that steam and possibly nitrogen in the upper volumes of the facility prevented the pressure decrease in the primary side. In the simulations this phenomenon was not so clear. In the APROS simulation the accumulator and primary side pressures decreased slowly and steadily in the beginning of this period. After that, the primary side pressure started to increase and the accumulator pressure stabilized to a constant value as the check valve in the accumulator line closed. In the TRACE simulation the primary pressure decreased slowly almost all the time and nitrogen was flowing to the primary side. Nitrogen and steam were not able to pressurize the upper plenum as much as in the experiment (Figure 11).



**Figure 11.** Pressures of the primary side, secondary side of the steam generator 1 and accumulator in the NCG-13 experiment and simulations.<sup>9</sup>

<sup>9</sup> Events in experiment: SOT = start of transient, ACCU = accumulator water injection start, SDE = secondary depressurization start, N2 = nitrogen injection start, HUP = core heat-up start, CPS = core protection system start, EOT = end of transient.

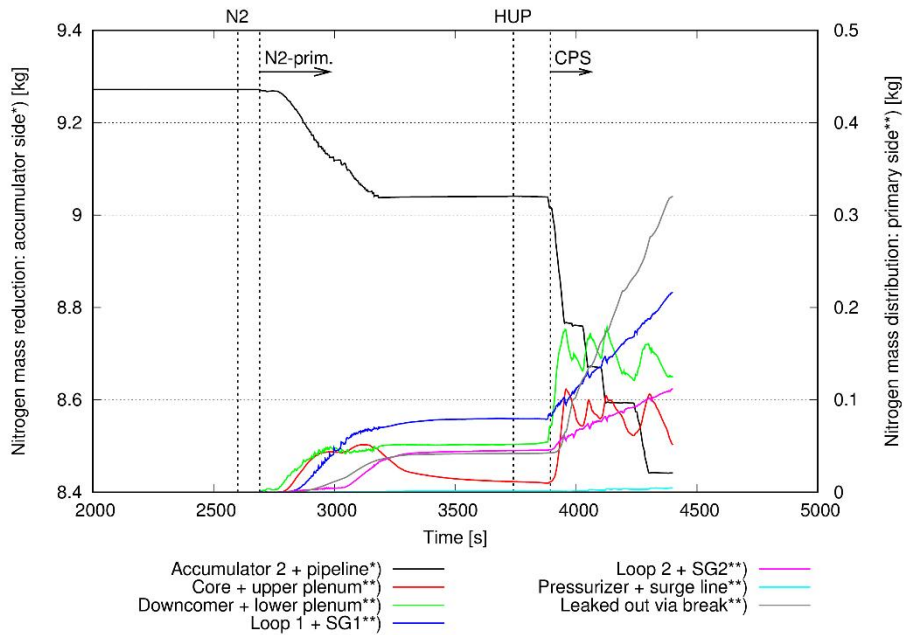


**Figure 12.** Nitrogen amounts in different parts of the primary system during the NCG-13 transient in the APROS simulation. (Points of event: black vertical lines and abbreviations in APROS simulation).<sup>10</sup>

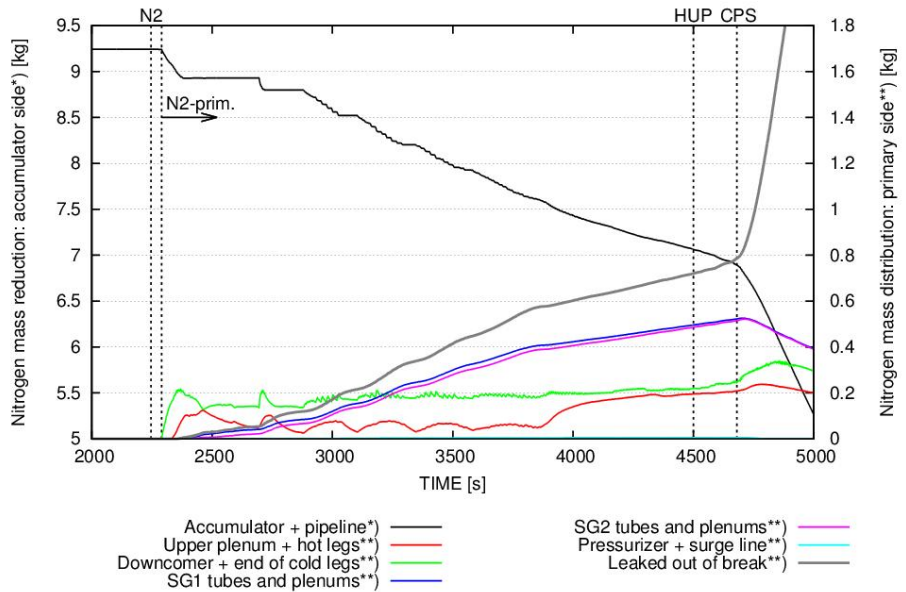


**Figure 13.** Nitrogen amounts in different parts of the primary system during the NCG-13 transient in the TRACE simulation. (Points of event: black vertical lines and abbreviations in TRACE simulation).<sup>7</sup>

The experiment results do not include any specific clear indication on the nitrogen distributions in the primary side during the transients. Yet, utilizing for example the pressure curves the favourable periods for the nitrogen flow entering the primary side can be estimated. Also some estimations can be made indirect-

<sup>10</sup> Events in simulations: N2 = nitrogen injection start, HUP = core heat-up start, CPS = core protection system start, N2-prim. = nitrogen start entering primary side.

ly on the nitrogen presence from the leak flow rate data. Using animation models allows deeper studies on the nitrogen locations and distributions in the simulations. The total amounts of nitrogen that were able to enter the primary side in these transients according to the simulation observations and estimations on the experiments vary from hundreds of grams to several kilograms. As the total duration of the simulations and experiments were different the nitrogen amounts entering the primary side varied and are not necessarily comparable. Figure 12 and Figure 13 present amount of nitrogen in different parts of the facility in the APROS and TRACE models in the NCG-13 case simulation.

In the simulations of the NCG-15 experiment the accumulator water injection ended slightly faster than in the experiment. For this reason the nitrogen connection line valve was also open earlier than in the experiment. Despite the early starting time of the accumulator nitrogen injection period, the nitrogen actually started to enter the primary side after several hundred hours after the initiation of the nitrogen injection system. There was a manometric cyclic behaviour in the experiment during the accumulator water injection period, notable from several parameters. The TRACE simulation model predicted the cyclic behaviour also but in the APROS simulation that was not so evident (Figure 14).

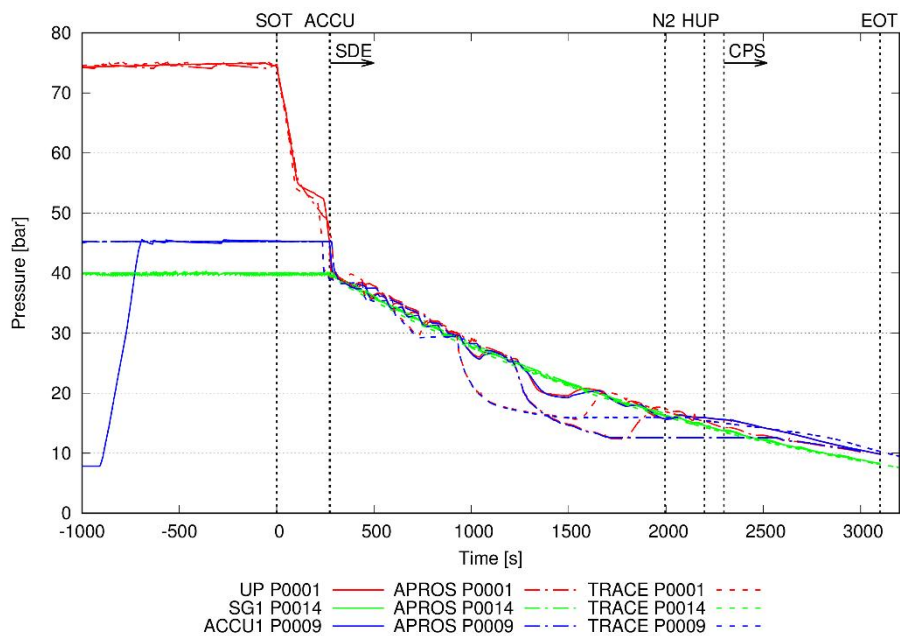


**Figure 14.** Pressures of the primary side, secondary side and accumulator in the NCG-15 experiment and simulations. The secondary side pressure of steam generator 2 was similar to that of the steam generator 1 and hence not presented here.<sup>11</sup>

The loop seal clearing strongly affected the conditions in the simulations of the NCG-15 case, i.e. in the redistributing the water amounts along the facility and contributing the core cooling capacities. Already during the accumulator water injection period the simulations experienced the core heat-up periods that were settled either with the loop seal clearings (TRACE, APROS) or with also a core protection system (APROS). The heat-up periods appeared also during the accumulator nitrogen injection period, once settled with the loop seal clearing and finally with clearings along with core protection system. The experiment was also a small core heat-up during the accumulator water injection period which was halted presumably by the accumulator water injection. In both simulations the final core heat-up occurred later than in the experiment (Figure 15).

<sup>11</sup> Events in experiment: SOT = start of transient, ACCU = accumulator water injection start, SDE = secondary depressurization start, N2 = nitrogen injection start, HUP = core heat-up start, CPS = core protection system start, EOT = end of transient, N2-prim. = nitrogen start entering primary side.

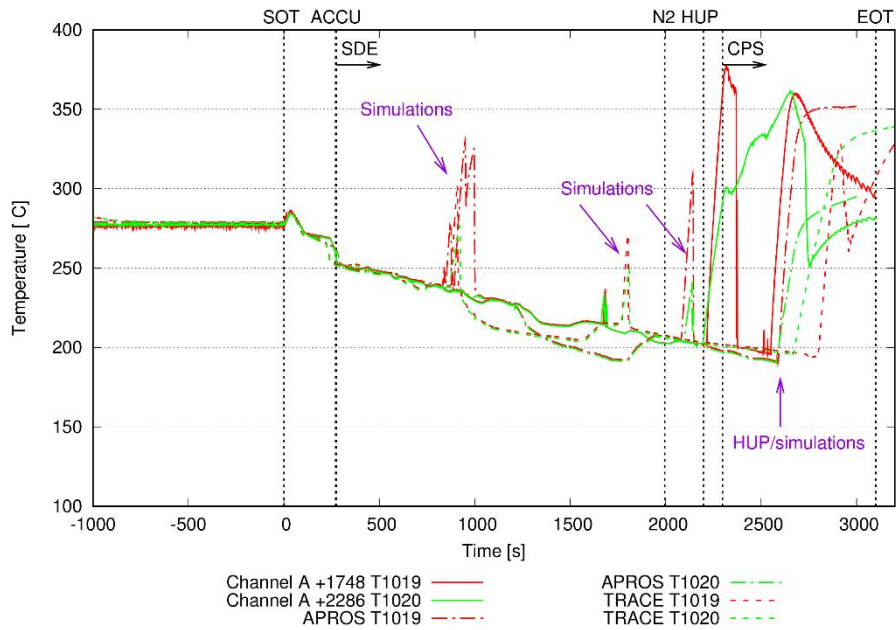


**Figure 15.** Surface temperatures of a heater rod in core channel A in the NCG-15 experiment and simulations.<sup>12</sup>

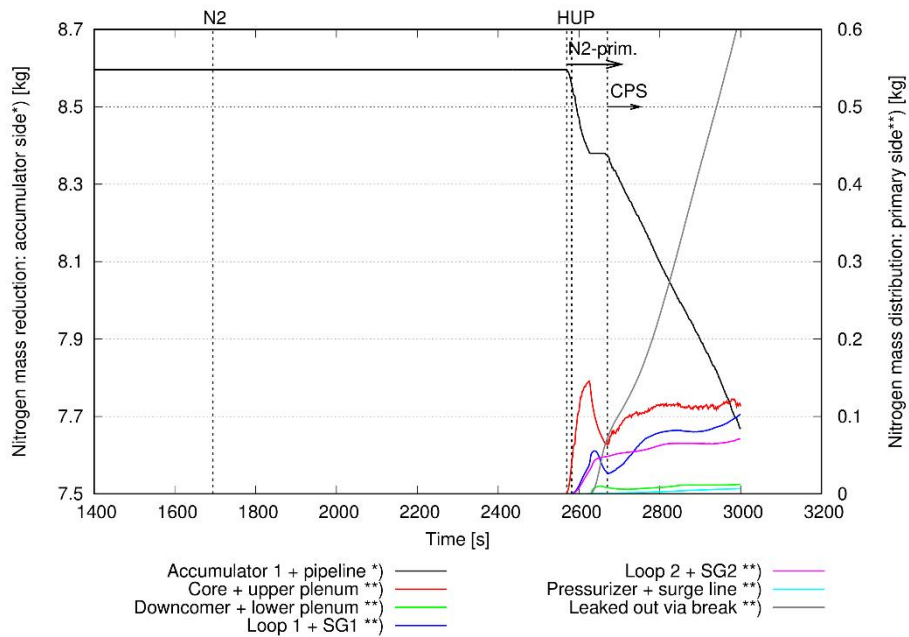


**Figure 16.** Nitrogen amounts in different parts of the primary system during the NCG-15 transient in the APROS simulation.<sup>13</sup>

<sup>12</sup> Events in experiment: SOT = start of transient, ACCU = accumulator water injection start, SDE = secondary depressurization start, N2 = nitrogen injection start, HUP = core heat-up start, CPS = core protection system start, EOT = end of transient.

<sup>13</sup> Events in simulations: N2 = nitrogen injection start, HUP = core heat-up start, CPS = core protection system start, N2-prim. = nitrogen start entering primary side.

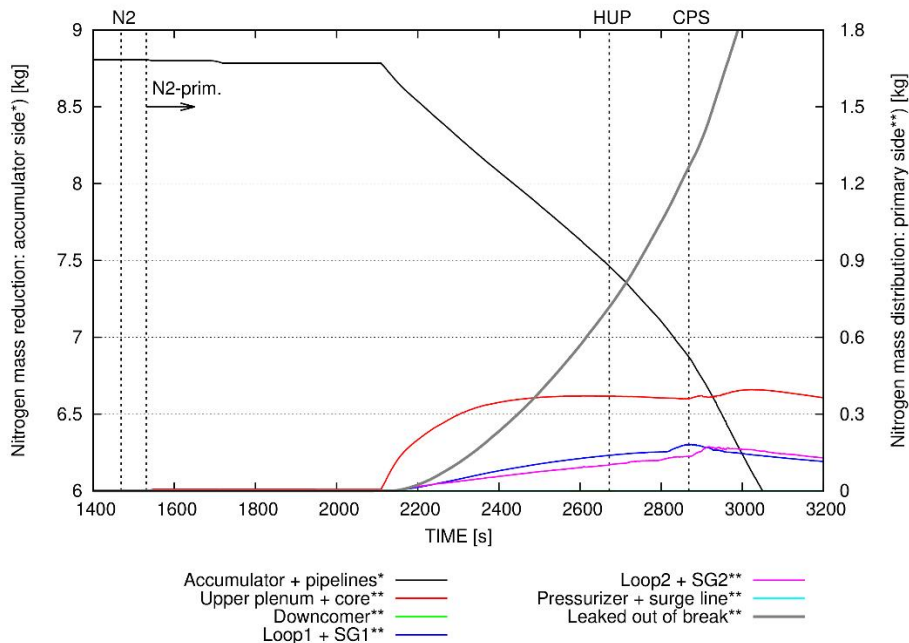


**Figure 17.** Nitrogen amounts in different parts of the primary system during the NCG-15 transient in the TRACE simulation.<sup>14</sup>

In the NCG-15 type transient the loop seal clearing behaviour is one major contributor in distributing the nitrogen into the cold leg end and downcomer parts (Figure 16 and Figure 17). In this type of transient the open loop seals set up an open path for the nitrogen to exit from the primary system.

In general both APROS and TRACE simulation models were able to calculate the nitrogen experiments moderately well, considering the overall duration of the transients, as well as the phenomena and conditions connected to both transient cases. The amount of the leaked water in both transients was predicted reasonable well in both simulations though some occasional discrepancies appeared in the leak flow rate due to differences in the conditions compared to the experiment. In general the simulations calculate the cases slightly longer than what was measured in the experiments.

Potential subjects for further investigation with aim to check and improve the behaviour of both simulation models include various issues. The nodalization of the top part volumes in the downcomer and upper plenum affect the overall mixing and the model choices could be reconsidered. Heat losses and large steel constructions in the upper parts of the facility (pressurizer, upper plenum, downcomer, secondary side of steam generator) affect the conditions during transients. The material properties and adjustment of the heat losses at these parts of the simulation models could be re-evaluated and checked against the proper experiment data. Yet, this is challenging because of the limited amount of the reference instrumentation probes in those volumes in the test facility. Also the manner the check-valves are simulating the real valve behaviour could be rechecked.

The choices for the suitable correlations in calculation for both codes in various places of the facility need to be confirmed, e.g. correlation choices utilized during condensation, counter-current flow and heat transfer situations. Choices against the code defaults could be tested to analyse the effects more deeply.

Considering the possibilities in general to express a chosen specific individual parameter along all the simulation model nodes visually with an animation model is an appealing issue. The node level analysis benefits of such visual observation possibility. This is present and possible with the TRACE code model utilizing the animation modelling part of the SNAP interface that is part of the TRACE code system pack-

<sup>14</sup> Events in simulations: N2 = nitrogen injection start, HUP = core heat-up start, CPS = core protection system start, N2-prim. = nitrogen start entering primary side.

age. The TRACE animation model is already fully representative to be utilized in studying chosen parameter variations along the whole model during a transient. As such an animation modelling possibility is not available with APROS, the animation model of the APROS model nodalization is under construction using the SNAP interface and functionality.

## Facility for research on passive heat removal

Many currently marketed LWR designs feature varying numbers of naturally circulating decay heat removal loops. Large diversity of design configurations is available. Some vendors connect the loops to the primary system; Isolation Condensers (IC) or Emergency Condensers (EC) of BWRs and Passive Residual Heat Removal Systems (PRHRS) in PWRs. Some connect to the secondary side; Passive Heat Removal System – Steam Generators (PHRS-SG) in VVERs. Many vendors connect loops even to the containment; Containment Cooling Condensers (CCC), Passive Containment Cooling Systems (PCCS), (both in BWRs) and Passive Heat Removal System – Containment (PHRS-C) in VVER.

Design details, e.g. the exact geometry of the heat exchangers, vary a lot between different vendors. Most designs rely on a water pool outside the containment as the heat sink, however. Moreover, the general features of naturally circulating loops are similar in all designs. These safety systems are designed to operate without an external power source and relying on relatively small gravitational pressure differences. The vendors are in the possession of design-specific performance data for the systems, but the coverage of the data is not widely known. In particular, it is unclear as to what extent the vendor testing covers phenomena and inherent failure mechanisms that could prevent or hamper the intended operation of the system. It is particularly noteworthy that the containment cooling loops often operate at low (~atmospheric) pressure, meaning that they are susceptible to boiling oscillations due to large water-steam density differences. While oscillating flow may be an efficient heat removal mechanism, it causes dynamic loads and consequent fatigue on system piping, containment penetrations, pipe supports, and associated vessels.

At LUT, tentative studies have been on-going on the fundamentals and operation modes of passive heat removal systems, first by preparing a general review /10/ within the INTEGRA project. The review on passive heat removal system characteristics includes term descriptions and passive heat removal characterizations. Further, the review presents a collection of various concerns and hazards derived from references under the topic of endangered operability of a passive heat removal system. The review collects issues on factors that can hamper operability or block the safety system functions. The review also presents descriptions of the today utilized or designed passive heat removal systems for the NPP types in Finland (operating, under construction or under application process). The review includes a selection of some publicly available references with more information on these systems.

The review also describes the LUT experimental thermal-hydraulic research efforts so far on the cases where the focus has been set on passive systems or parts of those systems. The review shows possibilities and expertise at LUT premises to provide further thermal-hydraulic experimental studies on the passive heat removal systems. The review provides based arguments on chosen path for further experimental studies. The review presents a passive containment cooling system (refers to the PHRS-C system of AES-2006 design) that was chosen as the subject for further practical experimental thermal-hydraulic studies.

The selected passive system to be studied in more detail at LUT was chosen to be an open passive heat removal system (Figure 18). The plan is to build a model of an open type passive heat removal loop, with open pipeline connections to the water pool side, according to the reference passive containment heat removal system.

The reference PHRS-C system is comprised of heat exchangers located in the dome part of the containment, emergency heat removal water tanks that are located outside the containment, and connecting riser and downcomer pipelines in between. The PHRS-C system includes four identical and independent subsystems of which each subsystem includes four heat exchanger loops. In the LUT test facility under design phase, one heat exchanger loop will be modelled.

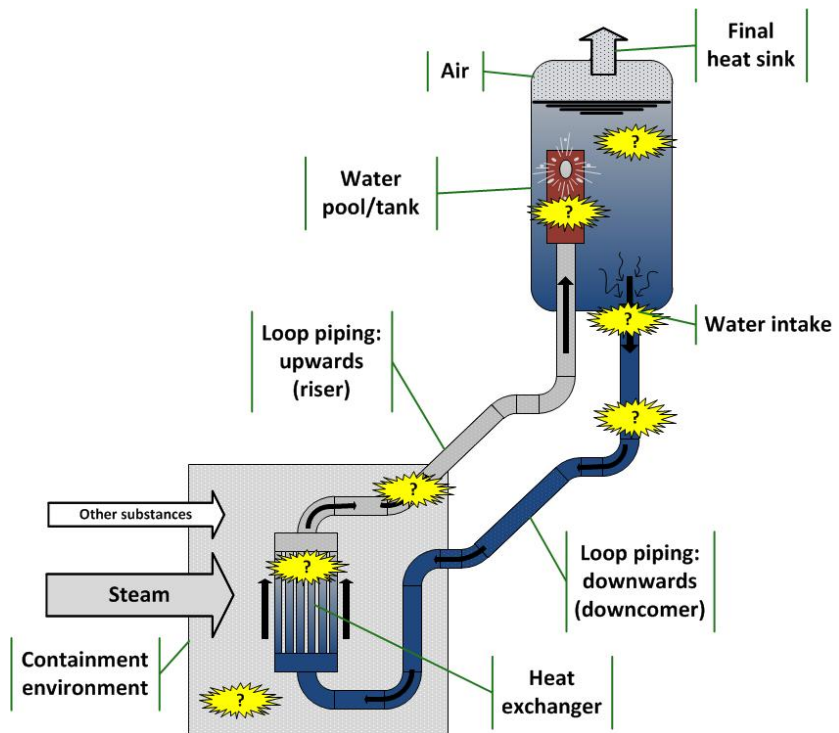


**Figure 18.** Sketch of an open natural circulation loop system.

In the actual design process /11/ of the new test facility, the principle was to model the natural circulation of the heat removal loop as representatively as possible. Further, the structure of the heat exchanger, as well as the heat exchange conditions, were emphasized in the design. Concerning the modelling of the natural circulation conditions, the clearest option would have been to maintain the elevations, i.e. to scale the heights 1:1 compared to the reference system. In practice, this proved to be impossible in the design of the facility due to the LUT laboratory space restrictions and limitations. Hence, two different height scales, 1:3 and 1:2, were considered in the design process.

In addition to heights, the riser and downcomer pipeline diameters needed to be scaled down. The chosen scaling methodology for the diameters was to maintain the relative gravitational and frictional pressure losses between the test facility and the reference system. Together with the riser and downcomer diameter calculation, flow velocities and mass flows in the loop and in the heat exchange tubes, as well as needed number of the heat exchange tubes in relation to the heat exchange power, were calculated in order to model the whole process of the system as accurately as possible.

As a result of the design process it was tentatively decided that 1:2 height scale will be applied for the test facility. The riser pipeline inner diameter was tentatively chosen to be the commercial pipe NS100 (114,3x2,5 mm, inner diameter 109,3 mm). The downcomer pipeline inner diameter was tentatively chosen to be the commercial pipe NS80 (88,9x2,5 mm, inner diameter 83,6 mm). The heat exchanger will be comprised of approximately 12–18 heat exchange tubes with an inner diameter of 32 mm, which is the same as in the reference system. The final number of heat exchange tubes will be decided later. The heat exchanger will be placed inside a vessel representing the containment, and representative conditions, i.e. temperature and pressure, will be created inside the vessel. The heat exchanger is not designed to be located fully inside the containment vessel, but the heat exchange tubes will penetrate the bottom of the vessel. This is due to the aim to be able to measure mass flows inside single heat exchange tubes, and the measuring is practically easier to conduct outside the vessel. The effective height, i.e. the vertical tube parts, of the heat exchanger inside the vessel will be approximately half of the corresponding height in the reference system. The external water storage tank will be placed on the balcony of the laboratory. The tentative structure of the LUT test facility is shown in Figure 19.

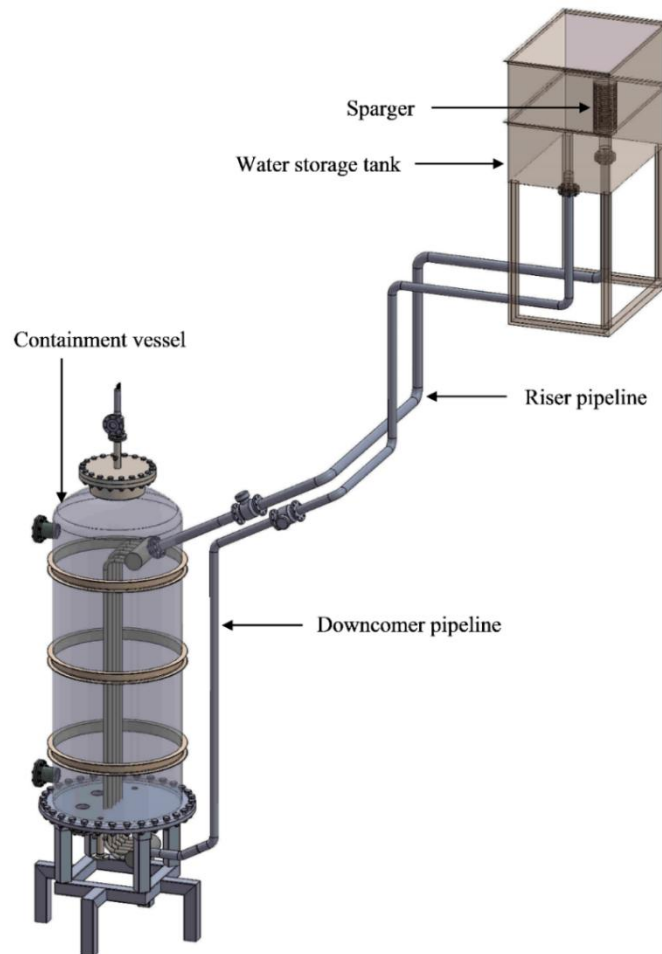


**Figure 19.** Tentative structure of the LUT test facility.

In the design process a lot of presumptions, deductions and approximations had to be made. This is due to the fact that the information regarding the reference system has been found in public sources, mainly in journal articles, and the sources didn't offer all the necessary details.

A TRACE model of the forthcoming test facility with tentatively chosen parameters will be made, and the functioning of the system will be tested with the model.

## **Acknowledgement**

The OECD/NEA PKL Phase 3 project was performed with the financial support of the Finnish Research Programme on Nuclear Power Plant Safety (SAFIR2014 and SAFIR2018), the Finnish power company Teollisuuden Voima Oy (TVO), and the partners participating in the OECD/NEA PKL Phase 3 project. The authors are grateful for their support to OECD Nuclear Energy Agency (NEA), the members of the SAFIR2014 and SAFIR2018 Reference Group 4 and the members of the Program Review Group and the Management Board of the OECD/NEA PKL Phase 3 project. The data from the experiments in the OECD/NEA PKL Phase 3 project will be available to the NEA member countries via their CSNI representative organizations three years after the end of the project.

## References

- /1/ Vesa Riikonen, Virpi Kouhia, Otso-Pekka Kauppinen, PWR PACTEL nitrogen experiments, Research report INTEGRA 1/2016, Lappeenranta University of Technology / Nuclear Engineering, Lappeenranta, 2016, pp. 23 + 17.
- /2/ Otso-Pekka Kauppinen, Vesa Riikonen, Virpi Kouhia, Juhani Hyvärinen, Analysis of reverse flow in low-rise inverted U-tube steam generator of PWR PACTEL facility, The 16th International Topical Meeting on Nuclear Reactor Thermal Hydraulics, NURETH-16, Chicago, USA, August 30-September 4, 2015, 2015.
- /3/ Otso-Pekka Kauppinen, Virpi Kouhia, Vesa Riikonen, Juhani Hyvärinen, Heikki Sjövall, Computer analyses on loop seal clearing experiment at PWR PACTEL, Annals of Nuclear Energy, Volume 85, 2015, Elsevier, 2015, pp. 47-57.
- /4/ Virpi Kouhia, Otso-Pekka Kauppinen, Simulations of PWR PACTEL nitrogen experiments, INTEGRA 2/2016, Lappeenranta University of Technology / Nuclear Engineering, Lappeenranta, 2016, pp. 64 + 4.
- /5/ <https://www.oecd-nea.org/jointproj/pkl-3.html>
- /6/ Vesa Riikonen, Virpi Kouhia, Otso-Pekka Kauppinen, Cool down under Natural Circulation Conditions in Presence of Secondary side Isolated Steam Generators, Research Report, PAX 1/2013, Lappeenranta University of Technology / Nuclear Safety Research Unit, Lappeenranta, 2013, pp. 17 + 3.
- /7/ Vesa Riikonen, Virpi Kouhia, Otso-Pekka Kauppinen, Station blackout experiments, Research Report, PAX 1/2014, Lappeenranta University of Technology / Nuclear Safety Research Unit, Lappeenranta, 2014, pp. 20 + 18.
- /8/ Vesa Riikonen, Virpi Kouhia, Otso-Pekka Kauppinen, PWR PACTEL flow reversal experiments, Research Report, INTEGRA 1/2015, Lappeenranta University of Technology / Nuclear Engineering, Lappeenranta, 2015, pp. 10 + 3.
- /9/ Virpi Kouhia, Vesa Riikonen, Harri Partanen, Antti Räsänen, Otso-Pekka Kauppinen, Joonas Telkkä, Lauri Pyy, General Description of the PWR PACTEL test facility - third edition, Technical report, PAX 2/2014, Lappeenranta University of Technology / Nuclear Safety Research Unit, Lappeenranta, 2014, pp. 28 + 118.
- /10/ Virpi Kouhia, Otso-Pekka Kauppinen, Review on factors affecting the operation of passive heat removal circuits, Research report, INTEGRA 2/2015, Lappeenranta University of Technology / Nuclear Engineering, Lappeenranta, 2016, pp. 58.
- /11/ Joonas Telkkä, Otso-Pekka Kauppinen, Virpi Kouhia, Harri Partanen, Facility for research on passive heat removal, Research report, INTEGRA 3/2016, Lappeenranta University of Technology, Nuclear Engineering, Lappeenranta, 2016, pp. 22 + 3.

## 5.4 Development and validation of CFD methods for nuclear reactor safety assessment (NURESA)

Timo Pättikangas<sup>1</sup>, Juhaveikko Ala-Juusela<sup>2</sup>, Ville Hovi<sup>1</sup>, Risto Huhtanen<sup>1</sup>, Ismo Karppinen<sup>1</sup>,  
Joona Leskinen<sup>1</sup>, Giteshkumar Patel<sup>3</sup>, Juho Peltola<sup>1</sup>, Tommi Rämä<sup>4</sup>, Timo Siikonen<sup>2</sup>, Vesa Tanskanen<sup>3</sup>,  
Timo Toppila<sup>4</sup>

<sup>1</sup>VTT Technical Research Centre of Finland Ltd  
P.O. Box 1000, FI-02044 Espoo

<sup>2</sup>Aalto University  
P.O. Box 11000, FI-00076 AALTO, Finland

<sup>3</sup>Lappeenranta University of Technology  
P.O. Box 20, FI-53851 Lappeenranta, Finland

<sup>4</sup>Fortum Power and Heat Ltd  
P.O. Box 100, FI-00048 FORTUM

### Abstract

Computational Fluid Dynamics (CFD) methods are developed and validated for the identified most important topics in nuclear reactor safety assessment. International single-phase mixing benchmarks are participated and spray experiments performed at LUT are modelled in co-operation with Swedish partners. Models for the departure from nucleate boiling (DNB) are developed for the OpenFOAM code and co-simulation of NPP components with CFD code and Apros system code are performed.

### Introduction

The project consists of four Work Packages (WP), where Computational Fluid Dynamics (CFD) methods are developed and validated for nuclear reactor safety assessment. The Work Packages deal with mixing and stratification of gases and liquids, modelling of spray and stratification experiments with the PPOOLEX facility, development of boiling models for the OpenFOAM CFD code and coupled simulations of the primary circuit of PWR by using CFD code and Apros system code.

In WP 1, the international blind benchmark in the Hydrogen Mitigation Experiments for REactor Safety (HYMERES) programme has been participated. The benchmark exercise was PANDA experiment HP1\_6\_2, which focussed on the hydrogen stratification and erosion of density layer by turbulent mixing processes. The benchmark was calculated by using the ANSYS Fluent CFD code.

In WP 2, spray and stratification experiments performed with the PPOOLEX facility at LUT have been modelled with CFD simulations. CFD model for the PPOOLEX spray tests was constructed and a pre-simulation of an experiment was performed. In addition, stratification and mixing experiment of the water pool in the wet well compartment was calculated.

In WP 3, OpenFOAM CFD solver is being developed and validated for nuclear reactor safety assessment. At VTT, subcooled nucleate boiling and wall heat transfer models have been integrated into the Eulerian two-phase solvers of the official OpenFOAM release. At Aalto University, heat transfer in fuel rod bundles has been calculated with OpenFOAM. At LUT, OpenFOAM simulations of POOLEX chugging tests have been done and models for direct-contact condensation have been developed. In the in-kind contribution of Fortum, heat transfer in VVER-440 fuel rod bundle has been calculated.

In WP 4, coupled simulation of VVER-440 steam generator with ANSYS Fluent and Apros 6 has been performed. The secondary side of the steam generator has been modelled with Fluent CFD code, which has been coupled with Apros model of generic VVER-440 nuclear power plant.

In the following, each Work Package of the project is discussed in more detail.

## Hydrogen stratification and erosion of the stratified layer

Blind simulation of the HYMERES experiment HP1\_6\_2 was performed in order to validate the computational methods of the ANSYS Fluent CFD code. The test case was erosion of density stratified gas layer by using a jet plume. The jet did hit an obstruction plate before entering the density gradient layer.

The experiment was performed with the PANDA-facility located at PSI in Switzerland. The experimental layout consisted of two vessels connected with a pipe. Volume of each vessel was about 100 m<sup>3</sup>, height was about 8 m and diameter 4 m. The test facility is illustrated in Figure 1.

Initially, the vessels were filled with pure steam, but at the top of Vessel 1 a lighter mixture was arranged by using helium injection. Experiment started from still flow conditions, where the initial temperature was 107 °C. Pressure was regulated to the nominal value of 1.3 bar with a valve at the top of Vessel 2.

In the experiment, the stratified helium layer was destroyed by vertical steam jet that was injected towards the helium layer. The steam jet did first hit an obstruction plate that was located between the injection pipe and the helium layer. Part of the steam plume was able to circumvent the obstruction plate and eroded the stratified helium layer. The flow velocity in the test facility is illustrated in Figure 2.

In the blind simulations, the calculated temperatures were to be higher than the experimental results already when the jet hit the obstruction plate. This was a common feature in the simulations of all participants of the blind benchmark (Andreani et al., 2016). It seemed that the steam jet was too solid and the unsymmetry of pipe exit flow was not properly taken into account. In addition, the importance of radiation heat transfer was discussed after the blind benchmark. In the specifications, it was advised to be neglected.

Post-calculations of the experiment have later been performed in another project.

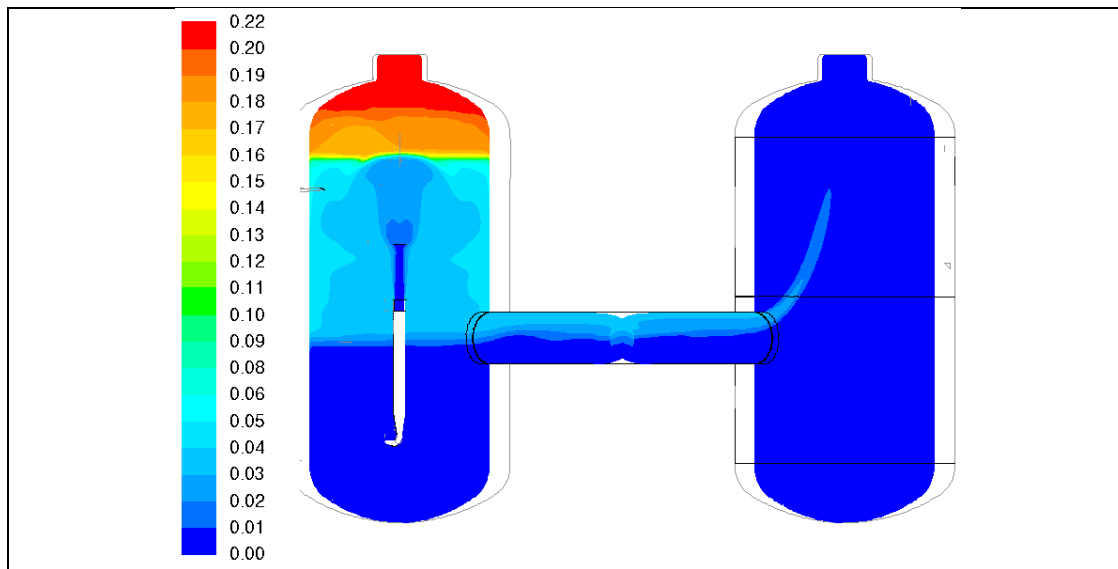


**Figure 1.** Volume fraction of helium in two vessels of the PANDA facility. CFD calculation of the OECD/NEA HYMERES benchmark HP1\_6\_2.

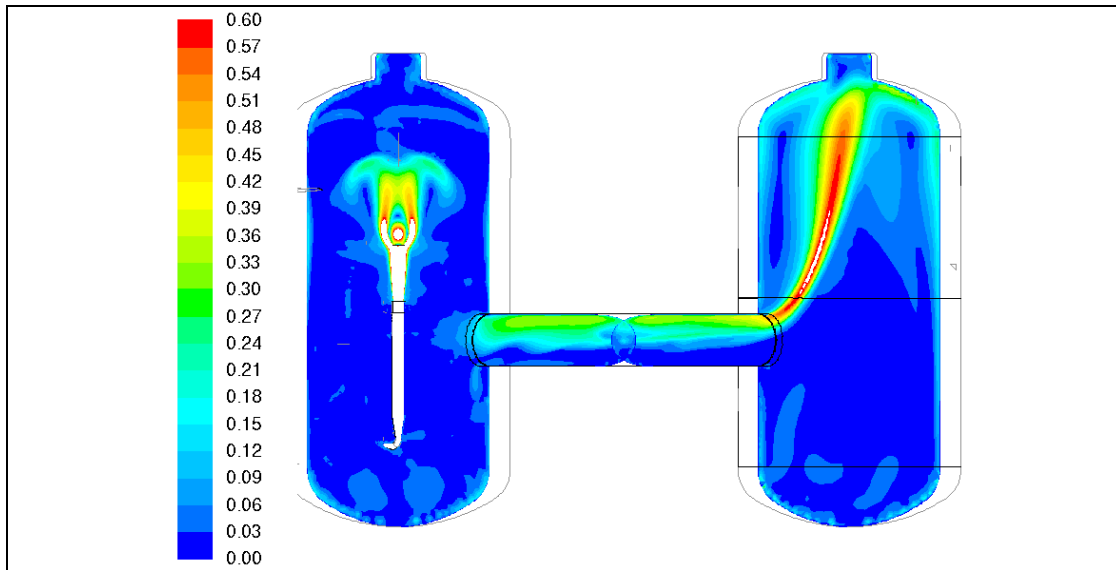


**Figure 2.** Velocity magnitude [m/s] in the two PANDA vessels at time 300 s. The vertical steam jet hitting on the obstacle plate can be seen in the left vessel.

### CFD modelling of PPOOLEX experiments

Pre-calculation on the effect of sprays in the PPOOLEX facility was performed by using ANSYS Fluent CFD code. PPOOLEX is a downscaled model of BWR containment, where spray have been installed in the wet well compartment. The goal is to study the effect of the wet well sprays on the thermal stratification of the pressure suppression pool.

In the simulation, the initial state of the PPOOLEX facility was carefully initialized to a typical situation that has occurred at late stage of recent pool stratification experiments (Laine et al., 2015). The initial pressure in the vessel was 2.75 bars. The temperature in the drywell was initially 133 °C and the drywell was filled with water vapour. The gas space of the wetwell was stratified: the temperature on the water surface was 40 °C and the temperature at the ceiling was 50 °C. The water pool was also stratified: the temperature at the bottom of the pool was 25 °C and on the water surface 40 °C.

The initialized flow field was first calculated without any sprays for 21.5 s, which ensures formation of proper hydrostatic pressure in the water pool and the gas space of the wetwell. At time  $t = 21.5$  s, the wetwell sprays were turned on. The flow rate of water from each spray nozzle was 17.8 litres/min, which means that within 60 s time the water level did rise by 1.5 cm. In the simulation, the temperature of the spray droplets was 10 °C.

In Figure 3, the velocity of the spray droplets is shown. The initial velocity of the droplets was 9.8 m/s and the mass weighted average velocity near the pool surface was 3.0 m/s. The droplets provide a mass, momentum and enthalpy sources on the pool surface. In the CFD simulation, the cooling of the water surface by the spray droplets was resolved. When the sprays had operated for 60 s, the liquid-water temperature on the pool surface varied between 31...34 °C. According to the simulation, the pool is partially mixed and the temperature at the pool bottom increases slightly.

According to the simulation, it seems that the cooling of the pool surface by spray eventually mixes the pool. The length of the simulation is, however, only 60 s, which is fairly short. Longer simulation would be needed to see full mixing of the pool.

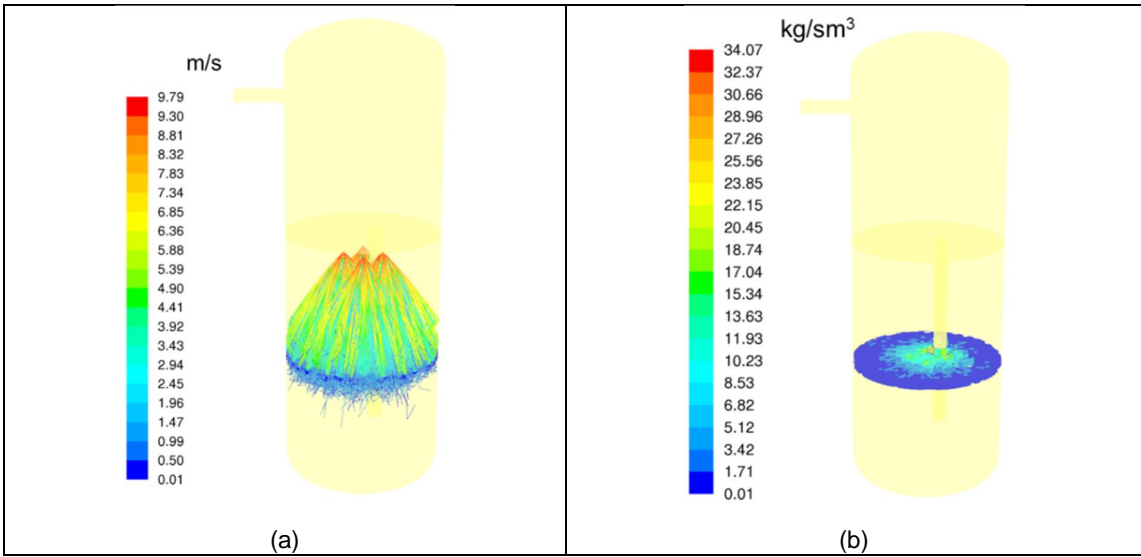


**Figure 3.** (a) CFD model of the wet well compartment of the PPOOLEX facility, where four spray nozzles are located near the ceiling of the wet well. (b) Source term of mass from the spray droplets on the surface of the water pool of the wet well.

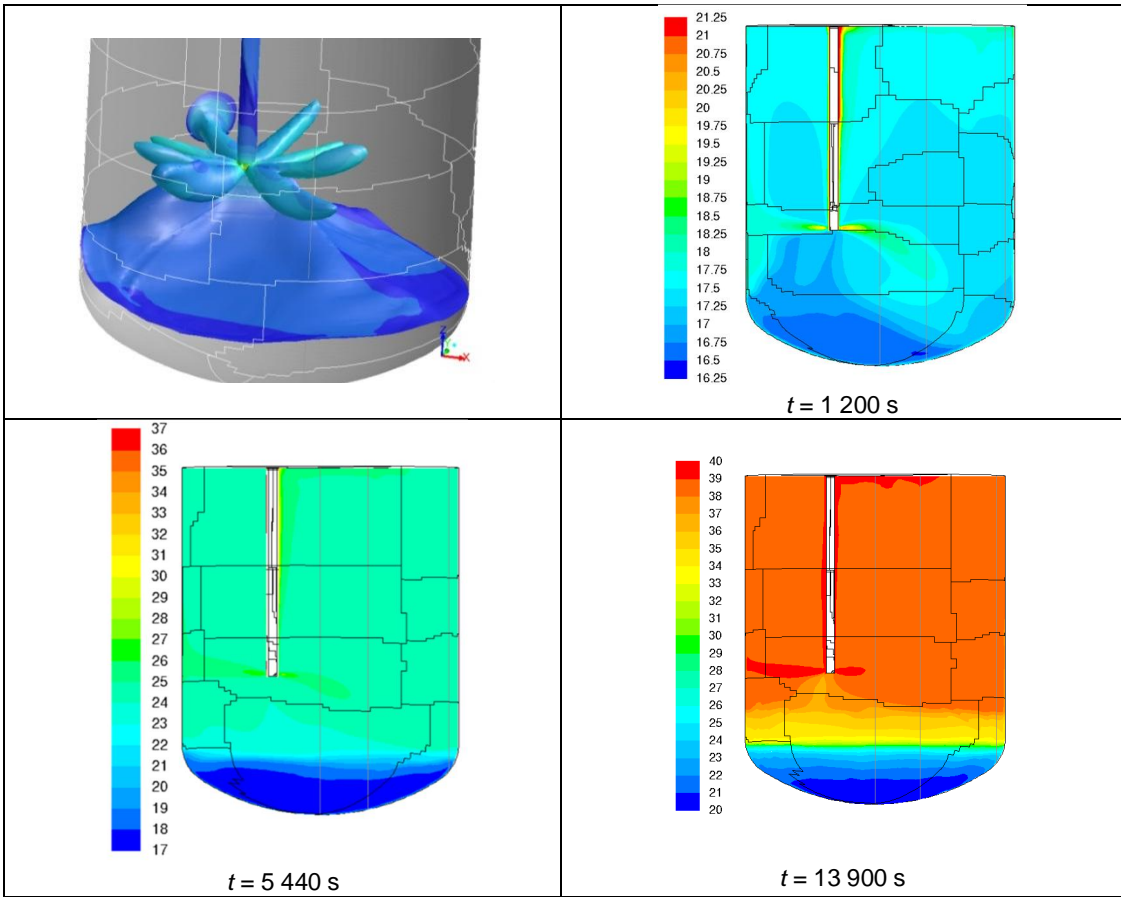


**Figure 4.** Time evolution of the thermal stratification of the pressure suppression pool. Formation of the thermal stratification is shown in the experiment at time  $t = 1\,200$ ,  $5\,440$  and  $13\,900$  s.

Thermal stratification of the pressure suppression pool of PPOOLEX was also studied in experiments, where steam is injected into the water pool through sparger. In the stratification phase of the experiment SPA-T1, steam was injected into the pool at a mass flow rate of 30 g/s for time 13 650 s (Puustinen et al., 2015). Then the mass flow rate was increased to 123 g/s in order to mix the pool.

The flow of water induced by the steam jets through eight sparger holes is illustrated in the top left frame of Figure 4, where an isothermal surface of liquid water is shown. The time evolution of the thermal stratification of the pool is also shown in Figure 4 at different instants of time. The temperature of the pool increases gradually during the injection of steam and sharp thermal gradient is formed below the sparger.

Comparison to the measurements of Puustinen et al. (2015) shows that the simulation predicts the temperature trends over time rather well. However, during the long transient the calculated mixing between the lower part and upper part is too strong. This might be corrected by adding grid resolution in the density and velocity gradient layer near the injection.

Due to the excessive mixing during stratification phase the predicted thermal transient at the mixing phase is milder than in the experiments. Mixing itself is predicted properly.

## **OpenFOAM solver for nuclear reactor safety assessment**

In commercial CFD software, the source code and the implementation of the numerical methods are not openly available. Thus, the possibilities to modify the solver or to include new models are limited. In addition, the license policy prevents effective utilization of parallel computer resources. The use of open-source software in the nuclear safety analysis would increase its transparency and improve opportunities for co-operation, as everyone would have access to a common software platform. The cost of parallel computational capacity has continuously been decreasing and the lack of licensing fees would allow this capacity to be utilized more effectively. This would improve the accuracy and reliability of modelling and increase the number of situations where CFD methods can be utilized.

The use of open source CFD software, especially OpenFOAM, is becoming more popular in industrial applications. In Finland, OpenFOAM is used at technical universities and it has been applied in cases brought up by the industry. In the previous SAFIR2014 program, OpenFOAM was found to be a viable platform for nuclear reactor safety (NRS) applications and a solver capable of simulating subcooled nucleate boiling was developed.

The long-term goal is to develop a general-purpose two-phase CFD solver for NRS assessment in co-operation with international partners. Close cooperation with the OpenFOAM Foundation makes possible to include the basic functionality needed in two-phase NRS application into the official releases of OpenFOAM. This provides a transparent and publicly available software platform that allows efficient international co-operation. According to the experiences obtained during the SAFIR2014 programme, inclusion of the main features of the developed models in the official releases is important for cost-effective and sustainable progress in model development.

At Aalto University, the work has concentrated on the simulation of heat transfer in a VVER-440 fuel rod bundle. Most of the work has been done on single-phase flows, where the effects of computational grid and turbulence modelling choices have been tested. In addition, the subcooled nucleate boiling capability developed in the project has been tested.

A full-length VVER-440 bundle has been simulated, where symmetry has been utilized to decrease the size of the computational domain to limit the required computing time. The heat flux distribution has been assumed uniform in all rods. Figure 5 shows a comparison of the temperature distribution at different cut planes obtained with the single- and two-phase solvers. The computational grid used in the single-phase simulation is denser than in the two-phase simulation. Figure 5 also shows a comparison of 600 K temperature iso-surfaces from both simulations.

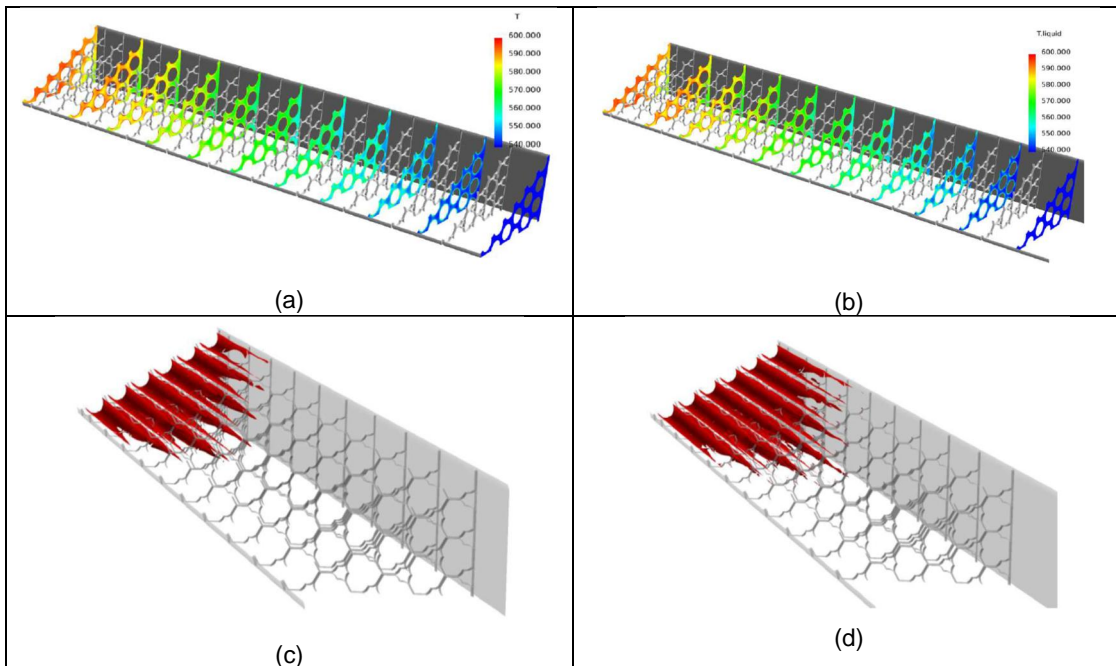


**Figure 5.** (a) Temperature distribution in single-phase simulation (b) Temperature distribution in two-phase simulation (c) 600 K temperature isosurface in single-phase simulation (d) 600 K temperature isosurface in two-phase simulation.

At Fortum, the goal for 2015–2018 is to calculate the Loviisa NPP fuel rod bundle by using OpenFOAM with realistic boundary conditions and including heat transfer from fuel rods. In 2015, a small one subgrid scale (app. 0.25 meters) fuel bundle model was simulated to test the OpenFOAM models and in year 2016 full-length fuel bundle (app. 2.6 meters) was simulated by using the same solver attributes.

The computational mesh of the fuel bundle model was made with better resolution than previous ones for increased accuracy. It consists of approximately 58 million cells. However, some of the cells were of lower quality. Hence the OpenFOAM solver was modified by VTT so that the highly skewed cells were solved with 1<sup>st</sup> order discretization (normal cells were solved with 2<sup>nd</sup> order discretization) in order to reach better convergence. General geometrical overview of one subgrid model and surface mesh are presented in Figure 6.

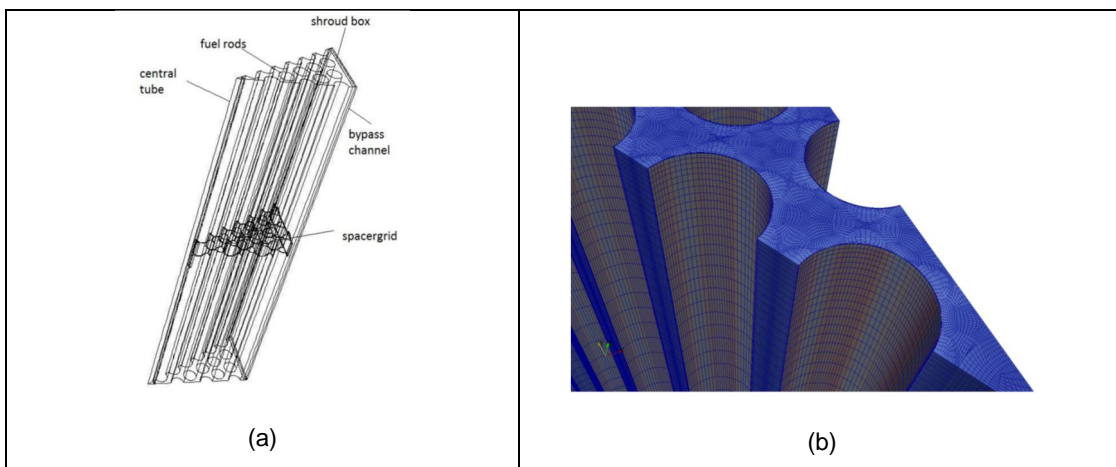


**Figure 6.** (a) General geometry of one subgrid model. (b) Surface mesh of the model.

The temperature rise in the fuel subchannels solved with OpenFOAM were compared to the results solved with ANSYS Fluent. Temperature rise in one subchannel is 40 – 50 K. The difference of the temperature rise between Fluent and OpenFOAM results is below 3% in all of the subchannels. Model outlet temperatures are presented in Figure 7.

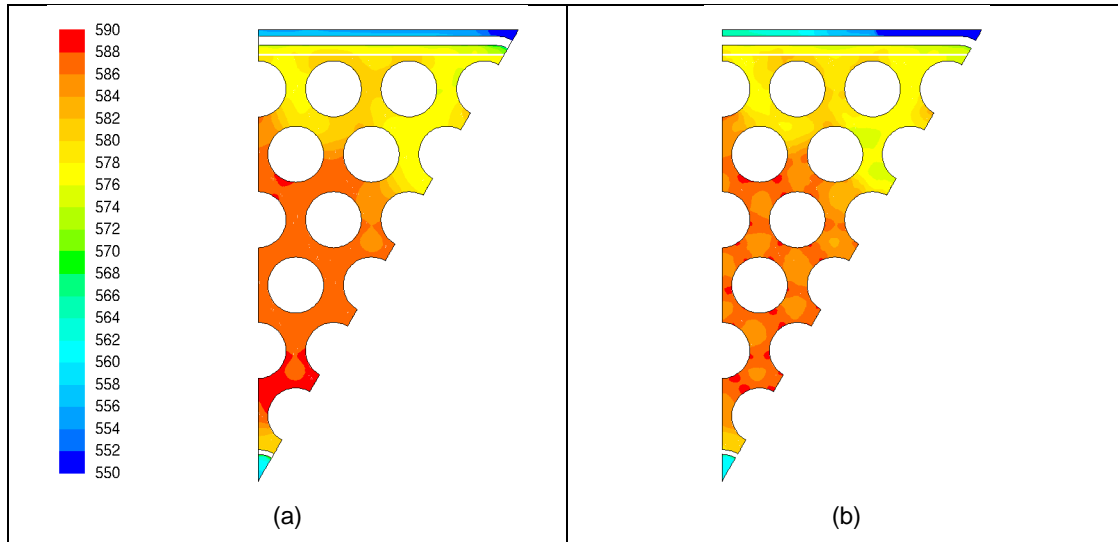


**Figure 7.** (a) Fuel bundle outlet temperature [K] of the ANSYS Fluent solution. (b) Fuel bundle outlet temperature [K] of the OpenFOAM solution.

At LUT, both 2D and 3D simulations of the chugging direct-contact condensation (DCC) mode of boiling water reactor (BWR) suppression pool were performed during 2015–2016 by using the Eulerian-Eulerian two-fluid approach of the OpenFOAM CFD code. The results were compared to the previous results obtained with the NEPTUNE\_CFD code and to the PPOOLEX test of the Lappeenranta University of Technology (LUT). The interfacial heat transfer between steam and water was modelled by employing different DCC models. In OpenFOAM simulations, the effect of turbulence modelling was studied by applying the standard  $k-\varepsilon$  (Sk- $\varepsilon$ ) model of Launder and Spalding (1974) and Lahey  $k-\varepsilon$  model (Lk- $\varepsilon$ ) of Lahey (2005).

The simulations of open-top pool POOLEX STB-28 test case showed that the incompressible two-phase flow solver of OpenFOAM was inappropriate for chugging. The two-phase compressible solver of OpenFOAM predicted notably higher DCC rates and chugging as well. Both qualitative and quantitative differences were observed between the numerical results of the OpenFOAM and the NEPTUNE\_CFD simulations, and the experimental results. Regardless of qualitative differences, it was concluded that the compressible two-phase solver of OpenFOAM is sufficient to invoke chugging phenomenon even without as sophisticated steam tables as NEPTUNE\_CFD has.

2D-axisymmetric simulations were performed for the PPOOLEX DCC-05-4 test case in order to simulate full drywell-wetwell system. Various modelling issues, e.g., the performance of different DCC models, the influence of turbulence modelling, interfacial momentum transfer, geometry and interface initialization were briefly studied with both NEPTUNE\_CFD software and the OpenFOAM CFD code. In OpenFOAM simulations, the Lk- $\varepsilon$  model yielded higher DCC rate due to the higher level of turbulence kinetic energy generation than the Sk- $\varepsilon$  model with the applied DCC models. Overall, the OpenFOAM simulations predicted higher DCC rates than the NEPTUNE\_CFD simulations. Subsequently, intense condensation resulted, which prevented much bubble growth at the exit of blowdown pipe. As a result, the interfacial area and bubble sizes in OpenFOAM cases were smaller than in the experiment and in the NEPTUNE\_CFD cases.

The bubble volume and the chugging frequency during the blowdown were obtained from the test data by using a pattern recognition algorithm of Hujala (2013). Figure 8 shows the FFT of the bubble volume in the PPOOLEX DCC-05-4 experiment and in the corresponding 2D-axisymmetric OpenFOAM and NEPTUNE\_CFD simulations.

In OpenFOAM simulations, some chugging frequencies were in the range of 0.5-3.3 Hz, but high frequency oscillations of 20-25 Hz seemed to be more dominant and these frequencies do not match either with NEPTUNE\_CFD or with test results. The OpenFOAM simulations failed to capture natural 50 Hz interface oscillation of condensing bubble.

The Rayleigh-Taylor Interfacial (RTI) area model of Pellegrini et al. (2015) was employed for the interfacial area modelling in NEPTUNE\_CFD simulations. Chugging and natural oscillation occurred with the Rayleigh-Taylor instability model at realistic frequencies, which demonstrated, that the increase of the interfacial area predicted by the model was within the correct order of magnitude. Due to that, DCC rate increased favourably. The implementation of RTI model to OpenFOAM is in progress. The other reasons for different condensation rates between the codes should be studied as well. The interfacial turbulence modelling is one likely reason for the different result.

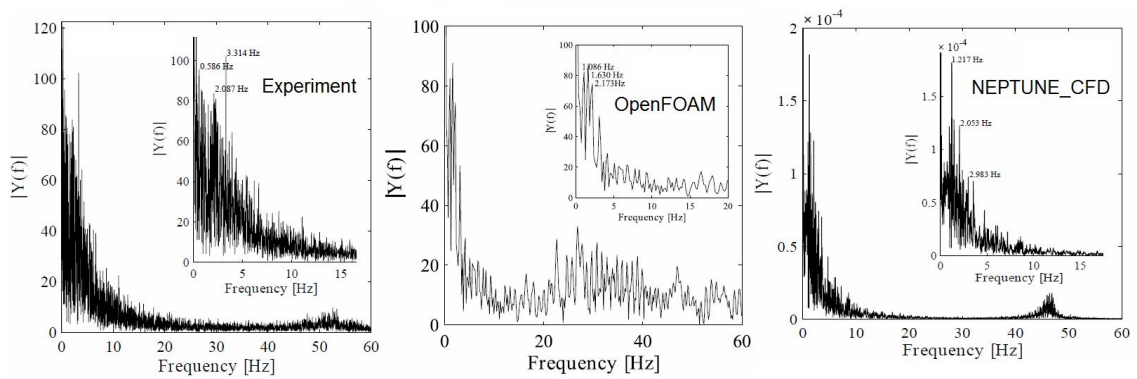


**Figure 8.** FFT from the recognized bubble volume in the PPOOLEX DCC-05-4 experiment, and in the corresponding 2D-axisymmetric OpenFOAM and NEPTUNE\_CFD simulations.

At VTT, the boiling and condensation models previously developed in the SAFIR program were during 2015 included in the two-phase solvers of the official OpenFOAM release in co-operation with the OpenFOAM Foundation. The goal was to avoid excessive maintenance of a separate solver code that structurally differs from the official OpenFOAM release. Even more importantly, the commonly available code allows efficient co-operation with OpenFOAM developers and other international partners. This has already resulted in improved solver performance and usability.

In 2016, the wall boiling models were extended to high void fractions and a framework was implemented for runtime selectable heat flux partitioning and wall boiling submodels. The boiling and condensation models were coupled to the Interfacial Area Transport Equation model (IATE) that allows modelling of bubble coalescence and break-up. The implemented models have been tested in simulations of DEBORA, NUPEC PWR Subchannel and Bundle Test (PSBT) and Large Water Loop (LWL) experiments.

The implemented models can be used by installing OpenFOAM development version from the OpenFOAM Foundation code repository. The thermal phase change and wall boiling support is included in a general-purpose two-phase solver called reactingTwoPhaseEulerFoam. The thermal phase change models consist of a two-resistance interfacial heat transfer formulation with user selectable heat transfer correlations and thermal diffusivity wall function that implement a version of the RPI wall-boiling model. The wall-boiling model has user selectable submodels for bubble departure diameter and frequency as well as nucleation site density. There are also user selectable correlations for the partitioning of the wall heat flux between the phases, which allows implementation of correlations that attempt to predict Departure from Nucleate Boiling (DNB). The selection of the implemented submodels can be easily extended by the users.

Figure 9 shows comparison of simulation and experimental results for the DEBORA5 subcooled nucleate boiling experiment (Manon, 2000). The simulated geometry is a 5 m long vertical pipe with a diameter of 19.2 mm. The heated section is 3.5 m tall and flowing liquid is R-12 at 26 bar pressure. Simulation results are shown for different turbulent dispersion coefficients and different bubble diameter modelling choices. The Lahey  $k-\epsilon$  turbulence model is applied with the Lopez de Bertodano turbulent dispersion model.

The simulation results show that with these models the turbulent dispersion coefficient has to be decreased to match the measured void fraction profile, if constant bubble diameter taken from the experimental results is used. If the Interfacial Area Transport Equations (IATE) model is instead used to determine the bubble diameter profile, the results are sensitive to the choice of the bubble departure diameter model. With the default coefficients both Tolubinski-Kostanchuk and Unal model predict departure diameters that are larger than the bubbles measure in the experiment. This delays the condensation of the vapour bubbles and results in the excessive void fraction and under predicted liquid temperature. The Tolubinski-Kostanchuk default coefficients have been fitted to pressurized water data and may not be realistic with the R-12 fluid used in the experiment. If the reference diameter of the bubbles is modified to match the measured diameter of the experiment (0.6 mm to 0.42 mm), the results match the experimental values quite well except for liquid superheat near the wall.

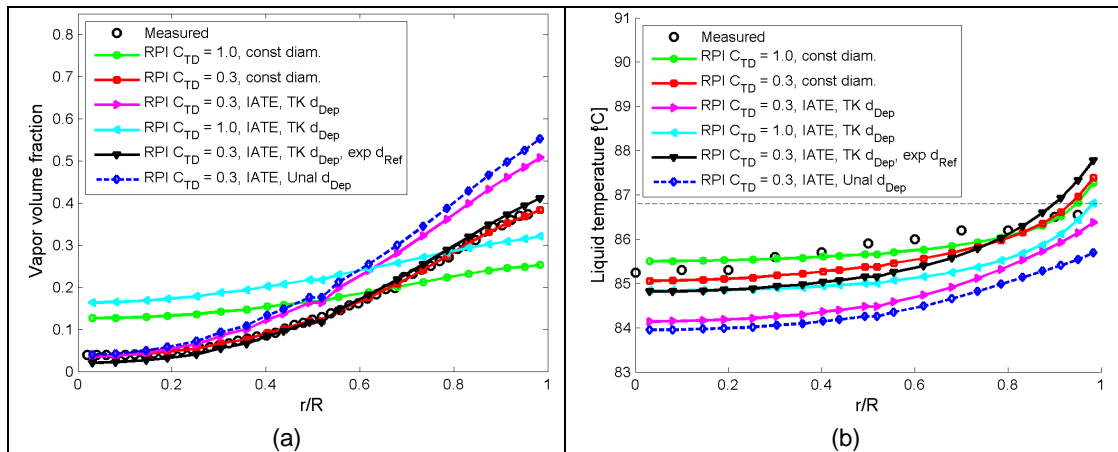
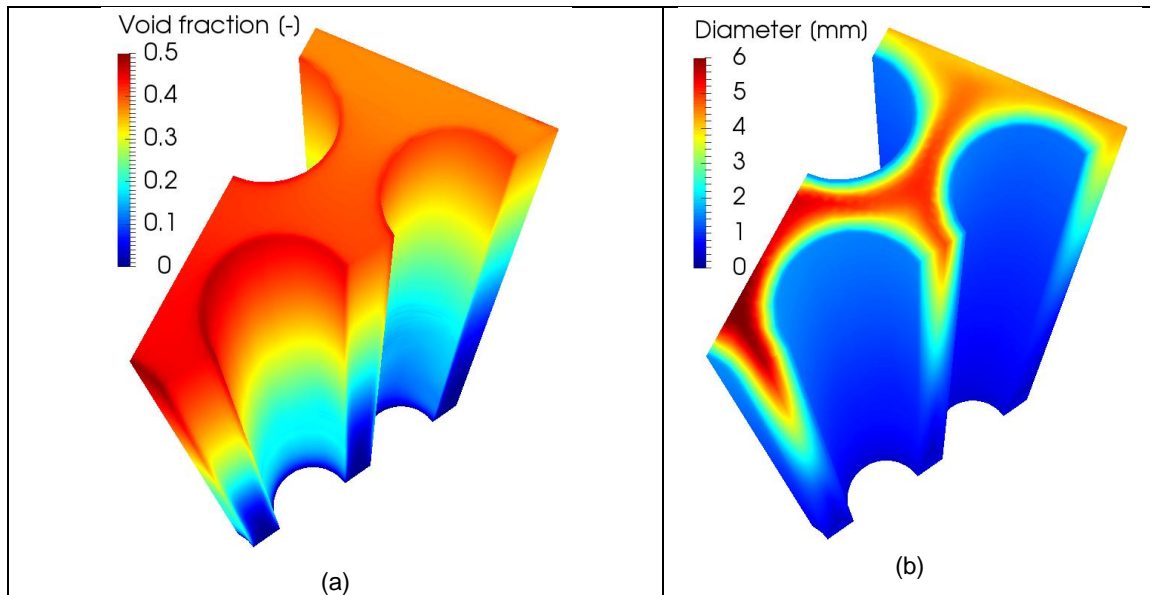


Figure 9. (a) Radial void fraction and (b) liquid temperature profiles of DEBORA5 simulations.



**Figure 10.** Void fraction (a) and bubble diameter (b) contours from a Large Water Loop simulation. The geometry has been scaled down vertically 1:50 for visualization.

Simulation to test the behaviour of the models when approaching Critical Heat Flux (CHF) are ongoing. The present test case is the Large Water Loop (LWL) facility at the Nuclear Machinery Plant, Skoda, Plzen Ltd. It is a 19-rod hexagonal bundle with pressurized water and the working fluid with thermal parameters similar to PWR reactors. Rods are heated electrically and the heated length is 3.5m. In the present simulation, spacer grids are neglected and symmetry is used to reduce to the computational domain to 1/12<sup>th</sup> of the full bundle. The whole 3.5 m heated length is simulated with fully developed inflow conditions. Figure 10 shows an example of calculated void fraction and bubble diameters. The closure models used in the presented simulation are the same as those used in the above DEBORA simulations with the IATE model and Tolubinki-Kostanchuk bubble departure diameter model. The LWL simulations will be continued to study the behaviour of the numerical model near CHF.

### Coupled CFD-Apros simulations of NPP components

Coupling of Apros system code and CFD code enables detailed three-dimensional modelling of one process component that is connected with a complicated system of pipelines and other process components. Two different types of coupling can be readily identified. In one-way coupling, Apros simulation provides boundary conditions for the CFD calculation, but no feedback from the CFD calculation to the Apros simulation occurs. In two-way coupling, the CFD code also provides boundary condition for the Apros simulation.

In 2016, coupling features of Apros 6 have been tested by coupling generic VVER-440 power plant model with CFD model of the steam generator. The plant model has been modified by replacing one of the steam generator models with an Apros model that describes the primary tubes in detailed manner. The plant model has then been coupled with the CFD model of the secondary side of the steam generator.

In Figure 11, the couplings of the codes are illustrated. The primary circuit is coupled to the CFD model of the steam generator, where heat transfer from the primary tubes to the secondary side is described in the ANSYS Fluent CFD model. The outflow of the steam generator is coupled to the Apros model of the steam line. The CFD model includes pressure difference measurement, which provides information to the water level control of the Apros model. Finally, feed water injection from Apros is coupled to the CFD model.

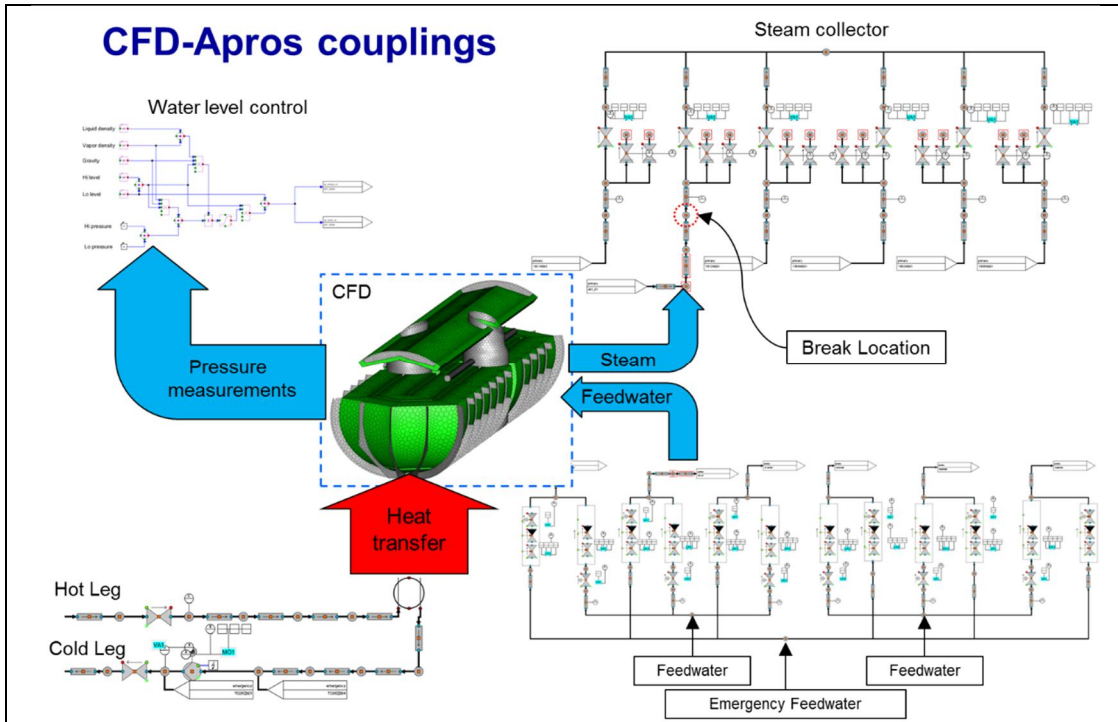


**Figure 11.** Two-way coupling of CFD model of steam generator with Apros 6 model of generic VVER-440 nuclear power plant.

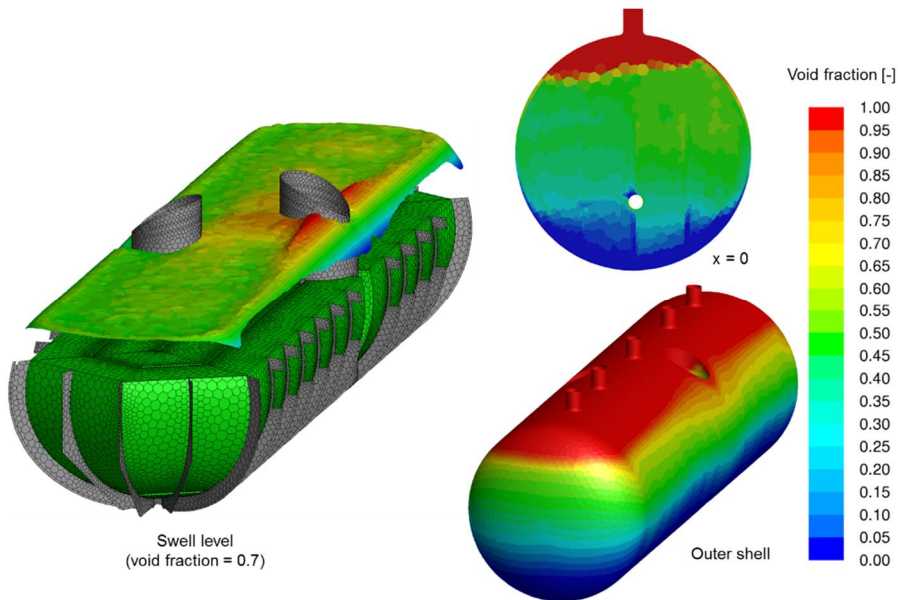


**Figure 12.** Stationary state of the VVER-440 steam generator at operational power calculated with two-way coupling of CFD model and Apros 6 plant model. Calculated swell level (left) and void fraction (right) are shown.

Two-way coupling has first been tested by calculating stationary operational state of the steam generator, which is illustrated in Figure 12. In the swell level, the difference between the hot and cold sides is

clearly visible. Near the hot collector, the swell level is higher than near the cold collector. The difference between the hot and cold sides is also clearly visible in the void fraction, which is larger on the hot side as is expected.

The model is being tested for the calculation of Main Steam Line Break (MSLB), which causes strong pressure transient on the secondary side of the steam generator. The two-way coupling with the plant model provides realistic boundary conditions for the behaviour of the primary circuit and feed water injection during the transient.

## Conclusions

In the calculations of thermal stratification and mixing, CFD calculations have provided quantitatively fairly accurate results. Experiment lasting almost four hours was calculated successfully. The quality of the numerical mesh was, however, once again found important for minimizing numerical diffusion, which mitigates thermal gradients in numerical results.

The role of the radiative heat transfer in containments should be further investigated. The results of the OECD/NEA HYMERES benchmark HP1\_6\_2 suggested that radiative heat transfer has an important role in some situations.

OpenFOAM has been shown to be useful tool in single-phase calculations of heat transfer in fuel rod bundles. The boiling models implemented in OpenFOAM have been validated against several experiments. The two-phase models implemented in the official release of OpenFOAM provide an efficient platform for further international development and validation work.

## Acknowledgement

The authors thank Mr. Markku Puustinen, Mr. Lauri Pyy and the staff of the INSTAB project for the data and co-operation in the modelling of PPOOLEX experiments.

## References

- Andreani, M., Daqiang, Y., Gaikwad, A.J., Ganju, S., et al., Synthesis of a blind CFD benchmark exercise based on a test in the PANDA facility addressing the stratification erosion by a vertical jet in presence of a flow obstruction, Application of CFD/CMFD Codes to Nuclear Reactor Safety and Design and their Experimental Validation, CFD4NRS-6, OECD/NEA & IAEA Workshop, September 13-15, 2016, Cambridge MA - USA.
- Hovi, V., Pättikangas, T., and Riikonen, V., 2016. Coupled one-dimensional and CFD models for the simulation of steam generators. Nuclear Engineering and Design 310 (2016), 93-111.
- Hujala, E., 2013. Evaluation of Bubble Formation and Break Up in Suppression Pools by Using Pattern Recognition Methods. Master thesis. Lappeenranta University of Technology. LUT Energy, Lappeenranta, Finland.
- Lahey, R., 2005. The simulation of multidimensional multiphase flows. Nucl. Eng. & Design 235, 1043-1060.
- Laine, J., Puustinen, M. and Räsänen, A., 2015. PPOOLEX experiments with a sparger. Nordic nuclear safety research, NKS-334.

- Launder, B., Spalding, D., 1974. The numerical computation of turbulent flows. *Comput. Meths. App. Mech. Eng.* 3 (2), 269–289.
- Manon, E., Contribution à l'analyse et à la modélisation locale des écoulements bouillants sous-saturés dans les conditions des Réacteurs à Eau sous Pression (Ph.D. Thesis), Ecole Centrale Paris, 2000.
- Pellegrini, M., Naitoh, M., Josey, C., Baglietto, E., 2015. Modeling of rayleightaylor instability for steam direct contact condensation, in: *The 16th International Topical Meeting on Nuclear Reactor Thermal Hydraulics (NURETH-16)*, Chicago, IL, August 30-September 4, p. 15.
- Puustinen, M., Laine, A. and Räsänen, A., 2015. Additional sparger tests in PPOOLEX with reduced number of injection holes. *Research Report INSTAB 1/2015*. Lappeenranta University of Technology. Lappeenranta 25.1.2016. 24 p. + app. 15 p.

## 5.5 Uncertainty and sensitivity analyses for reactor safety (USVA)

Asko Arkoma<sup>1</sup>, Torsti Alku<sup>1</sup>, Timo Ikonen<sup>1†</sup>, Maria Pusa<sup>1†</sup>, Elina Syrjälähti<sup>1</sup>, Ville Valtavirta<sup>1</sup>, Aarno Isotalo<sup>2†</sup>, Aapo Taavitsainen<sup>2†</sup>, Risto Vanhanen<sup>2†</sup>

<sup>1</sup>VTT Technical Research Centre of Finland Ltd  
P.O. Box 1000, FI-02044 Espoo

<sup>2</sup>Aalto University School of Science (currently working elsewhere)  
P.O.Box 11000, FI-00076 Aalto

†currently working elsewhere

### Abstract

In USVA, multidisciplinary uncertainty and sensitivity studies in reactor safety are done. The most important accomplishments of the project in 2015-2016 include a thorough comparison on statistical sensitivity analysis methods in the context of fuel behavior modelling (Ikonen, 2015, 2016), sensitivity analysis of local uncertainties in a 4-code calculation chain of a large break loss of coolant accident (LB-LOCA) (Arkoma and Ikonen, 2016a,b) and the development of an automated uncertainty analysis calculation system for the CASMO-4 – SIMULATE-3 calculation chain (Pusa, 2016). A Master's thesis was finalized at Aalto University on the combined uncertainty analysis of coupled neutron transport and fuel behaviour codes (Taavitsainen, 2016).

### Introduction

The general goal of the USVA project is to develop methods and practices in uncertainty and sensitivity analyses of multiphysics problems and calculation sequences in reactor safety. The goal supports the long-term aim of establishing a comprehensive methodology for uncertainty and sensitivity analysis for the entire reactor safety field. The project builds on the existing expertise in uncertainty and sensitivity analysis at VTT and Aalto University, and gathers the on-going research activities under one project. Also new experts in this area are trained. USVA promotes activities at the interfaces of the different disciplines in reactor safety.

In 2015, USVA had a high scientific level with a total of five peer-reviewed scientific papers (Ikonen, 2015, 2016; Arkoma and Ikonen, 2016a; Pusa, 2016; Vanhanen and Pusa, 2015). In addition, one special assignment was completed (Taavitsainen, 2015). In 2016, two scientific papers were prepared: conference paper on statistical and sensitivity analysis on LOCA (Arkoma and Ikonen 2016b), and a journal manuscript on CASMO-4 – SIMULATE-3 uncertainty propagation sequence (Pusa and Isotalo, 2016). Also, a Master's thesis was finalized at Aalto University (Taavitsainen, 2016). In addition, two extensive literature reviews have been done (Alku, 2017; Arkoma, 2016).

Many of the tasks in USVA are related to the topics of OECD/NEA Benchmark for Uncertainty Analysis in Modelling (UAM) for the Design, Operation and Safety Analysis of LWRs. The members of USVA have had an active participation in this benchmark during the first two years of USVA.

In the following, the various research topics studied in USVA 2015-2016 are explained item by item.

## Analysis of rod failures in LB-LOCA

A LB-LOCA in an EPR type power plant has been previously evaluated at VTT with statistical methods. In the analysis, the FRAPTRAN-GENFLO fuel behavior and thermal hydraulics code was used to estimate the percentage of failing rods in 59 global scenarios (Arkoma et al., 2015, 2016b). Each of the global scenarios involved calculating boundary conditions for the transient with APROS. In each of the global scenarios, 1000 FRAPTRAN-GENFLO simulations were performed, and in the worst scenario with respect to the number of failing rods, all the 63 835 rods were simulated. This data was made use of in the sensitivity analysis in USVA. Also, a comprehensive literature review on internationally applied uncertainty and sensitivity analysis methods in fuel modelling was done (Arkoma, 2016).

## Sensitivity analysis of local uncertainties in LB-LOCA simulations

In a previous statistical analysis on rod failures (Arkoma et al., 2015), the percentage of failing rods was analysed, but the underlying cause of rod failures was left undetermined. In 2015, the effect and importance of various local parameters, i.e. the location related parameters and the sampled fuel manufacturing parameters, to the outcome of chosen output parameters was studied (Arkoma and Ikonen 2016a). The results were further disseminated in TopFuel 2016 conference (Arkoma and Ikonen, 2016b), including some updates to the previous results (Arkoma et al., 2015; Arkoma and Ikonen 2016a).

At the moment, only the worst global scenario is considered but later on it is possible to include also the sensitivities of the global factors. The data originates from a 4-code chain: SIMULATE 3 (steady-state power histories), FRAPCON (steady-state fuel behaviour), APROS (transient power and thermal hydraulics), and FRAPTRAN-GENFLO (transient fuel behaviour). Due to complexity of the existing data, first the relevant input parameters for the sensitivity analysis have to be specified. Data visualization with a cobweb graph (Fig. 1a) is used for the screening. Then, selected sensitivity measures (Fig. 1b) are calculated between the chosen input and output parameters. The sensitivity indices calculated are the Borgonovo's delta measure, the first order Sobol' sensitivity index, and squared Pearson correlation coefficients. The first mentioned is a novelty in this context. As an outcome, the most relevant parameters with respect to the cladding integrity were determined to be the decay heat power during the transient, the thermal hydraulic conditions in the rod's location in the reactor, and the steady-state irradiation history of the rod as represented in this analysis by the rod burnup. Meanwhile, the tolerances in fuel manufacturing parameters were found to have negligible effect on cladding deformation. The outlined analysis procedure is general, and could be useful in analysing other types of complicated calculation sequences or simulations that produce correlated and sparse data.

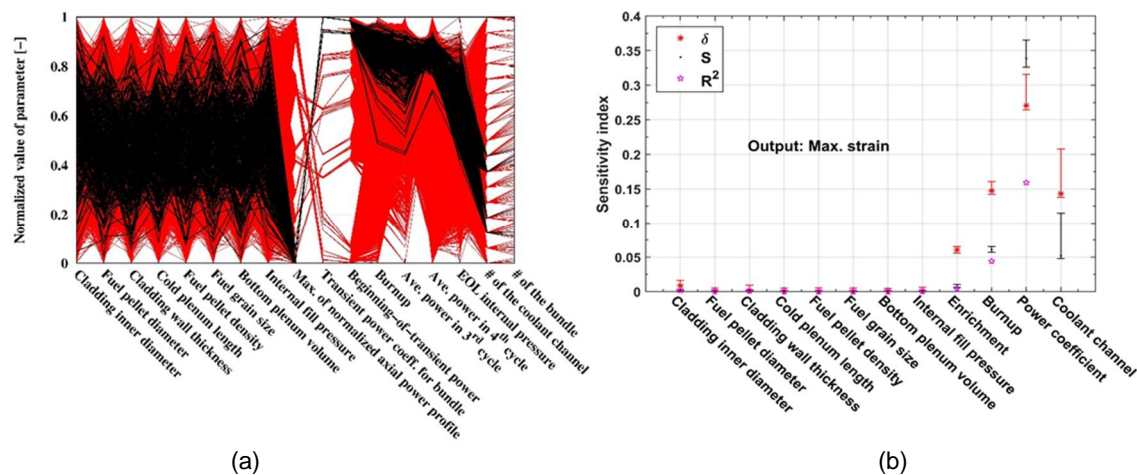


**Figure 1.** (a) Cobweb graph used for screening the most important input parameters. (b) Calculated sensitivity indices (Arkoma and Ikonen, 2016b).

## Applying Support Vector Machines to predict fuel failures in LOCA

As a part of the EPR LOCA analysis (Arkoma et al., 2015), the applicability of neural networks to predict the number of failing fuel rods was tested. A network was trained using the 1000 simulations from the worst global scenario. The network predictions were then compared to FRAPTRAN-GENFLO simulations results of all the rods in the reactor. It was discovered that the rods calculated by FRAPTRAN-GENFLO to survive were well predicted by the network to survive. However, a significant number of rods calculated to fail were not correctly predicted by the network. This can be understood by the fact that the number of failing rods used in teaching the network was very limited.

An alternative way to produce predictions from the existing data is to apply support vector machines (SVMs). SVMs have some advantages over neural networks; in this analysis, better performance in classification of the rods into failed/non-failed was expected. The analysis by SVM's has been initiated in 2016, divided into four phases: in the first phase, an SVM is fitted using the existing data from the 1000 FRAPTRAN-GENFLO simulations. The sensitivity analysis done in 2015 (Arkoma and Ikonen, 2016a), helps in selecting the relevant input variables used for fitting the SVM. In the second phase, the fitted SVM is applied with new input parameter values to obtain more predictions of rods that could possibly fail. In the third phase, additional FRAPTRAN-GENFLO simulations are made using the input values of those rods that the SVM predicts to fail. Now we have more simulation results regarding the failing rods, and the SVM may be improved with this data. Fitting the SVM anew is the last phase. With this procedure, and by using SVMs, the accuracy of the predictions is improved substantially, as seen in Fig. 2. In the coming years of USVA, the SVM's will be applied for each global scenario to capture the global effects. In addition, the SVM model can be used in sensitivity analysis within the global scenarios.

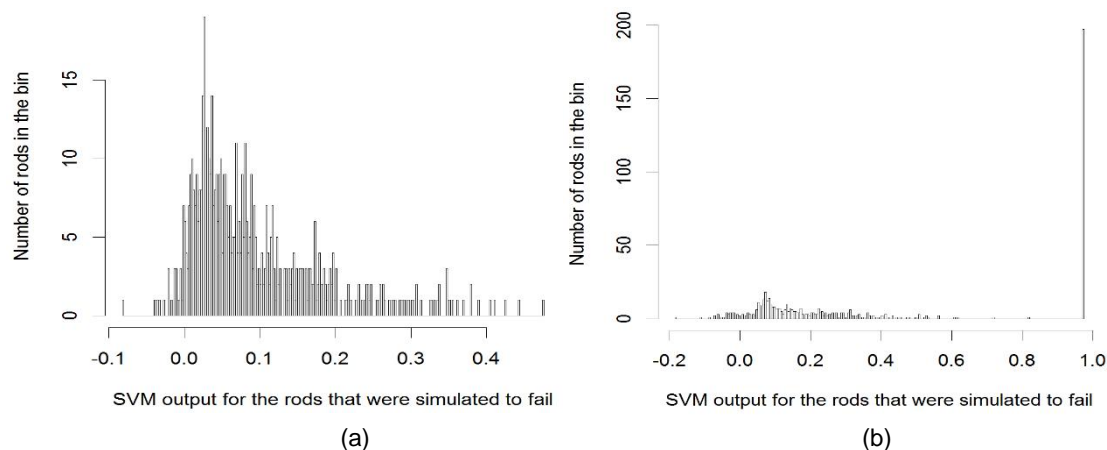


**Figure 2.** SVM outputs that correspond to failed rods in FRAPTRAN-GENFLO simulations of all those rods in the reactor that had been in-core for two cycles. The first SVM predictions (a) did not succeed so well (zero stands for survival of rod, unity being the rod failure), but after selecting new cases with the SVM that are susceptible to failure (SVM predictions > 0.1) and training the SVM anew, the SVM predictions are substantially improved (b). Here, SVM was used in regression mode, which produces non-binary outputs. In classification mode, binary information with probabilities whether the rod is predicted to fail or not, is obtained.

### Methodology for determining input uncertainties in thermal hydraulics simulations

In the OECD/NEA PREMIUM benchmark, it was distinguished that the methods for the uncertainty assessment of thermal hydraulics codes' models needs to be further studied. Particularly, the identification of the uncertain input parameters and defining their PDFs for the physical models that the thermal hydraulic

safety codes rely on, is challenging. These models have been built based on fitting to experimental data and laws of physics. To start with, a literature review was prepared (Alku, 2017). In the review, the existing methods used to quantify the uncertainty in thermal hydraulics codes were studied. In addition, methods used in other disciplines were considered and their applicability to nuclear safety codes were studied. The first objective of the review was to be able to identify the most promising approaches and to set up guidelines on the research for the upcoming years. In the report, the methods introduced in the PREMIUM benchmark were briefly presented before standard methods for solving inverse problems in the field of statistical inversion theory were described. A combination of existing methods in engineering physics is proposed as the solution to the quantification problem. The work will continue based on the recommendations of the review.

### Sensitivity analysis of fuel behavior

The influence of uncertainties in fuel performance simulations was studied (Ikonen, 2015, 2016). Based on previous experience, there was a need to review the various commonly used and also novel statistical methods that could be used to extract sensitivity information from the computational model. Several global sensitivity analysis methods were compared to assess their efficiency and applicability to nuclear fuel performance simulations (Fig. 3). The implications of large input uncertainties and complex models were analysed. Such a comparison was done on an existing data set of steady-state FRAPCON simulations, revealing several intricacies in the data. Depending on the considered output, the required fidelity varies. Hence, relying on a simple analysis method is not advisable. Instead, as a result of the work, a strategy is proposed that uses a mixture of various methods efficiently, so that comprehensive information can be extracted at a modest computational cost.

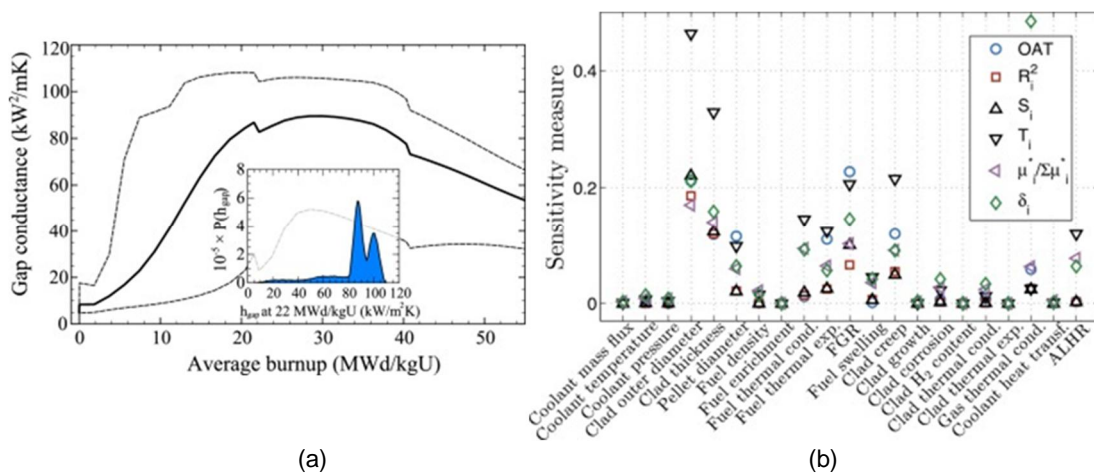


**Figure 3.** (a) The uncertainty distribution of the gap conductance, and (b) the sensitivity measures evaluated for the various input factors at the burnup of 22 MWd/kgU in a TMI-1 PWR rod according to FRAPCON simulations (Ikonen, 2016). The scatter in the sensitivity measures between the various methods and the multimodal probability distribution reveal the complexity of the data that calls for specific sensitivity analysis strategies.

### Method for the uncertainty analysis of nuclear fuel and neutronics

In the framework of coupled code systems, the objective was to study the combined uncertainty analysis of coupled neutron transport and fuel behaviour codes for a simple test case. A Master's thesis was written on the subject (Taavitsainen, 2016). Firstly, a computational system coupling the fuel behaviour code

FINIX and the reactor physics code DRAGON was set up and applied to the PWR pincell test case of UAM benchmark. A special assignment was completed on constructing the FINIX-DRAGON calculation system (Taavitsainen, 2015). Secondly, the nuclear data code NJOY was coupled to the calculation system to allow uncertainty analysis. The most important aspect was to find out if the uncertainties in nuclear fuel modelling and neutronics modelling may be handled separately. As an outcome, these may indeed be propagated separately.

A methodology named “CFENSS-SRS” (Coupled Fuel Behaviour and Neutronics Stochastic Sampling with Simple Random Sampling) was developed for the purpose of this work. The method applies the statistical uncertainty analysis to univariate nuclear fuel parameters and correlated neutron cross sections (Taavitsainen, 2016).

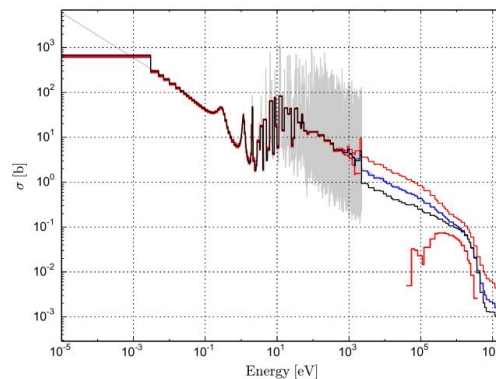


**Figure 4.** Nuclear data random sampling for the capture cross section of U-235. The red curves bound a 95% normal distribution confidence interval on both sides of the blue best estimate average curve. The black curve represents the perturbed average cross sections while the whitened background curve is for the pointwise data. Occasionally the lower red curve disappears by dropping to negative values and outside the used scale. (Taavitsainen, 2016)

#### **Nuclear data uncertainty propagation in full-core calculation sequences**

In the context of calculation sequences, the idea was to continue the work carried out in the CRISTAL project of SAFIR 2014 programme. Adjoint-based sensitivity and uncertainty analysis capability had previously been implemented to the assembly-level reactor physics code CASMO-4. In USVA, the implementation enabled the uncertainty analysis of assembly constants that were then passed on to codes simulating a full reactor core. In order to be able to propagate uncertainty through core-level simulations in a consistent manner, the methodology was extended to reflector regions. An automated calculation system was developed for propagating nuclear data uncertainty through assembly-level homogenization calculations with CASMO-4 in fresh fuel cases. Nuclear data uncertainty was propagated through the CASMO-4 – SIMULATE-3 (see Fig. 5) and CASMO-4 – TRAB3D-SMABRE calculation sequences with application to the PWR TMI-1 scenario. The results were published in (Pusa, 2016). The differences between covariance libraries have been studied, and a journal paper was published on the topic in 2015 (Vanhanen and Pusa, 2015). In addition, one objective was to test the methodology for a transient simulation with TRAB-3D/SMABRE (Fig. 6). All these goals were achieved.

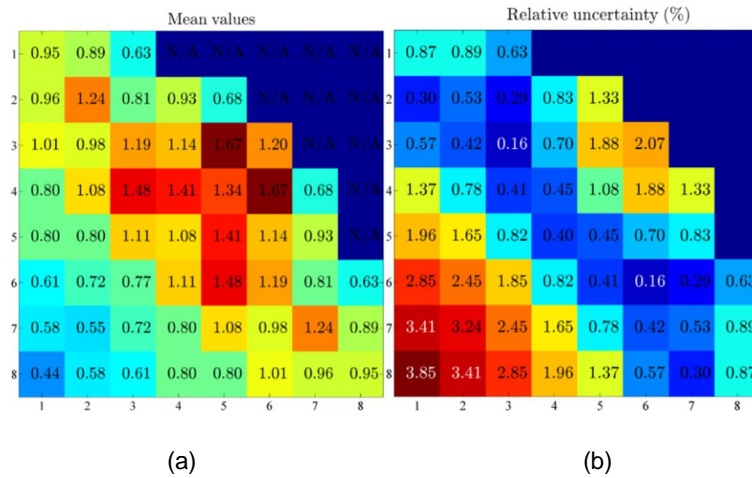


**Figure 5.** (a) Radial power distribution, and (b) respective uncertainties for a PWR modelled using CASMO-4 -- SIMULATE 3 uncertainty analysis sequence (Pusa, 2016).

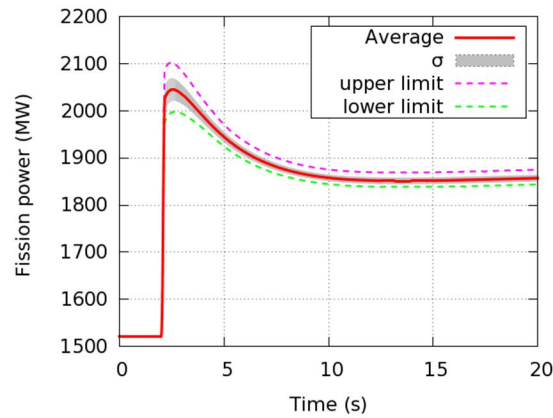


**Figure 6.** PWR control rod ejection transient simulated with CASMO-4 – TRAB3D uncertainty analysis sequence.

As mentioned above, the previously implemented uncertainty analysis capability CASMO-4 – SIMULATE-3 calculation sequence is based on the two-step approach. Namely, the adjoint-based method is used to compute the sensitivity profiles of assembly constants after which the corresponding uncertainties are propagated statistically through core-level simulations. In 2016, the two-step method was compared with a statistical approach. In the statistical approach, a large number of cross-section libraries were generated with Serpent using random samples of nuclear data. The two approaches were found to produce consistent best estimates, but unexplained deviations still remained in the uncertainties. A journal article on the CASMO-4 -- SIMULATE-3 uncertainty propagation sequence was finalized without the Serpent results, and the manuscript was submitted to Annals of Nuclear Energy (Pusa and Isotalo, 2016).

## Future plans

The research into using Support Vector Machines (SVMs) as a low computational cost statistical analysis tool for predicting rod failures in LB-LOCAs continues in the upcoming years. The possibility to also use the SVMs for sensitivity analyses regarding the cladding integrity will be one of the research topics while the other includes applying SVMs to multiple of the global scenarios included in the LB-LOCA analysis (Arkoma et al., 2015, 2016b).

The first half of the USVA project included a literature review that studied different methods for quantifying uncertainties in the physical models of thermal-hydraulic codes used in nuclear safety applications. Multiple suitable methods could be identified in the review and the application of these methods to a proof-of-concept uncertainty quantification problem will be accomplished in the latter half of the project.

Two new directions of research will also be started on the second half of the project:

Firstly, methods for uncertainty quantification in coupled fuel performance - reactor dynamics are developed. The initial focus will be in the accounting for the burnup dependence of the initial state of the transient.

Secondly a novel collision history based methodology for Generalized Perturbation Theory (GPT) based sensitivity/uncertainty analyses will be implemented in the Serpent Monte Carlo code. This methodology has applications in quantifying sensitivities/uncertainties coming not only from nuclear data (cross sections, fission spectra, scattering distributions) but also from temperature and density distributions or nuclide concentrations, which is promising for future research in the uncertainty quantification in coupled calculations and burnup calculations.

## References

- Alku, T., 2017. Methods for the quantification of uncertainties related to Apros' physical models, VTT Research report, VTT-R-00571-17
- Arkoma, A., 2016. Uncertainty and sensitivity analysis methods in nuclear fuel modelling – a literature review, VTT Research Report, VTT-R-05086-16
- Arkoma, A., Hänninen, M., Rantamäki, K., Kurki, J., and Hämäläinen, A., 2015. Statistical analysis of fuel failures in large break loss-of-coolant accident (LB-LOCA) in EPR type nuclear power plant, Nuclear Engineering and Design Vol. 285, pp. 1–14
- Arkoma, A., Ikonen, T., 2016a. Sensitivity analysis of local uncertainties in large break loss-of-coolant accident (LB-LOCA) thermo-mechanical simulations, Nuclear Engineering and Design Vol. 305, pp. 293-302. <http://dx.doi.org/10.1016/j.nucengdes.2016.06.002>
- Arkoma, A., Ikonen, T., 2016b. Statistical and sensitivity analysis of failing rods in EPR LB-LOCA. In proceedings of: TopFuel 2016, Boise, Idaho, U.S.A., September 11-16, 2016, Paper no. 17570
- Ikonen, T., 2016. Comparison of global sensitivity analysis methods – Application to fuel behavior modeling”, Nuclear Engineering and Design, Vol. 297, pp. 72-80  
<http://dx.doi.org/10.1016/j.nucengdes.2015.11.025>
- Ikonen, T., 2015. Global sensitivity analysis in fuel performance modelling, In proceedings of TopFuel 2015, September 13–17, Zurich, Switzerland
- Vanhanen, R. and Pusa, M., 2015. Survey of prediction capabilities of three nuclear data libraries for a PWR application. Annals of Nuclear Energy, Vol. 83, pp. 408-421  
<http://dx.doi.org/10.1016/j.anucene.2015.03.044>

- Pusa, M., 2016. Uncertainty analysis of assembly and core-level calculations with application to CASMO-4 and SIMULATE-3, in proceedings of PHYSOR 2016
- Pusa, M., Isotalo, A., 2016. Uncertainty analysis of assembly and core-level calculations with application to CASMO-4 and SIMULATE-3. Manuscript submitted to Annals of Nuclear Energy
- Taavitsainen, A., 2016. CFENSS-SRS method for the uncertainty analysis of nuclear fuel and neutronics, Thesis for the degree of Master of Science in Technology, Aalto University, School of Science.
- Taavitsainen, A., 2015. Coupled FINIX-DRAGON Calculation Chain for an LWR Pin Cell Case, Special Assignment, Aalto university

## 6. Structural integrity

### 6.1 Condition monitoring, thermal and radiation degradation of polymers inside NPP containments (COMRADE)

Konsta Sipilä<sup>1</sup>, Harri Joki<sup>1</sup>, Tiina Lavonen<sup>1</sup>, Antti Paajanen<sup>1</sup>, Sami Penttilä<sup>1</sup>, Marcus Granlund<sup>2</sup>, Anna Bondesson<sup>2</sup>, Anna Jansson<sup>2</sup>

<sup>1</sup>VTT Technical Research Centre of Finland Ltd  
P.O. Box 1000, FI-02044 Espoo

<sup>2</sup>SP Technical Research Institute of Sweden  
Brinellgatan 4 Box 857, SE-501 15 Borås

#### Abstract

Polymer based materials are used in wide range of applications inside nuclear power plant containments e.g. cables, sealants, paint coatings, lubricants and greases. During their designed life time and accidental scenarios they are exposed to stressors such as heat and ionizing radiation. COMRADE was developed to gain better understanding in setting acceptance criterion for polymer components, search for representative components for ageing studies, studying ageing effects on polymers experimentally and by means of computational material science. After one year of studies, preliminary acceptance criterion has been set for EPDM o-rings, which will be defined in more detail during future studies and broadened to include different materials and o-ring sizes. Attempt towards acquiring “in service” materials for ageing studies has been broadened to comprehend also currently running nuclear power plants. As part of modelling work it was concluded that modelling tools for the ageing of semi-crystalline polymers is currently lacking and future work is focused on that. The synergistic effects of radiation and heat were evaluated on EPDM and CSM and it seems that during a DBA, the radiation is more detrimental for EPDM than heat, as increasing temperature (up to 125°C) can hinder the degradation when simultaneous irradiation treatment is applied. For oxidation profile measurements it was concluded that ToF SIMS would be the most suitable technique out of two others tested. Finally, different semi-empirical methods were identified which could be used in evaluation of severity of dose rate effect if sufficient experimental data existed.

#### Introduction

Different polymer based materials are widely used in various applications in nuclear power plants and inside containments, e.g. cable jacketing/insulators, sealants, paint coatings, lubricants and greases. As any other material or component, polymers are susceptible to ageing. Elevated temperature, ionizing radiation and moisture are considered to be the most important ageing stressors and they tend to interact with the polymer structure in different ways. In addition to these ageing stressors, properties of polymer blend,

e.g. crystallinity degree, amount of fillers and antioxidants, has an effect to the ageing behaviour. Thus the degradation mechanism can be quite complex.

Proper ageing management procedures are based on knowledge on the ageing behaviour and how to set correct requirements for the used polymer components that they will endure their designed lifetime. The ageing behaviour needs to be known when polymer components are qualified. Accelerated ageing is used as part of the artificial ageing of the qualified polymer and the ageing mechanism should be the same as in the real service environment in order to yield in identical ageing conditions. Thus the effects of dose rate and temperature to the ageing mechanism must be known as well as the synergistic effects rising from the simultaneous and/or sequential exposure to ionizing radiation and excess heat.

The requirements that guarantee the proper and safe use of a polymer or any other component are defined as acceptance criteria and they can be used as part of qualification or annual inspections of components. An acceptance criterion for a polymer component is usually a material property that represents the material health, e.g. for cable jacketing materials typical acceptance criterion is 50% of elongation at break and in case of sealants compression set is used. However, the use of such secondary material properties that do not represent the actual functional property of the component (such as tightness of a sealant) must be used with care and excess amount of data should exist which correlates the secondary material property to the actual functional property. In addition destructive measurements cannot be conducted on materials that are already in use. Thus there is a demand for non-destructive techniques that can be used in inspections and qualifications of polymer components as well as defining acceptance criterion for specific component types. These techniques should also provide a possibility to extrapolate the remaining lifetime for components.

COMRADE is developed based on input from a feasibility studies from Energiforsk AB [Granlund et al. 2015] and STUK [Penttilä et al. 2016] and through discussions between VTT, SP and the Nordic NPPs through Energiforsk. When developing COMRADE it was understood that there are gaps in knowledge for setting functional based acceptance criteria at the nuclear power plants. Furthermore a need in gaining a better understanding on how a polymeric component reacts to different levels of low dose ionizing radiation and synergistic effects between thermo-oxidative and radiation degradation was identified. These issues are furthermore studied in three different work packages (WPs) and their content and results are described below.

## **Development of condition monitoring methods for polymeric components including low dose rate radiation exposure**

The first year of COMRADE project has been concluded and WP1 is at the final stage of the first ageing test. A peroxide cured EPDM o-ring at standard cord size 3.53 mm and test sheets from the same batch for dumb bells provided by James walker Ltd was used for the test. Test blocks for tightness test of the o-rings were manufactured by SP fitted to the correct o-ring size. The accelerated ageing test was done in sequence irradiation – heat – irradiation – heat at three different temperatures. Both o-rings and dumb bell test specimen were used in the accelerated ageing. In parallel to the samples treated by radiation the same set of samples were aged in heat. The starting point and the second evaluation point was completed and presented at the workshop in September. The third evaluation was completed in middle of January 2017 and the fourth and last was completed in the middle of February.

In task 1.2 Implementation phase, there was a specific question from one of the plants regarding distinguishing between sulphur and peroxide cured EPDM. The use of XRF-analysis was tested to analyse the sulphur content from the Sulphur cured o-rings. Reference measurements on peroxide cured o-rings were also conducted in order to evaluate whether the method could detect the sulphur from the vulcanisation system used in the o-rings.

## Methods

The ageing was completed using both radiation and heat. During the ageing samples were taken out to be analyzed at 4 evaluation points plus a reference sample. At each evaluation properties tested were oxidation induction temperature (OITe), tensile, hardness and compression set. Fourier Transform Infrared spectroscopy (FTIR) was tested but did not provide any details due to the carbon black filler. Nuclear Magnetic Resonance (NMR) was tested for 3 samples to see if any conclusions could be made. Relaxation was not tested due to the samples being too thin but this will be included in the 2017 test instead.

The tightness test was done using a blaster for hoses. The pressurized medium was water at room temperature and the maximum pressure was set to 110 bar for 45-60 seconds. The ramp up from 1 to 110 bar was done in 60 seconds. The test was done using the sample holder in figure 2. The o-ring was mounted in its position (red arrow figure 2) and screwed together. The o-ring was placed on a flat surface with support on the outer diameter. An air screw on top of the test block was closed after filling of water. The test block was tested initially without a o-ring to see at what pressure leak started. At 10 bar first leak indication was shown and at 30 bar a continuous flow of water came through the leak indicators. The leak indicator can be seen in figure 3 marked by red arrow. After the analysis of the samples they are scrapped.

Differential Scanning Calorimeter (DSC – OITe) test was conducted on samples prepared from the used dumb bells. The testing procedure followed ISO 11357-6.

The tensile test was done according to ISO 37. Sample dimensions of 85 x 10 x 2 mm were used. At the initial sampling (reference point) a series of 10 samples were tested. This was done to achieve a better understanding on how much the samples may differ. For each sampling point two samples were available for testing.

Hardness was measured using the dumb bells. The measurement followed standard IRHD-m (Shore A) and three measurement points leading to an average value.

Compression set was measured on the o-rings. After the tightness test the o-rings were placed in the constant climate enough time to dry up. The test was done according to standard ISO 815.



**Figure 1.** Test block not mounted to the left and mounted to the right.

## Materials

A peroxide cured Ethylene Propylene Diene Monomer (EPDM) has been used for the ageing study. This was chosen based on a request from the Industry team where the most suitable material to test was asked for. The delivered samples were

- o-rings (42 pcs of 50-217 with cord diameter of 3.53 mm)
- sheets (4 test pieces 2 x 290 x 290 mm)

## Accelerated ageing

The accelerated ageing was done in sequence with radiation – heat – radiation – heat. A study in WP3 is done to the sequence of ageing which can be taken into account for the next ageing test. It has been shown that starting with radiation creates more degradation than starting with heat. A parallel aging was done without the radiation treatment. In total 6 months of heat treatment and 14-18 kGy in total dose was used in the ageing process.

The thermo-oxidative ageing was done using 3 different temperatures; 90°C, 120°C, 140°C. The ovens did not have any controlled air flow. A monitoring system was used to monitor the temperature and the curves are available in the project report. The treatment was done according to the following time periods 2 months, 1 month, 2 month, 1 month.

The radiation treatment was done at VTT Technical Research Centre of Finland Ltd. The Gammacell® 220 used a Co-60 source with dose rate 67.35 Gy/h (measured 2016-03-06). The typical dose distribution of the sample cell can be found in the project report. Because of the dose distribution not being 100% in the entire chamber a time correction to the irradiation time depending on the size of the sample was done. The cell dimensions are height: 20.6 cm and inner diameter: 15.2 cm. This sets limitations on how large o-rings can be tested. The irradiation treatment is done in 2 sequences, as explained in the Accelerated ageing section, during 13 days per sequence with dose rate of 29 Gy/h leading to a total dose of 7-9.07 kGy per sequence. Dose rate 29 Gy/h was achieved by using lead shielding with 2.74 cm thickness. The dose rate was calculated based on the material in the test block and the wall thickness of the test block. The temperature in the cell is around room temperature (23°C). The chamber is tight and filled with air from the start.

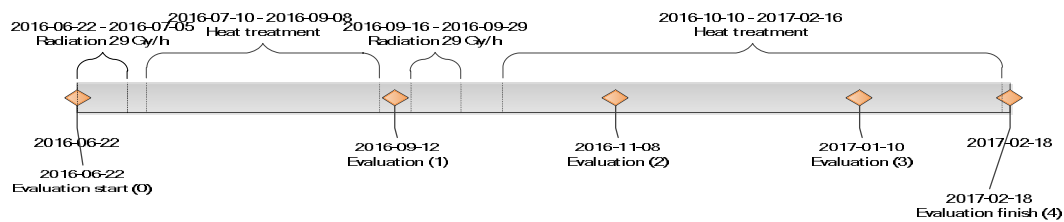


**Figure 2.** The time line for ageing process.

## Results and discussion

OITe measurement results are presented in Figure 3. As can be seen, there is very little difference between the irradiated and non-irradiated samples. It seems to be the temperature that provides a greater difference to the OITe. Tensile testing results are presented in Figure 4. The results do not show a similar trend as for the compression set. However, a difference between the irradiated and non irradiated samples is difficult to distinguish. There is very little difference between the irradiated and not irradiated samples as can be seen from Figure 5. Compression set measurement results are presented in Figure 6. A reference sample was made in 23°C with holding time of 72 hours resulting in 4,9%. Average thickness for the o-rings were used measured on 10 samples being 3,517 mm. There is a variation in the testing with 17%-22% compression giving us a similar measurement error in the reported values. There is very little difference between the irradiated and not irradiated samples.

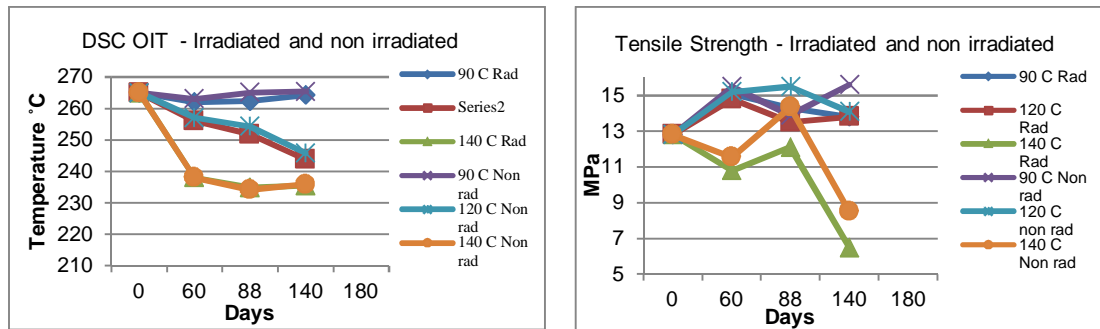


**Figure 3 and 4.** DSC OITe and Tensile strength for irradiated and non-irradiated samples.

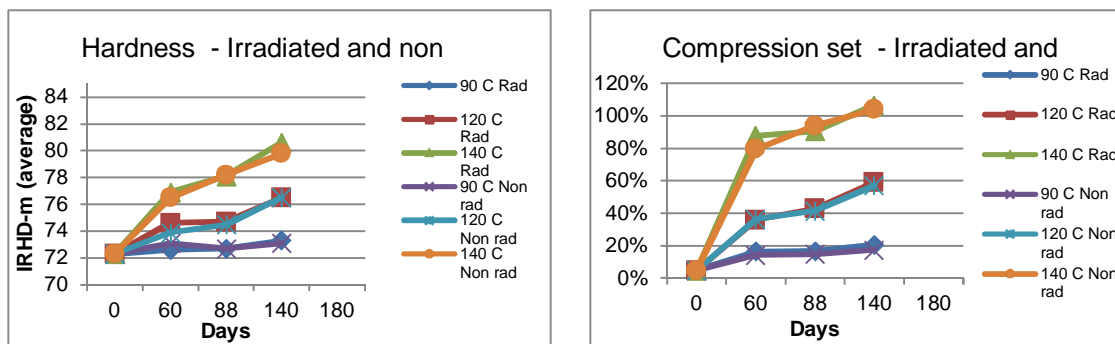


**Figure 5 and 6.** Hardness and compression set for irradiated and non-irradiated samples.

The first goal of this work package was to correlate a function, in this case tightness, to a material property. The tightness failed for the first time for the o-ring running in 140 °C (both irradiated and not irradiated) at evaluation 3. This is after 5 months of heat and 4 weeks of irradiation. The material property is compression set (105%), hardness (80), elongation at break (50%), tensile strength (7,5 MPa) and DSC – OITe (235,9°C). As can be seen in evaluation 2 for the same temperature the function is still working even though material property for compression set being above 90% and elongation at break with a decrease of 41% thus indicating severe material degradation. This indicates that very high material degradation is needed before the o-ring stops to function. The NMR indicates that there are differences between the irradiated and non-irradiated samples. It is difficult to see though how this would help the end of life estimation but a further analysis to the peak in the irradiated samples would be of interest. An evaluation of the o-rings that started to leak would also be of interest to see if the peak grows. Based on the current ageing treatments, the end of life criteria defined as different material properties are shown in Table 1.

**Table 1.** Summary of properties for the initial value and for when it has reach the end of life for the function tightness.

Property	End of life	Initial value
Compression set	105%	4,9%
Hardness	80	72,3
Elongation at break	50%	182%
Tensile strength	7,5 MPa	12,8 MPa
DSC – OITe	235,9°C	265°C

End of life is defined as when the o-ring stops to function. This has however yet only been reached for the ageing running in 140°C. By looking at the trends for the ageing running in 90°C and 120°C it may not be reached in the last month of aging. A faster degradation could occur so until the last evaluation has been completed it cannot be said for sure that it will not reach the end of life criteria.

No experimental test has been done using material from a power plant. The pre study in WP2 will show what material is available and after that a small scale test can be started in WP1 to achieve the goal to validate the test method for the function of tightness. This will further be strengthened once the modeling in WP1 task 1.3 has been compared to the result from the small scale test. If a leaking, or otherwise failed polymeric component, can be found in the power plants it would be interesting to have those in the small scale test as well.

The Arrhenius diagram plotted in the project report shows 3 different activation energies for the 3 different temperatures. Looking at the curve with or without radiation there is very little difference indicating the gamma radiation absorbed during normal service life to have little effect in the overall change in material property on a macro scale. For the second ageing test a change in sampling will be done due to this. As it was tested in the first ageing the sampling was taken after radiation plus heat. In the second aging the sampling will be done directly after irradiation to see if a larger difference can be seen.

An evaluation of material properties looking at thickness profile of the o-ring was not done since the samples were thin (3,5 mm). The expectation on the samples was that it would be difficult to see the difference on the surface compared to the bulk of the o-ring. This will however be studied in the next ageing test where the thickness will be around 7 mm.

## **Survey on polymeric materials available for ageing studies from Barsebäck plant under decommissioning**

Acquiring aged components from real service conditions and studying their material properties could provide more detailed information on degradation mechanisms and kinetics occurring in real service conditions. This information would be valuable when accelerated ageing treatments that aim to simulate the real ageing conditions are validated. The available materials can be used to verify the O-ring condition monitoring method developed in COMRADE-project (WP1) and degradation process studies (WP3).

Two material experts related to Barsebäck polymer components were interviewed in order to clarify whether the used components could be taken out from the plant for ageing studies. The polymer components available for ageing study and which service conditions are well documented are few in numbers. Also radiological clearances and the related precautions to working with decontaminated materials yield in complicated and costly material acquisition. More feasible way to obtain used materials from properly documented service environments would be acquiring materials from running plants during annual take outs. For this purpose a questionnaire is introduced to NPP polymer material experts (via COMRADE industry group) to obtain data on different polymers available to study. The questionnaire will compile the materials that interesting for industry and the project team, materials available from different Nordic NPPs and their service history. This work will be continued within COMRADE-project during year 2017.

## **Polymer ageing mechanisms and effects inside NPP containments**

The ageing environment for polymers within the containments of NPPs is rather complicated. During normal service of NPP the temperature within the containment can be tens of degrees beyond room temperature. Also radiation levels can vary from less than mGy/h to Gy/h. [Penttilä, 2016] So called hot spots with elevated temperature and higher dose rates are located in the vicinity of steam generator tubing or in process valves. Thus polymer components are subjected to various stressors such as heat, radiation and moisture. In the both cases of thermal and radiation ageing, oxidation is considered to be the most common and dominating degradation mechanism. [Bartonicek & al] Oxidation of polymers is due to polymer

radicals that are formed by thermal or radiation energy. These radicals react with oxygen forming peroxy radical which further reacts with the polymer chain forming hydroperoxide and polymer radicals. Hydroperoxide thermally decomposes to species that cause chain scission. Under radiation oxygen diffusion can be thus detrimental for polymers in room temperature and it is accelerated by increased temperature. The further complicating factor is diffusion-limited oxidation which has an effect to the oxidation behaviour of polymers. [Celina & al]

In Work Package 3 the effects of radiation and heat on polymer degradation are evaluated. Relevant issues that are under interest and have an effect to practical applications include use of modelling tools in simulating polymer ageing mechanism and possible development of predictive ageing methods based on computational material science, ageing effects and procedures in simulated accidental conditions, diffusion limited oxidation and dose rate effect.

### **Modelling tools for synergistic effects of radiation and heat**

A literature survey was completed in 2016 on the synergistic effects of temperature and radiation in polymer ageing, and on possible ways of considering them in the lifetime prediction of nuclear power plant components. The following topics were looked into in more detail: the proposed mechanisms behind the synergistic effects, material modelling methods feasible for studying ageing and an overview of previous research related to the topic.

The mechanisms underlying combined thermal and radiation ageing can be exceedingly complex, involving various chemical and physical processes across multiple structural and time scales. Probably due to this, practical lifetime prediction methods are semi-empirical and based on accelerated ageing experiments. Methods applicable to combined thermal and radiation ageing include the superposition of time-dependent data method, and the superposition of dose-to-equivalent-damage data method. The semi-empirical methods are limited in their predictive capability, as they cannot address possible changes in the dominant ageing mechanisms. For this reason, anomalous ageing phenomena such as the reverse temperature effect can render their predictions useless.

Mechanistic details of both thermal and radiation ageing can be addressed with the theoretical tools of computational materials science, as can be seen from Figure 7. For example, electronic structure calculations can be used to assess the feasibility of proposed reaction paths, and to predict the associated kinetics. At the other end of the spectrum, finite element analysis can be used to study how ageing-induced microstructural changes translate into the degradation of mechanical properties. Nevertheless, there remains a formidable gap between the present multi-scale materials modelling capabilities and practical lifetime prediction. Bridging the gap is clearly beyond the resources available in the context of the SAFIR2018 programme. However, modelling focused on a particular synergistic mechanism or some other relevant detail of the ageing process is feasible.

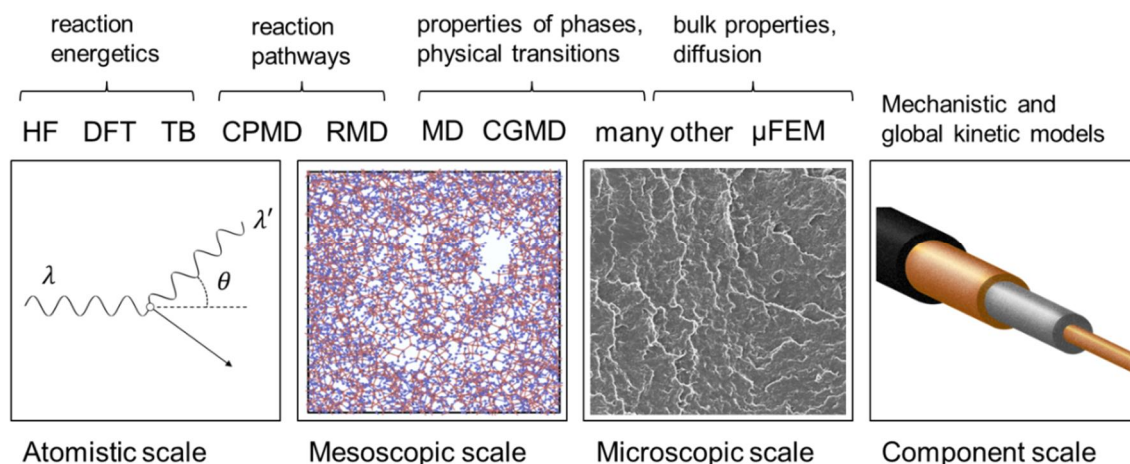


**Figure 7.** Scales and processes of thermal and radiation ageing coupled with numerical modelling methods. Abbreviations for the following modelling techniques: HF = Hartree-Fock method, DFT = Density-functional theory, TB = Tight-binding method, CPMD = Car-Parrinello molecular dynamics, RMD = Reactive molecular dynamics, MD = Classical molecular dynamics, CGMD = Coarse-grained molecular dynamics, FEM = Finite element method.

### Polymer ageing during DBA

During a DBA polymer components will be exposed to high temperatures and dose rates. It is not clear that which stressor causes greater amount of degradation to the polymer, and does the exposure to these two stressors yield in any synergistic effects? In order to clarify this, two commonly used rubber compounds peroxide vulcanized EPDM and CSM (tradename Lipalon) rubber cable jacketing materials were artificially aged thermally and irradiated by using gamma radiation. Total of nine different absorbed dose and temperature combination were used as ageing environment where the “worst” case was defined to be similar to those conditions present during a DBA i.e. dose rate 390 Gy/h, absorbed dose 228 kGy and temperature of 125°C. The aged samples were studied by tensile testing, hardness measurements and DSC analysis.

Tensile strength was not thought to be a good indicator for material degradation for these materials since it was not effected very strongly by the ageing treatments, except slightly after exposure to the most aggressive ageing environments. Similar observations were made in the case of hardness. A sufficient amount of degradation needs to be generated before hardness could be used as a degradation indicator. Elongation at break was clearly better criteria to evaluate the degradation of the materials. DSC analysis was considered to be sensitive in ageing detection when EPDM samples were studied and the results were aligned with the elongation at break results. However, the small sample size which was analysed could yield in some uncertainty in the results due to heterogeneities in sample structure and more accurate results would require several analyses. In case of CSM samples DSC is not applicable when detection of ageing is considered.

Based on the elongation at break results obtained with EPDM samples, it can be stated that moderate increase (ca. 75-125°C) in temperature during exposure to ionizing radiation hinders the degradation process, as shown in Figure 8. In addition, plane thermal ageing (equivalent to the thermal ageing component during simultaneous ageing) did not result in any changes in elongation at break. The observations made are opposite to what have been previously reported in literature [Ito 2007, Placek et al. 2008]. It was thus speculated that base polymer in the studies is the same but the different additives used can vary significantly between different EPDM blends which could have an effect to the nature and magnitude of the synergistic degradation yielding from exposure to heat and gamma radiation.

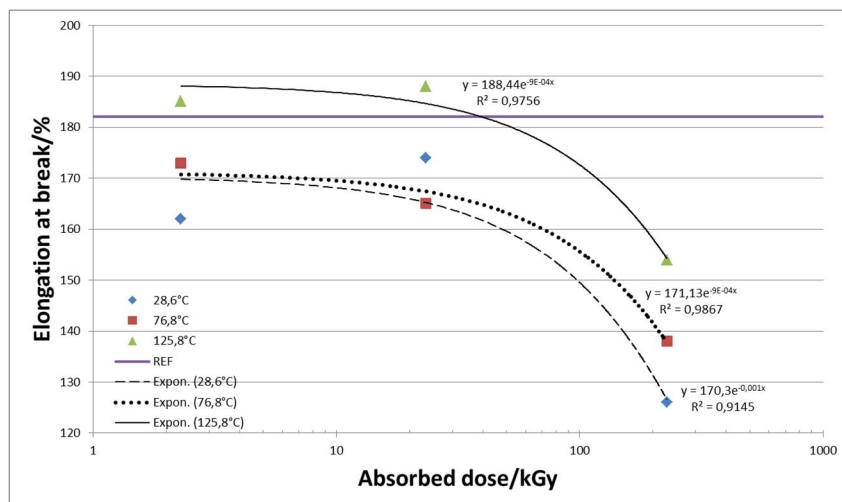


**Figure 8.** Elongation at break as function of absorbed dose for EPDM. Results obtained experimentally at 28,6°C are marked as blue diamonds, 76,8°C red squares and 125,8°C green triangles. Purple line indicates results obtained with reference samples. The fitted exponent functions are plotted as dashed, dotted and solid curves at temperatures of 28,6°C, 76,8°C and 125,8°C, respectively.

CSM (Lipalon) seemed to be more susceptible to both irradiation and thermally induced ageing and only small synergistic effects rising from simultaneous exposure to radiation and heat could be observed. Thermal ageing at 125°C resulted in clear decrease in elongation at break. Only slightly larger decrease was observed at 125°C when irradiation was conducted simultaneously. Simultaneous exposure to increasing temperature with irradiation resulted in increasing degradation as can be seen from Figure 9. This behaviour was opposite to what was observed on EPDM samples.

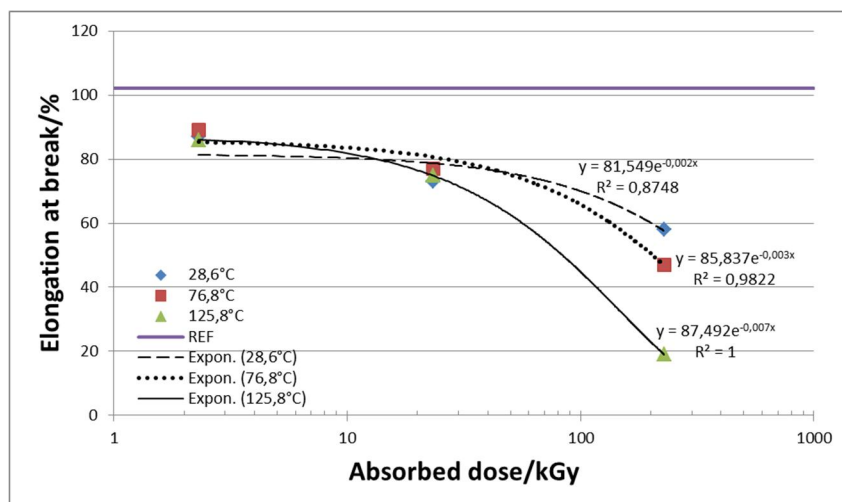


**Figure 9.** Elongation at break as function of absorbed dose for Lipalon. Results obtained experimentally at 28,6°C are marked as blue diamonds, 76,8°C red squares and 125,8°C green triangles. Purple line indicates results obtained with reference samples. The fitted exponent functions are plotted as dashed, dotted and solid curves at temperatures of 28,6°C, 76,8°C and 125,8°C, respectively.

### Synergy effects between radiation and heat and oxidation depth

The focus of this subtask is on evaluating applicability of different techniques on measuring the oxidation profile created on EPDM samples during accelerated ageing. These techniques include differential scanning calorimetry (DSC), time of flight secondary ion mass spectroscopy analysis (ToF SIMS) and Fourier transmission electron microscopy (FTIR). Obtaining homogenous ageing is required when polymer components are artificially aged to correspond the ageing condition that they will reach after normal service conditions (low dose rate and temperature). These different analytical techniques that could be used in oxidation profile measurements are required to use properly in order to distinguish homogenous vs. heterogeneous ageing from each other after accelerated ageing treatments.

The studied material was sulphur and peroxide cured EPDM rubber and it was aged to three different conditions: thermally aged, gamma radiated and simultaneously (peroxide cured EPDM sequentially) thermally and gamma radiated. The overall condition of samples was evaluated by tensile testing (i.e. tensile strength, elongation at break and modulus at 100% strain). The aim was to study ageing induced oxidation from surface towards the bulk with each technique.

Based on the results obtained with ToF-SIMS, it can clearly detect the oxidation occurring in the vicinity of surfaces of the aged samples. An example of formed two dimension oxidation graph is shown in Figure 10. The carbon black filler did not disturb the analyses. Based on the results alone no clear correlation to the material condition (i.e. material properties measured in tensile testing) could be drawn. The obtained oxidation profile thicknesses seemed to vary when repetition measurements were conducted. During repetition measurement the analysis spot changes which would indicate that material is oxidised quite heterogeneously or the material itself would be heterogeneous (at least at the analysis range ca. 0,1 $\mu$ m). Also the effect of uneven cross section surfaces contributes to the measured intensities. However, improvements in sample cross section surfaces and increasing the number of analysed samples is considered to lead to more reliable evaluation of the oxidation profile thicknesses.

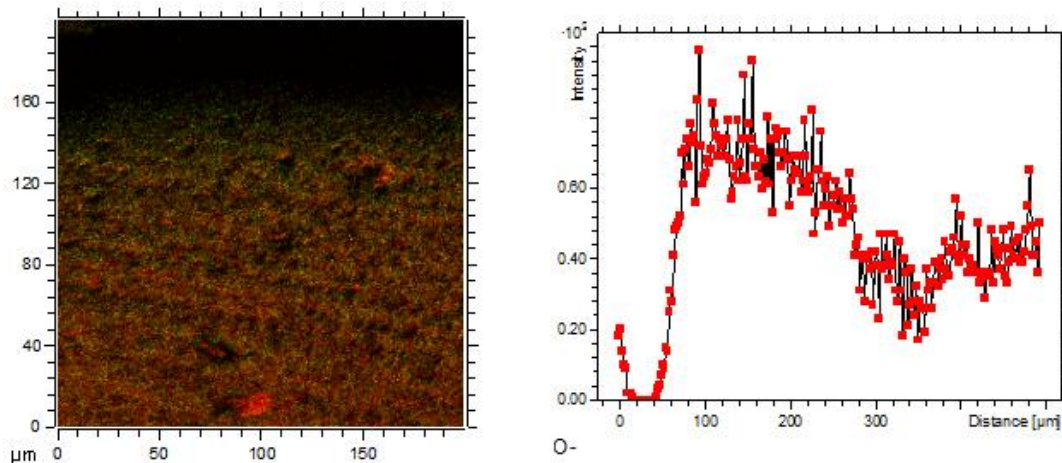


**Figure 10.** On left, two dimension quantitative oxidation graph obtained with sample irradiated and exposed to thermal ageing with even cross section surface. Surface is on top and oxygen illustrated as green colour. On right measured oxidation profile where profile thickness ca. 240  $\mu\text{m}$ .

FTIR measurements were conducted on rubber samples that contained clay instead of carbon black. The samples that contained carbon black could not be analysed due to the absorbed infrared light used by the technique. According to the results no oxidation products were found in the surface or bulk material that were expected. However, changes in absorption bands were observed due to the ageing treatments. More detailed analysis of these findings would require data on the ingredients of the studied EPDM

blend (which was not available). FTIR method seems to be sensitive to detect different compounds from surfaces and also bulk, when sample preparation is conducted with care.

DSC analyses were conducted on peroxide cured samples. Exothermic behaviour was recorded as a function of time and OITs were defined on each sample. The technique was sensitive to detect changes in polymer structure/constituent. However, the more detail evaluation of the exothermic peaks re-recorded would require detailed data on the ingredients of the EPDM blend. Also the resolution of technique in formation of oxidation profile is limited to the thicknesses of samples prepared. During sample preparation it was noted that thinner samples than 200  $\mu\text{m}$  are challenging to prepare limiting thus the analysed areas/spots along the profile to 200  $\mu\text{m}$  thick, at the best. This is considerably greater than in case of ToF SIMS.

### **Evaluation of damage caused by dose rate effect to polymer components used within containments**

This subtask concentrates on the irradiation based degradation of polymers and more precisely on methods that can be used in evaluation of dose rate effect as function of dose rate i.e. predicting from experimental data whether equivalent absorbed dose at lower dose rates causes more degradation in polymer than the corresponding equivalent absorbed dose at higher dose rates. These kinds of models could provide cheaper and more practical way to approach the existence of dose rate effect on certain polymer grades than time consuming low dose rate irradiation experiments. Applicable method would ease the recognition of the existence and severity of the dose rate effect so it could be taken into account when polymer component lifetime is predicted during qualification.

Ionizing radiation induces excited states in atoms that form the polymer structure and these unstable radicals will react with the surrounding material. This will ultimately lead to changes in polymer chain structure (e.g. chain scission) and degradation of macroscopic material properties will be observed. Dose rate effect is apparent phenomenon on many polymer grades that has effect on the amount of degradation that the polymer is experiencing in ionizing radiation environments. The phenomenon yields either from physical or chemical aspects. At high dose rates diffusion limited oxidation (DLO) effects become evident cause for dose rate effect and at low dose rates more complex chemical reactions determine the magnitude of dose rate effect. Very large dose rates are used during the accelerated ageing in many of the current qualification processes due to the high cost of the irradiation treatments. This would yield in neglecting the additional degradation rising from the dose rate effect in cases when the irradiation treatment should simulate the ageing during the designed service life or even DBA.

There are few semi-empirical methods that can be used in predicting the magnitude of degradation caused by the dose rate effect. Power law method and the two methods based on superposition are shown to function in the dose rate effect modelling on many polymer grades excluding those which have tendencies towards complex dose rate effects. For these materials sufficiently working method to predict dose rate effect behaviour in the vicinity of thermal transient temperatures is currently lacking. However, the use of these methods requires additional experimental data obtained in ionizing radiation and thermal environments which is costly. Thus using already existing experimental data could be used in estimation of dose rate effects. This would be possible in case of CSPE where differences in degradation data between different material manufacturers are remarkably low when the data is superposed and dose rate effects evaluated.

## **Conclusions**

COMRADE was established to provide better understanding on different polymer ageing, qualification and ageing management issues. Project consists of three different work packages that concentrate on condition monitoring techniques, mapping suitable components for ageing studies and studying ageing mechanisms and effects inside NPP containments, both experimentally and by using computational methods.

The work continues until the end of the current programme and after one year of project work, following conclusions/observations could be drawn:

- By artificially ageing EPDM o-rings and testing them with a certain sequence, an acceptance criteria based on the functionality of the o-rings could be suggested.
- Peroxide cured EPDM grade can be distinguished from sulphur cured grade by using XRF.
- Material acquisition from closed down Barsebäck NPP can be tedious and the documentation of polymer components seems insufficient for the purpose of ageing studies. Thus material acquisition from running plants would seem to be more reasonable.
- There remains a formidable gap between the present multi-scale materials modelling capabilities and practical lifetime prediction and bridging this gap would require greater resources than currently available. Thus more limited and still relevant ageing phenomena can be dealt in modelling point of view, such as the reverse temperature effect on semi-crystalline polymers.
- Synergistic effects yielding from heat and ionizing radiation can be either beneficial or detrimental for polymers, depending on the polymer type. The mechanism behind synergy needs to be studied in more detail.
- Applicability of three different techniques, which were used to study the oxidation in the vicinity of surfaces of artificially aged samples, was evaluated. ToF SIMS seemed to be the most promising technique with good sensitivity and resolution. In future work more attention should be drawn to sample preparation, in order to avoid erroneous measurement signals yielding from surface roughness.
- Some semi-empirical models for predicting ageing behaviour based on experimental data exists. The application of these models to predict effects of ionizing radiation at relatively low dose rates is possible if suitable artificial ageing data is available.

## Acknowledgement

Energiforsk, Finnish State Nuclear Waste Management Fund (VYR), Swedish Radiation Safety Authority (SSM) and VTT Technical Research Centre of Finland Ltd are greatly acknowledged for funding this work.

## References

- Bartoníček, B. Hnát, V. & Placek, V. 2001. Ageing Monitoring of Plastics Used in Nuclear Power Plants by DSC. *Journal of Thermal Analysis and Calorimetry*, Vol. 64. 571-576 p.
- Celina, M. Gillen, K. T. Wise, J. & Clough, R. L. 1996. Anomalous Ageing Phenomena in a Crosslinked Polyolefin Cable Insulation. *Radiat. Phys. Chem.* Vol. 48, No. 5. 613-626 p.
- Granlund, M. Almström, S. Jansson, A. Bondesson & Eriksson, J. 2015. Feasibility Study Acceptance Criteria For Polymers. *Energiforsk report* . 2015:157. 44 p.
- Ito, M. 2007. Degradation of elastomer by heat and/or radiation. *Nuclear Instruments and Methods in Physics Research B*. 265. 227-231 p.
- Penttilä, S. Saario, T. & Sipilä, K. 2016. Polymeerien säteilykestävyyden arvioinnin ja tarkastettavuuden perusteiden selvitys. *VTT-Customer report*. 50p.
- Placek, V. Kohout, T. Hnát, V. & Bartoníček, B. 2008. Assessment of the EPDM seal lifetime in nuclear power plants. *Polymer Testing*. 28. 209-214 p.

## 6.2 Analysis of fatigue and other cumulative ageing to extend lifetime (FOUND)

Juha Kuutti<sup>1</sup>, Otso Cronvall<sup>1</sup>, Ahti Oinonen<sup>1</sup>, Aapo Ristaniemi<sup>1</sup>, Qais Saifi<sup>1</sup>, Tommi Seppänen<sup>1</sup>, Antti Timperi<sup>1</sup>, Tero Tyrväinen<sup>1</sup>, Iikka Virkkunen<sup>2</sup>

<sup>1</sup>VTT Technical Research Centre of Finland Ltd  
P.O. Box 1000, FI-02044 Espoo

<sup>2</sup>Aalto University  
P.O. Box 11000, FI-00076 AALTO

### Abstract

A summary of the results obtained in the SAFIR2018 FOUND project during the years 2015-2016 is presented. The project is focused in ageing and failure assessment of NPP components. The main results include a broad review of the ageing of the BWR RPV and its internals, new experimental research on the primary water affected fatigue, reviews and developments of various failure assessment methods, thermal fatigue assessment methods, risk informed methods and methods to assess the dynamic response of piping systems. In addition, novel experimental research and results on the residual stresses in NPP piping components that have been in service for decades are presented.

### Introduction

The project FOUND concerns cross-disciplinary assessment of ageing mechanisms for safe management and extension of operational plant lifetime. It develops deterministic, probabilistic and risk informed approaches in computational and experimental analyses.

The focus areas are: Remaining lifetime and long term operation of components having defects; Susceptibility of BWR RPV internals to degradation mechanisms; Fatigue usage of primary circuit, with emphasis on environmental effects and transferability; Fatigue and crack growth caused by thermal loads, with emphasis on modelling; Development of RI-ISI methodologies, NPP piping analysis methods; Residual stresses in BWR NPPs. The research performed and the obtained results on each of these is described in the following.

### Remaining lifetime and long term operation of components having defects

With the modern developing NDE methods more indications are found year by year. The computational assessment of flaw behavior due to fatigue or stress corrosion cracking under operational loading including residual stresses is important for determining remaining lifetime of components. In the lifetime assessment of components, numerical methods for computing the component stress state, possible welding residual stresses are in practical use. The evaluation of the operational stresses may not be straightforward, for example in case of thermal loads where there might be significant uncertainties in the assessment caused by the complex thermohydraulic phenomena.

#### Treatment of uncertainties in structural analyses

Often the uncertainties are treated using safety factors. A review of the safety factor assessment practices was performed in the project (Cronvall 2015). This work provided a short introduction for considering the uncertainty and probability effects in typical structural integrity analyses of NPP piping components. It was found that the multitude of different safety factor definitions and a mixture of conservative and best-estimate assumptions makes it difficult, or even impossible, to define what is the total safety margin of a structure or component. Different types of input data have differently determined safety factors which are

not compatible with each other. Structural integrity analyses of structures and components would benefit from more specific definitions of the safety factors. Currently the evaluation of the total safety margin values has to be done with probabilistic terms by risk analysis approach. One possible future development would be probabilistic case studies that consider the full analysis chain, from load determination to calculation of the component stresses and evaluation of defect behavior inclusive of sensitivity analyses to determine the conservatism of analysis phases. The harmonization of the safety parameter definitions, such that all factors affecting the final result with equal weight are treated uniformly, is still an open issue. The importance of these issues increases due to plant ageing and a possible lifetime extension. The input data and related safety factors applicable for the design stage may differ from those applicable after e.g. 30 years of plant operation.

Another common approach related to risk analysis is sensitivity analysis with respect to the unknown parameters. For the thermal loads, this uncertainty analysis was performed in the project (Timperi & Cronvall 2016) by utilizing different methods to estimate the stresses due to thermal mixing. There were notable differences between the resulting stresses evaluated using the approaches, but the envelope of the results was covered by the safety factors typically proposed for thermal loads.

#### Flaw assessment methods

In addition, there is uncertainty concerning how to computationally assess the possible flaw behavior under the complex cyclic, thermal or residual stress loads. The numerical determination of crack criticality and possible growth is not straightforward due to the limitations of common methods to evaluate the parameters describing the crack loading. The traditional methods and parameters, such as the J-integral, are not directly suited for these cases. For this purpose, an effort was made to extend the J-integral field of applicability to cover cyclic and non-proportional loading cases in (Kuutti 2016). Example results of this research are shown in Figure 1. The figure presents a comparison of the crack driving forces computed with the implemented J-integral routine with the corresponding results obtained with the Abaqus built-in routine.

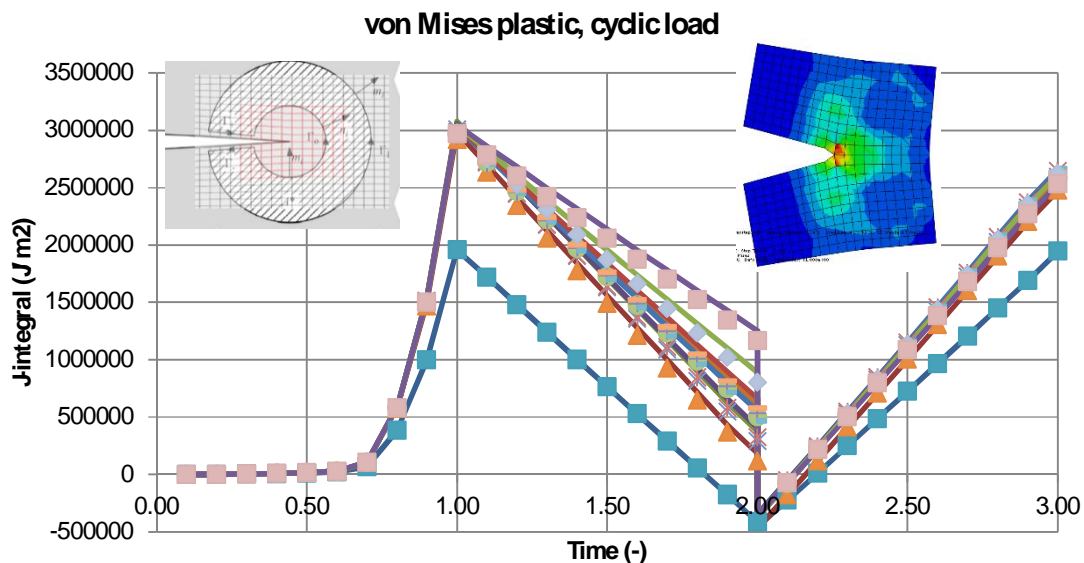


**Figure 1.** Contour integrals evaluated (solid lines) for a residual stress case compared with the results calculated by Abaqus (markers). Load is applied at time=0, reversed at time=1 creating a residual stress field at time=2. The load is re-applied again at time>2.0.

The flaw assessment is often performed using standardized engineering tools. For flaws in nuclear components, the ASME Section XI (ASME 2015) rules and methods are often applied to assess the flaw criticality. The present capabilities for the computation of the time and/or load cycles to reach the maximum

allowable crack sizes, as determined by the ASME code, are based mainly on engineering solutions, leading often to conservative results. Other engineering methods such as the BS 7910 (British Standards Institution 2015) method can be utilized in the NPP component assessments with reasonable justifications. The relation between the different methods is not fully established and a FAD based approach might be beneficial over the ASME XI rules. This aspect was studied in (Kuutti 2017a). The results show that, in most cases, the ASME rules and the FAD approach yield to similar results but significant differences may exist in more complex cases. An example comparison between the approaches is shown in Figure 2.

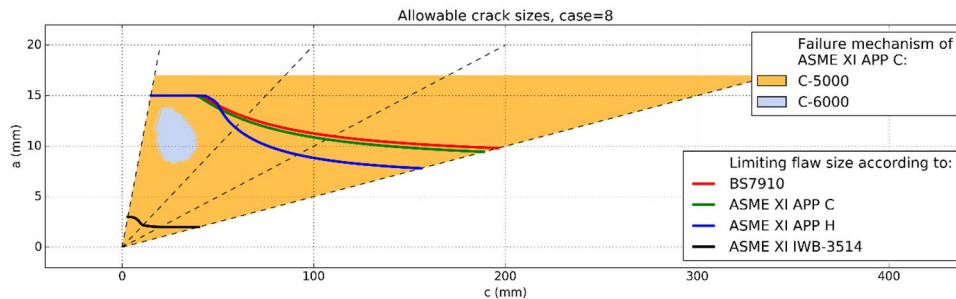


**Figure 2.** Comparison of allowable flaw sizes determined by the BS 7910 and ASME XI Appendix C and H procedures. The studied case is an axial inside surface flaw in a ferritic pipe under internal pressure.

## Susceptibility of BWR RPV and its internals to degradation mechanisms

This part of the project concerns the susceptibility of boiling water reactor (BWR) reactor pressure vessel (RPV) and its internals to various degradation mechanisms. This work consists of the following three main parts: (a) literature survey and review; (b) component specific survey on susceptibility to degradation mechanisms; (c) computational analysis approaches, tools and examples. A doctoral dissertation (Cronvall 2017) is being prepared in the work. Below, the original features of the work are described first. Introduction and scope of the work are described next.

The work then moves on to a literature survey on degradation mechanisms that can/could affect the BWR RPV and/or its internals. This includes an overview and detailed phenomenological descriptions of these degradation mechanisms. Interaction of degradation mechanisms is considered too. The relevant degradation mechanisms include: irradiation embrittlement (IE), thermal embrittlement (TE), fatigue crack growth (FCG), intergranular stress corrosion cracking (IGSCC), and irradiation accelerated stress corrosion cracking (IASCC). Next, the observed cracking degradation history of BWR RPVs and their internals is described component specifically in more detail with representative examples.

The work then moves on to describe in detail the major practical aspects of the relevant degradation mechanisms that affect the BWR RPV and its internals, and to evaluate the potential significance of their effects on the continued performance of safety functions of the considered components throughout the plant service life.

This is followed with an investigation on the susceptibility of the BWR RPV and its internals to degradation. Of BWR plants, the scope of this work concerns those designed by ABB, focusing on the third generation. The internals determined as significant in TVO report (Lemettinen 2016) and IAEA-TECDOC-1471 (IAEA 2005) were selected to be considered in this work. These components are from TVO units OL1/OL2. Altogether 31 components were selected for more detailed consideration. These components include RPV, Steam separator support legs, Steam outlet nozzles, Feedwater nozzles, Control rods, Core shroud, Core spray nozzles and Control rod guide tubes at the RPV bottom. The summary on component specific susceptibility of BWR RPV and its internals is presented in Table 1.

**Table 1.** Summary on component specific susceptibility of BWR RPV and its internals to relevant degradation mechanisms. Here susceptibility is denoted with "X".

Component	Degradation mechanism							
	Irradiation embrittlement	Thermal embrittlement	Fatigue crack growth	IGSCC	IASCC	General corrosion	Erosion-corrosion, FAC	Mechanical wear
Flange cooling spray piping			X	X				
Long nozzle pipes in cooling spray piping			X	X				
Evacuation pipe			X	X				
Spring beams and support brackets			X	X				
Steam dryer			X	X				
Steam outlet nozzles		X	X					
Steam separator stand pipes, pipe bundles and supports			X	X				
Feedwater nozzles	X	X	X	X	X			
Feedwater spargers			X	X	X			
Boron spray nozzles and piping			X	X	X			
Core spray piping inside and outside core shroud cover			X	X	X			
Control rods, control rod guide tubes			X	X	X			
Core shroud, core shroud support			X	X	X			
Pump deck			X	X	X			
Main circulation pump nozzles		X	X	X				
Core shroud support legs			X	X				
Instrumentation guide tubes and nozzles			X	X	X			
Control rod guide tubes and nozzles at RPV bottom		X	X	X				
Cylindrical RPV shell	X	X	X					
RPV bottom, flange, head and head bolts		X	X					
RPV support skirt		X						
Shutdown cooling nozzles, core spray nozzles	X	X	X	X	X			

The loads specific to the BWR RPV and internals are described next. These components experience several kinds of loads. They are in contact with hot and moving liquid coolant during normal plant operations. The coolant saturation temperature corresponding to the system pressure is just below 290 °C (TVO 2011). Internal components located in the vicinity of the core are also exposed to fast neutron fluxes ( $E > 1.0$  MeV) and gamma irradiation. The operating environment inside a BWR RPV generates many loads that are considered to propagate ageing related or time dependent degradation mechanisms. In the top level these can be divided into applied loads, environmental loads and manufacturing induced loads.

The work then moves on to describe the screening process for the considered components. For NPPs the purpose of a screening process is to select the components for further analyses, especially for degradation potential analyses. More specifically, these analyses are here called time limited ageing analyses (TLAAs). The objective of the TLAAs is to identify the degradation mechanisms of components and the increase in failure occurrences, to assess the remaining lifetime of components and to find suitable means to prevent or mitigate the effects of ageing degradation. The applied screening process is based on those by IAEA (IAEA 1992) and EPRI (Tang 2006). All considered components were screened.

Computational approaches, tools and analyses are described next. The covered computational approaches apply mainly structural mechanics and fracture mechanics. Temperature distributions, stresses and strains for the analyzed components are computed with general purpose FE codes and/or with analytical equations, where applicable. In most TLAAs, fracture mechanics based analysis code VTTBESIT is used. This code comprises parts developed by VTT (Vepsä 2004, Cronvall & Vepsä 2012) and by IWM (Varfolomeyev et al. 1996, Busch et al. 1995, 1995). Both deterministic and probabilistic crack growth computation procedures are presented. Computational developments are described next. These concern

new equations for stresses and strains in multi-metal hollow cylinder as well as new equations for inverse computation of temperatures in bi-metal pipe. The focus of the work is on the TLAAAs. Of the 31 considered components, 12 components screened in. Several of these components are assessed to be susceptible to more than one degradation mechanism. These components include all those mentioned above in the connection of susceptibility of BWR RPV and its internals to degradation.

The work then moves on to the TLAAAs for the components that screened in. Of the relevant degradation mechanisms, the performed TLAAAs concern IE, TE, FCG, IGSCC and IASCC. The maximum component specific number of TLAAAs is four, which concerns the Feedwater nozzles, Shutdown cooling nozzles and Core spray nozzles. The TLAAAs for the RPV cover 80 years of operational lifetime, whereas those for other components cover 60 years. According to the TLAA results the crack growth is in most cases very slow. In addition, the obtained crack growth results are also conservative. Firstly, it was assumed that initial cracks exist/nucleate from the start of the plant operation, whereas in reality it usually takes several years, even more than a decade, for a crack to nucleate from dormant microscopic size to macroscopic size capable to grow. Secondly, the end-of-life (EOL) crack sizes are computed according to Section XI of the ASME code (ASME 2015) using safety factors given therein for load induced primary stresses. In a couple of cases the computed crack growth is of significant scale. For instance, according to the TLAA results IGSCC can grow quite rapidly in Core shroud support leg weld. Concerning all performed TLAAAs, crack growth is in all cases so slow, that any growing crack would be found in the inspections well before it reaches any critical size. In most cases the resulting crack growth is negligible.

As the main argument of this work concerns the RPV, the TLAA results concerning it are summarized in the following. This component is affected by altogether three degradation mechanisms: IE, TE and FCG. However, the effect of TE is included in the empirical models for IE. According to the IE TLAA results the maximum stress intensity factor values for Appendix G of ASME Section XI (ASME 2015) reference crack in the RPV shell remain well below the corresponding fracture toughness values that have decreased during 80 years of plant operation. The actual structural integrity margin is considerably larger than what the results show, as the computation procedure includes several conservative assumptions. Thus, even after 80 years of plant operation there is a large structural safety margin for the RPV against IE. The crack growth for FCG in the RPV shell is slow in all cases for 80 years of plant operation, even for the largest initial crack postulate. The maximum crack growth through wall within 80 years is approximately 4.6 mm for this crack postulate with initial depth and length of 20 and 120 mm, respectively. The crack growth for FCG remains well under maximum EOL crack depth for 80 years of plant operation.

This work is not yet complete. Some TLAAAs still need to be done, and the new computational developments need to be validated.

## **Environmental fatigue of primary circuit**

One of the recognized degradation mechanisms of pressure boundary components in nuclear power plants is fatigue. Fatigue damage in NPP pressure vessels and piping originates from mechanical or thermal stresses experienced during transients such as start-up or shut-down. In NPPs evaluation of fatigue is based on local strain approach, codified stress analysis and material specific design curves. These design curves are derived from room temperature (RT) strain-controlled low cycle fatigue (LCF) test results and are included in design codes such as Section III of the ASME B&PV Code (ASME 2009).

Effects of plant relevant service conditions are however difficult to quantify, challenging the transferability of laboratory data. Experimental work in simulated reactor water has aimed at solving these uncertainties since the 1980's. The current consensus is that reduction in fatigue life in pressurized hot water can be accounted for by using  $F_{en}$  reduction factors, described in NUREG report 6909, for example (Chopra & Stevens 2014).  $F_{en}$  is defined as the ratio of fatigue life in air to fatigue life in water. For austenitic stainless steels,  $F_{en}$  is a function of strain rate, temperature and dissolved oxygen. Decreasing strain rate and/or increasing temperature increase the calculated  $F_{en}$ .

Unfortunately, most of the generated data to date has come from non-standard test procedures or specimens to avoid numerous difficulties of performing standard LCF tests in pressurized hot water. In order to

generate design compatible data and importantly, to meet requirements of the 2002 STUK guidelines update (STUK 2002) regarding environmentally assisted fatigue, a miniature fatigue device was first developed at VTT. During SAFIR2010 (Solin et al. 2011), a tailored-for-purpose fatigue device “FaBello” was designed and verified for ASTM E 606 compliant fatigue testing in simulated reactor coolant. In SAFIR2018, FaBello is used to generate qualified data in support of a new mechanism informed, plastic strain rate based  $F_{en}$  model.

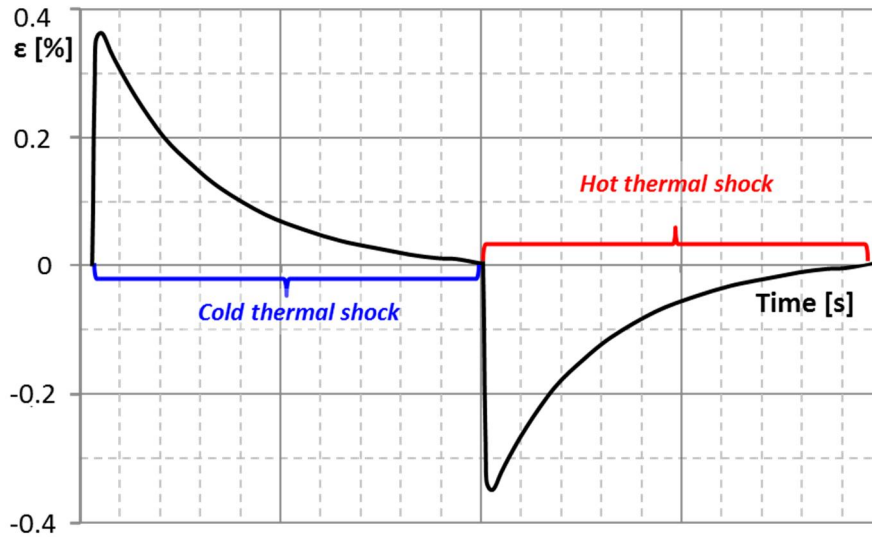


**Figure 3.** Schematic of a safety injection system transient.

#### Experiments in simulated PWR water

In this part of the project, two series of four tests for niobium stabilized AISI 347 stainless steel have been performed in 325 °C pressurized water. The selected strain waveforms were inspired by a typical transient experienced in the primary circuit safety injection system, Figure 3. This waveform was linearized and shortened for testing purposes, as shown in Figure 4. The use of reversed order dual strain rate waveforms for the rising ramp was selected to be able to easily compare effects of plastic strain rate. Decreasing ramps were always run with a fast strain rate, because environmental effects are considered negligible. In the 2015 tests, nominal total strain amplitude was 0.35% with the strain rate change taking place at zero strain. In 2016, nominal total strain amplitude was 0.3% with the strain rate change at -0.15% strain.

A description of the pneumatic bellows based FaBello test device is given in (Seppänen et al. 2015). Standard polished 8 mm diameter test specimens (Figure 5) were used. All tests were done fully reversed ( $R=-1$ ) and strain was directly controlled from specimen mid-section. The two strain rates used in 2015-16 were 0.01%/s and 0.0004%/s ( $1 \cdot 10^{-4} \text{ s}^{-1}$  &  $4 \cdot 10^{-6} \text{ s}^{-1}$ ). The latter strain rate is considered a saturation rate, below which environmental effects saturate at their maximum value (Chopra and Stevens 2014).

The results from 2015 were first presented in (Seppänen 2016) and reanalyzed in (Seppänen et al. 2016a). Provisional results from 2016 were first presented in (Seppänen et al. 2016b). The final results are presented in an upcoming paper (Seppänen et al. 2017). All of the 2015-16 results are shown in Figure 6. The air curve to which  $F_{en}$  is measured is labelled NUREG/CR-6909 Mean, which is the mean curve used to obtain the current ASME III design curve. For each waveform, nominal expected  $F_{en}$  values were calculated according to the equations in (Chopra and Stevens 2014) and resulting expected fatigue lives are shown as color coded dashed lines.

Since most data points are to the right of their corresponding expected lives in water, the NUREG  $F_{en}$  equation generally gives a conservative estimate. For the case of fast-slow strain rate tests, two data points out of four resulted in higher than expected experimental  $F_{en}$  values. This supports the hypothesis of

plastic strain rate having an important role, as plastic strain quickly accumulates after yielding has taken place. Conversely, the results suggest that the initial fully elastic part of a tensile ramp may not have a detrimental effect at all. Presently however, the entire ramp from minimum to maximum strain is considered when calculating  $F_{en}$  factors, with equal weight being given to all parts of the ramp.

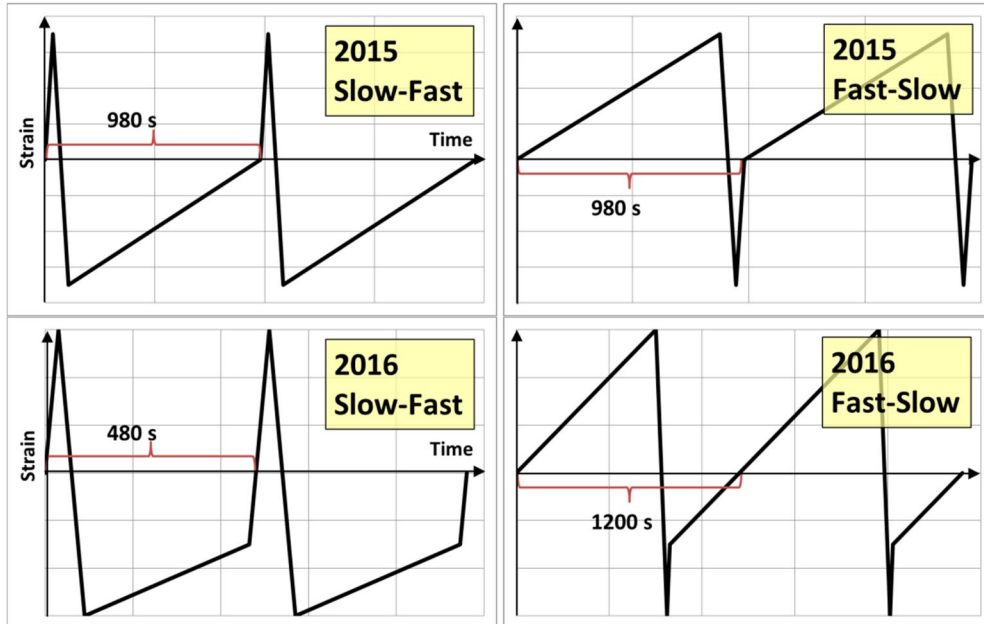


Figure 4. Strain waveforms for 2015-16.

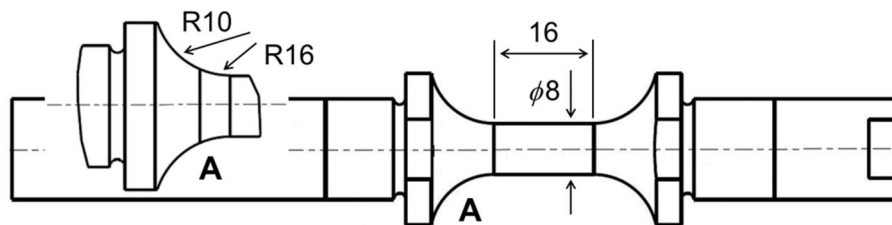
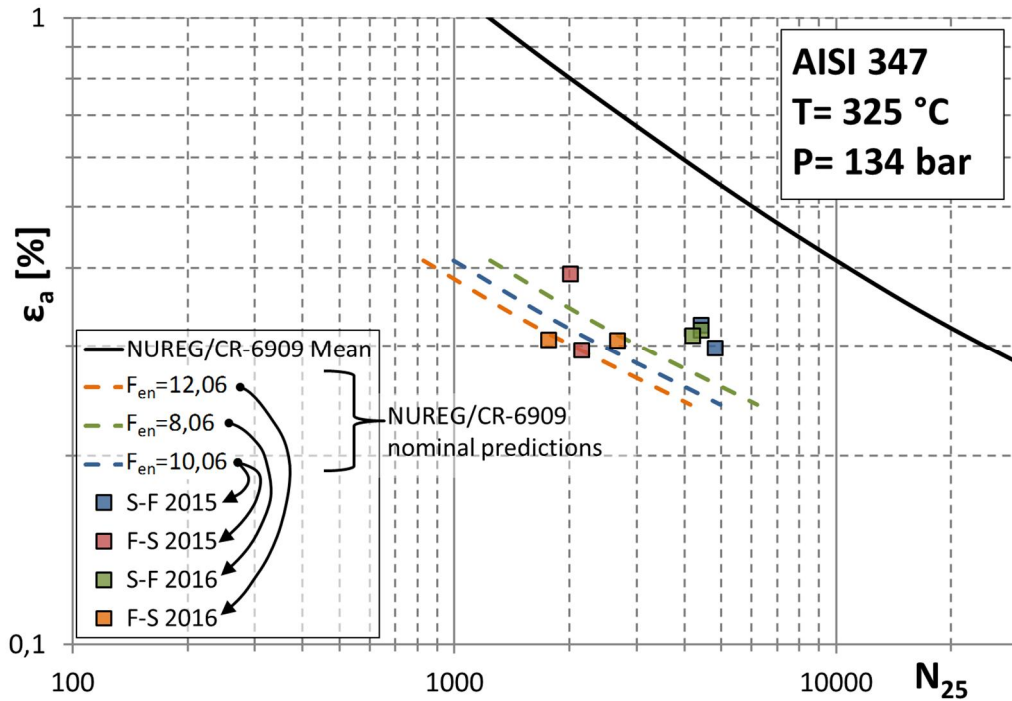


Figure 5. Specimen geometry for PWR water.

Figure 7 shows the results as  $F_{en}$  values. Included here are also the design  $F_{en}$  values. Test data in 325 °C is not directly comparable to design code requirements and therefore a temperature correction is necessary. Neglecting this correction would result in accounting for temperature twice. The correction is done by multiplying the fictitious elastic stress intensity ( $S_a = E \cdot \epsilon$ ) at test temperature by the ratio of elastic modulus at room temperature to elastic modulus at test temperature. Because  $E$  decreases as temperature increases, the shift to higher design strain amplitudes and therefore lower design  $F_{en}$  factors is easy to understand. After design modification, all  $F_{en}$  values are well below the estimated.

After two sets of experiments in simulated PWR water, it is clear that strain waveform does influence the fatigue life. If research continues to show a negligible effect of elastic strain rate as is expected, it is necessary to rewrite the  $F_{en}$  methodology to account for this. For plant relevant transients where strain rate and temperature are far from constant, this is especially important for realistic estimation of fatigue usage. Nonstabilized stainless steel AISI 304L will be used for simulated PWR water tests during the second half of SAFIR2018. This allows a comparison between different alloys, but alloy 304L is also more directly

comparable to the database of the NUREG report (Chopra and Stevens 2014), which is based entirely on nonstabilized alloys.



**Figure 6.** Fatigue test results in PWR water compared to the NUREG/CR-6909 mean curve and nominal expected  $F_{en}$ .

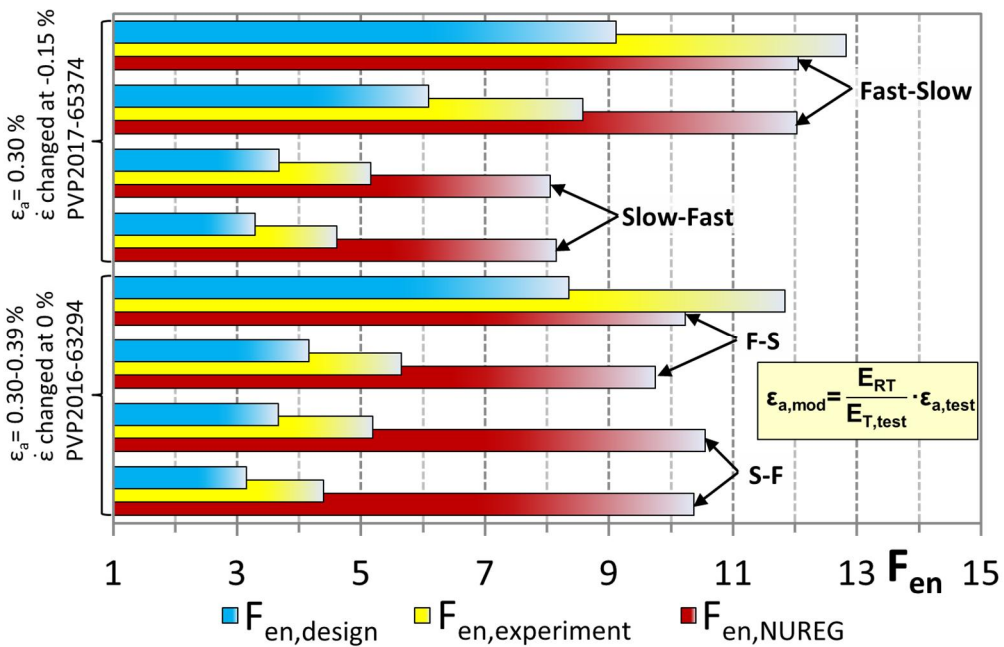


**Figure 7.** Comparison of predicted and experimental environmental effects.

## Modelling of thermal fatigue

This part of the research project focuses in evaluating the fatigue caused by thermal mixing loads both in the high-cycle and low-cycle regimes.

### High-cycle thermal fatigue

Thermal mixing of hot and cold water with large temperature differences has led to fatigue and crack growth e.g. in piping T-junctions. Computational fluid dynamics (CFD) and structural calculations of thermal mixing in a T-junction were performed with the commercial Star-CCM+ and Abaqus codes (Timperi 2016, 2017a). In large-eddy simulations (LES), the fluctuating wall heat fluxes obtained with different wall treatments and meshes were compared. In the structural calculations, turbulent thermal loads from LES were applied for 3D modelling while turbulent, spectrum and sinusoidal loads were applied in 1D modelling. Crack growth results using the 1D and 3D models and the different thermal loads were compared.

LES showed increase in peak root-mean-squared (RMS) temperatures with local mesh refinement, and hence too low peak values were obtained with wall functions. The peak RMS values occurred locally near the T-junction requiring a dense mesh, whereas a coarser mesh was sufficient for downstream locations. Peak wall heat fluxes were significantly affected by mesh, wall treatment and sub-grid scale model. Wall functions were unable to describe high heat fluxes at a sharp T-junction corner, but otherwise the peak RMS values were fairly close to a wall-resolved case. This is in contrast to Pasutto et al. (2009) and Jayaraju et al. (2010) and more in line with Howard and Serre (2017). Wall functions showed lower instantaneous wall heat fluxes than wall-resolved LES, but there was considerable difference in the frequency content between the two wall treatments.

Crack growth times with the 1D sinusoidal method spanned several orders of magnitude depending on frequency. The worst-case frequency was from 0.05 to 0.3 Hz depending on pipe wall thickness. The worst-case frequencies resulted in considerable over-conservatism compared to a realistic turbulent load, however the conservatism level is largely case-dependent. Circumferential and axial cracks had initially similar growth rate, but the axial crack grew faster for larger depths. Growth rates for thin and thick pipe walls showed significant differences only for deeper cracks. 1D and 3D models with corresponding turbulent thermal load agreed well with each other. Comparison of crack growth rates and times for various calculations is shown in Figure 8.

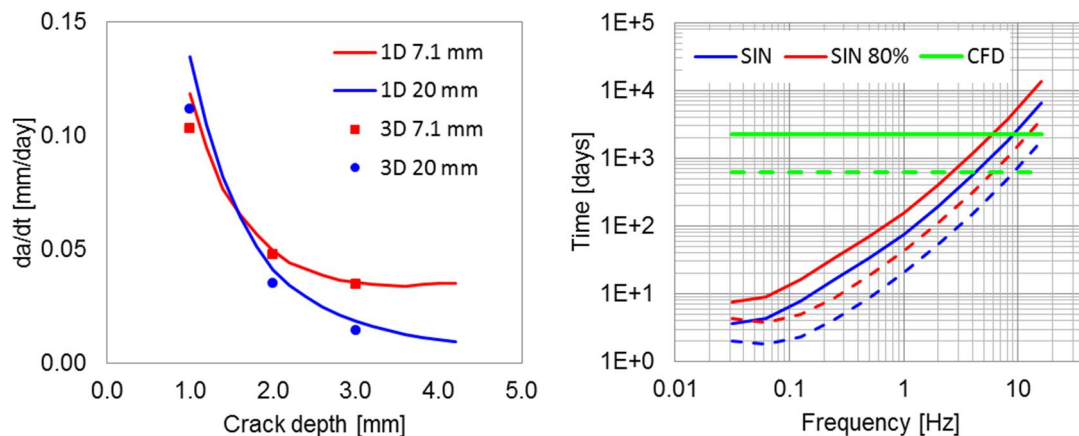


**Figure 8.** Left: Crack growth rates for 1D and 3D calculations with wall thickness 7.1 and 20 mm. Right: Crack growth times with different thermal loads for circumferential (solid lines) and axial (dashed lines) cracks.

### Low-cycle thermal fatigue

In some cases the thermal cycling causes irreversible deformations in the pipe wall. In these low-cycle thermal fatigue cases, severe cracking may occur at a small number of cycles. Due to the cyclic plastic and thermal effects, the traditional fracture mechanical tools are ill-suited to for the evaluation of the susceptibility to cracking and the possible flaw growth rate. The first attempt to predict the low-cycle thermal fatigue combined the experimental information on crack formation with the simulation results on the flaw loading (Virkkunen et al. 2013, 2015). The strain-life plot is shown in Figure 9. An example of simulated crack opening stress distributions over a single thermal cycle is shown in Figure 10.

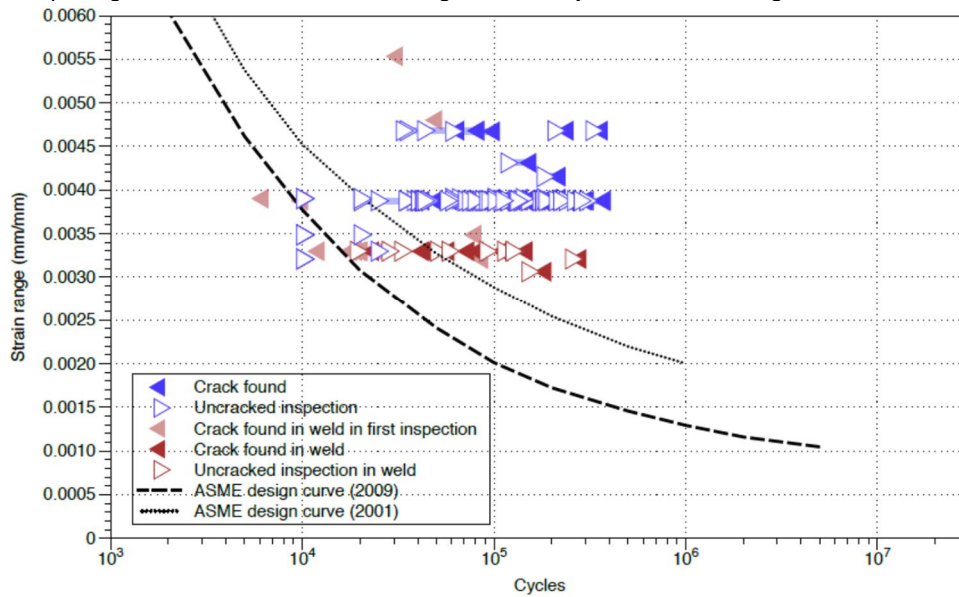


**Figure 9.** S-N plot with the selected Trueflow fatigue data. Clean inspections (no crack) are shown with open triangles. Inspections where a flaw was found are shown with filled triangles. The strain ranges are obtained through FE analyses.

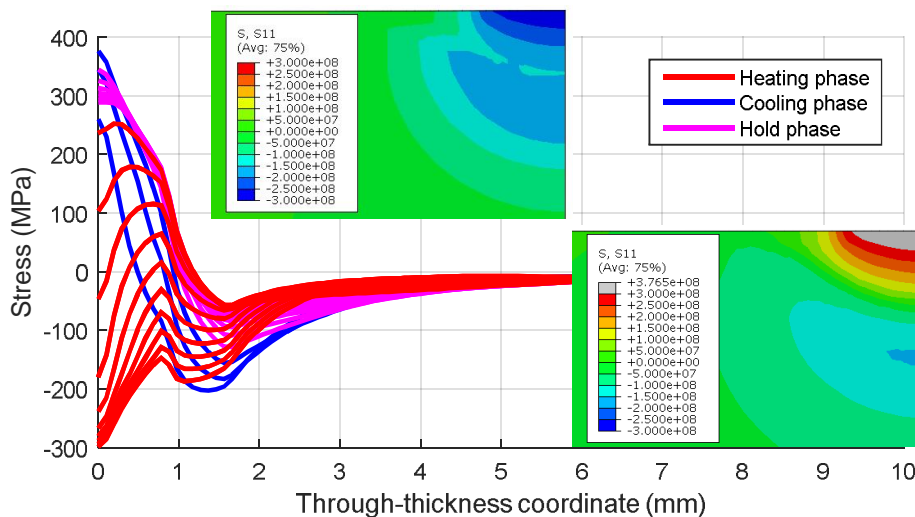


**Figure 10.** Through-thickness stress distributions and spatial crack opening stress distributions for a rectangular plate heated and cooled on a limited area on the top surface. Contour plots [Pa] shown for time instant of maximum and minimum crack opening stress.

This approach provided realistic estimates for the relation between the strain amplitude caused by the thermal load and cycles to failure. An accurate estimation of the flaw growth rate requires more advanced fracture mechanical tools such as those presented in (Kuutti 2015, 2017b). Therein, crack growth rates of the same experiments were simulated. The growth rate was computed using two approaches: by considering the intact specimen stresses and a handbook stress intensity factor solution and by FE-simulations where the actual crack was included. A relation between the crack tip opening displacement and J-integral was proposed to be used for characterizing the crack driving force for low-cycle thermal fatigue. The comparison of the obtained results (Figure 11) shows that the typical crack growth models based on the linear crack driving force parameters cannot be reliably predict the actual crack growth rate for the studied specimens. The study highlights the limitations and conservatism of the traditional approaches in lifetime assessment of components under low-cycle thermal loading. The proposed approach appears to be feasible in obtaining more realistic crack growth rate estimates but is likely too laborious for quick engineering assessments.

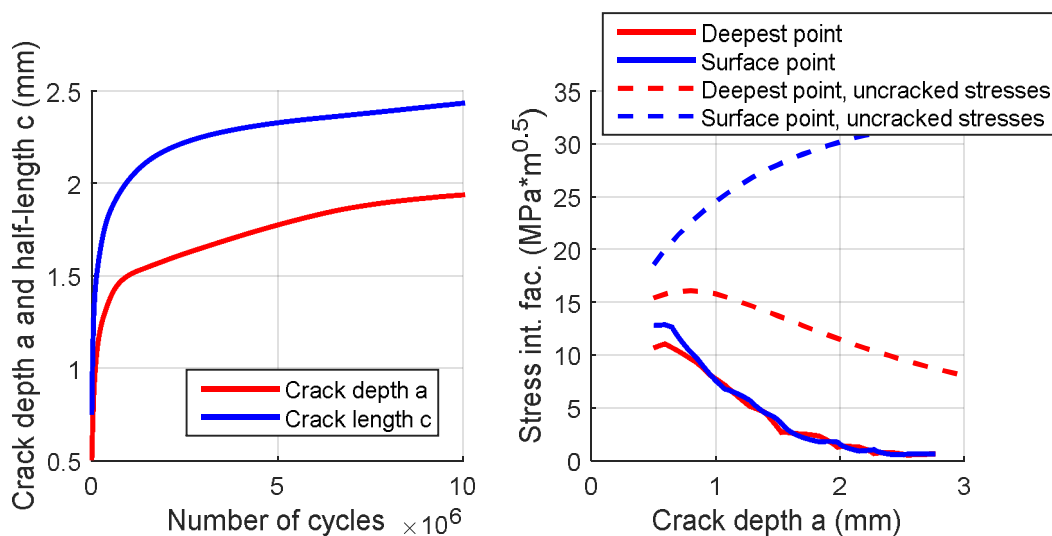


**Figure 11.** Crack size (left) and stress intensity factors (right) calculated in a low-cycle thermal fatigue crack growth assessment. In the right plot, the stress intensity factors calculated using the uncracked stress distributions are shown for comparison.

## Development of RI-ISI methodologies

The goal of risk informed in-service inspection (RI-ISI) analyses of NPP piping systems is to optimize the inspections so that they are targeted to sites with highest risk. With RI-ISI, the safety of the NPPs can be improved, the irradiation dose to inspection personnel can be decreased, and financial savings can be achieved by removing from the inspection programs sites with small risk but poor approachability. RI-ISI is a multi-disciplinary topic, combining e.g. risk analysis, structural reliability, fracture mechanics and non-destructive inspection techniques. For Finnish NPPs, RI-ISI is a very topical issue. The YVL guidelines (STUK 2014) state that the piping in-service inspection programme shall be prepared in a risk-informed manner and consequently the NPP licensees are starting to update their RI-ISI programs.

### VTT RI-ISI procedure

The VTT RI-ISI procedure (Oinonen 2017) is a combination of deterministic and probabilistic analysis tools for the evaluation of pipe failure possibilities and the risk informed planning of inspections. The procedure allows quantitative evaluation of the influence of different inspection intervals and inspection capability on the leak probability. The procedure combines deterministic fracture mechanical models describing

the crack growth with Monte-Carlo or Markov based probabilistic models to evaluate the leak probability and effect of inspections. An example result plot obtained with the VTT RI-ISI procedure is shown in Figure 12.

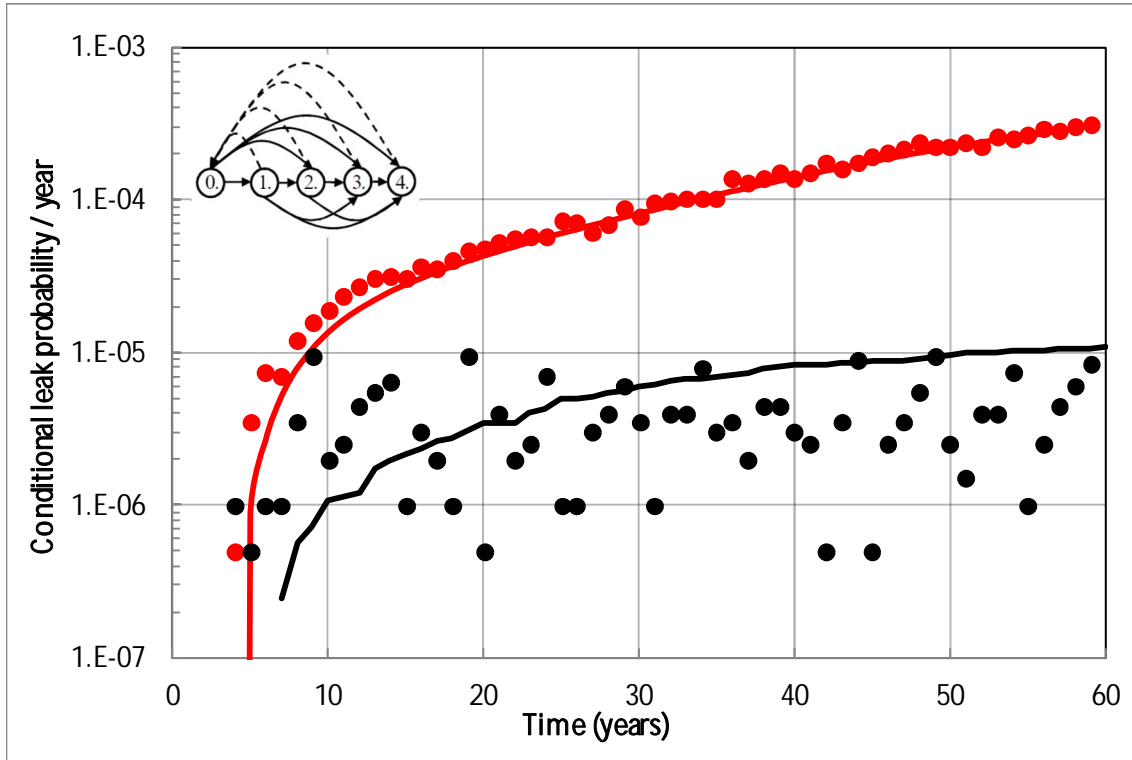


**Figure 12.** Conditional yearly leak probabilities simulated with the VTT RI-ISI Markov based procedure (lines) and Monte-Carlo based procedure (dots). The red line and dots denote cases without in-service inspections (flow of the ageing process along the solid lines in the subfigure) and the black line and dots denote cases with inspections (flow also along the dashed lines in the subfigure).

The on-going development of the VTT's RI-ISI procedure increases confidence in its results. In 2015, the VTT RI-ISI procedure was benchmarked (Heckmann and Saifi 2015). In the benchmark, the results obtained with the VTT RI-ISI procedure for a number of test cases were compared with results obtained with a corresponding probabilistic assessment tool used in Germany. The design examples covered both the BWR and PWR conditions, manufacturing defects and crack initiation, corrosive and fatigue crack growth, and in-service inspections. The results of both procedures are widely in a good agreement. Significant differences were mainly present due to the singular parameter combinations. The reasons for such systematic differences in the computed leak probabilities were identified in an extensive discussion. This analysis, based on the time-dependence of the annual leakage probability during operation, revealed the key ingredients that are considered as relevant for the differing leak probability evolutions.

The study of the effect of POD functions on the break probability (Oinonen 2015) is an example of work performed towards more accurate RI-ISI analyses and to reduce conservatism of the results. The effect of different POD functions was studied by break probability analyses carried out with the probabilistic VTT-BESIT code and a Markov application for representative nuclear power plant piping welds. The study shows that the difference in the results obtained with different POD definitions was marginal but the reduction of risk obtained with the inspections was clear.

#### **RI-ISI and PRA**

Another research topic addresses the connection between RI-ISI and PRA. Probabilistic risk assessment (PRA) is used to calculate the quantitative risk of nuclear accident and to analyze the importance of different systems and components. PRA's main purpose is to support risk-informed decision making. PRA also supports RI-ISI analyses by quantifying the consequences of pipe failures, see Figure 13. As identified in the research (Tyrväinen 2015, 2016), there is much to be gained from better connection and mutual support between PRA and RI-ISI. One possibility to bring RI-ISI and PRA closer would be to develop a software support for the better integration. Even common analysis software is a possibility. In addition, it would be beneficial to develop an automatic piping failure consequence calculator into the PRA software. Consequently, the research introduced a new RI-ISI feature which calculates CCDPs of piping component failures in PRA software FinPSA. The CCDPs of all piping component failures can be calculated automatically at once in the same RI-ISI table, based on the results of the PRA model. This feature does not complicate the PRA model at all, regardless of how many piping components are included. Currently, the RI-ISI feature calculates only CCDPs, but RI-ISI analyses require also failure probabilities of piping components. It could be possible to add failure probabilities to the RI-ISI table of FinPSA and implement some sort of inspection interval decision rules or optimization algorithm.

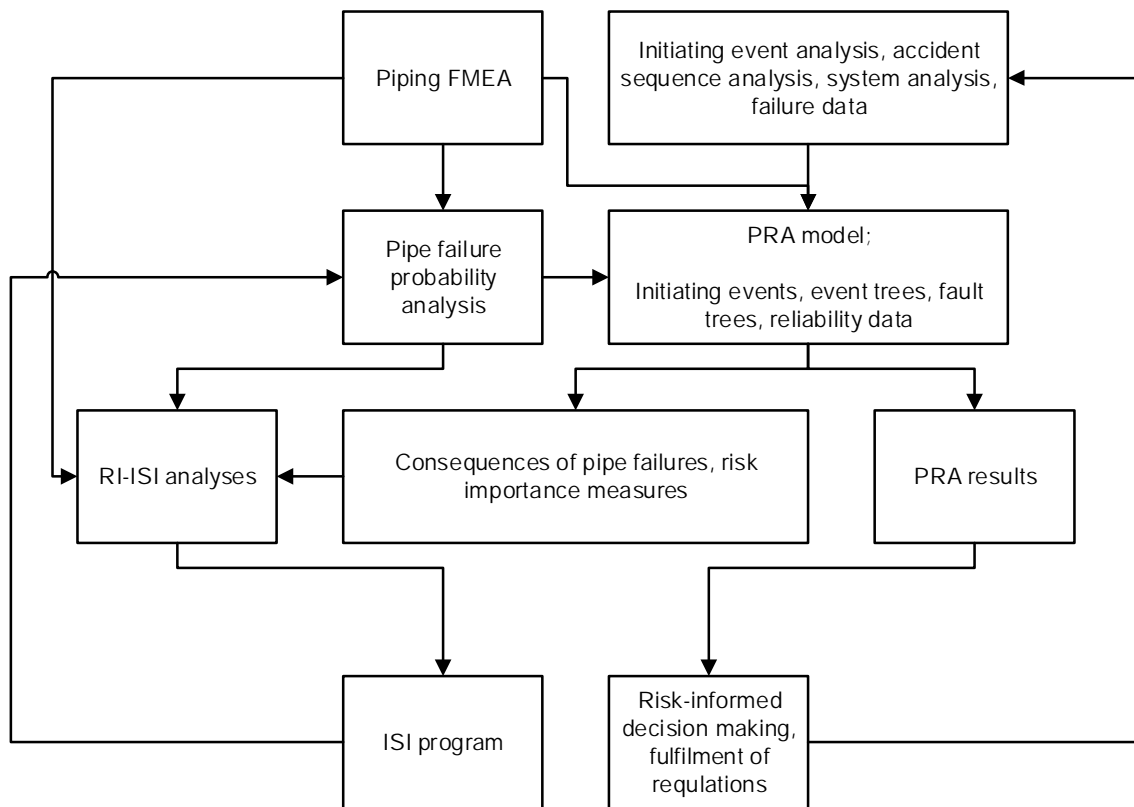


**Figure 13.** Simplified flowchart of RI-ISI and PRA and their connections.

### Research on NPP piping analysis methods

A part of the research focuses in the development of response assessment methods for NPP piping systems. The research performed so far include development of a linearization procedure to simplify complex nonlinear piping vibration assessments, development of a method to take into account the fatigue usage of a decaying stress or strain response, evaluation of different methods to combine the results from several

dynamic load cases into a resultant suitable for a design standard based assessment and a survey of suitable piping analysis benchmarking tools.

The performed survey (Oinonen 2016) is concerned with the qualification processes and benchmark problems for dynamical spectrum and time-history analyses of large-scale piping systems that are subject to typical NPP conditions. Safety-related applications of the design and maintenance standards for an assessment of the structural integrity of piping systems are addressed. Additionally, the piping component benchmarks involving the temperature loads, large deformations and plasticity are included. A summary of selected benchmark problems to exemplify software qualification for mechanical analyses of the large-scale piping systems and separate piping components is included.

A part of the research considered calculation of fatigue life for the final decaying part of damped vibration in case of response spectrum analysis (Timperi 2015). A procedure was proposed, where the decaying cycles were replaced with effective number of constant cycles, whose amplitude is that of the maximum resultant obtained from the spectrum analysis. The effective number of cycles was first studied analytically by assuming simplified expressions for the fatigue curve. For an analytical fatigue curve having 2 parameters, the effective number of cycles could be determined analytically and was independent of the initial amplitude. With a 3-parameter fatigue curve, the analytical expression corresponded to the real fatigue curve surprisingly well, but simplified expression for the effective number of cycles is not available. Also, the effective number of cycles becomes dependent on the initial amplitude for a realistic fatigue curve. A simple numerical method was proposed, where the effective number of cycles is determined by using the actual fatigue curve.

#### Combination of load cases

The primary stress limit equation in Section III of the ASME B&PV code requires calculation of a piping resultant moment by combining moments from simultaneous design loads. The combination procedure for dynamic time-history analyses may become computationally laborious depending on the level of required accuracy. This aspect was studied in (Timperi 2015, 2017b). To reduce unnecessary conservatism, the moment components applied in the summation equation can be selected physically from the same time instants, requiring a search of the maximizing instants from the time step combinations between the dynamic load cases. Combining the moments from time-history analyses was studied by using moments from dynamic piping analyses or by generating random moment signals.

The combination methods were first studied analytically and numerically by random moment signals. Combination methods were compared, where all possible time step combinations between different dynamic load cases are searched and where time-histories of each dynamic load case are searched separately. The latter case saved computational effort but was in general slightly more conservative than the former. However, if the algebraic signs of the moments are accounted for, the latter method may become too conservative compared to the former.

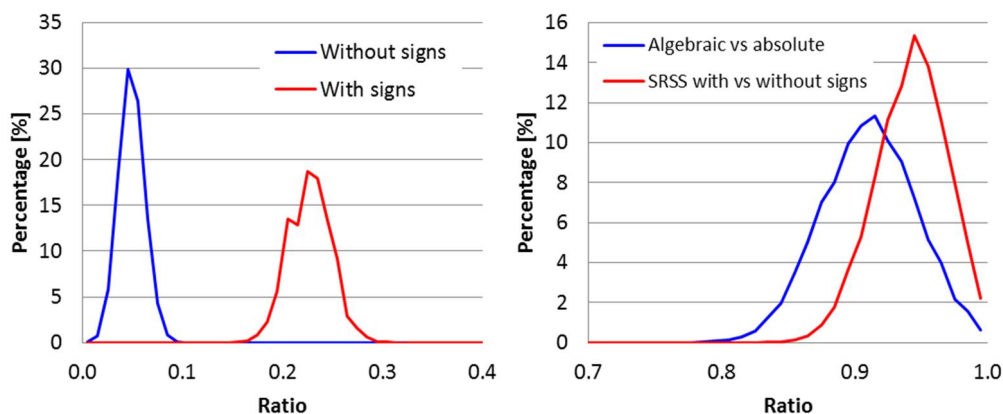


**Figure 14.** Left: Histograms of time step number ratios (reduced/original) with and without signs. Right: Histograms of resultant moment ratios for different summation methods.

Combination methods were then compared, where redundant time points are first removed to save the computational load. Methods were considered where the algebraic signs of the moments are either accounted for or not. When the signs were neglected, very large savings in the overall computing cost (i.e. many orders of magnitude) was achieved by removing the time points. On the other hand, the computational saving was only from one to two orders of magnitude when the signs were included. The former case with signs neglected was only slightly more conservative compared to the latter. In the considered signals, the positive and negative moment amplitudes were fairly similar and the moments oscillated around approximately zero mean value. Thus, taking the algebraic signs into account had a minor effect while neglecting the signs resulted in vast saving in the computing effort. It should be studied further whether it is possible to have more significant time point reduction when the signs are accounted for. Histograms of time step number and resultant moment ratios are presented in Figure 14.

### Linearization of nonlinear supports

In extreme dynamic load cases, plant piping supports keep the displacements of the pipes within acceptable limits. Studies (Ristaniemi 2015, 2016) were performed to investigate and develop linear modeling methods for nonlinear piping supports in dynamic analyses. In the study, a procedure to linearize nonlinear supports was presented. The purpose of the linearization procedure is to represent the nonlinear system as accurately as possible by an equivalent linear system. Using the linear system, computational effort can be significantly reduced. In the procedure, the nonlinear supports are replaced by linear springs or spring-dampers (Figure 15a,b). The equivalent spring and damping constants are typically found by an iterative procedure (Figure 15c).

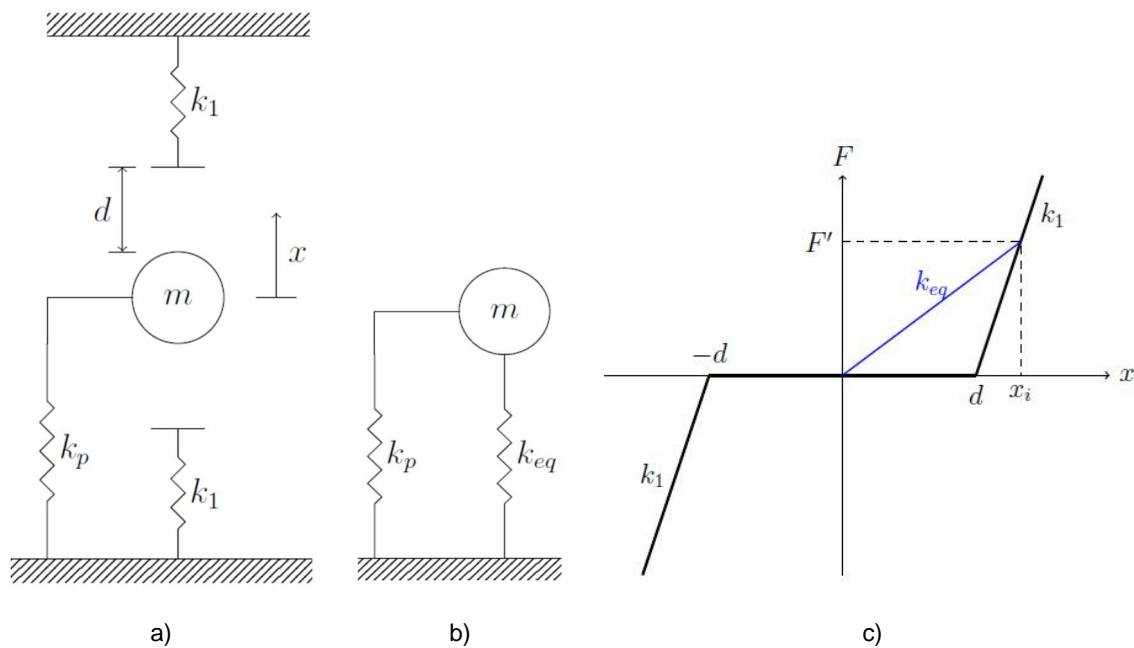


**Figure 15.** Schematic of a nonlinear piping support (a), its linearized representation (b) and an example of a method to determine the equivalent stiffness (c).

The linearization procedure was investigated using single and multiple degree-of-freedom examples. Linearization was then applied to a representative NPP piping and support configuration with four gap supports. It was found that the maximum displacements were of the same order of magnitude, though large differences occurred at single locations. The maximum support forces were generally much smaller

in the linear system due to the smaller linear stiffness. Example results from a seismic analysis of a linearized nonlinear system is shown in Table 2.

**Table 2.** Example results of a linearized simple piping system with nonlinear supports under seismic excitation.

Location	Nonlinear time history	Eq. linear time history	Eq. linear response spectrum (ABSSUM)	Eq. linear response spectrum (SRSS)
	Displacement (m)			
Node 3	0.1007	0.06658	0.06667	0.06568
Node 5	0.1007	0.10014	0.10005	0.10005
Node 7	0.1008	0.10006	0.10016	0.10016
Node 9	0.0926	0.06652	0.06681	0.06583
Force (kN)				
Node 3	1171.7	0	0	0
Node 5	2204.3	11.348	11.427	11.423
Node 7	1987.1	11.414	11.327	11.324
Node 9	0	0	0	0

## Residual stress relaxation in BWR NPPs

Residual stresses play a major role in stress corrosion cracking (SCC), which is identified as significant degradation mechanism for various BWR components. Experience from ageing NPPs shows slower stress corrosion crack growth in many components than would be expected under currently postulated stresses. Residual stress relaxation decreases the effective loads during the service life and therefore slows down SCC. The effect of residual stress relaxation on SCC is not, in general, considered in crack growth calculations although thermal and mechanical loads are known to relax residual stresses significantly. This is due to insufficient data available on the stress relaxation.

In the project, residual stress relaxation in BWR NPP was studied with co-operation of Aalto University and Teollisuuden Voima Oy. Previously used measurement methods are developed further, most notably the Contour method. In addition, residual stresses are measured from pipe sections removed from OL1 and OL2 and compared with other experimental data. The research outlined in the following is presented in detail in (Virkkunen and Toivonen 2016; Virkkunen 2017a, 2017b).

### Contour Method Development

Contour method is an experimental method to measure two dimensional residual stress maps of components. The method was introduced relatively recently (Prime, 2000) and has since found widespread use in various applications.

The contour method is a destructive method. The component to be measured is cut in two. If the sample was initially free from residual stresses, the cut surfaces remains plane. During the cutting, any possible

residual stresses on the cut plane and directed perpendicular to the surface are relieved by the introduction of the new free surface. The introduction of the free surface allows displacements on the new surface and thus relieves any possible stresses perpendicular to the cut surface. Consequently, any possible residual stresses on the cut surface are turned to displacements on the newly formed free surface. These displacements cause deviations from planeness of the cut surface and can be measured after the cut and used to compute residual stresses prior to cutting.

The surface measurement is typically done by 3D-coordinate measurement machine, though other measurement devices has also been used. The spatial resolution of the measurement is limited by the resolution of the measurement and subsequent smoothing required. With point-by-point measurements the measurement time increases rapidly with increasing spatial resolution. Measurements in 1 by 1 mm grid are commonly applied.

In current project, the spatial resolution of the contour method was significantly improved by adopting white light interferometry measurement to the cut surface. This development also vastly increased the amount of measurement data to be analyzed, and necessitated significant development of the measurement pipeline.

Figure 16a shows the final WLI contour measurement from the reference sample. The measurement clearly shows the expected contour caused by the four point bending used to prepare the reference sample. In addition, the contour shows greater detail than would be expected from traditional coordinate measurement system. To illustrate the effect of the added measurement detail, additional analysis was completed with averaging similar to what would have been necessary for coordinate measurement system. This image is presented in Figure 16b.

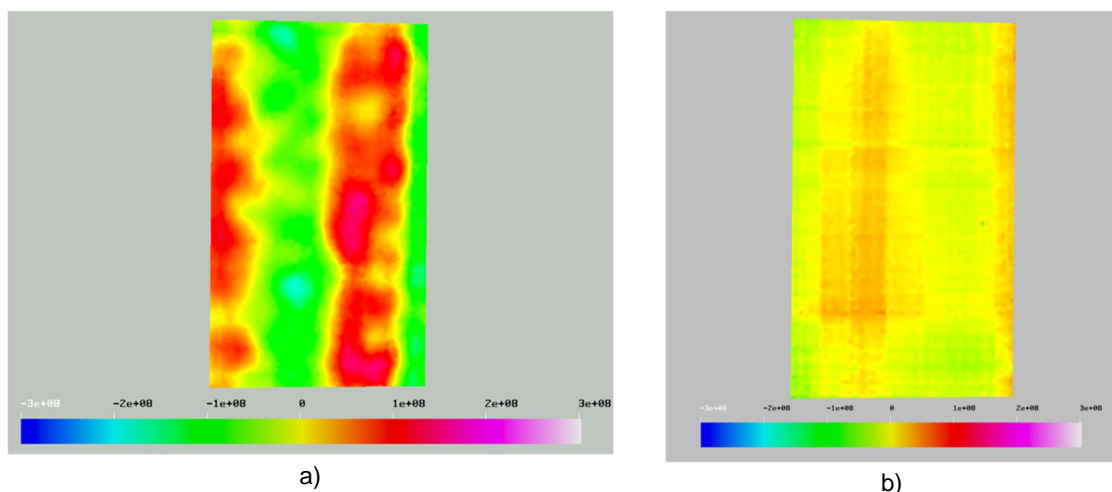


**Figure 16.** a) Final contour measurement on reference sample. b) Reference sample analyzed with smoothing similar to what would be necessary for coordinate measurement system.

#### Measurements from Removed Pipe Sections

Teollisuuden Voima provided a removed T-junction for residual stress measurements. Prior to measurement, the component had been cut in two. This was done for other investigations, but also provided measurement access to inner surface of the T-junction. The components had also been decontaminated prior to measurement. The sections were measured using X-ray diffraction and the contour method (using white light interferometry and the newly developed measurement pipeline). Contour measurements were completed on four sample surfaces. Typical results are shown in in Figures 17 – 18.

The results indicate, that service loads have caused some relaxation of residual stresses in the weld. The stresses are somewhat lower than were measured for the experimental pipe sections. Also, the tensile

stress region is confined more clearly inside the weld and there's a balancing compressive stress in the root area.

The previously developed WLI contour measurement proved invaluable in these measurements. With the numerous disturbances due to decontamination and sample removal, a more traditional contour measurement with lower spatial resolution would have been unable to discern the various effects and thus very limited information would have been obtained about the true residual stress state of the sample. In contrast, with the current measurement, these effects can be separated and accounted for.

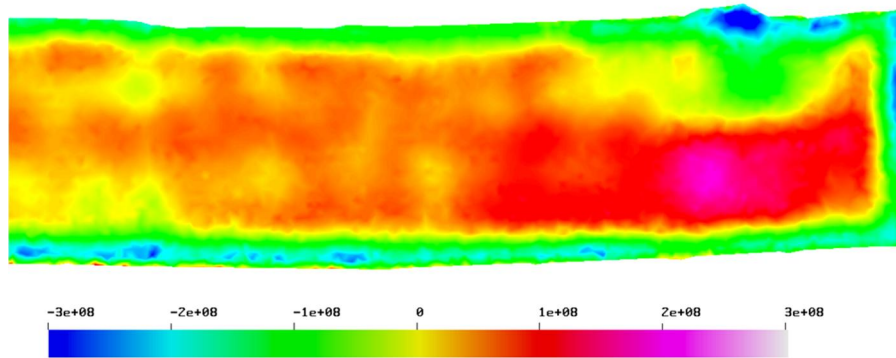


**Figure 17.** Contour measurements from weld sample A, weld 1 (stress in Pa).

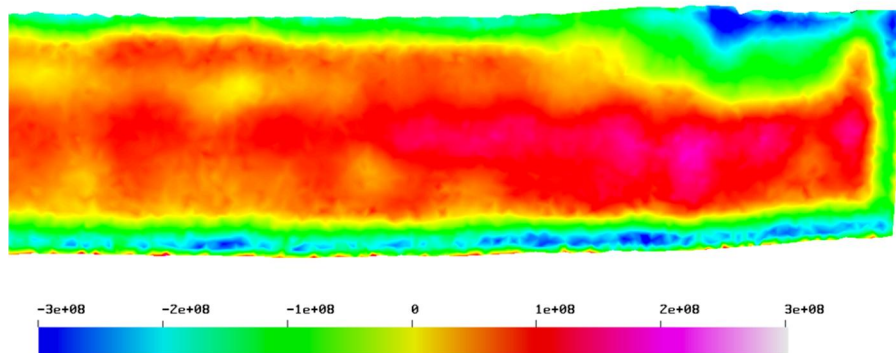


**Figure 18.** Contour measurements from sample B, weld 1 (stress in Pa).

### Concluding remarks

The FOUND project addresses several NPP ageing and component failure related aspects as described above. The research is still in progress and planned to continue in 2017 and 2018. The support from the SAFIR Reference Group 5, Teollisuuden Voima Oyj and the Swedish-Finnish Beräkningsgrupp (BG) is greatly acknowledged.

### References

ASME 2009. ASME Boiler and Pressure Vessel Code, Section III, Division 1, Appendices, Mandatory Appendix I Design Fatigue Curves, Addendum 2009b.

- ASME 2015. ASME Boiler and Pressure Vessel Code, Section XI - Rules for Inservice Inspection of Nuclear Power Plant Components.
- British Standards Institution 2015. BS 7910:2013+A1:2015 - Guide to methods for assessing the acceptability of flaws in metallic structures.
- Busch, M. et al. 1994. KI-Factors and Polynomial Influence Functions for Axial and Circumferential Surface Cracks in Cylinders. IWM-Report T 18/94, Fraunhofer-Institut für Werkstoffmechanik (IWM). 41 p.
- Busch, M. et al. 1995. Polynomial Influence Functions for Surface Cracks in Pressure Vessel Components. IWM-Report Z 11/95, Fraunhofer-Institut für Werkstoffmechanik (IWM), January 1995. 88 p.
- Chopra, O. and Stevens, G.L. 2014. "Effect of LWR Coolant Environments on the Fatigue Life of Reactor Materials", NUREG/CR-6909, Rev. 1, ANL-12/60 (Draft), U.S.NRC.
- Cronvall, O. & Vepsä, A. 2012. Further development and validation of probabilistic analysis application VTTBESIT. VTT Report VTT-R-01837-12, Technical Research Centre of Finland (VTT), Espoo, Finland. 49 + 7 p.
- Cronvall, O. 2015. Study on Status of Safety Margins Assessment Practices. VTT Research Report VTT-R-06265-15. Espoo: VTT.
- Cronvall, O. 2017. Susceptibility of BWR RPV and its internals to degradation mechanisms. Doctoral Dissertation. Unfinished Draft. 3.2.2017.
- Heckmann, K. and Saifi, Q. 2015. Comparative Analysis of Deterministic and Probabilistic Fracture Mechanical Assessment Tools. Paper for the European Technical Safety Organisations Network (ETSON) Award 2015.
- Howard, R.J.A and Serre, E., 2017. Large eddy simulation in Code\_Saturne of thermal mixing in a T junction with brass walls. International Journal of Heat and Fluid Flow. Article in press.
- IAEA 1992. Methodology for the Management of Ageing of Nuclear Power Plant Components Important to Safety. Technical Reports Series No. 338, International Atomic Energy Agency (IAEA), Vienna, 62 p.
- IAEA 2005. Assessment and management of ageing of major nuclear power plant components important to safety: BWR pressure vessel internals. IAEA-TECDOC-1471, International Atomic Energy Agency (IAEA), Vienna, Austria, 107 p.
- Jayaraju, S.T., Komen, E.M.J. and Baglietto, E., 2010. Suitability of wall-functions in large eddy simulation for thermal fatigue in a T-junction. Nuclear Engineering and Design, Vol. 240, pp. 2544–2554.
- Kuutti, J. 2015. Simulation of thermal cracking. VTT Research Report VTT-R-05024-15. Espoo: VTT.
- Kuutti, J. 2016. A J-integral calculation routine for Abaqus. VTT Research Report VTT-R-05842-16. Espoo: VTT.
- Kuutti, J. 2017a. Comparison of ASME XI and BS7910 allowable flaw sizes. VTT Research Report VTT-R-00597-17. Espoo: VTT.
- Kuutti, J. 2017b. Crack opening displacement as a crack driving force parameter for thermal fatigue simulations. VTT Research Report VTT-R-00087-17. Espoo: VTT.

- Lemettinen, P. 2016. OL1/OL2 Power Uprate - Risk Survey for Flow-induced Vibrations of RPV Internals. TVO Report 156094, Teollisuuden Voima Oyj (TVO), Eurajoki, Finland, 15.8.2016. 133 p.
- Oinonen, A. 2015. Effect of the Crack Detection Function on the Break Probability of Piping Welds. VTT Research Report VTT-R-05145-15. Espoo: VTT.
- Oinonen, A. 2016. A Review of Qualification of Nuclear Plant Piping Analyses. VTT Research Report VTT-R-03213-16. Espoo: VTT.
- Oinonen, A. 2017. VTTBESIMPROB 0.5 User Manual. VTT Research Report VTT-R-00159-17. Espoo: VTT.
- Pasutto, T., Péniguel, C. and Sakiz, M., 2009. Chained computations using an unsteady 3D approach for the determination of thermal fatigue in a T-junction of a PWR nuclear plant. In: 20th International Conference on Structural Mechanics in Reactor Technology Espoo, Finland, August 9–14, 2009.
- Prime, M.B. 2000. Cross-Sectional Mapping of Residual Stresses by Measuring the Surface Contour After a Cut. *J. Eng. Mater. Technol* 123(2), 162-168. doi:10.1115/1.1345526.
- Ristaniemi, A. 2015. Linearization of piping supports in dynamic analyses (Master's thesis). Espoo: Aalto University.
- Ristaniemi, A. 2016. Linearization of piping supports in dynamic response spectrum and time history analyses. VTT Research Report VTT-R-01434-16. Espoo: VTT.
- Seppänen, T., 2016. "Environmental Effect of Reactor Coolant on Fatigue of Stainless Steel", MSc thesis, Aalto University, Espoo.
- Seppänen, T., Alhainen, J., Arilahti, E. and Solin, J. 2015. "Experimental Methods for Direct Strain-Controlled Low Cycle Fatigue Tests in Simulated PWR Water", Paper 64, Proc. Fourth International Conference on Fatigue of Nuclear Reactor Components, Sevilla, Spain, September 28-October 1, 2015. 5 p.
- Seppänen, T., Alhainen, J., Arilahti, E. and Solin, J., 2016a. "Direct Strain-Controlled Variable Strain Rate Low Cycle Fatigue Testing in Simulated PWR Water", PVP2016-63294, Proc. ASME 2016 Pressure Vessels and Piping Conference, Vancouver, British Columbia, July 17-21. 2016. 5 p.
- Seppänen, T., Alhainen, J., Arilahti, E., 2016b. "Environmental Fatigue in Simulated PWR Water – Experiments with AISI 347", VTT Research Report VTT-R-05639-16. 11 p.
- Seppänen, T., Alhainen, J., Arilahti, E. and Solin, J., 2017. "Strain Waveform Effects for Low Cycle Fatigue in Simulated PWR Water", PVP2017-65374, submitted to ASME 2017 Pressure Vessels and Piping Conference. 7 p.
- Solin, J. et al. (9 authors) 2011., Fatigue of Primary Circuit Components (FATE), SAFIR2010, The Finnish Research Programme on Nuclear Power Plant Safety 2007–2010, Final Report. VTT Research Notes 2571, p. 368 – 380. [<http://www.vtt.fi/inf/pdf/tiedotteet/2011/T2571.pdf>]
- STUK 2002. Radiation and Nuclear Safety Authority: Ensuring the Strength of Nuclear Power Plant Pressure Devices. Guide YVL 3.5. Helsinki: STUK.
- STUK 2014. Radiation and Nuclear Safety Authority: In-service Inspection of Nuclear Facility Pressure Equipment with Non-destructive Testing Methods. Guide YVL E.5 / 20 May 2014. Second, revised edition Helsinki: STUK.

- Tang, H. T. 2006. Materials Reliability Program: Screening, Categorization, and Ranking of Reactor Internals Components for Westinghouse and Combustion Engineering PWR Design (MRP-191). Technical Report 1013234, Electric Power Research Institute (EPRI), California, U.S., 204 p.
- Timperi, A. & Cronvall O. 2016. Uncertainties in Stresses due to Thermal Mixing Loading. VTT Research Report VTT-R-00063-16. Espoo: VTT.
- Timperi, A. 2015. Study of Moment Combination and Effect of Damping in Dynamic Analyses. VTT Research Report VTT-R-05997-15. Espoo: VTT.
- Timperi, A. 2016. CFD and Structural Calculations of Thermal Mixing in a T-junction. VTT Research Report VTT-R-00221-16. Espoo: VTT.
- Timperi, A. 2017a. Spectrum Method for Modelling Crack Growth due to Thermal Mixing. VTT Research Report VTT-R-00137-17.
- Timperi, A. 2017b. Study of Moment Combination Methods for Dynamic Analyses. VTT Research Report VTT-R-00643-17. Espoo: VTT.
- TVO 2011. Nuclear power plant units Olkiluoto 1 and Olkiluoto 2. Teollisuuden Voima Oyj (TVO), PDF Publication in English, from <http://www.tvoy.fi>, 24 November 2011. 51 p.
- Tyrväinen, T. 2015. Connection between PRA and RI-ISI analyses. VTT Research Report VTT-R-04536-15. Espoo: VTT.
- Tyrväinen, T. 2016. Computation of consequences of piping component failures in PRA software. VTT Research Report VTT-R-04536-15. Espoo: VTT
- Varfolomeyev, I. et al. 1996. BESIF 1.0: Stress Intensity Factors for Surface Cracks under 2D Stress Gradients. IWM-Report T 14/96, Fraunhofer-Institut für Werkstoffmechanik (IWM), 42 p.
- Vepsä, A. 2004. Verification of the stress intensity factors calculated with the VTTBESIT software. Technical Research Centre of Finland (VTT), Research Group Structural Integrity, Research Report TUO72-044578. 40+2 p.
- Virkkunen, I., Kuutti, J., Miettinen, K. Trueflaw Fatigue Data – Crack Initiation Tests. (2013). TF Documentation number 288BDX066. 2013-12-05.
- Virkkunen, I., Kuutti, J., Miettinen, K. Trueflaw Fatigue data – Crack growth tests (2015). TF Documentation number 046BFX085. 2015-09-19.
- Virkkunen, I. and Toivonen, H. 2016. Contour Method Development, FE modeling of Residual Stresses Caused by Cyclic Thermal Loads. Aalto University, Research report, revision 2, 4.2.2016
- Virkkunen, I. 2017a. Measurement of residual stresses from BWR welds removed from service. Aalto University, Research report, Revision 1, 13.1.2017.
- Virkkunen, I. 2017b. Comparison of test samples and residual stresses from BWR welds removed from service. Aalto University, Research report, Revision 1, 29.1.2017.

### 6.3 Long term operation aspects of structural integrity (LOST)

Sebastian Lindqvist, Kim Wallin, Heikki Keinänen, Qais Saifi, Päivi Karjalainen-Roikonen

VTT Technical Research Centre of Finland Ltd  
P.O. Box 1000, FI-02044 Espoo

#### Abstract

The goal of this project is to develop the current structural integrity assessment methods for primary circuit through experimental and numerical investigations, and thus, improve the safety of the nuclear power plant. The obtained results during 2015-2016 are divided into four groups. Firstly, miniature sized fracture toughness specimens were validated and used to determine ductile-to-brittle temperature,  $T_0$ , of Barsebäck reactor pressure vessel weld. Secondly, related to dissimilar metal welds, inlay and overlay welding was investigated in cases of weld repair. Thirdly, two types of dissimilar metal welds were characterised. Tearing resistance was lowest at the fusion boundary and conventional specimens produce conservative results. The results show the effect of crack path on tearing resistance. Finally, based on experimental characterisation on dissimilar metal welds, a numerical model was built, and the tearing resistance and crack path was simulated. The tearing resistance gives a good fit to the experimental results, but to capture the crack path a refined numerical model, with thinner material zones, is required.

#### Introduction

The goal of SAFIR2018 subproject long term operation aspects of structural integrity (LOST) is to develop through experimental and numerical methods more accurate structural safety assessment methods to the nuclear power plant (NPP) end users and regulator. A systematic ageing management procedure is the basis for justifying the safe long term operation (LTO) of nuclear power plants. One fundamental part in this process is to assess the structural integrity of the NPP components such as reactor pressure vessel (RPV), pipes, welds and valves. In this project a comprehensive investigation is done considering the possibility of fast fracture in the upper shelf temperature regime of RPVs. Improved methods are developed for fracture toughness and crack driving force estimation of dissimilar metal welds (DMW). Also methods are developed for estimation of residual stresses in repaired DMWs, and the current methods for surveillance material testing are improved.

Project LOST is divided into two deliverables, “advanced structural integrity” and “dissimilar metal welds”. The “advanced structural integrity” includes research on fast fracture in upper shelf region and advances in surveillance specimens testing.

The investigation on fast fracture in upper shelf region is justified by the new YVL guidelines. Connected to the ageing of the material, the YVL guideline E.4, entitled “Strength analyses of nuclear power plant pressure equipment” contains in chapter 6 “Brittle fracture analysis”, section 6.8 “Other fast fracture considerations” the following paragraph: 616. *In connection with the strength analysis of Safety Class 1 pressure equipment, an assessment shall be given on the potential for a fast fracture occurring in the upper shelf area where temperatures exceed the transition temperature zone. This could occur in thick-walled components which undergo rapid cooling under high pressure. The adequacy of the toughness values of the upper shelf shall be analysed, where necessary. The methods and criteria used are subject to STUK's approval.*

Several studies have been published on the effect of temperature in the upper shelf region of nuclear pressure vessel steels. The resistance against fracture in upper shelf region decreases as the temperature gets higher. Practically no studies can, anyhow, be found on the effect of temperature gradient on fracture.

Therefore, the results will provide profound view on temperature effects on ductile fracture resistance behaviour of structural steels of NPPs in upper shelf region. Consequently, the results serve as input for structural integrity assessing in case of loss of coolant accident (LOCA) and LBB in NPPs.

The most recent innovation in surveillance specimen testing is miniature fracture toughness specimens, 4 mm thick C (T) specimens. The main activities related to these miniature C(T) specimens has been related to validation and standardisation of the specimen. VTT has already participated in one international round robin dealing with miniature size C(T) specimens. The benefit of miniature C(T) specimens is smaller material consumption in surveillance testing, thus the surveillance program will last longer. One Charpy-V specimen can be used to obtain 8 C(T) specimens. Thus already tested surveillance specimens can be reused.

Because the technique is quite new, the round robin activities continue with the aim of standardisation and evaluation guides of miniature size C(T) specimens.

Miniature C(T) specimens are also exploited in BREDA, a Scandinavian collaboration project. The goal with experiments carried out in BREDA is to decrease the uncertainty between experimental results from surveillance specimens, and the ageing behaviour of the RPV. IN the project the RPV trepan test samples are cut from Barsebäck 2 nuclear power plant. The work done in BREDA is carried out between Royal Institute of Technology-KTH, Stockholm, Chalmers Technical University – CTH, Göteborg and VTT Technical Research Center of Finland, Espoo. VTT is responsible for mechanical testing (tensile, Impact and fracture mechanical testing). A big part of the costs of mechanical testing at VTT is currently being included as support to a pilot project proposed under the auspices of Energiforsk (Swedish energy research).

The previous paragraphs described the state-of-the-art of “advanced structural integrity” deliverable. The second deliverable, “dissimilar metal welds”, includes investigations on residual stresses, material characterisation and local approach in DMWs. Dissimilar metal welds (DMW) are critical components of NPPs, because numerous flaws have been detected in these areas through non-destructive examinations (NDE) and DMWs contain regions that are prone to fracture.

The latest NDE methods tend to give more detailed information of existing defects/flaws in components. Flawed components can be repaired. When long term operation is considered of repaired components, an essential point is how to assess the usability and remaining lifetime that are affected by the residual stress state in the component. The overlay welding of components, e.g. bimetallic welds in nozzles, is a well-established repair technique in USA, especially in the case of circumferential flaws/cracks. The recent results show, however, that the situation may be different in the case of deep axial defects, for which overlay welding may lead to an unfavourable residual stress state. Most of the present computational approaches to model these are based on axisymmetric models. Three dimensional modelling may give more accurate results as compared to those obtained with axisymmetric models. Therefore, methods based on three dimensional modelling should be developed for assessment of residual stresses in repaired DMWs with axial defects.

Another goal for DMWs is to develop descriptive fracture toughness and crack driving force determination techniques, because current methods are developed for homogeneous specimens. Accurate fracture toughness determination of the most critical region in DMWs is important for LBB analysis that is used to ensure structural integrity. The development of descriptive fracture toughness and crack driving force determination techniques require both experimental and numerical work.

Descriptive fracture toughness values for DMWs are not easily achieved, because the current methods are developed for homogeneous materials. In DMWs the deformation of the material in front of the crack can be concentrated in a completely different manner than in homogeneous specimens. This difference in deformation behaviour can make the methods used for homogeneous specimens inapplicable for heterogeneous welds. Another problem is that in DMWs cracks can deviate away from their initial fracture plane. There is no standard that tells how to take into account crack deviation in fracture toughness measurements.

To overcome these difficulties in fracture toughness measurements and crack driving force determination of DMWs, both numerical and experimental investigations are required. Experimental methods are required to understand the material behaviour, determine accurate FE models and calibration parameters

for the numerical work. Numerical work is required to improve the analytical fracture toughness solutions and to improve the methods for crack driving force calculations in DMWs.

## Advanced structural integrity

### Miniature fracture toughness specimens

Miniature fracture toughness specimens, 4 mm thick C(T) specimens, were experimentally tested in [1] and [2] (Figure 1). In [1] the initiation location of brittle fracture was characterised and compared to standard sized specimens. The initiation location with respect to mid-plane of miniature C(T) specimens has the same distribution as conventional specimens, and side grooves have a minor effect on initiation location. These results validate the use of miniature C(T) specimens.

In [2] miniature sized C(T) specimens were experimentally tested to characterise the ductile-to-brittle transition temperature,  $T_0$ , in reference condition for reactor pressure vessel weld of Barsebäck 2.  $T_0$  is  $-98$  °C, which is a low value and brittle fracture at room temperature can be excluded.

This work is related to project BREDA, a Scandinavian collaboration project. The goal in BREDA is to estimate the representability of surveillance programs, by comparing the fracture toughness determined from surveillance specimens to fracture toughness obtained from reactor pressure vessel (RPV) wall. The RPV samples are extracted from Barsebäck 2 nuclear power plant. The project includes also an extensive microstructural characterisation.

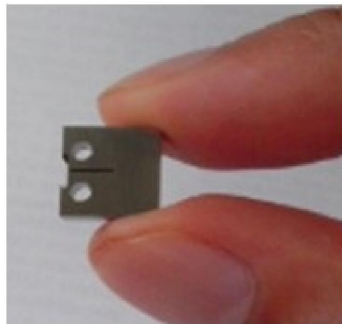


**Figure 1.** Newest innovation in surveillance specimen test techniques, miniature C(T) specimens. Four miniature C(T) specimens can be extracted from one Charpy-V specimen half.

## Dissimilar metal welds

### Residual stresses

Residual stresses due to overlay [3] and inlay [4] welding have been investigated by numerical simulations and literature surveys. On the basis of literature, weld inlay has been successfully applied in several cases. The good stress corrosion resistance obtained by inlay welding overrides the un-favourable effects of high tensile stresses. Numerical simulations predict that overlay welding reduces circumferential stresses especially near the inside surface. The results show that the decrease of the circumferential stress due to overlay welding is small at depths larger than half of the wall thickness from inner surface (Figure 2). The situation is the same in the case of combined inlay and overlay welding. The advantages/disadvantages of these two welding techniques are exploited when considering weld repairing.

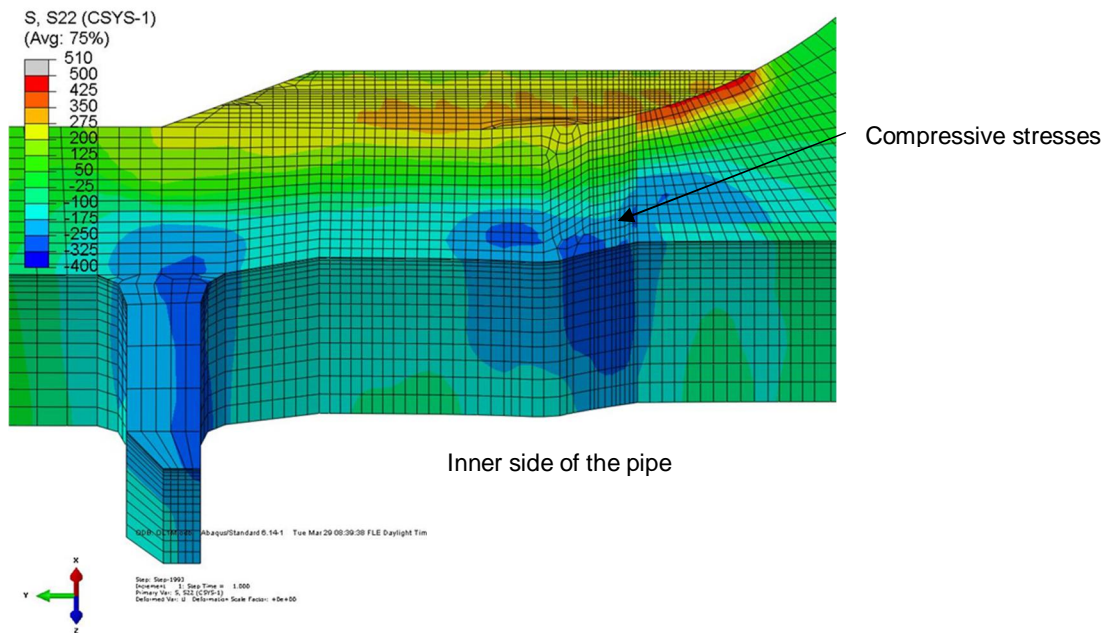


**Figure 2.** Computed hoop stress [MPa] of a dissimilar metal weld after overlay welding, a weld repair technique, at room temperature. The stresses are compressive close to the inner surface of the component.

## Material characterisation

Two different types of dissimilar metal welds, a VVER-type and a narrow-gap Alloy 52, have been experimentally characterised in [5] and [6]. In [6] tearing resistance is smallest at the fusion boundary (Figure 3). Tearing resistance is higher for HAZ cracks that initiate further away from the fusion boundary, even if the crack later on deviates to the fusion boundary. Furthermore, crack path analyses of SE(B) specimens show that if the initial crack is 20  $\mu\text{m}$  on weld metal side, then the tearing resistance is higher than at the fusion boundary. These results affect how the lower boundary values of DMWs shall be identified.

The effect of specimen configuration on tearing resistance was also investigated [6] and [7]. The results show that the conventional C(T) and SE(B) specimens produce conservative estimates of tearing resistance in comparison to SE(T) specimens. Tearing resistance is used to estimate the allowable crack size in the component. Therefore, a greater allowable crack size is obtained with SE(T) specimens.

In [5], the effect of DMW specific equations on tearing resistance was investigated. The results show that standard fracture toughness equations can produce non-conservative results compared to tearing resistance estimated with DMW specific equations. The only difference in DMW specific equations and standard solutions is the  $\eta$ -factor. The factor is affected by the properties of the surrounding materials and thus needs to be optimised for DMWs [8]. The investigation continues in 2017.

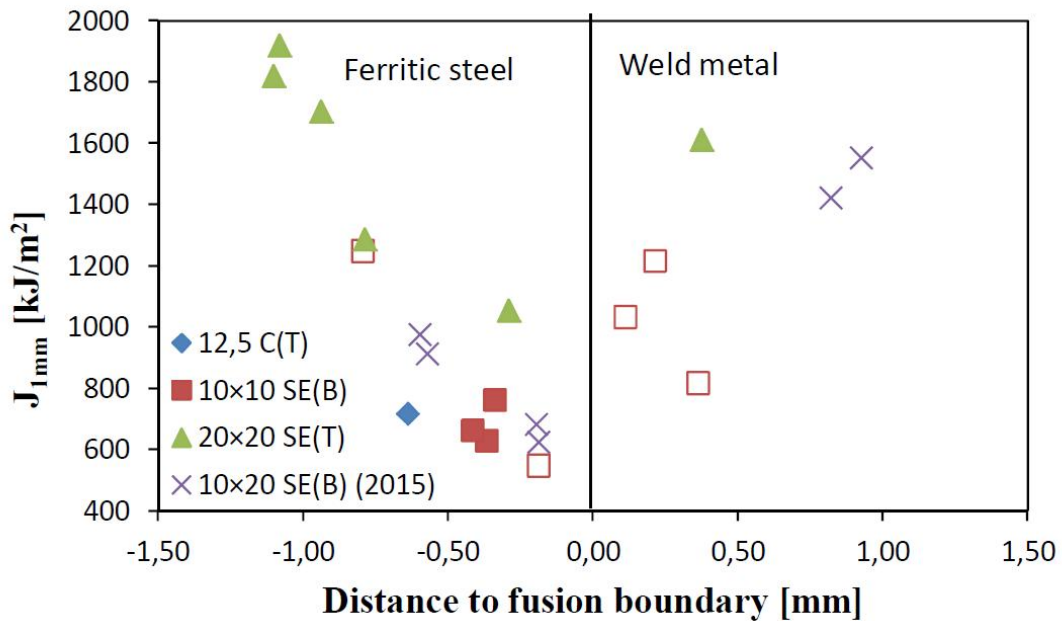


**Figure 3.** Tearing resistance,  $J_{1mm}$ , as a function of the initial distance of a crack to fusion boundary in a narrow-gap Alloy 52 dissimilar metal weld. The closer the crack is initially to the fusion boundary, the smaller is  $J_{1mm}$ .

### Local approach

Crack growth computation for two C(T) specimens were carried out by GTN model. The material was a DMW. The cracks were located in the ferritic HAZ, and the material properties in this region was characterised by 1 mm thick tensile specimens (Figure 4) and tearing resistance was characterised in [5]. Tearing resistance simulations yield a good fit with experimental results [9].

However, the numerical model is not able to predict the crack growth path. To model crack growth in HAZ of DMWs the thickness of the different material zones in HAZ has to be optimized [10]. The optimization is required to capture the effect of gradual strength changes on crack growth. The strength changes in HAZ occur over few mm, thus the thickness of the material zones in the numerical model have to be refined.

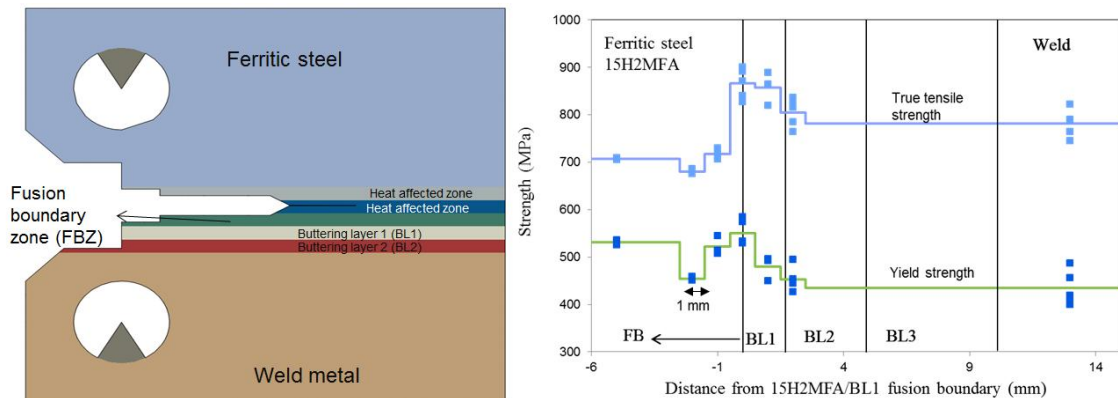


**Figure 4.** The material properties (right figure) of the different zones in the numerical model (left figure) were obtained from tensile tests with miniature tensile specimens capturing a 1 mm thick region.

The benefit with the used numerical model is simulations of crack growth. In previous models only static cracks can be analysed. The benefit with crack growth simulations in DMW interface region is increased understanding of the different material zones with different material properties on the crack growth path and tearing resistance.

## References

1. Wallin, K., Yamamoto, M. & Ehrnstén, U. 2016. Location of initiation sites in fracture toughness testing specimens – the effects of size and side grooves. Proceedings of the ASME 2016 Pressure Vessels and Piping Conference PVP2016.
2. Lindqvist, S. & Seppänen, T. 2017. BREDA: Fracture toughness measurements with miniature C(T) specimens in reference condition. Espoo: VTT. VTT Technology VTT-R-00140-17. 19 p. + app. 31 p.
3. Keinänen, H. 2016. Stresses due thick overlay welding. Espoo: VTT. VTT Technology VTT-R-00374-17. 28 p.
4. Keinänen, H. 2016. , Inlay welding as a nozzle repair method, literature survey of the residual stress computations. Espoo: VTT. VTT Technology VTT-R-01073-16. 17 p.
5. Lindqvist, S. 2016. Tearing resistance analysis of a VVER dissimilar metal weld mock-up. Espoo: VTT. VTT Technology VTT-R-03996-16. 24 p. + app. 23 p.
6. Lindqvist, S. 2016. , Dissimilar metal welds – the effect of crack path and specimen configuration on tearing resistance. Espoo: VTT. VTT Technology VTT-R-03998-16. 46 p. + app. 76 p.
7. Lindqvist, S. 2017. The effect of crack path on tearing resistance of a narrow-gap Alloy 52 dissimilar metal weld. Engineering fracture mechanics.
8. Lindqvist, S. 2015. Plastic  $\eta$ -factors for heterogeneous welds. Research Report. Espoo: VTT. VTT Technology VTT-R-03810-15. 29 p.
9. Saifi, Q. 2015. Crack Growth Computation in Dissimilar Metal Weld Joints by Local Approach. Research Report. Espoo: VTT. VTT Technology VTT-R-04464-16. 20 p.
10. Lindqvist, S. & Saifi, Q. 2017. Numerical prediction of tearing resistance and crack growth path in HAZ of a VVER dissimilar metal weld. Engineering fracture mechanics.

## 6.4 Mitigation of cracking through advanced water chemistry (MOCCA)

Tiina Ikaläinen<sup>1</sup>, Essi Jäppinen<sup>1</sup>, Timo Saario<sup>1</sup>, Konsta Sipilä<sup>1</sup>, Martin Bojinov<sup>2</sup>

<sup>1</sup>VTT Technical Research Centre of Finland Ltd  
P.O. Box 1000, FI-02044 Espoo

<sup>2</sup>University of Chemical Technology and Metallurgy  
1756 Sofia, Bulgaria

### Abstract

This project focuses on advanced water chemistry tools by which the formation of magnetite particulates in the pressurized water reactor (PWR) feed water line and their deposition into the steam generator (SG) can be minimised, and the resulting localised corrosion mitigated. As one of the main results octadecylamine, ODA, a film forming amine has been shown to reduce carbon steel corrosion rate in PWR secondary side conditions by a factor of x3. The main conclusion from the subproject on lead assisted stress corrosion cracking (PbSCC) is that a combination of a mechanical testing method, in this case the SSRT test method, in situ electrochemical methods and ex situ surface analytical methods are needed to gain further insight into the mechanism of PbSCC. Based on the results, the effect of Pb is to activate the surface so that any local corrosion mode, such as SCC, becomes practically impossible, and general corrosion is observed instead. However, if the environment changes to more oxidising one by as little as 0.1 V, Pb dissolves from the surface possibly as  $\text{PbCl}^+$ , leaving the surface in a semi-passive state and very susceptible to SCC.

### Introduction

Corrosion problems in the PWR secondary circuit are mostly related to deposition of magnetite into steam generator (SG) and enrichment of impurities into crevices within the circuit. The enrichment is typically driven by boiling. Water entering the crevices within a SG (e.g. between tube and tubesheet or under a magnetite deposit on a straight tube) boils letting volatile species escape as steam and leaving non-volatile species (salts, lead, copper etc) in the small water volume of the crevice. After some time of operation, the crevice chemistry can become very aggressive (either acidic or basic) due to impurity enrichment.

This project focuses on advanced water chemistry tools by which the formation of magnetite particulates in the feed water line can be mitigated and their deposition into SG can be minimised. To that end, the mechanism of lead assisted stress corrosion cracking as a major threat to SG integrity is researched. In addition, substitutes for using hydrazine, a potentially cancerous chemical used in PWRs, are studied.

### Mechanism of lead assisted stress corrosion cracking of carbon steel

The magnitude of corrosion damage around the SG tubes is typically enhanced by enrichment of impurities within crevices. This enrichment is driven by boiling, where water entering the crevices within a steam generator (e.g. between tube and tube-support or under a magnetite deposit on a straight tube) boils, allowing volatile species to escape as steam and leaving behind non-volatile species (salts, lead, copper etc.) in the small water volume of the crevice. Lead (Pb) has been detected in effectively all tube-support samples, crevice deposits and surface scales removed from steam generators. Typical concentrations seen are 100 to 500 ppm but in some plants, concentrations as high as 2,000 to 10,000 ppm have been

detected [Kim et al., 2005]. The cracking susceptibility is believed to have a strong dependence on the redox-potential of the crevice environment. Redox-potential, on the other hand, is affected by the amount of e.g. copper oxide in the crevice solution [Betova et al., 2015].

The PWR steam generator tube materials considered to be most resistive towards stress corrosion cracking (SCC), i.e. Alloy 600TT, Alloy 800 and Alloy 690 have each been shown to be susceptible to SCC enhanced by the presence of lead (PbSCC) [Kim et al, 2009]. In case of VVER-type PWRs, the steam generator tubing is most often stainless steel which has a relatively low susceptibility to PbSCC. However, the VVER steam generator body material, carbon steel, has been shown to be susceptible to PbSCC [Matocha et al., 2007].

The technique for studying SCC in this project is to perform slow strain rate tests (SSRT) in which a tensile specimen is loaded at a constant strain rate until fracture occurs. Susceptibility to SCC is deduced from the reduction in fracture strain as compared to that in an inert environment (e.g. air or the same environment but without the SCC promoting agent) and additionally from the morphology of the fracture surface.

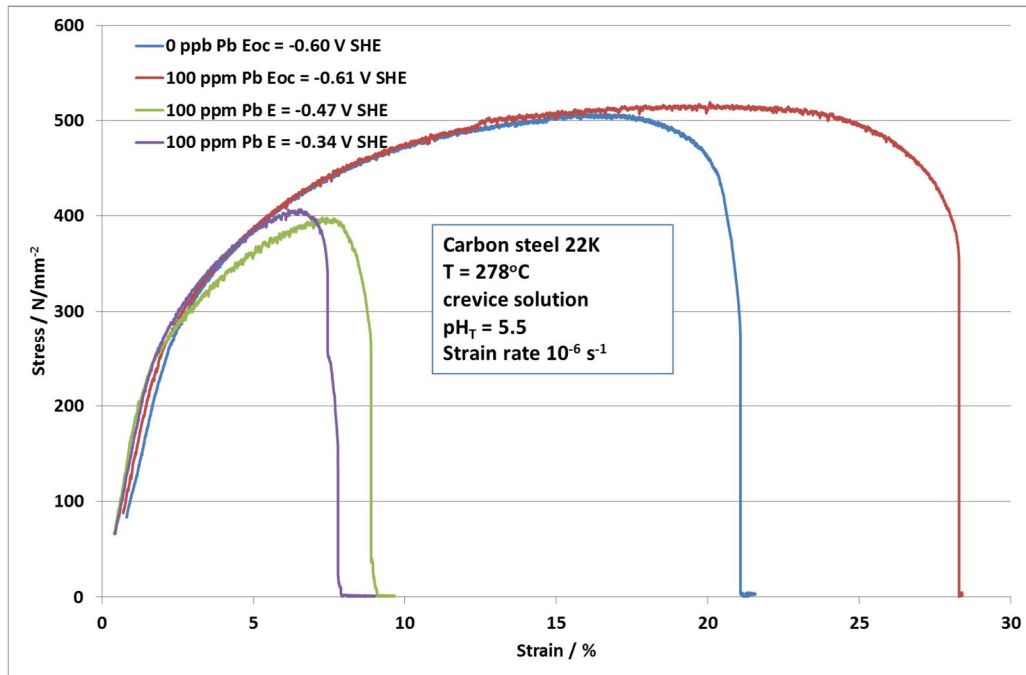


**Figure 1.** Comparison of stress-strain –curves of carbon steel 22K in crevice solution at T = 278°C with and without Pb, at corrosion potential and at slightly elevated potentials.

**Table 1.** SEM/EDS analysis results, surface of the SSRT-specimens, weighted average of oxygen, iron, sulphur and lead, a-%

Test	O	Fe	S	Pb
1	52.3	47.4	0.3	0
2	55.8	40.2	1.2	2.8
3	49.5	50.4	0.1	0
4	62.6	37.2	0.1	0.1

Figure 1 shows a comparison of stress-strain curves of carbon steel 22K in crevice solution at  $T = 278^{\circ}\text{C}$  with and without Pb, at corrosion potential and at slightly elevated potentials. Surprisingly, addition of 100 ppm Pb at corrosion potential is seen to increase the fracture strain from 22% to 28%, i.e. make the material more ductile. However, increasing potential (simulating slightly oxidising environment produced by e.g. oxygen leakage into the SG) results in a dramatic reduction of the fracture strain to values below 10%.

Electrochemical impedance spectroscopy (EIS) measurements revealed that in presence of 100 ppm Pb at corrosion potential there is practically no passive film on the surface of carbon steel 22K, i.e. the surface is in an active state and therefore any localised corrosion mode such as e.g. SCC becomes impossible. Ex situ studies of the exposed surfaces confirmed the presence of Pb on the surface at corrosion potential, but not at elevated potentials, Table 1. Current-voltage curves (i.e. polarisation curves) confirmed that the effect of Pb is to activate the surface and that at slightly elevated potentials a semi-passive surface film is formed on it. Thermodynamic phase stability calculations (Pourbaix-diagrams) revealed that at potentials about 0.1 V higher than the corrosion potential, Pb can dissolve from the surface as  $\text{PbCl}^+$ , in accordance with the SEM/EDS results shown in Table 1.

The main conclusion from this work is that a combination of a mechanical testing method, in this case the SSRT test method, in situ electrochemical methods and ex situ surface analytical methods are needed to gain further insight into the mechanism of PbSCC [Bojinov et al., 2016].

The system validation tests with carbon steel 22K in a representative slightly acidic crevice environment were rather successful. Based on the results, the effect of Pb is to activate the surface so that any local corrosion mode, such as SCC, becomes practically impossible, and general corrosion is observed instead. However, if the environment changes to more oxidising one by as little as 0.1 V, Pb dissolves from the surface possibly as  $\text{PbCl}^+$ , leaving the surface in a semi-passive state and very susceptible to SCC.

### **Effect of octadecylamine (ODA) on PWR feed water line corrosion**

There are three main routes to mitigate the corrosion problems caused by magnetite deposition on SG surfaces. The first one is to modify the water chemistry so that the source term of magnetite particles, i.e. corrosion of carbon steel components along the feed water line is minimised. This can be achieved e.g. by injecting a film forming amine into the secondary side loop or by controlling the secondary side water pH to be between 9.6 and 10, which coincides with the minimum in iron dissolution rate and thus minimises the

carbon steel corrosion rate. The second route is to select the water chemistry so that the magnetite particles keep in colloidal form and can be removed by filters before they have time to deposit into the SG. This can be done by adding a dispersant (such as polyacrylic acid, PAA) or by selecting a suitable combination of amines for the pH control. The third route is to prevent the detrimental action of the already existing magnetite deposits. This can be done by removing the deposits during outages frequently enough or by introducing crevice inhibitors (such as  $\text{TiO}_2$  or a film forming amine).

Film forming amines (FFA) have been found to be efficient in mitigating several of the detrimental aspects related to magnetite deposits. FFAs effectively reduce the source term, i.e. feed water line component corrosion by more than 90% [Betova et al., 2014], even at elevated pH close to 9.8. In addition, FFAs have been shown to be able to mitigate crevice corrosion, i.e. decrease the aggressiveness of existing crevices within SGs. As FFAs have so far been tried only in two PWR plants and one CANDU plant, (and of course in VVERs and conventional plants), there is a need for further studies on their application.

In the current project the effect of octadecylamine (ODA), one of the FFAs, on the corrosion rate of carbon steel and copper is studied using exposure coupons and in situ EIS as the main tools. Figure 2 shows a comparison of impedance spectra measured for carbon steel 22K at  $T = 228^\circ\text{C}$  in ammonia only (three repetitions) and ammonia with 20 ppm ODA (four repetitions). The impedance magnitude is about x3 higher with ODA, indicating roughly three times lower corrosion rate [Jäppinen et al., 2016a]. In case of copper a similar x3 reduction in corrosion rate was observed [Jäppinen et al., 2016b]. Reduction in the corrosion rate by roughly a factor x3 was confirmed also using conventional corrosion coupons exposed to the environment.

ODA is a film forming amine that can be used in the secondary side water of PWRs to mitigate corrosion within the feedwater line and thus also reduce magnetite deposition into steam generator, mitigating corrosion problems in the SG. ODA addition was found to have similar effect on the carbon steel corrosion rate whether it was added at the beginning of the exposure (fresh surface) or after a period of pre-oxidation of the carbon steel surface during which a stable magnetite film was grown. This indicates that ODA would possibly slow down also the corrosion of carbon steel at locations where flow assisted corrosion (FAC) takes place.

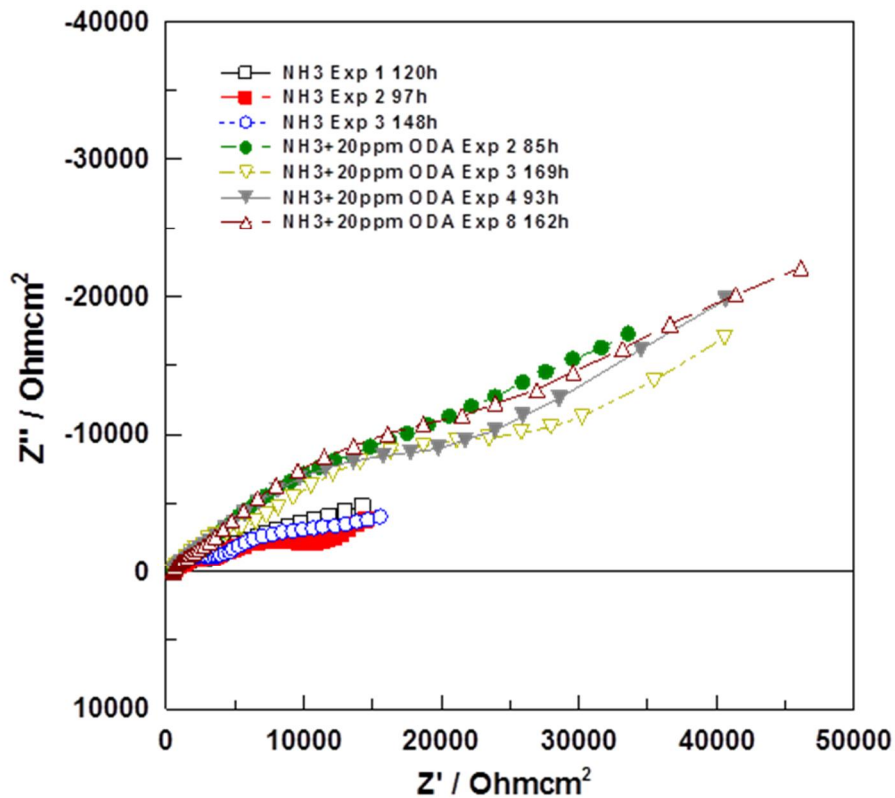


**Figure 2.** Impedance spectra of carbon steel (22K) at  $T = 228^{\circ}\text{C}$  in secondary side water treated with ammonia to  $\text{pHRT} = 9.2$  to  $9.8$ . Comparison of three repetitions without and four repetitions with 20 ppm added ODA as emulsion.

The main disadvantage of application of a film forming amine is that the on-line monitoring tools, e.g. conductivity sensors, unless withdrawn for the FFA application period, will also be covered with the thin FFA film and possibly lose their reliability. Removing and re-assembling the sensors before and after each FFA application campaign represents a notable effort which has to be considered when estimating the benefits of an FFA.

### Acknowledgement

Funding from Fortum Power and Heat Ltd and Teollisuuden Voima (TVO) Ltd is gratefully acknowledged.

## References

- Betova, I., Bojinov M. & Saario, T., State-of-the-art on SG corrosion problems – lead induced stress corrosion cracking. VTT Research Report VTT-R-03434-15, 2015.
- Betova, I., Bojinov, M. & Saario, T., Film-Forming Amines in Steam/Water Cycles – structure, properties, and influence on corrosion and deposition processes, VTT Research Report VTT-R-03234-14, 2014.
- Bojinov, M., Jäppinen, E., Saario, T. & Sipilä, K., Verification of a test method for lead assisted stress corrosion cracking of carbon steel, VTT Research Report VTT-R-05238-16, 2016.
- Jäppinen, E., Ikäläinen, T., Saario, T. & Sipilä, K., 2016a. Effect of octadecylamine on carbon steel corrosion under PWR secondary side conditions. Nuclear Plant Chemistry conference NPC 2016, Brighton, UK, 2-7th October 2016.
- Jäppinen, E., Sipilä, K. & Saario, T., 2016b. Effect of octadecylamine on copper and carbon steel corrosion under PWR secondary side conditions, VTT Research Report VTT-R-00275-16, 2016.
- Kim, D., Kim, M., Kwon, H., Hwang, S., Kim, J., Hong, J. & Kim, H., Oxide investigation formed on Alloy 600 in leaded aqueous solutions, 14th International Conference on Environmental Degradation of Materials in Nuclear Power Systems, Virginia Beach, 2009.
- Kim, U., Kim, K. & Lee, E., Effects of chemical compounds on stress corrosion cracking of steam generator tubing materials in caustic solution, Journal of Nuclear Materials, vol. 341, pp. 169-174, 2005.
- Matocha, K., Roznovska, G. & Hanus, V., The effect of lead on resistance of low alloy steel to SCC in high temperature water environments. In Corrosion issues in light water reactors – stress corrosion cracking. European Federation of Corrosion publications Number 51, eds. D. Feron and J-M. Olive. Woodhead Publishing Ltd, Cambridge, England, 2007.

## 6.5 Thermal ageing and EAC research for plant life management (THELMA)

Ulla Ehrnstén<sup>1</sup>, Matias Ahonen<sup>1</sup>, Juha-Matti Autio<sup>1</sup>, Mykola Ivanchenko<sup>1</sup>, Caitlin Hurley<sup>1</sup>, Aki Toivonen<sup>1</sup>, Roman Mougnot<sup>2</sup>, Risto Ilola<sup>2</sup>, Hannu Hänninen<sup>2</sup>

<sup>1</sup>VTT Technical Research Centre of Finland Ltd  
P.O. Box 1000, FI-02044 Espoo

<sup>2</sup>Aalto University  
P.O. Box 11000, FI-00076 AALTO

### Abstract

During the first two years of the THELMA project studies of thermal ageing of Alloy 690, started in the SAFIR 2014 ENVIS project have continued. The results show intergranular carbide precipitation, lattice contraction and increased hardness, indicative of ordering reaction. This may affect the long-term primary water stress corrosion cracking (PWSCC) resistance of pressurized water reactor (PWR) components. The studies on thermal ageing of Type 316L weld metals (similar to those used in EPR reactors) show spinodal decomposition, G-phase formation, decreased impact and fracture toughness and increased crack growth rate in BWR conditions. Nano-indentation and DL-EPR results are in good correlation with the degradation of mechanical properties and microstructural changes, implying that these methods could be used for prediction of plant aged boat samples. Initiation testing on austenitic materials (stainless steel and alloy 182) using tapered specimens show a decreasing apparent threshold stress with decreasing strain rate and a beneficial influence of polished versus ground surface, especially in BWR conditions.

### Introduction

The project THELMA, Thermal ageing and EAC (environmentally assisted cracking) research for plant life management, deals with nuclear materials behaviour in light water reactor (LWR) environments with special focus on determination of thermal ageing in austenitic primary circuit materials, i.e. stainless steel weld and cast materials and nickel-based Alloy 690. Further, precursors for environmentally assisted cracking initiation are studied and irradiated stainless steels are characterised for the OECD HALDEN project. THELMA also acts as the national forum for the EU-INCEFA+ project, aiming at an improved corrosion fatigue assessment for stainless steels in pressurized water reactor (PWR) environment. A doctoral thesis on low temperature crack growth was finalised during THELMA (Ahonen, 2015). The project results are intended for plant life management and failure analyses. A selection of results is presented in the following.

### Thermal ageing of stainless steel weld metals

Thermal ageing of stainless steel materials is known to occur in LWR conditions through spinodal decomposition, resulting in reduction of ductility and toughness. In THELMA, thermal ageing of Type 316 stainless steel weld metals is investigated in co-operation with Massachusetts Institute of Technology (MIT), USA. Stainless steel weld metals contain  $\delta$ -ferrite (>5%) to prevent hot-cracking during weld solidification. When  $\delta$ -ferrite undergoes spinodal decomposition it separates into a periodically spaced chromium-rich, iron-depleted  $\alpha'$ -phase (alpha prime phase), and an iron-rich, chromium-depleted  $\alpha$ -phase with a wavelength separation of approximately 5 to 10 nm. Additional microstructural changes occurring in the same temperature range are NiSiMo-rich G-phase precipitation,  $M_{23}C_6$  precipitation at  $\delta$ -ferrite-austenite phase

boundaries (with subsequent sensitization), as well as segregation of impurities. Mo-bearing steel, containing more Ni, such as Type 316, are more prone to G-phase precipitation compared to e.g. Type 304. The chemical composition of the weld material used in this investigation is shown in Table 1 (Lucas et al., 2015). The material was investigated in twelve different conditions: as-welded, aged 5000, 20000 and 40000 hours at 573 K (300 °C), aged 1000, 5000 and 10000 hours at 675 K (400 °C) and aged 1000, 5000 and 10000 hours at 703 K (430 °C).sensitization), as well as segregation of impurities. Mo-bearing steel containing more Ni, such as Type 316, are more prone to G-phase precipitation compared to e.g. Type 304. The chemical composition of the weld material used in this investigation is shown in Table 1 (Lucas et al., 2015).

An increase in indentation hardness (HIT) of the  $\delta$ -ferrite is clearly visible at each aging temperature, Figure 1. As the ageing temperature increases, so does the hardening rate of  $\delta$ -ferrite (about 7000 MPa after 40 000 hours at 573 K (300 °C) compared to 9300 MPa after 10 000 hours at 703 K (430 °C)). Indentation hardness of austenite remains the same during ageing, as expected. When comparing the different regions of the welds (root, middle, and crown), only small differences can be seen in the hardness values.

Double loop electrochemical potentiokinetic reactivation, DL-EPR tests, routinely applied to stainless steels for sensitisation determination, was applied to all materials using a stronger solution than normal. Only the weld materials aged and 703 K (430 °C) for 5000 and 1000 hours showed a proper reactivation peak. Post-test observations were conducted using scanning electron microscopy methods (SEM). Examination of the specimen surfaces showed no corrosion attack of the as-welded specimen and after 40 000 h at 573 K (300 °C), see , Figure 2 (a-b), whereas the specimens aged at 703 K (430 °C) for 5 000 and 10 000 hours show a clear corrosion attack on the entire surface. G-phase precipitation, confirmed by transmission electron microscope (TEM) observations, can be seen inside the  $\delta$ -ferrite grains (Ivanchenko, 2016). No  $M_{23}C_6$  precipitation could be observed, due to the low interstitial carbon content in these weld metals.

The impact energy and fracture toughness values are shown in Figure 3. The general trend in the Charpy-V impact toughness data decreases with increasing ageing time and temperature, as well as testing temperature. The decrease saturates rather quickly, when  $\delta$ -ferrite shows cleavage fracture. The general trend for the fracture toughness values is that the weld metal tested at 298 K (25 °C) shows the highest toughness, followed by the 561 K (288 °C) air toughness, and the in-situ boiling water reactor (BWR) environment toughness being the lowest (Lucas, 2011).

The investigations on thermally aged cast stainless steel from Ringhals 2 old steam generator elbows will be reported later, when more results have been obtained. The current results indicate degradation of mechanical properties and evidence of spinodal decomposition and G-phase formation also in the cast material (Bjurman et al., 2015 and 2016, Ivanchenko, 2016).

**Table 1.** Chemical composition of Type 316 weld metals

	C	Mn	Si	S	P	Cr	Ni	Mo	Cu
Weld wire—low ferrite (FN 10)	0.022	1.85	0.44	0.001	0.021	19.34	12.68	2.51	0.26
Weld wire—high ferrite (FN 14)	0.015	1.75	0.35	0.014	0.017	19.2	12.3	2.61	0.05

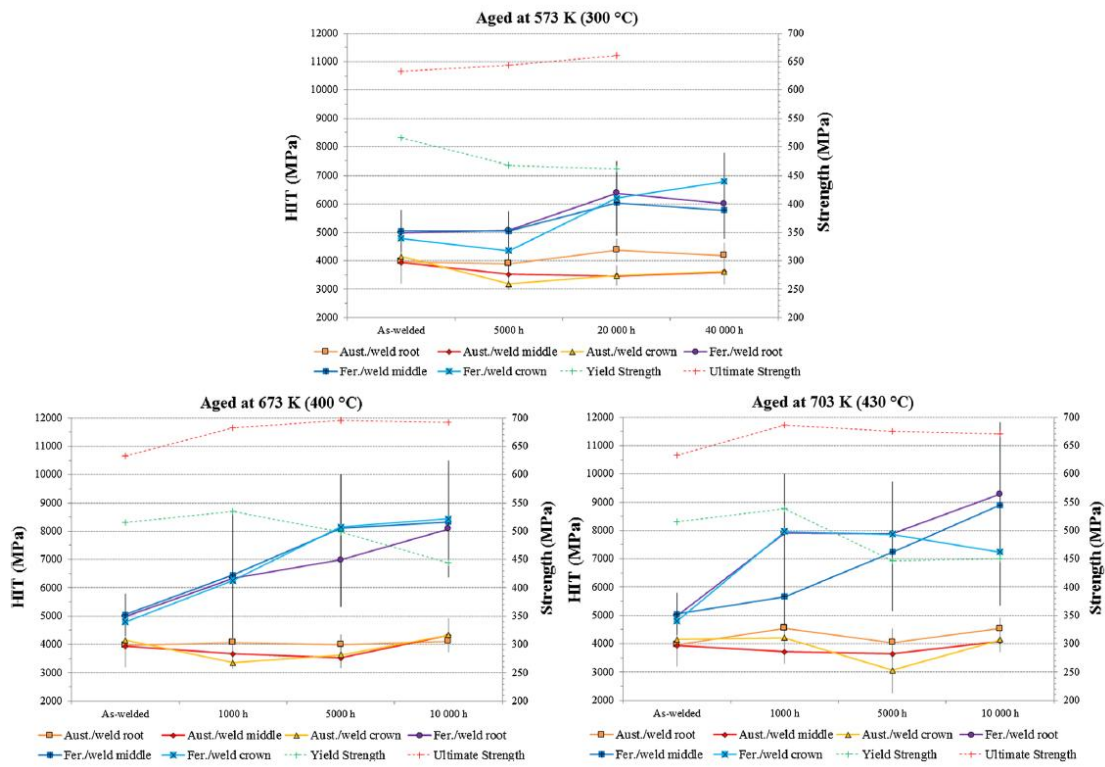


**Figure 1.** Nano-indentation hardness values for high-ferrite weld metal aged at 573 K, 673 K, and 703 K (300 °C, 400 °C, and 430 °C). In addition, yield and ultimate tensile strengths are presented with dashed lines and values on the secondary axis.

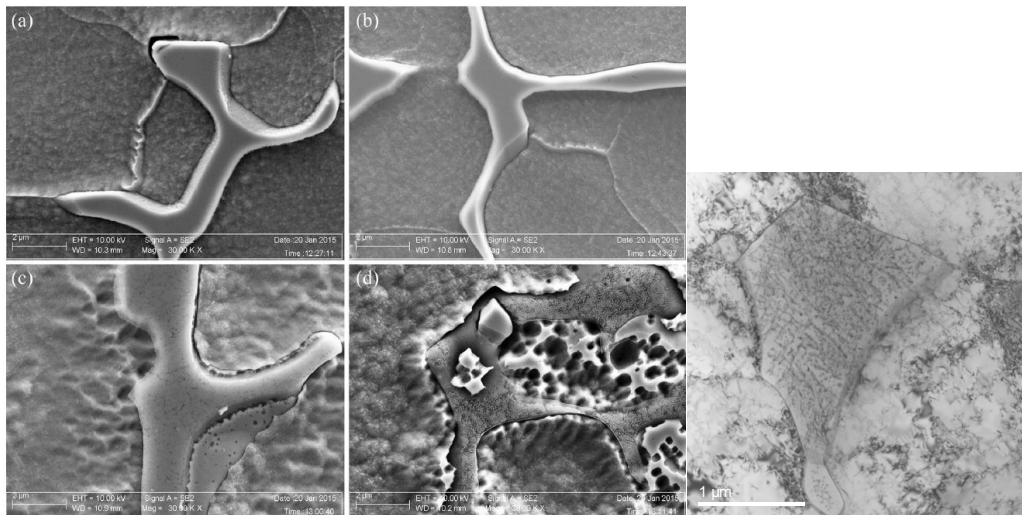


**Figure 2.** SEM micrographs of DL-EPR specimens tested in a 1M H<sub>2</sub>SO<sub>4</sub>+0.1M KSCN solution. (a) As-welded, (b) 573 K (300 °C)/40 000 h, (c) 703 K (430 °C)/5 000 h, (d) 703 K (430 °C)/10,000 h, (e) TEM-image showing G-phase.

(a)

(b)

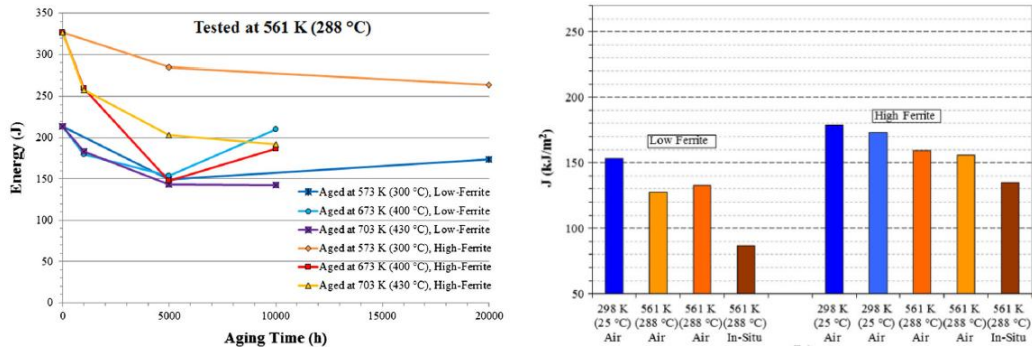


Figure 3. Impact energy (a) and fracture toughness (b) values for the materials.

### Thermal ageing and short range ordering of Alloy 690

Alloy 690 (Ni-30Cr-10Fe) is a nickel-base alloy which has been used to replace Alloy 600 since the 90s in order to improve the primary water stress corrosion cracking (PWSCC) resistance of components in pressurized water reactors. It is mostly used in the thermally treated (TT) condition Alloy 690 TT. Knowing the long-term behaviour of Alloy 690 components is of high importance to assure nuclear energy production, as they are used in critical applications such as the steam generator U-tubes and the reactor pressure vessel head penetrations. As with other commercial nickel-base alloys, Alloy 690 is subject to an ordering reaction during thermal ageing at temperatures under 550 °C. The main consequence of ordering is lattice contraction, which leads to increased hardness, ductility loss, change in the fracture mode from ductile to intergranular and heterogeneous planar slip. Most manufacturer data showing an excellent Alloy 690 long-term stability has been obtained at 565 °C and higher, but there is a strong probability that ordering can affect the long-term SCC resistance of Alloy 690 at lower temperatures, whether as an intrinsic driving force or as an additional factor. Thermal ageing of Alloy 690 has been studied in the SAFIR2014 ENVIS project, and is continued in 2018 THELMA project, and a doctoral thesis on the subject will be defended in 2017.

Two types of ordering occur in Alloy 690, i.e., short-range ordering (SRO) which is connected with the nearest neighbors of an atom, and long-range ordering (LRO) which describes the formation of an ordered super-lattice. LRO forms following a nucleation and growth process, with composition-dependent kinetics that typically requires ageing times over 10 000 h. SRO, however, develops rapidly at the early stages of ageing and its kinetics are independent of the chemical composition. The critical temperature for LRO is composition dependent and increasing the Fe content to more than 9 wt.% decreases the critical temperature from 550 °C to less than 420 °C, thus effectively reducing the temperature range in which the ordering reaction is possible (Mouginit et al. 2015, Mouginit et al., 2016).

Alloy 690 samples were prepared from a commercial melt from INCO to produce different levels of SRO. The iron content of the alloy is 9.18 wt.% Fe. All samples were solution annealed and water quenched. The first batch of samples was kept as-received solution annealed (SA). The second batch was 20% cold rolled (SACW). The third batch was heat treated at 700 °C for 17 h (TT). The fourth batch was heat treated at 700 °C for 17 h and 20% cold rolled (TTCW). Thus, a total of 20 different conditions is included in the work. The materials are studied using nano-indentation hardness, X-ray diffraction, SEM/electron back-scattered diffraction (EBSD) and TEM techniques.

The results show that intergranular (IG) carbide precipitation increased with ageing temperature. IG precipitates were identified mostly as Cr-rich M<sub>23</sub>C<sub>6</sub> carbides in non-cold-worked conditions, see Figure 4, while the larger precipitates, forming in recrystallized areas of cold work conditions aged at 550 °C were identified as  $\alpha$ -Cr, by TEM investigation. confirmed using TEM. Although 550 °C is usually considered too low for the formation of the  $\alpha$ -Cr phase, the large amount of deformation induced by cold work seems to

favor its precipitation. Diffusion-induced grain boundary migration was promoted at 475 and 550 °C, resulting in a typical wavy appearance of GB and bulged zones.

No direct observation of an ordered phase was achieved with TEM, but the formation of SRO was inferred from nano-hardness in all conditions, with a clear peak at 420 °C. The heat treatment of the TT condition increased the hardness and decreased the lattice parameter as compared to water quenching, implying the occurrence of ordering in Alloy 690 during the heat treatment, Figure 5. Indeed, the main microstructural change between TT and SA conditions consists of Cr-rich IG carbide precipitation, which decreases the hardness in the TT conditions due to a drop in solid solution hardening by carbon arising from carbide precipitation. Nonetheless, a higher hardness in TT conditions than in SA suggests the occurrence of SRO during thermal treatment, leading to a decrease in the lattice parameter and an increase in hardness. At higher temperatures, disordering affected these conditions more than the water-quenched conditions. Further, cold work promoted high strain levels prior to ageing. As a result, recrystallization and stress relaxation occurred in CW samples at higher temperatures and accentuated the effect of the disordering reaction. In addition, high levels of deformation due to CW promoted the extensive precipitation of  $\alpha$ -Cr in recrystallized areas upon ageing at 550 °C.

**Table 2.** Summary of material conditions used in the study (Mouginot et al., 2016)

As-received conditions	Code	Ageing temperature (°C)			
		350	420	475	550
SA + WQ	SA	SA350	SA420	SA475	SA550
SA + WQ + 20 % CW	SACW	SACW350	SACW420	SACW475	SACW550
SA + WQ + TT	TT	TT350	TT420	TT475	TT550
SA + WQ + TT + 20 % CW	TTCW	TTCW350	TTCW420	TTCW475	TTCW550

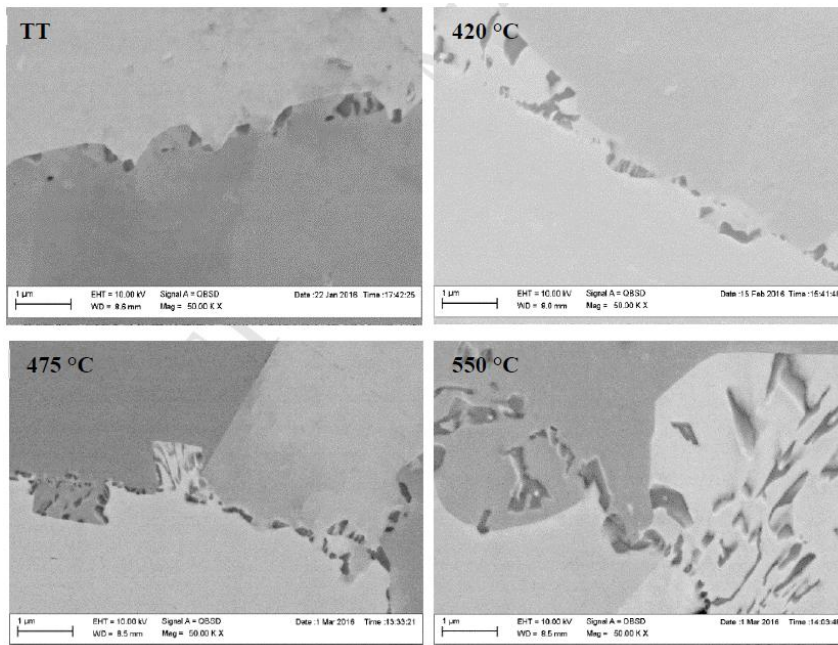


**Figure 4.** Evolution of IG carbide precipitation in TT-condition, before and after ageing at 420, 475 and 550 °C for 10 000 h.

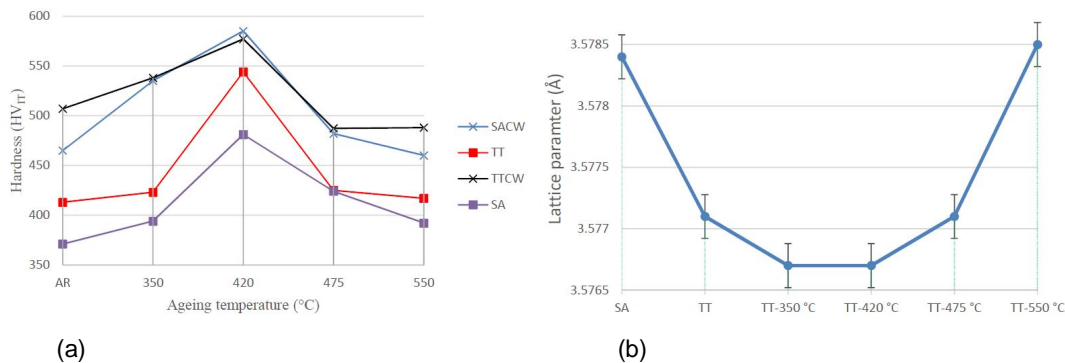


**Figure 5.** Nano-hardness (a) and lattice parameters (b), determined using X-ray diffraction, of as-received SA and TT samples, and of the TT condition after ageing at 350, 420, 475 and 550 °C for 10 000 h.

## Precursors for stress corrosion crack initiation in stainless steel

The role of cold work on the susceptibility of stress corrosion cracking (SCC) in metallic nuclear materials, especially austenitic stainless steels and nickel-base alloys, has been recognised for the past several decades and the first operational events occurred during the early days of commercial nuclear energy production. However, up to now harmonized international standards to recommend the component surface quality in LWR's are lacking. The MICRIN+ project, as part of the NUGENIA+ project, directly tackles this challenge by compiling relevant information on operational experience, specifications, codes and standards, as well as performing a tailored test program. The operational experience clearly shows the role of surface deformation on SCC initiation. Still, there are almost no national rules or guidelines on optimum surface treatment. This does not mean, that the nuclear industry would not have the knowledge, or that the rules and recommendations would not exist, but that these are internal rules, recommendations and specifications among licensees and manufacturers. Creating commonly accepted best practise and guidelines is considered very important. These must be based on a solid understanding and experimental proof on how surfaces can and should be optimised for mitigation to SCC.

However, initiation testing is both time consuming and challenging. A few test programmes have been and are performed using constant load testing, which is considered to be the most realistic testing method. Some of these tests are still running after more than a decade of testing. A reliable, accelerated test method is needed to assess, e.g., the role of surface treatment on SCC initiation susceptibility.

After writing a review on operational experience on the role of surface quality on SCC initiation and on national rules and guidelines on surface treatments (Nulife, 2012, Ehrnstén, 2015, Ehrnstén et al., 2016), a testing program was initiated between nine European laboratories to explore the appropriateness of using a tapered specimen type for accelerated initiation testing. The tapered specimen is attractive for determination of the apparent stress threshold, as the complete stress range can be tested in one single specimen, as seen in the schematically presented specimen in Figure 6. Two materials were tested, i.e., a stainless steel model alloy, alloyed with silicon to mimic irradiated stainless steel and Alloy 182, which was provided by SCK-CEN, Belgium, and cut from a dissimilar metal weld.

The results from the stainless steel test campaign showed a decreasing apparent stress threshold with decreasing strain rate. This is accordance with expectations, as the environmental effects are time dependent and slow processes. The data show quite high scatter, which at least partly is connected to challenges in interpretation of how an environmentally assisted crack can be separated from surface flaws and other surface details.

The results on Alloy 182 showed a similar decreasing apparent initiation stress threshold vs strain rate as the stainless steel material. These specimens were flat specimens, with one surface ground and the other polished, which resulted in a higher apparent stress threshold in BWR conditions, i.e., showing the detrimental effect of surface grinding on SCC crack initiation. The effect of surface condition was not as

evident in simulated PWR conditions. As for the stainless steel, also here, the difficulties in firm identification of cracks affected the results, resulting in rather large scatter (Kilian et al., 2016).

The results are promising, but far from enough for making recommendations on surface treatments. A proposal for further investigations, aiming at such recommendations, has been submitted to the Euratom H2020 programme.

The results from a Round Robin on crack initiation in Alloy 600 will be included in a later publication, when results are obtained from more participants. VTT has tested one specimen at 0.9YS without any crack initiation observed in simulated PWR conditions (Toivonen, 2016).

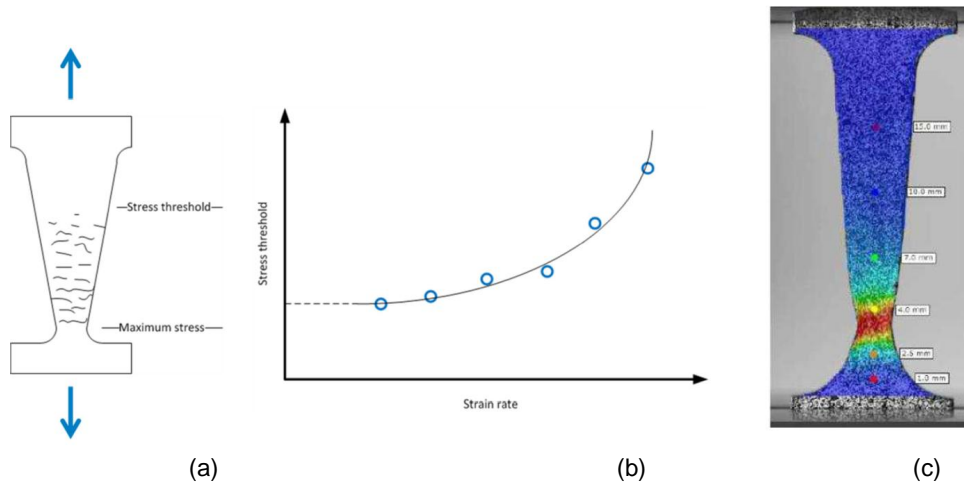


**Figure 6.** Schematic presentation of (a) a tapered specimen, (b) how the apparent initiation stress threshold is determined and (c) how the stress accumulates during straining, moving from the thinnest part to the thicker part of the specimen gauge length.

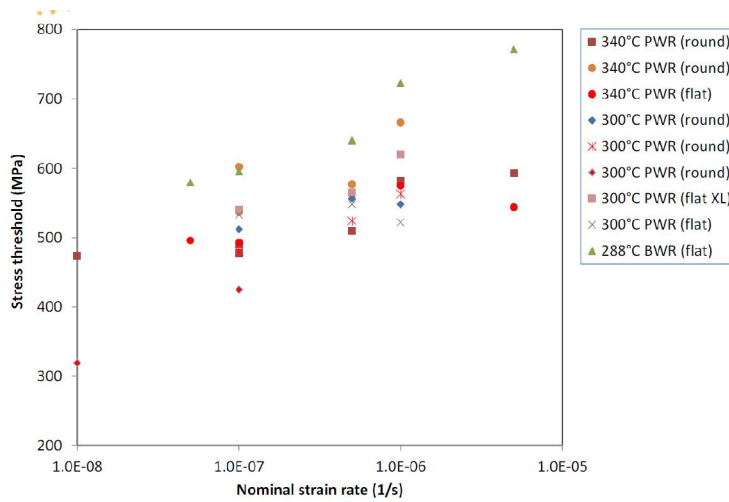


**Figure 7.** Summary of initiation test results using a model high-Si stainless steel.

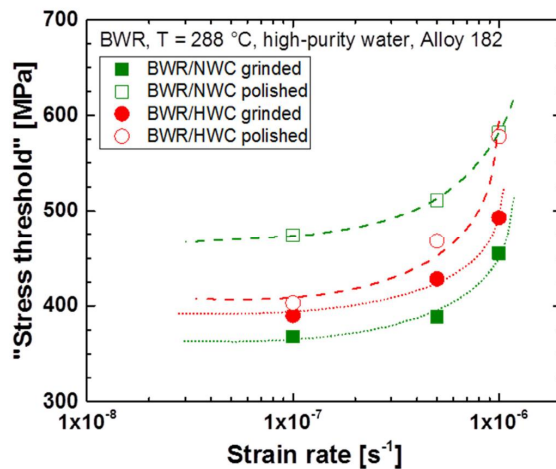


Figure 8. Summary of initiation test results for Alloy 182 in BWR environments.

### Towards improved assessment of corrosion fatigue

The effect of environment must be taken into consideration in fatigue life-time assessment of primary circuit component in Finnish NPP's. The current ASME assessment rules, applied by many, are also by many evaluated as overly conservative. Recent investigations on the role of hold times, which primary components typically are subjected to between the fatigue cycles, show a remarkable life-extending effect of these hold times. Due to this observation, and also other unexplored features, the EU-project INCEFA+ was initiated, aiming at the development of a new set of guidelines for environmental fatigue damage of nuclear power plant (NPP) components. The project was preceded with an in-kind project, in which all partners wrote reports on their position concerning corrosion fatigue strategies and important open issues. All these reports are available from the partners, and formed the basis for the proposal. The results of the INCEFA+ project, running from 2015-2019 will be interesting to the Finnish stakeholders, as the test matrix includes stainless steels used in all our NPP's and should produce about 200 new data points (Hurley, 2016).

Since the start of the project, the main focus has been on defining and agreeing upon common testing parameters and testing procedures. Testing, in air, has only recently started. The chemical composition of the materials is presented in Table 3 and the agreed test parameters in Table 4. The common material is Type 304L and specimens with specified surface condition have been delivered by EDF. Both solid polished and hollow CF specimens will be tested. The microstructures of the materials have been investigated by VTT, including determination of the grain size, which is ~80 μm in the common material, and e.g. smaller in the Type 316 and the Ti-stabilised material, see Figure 9. A [INCEFA+ public website](#) and [INCEFA+ ResearchGate](#) profiles have been created and are continually being updated with new public project information.

Table 3. Chemical composition of materials used for corrosion fatigue testing in INCEFA+

Material	C	Si	P	S	Mn	Cr	Ni	Mo	N	Nb/Ti
Type 304L <sup>15</sup>	0.029	0.37	0.029	0.04	1.86	18.0	10.0		0.056	
Type 304	0.029	0.37	0.028	0.0005	1.88	18.4	8.108	0.405	0.764	
Type 316L	0.021	0.26	0.033	0.003	1.69	17.5	11.14	2.15	0.12	
Type 321	0.102	0.52	0.023		1.45	18.1	9.79	0.023		0.61Ti
Type 347	0.031	0.325	0.03	0.004	1.86	17.3	9.12	0.38	0.021	0.357Nb

<sup>15</sup> INCEFA+ common material.

**Table 4.** Summary test parameters used in the strain-controlled tests in air and LWR environment

Test parameter	Low value	High Value
Environment	<i>air</i>	<i>LWR</i>
Temperature	<i>room temperature (RT)</i>	<i>300 °C</i>
Strain amplitude	<i>0.3 %</i>	<i>0.6 %</i>
Strain rate	<i>0.01 %·s<sup>-1</sup></i>	
Surface finish	<i>R<sub>a</sub> = 0.2 μm</i> <i>R<sub>t</sub> = 3 μm</i>	<i>R<sub>a</sub> = 7 μm</i> <i>R<sub>t</sub> = 50 μm</i>

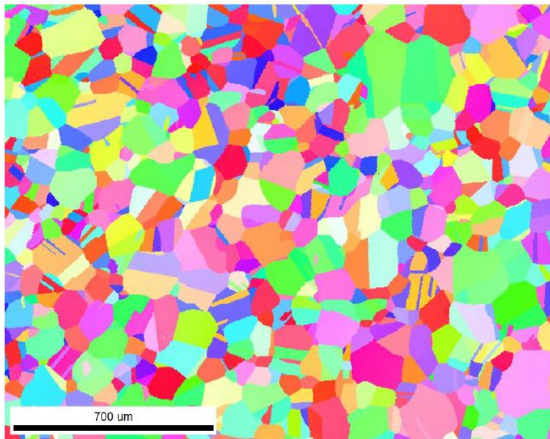


**Figure 9.** SEM/EBSD-image of Type 316 stainless steel with a grain size of 53 μm.

## Characterisation of irradiated stainless steel material

Structural materials in light water reactors are subject to irradiation-assisted stress corrosion cracking (IASCC). The initiation and propagation of IASCC cracks require a tensile stress, a corrosive environment and a susceptible material. Type 316 and 304 stainless steel are used as structural materials and are susceptible to IASCC. During reactor operation the neutron flux results in irradiation creep or irradiation stress relaxation. Hence, the initial stresses in structural components will vary during reactor operation. If the stresses decrease to zero due to irradiation stress relaxation, additional IASCC cannot occur thereafter. The purpose of one project in the OECD Halden programme is the measurement of irradiation creep and irradiation stress relaxation of common reactor structural materials in a thermal neutron reactor spectrum prototypic of PWRs and BWRs. VTT has performed the characterisation of selected materials from the Halden program as part of the SAFIR programme. The material which was selected for characterisation was from a creep test, in which the creep curve indicated shrinkage of the material in the beginning of the creep test, Figure 10.

The material was subjected to transmission electron microscopy characterization using a Philips CM200 FEG-STEM operating at 200 kV. Compositional analyses were carried out with a nominal probe size of 2 nm, utilising a Noran energy dispersive X-ray spectrum analyser (EDS). EDS spectra from background radiation from each specimen was recorded and afterwards subtracted from the spectra obtained during examination of the test material. A liquid nitrogen cold finger was also employed in order to help reduce hydrocarbon contamination in the microscope (Ivanchenko et al., 2016).

Secondary particles with a composition and morphology typical for steel manufacturing inclusions of MnO–Al<sub>2</sub>O<sub>3</sub>–SiO<sub>2</sub> type were observed. Typical irradiation damage defects such as planar defects, small

voids and dislocation loops were also observed in the material, see Figure 11. However, no features, which could explain a shrinkage of the material were found.

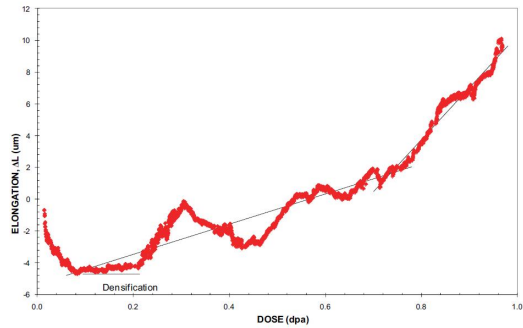


**Figure 10.** Type 304L irradiation creep tested at 290 °C and 100 MPa. The curve indicates lattice shrinkage in the beginning of the test.

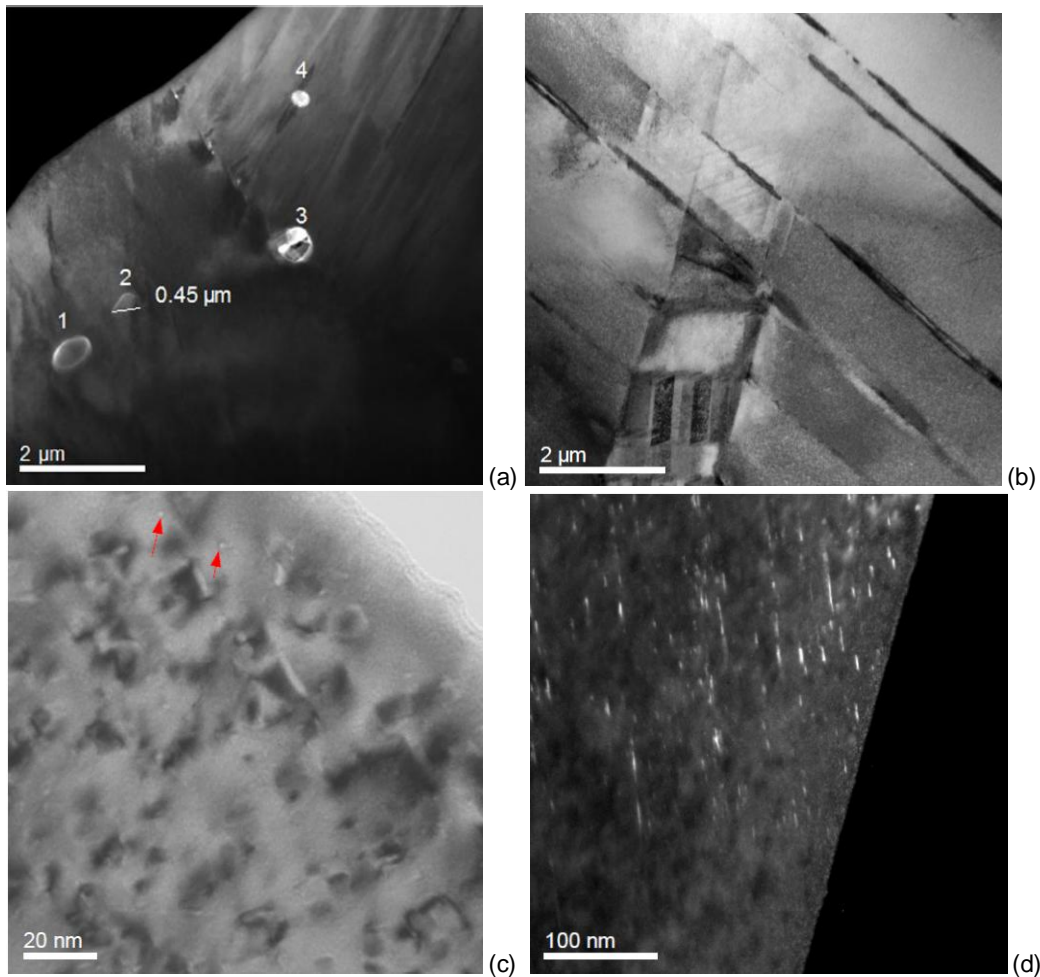


**Figure 11.** Secondary particles (a), planar defects (b), voids (c) and dislocation loops observed in the material.

## Acknowledgement

The weld metals were provided by MIT, USA, and the plant aged cast stainless steel by Ringhals Ab, Sweden. The Alloy 690 samples were aged and provided by the Korean Atomic Energy Research Institute (KAERI). XRD measurements were performed at the Helsinki University, Laboratory of Inorganic Chemistry. The irradiated stainless steel material was provided by IFE, Norway. The materials provided, as well as the funding from VYR, VTT Ltd, Halden and Aalto University are highly appreciated. The project manager appreciates highly the devotion of the project group to the different tasks in the project.

## References

- Ahonen, M. Effect of microstructure on low temperature hydrogen induced cracking behaviour of nickel-based alloy weld metals. VTT Science 105, 2015.
- Lucas, T., Forsström, A., Saukkonen, T., Ballinger, R., Hänninen, H. Effects of thermal aging on materials properties, stress corrosion cracking and fracture toughness of AISI 316L weld metal. Metallurgical Transactions A, Vol. 47A, August 2016, 3956-3970.
- Lucas, T. Doctoral Thesis, MIT, Cambridge, MA, 2011.
- Bjurman, M., Ivanchenko, M., Efsing, P., Ehrnstén, U., Hänninen, H. In Service Thermally Aged Cast Stainless Steel –Characterization by TEM and APT. Presentation at the EPRI International Light Water Reactors Material Reliability Conference 2016.
- Bjurman, M et al. Phase separation study of in-service thermally aged cast stainless steel - atom probe tomography- 17th International Conference on Environmental Degradation of Materials in Nuclear Power Systems – Water Reactors August 9-12, 2015, Ottawa, Ontario, Canada.
- Ivanchenko M. et al. Thermal aging induced phase transformations in nuclear grade type 316L stainless steel weld metal. Extended abstract in proceedings of "Material Issues in Design, Manufacturing and Operation of Nuclear Power Plants Equipment" MAINSTREAM-2016, 6-10.6.2016, St. Petersburg, Russia.
- Mouginot, R. et al. 17<sup>th</sup> International Conference on Environmental Degradation of Materials in Nuclear Power Systems – Water Reactors August 9-12, 2015, Ottawa, Ontario, Canada.
- Mouginot, R., Sarikka, T., Heikkilä, M., Ivanchenko, M., Ehrnstén, U., Kim, Y.S., Kim, S.S., H. Hänninen, Thermal ageing and short-range ordering of Alloy 690 between 350 and 550 °C, Journal of Nuclear Materials (2017), doi: 10.1016/j.jnucmat.2016.12.031.
- White paper on crack initiation of structural materials in LWRs. Nulife report 10(33), 2012.
- Ehrnstén, U., Progress report on projects MICRIN and MICRIN+, Mitigation of Crack Initiation VTT Research Report VTT-R-06104-15.
- Ehrnstén, U. et al. MICRIN+ State of the art report on surface requirements and practises for NPP primary components. Nugenia+ report, February 2016.
- Kilian R. et al. Draft NUGENIA Proposal for optimized surface conditions to mitigate in-service degradation (NUGENIA Position Paper), Nugenia+ report 27.09.2016.

Toivonen, A. SAFIR2018 THELMA 2016 - ICGEAC Inconel 600 Round Robin progress at VTT in 2016. VTT-R-05170-16, 17p.

Hurley, C., Progress report on INCEFA+ (Horizon2020) for SAFIR2018 – THELMA, VTT-R-06058-15.

Ivanchenko M., Karlsen W., Karlsen T. Microstructural TEM examination of 2 dpa irradiated 304L stainless steel extracted from a tensile creep specimen from IFA-669. Proceedings of the Fuels & Materials Session of the 39th Enlarged Halden Programme Group Meeting, EHPGM 2016, 8 - 13.05.2016, Sandefjord, Norway.

## 6.6 Non-destructive examination of NPP primary circuit components and concrete infrastructure (WANDA)

Tarja Jäppinen<sup>1</sup>, Miguel Ferreira<sup>1</sup>, Tuomas Koskinen<sup>1</sup>, Edgar Bohner<sup>1</sup>,  
Fahim Al-Neshawy<sup>2</sup>, Iikka Virkkunen<sup>2</sup>

<sup>1</sup> VTT Technical Research Centre of Finland Ltd  
P.O. Box 1000, FI-02044 Espoo

<sup>2</sup> Aalto University  
P.O. Box 11000, FI-00076 Espoo.

### Abstract

Addressing the Long Term Operation of nuclear power plants (NPP) beyond 40 years (and even beyond 60 years) will undoubtedly increase the occurrence and severity of known forms of deterioration. Therefore, there is a need to develop tools and methodologies that can maintain the safety while extending the operating lifetimes of NPP reliably. In WANDA that is the objective for the research.

Phased array ultrasonic testing on fatigue cracks with qualified procedures confirms that signal-to-noise -ratio between same size defects can vary a lot depending on the defect type and material anisotropy effect on the wave propagation. Simulation is a tool for NDT research at the present. That is used in WANDA project for SG magnetite deposit studies as well as for ultrasonic sound propagation studies.

New approach to determine POD curve with limited physical flaws was developed using a scanned UT-data from single flawed sample that was digitally altered and extended to provide unlimited variety of data files for POD determination. Inspectors were able to test capability of finding flaws and generate estimated POD curves with this process.

Multiple comparative NDE studies on reinforced concrete structures showed the promise of various techniques in evaluating concrete degradation, providing the basis of the conceptual designs for this study. A preliminary assessment of the basic restrictions and potential complexities involved with construction of large reinforced concrete mock-up has been conducted with a focus on defining the general requirements for the construction of the mock-up

### Introduction

The project WANDA – Non-Destructive Examination of Nuclear Power Plant Primary Circuit Components and Concrete Infrastructure, of the SAFIR2018 programme, focuses on the development and understanding of non-destructive examination (NDE) methods in two important nuclear power plant environments: primary circuit component materials and concrete infrastructure. The research work of primary circuit components concentrates on the ultrasonic testing of artificial defects, simulation, probability of detection (POD) and the measurement of magnetite in steam generator with eddy current techniques. The NDE research of concrete infrastructure focuses on the evaluation and calibration of the available NDE methods and monitoring systems for concrete structures. This is achieved through the design and construction of a real-scale reinforced concrete wall mock-up for NDE testing method development and education purposes. [Jäppinen & Ferreira, 2016]

The WANDA project seeks to maintain the high level of expertise of Finnish NDE research with regards to NPP component materials, and to initiate the development of competences directed toward the NDE research of reinforced concrete structures.

In-service inspection (ISI) programs play an important role in demonstrating sufficient structural integrity

of materials and components and guarantee the structural safety to continue NPP operation in a reliable and safe manner. ISI has an important role in identifying adverse environmental loadings or ageing effects before they potentially deteriorate structures compromising the safety of NPP. Therefore, profound understanding of the use and reliability of NDE methods is needed for safe operation of NPP. NDE plays an important role in the support of ageing management programs, where the renewal of an operating licence requires that NPP demonstrate that their facilities are ageing under controlled conditions.

## **NDE for primary circuit components**

Topics for the NDE research for components in the primary circuit in two first WANDA years have been non-destructive testing (NDT) of artificial defects of primary circuit components, simulation, probability of detection (POD) and the measurement of magnetite in steam generator (SG) with eddy current techniques. The development of the NDE techniques is done towards more reliable and efficient ISI to promote the safety of NPP.

The study with artificial defects is continued with fatigue cracks which are used as a reference when the performance of an NDT procedure is demonstrated. Test tube is presented in the Figure 1. According to the studies on the artificial defects [Leskelä & Koskinen, 2015] the ultrasonic response varies with the type of the defect and also with the technique used. In the report the inspections were done with three qualified phased array ultrasonic testing procedures using transmit-receive (TR) probes. All the techniques fulfilled the ASME Section XI code requirement for RMSE for length sizing and most techniques fulfilled the code requirement for RMSE for height sizing.

Shear wave (SW) techniques were generally performing well and the use of longitudinal waves (LW) is not essential. It was also noticeable that if scanning is done through the weld both shear wave and longitudinal wave techniques suffer from noise. If the only access to the defect is through the weld the use of longitudinal wave techniques might be required but it was observed that LW techniques were not always performing well enough with small defects. Combination of sectorial scan using shear waves and mode conversion utilizing the inside surface creeping wave showed good performance. Good coupling is important for the reliability and repeatability of an inspection. Large probe enables a good coverage for a single scan line thanks to the wide electronic linear scan. However, smaller probes are less susceptible for loss of proper coupling thus they are often preferable not only due to the better accessibility



**Figure 1.** Phased array ultrasonic examination of the open piping test block.

This research confirms the known facts for NDT of NPP ISI that signal-to-noise -ratio between same size defects can vary a lot depending on the defect type, the crack shape and morphology affects the detectability of the defect when skew angle is introduced to the flaw, anisotropic austenitic material affects

to the propagation of ultrasonic waves and the high noise level reduces the defect detection and sizing capability. This concludes to that ultrasonic examination and data analysis requires experience and knowledge of various kinds of indications. In Figure 2 the effect of austenitic stainless steel weld to the propagation of the ultrasonic sound.

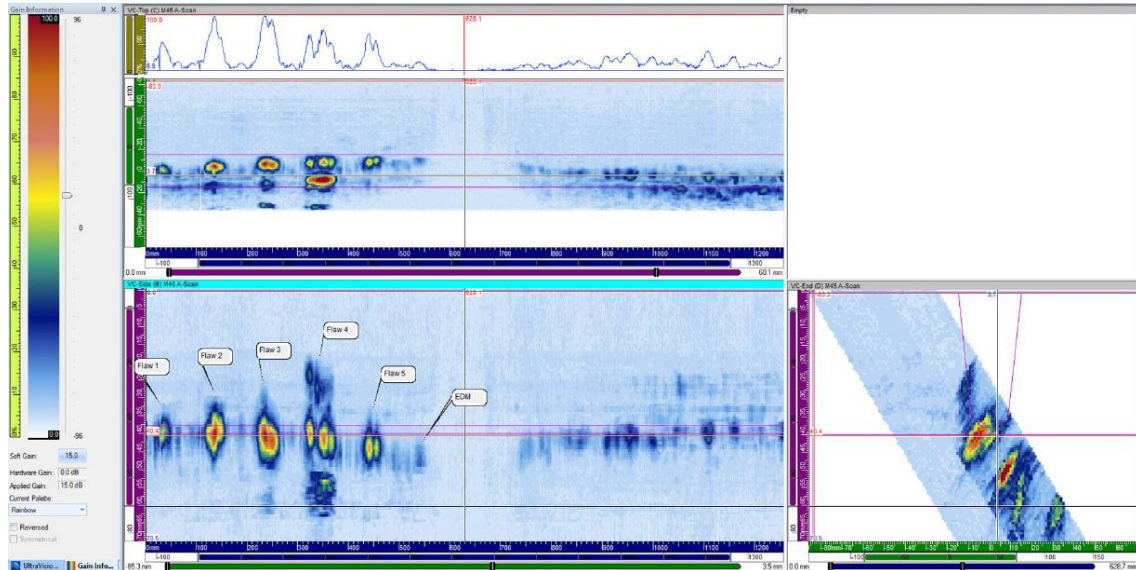


**Figure 2.** Phased array ultrasonic examination results with TRL technique at 45° longitudinal wave inspected from same of the weld.

Corrosion products depositing in the secondary circuit on steam generator tubing can accelerate localised corrosion and cause tubing degradation. In order to determine the extent and nature of deposit formation Eddy current method (ET) has been used as a detection method. In previous SAFIR projects an ET technique development has been carried out and now in WANDA the development work is moved to simulation to analyse different probe designs and to find a possible model for magnetite detection. In the year 2015 [Jäppinen & Pippuri, 2015] the work was done with two different simulation software, CIVA (analytical ray tracing method, developed for NDT applications) and COMSOL Multiphysics.

The simulation tools model the symmetric magnetite layer on the horizontal steam generator tube and the eddy current signal of the magnetite. In the test sets the coil distance and magnetite pile thickness were varied.

A goal for the future has been to model asymmetric magnetic layers on the tubes since the magnetite hardly stays symmetrical around the SG, at least when a deposit pile is formed. Both CIVA software and more flexible COMSOL Multiphysics software were used for modelling (Fig. 3). Results with both simulation software indicate that the best coil distance is 20 mm for the magnetite detection on a tube with outer diameter of 16 mm. Also this study proves that COMSOL is flexible and suitable software to model eddy current inspections.

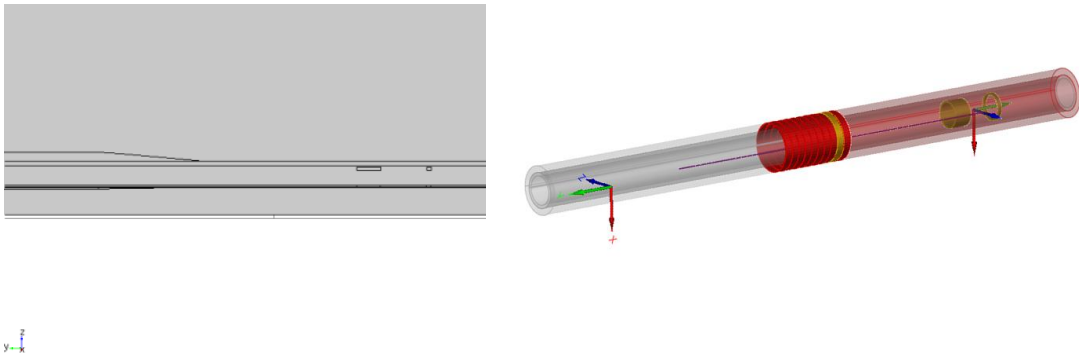


**Figure 3.** Close-up of the COMSOL (left) and CIVA (right) model geometry for the modelling of magnetite layer on the SG tubing.

In 2016 assessing NDE reliability with experimental and model assisted probability of detection (POD) for the nuclear industry was started in WANDA Ultrasonic testing is the main tool to inspect the structural integrity of pressurized components in nuclear power plants during in-service inspection. It is important to determine how probable it is to find a certain type and size of a flaw in order to choose to most effective method for different situations. POD curves are used to determine these probabilities. However, these POD curves require a lot of data points in order to be reliable, thus producing these curves is relatively expensive. This is why different simulation tools are used to reduce costs and reduce the amount of physical test pieces.

In present research, new approach to determine POD curve with limited physical training flaws was developed using previously developed eFlaw technology. With this technology, scanned UT-data from single sample was digitally altered and extended to provide unlimited examples of data files for POD determination.

A single weld test piece containing three cracks was used for this study. The test piece was welded austenitic stainless steel 321 pipe representing an actual geometry found in a nuclear power plant primary circuit. The weld was 30 mm wide and the pipe thickness was 40 mm. The outer diameter of the pipe was 400 mm. The weld inspected was a U-groove weld with 3 mm gap. The schematics for the pipe and the weld can be seen in Figure 4. Three circumferential straight artificial flaws were produced to the test piece with thermal fatigue by Trueflaw Ltd. The cracks were located in the heat affected zone.

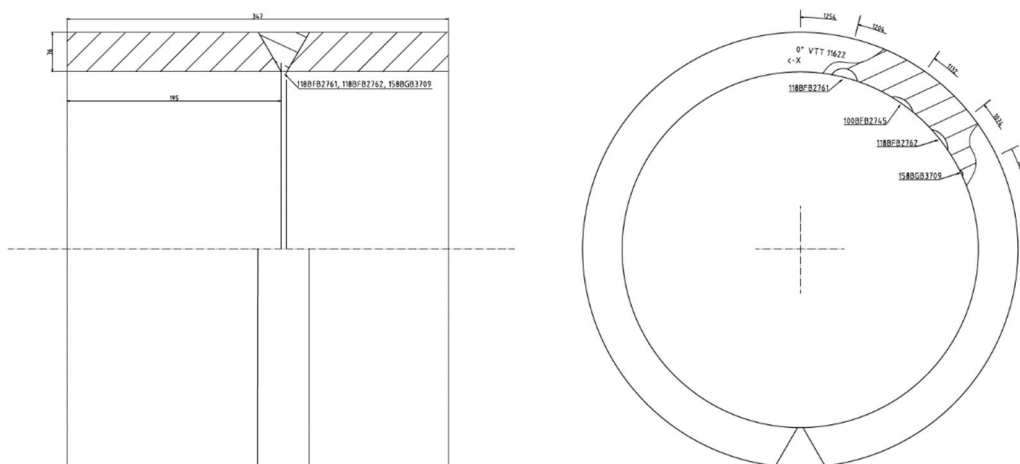


**Figure 4.** Used mock-up and flaw locations.

The mock-up was scanned with phased array ultrasonic system. The probe used was a 1.5 MHz transmit receive shear wave (TRS) probe with a wedge curved to the shape of the outer diameter of the pipe, and water was used as a coupling agent. Weld centerline was selected as the origin in the index direction. Scan axis was along the circumference of the pipe and index axis was set lengthwise of the pipe. The scan area was set 34 mm from the weld centerline to 54 mm from the weld centerline from both sides of the weld. Index resolution was 20 mm thus the number of scan lines was 2. The focal laws were set for 40° to 70° sectorial scanning with 1° step.

The scanned data was acquired in the UVData file format containing both the raw UT data and the necessary meta-data to interpret the various included signals. The raw UT data was extracted from the file and most interesting channels were selected for this initial study. The data contains wealth of other data, which will be exploited in further research. For this study, a single scan line with 45° beam angle was selected and extracted for further analysis. Figure 5 shows the extracted raw data as B-scan image with the flaw signals marked. In addition to the flaw signal, some locations without flaw signal were marked for removal and re-introduction. This was done to exclude the possibility that the re-introduction itself causes some detectable changes that the inspectors learn to look for.

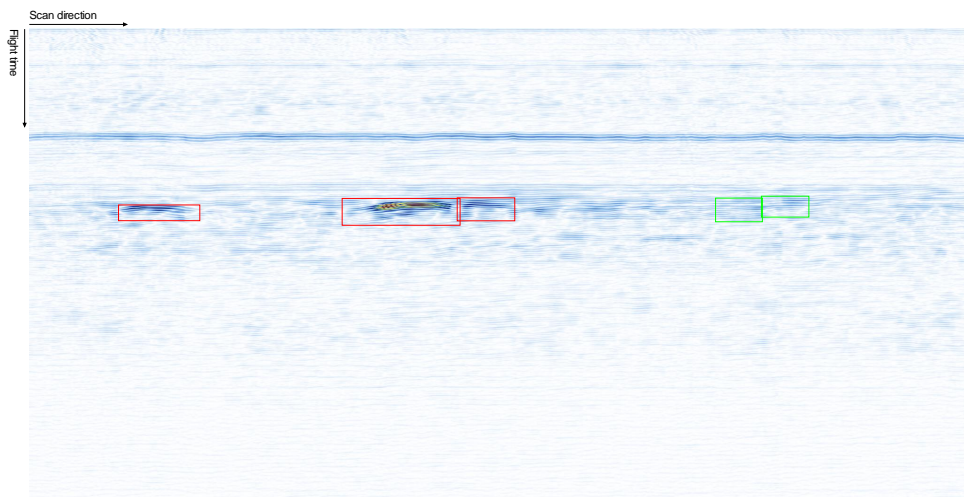


**Figure 5.** B-scan from the data, as acquired, with the flaw signals marked with red rectangles. Green rectangles show unflawed regions that were removed and re-introduced to study the possibility that the manipulation itself causes detectable changes.

It was taken as a premise, that the signal amplitude is the most significant feature of the crack signal from detection point of view. (Similar premise is used, e.g., in a vs.  $\hat{\alpha}$  POD analysis routinely conducted.) In particular, the crack amplitude (signal) in relation to the noise of the weld would be the most significant feature determining crack detection.

With this technique, it was possible to produce unlimited number of "virtual" data files with different flaw populations for POD determination.

With the ability to create flawed data files on demand, it was possible to gather hit/miss data from various inspectors and to generate POD curves on these data. To facilitate data collection, an online tool was created, which included most basic inspector views (B-view and slider control for data gain) and allowed indication of crack presence by simple click. With this (admittedly simplified) tooling, it was possible to gather quickly the data needed to use conventional statistical tools for POD determination.

Such tooling (albeit currently with limited number of real defects and simplified tooling) enables POD estimation with unprecedented ease and allows use of POD as feedback-tool for inspector training etc. Typical view from the online tool is shown in Figure 5.

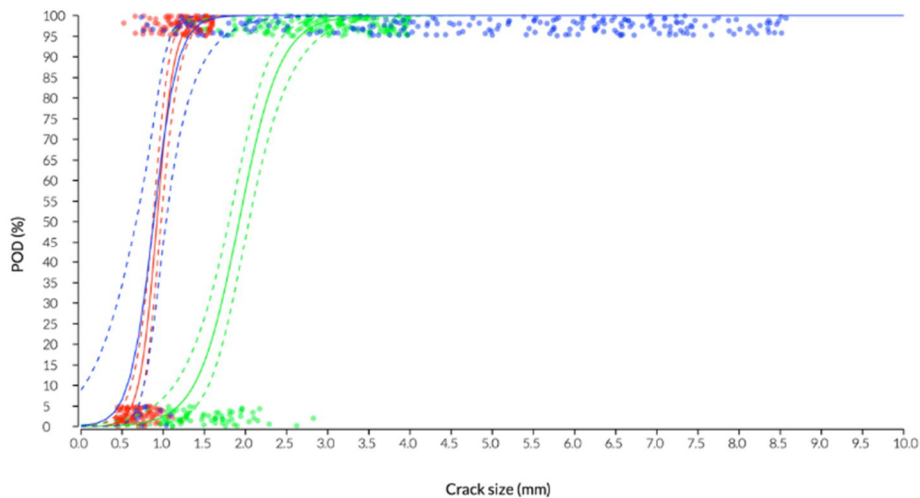


**Figure 6.** Computed POD curves from combined inspectors and separated in terms of the real crack sizes with points and curves showed in red, green and blue corresponding to original crack sizes of 1.6, 4.0 and 8.6 mm, respectively.

Even with the very limited number of actual physical cracks, the results were very promising. Inspectors were able to find flaws and generate a plausible POD curve (Fig 6.) with the application even with the lack of an A-scan image and with minimal information. The result indicates it is possible to emulate the amplitude response of a flaw and produce an amplitude response image for an inspector to evaluate. This in turn can be used to generate hit/miss data with real inspector response.

Further investigation is needed to confirm that the results generalize well to more diverse set of physical flaws. Also, the effect of more sophisticated tools for UT data-analysis needs more work.

## NDE for concrete infrastructure

The effects of potential deterioration of NPP concrete structures, systems and components (SSC) must be assessed and managed during both the current operating license period as well as subsequent license renewal periods. Reinforced concrete structures (RCS) differ to the many other mechanical and electrical components, as the replacement of these is impractical. Therefore it is clear that the safety issues related to plant aging and continued service of the concrete structures must become thoroughly resolved [Clayton & Hileman, 2012]. The inspection of NPPs concrete structures present challenges different from those of conventional civil engineering structures. As a result, there is a need for NDE of RCS to be able to undertake compliance testing, collection of specific data or parameters, condition assessments, and damage assessment.

NPP RCS present a unique challenge for development of performance acceptance criteria because of their large size, limited accessibility in certain locations, the stochastic nature of past and future loads, as well as that of mechanical and durability performance characteristics due to ageing and possibly degradation, and the qualitative nature of many non-destructive evaluation methods. Improved guidelines and acceptance criteria to assist in the interpretation of condition assessment results, including development of probability-based degradation acceptance limits, are required [Ferreira et al., 2016].

The application of NDE methods to NPP RCS has several challenges: infrastructure wall thicknesses (typically >1.0 m); dense and complex reinforcement detailing; penetrations or cast-in-place items; limited accessibility (i.e. liners or other components); severe environments; inaccessible structures; limited experience with NDE methods for NPP and lack of specific equipment or knowledge for NDE of NPP RCS [Wigenhauser et al., 2012].

It is understood that there is a clear need for means of ensuring concrete structures meet their design

criteria, during and immediately following construction, where NDE methods can provide quality control and verification. However, with time, NPP RCS are subject to ageing resulting in their degradation and consequently deterioration in their performance. NDE methods can be used to characterize material properties, measure performance, and provide valuable input for the assessment of the RCS performance.

NDE methodologies must continue to evolve. Research has shown the need for realistic specimens should be developed to allow direct comparisons between various techniques, with consideration given to ensuring a broad range of defects, and to ensure the probability of detection for a method can be properly determined [OECD/NEA, 2016].

The research in WP2 can be divided into three main areas addressing the review of NDE methods and monitoring of concrete performance (Task 1); the design and construction of a test mock-up of a reinforced concrete containment wall (Task 2), and the assessment of NDE and monitoring methods (Task 3). An additional fourth task represent an initial effort looking into the probability of detection methodology applied to concrete structures.

**Task 1 – Review of NDE methods and monitoring of concrete performance** included the preparation of three literature reviews summarizing the current use of NDE methods, sensors and monitoring systems for RCS, and a summary of NDE research on reinforced concrete with relevance to NPP.

The first research report [Al-Neshawy et al., 2016a], entitled *NDE of thick-walled reinforced concrete structures – Selection matrix for non-destructive evaluation of NPP concrete structures*, draws on previous studies to focus the advantages and disadvantages of different NDE methods for RCS. In the report, NDE methods currently in use are critically assess, and a selection matrix for NDE of NPP RCS is proposed. The selection matrix is proposed to address a need of NPP infrastructure evaluation in Finland. The ultimate goal of the NDE selection matrix is to identify and describe the effective use of NDE methods that can detect and characterize deterioration in NPP concrete structures especially considering the ageing phenomena affecting RCS [Al-Neshawy et al. 2016b].

The second research report [Bohner et al. 2016], entitled *NDE of thick-walled reinforced concrete structures – Technologies and systems for performance monitoring*, assesses monitoring technologies and sensing techniques for RCS. The work focuses on identifying the potentials of different available techniques, equipment and/or procedures. The review includes a determination of existing monitoring methods and techniques as well as the identification of limitations and restraints of the technology readiness with respect to their application in thick-walled RCS, as commonly used for e.g. NPP containments. The technologies are shortly described by taking into account the history and background of sensor development, working principle, signal type, existing experiences with the technology as well as advantages and disadvantages of the use and operation of the sensor. In addition, data acquisition systems of automated multi-sensor monitoring systems are presented and evaluated.

The third research report [Ferreira et al. 2015], entitled *NDE of thick-walled reinforced concrete structures – International research review*, provides an overview of the research on NDE methods being used for NPP and similar type structures. It focuses on the difficulties that have been encountered, and what has been achieved in the respective research projects. An overview of NPP concrete structures in Finland is given, including a brief section on testing and inspection requirements according to the YVL guidelines. This is followed by a compilation of information from other related research projects, and the lessons learnt relevant to the construction of a mock-up. The output from this report contributes to an improved basis for the preparation of the mock-up design.

These three reports will provide the basis for defining the design criteria for the mock-up of a testing element (geometry, concrete characteristics, reinforcement, testing, monitoring, type and layout of sensors, location and size of defects, NDE methods, etc.).

**Task 2 – Design and construction of a test mock-up of a reinforced concrete containment wall** concentrates on the design of the mock-up wall, and its construction. To determine the design requirements for a NPP mock-up concrete specimen, several meetings were held with the Finnish regulator STUK and operating utilities (TVO and FORTUM), and also with The Finnish Transport Agency who is responsible for

the maintenance of Finland's transport system, to roadmap relevant aspects related to NDE of NPP RCS. The discussions were guided by the following topics [Al-Neshawy, et al, 2016c]:

- NDE of concrete: defects, cracks, quality control issues, material and structural properties, complicated geometries, lack of access, etc.;
- NDE of steel: reinforcement (concrete cover detection, corrosion of reinforcement, definition of layout), prestressed reinforcement (corrosion, grouting defects, prestress loss), and liner (corrosion, detachment, concrete NDE behind liner);
- Monitoring: automatization – systems, data analysis, alerts, use of data;
- Others aspects: inclusions, pipings, joints, leaking containments, etc.;
- NDE technologies: special interests, new technologies.

The focus of the meetings was on defining research actions to address specific NDE and monitoring interests and knowledge gaps that can improve the reliability, sustain the safety, and extend the life of operating reactors. A list of structural flaws for inclusion in the test specimens has been compiled based on examinations of previous NPP structure failures and the processes that lead to the deterioration of these structures [Clayton et al, 2014]. These discussions and studies have identified a series of issues and limitations:

- Every NDE method has some limitations, generally perform well on relatively thin concrete structures, however better understanding is required to see how these methods perform on thick and heavily RCS;
- Based on NPP structural typology, it is clear that there is a need for testing concrete specimens much larger and more heavily reinforced than typically tested due to representativeness, thick-walled challenges, boundary conditions, etc.;
- Deterioration of RCS of NPP are typically in the form of cracking, spalling, general deterioration, delamination cracks/gaps near layers of reinforcement;
- Examination of NDE test specimens with intentional defects has shown current NDE method limitations. These NDE test specimens also tested the creation of realistic flaws to simulate defects created by construction methods;
- Examination of volumetric imaging techniques (beamforming and multi-transducer array) have shown it possible to detect structures at greater depths that may be obstructed by reinforcement closer to the surface.

An in-situ mock-up that is representative of NPP containment concrete cross sections is needed for NDE and testing of instrumentation and measurement techniques. Adequate test mock-ups play a key role, since they can provide defined conditions under which the different NDE concrete measurement methods can be evaluated. Material properties as well as the location of reinforcement, tendon ducts, and test flaws must be well documented. The test blocks can provide more defined conditions, since the critical parameters can be controlled during the block fabrication. Defects in concrete structures can be due to poor workmanship quality during the construction process, or due to deficient structural design and detailing. In existing structures, deterioration typically is related to construction defects, structural defects and cumulative degradation defects of concrete with time. The most common types of defects in concrete structures are: dimensional errors; finishing errors; honeycombing; cracking, delamination due to structure stresses or deterioration mechanisms; embedded foreign objects in the concrete; voids adjacent to liner and voids in grouted tendon ducts for the post-tensioned structures. Exposure to the environment (e.g., temperature, moisture, cyclic loadings, etc.) can produce degradation of reinforced concrete structures throughout its service life.

One of the critical purposes of the mock-up will be to determine how the current NDE methods are able to determine various forms of degradation. There are two critical trade-offs to account for within the space constraints of the mock-up when determining the simulated defects in the conceptual design. This includes the determination of how realistic versus how controlled each defect should be as well as a determination of the detection/characterization difficulty each defect should achieve [Clayton, et al, 2014].

In the first trade-off, defects used in the mock-up should be modelled to represent activities that may actually occur (or have been documented to have occurred) during the construction process and/or cumulative deterioration and degradation of the concrete with time. Note that, designing defects for the mock-up solely to be repeatable and not realistic can lead to the wrong conclusions when evaluating the various NDE methodologies. For example, the NDE attributes determined to be desirable based on good performance on the test block may not be useful for evaluation of commercial concrete NPPs if the defects are not realistic enough. This distinction is fundamental as the latter is the main objective of this study.

With regard to the second trade-off, the conceptual design of the mock-up should include sufficiently challenging defects that even the superior performing NDE methods cannot fully identify. This will ensure that limitations of even the most advanced methods are able to be quantified. At the same time, some of the defects should be identifiable by a majority of the methods. This will ensure that the methods that are not close to the desired achievement can be eliminated from consideration, while the baseline level of achievement of the methods performing well can be identified [Clayton, et al, 2014].

For the construction of the mock-up, types of simulated defects and materials/methods used should be considered, for example:

- Delaminations could be imitated by using 0.05 mm plastic sheets and 0.25 mm cloth squares [Wimsatt, et al. 2014];
- Air-filled voids could be constructed by inserting foam squares 13 mm thick in vacuum-sealed plastic bags [Wimsatt, et al. 2014];
- Water-filled voids could be constructed by placing water-filled bags within vacuum-sealed plastic bags and carefully padding the defect with concrete;
- Cracks using carefully created laminar sheets of different densities;
- Honeycombing by glueing large aggregates carefully;
- Corroded reinforcement steel with reduced cross section by prior removal
- Voids in grouted ducts using polyurethane foam;
- Insufficient (inadequate) concrete cover depth.

**Task 3 – Assessment of NDE and monitoring methods.** This task addresses the evaluation and calibration of NDE methods and sensors and monitoring methods for performance assessment of RCS. A testing program will be defined which will cover calibration of test methods, correlation between test methods, effect of time dependency and testing conditions on test methods, accuracy of test methods, among other aspects yet to be defined. The focus will be on existing test methods and the availability of new test methods, especially considering the difficulties associated with NPP RCS.

Even though on-site testing of concrete in NPP structures typically only allows for one-sided access, the mock-up is designed to allow for testing access on both sides of the wall with the understanding that the testing on each side of the wall can be treated as an independent measurement. The reinforcement pattern can be similar for both sides of access, allowing evaluation of the effect of different depths using only one defect by comparing results of testing on both sides of the specimen. Although access to both sides would allow for test methods using two-sided access measurements, the testing should focus on one-side per measurement to simulate realistic containment wall access conditions.

A monitoring program will be defined that covers calibration and validation of sensors, correlation between different NDE methods and sensors, effect of time dependency and testing conditions on sensors results, resolution and accuracy of sensors, among other aspects yet to be defined. The focus will be on the available and new sensors and monitoring systems.

Sensor-based monitoring systems can be used to continuously follow the performance of the structures in real-time, mostly over long time periods starting with the manufacturing of the structures. The application of both, NDE methods and monitoring systems, allows for the best performance assessment by generating partly redundant data and using synergetic effects [Bohner et al. 2016].

Since the mock-up most likely will be located outdoors, it is beneficial to monitor the state and condition of the wall at the time of NDE testing. Certain NDE methods might utilize this information as input data for data analysis and assessment of the technologies tested. The monitoring plan will address [Al-Neshawy,

et al. 2016c]: monitoring of relative humidity and temperature; monitoring early age cracking of the mock-up wall; and the monitoring of reinforcement corrosion;

An important aspect of the mock-up is to allow for continuous long term testing. The intention is for the specimen to be available for a long period of time (i.e.: more than 20 years) which allows for different/new equipment to be assessed in a well-documented situation, and to assess in real-time the effects of ageing of RCS. Furthermore, the mock-up will be available for users of NDE equipment to test and calibrate performance accordingly. The education of a new generation of engineers with NDE experience is another goal. The mock-up will allow for the training of young engineers in the use of different NDE equipment and in the development of expertise with RCS similar to that of NPPs.

**Task 4. Probability of Detection methodology applied to concrete NDE.** For the in-service condition assessment of reinforced concrete structures, it is necessary to qualify and quantify the extent of the defects using a range of NDE methods. The analysis and reliability check of the data produced by these tools and methods gives a large amount of information over a long time period. For evaluating the capability of these NDE methods, the determination of the Probability of Detection (POD) is an essential methodology [Kessler and Gelhen, 2015]. The capability is defined as the probability of detecting a defect with a particular size under specified inspection conditions and a defined procedure. In this task, an overview of the current state-of-the-art review will be prepared on the use of the probability of detection curve in the field of reinforced concrete structures NDE

## Conclusions

The Finnish national Research Programme on Nuclear Power Plant Safety (SAFIR2018) is guiding research towards nuclear power plant safety. In the SAFIR2018 research programme, the project NDE of nuclear power plant primary circuit components and concrete infrastructure (WANDA) is focusing on the development and understanding of NDE methods, with special focus on reactor internals and more recently concrete infrastructure.

The main motivation of the WANDA project is to maintain the level of expertise of Finnish NDE research of the NPP component materials and to raise that of NDE research on concrete infrastructure.

The different research topics in WANDA are strongly linked by the common factor of NDE. In fact many methods and technology are similar but differing in application and analysis. For this reason the sharing of competence is in vital importance to push the known boundaries of NDE.

The studies on fatigue cracks were continued with three qualified phased array ultrasonic testing procedures using transmit-receive probes. Shear wave techniques were generally performing well and the use of longitudinal waves is not essential. If scanning is done through the weld both shear wave and longitudinal wave techniques suffer from noise. The tests confirm that signal-to-noise -ratio between same size defects can vary a lot depending on the defect type and mostly anisotropic austenitic material affects to the propagation of ultrasonic waves and the high noise level reduces the defect detection and sizing capability.

Simulation is a tool for NDT research at the present. That is also in steam generator magnetite deposit studies. In WANDA the development work was moved to simulation and to analyse different probe designs and to find a possible model for magnetite detection. The work with two different simulation software, CIVA and COMSOL Multiphysics showed both suitability to model magnetite on SG tubing.

In present research, new approach to determine POD curve with limited physical training flaws was developed using previously developed eFlaw technology. With this technology, scanned UT-data from single sample was digitally altered and extended to provide unlimited examples of data files for POD determination. The scanned data was acquired in the UVData file format containing both the raw UT data and the necessary meta-data to interpret the various included signals. The raw UT data was extracted from the file and most interesting channels were selected for this initial study. A single scan line was selected and extracted for further analysis. In addition some locations without flaw signal were marked for removal and re-introduction. Even with the very limited number of actual physical cracks, the results were very promising. Inspectors were able to find flaws and generate a plausible POD curve with the application even with the

lack of an A-scan image and with minimal information.

A study of NDE for detection of defects in NPP reinforced concrete mock-ups is an essential component in defining the most promising techniques and directing the R&D efforts in this field. For the success of such an approach, a realistic containment mock-up is to be built. This mock-up will house various defects, well defined, and realistic to be evaluated by existing NDE methods. It is also critical that the evaluation mock-up and embedded defects is representative of in-service NPP structure concrete.

Multiple comparative NDE studies have been conducted on reinforced concrete structures that are not as thick or heavily reinforced as typical NPP reinforced concrete structures. Results of the comparative studies on these specimens showed the promise of various techniques in evaluating concrete degradation, providing the basis of the conceptual designs for this study.

A preliminary assessment of the basic restrictions and potential complexities involved with construction of large reinforced concrete mock-up has been conducted with a focus on defining the general requirements for the construction of the mock-up.

## References

- Al-Neshawy, F., Ferreira, M., Bohner, E., 2016a. NDE of thick-walled reinforced concrete structures – Selection matrix for non-destructive evaluation of NPP concrete structures. VTT Research Report. VTT-R-00215-16. 90p.
- Al-Neshawy, F., Sistonen, E., Ferreira, M., Bohner, E., Puttonen, J., 2016b. Selection Matrix for Non-Destructive Testing of NPP Concrete Structures. 19th World Conference on Non-Destructive Testing (WCNDT 2016). 13-17.6.2016, Munich, Germany, 9 p.
- Al-Neshawy, F., Ferreira, M. & Bohner, E. 2016c. Pre-design considerations for large-scale NDE mock-up. Espoo. VTT Research Report. VTT-R-00645-17. 30pp.
- Bohner, E., Kuosa, H., Al-Neshawy, F., Ferreira, M., 2016. NDE of thick-walled reinforced concrete structures – Technologies and systems for performance monitoring. VTT Research Report. VTT-R-00449-16. 63p.
- Clayton, D., Hileman, M., 2012. Light Water Reactor Sustainability Nondestructive Evaluation for Concrete Research and Development Roadmap. ORNL/TM-2012/360. OAK Ridge National Laboratory. 72p.
- Clayton, D., Khazanovich, L., Hoegh, K., Hileman, M., (2014) Preliminary Conceptual Design of a Thick Concrete Nondestructive Evaluation Specimen. ORNL/TM-2014/146. OAK Ridge National Laboratory.
- Ferreira, M., Bohner, E., Al-Neshawy, F., 2015. NDE of thick-walled reinforced concrete structures – International research review. VTT Research Report. VTT-R-04696-15. 36p.
- Ferreira, M., Bohner, E., Calonius, K., 2016. Acceptance criteria for maintenance of concrete structures in the nuclear industry - A Preliminary Study. Energiforsk AB. REPORT 2016.xxx. 65 p. (in publication)
- Jäppinen, T. & Pippuri, J., 2015. CIVA and COMSOL Simulation of Eddy Current Signal from the Magnetite Layer on SG tubing. Espoo. VTT research Report. VTT-R-00550-16. 13 p.
- Jäppinen, T., Ferreira, M., NDE Research of Nuclear Power Plant Primary Circuit Components and Concrete Infrastructure in Finland. 19th World Conference on Non-Destructive Testing (WCNDT 2016). 13-17.6.2016, Munich, Germany (2016), 7 p.

- Kessler, S., Gehlen, C. (2015). Probability of Detection of corrosion detection in reinforced concrete structures. International Symposium, Non-Destructive Testing in Civil Engineering (NDT-CE). September 15 - 17, 2015, Berlin, Germany.
- Leskelä, E. & Koskinen, A., 2015. Phased array ultrasonic examination of mechanical fatigue cracks in austenitic piping test block. Espoo. VTT research Report. VTT-R-00542-16. 40 p. + app. 86 p.
- OECD/NEA, 2016. Final Report of Assessment of Structures subjected to Concrete pathologies (ASCET) phase. OECD, Nuclear Safety, NEA/CSNI/R(2016)13 .
- Wiggenhauser, H., Helmerich, R., Karuse, M., Mielentz, F., Niederleithinger, E., Taffe, A., Wilsch, G., 2013. Non-destructive testing of NPP concrete structures. Sate of the art report. BAM - Bundesanstalt für Materialforschung und –prüfung. 119p.
- Wimsatt, A., White, J., Leung, C., Scullion, T., Hurlebaus, S., Zollinger, D., Grasley, Z., Nazarian, S., Azari, H., Yuan, D., Shokouhi, P., Saarenketo, T., Tonon, F., (2012) Mapping Voids, Debonding, Delaminations, Moisture, and Other Defects Behind or Within Tunnel Linings SHRP 2 Renewal Project R06G. Transportation Research Board. 555 p.

## 7. Research infrastructure

### 7.1 Development of thermal-hydraulic infrastructure at LUT (INFRAL)

Joonas Telkkä, Elina Hujala, Lauri Pyy

Lappeenranta University of Technology  
P.O. Box 20, FI-53851 Lappeenranta, Finland

#### Abstract

The aim of the INFRAL project is to develop the thermal hydraulic measurement infrastructure of the LUT nuclear safety research laboratory, to secure the operability of the existing test facilities and to launch a study on the new large-scale integral test facility. During 2015–2016, the so-called advanced measurement techniques, i.e. particle image velocimetry (PIV), wire-mesh sensors (WMSs) and high-speed cameras (HSCs) have been versatilely used in different research projects. The expertise on these measurement systems, as well as on the related data processing procedures, has taken big leaps forward. The study on the new modular integral test facility was launched in 2016. The survey of the research based requirements for the new test facility was conducted on the national level to ensure that the needs of Finnish stakeholders will be fulfilled. In addition, international trends and needs for the thermal hydraulic experimental research were studied to enable participation to various joint international projects in the future. International co-operation with other top-level universities and research institutes has continued, and LUT has formed valuable connections to institutes such as ETH Zurich, Paul Scherrer Institute and University of Michigan.

#### Introduction

In the SAFIR2014 programme, the research project ELAINE was launched for the enhancement of measurement instrumentation available for the thermal hydraulic experiments in Lappeenranta University of Technology (LUT). Significant milestones in the project were the acquisitions of a particle image velocimetry (PIV) measurement system, wire-mesh sensor (WMS) electronics and a system of three modern high-speed cameras (HSC). In addition to acquisitions of experimental hardware, a new data storage system for the experimental data (EDS) was developed and taken into active use. In addition, one important task in the project was the maintenance of the (PWR) PACTEL test facility in order to secure its operability and availability for the experiments.

In the SAFIR2018 programme, the INFRAL project was launched in 2015, and it aims for the further development of the techniques related to the advanced measurement techniques and their applications. The goal is to build good in-house expertise in the use of the acquired techniques to facilitate the needs of

computational modellers in the future experiments in the best way technically possible. The CFD grade measurements can give new insights into the physics behind the different flow phenomena that may ultimately lead to improvements in the safety of nuclear power plants. Further, the goal of the INFRAL project is to secure the operability of PACTEL test facilities and to launch a study on the new major test facility to prepare for the post-PACTEL era.

Both in 2015 and 2016 the INFRAL project has been divided into four different work packages. The first work package (Advanced measurement techniques) includes activities that are related to the use of advanced measurement techniques in LUT. Part of the work is to develop analytical tools to extract the needed data from the measurements. The other part is to study the applicability of the techniques for different flow problems and to develop new measurement solutions. The second work package (Maintenance and equipment) aims on the maintenance of (PWR) PACTEL and other test facilities, and it comprises the yearly inspections, calibrations etc.

The third work package (Modular Integral Test Facility, MOTEL) aims on designing and constructing a new large-scale integral test facility in LUT laboratory. The fourth work package (Project management, international co-operation and publications) includes the tasks related to the project management and participation to the reference group meetings and seminars. Also international co-operation actions, such as research visits, are a part of the work package.

## **Advanced measurement techniques**

The work package 1 of the INFRAL project consists of research topics that are related to the study and application of the so-called advanced measurement techniques: particle image velocimetry (PIV), wire-mesh sensors (WMSs) and high-speed cameras (HSCs). The measurement systems were acquired to LUT already during the previous project (ELAINE) in 2011–2014. During the on-going SAFIR2018 research programme the advanced measurement systems have been developed further and used in various applications. Some of the application targets are also related to non-SAFIR projects. The PIV measurement system, in particular, has been versatilely used in many different projects during 2015–2016. The tasks in the work package 1 are the following:

- Advanced and combined use of PIV/WMS/3D Cam systems (T1.1)
- Evolutionary WMS applications (T1.2)
- Improvement of 3D High-Speed Camera data analysis (T1.3)
- New applications of advanced measuring techniques (T1.4)

The task 1.1 supports the use of advanced measurements techniques in LUT. In 2015 the particle image velocimetry system was upgraded for shadowgraphy use with add-on components (software+hardware). Therefore, no conventional PIV measurements were performed in 2015. Shadowgraphy is used to size water droplets with the help of bright backlight that creates a measurable edge of the particle's cross section. The end result is a droplet distribution from the measurement area, which can be used to determine the spread parameter for Rosin-Rammler distribution used commonly for droplet mass fraction frequency distributions. A test facility with easy-to-control environment was created and successfully tested during 2015. Figure 1 shows the workflow of a shadowgraphy analysis. The work is also related to the INSTAB project [1].

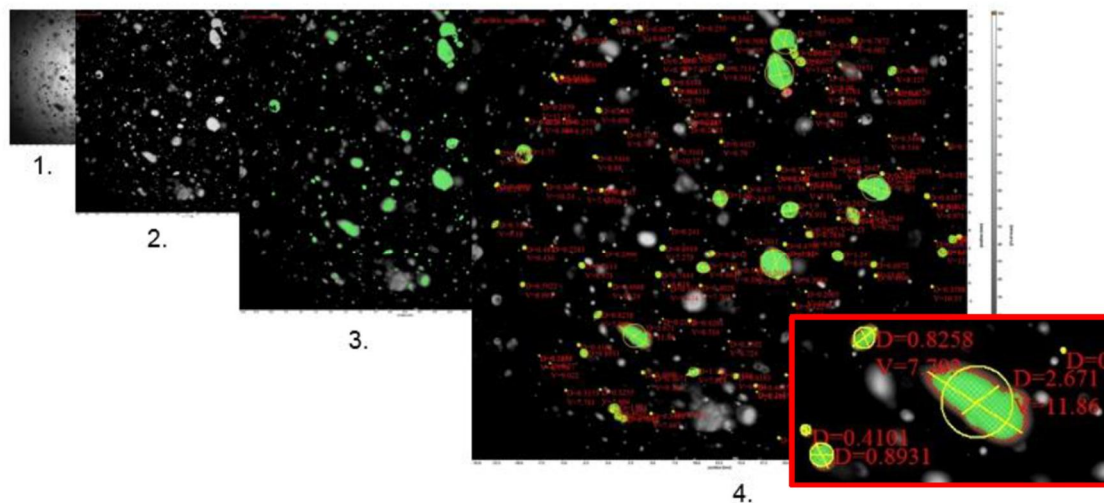


**Figure 1.** The workflow of droplet shadowgraphy measurements. Analysis of the water droplets from the spray nozzle. 1. Raw image. 2. Processed image. 3. Droplet recognition. 4. Droplet properties (size, velocity, ...).

In 2016, the PIV system was mainly utilized in contract measurement schemes. In December 2016 PIV was applied within the SPA-T8R and SPA-T9 test series where thermally separated layers of water were mixed with a sparger using different amounts of outlets open within the sparger. The test series was a part of the INSTAB project. As it has been found out before in case of condensation, the optical aberrations create too challenging environment for successful PIV measurements. Another downside with the existing system is the low frequency of the laser and the cameras. Hence they don't work well with the fluctuating water phase even without any optical aberrations, causing problems with time-averaging. Preliminary qualitative inspection of SPA-T8R and SPA-T9 results show that similar flow structures appear roughly for few seconds, and with a low-speed PIV system only 2–40 image pairs can be measured in theory. One possibility to achieve better velocity data would be to update the laser for one with kilohertz range in order to capture hundreds of image pairs. This would improve the reliability of the time-averaged velocity fields, or makes possible to execute time-resolved PIV (TR-PIV) when the phenomenon is very short and unrepeatable. Naturally, optical aberrations would still appear when condensation of steam occurs near the field-of-view (FOV) or between cameras and the FOV. With higher water temperatures the fluorescent tracer particles also fall to the bottom of the PPOOLEX vessel, creating yet another problem for PIV measurements as the seeding density gets lower with the elevating temperature. The work to overcome these challenges technically still continues.

In December 2016 a new set of sCMOS cameras were acquired to update the PIV system. This update will double the measurement frequency to 15 Hz (7 Hz before) making the laser unit the limiting component frequency-wise. The biggest advantage of the sCMOS cameras is the better chip design compared to the existing ImagerX Pro cameras. The chip can withstand more reflection making it easier to apply in the challenging measurement environments as well as better overall performance for shadowgraphy measurements. The new cameras will be operational by the end of February 2017.

The contract measurements with PIV involved three different measurement schemes in 2016, where the most challenging scheme was the measurement of 8 MW gas burner in a chamber. Measurement experience was also gathered from a simple airflow (stereo-PIV) and water flow within a channel (planar-PIV), which were more traditional measurements with more easily controlled and optically sturdier environments.

The shadowgraphy extension of the PIV system was not utilized in 2016 for measurement activities, but the capability to execute new shadowgraphy measurements exists. A master's thesis "Spray Droplet Size Distribution Measurement" by Dmitry Skripnikov was finalized in September 2016 [2]. The thesis emphasized in handling of shadowgraphy droplet distribution data and ways to validate CFD (ANSYS Fluent)

results with droplet mass fraction frequency distribution by providing correct spread diameter for Rosin-Rammler droplet number and volume distributions. The thesis was graded 4 (very good).

Within the task 1.2 the advanced applications for the wire-mesh sensor technique have been actively studied in LUT. The axial sensor design (the AXE sensor, presented in figure 2) was designed and constructed in the previous ELAINE project in the SAFIR2014 programme to tackle the problems related to the measurement of the axial flow behavior. Like the name of the sensor states, it is installed axially into the centreline of the flow channel to study the axial flow dynamics of the two-phase flow. The sensor has 16 x 128 wires placed with the 3 mm x 3 mm spatial resolution over the area of 45 x 381 mm<sup>2</sup>.

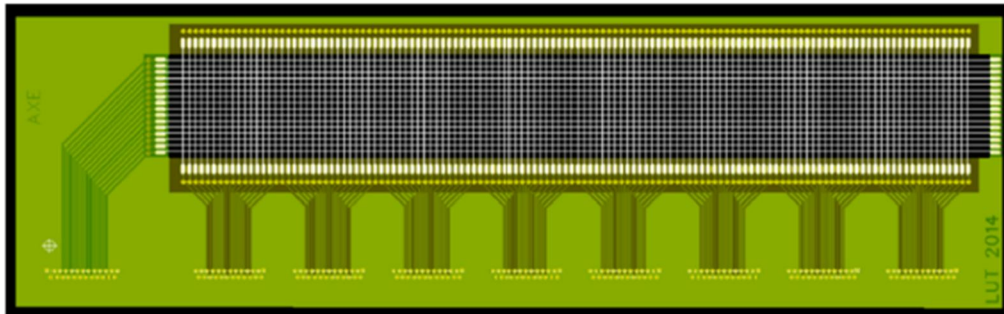


**Figure 2.** The AXE sensor design.

In 2015, the applicability of the AXE sensor was studied under various flow conditions in the HIPE (Horizontal and Inclined Pipe Experiments) test facility. The first measurement results were presented in the NURETH-16 conference (September 2015, Chicago, U.S.) [3].

The results from the axial WMS measurements were also presented in the SWINTH-2016 workshop in June 2016 [4]. The participation to the workshop also supported the use of all kinds of advanced measurement techniques as the workshop was intended for researchers who are developing and applying these techniques in practice. Example of the results from the axial WMS measurements is presented in Figure 3. The figure presents time-averaged void fraction distributions in the flow channel of the HIPE facility. These are measured with different pipe inclinations with both traditional radial, and axial wire-mesh sensors.

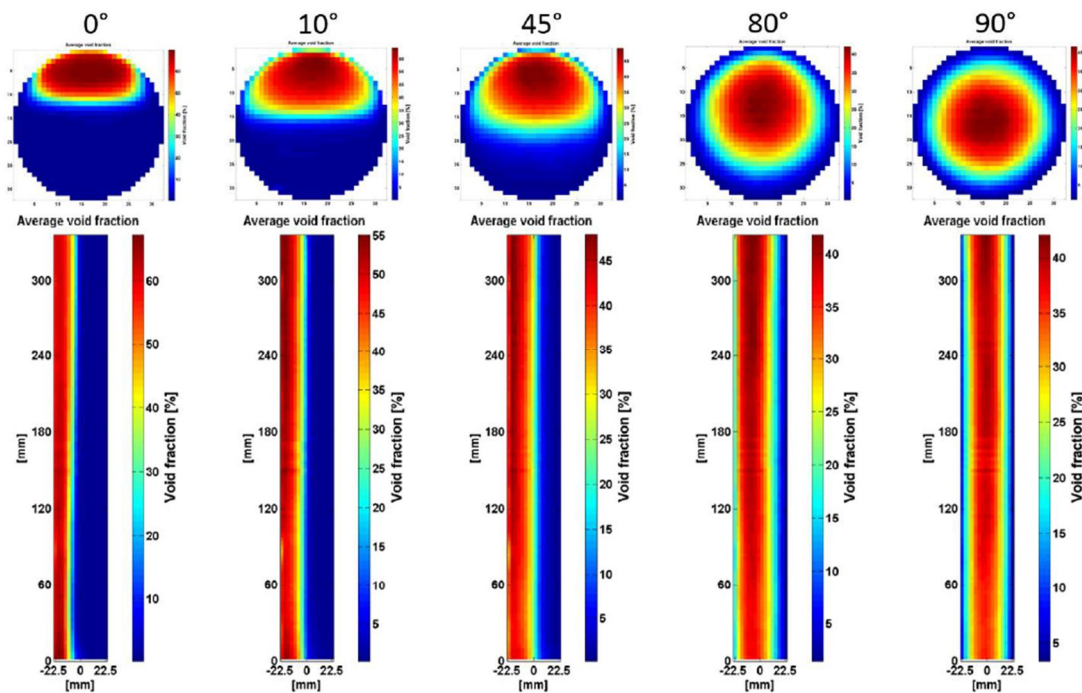


**Figure 3.** Time-averaged void fraction distributions ( $J_L=1.2$  m/s,  $J_G=0.6$  m/s), horizontal to vertical. [4]

It can be stated, based on the conducted measurements that the axial sensor design has advantages and drawbacks. The sensor can be applied to study the axial behavior of the two-phase flow. However, the sensor itself has noticeable effects on the flow velocities as the comparative experiments with the traditional WMSs revealed. In 2016, the axial WMS technique was studied further. Two separate swirling devices with different blade angles (30 ° and 60 °) were designed and manufactured. The swirling devices were applied to the HIPE test facility to create a swirling two-phase flow. Two identical series of experiments were conducted separately with both swirling devices using both axial and radial sensors under swirling two-phase flow conditions. The set-up of the experiments is presented in Figure 4. The test matrix of these experiments, i.e. the pipe inclinations and superficial water and air flow rates, was the same as in the previous experiments without the swirling devices. The data analysis of the swirling two-phase flow measurements will be done in 2017, and the results will be compared to those of the previous measurements.

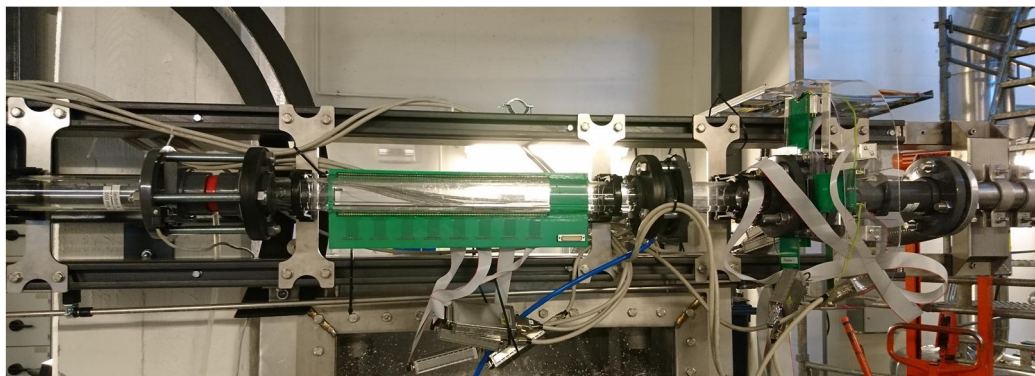


**Figure 4.** Set-up of the WMS measurements with a swirling device (horizontal flow case). The swirling device is on the left (red color), the axial sensor in the middle, and the two radial sensors are on the right.

In addition to developing own WMSs in the LUT laboratory, the development of the so-called high temperature and high pressure WMS technique at ETH Zurich and Helmholtz-Zentrum Dresden-Rossendorf (HZDR) has been followed. The new design of the sensor was developed [5] in order to simplify the manufacturing process compared to the previously developed one [6]. The high temperature/high pressure WMS technique was also presented in the SWINTH-2016 workshop where good knowledge of it was acquired [7]. The sensors can operate at temperatures potentially up to 350 °C and pressures up to 22 MPa [7].

The technique has already been used at HZDR, and there has been communication between LUT and HZDR/ETH Zurich regarding this issue. HZDR has already gained some promising results from the conducted measurements, and hence in principle the functioning of the high temperature/high pressure WMS technique has been confirmed. There have been preliminary plans of applying this technique to the forthcoming modular integral test facility, MOTEL, which is under design at LUT. The temperature and pressure levels will be so high in the test facility that the traditional WMSs cannot be applied to it. High temperature/high pressure WMSs could offer a novel means of void fraction measuring in challenging circumstances. Concerning the characteristics, restrictions, economic requirements etc. of the HT/HP WMS technique, a research visit to HZDR/ETH Zurich has been planned. The visit will probably take place during the first half of 2017.

The actions in task 1.3 are related to the improvement of high-speed camera data analysis procedures using the PPOOLEX experimental data. During the year 2015, the pattern recognition algorithm was improved to be more accurate. The challenge was to combine all three video directions together due to a large amount of swarm of small bubbles especially on the bottom and the right side cameras. Most of the evaluations and calculations were made by using the left side camera only, but other cameras were used for the confirmation of the results. The evaluations of the volume and the surface area of the bubbles were performed too. From the bottom camera images, the form of the bubbles were evaluated symmetrical. From the left side image, the 3D model was produced, and the volume and the area of the bubble calculated. Error of the volume and the area estimation is less than 15 percent for the pure sphere. Also the accelerations and the velocities of the bubbles were evaluated.

The chugging frequencies were evaluated by using the pattern recognition algorithm. Figure 5 shows the cross-sectional areas of the bubbles obtained on the basis of the images from the side cameras compared to the pressure measurements  $p_5$  below the pipe's outlet and  $p_6$  at the bottom of the pool. It can be clearly seen that the greatest pressure changes appear immediately after the largest bubbles.

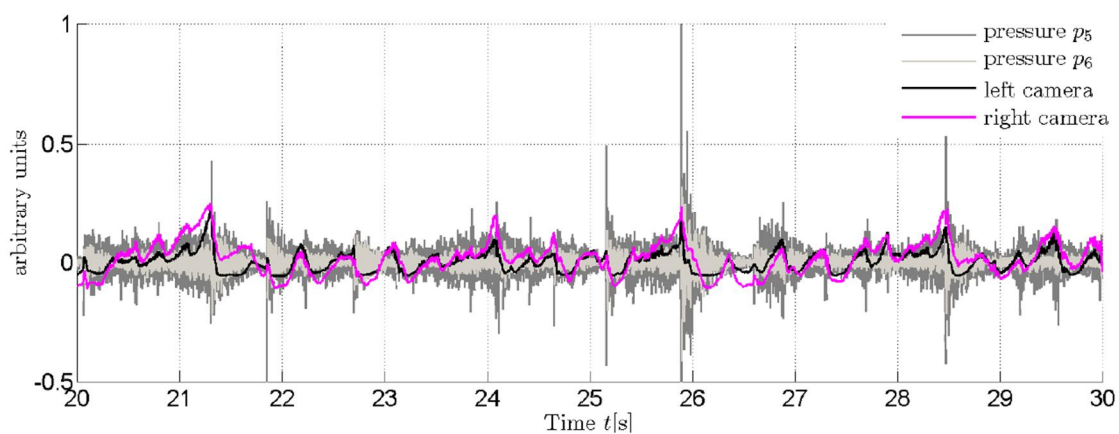


**Figure 5.** A sample of cross-sectional area change (difference between the measured and mean area) of the bubbles compared to the pressure  $p_5$  outside the pipe outlet and pressure  $p_6$  at the bottom of the pool in arbitrary units in the DCC-05-4 experiment (PPOOLEX).

In 2016, only analysis of the old experiments were made, and there were no new measurements with high-speed cameras concerning pattern recognition. During 2016, the pattern recognition algorithm made for the DCC-05 experiments was improved, and the data analysis methods were added. The old challenges, with combining all three video directions together due to a large amount of small bubbles especially on the bottom and the right side cameras, still occur. Hence, most of the evaluations and calculations were made using the left side camera only, and other cameras were used for the confirmation of the results. The evaluations of the volume and the surface area of the bubbles were performed. From the bottom camera images, the form of the bubbles were evaluated symmetrical. From the left side image, the 3D model was produced, and the volume and the area of the bubble calculated. Calculation methods were enhanced. Error of the volume and the area estimation was less than 10 percent for the pure sphere. Also the accelerations and the velocities of the bubbles were evaluated. The full DCC-05 part 4 video material was analyzed and the different frequencies were assessed at separate phases of the bubbles. The preliminary results have been published in [8] and more detailed analysis will be presented in another journal article and in the NURETH-17 conference in 2017.

The TRA-04 experiments pattern recognition procedure and data analysis were started in 2016 and will be continued in 2017. The chugging frequencies can be estimated by using Fast Fourier Transform (FFT) to the bubble volume data obtained with pattern recognition. Wavelet Transform analysis has also been used in denoising of the signal.

The goal of the task 1.4 is to follow the state-of-the-art of advanced measurement techniques and their applications in experimental thermal hydraulic research in universities and research institutes across the world. The task is comprised of following the journal articles and conference papers on the field, communication with other experts, as well as participating in conferences/seminars and doing research visits to other universities/research institutes. The followed measurement techniques include also other techniques and systems than those in use in the LUT laboratory, such as tomography measurement systems. Also completely new advanced measurement techniques are surveyed. One example of recently developed measurement techniques is the distributed temperature sensor (DTS) based on Rayleigh-backscatter phenomenon. The sensor enables the measurement of temperature distribution in high detail in different geometries, such as a slab or a rod [9]. Different applications of the DTS technique are presented in Figure 6.

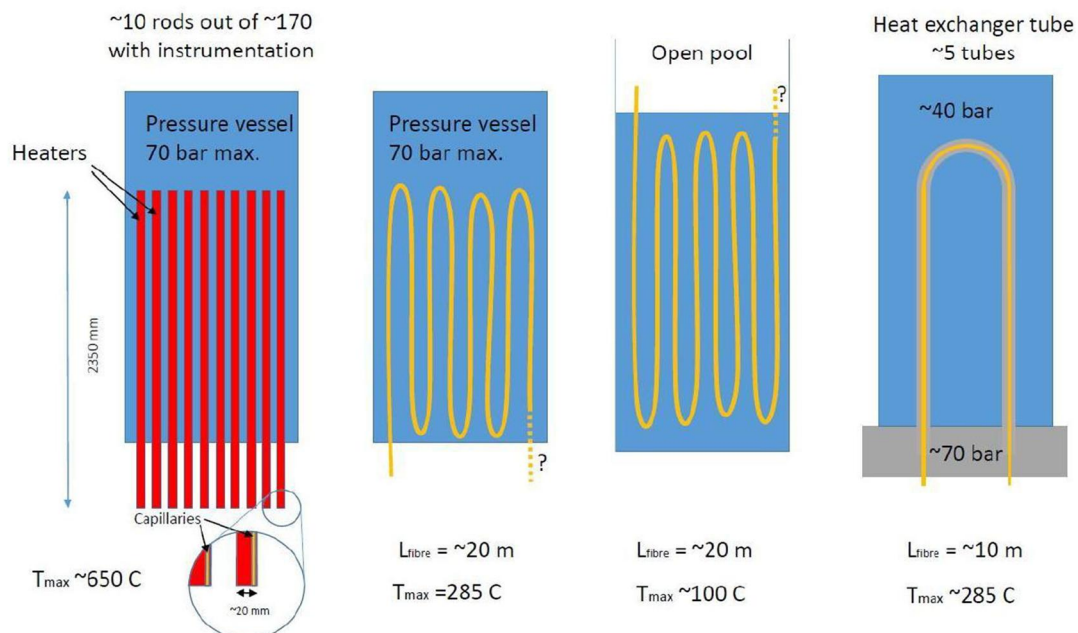


**Figure 6.** Different applications of the distributed temperature sensor based on Rayleigh-backscatter phenomenon.

The distributed temperature sensor technique was presented also in the SWINTH-2016 workshop, where more information concerning it was acquired. Regarding the characteristics of the DTS technique, temperatures up to 850 degrees Celsius can be measured. The technique can measure the temperature profile along the length of the fibre at an accuracy comparable to thermocouples and sampling rates  $< 1$  Hz. Obtaining a full profile, instead of a few point values, would represent a major advance in providing temperature data for understanding of physics and validation of codes. Point resolution and temperature resolution in DTSs are mutually exclusive to some degree. If accurate temperature measurement is preferred, the spatial resolution suffers. And the other way around, if spatial resolution is of importance, the measurement accuracy weakens. [10]

There have been preliminary plans for utilizing distributed temperature sensors in the LUT laboratory in the future. One intended target of application for the DTS is the forthcoming modular integral test facility, MOTEL, which design is on early phase. In addition to conventional point-form measurements, such as thermocouples and pressure sensors, the facility will be supplied with 2D/3D capable measurement techniques in order to provide data for 2D/3D modelling for code validation purposes.

In addition to the DTS technique, the development of different tomography measurement systems has been followed. The research visit to University of Michigan (UMICH), which took place in September–October 2016, provided lots of important information concerning tomography systems and their characteristics, such as technical and economic requirements. Two researchers from LUT attended the research visit, and during the visit the tomography measurement systems of UMICH Nuclear Engineering and Radiological Sciences department were introduced.

The department has an X-ray imaging system, as well as a gamma tomography measurement system on a testing phase. There was also an opportunity to conduct some hands-on measurements with the X-ray system. The introduction to the tomography systems and the discussions concerning them were valuable in terms of learning characteristics and limitations related to the systems and their implementation. As mentioned above, a new large-scale test facility is under design at LUT, and all the information concerning advanced measurement techniques is beneficial in designing the instrumentation for the forthcoming facility. Tomography systems, which could enhance e.g. void fraction measuring possibilities, are among the potential advanced measurement systems to be applied in the facility at some point in the future.

## **Maintenance and equipment**

The second work package of INFRAL aims on the maintenance of (PWR) PACTEL and other test facilities in LUT laboratory. The maintenance actions ensure the availability of the facilities for the thermal hydraulic experiments conducted in other research projects, such as INTEGRA and INSTAB.

The periodical inspections of the pressure vessels are performed in accordance to the legislation regarding pressure vessels and equipment. Aged components in the facilities are replaced and the operability of the systems is ensured by purchasing spare parts to replace broken ones. Typically, these parts include moving parts such as valve and automation components, but also parts for control and data acquisition systems.

Due to the upgrades in the power grid automation operated by the local power utility, the use of the PACTEL test facility has raised concerns as the unbalanced phase control system used in the core simulator trips the utility's phase trip alarms. In 2015, the replacement of the core simulator power control equipment was evaluated. The hardware was purchased in 2016. Also the power measurement system of PACTEL has been renewed.

In 2015, the procurement process of a computer for the post-processing of computational and experimental data was started, and the computer was taken into operation in 2016.

In 2016, the upgrade of power transformers has been prepared to increase the electrical power available for the thermal hydraulic experiments (1 MW  $\rightarrow$  appr. 2.5 MW). The upgrade will enable higher heating power to be available for new experimental facilities, such as MOTEL. The higher heating power enables

new research topics such as more realistic critical heat flux studies with different fuel geometries. The power transformer upgrade process has been postponed, and the options for the upgrade are being studied.

The general maintenance of PACTEL has continued as planned. The yearly calibrations and inspections have been carried out, and some of the components, such as pressure and pressure difference gauges, have been renewed.

## **Modular Integral Test Facility (MOTEL)**

The work package 3 of the INFRAL project aims on surveying different possibilities to construct an integral test facility as a successor of (PWR) PACTEL. This upfront planning helps to construct the facility without delays in the future. In 2015, a project proposal was submitted to the Academy of Finland on the topic. The work package started in 2016 with the study of the research based requirements for the new test facility, MOTEL (Modular Test Loop).

The survey of the research based requirements for the new modular integral test facility was conducted on the national level to ensure that the needs of Finnish stakeholders will be fulfilled. In addition, international trends and needs for the thermal hydraulic experimental research were studied to enable participation to various joint international projects in the future.

In 2016, a research report concerning the research based requirements for the new facility was written [11]. The key design feature of the test facility is modularity, which means that the facility will be built of interchangeable parts that enable easy modifications of the facility. Hence, the facility will be able to represent widely different types of nuclear power plants, VVERs, PWRs, BWRs and SMRs (Small Modular Reactors), in contrast to traditional large scale thermal hydraulic test facilities that refer to only one plant design.

The facility is intended to allow study of both local phenomena and system level behavior. The purpose of the experiments to be conducted is to gather data, which can be used as such but also for computer code validation.

Considering domestic research requirements in Finland, the new test facility should be able to model at least the primary circuit of the EPR and AES-2006 type pressurized water reactors, containment of a boiling water reactor, as well as small modular reactors. Internationally, in the field of thermal hydraulic research important areas in the future will include multi-dimensional, i.e. two- and three-dimensional, modeling, as well as research of passive features and passive safety systems of nuclear power plants. These aspects will be taken into account in designing the new facility.

MOTEL will be designed to model normal operation at full power and in shutdown conditions, as well as operation under transients, accidents and severe accidents, with emphasis on the coolability of nuclear fuel after reactor shutdown and phenomenological reliability of the decay heat removal from the reactor.

Components of interest are fuel bundles (the heat source), flow paths to heat sinks such as steam generators or dedicated heat exchangers, and the various geometries of steam generators and heat exchanger tube bundles. Specific interest is in stability of loop flows, heat transfer phenomena, and 2D/3D flow behavior and flow distribution in bundles. In particular, on multidimensional flow behavior in the reactor core will be focused more than before. To properly represent 2D/3D flow fields, a new scaling approach which enables larger component diameters, more realistic L/D ratios than in earlier facilities, and a reduction of component and system height, will be necessary.

The scaling of MOTEL seeks to optimize geometric and parametric representation of multiple nuclear power plant types while keeping the cost of the facility within manageable limits.

In 2016, the actual design process of MOTEL started with a survey of the options for the first heater element. The design and the construction of the facility are done with a funding from the Academy of Finland.

## Project management, international co-operation and publications

The work package 4 includes the tasks related to the project management and participation to the reference group meetings and seminars. Also international co-operation activities are a part of the work package.

The building of expertise on the advanced measurement techniques requires collaboration with other research institutes who are using the same techniques for thermal hydraulic studies. The exchange of experiences on advanced measurements have continued with institutes such as Paul Scherrer Institute (PSI, Switzerland), ETH Zurich, Helmholtz-Zentrum Dresden-Rossendorf and University of Michigan.

In September–October 2016 two researchers from LUT made a research visit to University of Michigan. The first visit to UMICH took place in November 2014, and since then the thermal hydraulic measurement infrastructure at UMICH had developed significantly. The purpose of the visit was to get familiar with some of the measurement systems that don't exist at LUT laboratory, for example the LDV (laser doppler velocimetry) system and the tomography systems, deepen the knowledge and know-how on PIV and WMS measurement techniques and data processing procedures, as well as to network with other experts on the field and enhance the good connections with UMICH. Communication with UMICH will continue in the future regarding e.g. the WMS data processing procedures.

The co-operation with other institutes will continue in the future, too. For example communication with HZDR/ETH Zurich concerning the high temperature/high pressure wire-mesh sensors will continue, and tentative plans for a research visit have been made.

## References

- [1] Pyy, L. 2015. Single spray nozzle tests. Research Report INSTAB 2/2015, Lappeenranta University of Technology. 25 p.
- [2] Skripnikov, D. 2016. Spray Droplet Size Distribution Measurements. Master's Thesis, Lappeenranta University of Technology. 69 p.
- [3] Ylönen, A. & Hyvärinen, J. 2015. Study of Two-Phase Pipe Flow using the Axial Wire-Mesh Sensor. Proceedings of the 16<sup>th</sup> International Topical Meeting on Nuclear Reactor Thermal Hydraulics (NURETH-16), Chicago, U.S., August 30–September 4, 2015. 10 p.
- [4] Ylönen, A., Varju, T. & Hyvärinen, J. 2016. Estimation of Velocity Fields from the Axial Wire-Mesh Sensor Data. Proceedings of the Specialist Workshop on Advanced Instrumentation and Measurement Techniques for Nuclear Reactor Thermal Hydraulics (SWINTH-2016), Livorno, Italy, June 15–17, 2016. 15 p.
- [5] Kickhofel, J. 2015. Wire Mesh Sensor for High Temperature High Pressure Applications. Proceedings of the 16<sup>th</sup> International Topical Meeting on Nuclear Reactor Thermal Hydraulics (NURETH-16), Chicago, U.S., August 30–September 4, 2015. 12 p.
- [6] Pietruske, H. & Prasser, H.-M. 2007. Wire-mesh sensors for high-resolving two-phase flow studies at high pressures and temperatures. *Flow Measurement and Instrumentation* 18 (2007), 87–94. 8 p.
- [7] Kickhofel, J., Yang J. & Prasser, H.-M. 2016. Designing a High Temperature High Pressure Mesh Sensor. Proceedings of the Specialist Workshop on Advanced Instrumentation and Measurement

- Techniques for Nuclear Reactor Thermal Hydraulics (SWINTH-2016), Livorno, Italy, June 15–17, 2016. 12 p.
- [8] Patel, G., Tanskanen, V. Hujala E. & Hyvärinen, J. 2016. Direct contact condensation modeling in pressure suppression pool system. Nuclear Engineering and Design, Available online 13 September 2016, ISSN 0029-5493. 15 p.
- [9] Gerardi, C., Bremer, N., Lisowski, D. & Lomperski, S. 2015. Distributed Temperature Sensor testing in Liquid Sodium. Proceedings of the 16<sup>th</sup> International Topical Meeting on Nuclear Reactor Thermal Hydraulics (NURETH-16), Chicago, U.S., August 30–September 4, 2015. 10 p.
- [10] Lomperski, S., Bremer, N., Gerardi, C. & Lisowski, D. 2016. Performance Assessment of a 50 m-long Fiber Optic Distributed Temperature Sensor in a Fluid Dynamics Experiment. Proceedings of the Specialist Workshop on Advanced Instrumentation and Measurement Techniques for Nuclear Reactor Thermal Hydraulics (SWINTH-2016), Livorno, Italy, June 15–17, 2016. 11 p.
- [11] Telkkä, J. & Hyvärinen, J. 2016. Research based requirements of MOTEL. Research Report INFRAL 1/2016, Lappeenranta University of Technology. 22 p.

## 7.2 JHR collaboration & Melodie follow-up (JHR)

Santtu Huotilainen, Ville Tulkki, Petri Kinnunen

VTT Technical Research Centre of Finland Ltd  
P.O. Box 1000, FI-02044 Espoo

### Abstract

Jules Horowitz Reactor (JHR), a new European material testing reactor (MTR), is currently under construction at CEA Cadarache research centre in France. The JHR consortium has set up three working groups (WG) to determine experimental needs and plan future experiments. After gathering information on the topics of interest for the first experiments from the JHR consortium members, and creating the ranking grids for the selection of the topics, the WGs agreed on fuel and material irradiation experiments, which would become the first experiments planned and performed by the international JHR consortium. The position paper, which describes these pre-JHR experiments proposed by the WGs, was drafted and delivered to the JHR governing board in 2016. The Melodie, Mechanical Loading Device for Irradiation Experiments, delivered to CEA in 2012 as a part of the Finnish in-kind contribution to the international JHR project, is a device for the study of the irradiation creep of a Zircaloy-4 fuel cladding tube specimen. The instrumented test device has the capability to control the biaxial loading and to measure the biaxial strain of the specimen online. The Melodie in-core experiment started in May 2015 and lasted for six reactor cycles. The results of the in-core experiment have not been fully analysed yet, but some initial results are available. The LVDT5, measuring the axial strain, produced consistent low-noise data in just one week, making it possible to analyse the value of the axial creep strain. The behaviour of the loading frame, the gas management system and the data acquisition system was reliable throughout the experiment, which indicates the potential of the technology considering future experiments.

### Introduction

Jules Horowitz Reactor (JHR), a new European material testing reactor (MTR), is currently under construction at CEA Cadarache research centre in France. Finland is participating in the construction with a 2% in-kind contribution, which includes Underwater Gamma spectrometry and X-ray radiography (UGXR) and Hot-cell Gamma spectrometry and X-ray radiography (HGXR) systems as well as a Mechanical Loading Device for Irradiation Experiments (MeLoDIE). With this in-kind contribution, Finland will have the possibility of utilising the new JHR research infrastructure dedicated to nuclear safety related research. Furthermore, the in-kind contribution enables access to the results of the future experiments.

JHR will offer modern irradiation experimental capabilities to study material & fuel behaviour under irradiation. JHR will be a flexible experimental infrastructure to meet industrial and public needs within the European Union related to present and future Nuclear Power Reactors. JHR is designed to provide a high neutron flux (twice as large as the maximum available today in MTRs), to run highly instrumented experiments to support advanced modelling giving prediction beyond experimental points, and to operate experimental devices giving environmental conditions such as pressure, temperature, flux, and coolant chemistry relevant for example for water reactors, for gas cooled thermal or fast reactors, and for sodium fast reactors. These objectives require representative tests of structural materials and fuel components, as well as in-depth investigations with separate-effect experiments, coupled with advanced modelling.

According to the consortium agreement, JHR is aimed to become an international user facility with the model of the Halden Reactor Project with multinational projects and proprietary experiments. Consequently, CEA is preparing, with the support of the OECD/NEA, a joint programme, which has the strategic scope

to address fuel and material issues of common interest that are key for operating and future NPPs (mainly focused on LWR).

The JHR consortium has set up three working groups (WG) to determine experimental needs and plan future experiments. To have our national interests brought forward and to be able to follow and participate in the planning of the experiments, VTT has named participants to each of the three WGs. The WGs hold meetings twice a year, and in spring an annual JHR Technical Seminar is held, where the outcomes of the WG meetings and the progress of in-kind work are presented.

The Melodie, Mechanical Loading Device for Irradiation Experiments, was delivered to CEA in 2012 as a part of the Finnish in-kind contribution to the international Jules Horowitz Reactor (JHR) construction project. It is a device for the study of the irradiation creep of a Zircaloy-4 fuel cladding tube specimen. The instrumented test device has the capability to control the biaxial loading and to measure the biaxial strain of the specimen online.

After the delivery of the Melodie sample holder, the experimental setup was completed with the addition of a glove box containing a gas management system and a safety box to allow the independent operation of the setup. After some modifications and extensive preliminary testing, the experimental setup was finally ready to be transferred to the Osiris reactor building in the end of March 2015.

The in-core experiment was started on 7 May, 2015. With the final shutdown of the Osiris reactor taking place at the end of 2015, a total of six reactor cycles of irradiation were planned for Melodie. Because of the definitive time limit, some of the original experimental objectives had to be condensed or omitted. However, the main objectives were retained.

## **JHR collaboration progress in 2015–2016**

The planning of the future experiments in JHR has been launched within three working groups (WG), namely Fuel WG (FWG), Materials WG (MWG), and Technology WG (TWG). The objective of these working groups is to advise the Governing Board (GB) on potential scientific topics of interest for future R&D programs in JHR, through proposal of joint international programs or multi-lateral programs. This is done by determining experimental needs, planning future experiments, and developing experimental devices and infrastructure. Some of the experimental devices are based on existing technologies, but also new types of devices are being developed, extending the experimental capabilities and bringing new information on the subjects studied.

In 2015, the MWG and FWG held a common meeting in Rez, Czech Republic in January. TWG held a meeting in February. In the MWG and FWG common meeting the ranking grids for potential topics of interest for future experiments in JHR were discussed, and a common set of criteria for carrying out the ranking was established.

The fifth annual JHR Technical Seminar was held at CEA Cadarache in April 2015. The feedback from the three WGs had more emphasis in the seminar program than in previous years, which allowed a wider discussion about the role of the WGs and about the roadmap for their work.

Another WG meeting took place in October 2015 in Studsvik, Sweden, with all three WGs together. In this meeting the WGs discussed the contents of a synthesis document that would be delivered to the GB by the end of October 2015 and a position paper to be delivered by the end of December 2015. The synthesis document describes the work carried out by the WGs and the objectives for the future. The position paper includes a proposal for two irradiation experiments to be carried out before the start-up of JHR.

To fulfil the objective set for the WGs, the participants had identified open issues in the field of nuclear fuel and nuclear materials development and qualification, elaborated shared criteria to define the ranking grids to identify issues of common interests for participants taking into account their potential scientific and/or industrial interests, assessed the grid and selected a first set of potential joint or multilateral experiments in JHR, with special attention to programs which could fulfil the needs of both FWG and MWG. Furthermore, the WGs defined initial technical specifications for the first experimental program (irradiation and PIE), and considered the feasibility of these first programs, in particular the possible role of existing

MTRs associated with hot labs as support for qualification and/or benchmarking experiments and the added value offered by the JHR.

The ranking grids were first formed separately in MWG and FWG. In the WG meeting in January 2015, the results of the grid formation so far were discussed, still separately between the two WGs, and the grids were updated, after which the two WGs presented their results in a joint session. The need for creating a common set of criteria for ranking the contents of the grids was expressed, and by the end of the meeting initial criteria were established. The members of the consortium were subsequently asked to use the selected criteria to rank the contents of the grids. Answers were received from several but not all members. The ranking grids of potential topics of interest remain open for discussion, corrections and additions.

Another outcome of the WG meetings was to investigate the opportunity to define an experimental program of common interest to be eventually performed within one of the operating research reactors according to the priorities set by the WGs and with regard to the preparation of future irradiation programs in JHR. In addition to the scientific and technical aspects, such consensus on JHR validation/qualification experiments will enhance the way of working together within the consortium as well as the preparation of being efficient together once the JHR is in operation.

In the first WG meeting of 2016, organised by the Israel Atomic Energy Commission (IAEC) in the Soreq Nuclear Research Centre in Israel, the synthesis document was briefly reviewed once more, and a TWG memo to be attached to the synthesis document was presented. The attachment was not included in the version sent to the GB in December 2015, but it was later added in the revision of the document. It was pointed out that the executive summary of the synthesis document is important, expressing the consensus of the three WGs.

The position paper was drafted by Mr Bignan and the convenors and secretaries of the WGs, and a version ready for submission to the GB was presented to the members of the WGs. The contents of the paper and the objectives of the WGs with regard to future work were then discussed. The participants agreed it is important that potential partners outside the JHR consortium are given a clear idea of the scientific and technological objectives of the planned experimental campaigns, and participation is encouraged.

Presentations about the HFR research reactor at JRC Petten, the hot cell facility in Rez and the BR2 reactor were given by Mr Elio d'Agata, Mr Marek Miklos and Mr Brian Boer, respectively. These presentations were given with regard to their potential role in the the planned pre-JHR irradiation experiments.

The WG meeting in Israel included parallel sessions of FWG and MWG, with the members of TWG participating in both sessions. In the MWG session, the main focus was in the specifications of the first material irradiation experiment presented in the position paper. The goal of the experiment is to study the effect of the neutron spectrum on the irradiation damage production and the mechanical behaviour of the material. Therefore, it is planned to irradiate specimens in two different spectra to same doses. The material selected for the irradiation experiment was decided to be stainless steel, but a more specific selection of the material was not made. It was pointed out that the specimens must all be from the same material heat, and in addition to the specimens prepared for the irradiation experiment also non-irradiated specimens must be available for comparison in the post-irradiation examination. During the meeting there was discussion about the test parameters, since the parameters first proposed in the draft version of the position paper had been changed between the distribution of the draft and the meeting. The iteration of the parameters considering the experimental objectives and the test environments was continued in the discussion, but no definitive decisions were made.

FWG discussed the prospects of the fuel experiment. A power transient or ramp experiment had been determined to be the most appropriate type of an experiment, given the experimental devices available in the start-up of JHR. However, CEA considered that the irradiation devices used in OSIRIS are the viable reference to the JHR and that there is little more that could be done to assist in the commissioning phase of JHR by the experiments in the other reactors. As such the justification for the experimental campaign was not clear. However, a twin experiment with sibling rods to demonstrate JHR capabilities was considered to be of both technical and scientific value. First sibling rod would be irradiated in BR2 and second in JHR. The test would be a stepwise ramp experiment to a very high power in order to observe the fuel microstructural changes while at the same time ensuring the integrity of the fuel rod. For reference, Mr

Francesco Corleoni from Studsvik showed the xM3 experiment performed at Studsvik R2 reactor in 2005, which had experienced central melting of the fuel while maintaining rod integrity. Potential rods and PIE were also discussed, and it was acknowledged that the transfer of irradiated fuel would be a major cost issue.

In the second WG meeting of 2016, which was organised by SCK.CEN in Mol, Belgium, the participants discussed the FIJHOP (Foundation for future International Jules HOrowitz experimental Programs) project proposal submitted in the H2020 October call. The main general objective of the 5-year project, with a total of 20 partners including the 12 JHR consortium members, is to prepare for the future joint international experimental programs performed in JHR by utilising the existing European material testing reactors (MTR), namely BR2, HFR and LVR-15 reactors. The FIJHOP project would essentially include the pre-JHR experiments initially discussed in the previous WG meeting. The discussion continued with the iteration of the detailed specifications of the experiments. Some participants questioned the selection of JRQ material as the other choice alongside stainless steel and were questioning the objectives of the JRQ irradiation. Initially designed as a reference material for the study of irradiation damage in RPV steels, the JRQ steel, which has higher amounts of alloying elements than RPV steels, has been found to be very heterogeneous. Therefore, the selection of the material for specimen manufacturing is important, as specimens manufactured from different locations of the original JRQ steel plate can have very different mechanical properties.

There was also general discussion about the main scientific objective of the FIJHOP project, the study of the neutron spectrum effect on material microstructure and mechanical properties. The subject is very difficult to study experimentally, since the alteration of the neutron spectrum usually has an effect on the neutron flux and temperature.

In the fuel session, EdF presented its views on the future fuel experiment. EdF is interested in investigating the current limit of 1% cladding deformation and its possible extension, as well as incipient fuel melting limit. Also release after failure is based on very conservative tests/assumptions, so in the future source term measurement during rod failure would be an interesting test. According to the analysis on the FIJHOP proposal EdF considered that whereas the slow ramp rate was fine, high BU or high terminal level would not necessarily be reached nor would the cladding outer diameter be measured. FIJHOP test should be complemented by other tests afterwards.

In the general discussion on the FIJHOP proposal, the variety of the codes used in the work, and what is actually calculated, was debated in length. This will be further detailed if the funding is received. Two alternative scenarios for the final part of the irradiation were described to be decided later on, both of which would aim for 10% fuel melting in the high power section of the segment. The challenge will be that the temperature measurement will not be conducted at the highest power position but a bit below it. Also, the determination of the possible melting afterwards will be difficult as destructive PIE was not included in the project due to budgetary reasons. However, some indications will be seen from the gamma scanning as the volatile species should be redistributed in the molten region.

A second fuel irradiation proposal for a future European Commission call was discussed. Basically it would be a similar irradiation, but the uninstrumented rod would be removed from the reactor at given points, measured at hot labs and returned to the reactors for continued irradiation. This would complement the FIJHOP irradiation, being in principle a similar irradiation scheme but providing information on cladding deformation.

## **Results of the JHR collaboration**

The synthesis document describing the work carried out by the WGs and the objectives for the future was distributed to the WGs for review in mid-December 2015. After a review round, a revised version of the document was delivered by the WGs to the JHR governing board in early 2016.

After gathering the information about the potential topics of interest for the first experiments from the JHR consortium members, and subsequently creating the ranking grids for the evaluation and selection of the topics, the WGs agreed on a fuel irradiation experiment and a material irradiation experiment, which

would become the first experiments planned and performed by the international JHR consortium. The position paper, which describes these pre-JHR experiments proposed by the WGs, was drafted and delivered to the governing board in 2016.

Based on the work carried out by the WGs and described in the synthesis document and the position paper, a project proposal was drafted during the summer 2016 and submitted to the European Commission H2020 October call on the 5<sup>th</sup> of October 2016. The FIJHOP project consortium gathers a total of 20 partners, including the 12 JHR consortium members. The work started within the JHR WGs will continue in the 5-year FIJHOP project, leading to the first experiments in the JHR in early 2020s.

## Melodie follow-up

The Melodie, Mechanical Loading Device for Irradiation Experiments, was delivered to CEA in 2012 as a part of the Finnish in-kind contribution to the international Jules Horowitz Reactor (JHR) construction project. It is a device for the study of the irradiation creep of a Zircaloy-4 fuel cladding tube specimen. The instrumented test device has the capability to control the biaxial loading and to measure the biaxial strain of the specimen online.

The Melodie experimental setup includes a sample holder, a Chouca irradiation capsule, a glove box containing a gas management system and a safety box for the sample holder, another glove box for the Chouca capsule, above-water lines and underwater lines for connecting the pneumatic and electrical lines between the glove box and the sample holder, and a Moog standalone servo controller for the control of the experimental pneumatic lines and for data acquisition.

The upper part of the Melodie sample holder, with the interface to the Chouca capsule and to the underwater lines, was manufactured by Soterem (Toulouse, France) according to the French RCC-MX nuclear construction code. The Chouca capsule is a material irradiation device used by CEA in the Osiris reactor. It has a double wall tube structure with electrical heaters on the level of the reactor core for controlling the temperature profile. The gas management system is based on a system previously used with pneumatic loading devices at VTT, with the addition of a standalone pressurisation loop. The safety box is an interface between the gas management system and the sample holder, and it also connects the Melodie experimental system to the Osiris safety systems.

The main goal of the Melodie in-core experiment was to act as a prototype for future instrumented material experiments in the JHR. Therefore, the instrumentation in the Melodie sample holder, including the pneumatic mechanical loading units and LVDT (Linear Variable Differential Transducer) sensors, had to be tested and their operation validated in reactor environment.

Zircaloy-4 was chosen as the material of the specimen, because it is well known and the results of the experiment can be compared to data already available. Potentially it was also possible to produce new creep data, especially to study the performance of the cladding in the early stages of creep or in transient situations, because of the online control and measurement.

Being delayed from the original scheduled start of the irradiation, and the shutdown of the Osiris reactor nearing, the experimental objectives were revised and the plan was to test all possible features and capabilities of the device in a short amount of time. Typically, creep is a slow deformation process under stress and temperature over a relatively long time period. In this case, however, the original plan of performing an irradiation creep test by keeping constant irradiation and stress conditions during one or more reactor cycles without changes was abandoned. Instead, the stress levels were varied within a single reactor cycle to be able to test the performance of the device efficiently.

The Melodie sample holder was placed in the position 24NE of the Osiris reactor core, with an average fast neutron flux of  $1.2 \times 10^{14}$  n/cm<sup>2</sup>s. The target temperature for the Zy-4 specimen was 350 °C. The temperature of the specimen could be controlled to some extent with the electrical heaters of the Chouca to have as flat a temperature profile as possible.

In-core experiments are divided into cycles based on the reactor operating schedule. In Osiris, each cycle was 18 to 25 days long, and between the cycles there were outages of about 10 days each. From August to September, a longer maintenance outage was scheduled, and there was no irradiation cycle.

Therefore, the Melodie experiment, started in May 2015, had six cycles of reactor time before the shut-down of Osiris at the end of 2015.

During the in-core experiment, the Melodie sample holder was inserted into the Chouca capsule. The bottom part of the sample holder was submerged in NaK, which prevented oxidation and acted as a thermal conductor. The rest of the Chouca was filled with helium gas. Helium was also used in the pneumatic loading units and the mover because of its low activation under irradiation. The pneumatic and electrical lines of the sample holder were connected to the gas management system and the Moog controller. The Moog controller was used together with the glove box for adjusting the pressure in the four experimental pressure lines. LVDT and pressure sensor signals were recorded with a selected acquisition rate, and the recorded files were transferred to a computer during operation. Data was recorded also to the Osiris database via the local network. The Osiris database contains the data from the same experimental signals as the Moog, plus data from all 12 thermocouples, the reactor linear power, and the control rod positions.

## **Results of the Melodie in-core experiment**

The first cycle of the Melodie in-core experiment started on 7 May, 2015. The goal was to first ensure the instrumentation is working the same way as out-of-pile. During the first diameter scans with the DG after the start of the cycle it was immediately observed that the DG does not show similar behaviour as out-of-pile. The signal had a lot of disturbance and was not consistent between the scans. It was concluded that the disturbance was most probably due to temperature changes in the sensor. The tests with the DG continued throughout the reactor cycle with varying scanning speeds. Because of the lack of repeatability in the measurement the problem was difficult to analyse more closely. The temperature profile was also adjusted with the electrical heaters in the Chouca to see if it had any influence on the DG signal, but it was found not to mitigate the problem.

After discovering the problems with the online measurement capability of the DG, the second reactor cycle was dedicated to axial strain measurement. During the preliminary tests and also the first reactor cycle the focus had been on the diameter measurement, and little emphasis had been put on the behaviour and tuning of the LVDT5. Therefore, the interpretation of the axial strain measurement was not as straightforward as expected. The LVDT5 signal was working, but taking into account the thermal expansions and elastic deformations of the loading frame was difficult. It was decided to continue gathering data and simultaneously trying to perform initial analysis on it to be able to conclude whether the measurement was producing rational results or not. This work continued in the third cycle.

The axial strain measurements continued, and early in the third cycle the LVDT5 produced consistent low-noise data making it possible to analyse reliably the value of creep in one week (Figure 1). The stress level was changed twice, and the creep rate with stress levels of 60 MPa, 110 MPa and 60 MPa was measured during the third reactor cycle. However, in the end of the cycle the strains measured during the cycle were compared to those measured in room temperature before and after the cycle, and there was a discrepancy between the measurements, indicating that further analysis was needed.

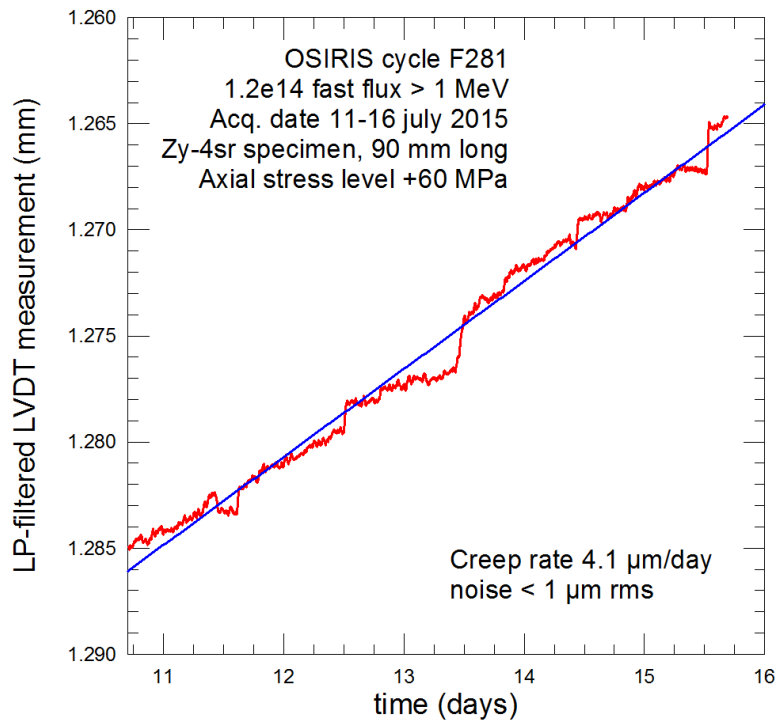


**Figure 1.** Axial creep strain measurement with 60 MPa stress and  $345 \pm 5$  °C.

During the long summer outage after the third cycle, it was discovered in out-of-pile measurements that the impedances of the LVDT5 coils were strongly drifting, suggesting some degree of damage in the sensor. In the DG, however, there was no noticeable change in the electrical signals compared to the measurements before the start of irradiation, and the scanning diameter measurement seemed to be working fine out-of-pile.

The fourth cycle was dedicated to offline hoop strain measurement. The diameter was measured before and after the cycle to have an integrated measurement over the cycle. These offline measurements were repeated later after each of the remaining cycles.

In the fifth cycle the focus was back on the axial strain measurement. The goal was to repeat the measurement carried out in the third cycle. After the fifth cycle the Melodie device was brought to the hot cells in the Osiris reactor building for changing the Chouca. The sample holder was extracted from the original Chouca and inserted into a new one. The new Chouca has a slightly different design in terms of the gas gap between the two tubes, which has an effect on the temperature profile on the core level. The change of the Chouca was planned already after the first cycle, when the behaviour of the system was found not to be satisfying with regard to the DG measurement. However, it was not carried out until the last outage because of the other tests performed during the reactor cycles and also because of the preparations needed for the change procedure.

In the sixth and last reactor cycle the goal was to test the behaviour of the DG in the new Chouca. The behaviour was not very different from the first cycle, which confirmed the assumption formed after the first cycle that the inherent performance of the sensor is too sensitive to the harsh environment of the Osiris reactor and the solution is beyond our reach during the time frame of this experiment. The remaining days of the last cycle were again dedicated to the axial strain measurement.

## References

- Al-Mazouzi, Abderrahim, Marek Miklos, and Petri Kinnunen. "Synthesis Document." Memo, Fuel, Materials and Technology Working Groups, JHR Consortium, 2015.
- Bignan, Gilles, Abderrahim Al-Mazouzi, Marek Miklos, and Petri Kinnunen. "Position Paper." Position Paper, Fuel, Materials and Technology Working Groups, JHR Consortium, 2016.
- Bignan, Gilles, and Jérôme Estrade. "The Jules Horowitz Reactor: A new high performance MTR (Material Testing Reactor) working as an international user facility in support to nuclear industry, public bodies and research institutes." *16th Meeting of the International Group On Research Reactors (IGORR)*. Bariloche, 2014.
- Bignan, Gilles, and Nicolas Waeckel. "The key-role of material testing reactors in support to nuclear industry: Example of JHR and of the ICERR scheme." *IAEA International Conference on Research Reactors: Safe Management and Effective Utilization*. Vienna: IAEA, 2015.
- Guimbal, Philippe, et al. "Status of the MeLoDIE experiment, an advanced device for online biaxial study of the irradiation creep of LWR cladding." *3rd International Conference on Advancements in Nuclear Instrumentation, Measurement Methods and their Applications (ANIMMA)*. Marseille, 2013.
- Huotilainen, Santtu. *Development and 3D design of an in-reactor material creep test device*. Master's thesis, Espoo: Aalto University, 2010.
- Huotilainen, Santtu. *Progress report on JHR collaboration*. Espoo: VTT-R-06014-15, 2015.
- Huotilainen, Santtu. *Technical report on the Melodie in-core experiment*. Espoo: VTT-R-06016-15, 2015.
- Tähtinen, Seppo. *Melodie sample holder - development and performance*. Espoo: VTT-R-00516-13, 2013.

### 7.3 Radiological laboratory commissioning (RADLAB)

Wade Karlsen

VTT Technical Research Centre of Finland Ltd  
P.O. Box 1000, FI-02044 Espoo

#### Abstract

The RADLAB project executes the renewal of the radiological research infrastructure hosted by VTT, embodied in the new VTT Centre for Nuclear Safety. In the first half of the SAFIR 2018 programme, the RADLAB project has overseen the design and fabrication of new hot cells for testing and characterization of activated reactor structural materials. It has also executed the procurement of key hot laboratory equipment, the design, fabrication and installation of self-built research facilities, the design, fabrication and installation of materials handling and storage facilities, and contributed to the full laboratory infrastructure commissioning and ramp-up of operations for both reactor safety and final repository research. The hot cells have been designed and manufactured on a contract with Isotope Technologies Dresden, GmbH, all the main key devices have been procured, and the radiological operation permit for the radiochemistry and microscopy facilities has been granted. The installation and commissioning of the new hot cells is on track for 2017.

#### Introduction

During the SAFIR2018 research programme, the Finnish radiological research infrastructure renewal reaches a crescendo as a significant new research capacity is realized, the VTT Ltd. Centre for Nuclear Safety (CNS). The VTT CNS and its hot cell facility is a national infrastructure hosted by VTT, and is considered an important element in fulfilling the national requirements for independent competencies for domestic nuclear power generation. As such, from 2016 onward, the Finnish State Nuclear Waste Management Fund (VYR) has supported the renewal of the radiological laboratory research infrastructure via three instruments: 1) the research and infrastructure instrument, generally comprised mainly of personnel, travel and associated research execution expenses; 2) a special allocation for supporting the VTT Ltd. Centre for Nuclear Safety radiological laboratory facility expense, and 3) a special allocation for supporting the VTT Ltd. Centre for Nuclear Safety radiological laboratory equipment investment expenses as investment aid. All three instruments are jointly supported by the SAFIR2018 (nuclear power plant safety) and KYT2018 (nuclear waste management) research programs.

This RADLAB project is the continuation of the REHOT project that was in the SAFIR 2014 program and the first year of the SAFIR 2018 program. The RADLAB project is an integral part of the overall infrastructure renewal process surrounding the VTT CNS, in support of both reactor safety and nuclear waste management (NWM) research. While the former REHOT project focused mainly on the design, construction and equipping of the new CNS facilities, as shown in the schematic of Figure 1, the RADLAB project spans the move from the existing facilities at Otakaari 3 (OK3), to the new facilities located at Kemistintie 3 (KM3), and features the commissioning of equipment and ramping up of the infrastructure in the new facilities.

The design of the VTT CNS in its current rendition has been on-going since 2012 in the REHOT project [1, 2]. The facility is owned by the Finnish State real-estate company Senaattikiinteistöt, with VTT renting the building from them as the facility users. As such, the facility design process was carried out in close

cooperation between VTT researchers (the facility users) and the design team employed by Senaatti-kiinteistöt. Regulation and oversight by the authorities has involved the local municipal government, building department and emergency services, as well as Radiation and Nuclear Safety Authority, Finland-STUK.

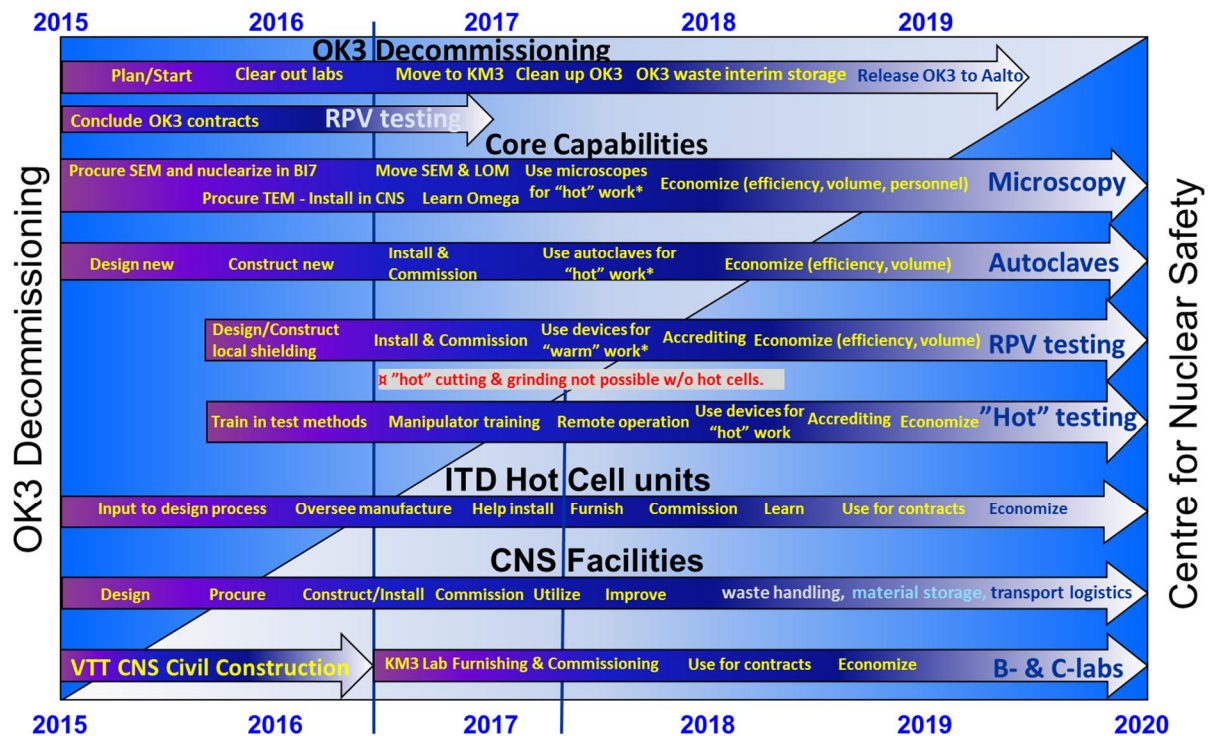


**Figure 1:** Radiological laboratory infrastructure renewal process comprised of simultaneous decommissioning of facilities at Otakaari 3 (OK3) and equipping and commissioning of the Centre for Nuclear Safety.

The location and position of the new VTT CNS in Otaniemi is shown in Figure 2. Since the safe shipment of radioactive materials can involve large trucks, the location enables driving and turning access for large tractor and trailer combinations. As visible in the site layout (Figure 2), the facility includes an office wing and a laboratory wing nestled amongst the trees. The office wing is 3,300 m<sup>2</sup> and includes a ground-level conference centre, above which are three floors of modern, flexible office space for 150 people. It features an architecturally striking, angular facade on the Kivimiehentie street side, producing the distinct, yet complementary appearance shown in Figure 2, blending in with the natural surroundings. The office wing houses nuclear sector researchers in areas such as computerized fluid dynamics, process modelling (APROS), fusion plasma computations, severe accidents, core-computations, nuclear waste-management and safety assessments, as well as the staff working in the laboratory wing. The laboratory wing is a more conventional, rectangular wing, and includes a basement level and two floors of laboratory space. The laboratory activities include research involving radiochemistry, aerosols, nuclear waste management, dosimetry, failure analysis as well as mechanical and microstructural characterisation of structural materials. Shipping radioactive materials into and out of the facilities occurs through a gated courtyard and covered loading dock at the basement level, at the rear of the building.

Over the course of the SAFIR2014 program, the renewal of the hot cell infrastructure made great strides forward in the REHOT project. The process was initiated in 2008 with preliminary assessment of the needs and options as a part of the SAFIR2010 AKTUS project, after which a draft facility design was made in collaboration between VTT and A-Insinöörit, the engineering company employed by Senaatti-kiinteistöt. This was subsequently turned into an engineering design during 2012. Over the 2013 period the floor

plans of the facility were subjected to further modifications, and then the detailed design process was carried out to generate the detailed layouts of furnishings and building systems on a room-by-room basis [3]. In 2013, the draft plans of the laboratory facility, the activities and the practices that would be employed, were presented to STUK's radioactive facilities evaluators for review. A preliminary, non-binding assessment was received with some specific recommendations for improvement, which were then implemented into the design.



**Figure 2:** VTT Centre for Nuclear Safety in Otoniemi.

With regard to the hot cells themselves, a significant milestone in 2013 was the execution of a hot-cell conceptual design and preliminary cost estimate, which was made on a contract with Merrick & Company [4]. A reassessment of the design was then carried out by VTT and utilized for the tendering process for the engineering design and fabrication of the hot cell facilities, carried out in 2014 [5]. The contract was awarded to Isotope Technologies Dresden GmbH (ITD).

The ground breaking for the CNS began immediately in 2014, so during the SAFIR2018 programme the CNS progresses through the construction and commissioning stage of the radiological laboratories, including the hot cell facilities. Although the renewal of the research environment does not provide time for significantly modifying the goals set for the programme, it creates new possibilities for research with its new hot cell and laboratory facilities and equipment needed for research on reactor structural materials and nuclear waste management.

The CNS and its hot cell facilities enable **progress beyond the state-of the art** on many fronts. The modern laboratory facilities provided by the CNS raises the level of technological prowess, in tandem with enhancing radiation safety. By bringing most of the VTT nuclear sector researchers together under the same roof, the capacity to act together in wide-ranging national programs is enhanced. Likewise, the CNS provides a common radiological facility housing radiochemistry laboratories, modern microscopy and analytical capabilities, and mechanical testing of radioactive materials. This offers a better platform for national multidisciplinary collaboration.

The technological enhancement enables a higher scientific level in research results. This in turn is essential for participation in international research projects and programmes, as well as for enabling high-level research in support of doctoral programs. The enhanced radiation safety offered is also beneficial for providing an environment amenable to hosting visiting researchers, whether as part of domestic degree programs, or of international consortium research projects.

With respect to the hot cells themselves, the greatest change is the essential improvement of research capacity for highly radioactive, neutron-irradiated, austenitic stainless steels and freshly irradiated pressure

vessels steels. And as a national research infrastructure coupled with Finland's share of the Jules Horowitz Material Test Reactor (JHR), **for the first time in the history of Finnish nuclear R&D** the country will have the possibility to carry out the whole material testing chain, starting from neutron irradiation in the JHR core, through to comprehensive mechanical, microstructural and analytical post-irradiation examinations (PIE) in the CNS radiological facilities.

## Objectives and expected results

As was outlined in the REHOT 2015 project report "Roadmap for the VTT Centre for Nuclear Safety Research Infrastructure" [6], the infrastructure for radioactive materials research and testing involves facilities, equipment and competent users. The RADLAB project is the means by which the infrastructure renewal is executed by the personnel involved in carrying out the work. This includes design input and oversight of ITD in designing and manufacturing the hot cells, but also in training of personnel, adopting a new safety culture, executing the key equipment procurement processes, nuclearization of equipment going into the cells, and the design, procurement and installation of the other research devices and process equipment supporting the radioactive materials handling and storage.

The ultimate objective of the hot cell contract with ITD is to achieve safe, functional hot cells in a cost effective manner, which are appropriate to the specified research and testing needs.

The primary objective of the equipment procurement is to acquire the most suitable and cost effective hot laboratory, hot cell and ancillary devices and instruments for the specified needs. The end result is therefore delivery of each purchased piece of equipment, and demonstrated functionality of each self-built device.

The overall objective of the equipment nuclearization and installation (whether purchased or self-built), is to achieve safe functionality of the device in its application for radioactive material handling or testing, whether it is a self-built "hot" autoclave system, a stand-alone device like a "hot" SEM, or a device deployed inside one of the hot cell chambers. In the case of the hot cell suite manufactured by ITD, a full Factory Acceptance Test (FAT) and Site Acceptance Test (SAT) procedure is specified in the contract.

## Exploitation of the results

While the principle goal of the RADLAB project is to execute the infrastructure renewal, the exploitation of that result is firstly achieved by *demonstration of the functionality* of the facilities for producing mechanical and microstructural data and results of radioactive materials in conditions that are in line with the ALARA principle expected of contemporary radiological facilities. The goal of the programme period will be to demonstrate the research capacity of the facility for use in increasing the overall understanding of the effect of radiation on nuclear power plant structural materials. The primary areas of research involve life cycle extension, reactor pressure vessel steels, austenitic stainless steels (internal components), but as new topics there is irradiated fuel element structural parts and fuel cladding materials (GEN III-IV), and consideration also of capabilities to research irradiated concrete. Source material for such tests and examinations should ideally be from materials harvested from NPPs, both domestic and international. With particular regards to testing and characterizing materials from in-core irradiations and tests, the Halden Reactor Project provides materials from real plants, and the Jules Horowitz Reactor project is being followed-up in collaboration with a separate project in SAFIR2018.

On another level, the VTT CNS gathers much of the VTT Nuclear Safety research personnel earlier scattered in Otaniemi, into a single, compact location. This will *promote synergism* between researchers across topics and facilitate closer collaboration between experimental and modelling work. A first tangible step in this direction is collaboration between the JHR and PANCHO projects realized in SAFIR2018, in which biaxial creep experiments on fuel cladding material in JHR are joined with cladding creep modelling work in PANCHO, which involves VTT researchers that are housed in the office wing of the VTT CNS.

The proximity of the VTT CNS to Aalto University also help to *strengthen the symbiotic relationship* that exists between the two institutes. The existence of shared facilities and equipment will promote the syner-

gy of Finnish research on existing and future reactor concepts. Finally, modern radiological research facilities strengthen Finland's capacity and capability to *contribute to international projects* as an equal partner or even leader.

## Results

The project is executed in 5 main work packages, the results of which are described in the following sections. The first one is focused on the hot cell fabrication, installation and commissioning process, which involved not only participation in the execution of the hot cell contract with ITD, but also continued development of the hot cell functions and training of operators for the hot cell facilities. In the second work package the hot laboratory equipment is procured, which involves not only executing the procurement process for each device, but also managing the overall investment schedule. The third work package focuses on self-built research facilities, including their design, fabrication and installation, as well as device adaptation for use in the hot cell theatre with appropriate modifications for e.g. remote operation and radiation protections ("nuclearization"). In the fourth work package the facilities for handling and storage of radioactive materials and waste are designed, fabrication and installed. Finally, in light of the integral nature of this work with the realization of the VTT CNS, the fifth work package focuses mainly on the organization of the VTT CNS, commissioning, and ramp-up of the infrastructure utilization.

### Hot cells (WP1)

Over the 2015-2016 period the hot cells work package involved executing the hot cell contract with ITD, as well as developing the hot cell functions and training of personnel at VTT for the new hot cell environment. The engineering design of the hot cells was mainly executed in 2015. More detailed descriptions of the hot cell design features are given in separate reports [7,8]. Figure 3 shows the final design of the cells on the main floor. They consist of a main hot cell block arranged in two rows of 6 work-stations on each side, connected by a conveyor cell between them, and a separate, lighter cell having a shielded glove-box on one end. Additionally, in the basement there is a large cell for receiving and unloading radioactive transports. It has two work stations and an elevator connected to the upstairs conveyor cell, enabling transfer of radioactive materials directly from the basement to the main block of hot cells. Most of the manufacturing of the new hot cells took place in 2016. Figure 4 illustrates how the hot cells are constructed of a steel beam framework with a stainless steel containment.

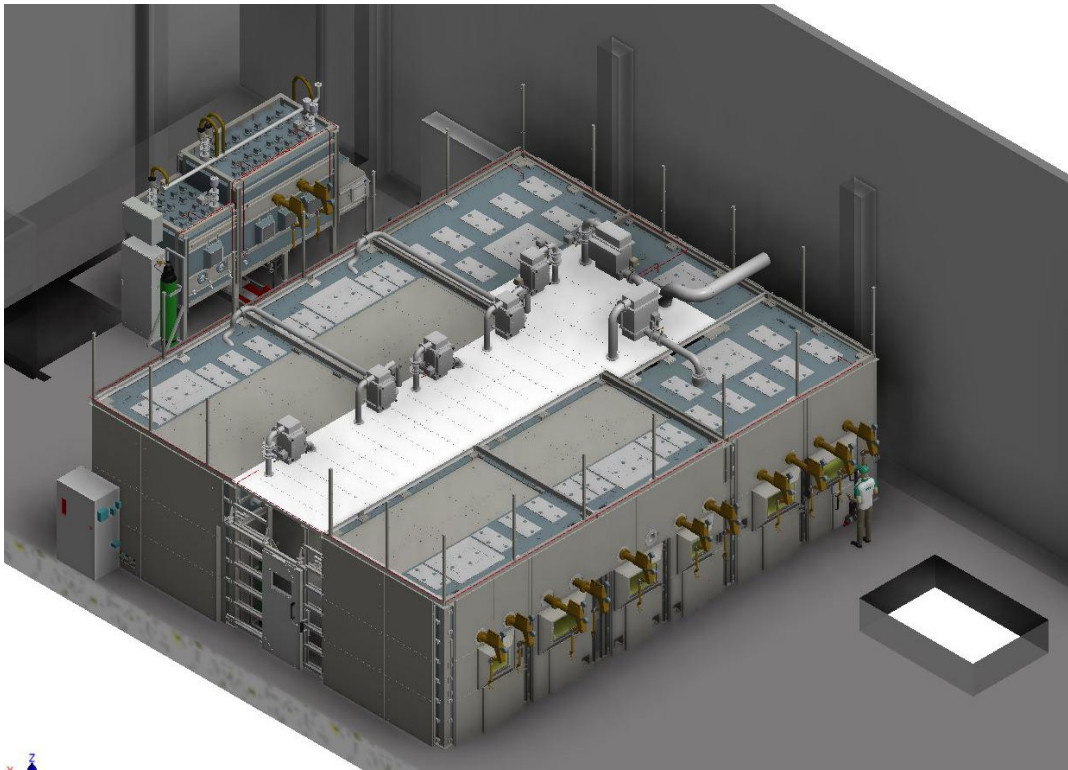


**Figure 3:** Hot cells on the main floor.



**Figure 4:** The hot cells are constructed from steel beams bolted together to make a frame that will support lead shielding bricks, and a stainless steel containment within which the radioactive materials are handled.



**Figure 5:** The finished features in a typical hot cell unit feature leaded glass windows and manipulators at each work station, double door transfer between cells, and a docking port in the table level of some cells.

In 2015 the Quality Assurance and documentation oversight at VTT was aided by a sub-contract with Qualifinn Oy for evaluating the Engineering Design Quality Plan presented by ITD. This work continued in 2016 for evaluating the Manufacturing Quality Plan of ITD [9]. Factory acceptance tests were conducted on several different occasions in the autumn, as each hot cell subassembly was pre-assembled in ITD's Dresden factory. Figure 5 shows examples of finished features in a typical hot cell unit, with leaded glass windows and manipulators at each work station, double door transfer between cells and a docking port in the table level of some cells. Installation of the hot cells in VTT's facilities commenced on the first day of 2017.

To make use of the infrastructure, there is a need to establish a safe, effective and efficient radiological workforce meeting the research and testing needs of the Finnish nuclear sector. The effective utilization of the remote-handling hot cells includes things like skilful manipulator operation, visualization with remotely-operated cameras, and development and utilization of in-cell tools and aids. Therefore, in 2016 one of VTT's hot cell engineers spent 3 months at the Paul Sherrer Institute, where he became more familiar with remote preparation and handling of metallography specimens for analyses by EPMA and SIMS, carrying out mechanical testing in a hot cell, and utilization of robotic manipulation in a hot cell setting.

### **Equipment procurement (WP2)**

Over the 2015-2018 period, the equipment procurement work package executes the procurement process for the hot laboratory equipment. The equipment is comprised of "standard" factory-produced devices related to the testing and research to be carried out in the hot cells and microscopy facilities. The process for each piece of purchased equipment involves carrying out the multistage competitive bid process involving information gathering, technical specification development, supplier identification, tendering, ordering, factory acceptance testing, and then taking delivery and commissioning of the device. Table 1 shows the

pieces of equipment in the 2015-2016 RADLAB procurement portfolio, along with their intended purpose. To guide the selection of key pieces of equipment, more extensive investigations were made to identify the important characteristics, such as for the mechanical testing devices [10] and the electron microscopes [11,12]. Not all pieces of equipment were ultimately purchased with the investment aid instrument, but rather, some were purchased as a part of VTT's own investments. The 2015–2016 RADLAB project years were the most intensive equipment investment years, so some of the more significant devices are highlighted in the paragraphs following the table.

**Table 1:** Devices in the procurement process in the 2015-2016 RADLAB period.

Device	Purpose
<b>Mechanical testing devices</b>	
MTS Hydraulic mechanical test station (MTS)	Pre-fatiguing and mechanical testing of irradiated materials. Includes environmental chamber for test temperatures between -150 and 550°C.
In-cell Zwick HIT50 with semiautomatic tempering and feeding unit RoboTest I, integrated into hot cell.	Instrumented impact test on subsized Charpy 3x4x27 mm and 5x5x27 mm specimens at temperature range from -180 to 600°C, with autofeeding. RPV surveillance tests with subsized specimens, irr RPV materials, irr. material from research reactors and programmes.
Zwick RKP450 with semiautomatic tempering and feeding unit RoboTest I <i>in local shielding.</i>	Instrumented impact tests on reference and low-level Charpy-V 10x10x55 mm and 5x10x55 mm specimens at temperature range from -180 to 300°C, in local shielding (device is too big to justify full shielding, as is only relevant to surveillance and reference tests.)
In-cell Zwick Z250SW universal testing machine with environmental chamber	Mechanical testing, e.g., fracture mechanical and tensile tests with 3PB and C(T) type specimens at temperature range from -150 to 400 °C.
Struers DuraScan 80 automatic hardness tester	Hardness measurement.

Table 1 (continued): Devices in the procurement process in the 2015-2016 RADLAB period.

Device	Purpose
<b>Mechanical testing support devices</b>	
In-cell piezomatic fatigue cracking device with specimen feeding cartridge.	Pre-fatigue cracking of 3PB specimens from 3x4x27mm to 10x10x55 mm, in a hot-cell-ready, semi-automatic fashion.
Digital video microscope. (several options)	Dimensional measurements of test specimens before and after mechanical tests, e.g., dimensions, notch depth/geometry, lateral expansion, reduction of area, etc. in remote setting of hot-cell.
GF AgieCharmilles-Wire EDM CUT200	For accurate and high-quality electro-discharge machining of radioactive materials for producing test specimens from bulk material. Programmable remote operation enables installation in a cell. Key device for e.g. producing multiple test specimens from a single Charpy, extracting a crack from a failed component, or producing blanks for microscopy specimen production.
Centrifuge water circuit for EDM	For separating out cutting debris from water circuit before it reaches the filter systems, which concentrates the radioactivity for more compact disposal and reduces the frequency of filter changes.
KUKA Robotic manipulator	For piloting programmable remote operations like EDM filter changing, machining open of surveillance capsules, and precise picking-and-placing operations.

Manipulator practice/mock-up station	Pair of master-slave manipulators in a framework, for training future hot-cell workers and for aiding in the nuclearization of in-cell equipment for remote operation.
<b>Materials characterization equipment and devices for microscopy "glovebox"</b>	
FEG-SEM	Topographical imaging of fracture surfaces and other component and material failure features, imaging at scales of mms down to nms. With electron backscatter diffraction (EBSD), crystallographic information can be gained to sub-micron resolution. With energy dispersive and wavelength dispersive spectrometers, elemental analyses can be achieved over wide range of periodic table, even with some accuracy for elements of low-atomic number, and mapping to sub-micron resolution.
Transmission Electron Microscope- TEM with EDS and EELS.	Microstructural characterisation and elemental analysis of materials from sub-micron to atomic scales, including detailed crystallographic information on selected locations, mapping of lattice orientation, and discrimination between phases. High-count silicon-drift energy dispersive spectroscope (EDS) and electron energy loss spectrometer (EELS) spectrometer of the instrument enables simultaneously gathering elemental distribution through the microstructure, including of radioactive samples whose radiation would otherwise overpower the EDS spectrometer.
Struers CitoPress and CitoVac	Remote hot and cold moulding of radioactive metallography specimens, e.g. for cross-sections of cracks and defects, macroheterogeneity assessment, etc.
Struers Tegrapol/ force with doser unit.	Remote preparation of metallographic sections of irradiated materials by grinding and polishing.
Digital microscope. Several options.	Observation of sample surfaces following e.g. fracture testing or initial grinding for metallography.
<b>Environmental testing of materials</b>	
Autoclave electronics renewal	IASCC/SCC susceptibility studies of irradiated and contaminated structural materials in simulated LWR coolant (crack growth rate measurements, crack initiation susceptibility measurements, benchmarking of different materials).
Water circuit	
New autoclave unit.	

Table 1 (continued): Devices in the procurement process in the 2015-2016 RADLAB period.

Device	Purpose
<b>Equipment for reception cell</b>	
Auxiliary in-cell devices for affixing, and handling of bulky items.	Handling of different types of bulky active material blocks, e.g., preparing for failure analysis, surveillance capsules, etc.
Commercial or purpose build CNC milling and sawing device. (Several options)	Opening of various types of surveillance capsules coming from different types of nuclear reactor pressure vessels.
<b>Radioactive material transport and storage</b>	
New small transport cask	For road transport of smaller radioactive materials beyond Finnish borders, replacing current cask allowed only in Finland.
Large transport cask	For road transport of larger radioactive materials in Finland and outside of Finland. EPR surveillance capsules do not fit in current cask.
Facility cask for SEM specimens	Safe transfer of rad specimens from preparation in shielded glove-box, to the SEM airlock.
Self-propelled heavy pallet truck	For moving of heavy transport casks through the basement transport airlock, and movement of the cask to the ports in the basement reception cell. The reception cell is designed around the use of such a pallet truck.

Free-standing light bridge crane.	For manoeuvring waste drums in waste storage, to sort, place and stack behind shielding blocks.
Rad waste drying and compacting	Preparation of very low radioactive and contaminated waste from laboratory processes for more efficient storage in waste drums.
Radioactive specimen storage facility.	Safe and organized storage of radioactive specimens, including archiving of important test pieces. Currently a large number of RPV materials are being stored, especially for Loviisa plants.
Radioactive material database system; Realized as a tailor-made system by an external contractor.	Collection and storage of key technical information about tested and researched materials within the radiological facility in a uniform and useful format, in a system that can be maintained over the long-term. Streamline processes and reduce human errors. Enable real-time presentation of total radioactivity in storage and at workstations within the radiological facility.
<b>Radiation detection and monitoring of radiological facility &amp; personnel</b>	
Personnel dosimeters	Personal radiation exposure monitor for the workers in the hot cell and radiological facilities.
Contamination detectors	Detection of radioactive contamination on objects or personnel at control points of the radiological facilities.
Background radiation monitors	Monitoring of background radiation levels in rooms of the radiological facilities, as a safety precaution to minimized accidental, undue exposure of rad workers.
Radionuclide measuring system.	Measurement of the radiological spectrum of contaminated and radioactive substances, particularly waste packed in drums, and materials packaged for transport.
<b>Technical support facilities</b>	
Machining, welding, mechanical tools etc.	To provide machining, welding and mechanical support capabilities for adapting equipment to remote operations, repairing in-cell (contaminated) equipment, and producing jigs, fixtures, etc. for aiding in-cell operations on an ad hoc, rapid turn-around basis.

### Mechanical testing devices

Firstly, in order to enable integration by ITD into the respective hot cells, the in-cell mechanical testing devices were an essential investment that had to be defined already early in the hot cell design process in 2015. As described in more detail in [10], the first priority in defining the mechanical testing activities and equipment requirements arises from the execution of the pressure vessel steel irradiation surveillance programs, particularly the capability to determine material strength and toughness properties. The second priority, although almost equally important, is the ability to prepare sub-size test specimens and reconstituted specimens to increase usage and the number of data points obtained from the limited amount of reactor-irradiated material available. To enable multi-purpose testing it was concluded that impact testing devices as well as universal tension/compression devices were required.

The basic requirements for an impact tester are capabilities to carry out conventional and instrumented impact tests and dynamic fracture mechanic tests in the temperature range from about -100°C to about 300°C, according to requirements set by relevant testing standards and accredited testing laboratory procedures. The most commonly used test specimens are Charpy-V specimens with dimensions of 10x10x55 mm and sub-size Charpy-V specimens down to dimensions of 3x4x27 mm. Basically, the specimen size requirements means that there is a need for two impact hammers, e.g., one with a maximum energy of 300 J and other with maximum energy of about 50 J. Relevant testing standards and procedures are summarized in Table 2. The assessment conducted and reported in the separate report on the matter [10], concluded that small specimens could be tested with the smaller impact hammer integrated in the hot cell,

while the larger impact hammer would mainly be required for older “classical” impact tests. Since the latter is expected to eventually reduce in popularity with the increasing need to get more test data from a single specimen via small specimen techniques, a large impact hammer would be deployed as a locally shielded device in the new facilities.

**Table 2:** Most important impact testing standards for NPP reactor materials testing.

Standard	Description
ISO EN 148-1:2006(E),	Metallic materials-Charpy pendulum impact test-Part 1: Test method.
ISO EN 148-2:1998(E),	Metallic materials-Charpy pendulum impact test-Part 2: Verification of test machines.
ISO EN 148-3:1998(E),	Metallic materials-Charpy pendulum impact test-Part 3: Preparation and characterization of Charpy V reference test pieces for verification of test machines.
ASTM E 23-07a,	Standard Test Methods for Notched Bar Impact Testing of Metallic Materials.
ISO EN 14556:2000(E),	Steel-Charpy V-notch pendulum impact test-Instrumented test method.
T259-HC/CH-V-1b	Instrumented Charpy-V impact test

A good option identified for an instrumented pendulum impact tester is the Zwick RKP 450 model with 300 J pendulum arm and head. The basic instrument dimensions are 2000 x 1920 x 500 mm and weight without foundation is about 700 kg. In addition to the basic equipment, Zwick GmbH & Co can also supply the tempering and feeding unit, model TZE, covering the temperature range from -180°C to 300°C by using liquid nitrogen and resistance heaters for cooling and heating, respectively. In semi-automatic mode the specimen handling inside the tempering unit is performed by two manually operated pneumatic slides, and specimen alignment at the specimen support and the start of the test are done automatically, remotely.

One candidate for a smaller impact tester is the Zwick HIT50 model. The basic instrument dimensions are 1170 x 1180 x 500 mm and its weight is about 500 kg. This small impact tester can be mounted on a special instrument table, and therefore it is easier to install in a hot cell compared to large impact tester. The same tempering and feeding unit is also available for the Zwick HIT50 model.

For the universal testing machine (UTM), the first priority is the capability to carry out tensile and fracture toughness tests in the temperature range from -100°C to about 350°C, according to requirements set by relevant testing standards and accredited testing laboratory procedures. Relevant testing standards and procedures are summarized in **Table 3**. The most commonly used tensile test specimens are flat, miniature specimens with dimensions of 1x2x20 mm, or larger cylindrical specimens 4-6 mm in diameter. Fracture toughness specimens are either three-point-bend specimen with dimensions of 10/5x10x55 mm down to 3x4x27 mm or C(T) specimens with varying specimen width from 25.4 mm down to 4 mm. As a research institute, the capability to utilize other types of tensile test and fracture toughness specimens specified in the standard procedures was also considered.

Fracture toughness specimens are pre-cracked, and therefore a technical capability for fatigue pre-cracking is also needed. Fatigue pre-cracking is performed at ambient temperature, and while not as fast, standard UTMs can be employed. To increase throughput, a dedicated pre-cracking machine could be justified.

The second priority for the universal testing machine is the capability to carry out various other types of mechanical tests, e.g., high/low cycle fatigue, fatigue crack growth, constant load, thermal creep, shear punch tests etc. using various types of test specimens.

Due to the relatively large variety of different tests and test specimen geometries, two separate universal testing machines is the minimum foreseen for hot cell testing. Due to requirements for fatigue precracking and low/high cycle fatigue testing, at least one of the testing machines should be servo-hydraulic ma-

chine which is most suitable for the alternating loading mode requirements. It is noted that there are also similar versions of electromechanical machines available. For deployment in the new hot cells, a 100kN servo-hydraulic MTS device was purchased in 2015, while a Zwick Z250SW 250kN electromechanical universal testing machine was purchased for delivery directly to ITD in 2016 for integration into the new hot cell.

**Table 3:** Most important tensile and fracture toughness testing standards for NPP reactor materials testing.

Standard	Description
<b>Tensile test</b>	
ISO EN 6892-1:2009	Metallic materials. Tensile testing. Part 1: Method of test at room temperature
ISO EN 6892-2:2011	Metallic materials. Tensile testing. Part 2: Method of test at elevated temperature
ASTM E8/8M-11	Standard Test Methods for Tension Testing of Metallic Materials
ASTM E21-09	Standard Test Methods for Elevated Temperature Tension Tests of Metallic Materials
<b>Fracture mechanic test and prefatigue</b>	
ASTM E1921-08	Standard Test Method for Determination of Reference Temperature, $T_0$ , for ferritic Steels in the Transition Range
ASTM E1820-08	Standard Test Method for Measurement of Fracture Toughness
ESIS P2-92	Procedure for Determining the Fracture Behaviour of Materials
<b>Calibration</b>	
ISO EN 7500-1:2004	Metallic materials-Verification of static uniaxial testing machines-Part 1: Tension/compression testing machines-Verification and calibration of the force measuring system
ISO 9513	Metallic materials-Calibration of extensometers used in uniaxial testing

Once the two Zwick devices were selected for the in-cell equipment, the details were fixed in collaboration with ITD, including the details of the furnace, and then a final package price was negotiated with Zwick. The purchase orders for both mechanical test devices were approved in May 2016. The factory acceptance tests of both devices were carried out at Zwick's German factories in late November 2016, Figure 6. After acceptance (with modification requests relating to remote-opening mechanism of furnace door), they were then shipped to ITD for integration of the devices. The FAT of the cells with integrated devices took place on ITD's premises a couple of months later. The integrated devices are shown in the images in Figure 7.



(above) Zwick HIT50 small impact tester with semi-automatic, remotely operated specimen furnace and feeder.



(right) Zwick Z250SW 250kN electromechanical universal testing machine with environmental chamber.

**Figure 6:** Factor acceptance tests of the two Zwick mechanical testing devices took place at two different factories in Germany in November 2016. From there they were delivered to ITD for in-cell integration.

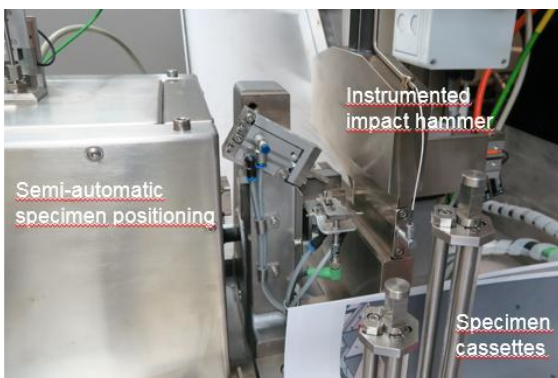
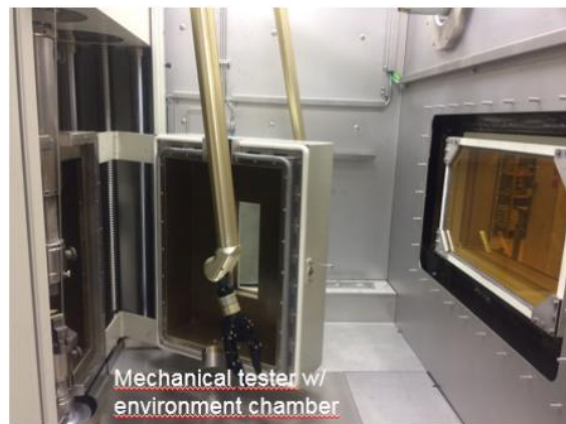
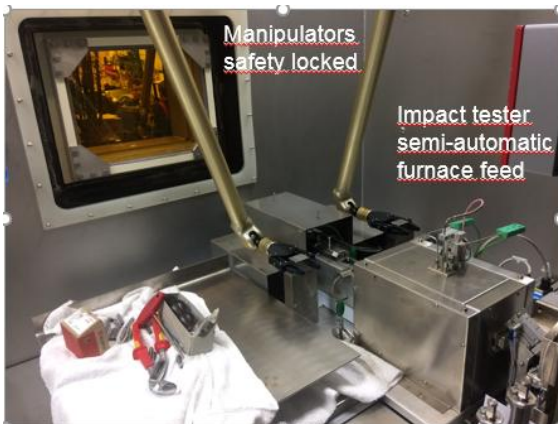


**Figure 7:** Factor acceptance tests of the two Zwick mechanical testing devices as they were integrated into the hot cells took place at ITD's factory.

## Analytical electron microscopes

Since the CNS laboratory was scheduled to be completed before the hot cells would be manufactured and installed, two other significant investments were the analytical electron microscopes.

As described in [12], a modern scanning electron microscope (SEM) equipped with a field emission gun (FEG) enables imaging to nanoscale, covering a wide field of study areas, from reactor pressure vessel (RPV) carbides distributions, to general lower magnification fractography. The strength of a FEG-SEM is the capability to span the magnification range from optical microscopy to transmission electron microscopy (TEM). Equipped with a carefully chosen variety of peripheral devices, it is a very versatile tool. Energy dispersive x-ray spectroscopy (EDS) is used for fast elemental mapping, electron back-scatter diffraction (EBSD) gives information on the crystallography of the material, residual strains, grain orientation, texture etc. Wavelength dispersive x-ray spectroscopy (WDS) widens the possibilities for elemental analysis in situations where EDS is inadequate; it enables higher spectral resolution, so that overlapping peaks in the EDS spectrum can be separated, and the elements identified with more confidence. This is very relevant to RPV steels, as there are significant overlaps on Mo and S and P, for example. WDS also enables quantifying the composition of micron-sized particles.

A focused ion beam (FIB) has become a widely used tool for location-specific microcross-sectioning, and in-situ sample preparation in the SEM. A FIB also enables preparation of site-specific TEM foils, and extraction of samples for atom probe tomography (APT). The low volume of APT samples and FIB-extracted TEM foils makes it possible to ship irradiated samples reasonably easy abroad for further analysis, while in-house sample preparation with a FIB equipped FEG-SEM ensures that samples are taken from a relevant area in the specimen. For general work in the FEG-SEM, a FIB is also very powerful, as initiation sites, crack tips, defects etc. can be cross sectioned accurately. Also, difficult to prepare samples like brittle (ceramic) or very soft and ductile (Cu) can be prepared more easily, and with better quality. Of particular importance, the minimal sample preparation prior to FIB microscopy of irradiated specimens can also lower the dose for laboratory personnel.

Based on points like those in the preceding paragraphs, and an assessment of the different suppliers of electron microscopes and peripheral devices, it was concluded in early 2015 that the optimal setup would be a Zeiss CrossBeam540 FIB-SEM equipped with an EDAX Triade EDS/EBSD/WDS analyser portfolio. The instrument was delivered in the last week of September 2015, and the analysers in January 2016.

The report [11] describes in more detail the characteristics of a modern analytical transmission electron microscope. It has a field emission electron source, and is operated at 200 kV. A Shottky emitter is the most common electron source, as it provides the most stable and intense electron probe currents. The instrument should have powerful energy dispersive X-ray emission (EDS) detection capability as well as possibility for

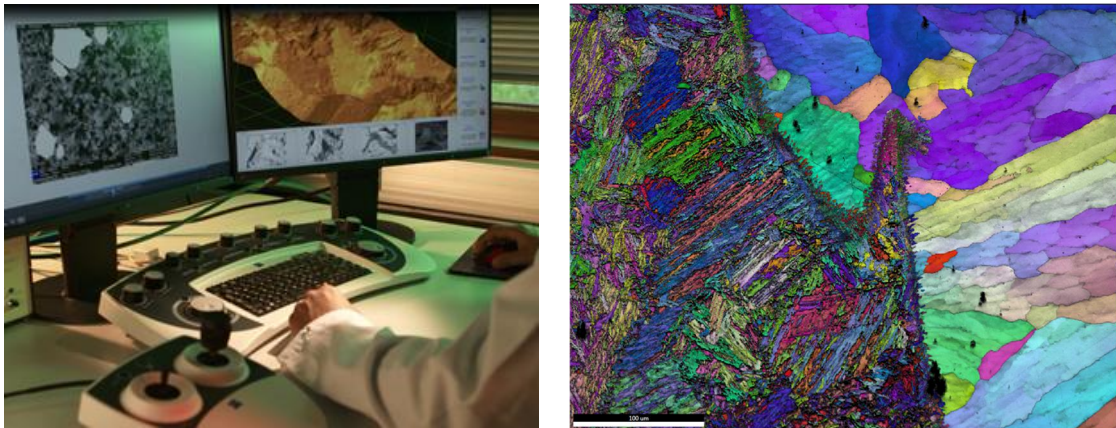
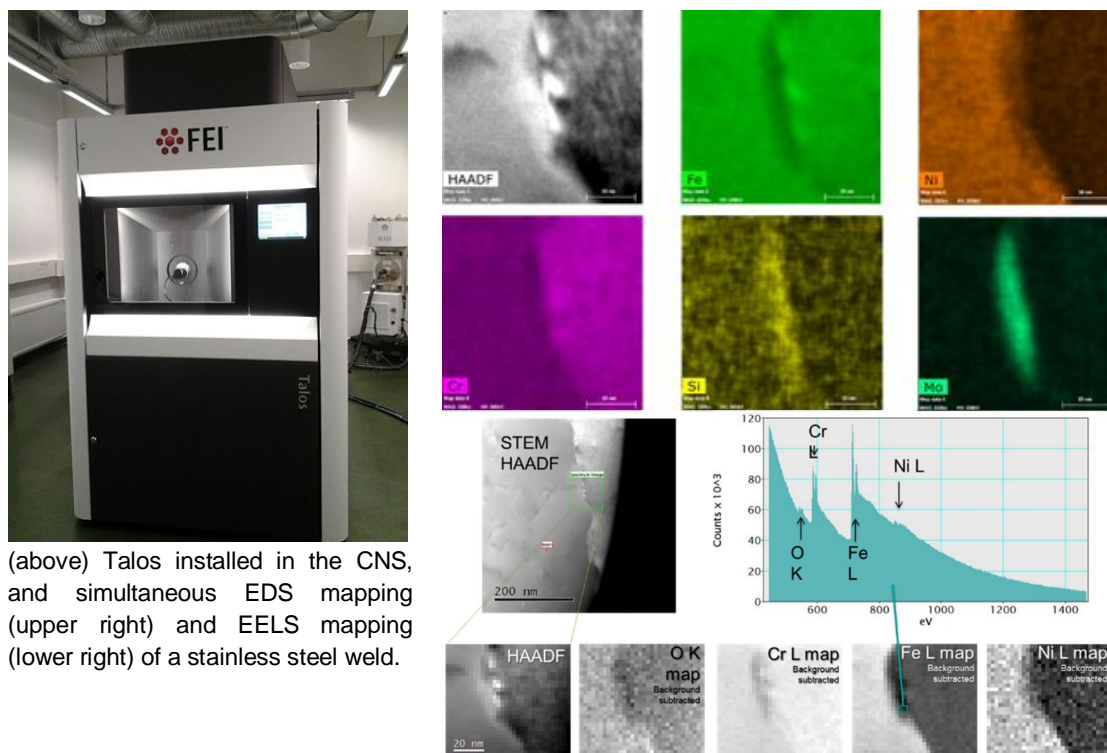


**Figure 8:** The Zeiss CrossBeam540 FIB-SEM was delivered in late September 2015 (left). The EBSD proved to be excellent, as shown in the example of a grain orientation map of an RPV weld fusion zone (right).

electron energy loss spectroscopy (EELS) coupled with either image filtering or electron spectroscopic imaging (ESI). In addition to standard bright- and dark-field imaging modes and selected area diffraction mode, a modern analytical TEM also has a scanning transmission mode (STEM) that can image the sample down atom resolution, and which can simultaneously use EDS and EELS spectroscopy on a selected location in the sample. A powerful variant of the STEM mode is Z-contrast imaging, showing atomic number contrast. This mode is especially important in the analysis of the small particles or inclusions etc.

Furthermore, a modern analytical FEG TEM has a very useful method called convergent beam electron diffraction (CBED), that utilises a nanometre range electron probe to provide diffraction data from very small areas or details on the sample. The method can be used in analysis of most of the important lattice defects in irradiated materials.

The preparations for procuring a new TEM was carried out for several years, but in 2015 it proceeded with more intense negotiations with the principal suppliers. While Hitachi was ultimately discarded, the JEOL microscope was left as the principle candidate. Then FEI reasserted their interest by offering their new Talos F200X FEG microscope. Introduction to a real FEI Talos was had at the M&M conference in August 2015, where other users and their accomplishments with the Talos instrument raised the level interest in procuring one. In late September 2015 two VTT microscopists visited the FEI demo center in Eindhoven to test a Talos with VTT's own (non-irradiated) foils. After FEI's Talos budgetary offer was proven to be competitive, an internal decision was reached to purchase at Talos with its built-in 4-sector EDS analyser and EELS system. VTT purchase approval was attained and signed by the VTT CEO in late 2015, and an informal order was placed with FEI for a Talos, to reserve a manufacturing window, while the formal procurement process was launched. Ultimately the new microscope was delivered directly to VTT's new CNS laboratories in June 2016.



(above) Talos installed in the CNS, and simultaneous EDS mapping (upper right) and EELS mapping (lower right) of a stainless steel weld.

**Figure 9:** The FEI Talos F200X FEG was delivered to the VTT CNS in June 2016.

### Research equipment (WP3)

The research equipment work package is mainly tasked with the development and construction of those research devices that are not readily available on the market, but rather, require custom design. Adapting devices for functionality in a remotely-operated, potentially contaminated environment (called “nuclearization”) is also carried out in this work package. Devices and adaptations are designed with the experts involved in utilizing the equipment for producing research results, and then made by in-house assembly of parts bought from component suppliers, or fabricated in-house or by outside shops.

**Hot autoclaves** enable safe mechanical testing of radioactive materials in well-controlled, simulated power plant water environments. The main use for such facilities currently is in assessing the susceptibility of stainless steel internals component materials to irradiation assisted stress corrosion cracking (IASCC), generally as a function of material irradiation condition, loading scenario, and water chemistry. The materials testing autoclaves and water circuit are located in a dedicated room of the basement of the CNS. An example of the typical water circuit is shown in Figure 8. The floor plan/placement of the hot autoclaves and water circuits for the new facility was first done in 2015, and the plans were updated in 2016. The design for the new autoclave is shown in Figure 9. A more detailed description of the hot autoclave facility is in [13].

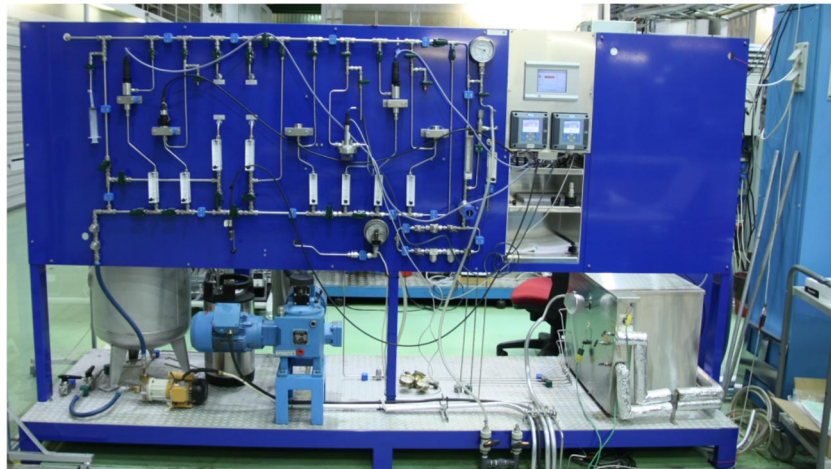


**Figure 10:** A water re-circulation loop in the laboratory for unirradiated materials testing, illustrating the design for a loop for irradiated materials testing. The total space needed for the loop is in the range of 4-5 m<sup>2</sup>.

1. Lid lift control
2. Venting valve
3. K-type temperature sensor
4. Drain valve
5. Lid lift mechanism
6. Displacement indicators
7. Stepper motors and worm gears
8. Autoclave
9. Load cells

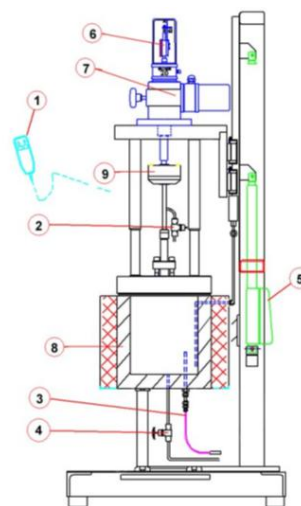


**Figure 11:** The hot autoclave design is comprised of the loading devices, the autoclave itself, and a mechanism for lifting the lid remotely.

In 2016, the needs for upgrades for old hot autoclaves (2) and water circuit (1) were identified and offers requested from suppliers. In the last pressure vessel/autoclave inspection a crack indication was found in one of the two old autoclaves. Due to the contamination and general condition of that autoclave, a decision was made to replace it instead of renewal. Components for the renovation of the other autoclave were ordered and delivered by the end of 2016. An offer for a new autoclave was requested and received.

RPV surveillance specimens are packed in stainless steel “cans” for irradiation in the power reactor. When the specimens are to be tested, they first have to be removed from the can by machining it open. The irradiated can and its specimens have a high level of radioactivity, so the machining operation has to be carried out remotely. Modelling of **surveillance capsule opening** by a roof-mounted power manipulator was done in 2015 to evaluate its potential. Successful remote machining of a capsule mock-up was subsequently demonstrated using the KUKA robotic manipulator pilot set-up [14], and that method was taken into the hot cell 3.1 design process as the primary machining method over the 3-axis milling machine.

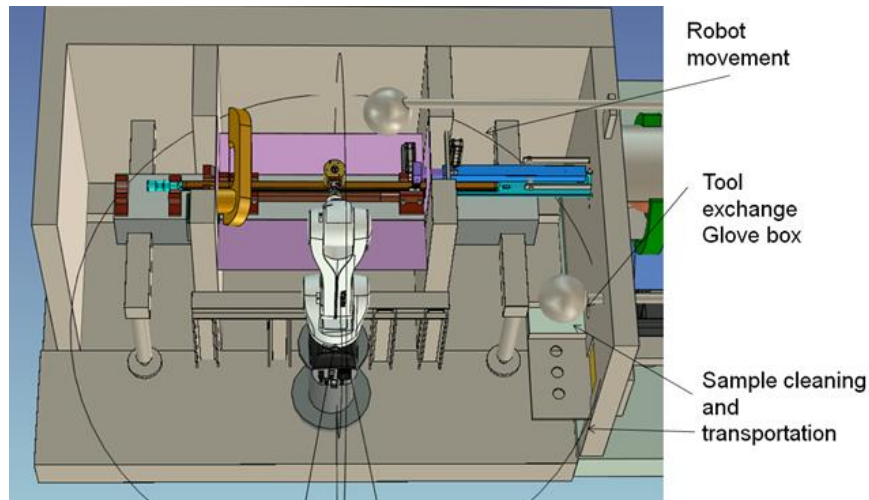


**Figure 12:** Modelling of KUKA robotic manipulator for cutting open a monolithic type surveillance capsule.

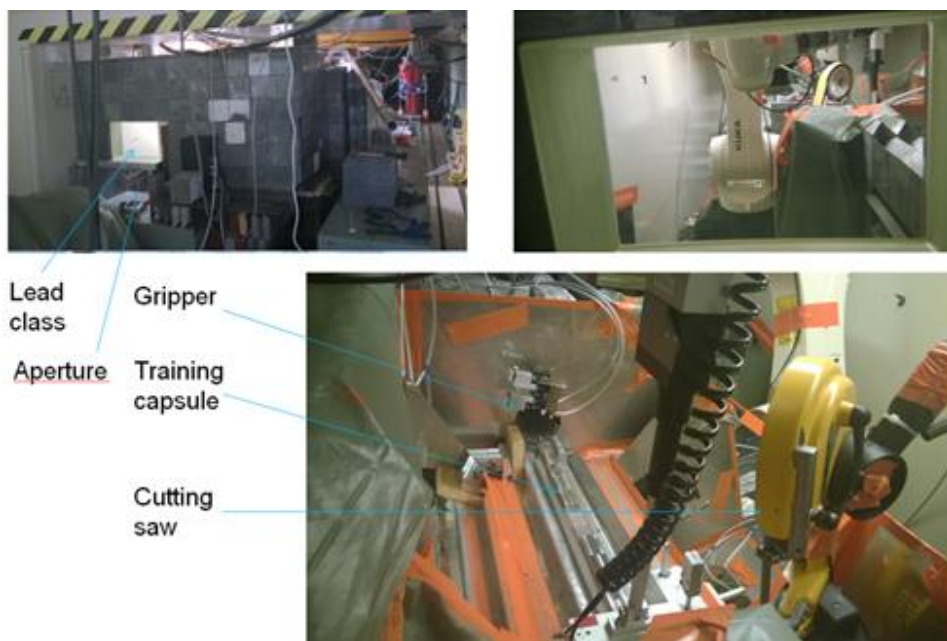


**Figure 13:** The pilot set-up with the KUKA successfully demonstrated the use of robotics in remote operation.

In parallel, testing the use of a conventional **3-axis machining station** for opening surveillance capsules was also undertaken in 2015, and potential suppliers for a 3-axis machining station equipped with CNC were still sought from within Finland. Then in 2016 a first conceptual design and cost estimate for a remotely-operated CNS machining station was made by Metecno Oy. This is shown in Figure 12. This was then iterated to an improved design that would be sufficient for making a purchase decision and procurement description in 2017. Purchase of the device is now on hold while efforts focus on getting the hot cells up and running. Nonetheless, the worktable in cell 3.1 is designed to accommodate either a conventional 3-axis mill, or a robotic machining manipulator.

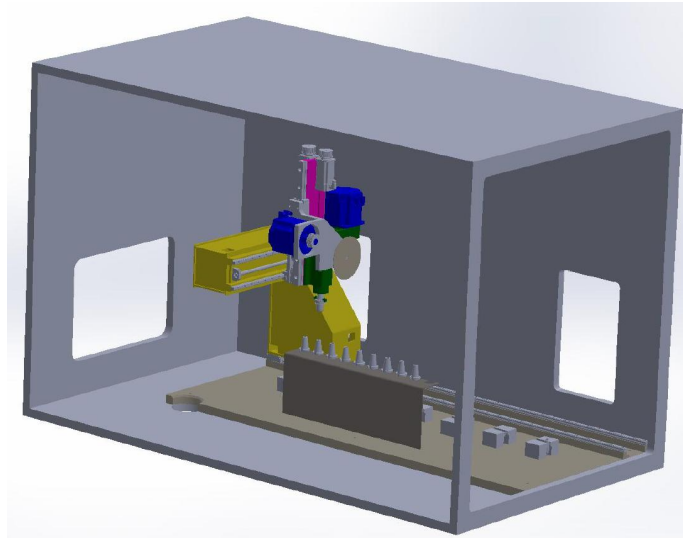


**Figure 14:** As an alternative means of machining open surveillance capsules, the use of a custom-build CNC 3-axis machining station was explored. A conceptual design and cost estimate was provided by Me-tecno Oy.

In the so-called “reconstitution” process, precision welding with low total thermal input is possible by electron beam welding (EBW). In 2016 some needed modifications to VTT’s **electron beam welder** (EBW) were identified to enable better functionality within the new hot cell environment, as shown in Figure 13. The decision was made to purchase the modification planning and execution from the EBW manufacturer. The modification is scheduled to be made in 2017 to coincide with for installation of the EBW into the new hot cell 1.2. It will facilitate remote operation of the chamber door, as well as easier replacement of the EBW filament from the small man-access in the rear of the hot cell.



**Figure 15:** VTT’s electron beam welder (left) will be modified for integration into the new hot cell (right).

In 2015, the culmination of the nuclearization progress of the pilot facility of the **electric discharge machine (EDM)** was reported in a comprehensive document [15]. The EDM is a key device for the cutting of radioactive materials, like accurate sample preparation for RPV surveillance programs. For proper function of the cutting procedure, the water must be very clean. The cutting debris is in the form of small particles suspended in water. In conventional machines these are filtered out via disposable filter cartridges, but

when machining radioactive materials, the debris-containing filter cartridges are a significant source of radioactivity. This is important both when needing to change the filters, and for disposal of the cartridges. Therefore, a new water purification method for the EDM was developed that employed a particle centrifuge and a reversible permanent filter, which succeeded in reduce the number of disposable cartridges required. Figure 14 shows the pilot set-up employed for testing the method, and Figure 15 shows the main components of the water circuit itself.

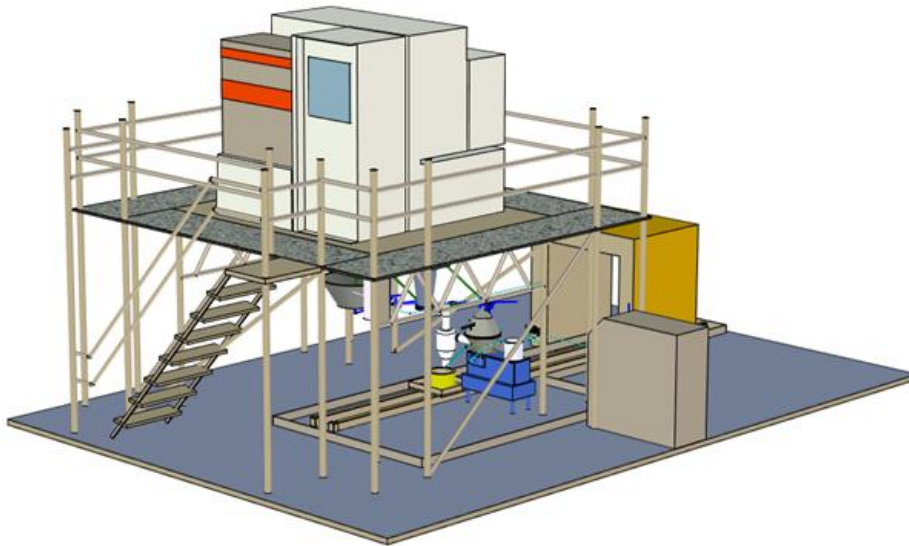


**Figure 16:** The electric discharge machine (EDM) was piloted with an external water circuit featuring a centrifuge to reduce the use of disposable filters, which are problematic when machining radioactive materials.

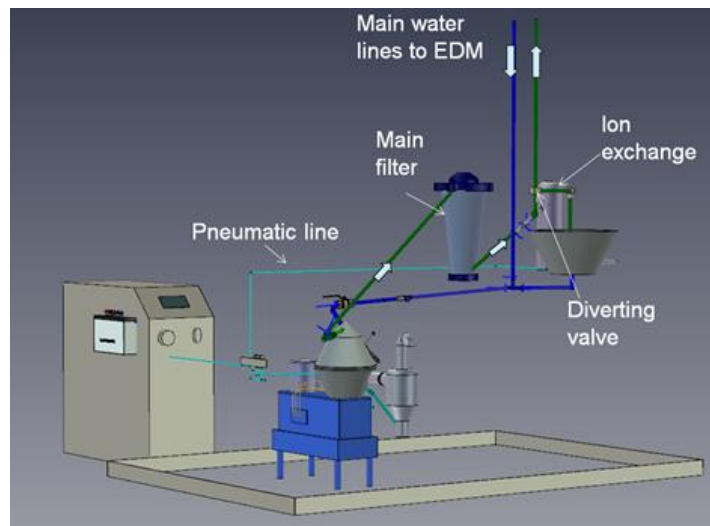


**Figure 17:** The main constituents of the EDM water circuit are the controller, centrifuge, (reversible) main filter, and diversion circuit through the ion exchange resin.

Finally, while the main equipment for testing and characterization of radioactive structural materials is located in the hot cells constructed by ITD, non-active materials, contaminated materials, and materials of low levels of radioactivity can be handled more quickly and easily in **locally shielded devices**. This can

relieve some of the workload of the hot cells themselves, and increase the overall capacity of the facilities. Thus, design work is underway for local shielding for a full-size 450 J instrumented impact hammer (replacing the old, outdated device that will be decommissioned with the OK3 facilities), and a universal mechanical testing device. The conceptual design of the local shielding for those devices took place in 2016, and the engineering design and fabrication will take place in 2017. Local shielding includes, at a minimum, a containment enclosure attached to the ventilation system so that any possible contamination is isolated. For lightly gamma irradiating materials, some local lead shielding is employed as needed. Handling is via glove-ports and utilizing hand tongs to offer a degree of radiation protection. Examples of local shielding solutions are illustrated in Figure 16.

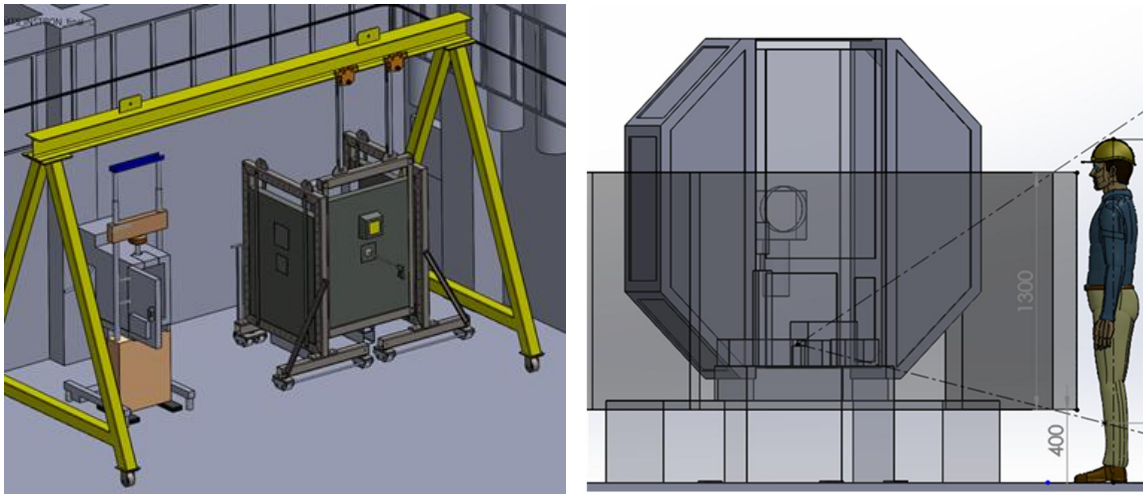


**Figure 18:** Local shielding is possible in cases where mechanical testing includes non-radioactive reference specimens and contaminated or radioactive specimens of relatively low total radioactivity.

### Supporting facilities (WP4)

The VTT CNS requires a number of self-built supporting facilities. In the 2015–2016 period, this work package has focused on the design, construction and installation of equipment for three main areas: laboratory radioactive waste handling, radioactive research material logistics, and orderly storage of radioactive specimens. The hardware for these systems are mainly located in the basement of the CNS.

The design requirements and some options for the **waste handling system** were conceptualized in earlier projects [16,17], and then elaborated in a report produced in 2015 project on a contract with Platom Oy [18]. A separate room is available for wet waste handling installations, including the EDM water loop and a water evaporation/re-condensation system. A separate room is also available for the dry waste handling installation, including waste sorting, drying and packing equipment. As shown in Figure 17, dry contaminated waste is stored in 200 litre barrels, shielded by a moveable wall of concrete blocks. The barrels are planned to be manipulated by an overhead bridge crane covering the storage area. In 2016 the main focus was on the dry-waste handling, and effort went to ensuring that the building fixtures, epoxy floor and final as-built dimensions were suitable for the purpose. The light-duty bridge crane model was identified for purchase, and the concrete shielding blocks were sourced.

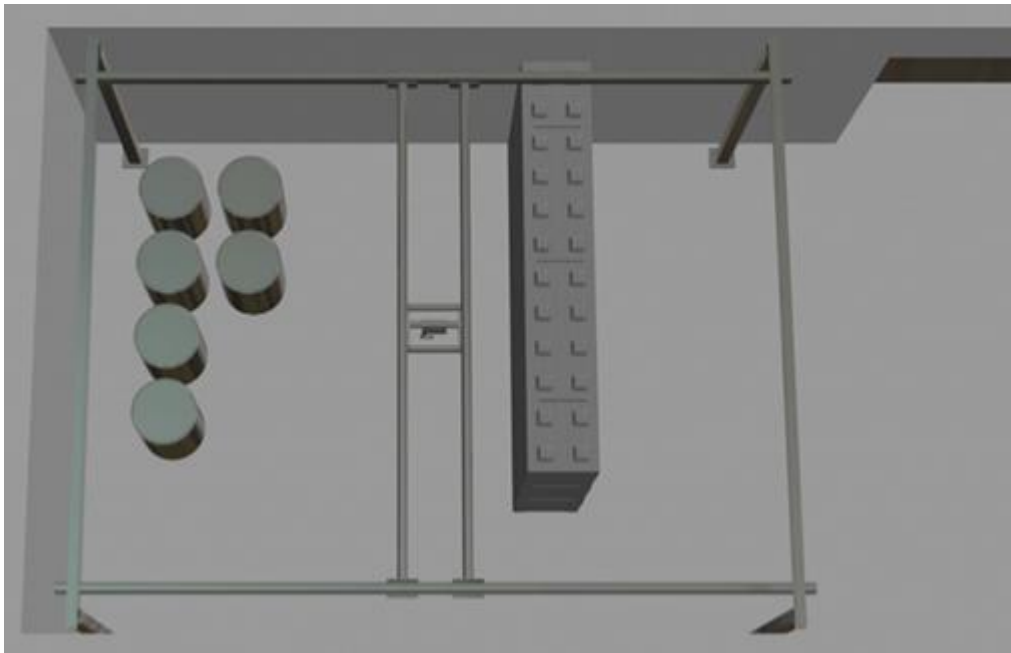


**Figure 19:** Dry contaminated waste is stored in 200 litre barrels, which are to be stored in a specific room in the basement of the CNS, shielded by a moveable wall of concrete blocks. The barrels are planned to be manipulated by an overhead bridge crane covering the storage area.

Means are required for safe and orderly interim storage of radioactive test materials. The location for a primary storage facility has been specified in the new CNS to take advantage of natural shielding offered by the surrounding granite base-rock. A comprehensive storage system consists of both a shielded storage device and the means for safely and orderly picking and placing of the radioactive materials. In 2016 the conceptual design of the **physical storage** device was completed and its engineering design and fabrication will be realized in 2017 on a procurement contract. It will consist of vertical stacks of baskets in an alpha-numerical matrix within a well of lead or steel radioactive shielding, as shown in Figure 18.

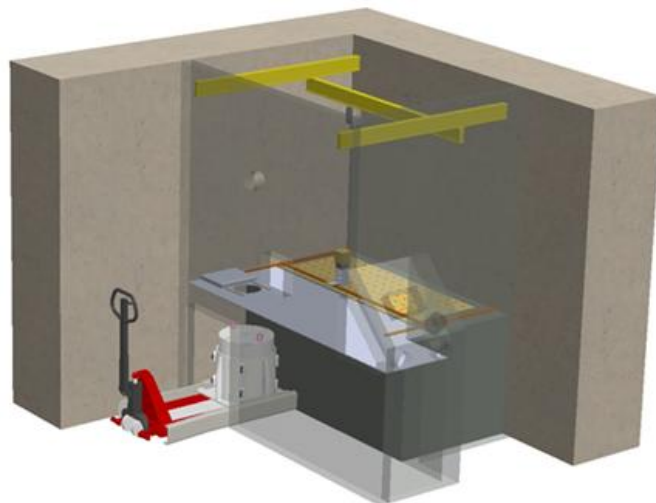


**Figure 20:** The physical shielded storage for radioactive specimens will consist of vertical stacks of baskets in an alpha-numerical matrix within a well of lead or steel radioactive shielding well.

Orderly storage also requires an inventory database for maintaining important specimen information and tracking its location in the facility when it is taken out of the storage facility. An important aspect of the move from the old OK3 facilities, is the orderly transfer to the new facilities of any radioactive specimens that cannot otherwise be returned to their origin by that time. To prepare for that, a new **specimen database** was conceptualized in 2015 on a contract with Fraktio Oy [19]. In the 2016 project, a contract was carried out with Ambientia Oy, to create the first version of a functional specimen database system. Now the existing materials inventory can be recorded in the database system, which can then form the basis for the inventory database system in the new facilities. The software tool, named “Pergament”, includes functionality for tracking specimens throughout the radiological facilities, as well as pinpointing storage locations in the central storage device. A screen shot from the software tool is shown in Figure 19. Radioactivities can be recorded for a piece of material, and then calculated for each of the subsequent specimens created from the material. Files affiliated with particular specimens, such as photographs, documentation and reports, can be appended to the database entries, and histories are recorded as the material and specimens move and evolve through the research and testing processes.

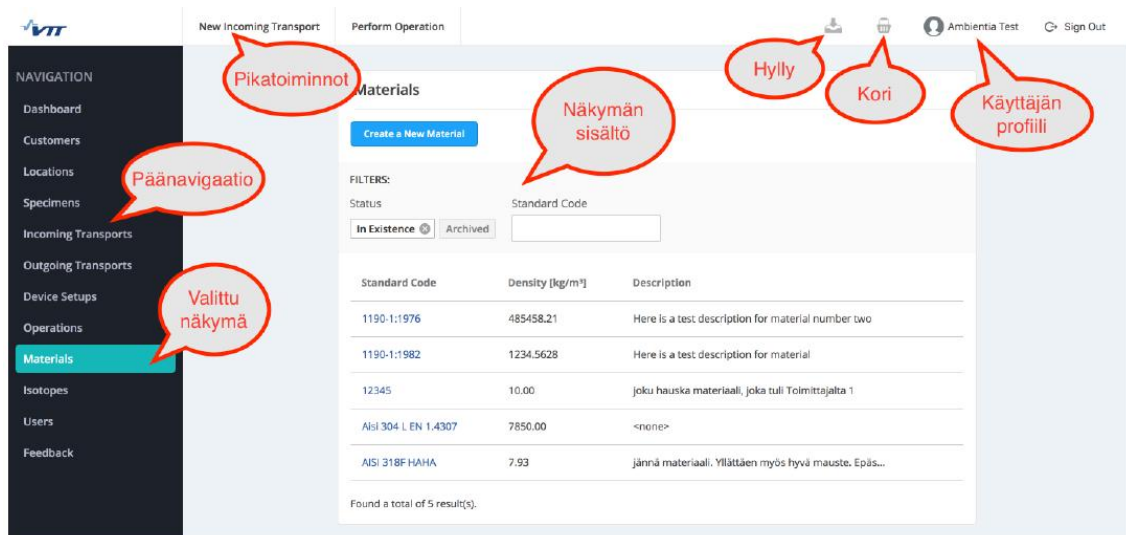


**Figure 21:** Screen shot from the “Pergament” radioactive specimen database tool, showing some of the features of the tool.

### Centre for Nuclear safety realization and commissioning (WP5)

Continuing the momentum built up in 2014, construction of the VTT Centre for Nuclear Safety (CNS) proceeded on schedule through 2015, and in 2016 the commissioning of the new facilities got underway. The ridge-raising celebration was held in the first week of June 2015, and the office wing was ready for move-in in January 2016. The construction progress is shown in Figure 22. In parallel, follow-up of the detailed facility design process mainly consisted of deciding particular details of specific aspects and cost-savings opportunities of the building systems, structures and furnishings, mainly with the help of the detailed 3-D design model and discussions held around drawings of particular features.

The Centre for Nuclear Safety commissioning project (KORY) held its kick-off meeting on 26.8.2015. The KORY coordinated the commissioning process of the new facility, involving familiarization with the functionality and maintenance of the facility technology, move-in and installation of end-user equipment, and assurance of building functionality. The members include key members from VTT (end-user), Senaatti-kiinteistöt (owner), A-Insinöörit (construction consultant), SRV (principle constructor), and the building facilities maintenance contractor.

Oversight by external stakeholders in the CNS included a site visit by TVO construction experts on 9.9.2015 to learn more about the design and construction choices of the facility, as well as an inspection tour on 24.9.2015 by STUK and EURATOM representatives for nuclear materials safeguards.

The laboratory wing was released to VTT on schedule, in May 2016. But many small fixes and changes were still carried out intensively in the weeks following, while equipment such as the high resolution, inductively coupled mass-spectrometer were moved into the facilities (). The radiological commissioning process was managed through a few meetings with STUK over the 2016 period, and the documentation was prepared and submitted for three different permits. In late January 2017, STUK approved the radiological facility permit enabling operation of the CNS radiochemistry and microscopy laboratories for radioactive materials analyses. At the same time the nuclear materials security permit granted the previous summer came into effect. The iodine laboratory of VTT Expert Systems received their complementing permit in autumn 2016. With the permits coming on line, it was a suitable time to hold a seminar detailing the new infrastructure capabilities more broadly. This Users' Group seminar was held on January 24<sup>th</sup>, 2016, and was followed by a tour of the new laboratories and the hot-cell installation site.



**Figure 22:** Progress on construction of the VTT Centre for Nuclear safety in 2015, as the building took on its final exterior appearance, CW from upper left, January, March, July and December 2015. In January 2016 the office wing was ready for move-in.



**Figure 23:** The laboratory wing was released to VTT in May 2016, after which equipment move-in began.

## References

1. Aho-Mantila, I., Ehrnstén, U., Jäppinen, T., Karlsen, W., Lappalainen, P., Lydman, J., Lyytikäinen, T., Mattila, M., Paasila, M., Toivonen, A., Tähtinen, S., Veivo, J. Hot Cell activities and design considerations. VTT Report VTT-R-05328-13. 56 p.
2. Ehrnstén, U., Autio, J-M., Karlsen, W. Hot cell microscopy activities and design considerations. VTT Report VTT-R-00629-14. 18 p.
3. Karlsen, Wade, The new VTT Centre for nuclear safety, 51st Annual Meeting of the Hot Laboratories and Remote Handling Working Group, HOTLAB 2014, 21 - 25 September 2014, Baden, Switzerland Proceedings. HOTLAB Steering Committee (2014), 18 p. <http://hotlab.sckcen.be/en/Proceedings>
4. Karlsen, W. Hot Cell Conceptual Design for VTT by Merrick & Company. VTT Report VTT-R-06084-13. 103 p.
5. Tähtinen, S., Karlsen, W. Engineering design and manufacturing of radioactive materials testing hot cells. VTT Report VTT-R-03470-14. 27 p.
6. Karlsen, W. Roadmap for the VTT Centre for Nuclear Safety Research Infrastructure, VTT Report VTT-M-06237-15.
7. Karlsen, W., and Tähtinen, S., VTT Hot Cell Conceptual Design by ITD, VTT Report VTT-R-02511-15. 16 p.
8. W. Karlsen, F. Butze "The new VTT hot cells," in Proceedings of the 52nd Annual Meeting of the Hot Laboratories and Remote Handling Working Group, HOTLAB 2015, September 27-30, 2015, Leuven, Belgium, 11p. <http://hotlab.sckcen.be/en/Proceedings>
9. Tähtinen, S., VTT Hot Cell Design and Manufacturing by ITD – Project Quality Plan - Manufacturing, VTT-R-04150-16, 29 p.
10. Tähtinen, S. REHOT - Mechanical testing. VTT Report VTT-R-00552-14. 31 p.
11. Tapper, U., Centre for Nuclear Safety Transmission Electron Microscope (TEM) Procurement, VTT Report VTT-R-04881-15, 13 p.
12. Autio, J.-M., Tapper, U., Centre for Nuclear Safety SEM Procurement, VTT Report VTT-R-00565-15. 17 p.
13. Toivonen, A., and Väisänen, P., REHOT 2015 D3.1.1 Descriptive report of "hot" autoclave facilities. VTT Report VTT-R-05721-15. 10 p.
14. Moilanen, P., Lappalainen, P., Planman, T. and Lyytikäinen, T., Remote opening of an irradiated surveillance capsule by robot, VTT-R-03965-16, 20 p.

15. Moilanen, P., Paasila, M., Lappalainen, P., Water purification system for the Electric Discharge Machine (EDM) VTT-R-05845-15, 36 p.
16. Aho-Mantila, I., Lappalainen, P., Lydman J., Paasila, M. Ydinturvallisuustalon hotcell -laboratorion jätteenkäsittelysuunnitelma, luonnos. VTT Report VTT-R-00580-14, 19 p.
17. Huotilainen, S., Ydinturvallisuustalon aktiivisten materiaalien jätteenkäsittelyn infran suunnittelu, VTT Report VTT-R-00179-15, 10 p.
18. Huotilainen, S., Ydinturvallisuustalon aktiivisten materiaalien jätteenkäsittelyn tekninen suunnittelu, VTT Report VTT-R-06012-15, 18 p.
19. Karlsen, W. and Paasila, M., Description of radioactive specimen storage database system, VTT Report VTT-R-00252-16, 31 p.

Title	<b>SAFIR2018 – The Finnish Research Programme on Nuclear Power Plant Safety 2015–2018</b> Interim Report
Author(s)	Jari Hämäläinen & Vesa Suolonen (eds.)
Abstract	<p>The Finnish Nuclear Power Plant Safety Research Programme 2015–2018, SAFIR2018, is a 4-year national technical and scientific research programme on the safety of nuclear power plants. The programme is funded by the Finnish State Nuclear Waste Management Fund (VYR), as well as other key organisations operating in the area of nuclear energy. The programme provides the necessary conditions for retaining knowledge needed for ensuring the continuance of safe use of nuclear power, for developing new know-how and for participation in international co-operation. Major part of Finnish public research on nuclear power plant safety is carried out in the SAFIR2018 programme.</p> <p>SAFIR2018 consist of four main research areas: (1) Plant safety and systems engineering; (2) Reactor safety; (3) Structural safety and materials; and (4) Research infrastructure. Research carried out in the projects is guided by six reference groups. The research results of the projects are published in scientific journals, conference papers and research reports.</p> <p>The programme management structure consists of the Management Board, three Steering Groups managing the research areas, six Reference Groups, and programme administration. SAFIR2018 Management Board consists of representatives of the Radiation and Nuclear Safety Authority (STUK), Ministry of Economic Affairs and Employment (MEAE), Fennovoima Oy, Fortum, Teollisuuden Voima Oyj (TVO), Technical Research Centre of Finland Ltd (VTT), Aalto University (Aalto), Lappeenranta University of Technology (LUT), the Finnish Funding Agency for Innovation (Tekes), and the Swedish Radiation Safety Authority (SSM).</p> <p>Research projects of the programme were chosen on the basis of annual call for proposals. The total volume of the SAFIR2018 programme in 2015–2016 was 15,5 M€ and 112 person years. Main funding organisations were the Finnish State Nuclear Waste Management Fund (VYR) with 9,3 M€ and VTT with 3,4 M€. The research was carried out in 28 projects during 2015 and 2016.</p> <p>The research in the programme has been carried out by VTT, LUT, Aalto, University of Oulu, Finnish Meteorological Institute, Finnish Institute of Occupational Health, SP Technical Research Institute of Sweden, Risk Pilot AB, Finnish Software Measurement Association FISMA, and IntoWorks. A few subcontractors have also contributed to the work in the projects.</p> <p>This report gives a summary of the research results of the SAFIR2018 programme during the years 2015–2016. More detailed statistical information of the programme and lists of project publications as well as the members of the Management Group, Steering Groups, and Reference Groups can be found in annual plans and reports on SAFIR2018 website <a href="http://safir2018.vtt.fi/">http://safir2018.vtt.fi/</a>.</p>
ISBN, ISSN, URN	ISBN 978-951-38-8524-3 (URL: <a href="http://www.vttresearch.com/impact/publications">http://www.vttresearch.com/impact/publications</a> ) ISSN-L 2242-1211 ISSN 2242-122X (Online) <a href="http://urn.fi/URN:ISBN:978-951-38-8524-3">http://urn.fi/URN:ISBN:978-951-38-8524-3</a>
Date	March 2017
Language	English
Pages	387 p.
Name of the project	The Finnish Nuclear Power Plant Safety Research Programme 2015-2018, SAFIR2018
Commissioned by	MEAE
Keywords	nuclear safety, safety management, nuclear power plants, human factors, safety culture, automation systems, control room, nuclear fuels, reactor physics, core transient analysis, thermal hydraulics, modelling, severe accidents, structural safety, construction safety, risk assessment, research infrastructure
Publisher	VTT Technical Research Centre of Finland Ltd P.O. Box 1000, FI-02044 VTT, Finland, Tel. 020 722 111



**SAFIR2018 –  
The Finnish Research Programme on Nuclear  
Power Plant Safety 2015–2018**  
Interim Report

ISBN 978-951-38-8524-3 (URL: <http://www.vttresearch.com/impact/publications>)  
ISSN-L 2242-1211  
ISSN 2242-122X (Online)  
<http://urn.fi/URN:ISBN:978-951-38-8524-3>

